Multiple freshwater mussel species of the Brazos River, Colorado River, and Guadalupe River basins
CMD 1—6233CS

Compiled on March 2, 2020

Principal investigators:
Timothy H. Bonner, Texas State University, Department of Biology
Edmund L. Oborny and Bradley M. Littrell, BIO-WEST, Inc.
James A. Stoeckel, Auburn University, School of Fisheries, Aquaculture, and Aquatic Sciences
Brian S. Helms, Troy University, Department of Biology & Environmental Sciences
Kenneth G. Ostrand, USFWS San Marcos Aquatic Resources Center
Patricia L. Duncan, USFWS Uvalde National Fish Hatchery
Jeff Conway, USFWS Inks Dam National Fish Hatchery

Table of Contents **Page**

Multiple freshwater mussel species of the Brazos River, Colorado River, and Guadalupe River basins

CMD 1—6233CS

Final Report

February 28, 2018

Principal investigators:

Timothy H. Bonner, Texas State University, Department of Biology
Edmund L. Oborny and Bradley M. Littrell, BIO-WEST, Inc.
James A. Stoeckel, Auburn University, School of Fisheries, Aquaculture, and Aquatic Sciences
Brian S. Helms, Troy University, Department of Biology & Environmental Sciences
Kenneth G. Ostrand, USFWS San Marcos Aquatic Resources Center
Patricia L. Duncan, USFWS Uvalde National Fish Hatchery
Jeff Conway, USFWS Inks Dam National Fish Hatchery

Table of Contents

The Texas Comptroller of Public Accounts office provided financial assistance for this study. We thank R. Gulley, M. Hope, and K. Horndeski of the Texas Comptroller of Public Accounts office for their support and coordination of our research activities. We also thank staff from Austin Ecological Field Office, Texas Parks and Wildlife, Lower Colorado River Authority, and Brazos River Authority for their assistance and coordination among our partners.

The findings and conclusions in this report presented by U.S. Fish and Wildlife Service project team members do not necessarily represent the views of the U.S. Fish and Wildlife Service.

Executive Summary

This comprehensive research project was initiated to quantify distributional, ecological, and biological information for five federal candidate freshwater mussel species in portions of the Colorado River basin, Brazos River basin, and Guadalupe River basin of central Texas. The five candidate freshwater mussel species were Smooth Pimpleback (*Cyclonaias houstonensis*, formerly *Quadrula houstonensis*), Texas Pimpleback (*Cyclonaias petrina*, formerly *Quadrula petrina*), Texas Fatmucket (*Lampsilis bracteata*), Texas Fawnsfoot (*Truncilla macrodon*), and False Spike (*Fusconaia mitchelli*). Field surveys were conducted in the lower Colorado River basin, middle Colorado River basin, upper Brazos River basin, Little River (a Brazos River tributary), and upper Guadalupe River to document current distribution, occurrence, abundance, population structure, and habitat associations of the candidate species. Applied research studies using respirometry, enzyme transport system (ETS) assays, and valve closure/movement experiments were conducted to evaluate the influence of thermal, hypoxia, suspended solids, salinity, and nitrogenous stressors on growth and survival of multiple candidate mussel species. Additional experimental trials evaluated the desiccation tolerances and behavioral responses to dewatering events for multiple candidate species. Stable isotope analysis was used to evaluate food resources being utilized by candidate mussel species and evaluate spatial and temporal variations in feeding across basins and seasons.

Previously established hydraulic model sites on the lower Colorado River were surveyed for freshwater mussels, and initial Habitat Suitability Criteria (HSC) were developed for multiple hydraulic variables and candidate species to be used in an ongoing environmental flow assessment. Robust design mark and recapture studies were initiated at two sites in the Colorado River basin to evaluate capture probabilities and assess population parameters such as abundance

and survival in relation to river discharge. Additionally, mark and recapture studies allowed for a quantification of movement and baseline growth for multiple candidate species. Lastly, development of facilities and protocols for captive propagation and rearing of candidate species was initiated at three separate U.S. Fish and Wildlife Service (USFWS) fish hatchery/research facilities. In aggregate, the research presented herein represents a substantial increase in available information on candidate freshwater mussel species. An overview of the more pertinent information for each species is provided below.

Smooth Pimpleback *Cyclonaias houstonensis*

Cyclonaias houstonensis was captured in three (lower Colorado River, middle Colorado River, and Little River) of the four survey basins where it had previously been documented. Although previously documented in the upper Brazos basin, including the Clear Fork Brazos River, live individuals were not observed during our surveys. In the lower Colorado River, *C. houstonensis* occurred at 31% of sites and ranked 3rd in relative abundance, accounting for 17% of all mussels observed. In the middle Colorado River, *C. houstonensis* occurred at 12% of sites, and ranked 10th in relative abundance (3%). In the Little River, *C. houstonensis* occurred at 40% of sites, and ranked first in relative abundance (42%). Among georegions, *C. houstonensis* was most common (15% occurrence among mesohabitats) and abundant (17% relative abundance) in Georegion 5 (Lowland). Across all survey basins, *C. houstonensis* was found in all mesohabitat types, although catch-per-unit-effort (CPUE; mussels/p-h) was lowest in riffles and backwaters and highest in mid-channel runs. Multivariate analysis of lower and middle Colorado River data demonstrated an association with run edge habitats and sand substrates. Initial habitat suitability criteria (HSC) generated for *C. houstonensis* generally support these results with the highest

utilization observed in moderate depths, moderate velocities, under low shear stress, with boulder, bedrock, and sand substrates.

Respirometry data suggests that increasing temperature to a maximum of 36 ºC results in increased metabolic demand which may cause *C. houstonensis* to be more susceptible to food limitation and subsequent growth limitations at higher temperatures. However, their ability to obtain oxygen from the water varied little with temperature, (*C. houstonensis* generally switched from aerobic to anaerobic respiration at around 2.0 mg/L dissolved oxygen [DO] regardless of temperature), and they were observed to have a short-term tolerance of low DO even at high temperatures. Optimal temperatures for respiratory enzymes (ETS) of temperature-acclimated mussels were 31.6°C for the Colorado River population and 27.6°C for the Navasota River population. Optimal ETS temperatures for non-acclimated animals were 30.5°C and 28.8°C for Colorado and Navasota river populations, respectively. Based on previous literature, optimal temperatures for mussel growth are likely a few degrees lower than those measured for enzymes. Onset of mussel mortality due to thermal stress was hypothesized to occur at 37.1°C for *C. houstonensis*, which was lower than the same value for *C. petrina* (38.9 ºC), but higher than values observed for *Lampsilis teres* (29.4 ºC), *Amblema plicata* (36.0 ºC), and *Fusconaia mitchelli* (29.4 ºC). Even at excessive concentrations (Turbidity ~75 NTU, TSS ~250 mg/L), there was little to no evidence that exposure to suspended solids resulted in valve closure. *Cyclonaias houstonensis* were more sensitive to salinity than turbidity, with salinities >2.5 ppt resulting in strong reductions in mussel gape. Total ammonia nitrogen (TAN) concentrations of 0.5 and 2 mg/L did not affect *C. houstonensis* respiration rates or ability to obtain oxygen from surrounding waters in the short term. However, frequency of valve closure did appear to increase at 2.0 mg TAN/L raising the possibility of negative impacts on filtration, respiration,

and fertilization efficiency during long-term exposure. A LT_{50} of 18.39 days during desiccation trials suggests *C. houstonensis* is moderately tolerant of desiccation. Currently available stable isotope data suggests the majority of the carbon assimilated by *C. houstonensis* is derived from coarse particulate organic matter (CPOM); however, whether this results from direct feeding on CPOM particles or a reliance on associated bacteria and fungi is unclear given current data.

Visual/tactile capture probability of *C. houstonensis* from the lower Colorado River mark recapture site ranged from 0.47 – 0.52. Population estimates suggest a population size of 350 – 400 individuals within one 300 m^2 area in Colorado County prior to flooding effects from Hurricane Harvey, and approximately 20 individuals after this event. Observed movement between primary sampling periods at both sites ranged from 0 – 24 meters (m), and averaged 3.96 – 12.4 meters. Observed growth rates averaged 1.3 – 1.4 mm/month in the lower Colorado River and 0.4 mm/month in the middle Colorado River. Although a wide variety of environmental parameters influence growth rates, growth rates were likely slower in the middle Colorado River due to the dominance of larger individuals.

Three USFWS hatchery/research facilities (San Marcos Aquatic Resource Center, SMARC; Inks Dam National Fish Hatchery, IDNFH; Uvalde National Fish Hatchery, UNFH) have developed infrastructure to house and propagate *C. houstonensis*, and attempts to collect gravid individuals from the wild and infest host fish will be initiated in spring 2018.

Texas Pimpleback *Cyclonaias petrina*

Cyclonaias petrina was observed in all three of the survey basins where it was historically documented. In the lower Colorado River, *C. petrina* occurred at approximately 13% of sites and represented 1.3% of all individuals captured, ranking 7th in relative abundance.

In the middle Colorado River, *C. petrina* was found at 15% of sites and ranked first in relative abundance (20%). The highest CPUE was within San Saba County downstream of the San Saba River confluence. In the upper Guadalupe River, *C. petrina* was observed at 20% of sites and ranked third in abundance (21%). Among georegions, *C. petrina* was most common (7.1% occurrence among mesohabitats) and abundant (37% relative abundance) in Georegion 3 (Llano Uplift). Across all survey basins, *C. petrina* was found in all mesohabitats, but mean CPUE was highest in run edge habitats and lowest in riffles. Multivariate analysis of lower and middle Colorado River data demonstrated an association with run habitats, swifter current velocities, and gravel and cobble substrates. Compared to all mussels in aggregate, initial HSC generated for *C. petrina* showed broader curves for mean column velocity, Froude number, Reynolds number, and shear stress, suggesting increased utilization of high energy environments.

Respirometry data suggests that increasing temperature to a maximum of 36ºC results in increased metabolic demand which may cause *C. petrina* to be more susceptible to food limitation and subsequent growth limitations at higher temperatures. Increased valve closure was noted at higher temperatures. However, their ability to obtain oxygen from the water varied little with temperature, and they were observed to have a short-term tolerance of low DO even at high temperatures. Optimal temperatures for electron transport system (ETS) enzymes of temperature-acclimated mussels were 35.3°C for the Colorado River population and 34.6°C for the Navasota River population. Optimal ETS temperatures for non-acclimated animals were 30.2°C and 28.5°C for Colorado and Guadalupe river populations respectively. Optimal temperatures for mussel growth are likely a few degrees lower than those measured for enzymes. Onset of mussel mortality due to thermal stress was hypothesized to occur at 38.9°C for *C. petrina*, which was higher than all other species tested (*C. houstonensis*, *Lampsilis teres*,

Amblema plicata, and *Fusconaia mitchelli*). Even at excessive concentrations (Turbidity ~75 NTU, TSS ~250 mg/L), exposure to suspended solids had little influence on valve closure. *Cyclonaias petrina* were more sensitive to salinity than turbidity, with salinities >2.0 ppt resulting in major decreases in gape and nearly complete valve closure by 4ppt. Total ammonia nitrogen (TAN) concentrations of 0.5 and 2 mg/L resulted in frequent valve closure events precluding the ability to measure effects on respiration rates and ability to extract oxygen from ambient water. High frequency of valve closure raises the possibility of negative impacts on filtration, respiration, and fertilization efficiency during long-term exposure to a greater degree than for *C. houstonensis*. Desiccation and dewatering trials suggest *C. petrina* is tolerant of short-term desiccation (LT_{50} of 32.04 days) and increases movement in response to dewatering, thus reducing their propensity for stranding. Currently available stable isotope data suggests the majority of the carbon assimilated by *C. petrina* is derived from coarse particulate organic matter (CPOM); however, whether this results from direct feeding on CPOM particles or a reliance on associated bacteria and fungi is unclear given current data.

Visual/tactile capture probability of *C. petrina* from the lower Colorado River mark recapture site ranged from 0.54 – 0.58. Population estimates suggest a population size of approximately 127 individuals within one 300 m^2 area in Colorado County prior to flooding effects from Hurricane Harvey, and approximately eight individuals after this event. Population estimates at the middle Colorado mark recapture site ranged from 255 – 490 individuals within 300 m^2. Observed movement between primary sampling periods at both sites ranged from 0 – 24 meters (m), and averaged 3.9 – 7.8 meters. Observed growth rates averaged 1.9 – 2.3 mm/month in the lower Colorado River and 0.6 – 0.8 mm/month in the middle Colorado River. Although a

wide variety of environmental parameters influence growth rates, growth rates were likely slower in the middle Colorado River due to the dominance of larger individuals.

The same three USFWS hatchery/research facilities have developed infrastructure to house and propagate *C. petrina*, and attempts to collect gravid individuals from the wild and infest host fish will be conducted in spring 2018.

Texas Fatmucket *Lampsilis bracteata*

Live *L. bracteata* were observed in two of the three survey basins where they were historically documented. In the upper Guadalupe River, they were observed at 40% of the sites sampled and ranked 1st in relative abundance (34%). Gravid females were observed in the upper reaches in Kerr County. In the middle Colorado River basin, *L. bracteata* was the rarest mussel encountered (0.4% relative abundance) and occurred at 2% of sites. None were observed in the mainstem, but a previously undocumented population was located at one site sampled in Cherokee Creek. In the lower Colorado River basin, *L. bracteata* were previously reported from lower Onion Creek but were not located at one site within Onion Creek in this study. *Lampsilis bracteata* was only found in Georegion 3 (Llano Uplift). Across basins, highest mean CPUE was in run edge habitats, and the species was not located in backwaters. Overall, they occupied swift current velocities in comparison to other species. In the upper Guadalupe River, they were found more often than expected over bedrock and gravel substrates.

Although laboratory studies are ongoing for this species, initial data demonstrates lower optimal temperatures than those observed for *C. houstonensis* and *C. petrina*, suggesting this species may be more thermally sensitive than the two *Cyclonaias* species. Of the three species, *L. bracteata* was also the quickest to succumb to desiccation (LT_{50} 2.86 days) and did not exhibit

a movement response to dewatering. In aggregate, this suggests that *L. bracteata* populations would be expected to exhibit greater impacts than the other two species from extreme low flows, which often result in high temperatures and potential desiccation. Not surprisingly, the distribution of *L. bracteata* seems to be associated with relatively persistent spring inputs. Currently available stable isotope data suggests that the majority of carbon assimilated by *L. bracteata* is derived from CPOM. However, carbon sources were much more variable for *L. bracteata* than for the other species examined, and were dominated by suspended particulate organic matter at certain sites/seasons. Stable isotope analysis is ongoing and additional data may help elucidate spatial and temporal patterns.

The same three USFWS hatchery/research facilities have developed infrastructure to house and propagate *L. bracteata*. Gravid females collected in spring and summer 2017 were used to infest host fish at both the SMARC and IDNFH facilities. Initial studies conducted at SMARC evaluated three potential host fish (i.e., Green Sunfish, Bluegill, and Blacktail Shiner) and found Green Sunfish to be the most suitable and efficient host. Subsequent inoculations using Green Sunfish resulted in production of 1,533 live juveniles. However, growth rates were slow and 100% mortality was observed within six weeks. As a result, future propagation efforts at SMARC will use filtered pond water instead of well water, and holding temperature will be increased from 21 to 25°C. Both Bluegill and Green Sunfish were inoculated at IDNFH and staff estimated 2,300 metamorphosed juveniles were produced. However, near total mortality was observed due to an issue with reduced source water oxygen content. This issue has been resolved by adding the ability for supplemental aeration to the system. Two juveniles which survived this event exhibited good growth rates over the course of the study. Although

propagation success was low in 2017, changes implemented at both facilities are anticipated to promote successful propagation of a larger number of *L. bracteata* in 2018.

Texas Fawnsfoot *Truncilla macrodon*

Live *T. macrodon* were observed in two of the four basins where they were historically documented. In the lower Colorado River, nine individuals (0.4% relative abundance) were present at seven survey sites (15% occurrence) in Colorado, Wharton, and Matagorda counties. In the middle Colorado River, *T. macrodon* were not captured during surveys. However, recently dead shells were found (with tissue still present) in San Saba County, and one juvenile individual was captured in this basin during mark recapture studies. This suggests the species persists in the middle Colorado basin. Although *T. macrodon* were documented in both the Little River and upper Brazos River basin, no live individuals were located in these areas during this study. Recent drought impacts in the Clear Fork Brazos River, an upper Brazos tributary where *T. macrodon* was previously reported, warrant the need for additional surveys to assess the current status of the species in this area. Among georegions, *T. macrodon* were mainly found in Georegion 5 (Tertiary). Across all basins, *T. macrodon* were found in run edge, pool edge, and backwater habitats with the highest mean CPUE observed in run edge habitats. Multivariate analysis of lower and middle Colorado River data demonstrated an association with run edges and clay, silt, and sand substrates. A total of 16 individual *T. macrodon* were captured from the mark recapture site in the lower Colorado River and one individual was captured from the mark recapture site in the middle Colorado River. Recapture data were insufficient to examine capture probability, population estimates, or growth rates. Observed movements between primary

periods ranged from 1 m to 20 m and averaged 6.6 m – 10.2 m, similar to that of larger bodied *Cyclonaias* mussels.

The same three USFWS hatchery/research facilities have developed infrastructure to house and propagate *T. macrodon*. However, given the difficulty in locating large numbers of individuals at any location, finding gravid females is challenging. Efforts to locate gravid females for propagation studies will continue in coming years.

False Spike *Fusconaia mitchelli*

Fusconaia mitchelli was previously reported in three of the five survey basins (i.e., middle Colorado River basin, upper Guadalupe River basin, and Little River basin), but no live individuals were observed during surveys as part of this project. The species is currently known to be extant in portion of the Little River basin, the Llano River, the San Saba River, and the lower Guadalupe River, with the highest abundances occurring in the lower Guadalupe River.

Ten individual *F. mitchelli* were collected from the lower Guadalupe River and used for non-acclimated ETS enzyme experiments. The optimal range of ETS enzyme activity for *F. mitchelli* was 26.5 – 28.8ºC, with a hypothesized onset of lethal effects at 31.0ºC. This estimated onset of lethal effects was second lowest among the five species examined, being slightly higher than that observed for *L. teres* (29.4ºC) and considerably lower than *C. petrina* (38.9ºC), *C. houstonensis* (37.1ºC), and *A. plicata* (36.0ºC).

The same three USFWS hatchery/research facilities have developed infrastructure to house and propagate *F. mitchelli*. However, given the difficulty in locating large numbers of individuals at any location, finding gravid females is challenging. Efforts to locate gravid females for propagation studies will continue in coming years.

In conclusion, this comprehensive research project was conducted to quantify distributional, ecological, and biological information for five federal candidate freshwater mussel species. Field surveys, applied research, mark-recapture studies, and captive propagation activities presented herein filled several key data gaps, which will facilitate upcoming state and federal conservation assessments.

Task 1: Freshwater mussel field surveys

Contributing authors: Brad Littrell, Kyle Sullivan, David Ruppel, Cody Craig, Peter Pfaff, Tim Bonner

Addresses:
BIO-WEST, Inc. San Marcos, Texas 78666 (BL, KS)
Texas State University, Department of Biology/Aquatic Station, San Marcos Texas 78666 (DR, CC, PP, TB)

Principal Investigators: Brad Littrell and Tim Bonner

Email: blittrell@bio-west.com, TBonner@txstate.edu

Literature review of target mussel distributions in Texas

Approximately 50 species of freshwater mussels reside in Texas, 15 of which are listed as state threatened (TPWD 2010). Of these 15 state threatened species, 14 are endemic to the region (Burlakova et al. 2011). In the central Texas province, which includes the Nueces-Frio, Guadalupe-San Antonio, Colorado, and Brazos basins, 6 endemic species are known to occur, 5 of which are pending review by the U.S. Fish and Wildlife Service (USFWS) for federal listing (USFWS 2011; Howells 2014). The most recent studies on the unionid assemblages of central Texas have focused on tributaries of each major basin, with less emphasis on the mainstem portions of these systems (Burlakova & Karatayev 2010; Randklev et al. 2017). Though several studies have begun to tackle these larger systems, such as the mainstem Guadalupe and Brazos rivers, a large data gap is present within the mainstem Colorado River (Burlakova & Karatayeu 2010; Randklev et al. 2009; Tsakiris & Randklev 2016; Tsakiris & Randklev 2016). Burlakova and Karatayeu (2010) surveyed several sites on the mainstem Colorado, but only did so in close proximity to public access sites. For the USFWS to make appropriate decisions on these candidate species, it is crucial to fill data gaps where adequate survey efforts are lacking.

Cyclonaias houstonensis (formerly in the genus *Quadrula*; Williams et al. 2017), Smooth pimpleback, is known to have occurred in the Colorado and Brazos River basins. Historically, *C. houstonensis* was considered rare where it occurred based on expert's inability to find large populations that persisted throughout its native range (USFWS 2011). In more recent studies, *C. houstonensis* was found in high numbers within the Brazos River basin, including tributaries such as the Little River and Yegua Creek, among others (Tsakiris & Randklev 2016; Randklev et al. 2017). Within the Colorado River basin, *C. houstonensis* was thought to be much less common. The majority of survey efforts have been focused within tributaries of the Colorado River, which includes the Llano, San Saba, Pedernales, Concho Rivers, with less emphasis on the mainstem Colorado (Randklev et al. 2017). Burlakova and Karatayeu (2010) found low densities of *C. houstonensis* in the Lower Colorado River, though few sites (N = 14) were surveyed.

Cyclonaias petrina (formally in the genus *Quadrula*; Williams et al. 2017), Texas pimpleback, is known to have occurred in the Guadalupe-San Antonio River and Colorado River basins. The range of *C. petrina* was historically believed to have been reduced substantially, and only occurred in four streams, the San Saba, Concho, Guadalupe, and San Marcos Rivers (USFWS 2011). Most recent surveys found live *C. petrina* in these four streams, as well as the Llano River (Randklev et al. 2017) and lower Guadalupe River (Tsakiris & Randklev 2016). Although Burlakova and Karatayeu (2010) surveyed a few sites in the mainstem Colorado River and observed no live *C. petrina*, extensive surveys within the Colorado River mainstem are lacking.

Lampsilis bracteata, Texas fatmucket, is known to have occurred in the upper reaches of the Colorado and Guadalupe-San Antonio basins within the Edwards Plateau. In the Colorado

River system, *L. bracteata* was historically found in the mainstem and tributaries, which includes the Pedernales River, Llano, San Saba, and Concho Rivers, and Onion, Jim Ned, and Elm Creeks (USFWS 2011). Based on the most current survey efforts, *L. bracteata* appears to be extirpated from the mainstem Colorado River, and is restricted to its tributaries, including the Concho, Llano, and San Saba Rivers (Burlakova & Karatayeu 2010; Randklev et al. 2017). Survey efforts by Randklev et al. (2017) found the San Saba River to have the densest populations where *L. bracteata* persists. In the Guadalupe River, *L. bracteata* was historically found from the lower reaches in Gonzales County to the headwaters in Kerr County, though individuals from the lower reaches were most likely misidentified *Lampsilis hydiana*, Louisiana fatmucket (USFWS 2011). Furthermore, *L. bracteata* was also historically found in several tributaries, which included the North Fork Guadalupe River, Johnson Creek, and Blanco River. In the San Antonio River, *L. bracteata* occurred at its confluence with the Medina River, upstream to the City of San Antonio. Additionally, *L. bracteata* historically occurred in two tributaries, the Medina River and Cibolo Creek, though no recent survey efforts have documented live individuals in the San Antonio River basin (USFWS 2011).

Truncilla macrodon, Texas fawnsfoot, was known to occur in the Brazos River and Colorado River basins. In the Brazos River basin, *T. macrodon* occurred from Fort Bend County, upstream to the confluence of the Clear Fork Brazos River (Randklev et al. 2009; USFWS 2011). Furthermore, this species historically occurred in tributaries of the Brazos River, which includes the Clear Fork Brazos, Navasota, Leon, Little, San Gabriel Rivers, and Deer and Yegua Creeks (Randklev et al. 2013; Tsakiris & Randklev 2016; USFWS 2011). The most recent survey efforts have found *T. macrodon* live in multiple tributaries, which includes Yegua Creek, Navasota, Little, Leon, San Gabriel, and Clear Fork Brazos Rivers, among others (Randklev et al. 2013;

Tsakiris & Randklev 2016; Randklev et al. 2017). In the Colorado River basin, *T. macrodon* occurred in the majority of the mainstem, from Wharton County to the headwaters, as well as tributaries in the Edwards Plateau. *Truncilla macrodon* was thought to be extirpated from the Colorado River until 2009, when live individuals were found within the lower reaches of the mainstem (Burlakova & Karatayeu 2011).

Fusconaia mitchelli, False spike, is known to have occurred in the Brazos, Colorado, and Guadalupe River basins. In the Brazos River basin, historic records occurred in the Little River system, which includes the Leon and San Gabriel Rivers, as well at the mainstem Brazos. *Fusconaia mitchelli* was known to have occurred in the mainstem Colorado River in San Saba County, as well as in the Llano River. Furthermore, *F. mitchelli* occurred in the Guadalupe River from Victoria county to Kerr County. For over 30 years, *F. mitchelli* was thought to be extinct until live individuals were collected within the lower Guadalupe River in Gonzales County (Randklev et al. 2012). Recent survey efforts by Tsakiris and Randklev (2016) found the species persists in the Lower Guadalupe River, though in low abundance. Since *F. mitchelli* was rediscovered as extant, more recent survey efforts have also found live individuals in both the Brazos and Colorado River basins. In the Brazos basin, live individuals were collected within Brushy Creek, Leon, San Gabriel, and Little Rivers. Additionally, one live individual was found in the Llano River (Randklev et al. 2017).

Part I: Study Objectives

The goal of this study was to provide information to evaluate the freshwater mussel communities in portions of the Colorado, Brazos, and Guadalupe River basins of central Texas, with an emphasis on investigating five federal candidates and petitioned freshwater mussel

species (i.e., *C. houstonensis*, *C. petrina*, *L. bracteata*, *T. macrodon*, and *F. mitchelli*). Specific task objectives for the five candidate species were to assess distribution, catch per unit effort, and population size structure. We separated the basins of interest into 5 sub-basins, including the Lower Colorado River basin (from Longhorn Dam to Bay City Dam), the Middle Colorado River basin (from O.H. Ivie Reservoir to Lake Buchanan), the Upper Brazos River basin (upstream from Possum Kingdom Reservoir), the Little River drainage (from the confluence of the Lampasas and Leon Rivers to the confluence with the Brazos River), and the Upper Guadalupe River basin (from Canyon Lake upstream to the confluence of the North and South forks).

Part I Methods

Study Area

The Colorado River is the largest river in Texas that is completely confined within the states borders. The headwaters originate in Dawson County in the Great Plains of west Texas, and flows southeast through the Edwards Plateau, where is receives large contributions from several spring-fed rivers, such as the San Saba, Pedernales, and Llano Rivers. The river then transitions to a large alluvial system, as it flows through the Gulf Coastal Plain, eventually draining into Matagorda Bay (Dahm et al. 2005). Several mainstem reservoirs occur on the Colorado, most notably the Highland Lakes, a series of seven reservoirs (Lake Buchanan, Inks Lake, Lake LBJ, Lake Marble Falls, Lake Travis, and Lake Austin) which separate the Middle Colorado from the Lower Colorado. For this study, the Middle Colorado River is defined as the segment between O.H. Ivie Reservoir and Lake Buchanan. The Lower Colorado River is defined as the segment from Longhorn Dam (forming Lady Bird Lake) to Bay City Dam, which

is 32 miles above the river's mouth at Matagorda Bay. The Lower and Middle Colorado river mainstem were each broken up into 5 reaches each. The Lower Colorado mainstem reaches included Longhorn Dam to Bastrop (Reach I; river mile [RM] 292 – 237), Bastrop to La Grange (Reach II; RM 237 – 174), La Grange to Columbus (Reach III; RM 174 – 132), Columbus to Wharton (Reach IV; RM 132 – 64), and Wharton to Bay City Dam (Reach V; RM 64 – 32). In addition to the mainstem, we surveyed in Onion Creek, a tributary of the Lower Colorado River. The Middle Colorado mainstem reaches included O.H. Ivie to State Highway (SH) 377 (Reach I; RM 608 – 553), SH 377 to SH 45 (Reach II; RM 553 – 529), SH 45 to SH 16 (Reach III; RM 529 – 493), SH 16 to Bend (Reach IV; RM 493 – 447), and Bend to Lake Buchannan (Reach V; RM 447 – 422). In addition to the mainstem, we surveyed in two Middle Colorado tributaries, Cherokee Creek and Pecan Bayou.

The Brazos River is the third largest river in the state of Texas, and originates in Stonewall County at the confluence of the Salt Fork Brazos and Double Mountain Fork Brazos Rivers. It flows southeast through the Great Plains before reaching the Gulf Coastal Plain, where it drains into the Gulf of Mexico. The Brazos River is 1390 km long and drains an area of about 115600 km^2 (Dahm et al. 2005). For this study, the area of interest includes the Upper Brazos River basin, from the headwaters to Lake Possum Kingdom. This includes the mainstem portion of the river as well as the Clear Fork Brazos River. Furthermore, because candidate species have been documented in the area, another sub-basin of interest within the Brazos River watershed is the Little River. This tributary to the Brazos originates at the confluences of the Leon and Lampasas Rivers in Bell County. It flows east for approximately 258 km before it meets with the Brazos mainstem, draining an area of about 12,485 km^2 (Rose & Echelle 1981).

The Guadalupe River originates in Kerr County in Hunt, at the confluence of the North and South Fork Guadalupe Rivers, and flows through the Edwards Plateau until it reaches the coastal plain, and eventually drains into San Antonio Bay. The Guadalupe River is a part of the Guadalupe-San Antonio basin and is approximately 370 km long, with the entire watershed draining an area of about 26,231 km^2 (Dahm et al. 2005). For this study, the area of interest includes the upper portion of the Guadalupe River, from its headwaters, downstream to Canyon Lake.

Survey Design

To delineate survey sites within each basin, we utilized aerial imagery to target areas with heterogeneous habitats. We chose sites within sections of each river with a mosaic of habitat types to investigate habitat associations among mussel communities, as well as candidate species. Habitat types were divided into mesohabitats, which included riffles, runs, pools, and backwaters. Dividing habitat types with a mesohabitat scale is useful for investigating habitat associations because they can be easily identified (Frissell et al. 1986). Moreover, due to differences in mussel abundance between bank and mid-channel habitats observed in previous studies (Brown & Banks 2001; Brim Box et al. 2002), we partitioned runs and pools into sub-mesohabitats to increase resolution and identify potential differences within these mesohabitats. As a result, we separated each site by six potential mesohabitat types: run bank, run mid-channel, pool bank, pool mid-channel, riffle, and backwater.

Within each mesohabitat type, we utilized qualitative surveys via timed visual and tactile search methods. A qualitative survey approach is an efficient search method to establish a list of taxa, as well as increase the detection probability of rare species (Vaughn et al. 1997; Strayer &

Smith 2003). At each site, we surveyed one of each mesohabitat type. If a particular mesohabitat type was absent within a site, we surveyed additional mesohabitat types present until a total of 6 mesohabitats were searched at each site. For each mesohabitat, areas with a maximum of 300 m^2 were marked off and initially surveyed for one person-hour (p-h). If we found no live mussels, that mesohabitat was complete. If live mussels were collected, we conducted a second p-h. If we collected a new species within the second p-h, a third p-h was conducted. We conducted additional one p-h searches until no new species were collected (Metcalfe-Smith et al. 2000). Once sampling efforts were complete, all native freshwater mussels were identified, enumerated, measured to the nearest millimeter (mm) shell length, and sexed (if applicable), before being returned to the area of capture.

Habitat Measurements

At each mesohabitat type, we estimated percent substrate composition based on the standard Wentworth particle size scale (Wentworth 1922). We utilized a Hach flowmeter and top-set wading rod to measure average depth (ft), mean water column velocity (ft/s), and benthic velocity (ft/s) at one point near the center of each mesohabitat. We used FST Hemispheres (Statzner et al. 1991) to quantify shear stress at one point within each mesohabitat. To measure substrate compaction (kg/cm^2), we took three readings from random points within the mesohabitat using a Humboldt soil penetrometer (Johnson & Brown 2000). Additionally, we recorded the percent coverage of other habitat parameters such as large woody debris, aquatic vegetation, and undercut banks. We used a HydroTech multiprobe water quality sonde to measure water quality parameters including temperature (°C), dissolved oxygen (mg/L, %

saturation), pH, conductivity (µS/cm), and turbidity (NTU). Lastly, we collected a GPS waypoint near the center of each mesohabitat.

Data Analysis

We analyzed average mussel catch-per-unit effort (CPUE; mussels/p-h) for all mussels in aggregate by basin, reach, and mesohabitat type. We assessed differences among reaches and mesohabitats with a nonparametric Kruskal-Wallis Test. If we observed significant differences among groups, a nonparametric pairwise multiple comparison using Dunn's Test with a Bonferroni adjustment was applied to identify between which groups differences occurred. Lastly, we constructed CPUE by site vs. river mile scatterplots to investigate relationships between relative abundance and longitudinal stream position. Tributary sites were not included in relative abundance vs. stream position analysis.

For candidate species, we evaluated each species average CPUE among basins, reach, and mesohabitats. We assessed differences among reaches and mesohabitats for each candidate species with a nonparametric Kruskal-Wallis Test. If we observed significant differences among groups, a nonparametric pairwise multiple comparison using Dunn's Test with a Bonferroni adjustment was applied. Lastly, we analyzed size structures of each candidate species within each basin by constructing length frequency histograms.

Part I Results

Freshwater mussel assemblages by reach and basin

Lower Colorado River Basin

We collected 2,327 live mussels representing 14 species across 49 sites (Table 1). The unionids collected in the Lower Colorado River contributed to 73% of all the individuals collected during our survey efforts across all basins. We observed live mussels at 26 sites (54%) surveyed. The most common species in this basin were *Lampsilis teres* (occurring at 46% of sites sampled), *Leptodea fragilis* (33% occurrence), *Amblema plicata* (33% occurrence), and *C. houstonensis* (31% occurrence). The unionid assemblage of the Lower Colorado was numerically dominated by *A. plicata*, which accounted for 57% of all live mussels collected. The second and third most abundant species were *L. teres* and *C. houstonensis*, which accounted for 16.9% and 16.6% of all live mussels collected, respectively. The remaining 11 species found within the Lower Colorado only accounted for 9.5% of all live unionids collected. The rarest species collected was *Uniomerus tetralasmus*, with only one individual observed at one site. Other infrequently documented taxa included *Quadrula apiculata*, *Toxolasma parvum*, *Utterbackia imbecillis*, and *T. macrodon* (Table 1).

Overall CPUE of unionids in the Lower Colorado River was 4.15 ± 1.34 (SE) mussels/p-h. Mean CPUE among reaches ranged from 0.67 ± 0.33 (SE) mussels/p-h in Reach I to 12.09 ± 6.01 (SE) mussels/p-h in Reach IV (Figure 1). Comparison of CPUE by Kruskal-Wallis analysis detected significant differences in reaches ($p = 0.02$). Despite this, pairwise multiple comparison using Dunn's Test did not provide evidence for where differences occurred. Longitudinal changes in CPUE were observed with increasing distance downstream from Longhorn Dam. CPUE was relatively low from RM 292 (Longhorn Dam) to RM 392, and only reached a maximum CPUE of 3.00 mussels/p-h. CPUE from about RM 240 to RM 188 was 0.00 mussels/p-h, which was the longest distance where no live unionids were recorded within the Lower Colorado River. CPUE began to increase at about RM 178 within Reach II, peaking at

approximately RM 110 within Reach IV, at a maximum of 51.60 mussels/p-h. After this peak, CPUE decreased rapidly, never exceeding 11.00 mussels/p-h for the remaining 70 river miles surveyed (Figure 2).

CPUE within individual mesohabitats ranged from 0.00 mussels/p-h to 124.30 mussels/p-h. Mean CPUE was highest in pool mid-channel habitats at 8.58 ± 4.57 (SE) mussels/p-h (range: 0.00 – 114.00 mussels/p-h). The lowest CPUE was observed within riffle habitats at 0.47 ± 0.47 (SE) mussels/p-h (range: 0.00 – 15.00 mussels/p-h) (Figure 3). Comparison of CPUE by Kruskal-Wallis analysis detected significant differences among mesohabitat types ($p = 0.001$). Pairwise multiple comparison using Dunn's Test detected CPUE within pool edge habitats was significantly higher compared to riffle habitats ($p = 0.008$) and run mid-channel habitats ($p = 0.03$), and CPUE was significantly higher in run edge habitats compared to riffle habitats ($p = 0.02$)

We observed live individuals of three (*C. houstonensis*, *C. petrina*, *T. macrodon*) of the four state-listed species historically known to occur in the Lower Colorado River basin (i.e., *C. houstonensis*, *C. petrina*, *L. bracteata, T. macrodon*; Howells 2014; Table 1). *Cyclonaias houstonensis* collected in the Lower Colorado accounted for 73% of individuals collected from all basins surveyed. Within the Lower Colorado, they were the third most abundant species encountered and occurred at 31% of sites. *Cyclonaias petrina* made up 1.3% of the Lower Colorado unionid community and occurred at 13% of sites surveyed. *Truncilla macrodon* was the least abundant candidate species collected live, numerically comprising 0.39% of the community and occurring at 15% of sites surveyed (Table 1). We observed no live *L. bracteata* in Onion Creek, although only one site was sampled as part of this study. Lastly, we observed no live *F. mitchelli* within the Lower Colorado basin.

Mean CPUE of *C. houstonensis* by reach ranged from 0.00 mussels/p-h in Reach I to 1.72 mussels/p-h in Reach IV (Figure 4). Comparison of *C. houstonensis* CPUE by Kruskal-Wallis analysis detected significant differences in reaches ($p = 0.003$). Pairwise multiple comparison using Dunn's Test detected CPUE was significantly higher in Reach III compared to Reach I ($p = 0.01$) and Reach II ($p = 0.04$). CPUE of *C. petrina* by reach ranged from 0.00 mussels/p-h in Reach I, II, and III, to 0.2 mussels/p-h in Reach IV (Figure 4). Comparison of *C. petrina* CPUE by Kruskal-Wallis analysis detected significant differences in reaches ($p = 0.01$). Pairwise multiple comparison using Dunn's Test detected CPUE was significantly higher in Reach IV compared to Reach I ($p = 0.04$) and Reach II ($p = 0.04$). CPUE of *T. macrodon* by reach ranged from 0.00 mussels/p-h in Reach I and II, to 0.06 mussels/p-h in Reach IV (Figure 4). Comparison of *T. macrodon* CPUE by Kruskal-Wallis analysis detected significant differences in reaches ($p = 0.03$). Despite this, pairwise multiple comparison using Dunn's Test did not provide evidence of where differences occurred.

Middle Colorado River Basin

We collected 492 live mussels across 42 sites, representing 12 species (Table 2). The unionids collected in the Middle Colorado basin contributed to 15% of all the individuals collected during total survey efforts across all basins. We observed live mussels at 34 sites (83%), which was the highest occurrence among all basins. The most common species in the basin was *L. fragilis*, which occurred at 61% of sites sampled. *C. petrina* and *L. fragilis* were the most abundant species, accounting for 19.7% and 19.5% of live unionids, respectively (Table 2). The rarest species were *L. bracteata* and *A. plicata*, accounting for 0.41% and 1.02% of the unionids collected, respectively (Table 2).

Overall CPUE of unionids in the Middle Colorado was 1.08 ± 0.24 (SE), the second lowest among basins. Mean CPUE among reaches ranged from 0.48 ± 0.14 (SE) mussels/p-h to 1.77 ± 0.67 (SE) mussels/p-h. The highest CPUE occurred in Reach IV at 1.77 ± 2.22 (SD) mussels/p-h (range: 0.00 - 8.00 mussels/p-h; Figure 5). Comparison of CPUE by Kruskal-Wallis analysis failed to detect significant differences among reaches ($p = 0.22$). We observed no distinct longitudinal patterns between total mussel CPUE and longitudinal stream location (Figure 6). Mean CPUE was 0.53 ± 0.41 (SE) mussels/p-h among three sites in Pecan Bayou and 1.00 mussels/p-h at one site in Cherokee Creek.

CPUE within individual mesohabitats ranged from 0.00 mussels/p-h to 21.33 mussels/p-h. The highest mean CPUE among mesohabitats occurred within run edge habitats, averaging 1.69 ± 1.01 (SE) mussels/p-h (range: 0.00 – 21.33 mussels/p-h). The lowest CPUE among mesohabitats was within riffle habitats, averaging 0.16 ± 0.1 (SE) mussels/p-h (range: 0.00 – 0.50 mussels/p-h; Figure 7). Comparison of CPUE by Kruskal-Wallis analysis failed to detect significant differences among mesohabitats ($p = 0.06$).

We observed live specimens of three (*C. houstonensis*, *C. petrina*, *L. bracteata*) of the five state-listed species historically known to occur in the Middle Colorado River drainage (i.e., *C. houstonensis*, *C. petrina*, *L. bracteata*, *T. macrodon*, *F. mitchelli*; Howells 2014) (Table 2). Among all basins of occurrence, 71% of the *C. petrina* collected occurred within the Middle Colorado basin, most of which were found at one site in San Saba County. *Cyclonaias houstonensis* occurred at 12% of sites, and accounted for 2.6% of the community (Tables 2). No live *T. macrodon* or *F. mitchelli* were observed during field surveys, although a live *T. macrodon* was taken from the middle Colorado River during mark and recapture study.

Mean CPUE of *C. houstonensis* by reach ranged from 0 mussels/p-h in Reach III and V, to 0.07 mussels/p-h in Reach IV (Figure 8). CPUE by Kruskal-Wallis analysis failed to detect significant differences in reaches ($p = 0.32$). Mean CPUE of *C. petrina* by reach ranged from 0 mussels/p-h in Reach II and V, to 0.57 mussels/p-h in Reach IV (Figure 8). CPUE by Kruskal-Wallis analysis failed to detect significant differences in reaches ($p = 0.12$).

Upper Brazos River

We collected one mussel across 10 sites in the Upper Brazos River Basin. One single *U. tetralasmus* was collected in the Clear Fork Brazos River, at Fort Griffin, in Shackleford County. Although sites on the Clear Fork Brazos River contained a diverse community of dead shell material, we observed no live unionids and few shells in the mainstem portion of the Brazos River basin upstream from Possum Kingdom Reservoir.

Little River Basin

We collected 320 live mussels representing five species across 10 sites in the Little River (Table 3). The unionids collected in the Little River represented 10% of all the individuals collected during total survey efforts across all basins. Live mussels were observed at seven sites (70%), second highest occurrence among basins. The most common species in this basin was *Cyrtonaias tampicoensis*, which occurred live at 70% of the sites sampled. *C. houstonensis* was the most abundant species, which accounted for 42% of all live mussels collected and occurred at 40.00% of sites surveyed. The second and third most abundant species were *A. plicata* and *C. tampicoensis*, which accounted for 23% and 21% of all live mussels observed, respectively. The

rarest species found live within the Little River was *L. fragilis*, with only 6 individuals collected, accounting for 0.02% of the mussel community (Table 3).

Overall mean CPUE of unionids in the Little River was 3.06 ± 1.15 (SE) mussels/p-h and ranged from 0.00 mussels/p-h to 9.00 mussels/p-h among sites. We observed no longitudinal patterns between CPUE and longitudinal river location (Figure 9).

CPUE within individual mesohabitats ranged from 0.00 mussels/p-h to 37.50 mussels/p-h. Mean CPUE was highest within pool edge habitats at 4.03 ± 4.02 (SE) mussels/p-h (range: 0.00 – 37.50 mussels/p-h). CPUE was lowest within riffle habitats at 0.11 ± 0.11 (SE) mussels/p-h (range: 0.00 – 1.00 mussels/p-h). (Figure 10). Comparison of CPUE by Kruskal-Wallis analysis failed to detect significant differences among mesohabitats ($p = 0.56$).

We observed live individuals of one (*C. houstonensis*) of the three candidate species that are historically known to occur in the Little River Drainage (i.e., *C. houstonensis*, *T. macrodon*, *F. mitchelli*; Howells 2014; Table 3). *Cyclonaias houstonensis* occurred at 40% of sites surveyed and was the most numerically abundant species encountered. No live *T. macrodon* or *F. mitchelli* were collected in the Little River.

In addition to native unionids, it is important to note that live zebra mussels *Dreissena polymorpha* were documented at the two upstream-most sites (State Highway 95, Bell County; FM 437, Milam County) in the Little River. Thirty-eight live zebra mussels were documented from five mesohabitats at these two sites.

Upper Guadalupe River Basin

We collected 47 live mussels representing five species across 10 sites (Table 4). The unionids collected in the Upper Guadalupe River contributed only 1.5% of all the individuals

collected during total survey efforts across all basins, the second lowest among all drainages surveyed. Live mussels occurred at 4 sites (40%) surveyed. *L. bracteata* was the most common and abundant species present, which occurred at 40% of sites surveyed, and accounted for 34% of the mussel community. The second and third most abundant species were *Toxolasma texasiense* and *C. petrina*, which accounted for about 28% and 21% of live mussels collected, respectively. *Toxolasma parvum* was the rarest species observed, occurring at 10% of sites, and accounting for 2.13% of the mussel community (Table 4).

Overall CPUE for unionids in the Guadalupe River was 0.50 ± 0.30 (SE) mussels/p-h, and ranged from 0.00 mussels/p-h to 3.00 mussels/p-h among sites. Longitudinal patterns were observed with increasing distance from the North and South Fork Guadalupe Rivers confluence. The highest mean CPUE was observed at RM 417.5 (3.00 mussels/p-h.), with the last occurrence of live mussels at approximately RM 393. No live mussels were observed between RM 393 and Canyon Lake (Figure 11).

CPUE within individual mesohabitats ranged from 0.00 mussels/p-h to 6.67 mussels/p-h. Mean CPUE was highest within run edge habitats, averaging 1.24 ± 0.76 (SE) mussels/p-h (range: 0.00 – 6.67 mussels/p-h). Mean CPUE was lowest within pool-mid channel habitats, where no live mussels were detected (Figure 12). Comparison of CPUE by Kruskal-Wallis analysis failed to detect significant differences among mesohabitat types ($p = 0.33$).

We observed two (*C. petrina*, *L. bracteata*) of the three candidate species historically known to occur in the Upper Guadalupe River Drainage (i.e., *C. petrina*, *L. bracteata*, *F. mitchelli*; Howells 2014; Table 4). *L. bracteata* and *C. petrina* accounted for 55% of the unionid community combined. We observed no live *F. mitchelli* in the Upper Guadalupe basin.

Candidate Species

Cyclonaias houstonensis

We collected a total of 533 live *C. houstonensis* within the Little (40% of sites), Lower Colorado (31% of sites), and Middle Colorado (12%) rivers. In the Lower Colorado River, we observed *C. houstonensis* from Fayette County, upstream of La Grange, downstream to Wharton County, between Wharton and Bay City (Figure 13). In the Middle Colorado River, we observed *C. houstonensis* from Coleman County to San Saba County, though its distribution was patchy with large gaps between site occurrences (Figure 14). In the Little River, *C. houstonensis* was the numerically dominant species and was found live in Milam County, from near Val Verde, downstream to Cameron (Figure 15).

Among basins within its historical range, the highest mean CPUE for *C. houstonensis* occurred within the Little River, averaging 1.27 ±0.73 (SE) mussels/p-h (range: 0.00 – 5.75 mussels/p-h) (Figure 16). Comparison of CPUE by Kruskal-Wallis analysis detected significant differences among basins ($p = 0.01$). Despite this, pairwise multiple comparison using Dunn's Test did not provide evidence for where differences occurred.

CPUE of *C. houstonensis* within individual mesohabitats ranged from 0.00 mussels/p-h. to 52.00 mussels/p-h. Mean CPUE was highest within run mid-channel habitats at 0.87 ± 0.46 (SE) mussels/p-h (range: 0.00 – 52.00 mussels/p-h; Figure 17). Comparison of CPUE by Kruskal-Wallis analysis detected significant differences among mesohabitats ($p = 0.02$). Pairwise multiple comparison using Dunn's Test detected CPUE was significantly higher in run edge habitats compared to riffle habitats ($p = 0.006$).

The size structure of *C. houstonensis* in the Lower Colorado River was dominated by size classes of 50 - 60 mm, with a few smaller individuals from 20 – 30 mm. In the Middle Colorado

River, all the *C. houstonensis* we observed were large individuals greater than 60 mm. The size structure of the Little River was dominated by size classes of 50 - 60 mm, with a few smaller individuals (30 – 40 mm) present (Figure 18).

Cyclonaias petrina

We collected a total of 140 live *C. petrina* within the Lower Colorado (13% of sites), Middle Colorado (15% of sites), and Upper Guadalupe (20%) rivers. In the Lower Colorado River, we observed *C. petrina* from Colorado County, upstream of Columbus, downstream to Wharton County, near Wharton, Texas (Figure 19). In the Middle Colorado River, we observed *C. petrina* from Coleman County to San Saba County, with the majority of occurrences within San Saba County (Figure 20). In the Upper Guadalupe River, we observed live mussels within the upper reaches in Kerr County, from Hunt, downstream to Center Point *(*Figure 21).

Among basins, *C. petrina* mean CPUE was highest within the Middle Colorado River at 0.18 ± 0.12 (SE) mussels/p-h (range: 0.00 – 4.44 mussels/p-h). Mean CPUE was lowest within the Lower Colorado River at 0.04 ± 0.03 (SE) mussels/p-h (range: 0.00 – 1.46 mussels/p-h) (Figure 22). Comparison of CPUE by Kruskal-Wallis analysis failed to detect significant differences among basins ($p = 0.76$).

Among mesohabitats, mean CPUE of *C. petrina* was highest in run edge habitats at 0.27 ± 0.2 (SE) mussels/p-h (range: 0.00 – 18.00 mussels/p-h), and lowest in riffle habitats at 0.01 ± 0.01 (SE) mussels/p-h (range: 0.00 – 0.50 mussels/p-h) (Figure 23). Comparison of CPUE by Kruskal-Wallis analysis failed to detect significant differences among mesohabitats ($p = 0.6$).

The size structure of *C. petrina* collected within the Lower Colorado River was dominated by individuals from 65 – 80 mm, but included a few individuals from 40 – 60 mm.

Size structure within the Middle Colorado River represented was dominated by individuals from 70 – 80 mm, and contained no individuals less than 50 mm. Within the Upper Guadalupe River, individuals from 55 – 60 mm were most common, with one individual at approximately 20 mm collected (Figure 24).

Lampsilis bracteata

We collected a total of 18 live *L. bracteata* within the Middle Colorado (2.4% of sites) and Upper Guadalupe (40%) rivers. In Middle Colorado River, we found no live *L. bracteata* within the mainstem, though two live individuals were collected in Cherokee Creek (Figure 25). In the Upper Guadalupe River, we observed *L. bracteata* in Kerr County, from Hunt to just upstream of Comfort (Figure 26). No *L. bracteata* were observed in the Lower Colorado River basin.

Among basins, mean CPUE for *L. bracteata* was highest within the Upper Guadalupe River, averaging 0.18 ± 0.09 (SE) mussels/p-h (range: 0.00 – 0.80 mussels/p-h; Figure 27). Comparison of CPUE by Kruskal-Wallis analysis detected significant differences among basins ($p = 0.001$). Pairwise multiple comparison using Dunn's Test detected that CPUE was significantly higher in the Upper Guadalupe compared to the Middle Colorado basin ($p < 0.001$).

Among mesohabitats, the highest mean CPUE occurred within run edges at 0.17 ± 0.11 (SE) mussels/p-h (range: 0 – 1.67 mussels/p-h). Mean CPUE was lowest within backwater habitats, where no live individuals were collected (Figure 28). Comparison of CPUE by Kruskal-Wallis analysis failed to detect significant differences among mesohabitats ($p = 0.1$).

Size structure of *L. bracteata* in the Upper Guadalupe was dominated by individuals 50 - 60 mm, with only one small individual (25 mm) collected (Figure 29). The two individuals collected from Cherokee Creek in the Middle Colorado basin were 48 and 64 mm.

Truncilla macrodon

Nine live *T. macrodon* were collected within the Lower Colorado River (15% of sites). We observed *T. macrodon* from Colorado County to Matagorda County (Figure 30). No live *T. macrodon* were found in the Brazos River upstream of Possum Kingdom Lake, including three sites within the Clear Fork Brazos River. No live *T. macrodon* were collected from the Little River.

CPUE of *T. macrodon* within the Lower Colorado averaged 0.02 ± 0.007 (SE) mussels/p-h (range: 0.00 – 0.22 mussels/p-h). Mean CPUE was highest within run edge habitats at 0.02 ± 0.008 (SE) mussels/p-h (range: 0.00 – 0.50 mussels/p-h). No live *T. macrodon* were observed in pool mid-channel, riffle, or run mid-channel habitats (Figure 31). Comparison of CPUE by Kruskal-Wallis analysis detected significant differences among mesohabitats ($p = 0.01$). Pairwise multiple comparison using Dunn's Test detected that CPUE was significantly higher in run edge habitats compared to run mid-channel ($p = 0.03$) and pool mid-channel ($p = 0.02$) habitats.

T. macrodon ranged in size from 18 – 54 mm, with the most frequently encountered size class being approximately 50 mm (Figure 32).

Fusconaia mitchelli

During our survey efforts, no live *F. mitchelli* were collected, though recently dead shells with nacre still intact were collected in the Little River.

Part 1 Synthesis

Cyclonaias houstonensis

Cyclonaias houstonensis is historically known from four of the five basins surveyed (i.e., Lower Colorado River, Middle Colorado River, Little River, and Upper Brazos River), and was located in three of these basins. It occurred at 31% of sites in the Lower Colorado River and was found from Fayette County downstream to Wharton County. In the Middle Colorado River, *C. houstonensis* was found patchily distributed (12% of sites) from Coleman County to San Saba County. Our results indicate *C. houstonensis* currently persists in the Middle Colorado River within Coleman County, which was uncertain prior to these surveys (USFWS 2016). In the Little River, it was the numerically dominant species and occurred at 40% of sites. Live *C. houstonensis* were not encountered in our surveys within the Upper Brazos River system, including the Clear Fork Brazos River.

Although visual and tactile surveys are biased towards large and sculptured individuals (Strayer & Smith 2003; Haag 2012), the presence of smaller *C. houstonensis* (20 – 40 mm) supports that recruitment has successfully occurred recently in the Lower Colorado River and Little River, though we cannot quantify recruitment based on these surveys. Within the Middle Colorado River, only large adults over 60 mm were encountered.

Across all basins, *C. houstonensis* was found in a variety of mesohabitats, with the highest CPUE in run mid-channel and pool mid-channel mesohabitats. Analysis revealed significantly higher CPUE in run edge mesohabitats than in riffles. Others have suggested that *C. houstonensis* prefers bank, backwater, and front of point bar habitats (Randklev et al. 2014).

Cyclonaias petrina

Live *C. petrina* were found in all survey basins where they were historically documented (i.e., Lower Colorado, Middle Colorado, and Upper Guadalupe). In the Lower Colorado River, we observed *C. petrina* at 13% of sites and located them from Colorado County, upstream of Columbus, downstream to Wharton County, near Wharton, Texas. In the Middle Colorado River, *C. petrina* were found at 15% of sites and located from Coleman County to San Saba County, with the majority of occurrences within San Saba County below the San Saba River confluence. Individuals collected below O.H. Ivie in Coleman County fill a distributional gap in the currently occupied range of this species (Randklev et al. 2017). In the Upper Guadalupe River, we observed live *C. petrina* at 20% of sites sampled and located them within the upper reaches in Kerr County, from Hunt, downstream to Center Point, Texas.

Among all basins, the smallest *C. petrina* collected were > 40 mm, excepting one 18 mm individual from the Upper Guadalupe River, which suggests recent recruitment in this population. Among mesohabitats, *C. petrina* mean CPUE was highest in run edge habitats and lowest in riffles. This differs from previous studies (Tsakiris & Randklev 2016; Randklev et al. 2017) that suggested riffle habitats were optimal for *C. petrina* in the lower Guadalupe River.

Lampsilis bracteata

Live *L. bracteata* were found in two of the three survey basins where they were historically documented (i.e., Upper Guadalupe, Lower Colorado, Middle Colorado). We observed *L. bracteata* restricted to the upper reaches of the Upper Guadalupe River from the confluence of the North and South Forks downstream to approximately Comfort. This distribution may be a result of water permanency in recent drought years, as portions of the Upper Guadalupe River closer to Canyon Lake experienced extensive desiccation during recent

drought years of 2011 -2013 (BL personal observation), whereas the river never went dry in Kerr County (Tara Bushnoe, Upper Guadalupe River Authority, personal communication). Similarly, recent surveys in Colorado River tributaries (San Saba, Llano, Pedernales rivers) found *L. bracteata* restricted to the upper reaches of these systems (Randklev et al. 2017), suggesting that water permanency associated with Edwards Plateau spring systems may be influencing distribution of this species. In the Middle Colorado, no *L. bracteata* were observed in the mainstem, but two live individuals were collected in Cherokee Creek. Based on known historical records (USFWS 2011), this represents a previously undocumented population. To confidently identify the extent of this population, further surveys are warranted. In the Lower Colorado River basin, *L. bracteata* has been previously reported from Onion Creek (Randklev et al. 2017). We only sampled one site in Onion Creek and did not observe *L. bracteata*.

The Upper Guadalupe River *L. bracteata* population was dominated by large adults of 50 – 60 mm, although one small individual of 25 mm was noted. Based on only one small individual collected, it is difficult to infer the level of recruitment within this system. However, it should be noted that we observed female *L. bracteata* gills fully charged with glochidia, which supports that spawning has successfully occurred recently on the Upper Guadalupe. The two individuals collected in Cherokee Creek within the Middle Colorado River basin were both larger adults (48 mm and 64 mm).

L. bracteata were found in four of the five mesohabitat types sampled, but were not located in backwaters. The highest mean CPUE was in run edge habitats. This association with edge habitats corroborates the work of previous researchers who have found *L. bracteata* in bank and pool habitats, but not in backwaters, mid-channel habitats, or riffles (Randklev et al. 2017).

Truncilla macrodon

Live *T. macrodon* were observed in one of the four basins during qualitative surveys. *Truncilla macrodon* were historically documented in all four basins (i.e., Lower Colorado River, Middle Colorado River, Little River, Upper Brazos River). In the Lower Colorado River, we collected a total of nine live individuals from Colorado, Wharton, and Matagorda counties, and found them in 15% of the sites sampled. In the Middle Colorado River, no live individuals were documented during survey efforts, but we found fresh dead adult *T. macrodon* shells (e.g., adductor muscle intact) in San Saba County. In addition, one live juvenile *T. macrodon* was collected during a mark-recapture study in San Saba County. The presence of fresh dead adult shells and one live juvenile indicates that *T. macrodon* persists within the Middle Colorado River in San Saba County, though likely in low abundance. Although live *T. macrodon* have recently been documented in the Little River in low abundance (Randklev et al. 2017), no live individuals were found during our surveys there. Additionally, despite relatively recent records of *T. macrodon* from the Clear Fork Brazos River (Randklev et al. 2017), we sampled three sites and did not locate any live individuals. It should be noted that the Clear Fork Brazos River contained a diverse community of dead shell material suggesting a once diverse mussel community, but this system experienced extensive desiccation in recent drought years of 2011-2013 (BL personal observation) and only one live mussel was documented in the Clear Fork Brazos River during these surveys. Therefore, the status of the *T. macrodon* population in this system is uncertain, and additional surveys are needed.

Although a low number of individuals were collected, one 18 mm *T. macrodon* was observed in the Lower Colorado River which suggests that reproduction has recently occurred.

Additionally, one live juvenile collected in the Middle Colorado River during mark recapture work suggests a reproducing population exists, although evidently in low abundance.

T. macrodon were found in run edge, pool edge, and backwater habitats, with the highest mean CPUE observed in run edge habitats. This association with edge habitats corroborates previous work in the lower Brazos River that suggests *T. macrodon* prefer bank habitats (Randklev et al. 2014).

Fusconaia mitchelli

Given recent and historical records, *F. mitchelli* was previously documented in three of the five survey basins (i.e., Middle Colorado River basin, Upper Guadalupe River basin, and Little River basin; Randklev et al. 2017). Although *F. mitchelli* is known to occur in Colorado River tributaries mentioned above, it has never been documented in the Lower Colorado River basin. Despite surveying over 62 sites in the Upper Guadalupe, Middle Colorado, and Little River basins, we observed no live *F. mitchelli*. It should be noted that we observed relatively recently dead shells (nacre still present) at one site on the Little River, near where other surveyors have recently located live individuals (Randklev et al. 2017).

Part 1. Tables

Table 1. Occurrence of freshwater mussel species within the Lower Colorado River basin.

Species	Lower Colorado River Basin			
	Total Live	**Percentage Live**	**Occurrence (Number of Sites)**	**Percentage Occurrence**
Amblema plicata	1325	56.94	16	33.33
Cyclonaias houstonensis	387	16.63	15	31.25
Cyclonaias petrina	30	1.29	6	12.50
Cyrtonaias tampicoensis	37	1.59	10	20.83
Lampsilis teres	394	16.93	22	45.83
Leptodea fragilis	64	2.75	16	33.33
Potamilus purpuratus	15	0.64	5	10.42
Pyganodon grandis	16	0.69	3	6.25
Quadrula apiculata	5	0.21	4	8.33
Toxolasma parvum	3	0.13	3	6.25
Toxolasma texasiense	34	1.46	5	10.42
Truncilla macrodon	9	0.39	7	14.58
Uniomerus tetralasmus	1	0.04	1	2.08
Utterbackia imbecillis	7	0.30	4	8.33
Total	**2327**		**26**	**54.17**

Table 2. Occurrence of freshwater mussel species within the Middle Colorado River drainage.

Species	Middle Colorado River Basin			
	Total Live	**Percentage Live**	**Occurrence (Number of Sites)**	**Percentage Occurrence**
Amblema plicata	5	1.02	2	4.88
Cyclonaias houstonensis	13	2.64	5	12.20
Cyclonaias petrina	97	19.72	6	14.63
Cyrtonaias tampicoensis	49	9.96	10	24.39
Lampsilis bracteata	2	0.41	1	2.44
Lampsilis teres	27	5.49	8	19.51
Leptodea fragilis	96	19.51	25	60.98
Potamilus purpuratus	20	4.07	10	24.39
Pyganodon grandis	33	6.71	13	31.71
Quadrula appiculata	70	14.23	11	26.83
Tritogonia verruccosa	54	10.98	11	26.83
Utterbackia imbecillis	26	5.28	8	19.51
Total	**492**		**34**	**82.93**

Table 3. Occurrence of freshwater mussel species within the Little River drainage.

Species	Little River Basin			
	Total Live	**Percentage Live**	**Occurrence (Number of Sites)**	**Percentage Occurrence**
Amblema plicata	75	23.44	4	40.00
Cyclonaias houstonensis	133	41.56	4	40.00
Cyrtonaias tampicoensis	66	20.63	7	70.00
Lampsilis teres	40	12.50	4	40.00
Leptodea fragilis	6	0.02	2	20.00
Total	**320**		**7**	**70.00**

Table 4. Occurrence of freshwater mussel species within the Upper Guadalupe drainage.

Species	Upper Guadalupe River Basin			
	Total Live	**Percentage Live**	**Occurrence (Number of Sites)**	**Percentage Occurrence**
Cyclonaias petrina	10	21.28	2	20.00
Lampsilis bracteata	16	34.04	4	40.00
Toxolasma parvum	1	2.13	1	10.00
Toxolasma texasiense	13	27.66	2	20.00
Uniomerus tetralasmus	7	14.89	1	10.00
Total	**47**		**4**	**40.00**

Part 1 Figures

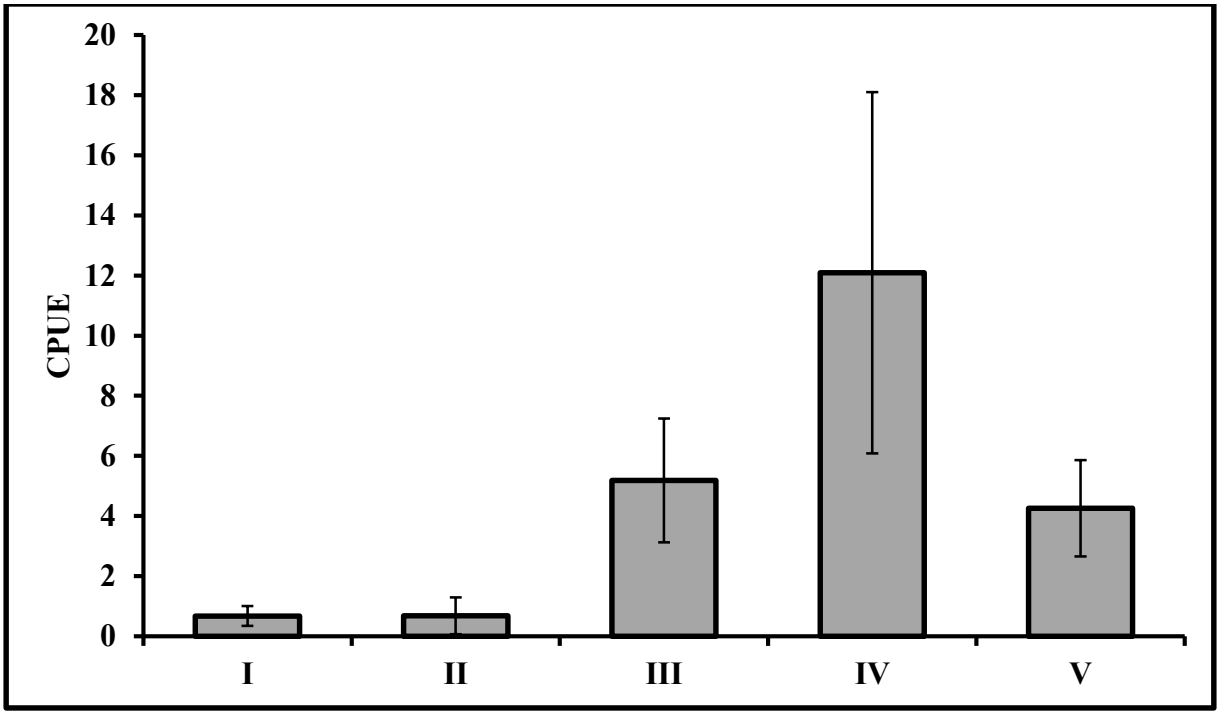

Figure 1. Catch-per-unit effort (CPUE; mussels/p-h) of unionids by reach within the Lower Colorado River drainage. Reach I - Longhorn Dam to Bastrop, Reach II - Bastrop to La Grange, Reach III - La Grange to Columbus, Reach IV - Columbus to Wharton, and Reach V - Wharton to Bay City.

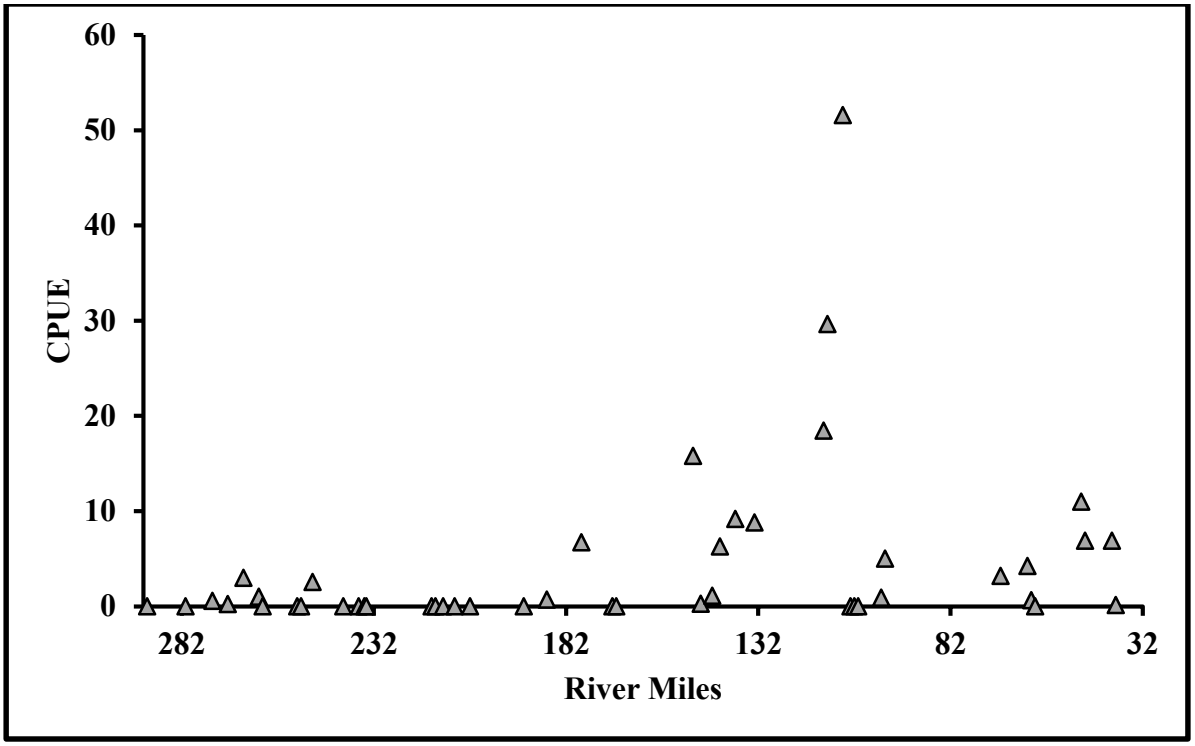

Figure 2. Catch-per-unit effort (CPUE; mussels/p-h) of unionids by river mile (RM) within the Lower Colorado River. For spatial reference, Longhorn Dam is at RM 292 and Bay City Dam is at RM 32.

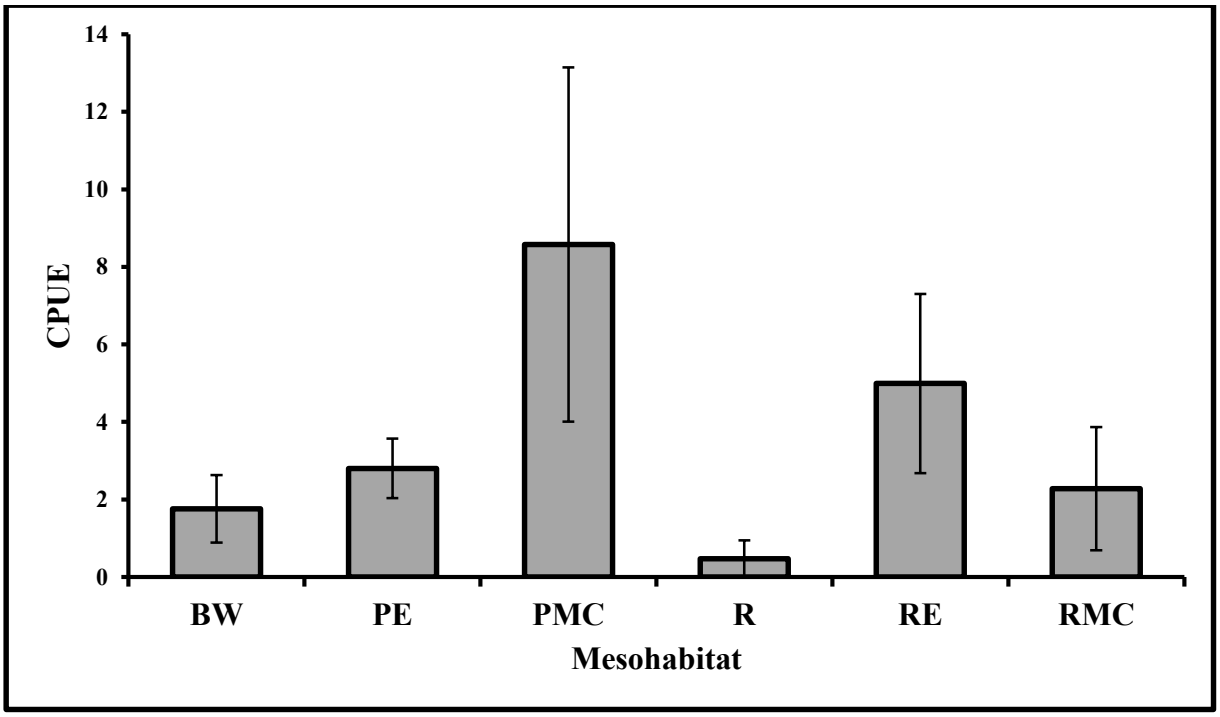

Figure 3. Catch-per-unit effort (CPUE; mussels/p-h) of unionids by mesohabitat within the Lower Colorado River drainage. BW = backwater, PE = pool edge, PMC = pool mid-channel, R = riffle, RE = run edge, RMC = run mid-channel.

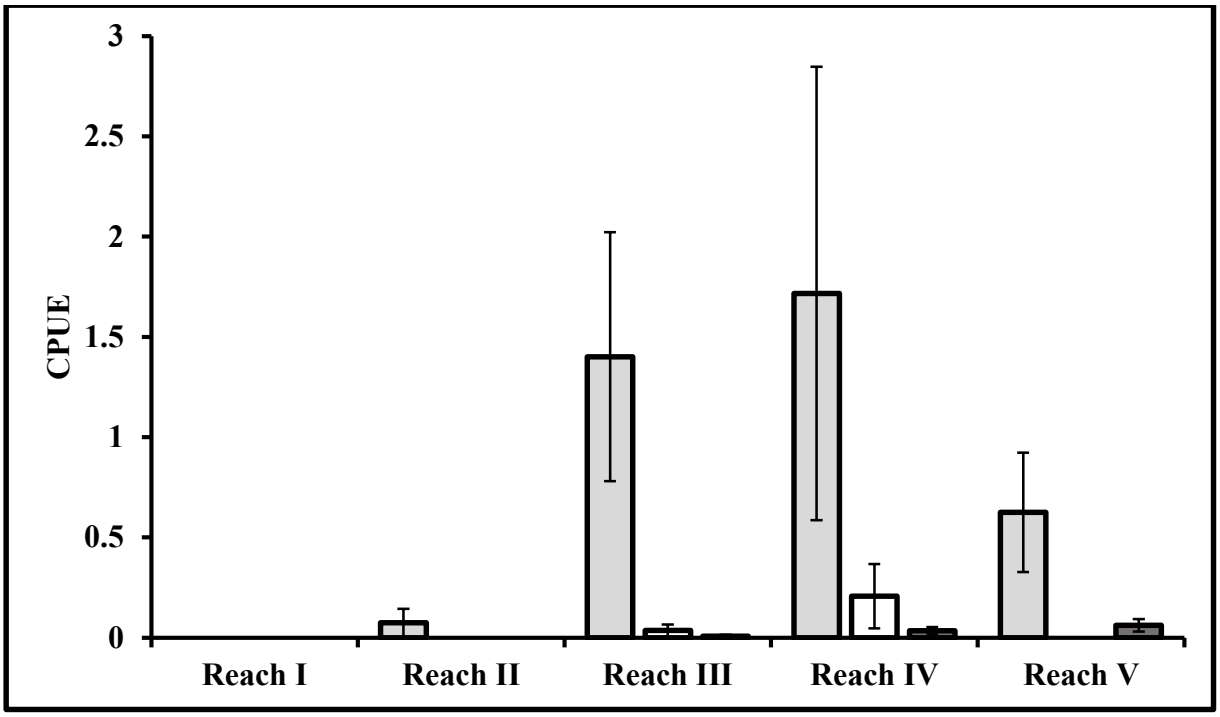

Figure 4. Catch-per-unit effort (CPUE; mussels/p-h) of *C. houstonensis* (light grey), *C. petrina* (white), and *T. macrodon* (dark grey) by reach within the Lower Colorado River drainage.

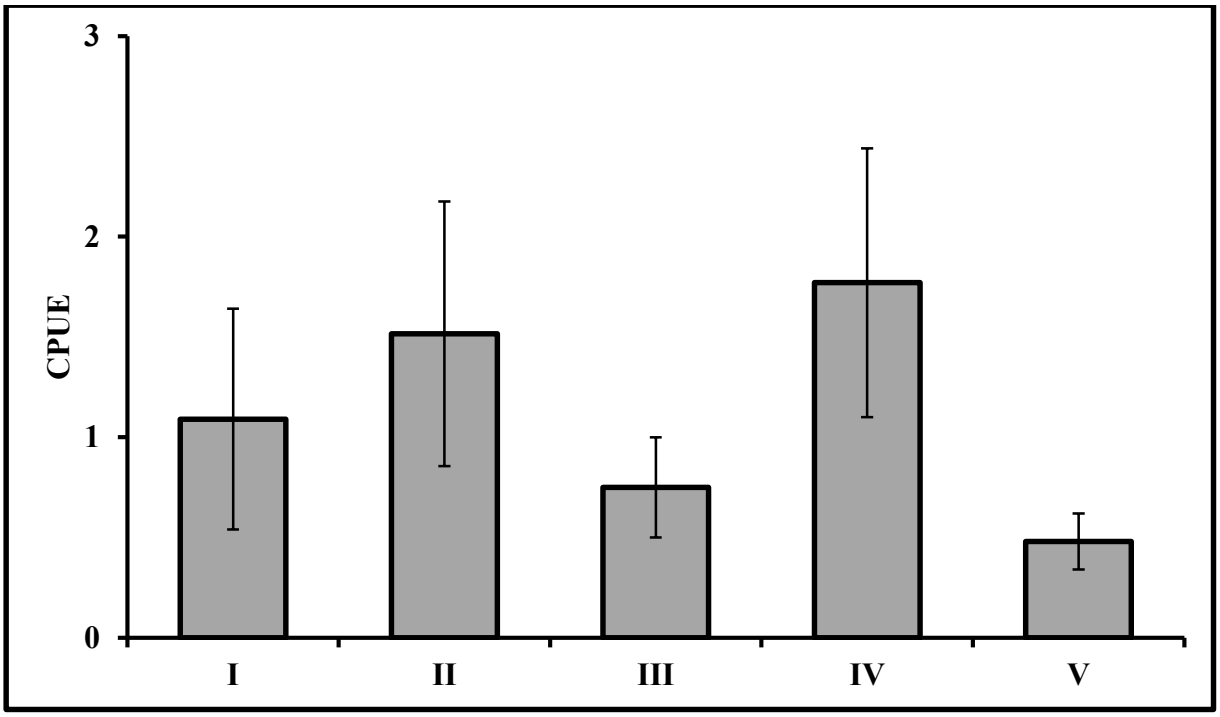

Figure 5. Catch-per-unit effort (CPUE; mussels/p-h) of unionids by reach within the Middle Colorado River drainage. Reach I - O.H. Ivie Reservoir to SH 377, Reach II - SH 377 to SH 45, Reach III - SH 45 to SH 16, Reach IV - SH 16 to Bend, and Reach V – Bend to Lake Buchannan.

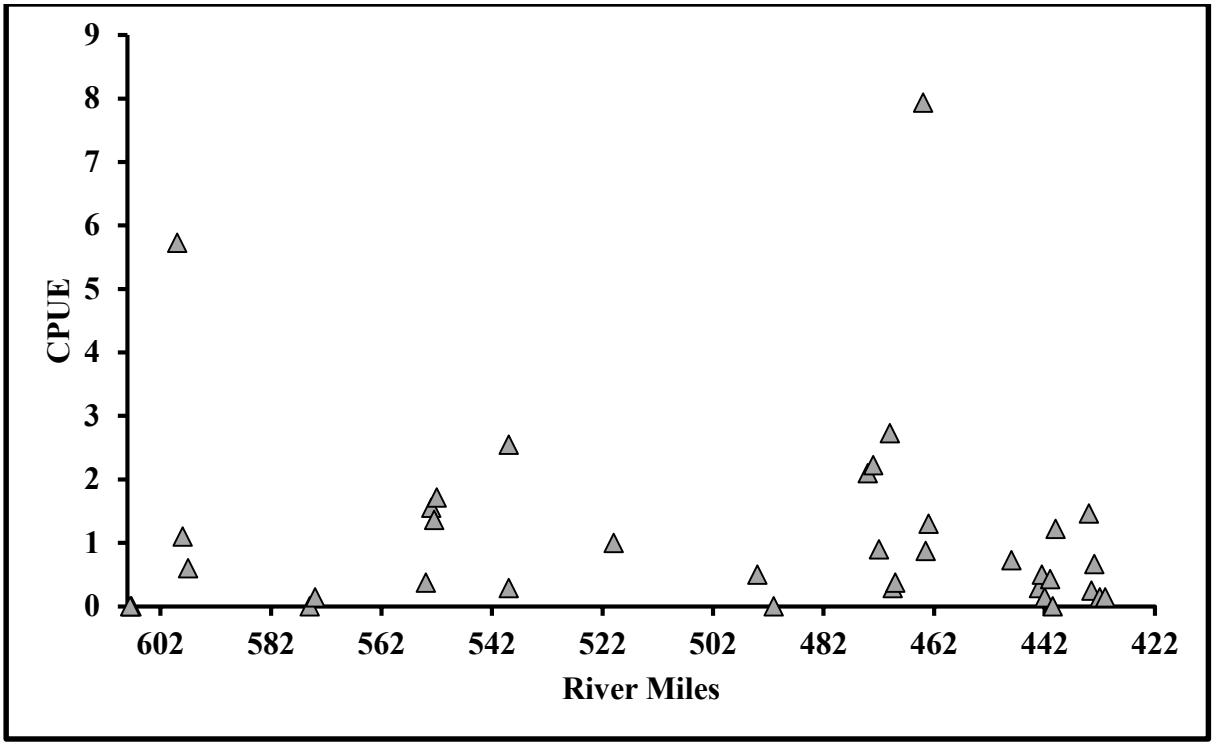

Figure 6. Catch-per-unit effort (CPUE; mussels/p-h) of unionids by river mile (RM) within the Middle Colorado River. O.H. Ivie Dam is located at approximately RM 608 and the headwaters of Lake Buchanan are located near RM 422.

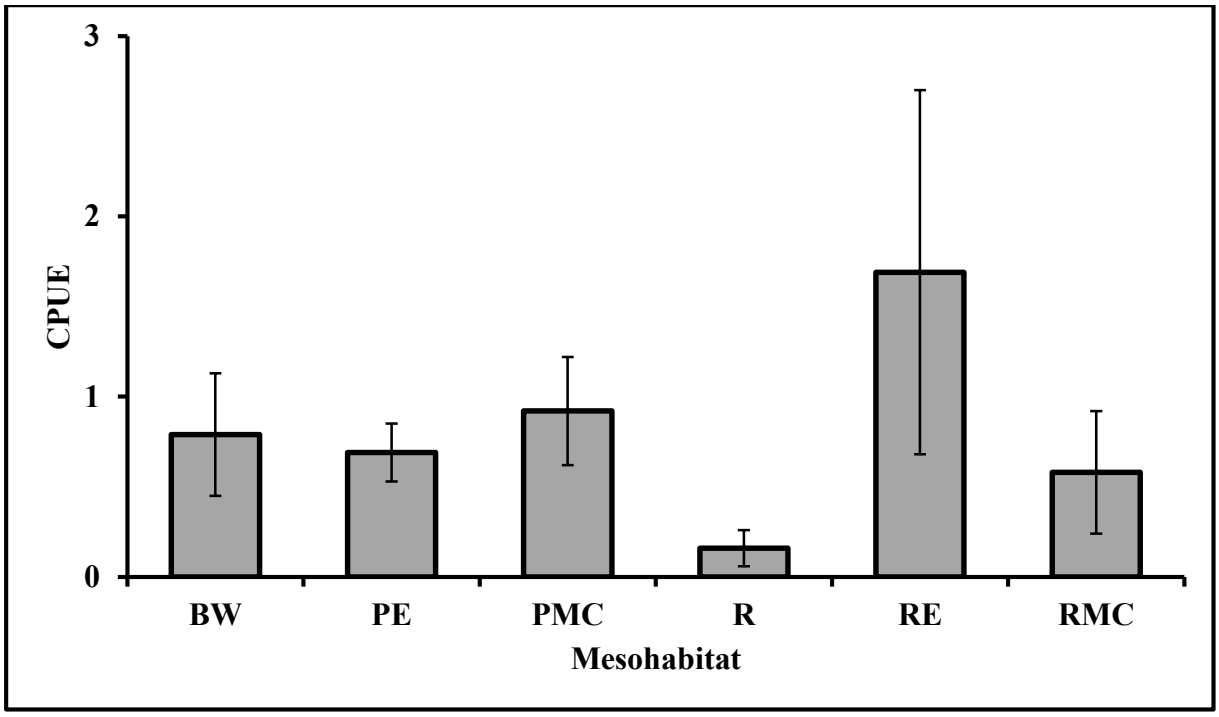

Figure 7. Catch-per-unit effort (CPUE; mussels/p-h.) of unionids by mesohabitat within the Middle Colorado River drainage. BW = backwater, PE = pool edge, PMC = pool mid-channel, R = riffle, RE = run edge, RMC = run mid-channel.

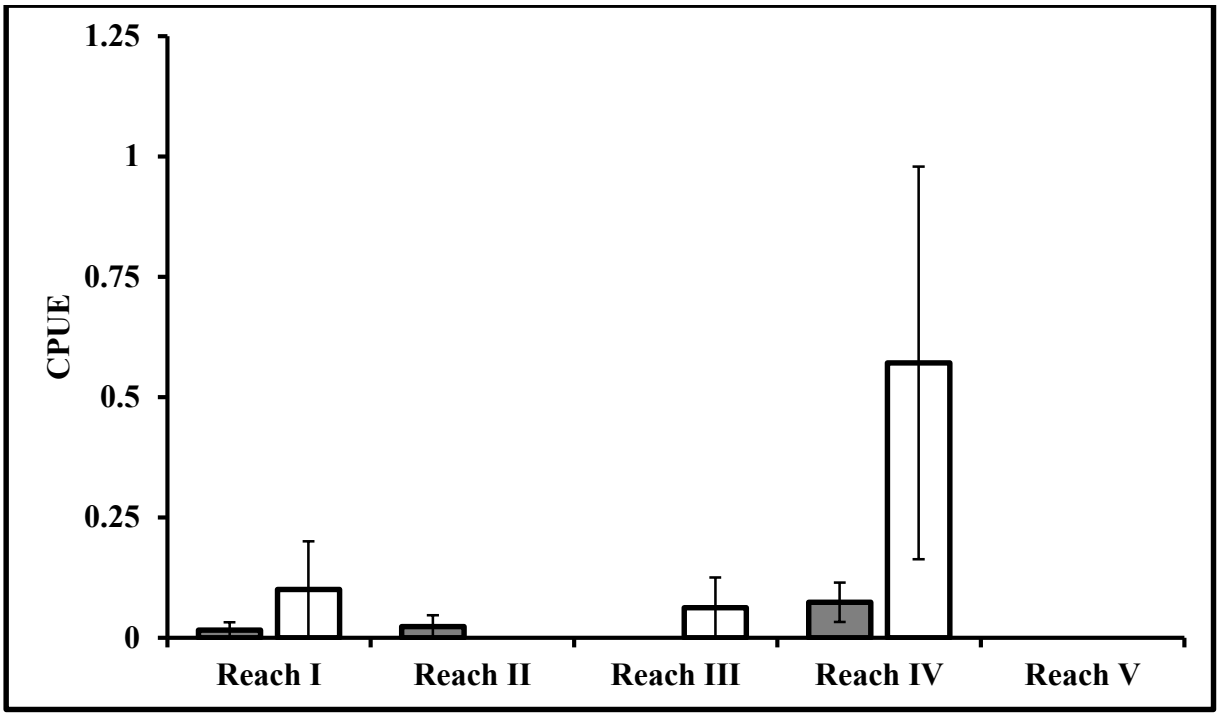

Figure 8. Catch-per-unit effort (CPUE; mussels/p-h) of *C. houstonensis* (dark grey) and *C. petrina* (white) by reach within the Middle Colorado River drainage.

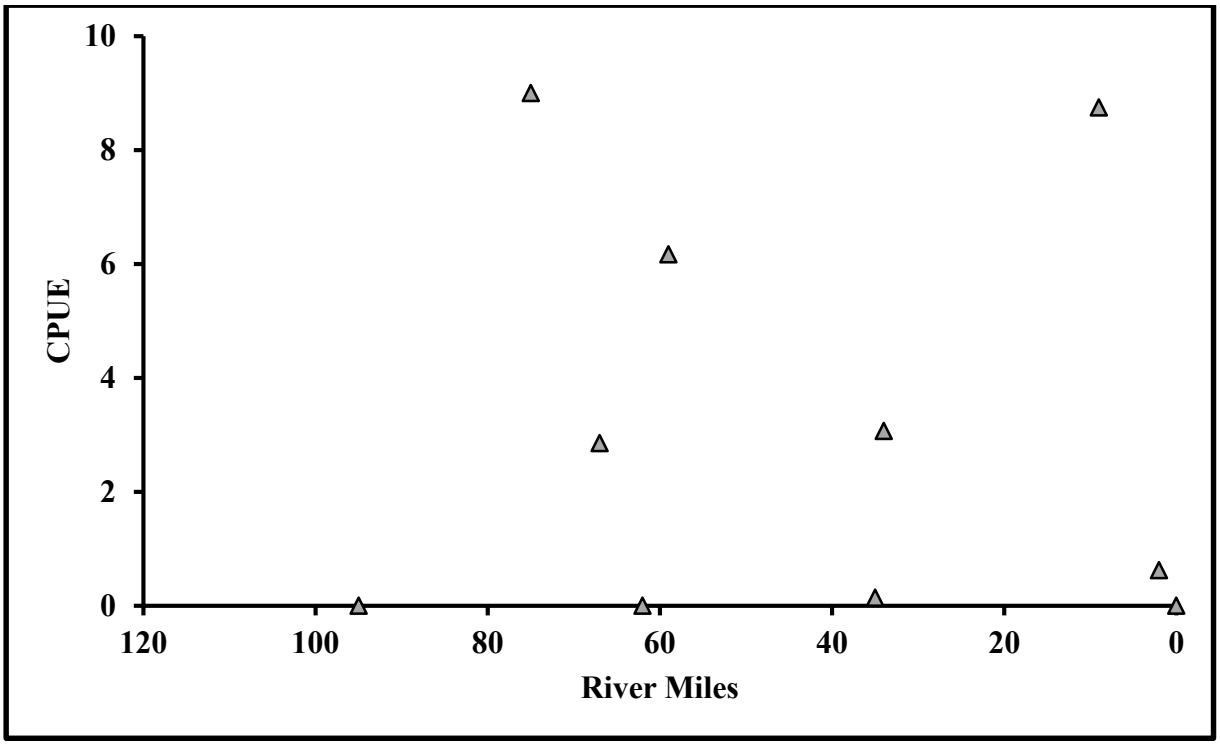

Figure 9. Catch-per-unit effort (CPUE; mussels/p-h) of unionids by river mile within the Little River. River mile 0 represents the confluence with the Brazos River.

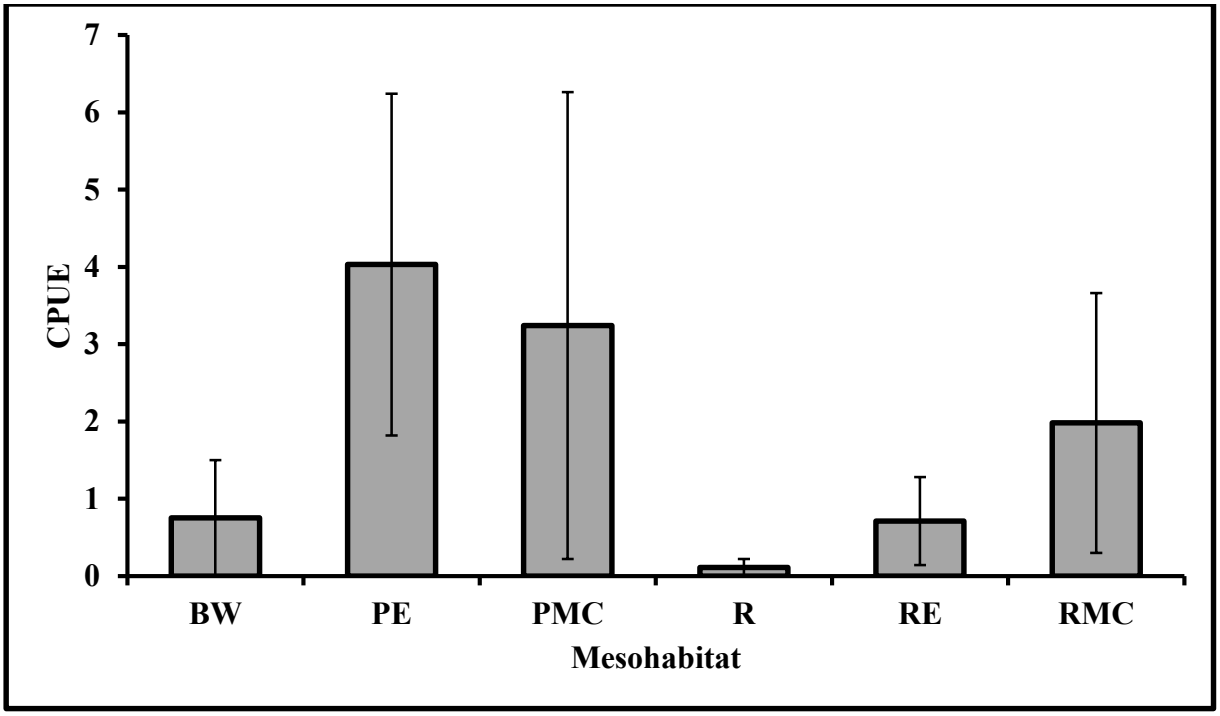

Figure 10. Catch-per-unit effort (CPUE; mussels/p-h.) of unionids by mesohabitat within the Little River drainage. BW = backwater, PE = pool edge, PMC = pool mid-channel, R = riffle, RE = run edge, RMC = run mid-channel.

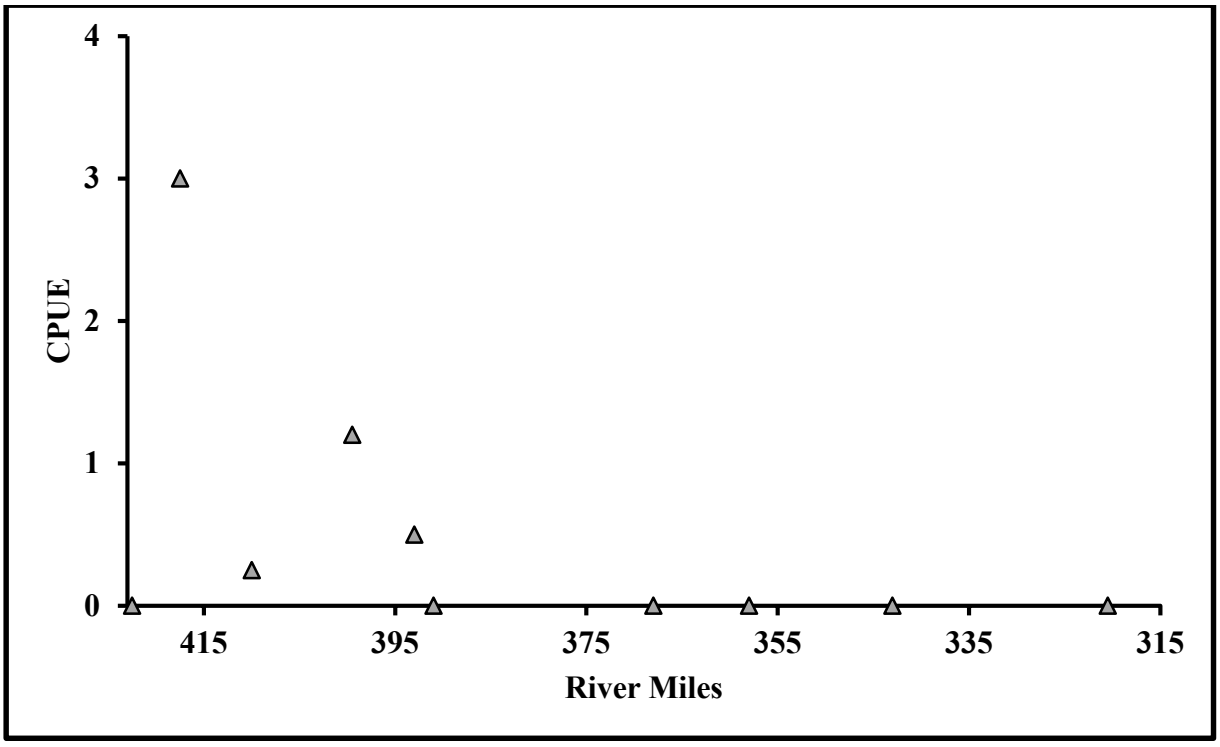

Figure 11. Catch-per-unit effort (CPUE; mussels/p-h.) of unionids by river mile within the Upper Guadalupe River. For spatial reference, the confluence of the North and South Fork Guadalupe River is at RM 423, and the headwaters of Canyon Lake are located at RM 315.

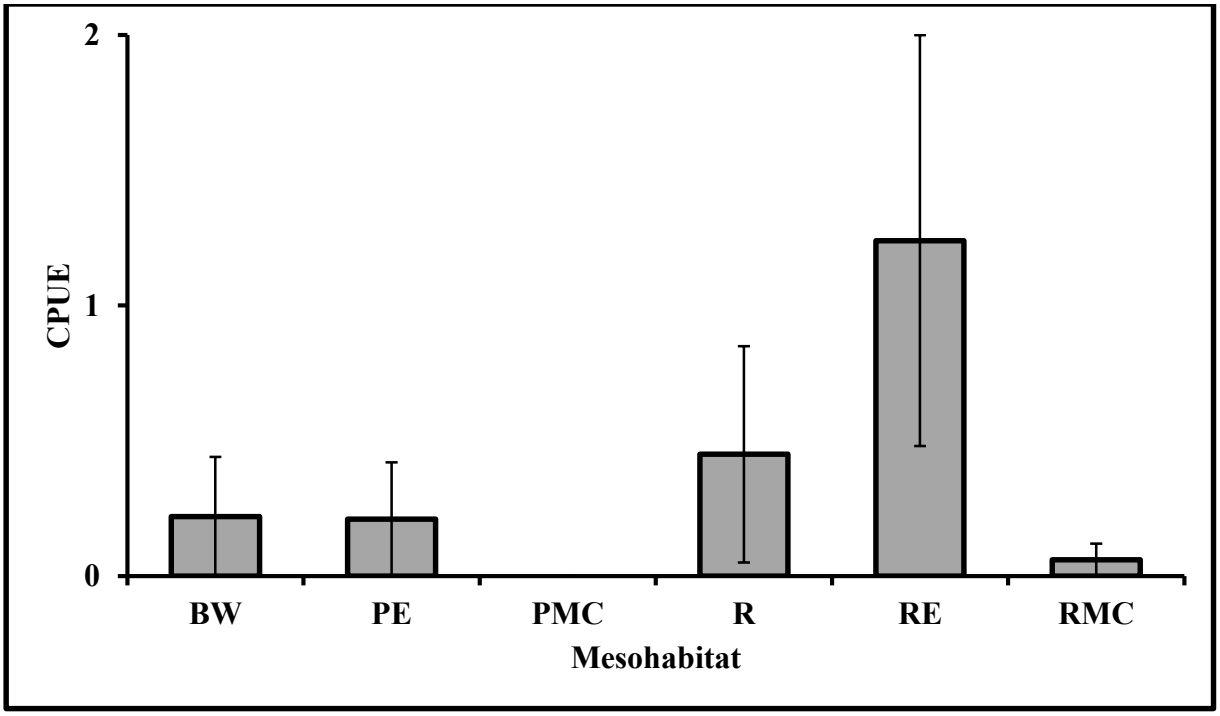

Figure 12. Catch-per-unit effort (CPUE; mussels/p-h.) of unionids by mesohabitat within the Upper Guadalupe drainage. BW = backwater, PE = pool edge, PMC = pool mid-channel, R = riffle, RE = run edge, RMC = run mid-channel.

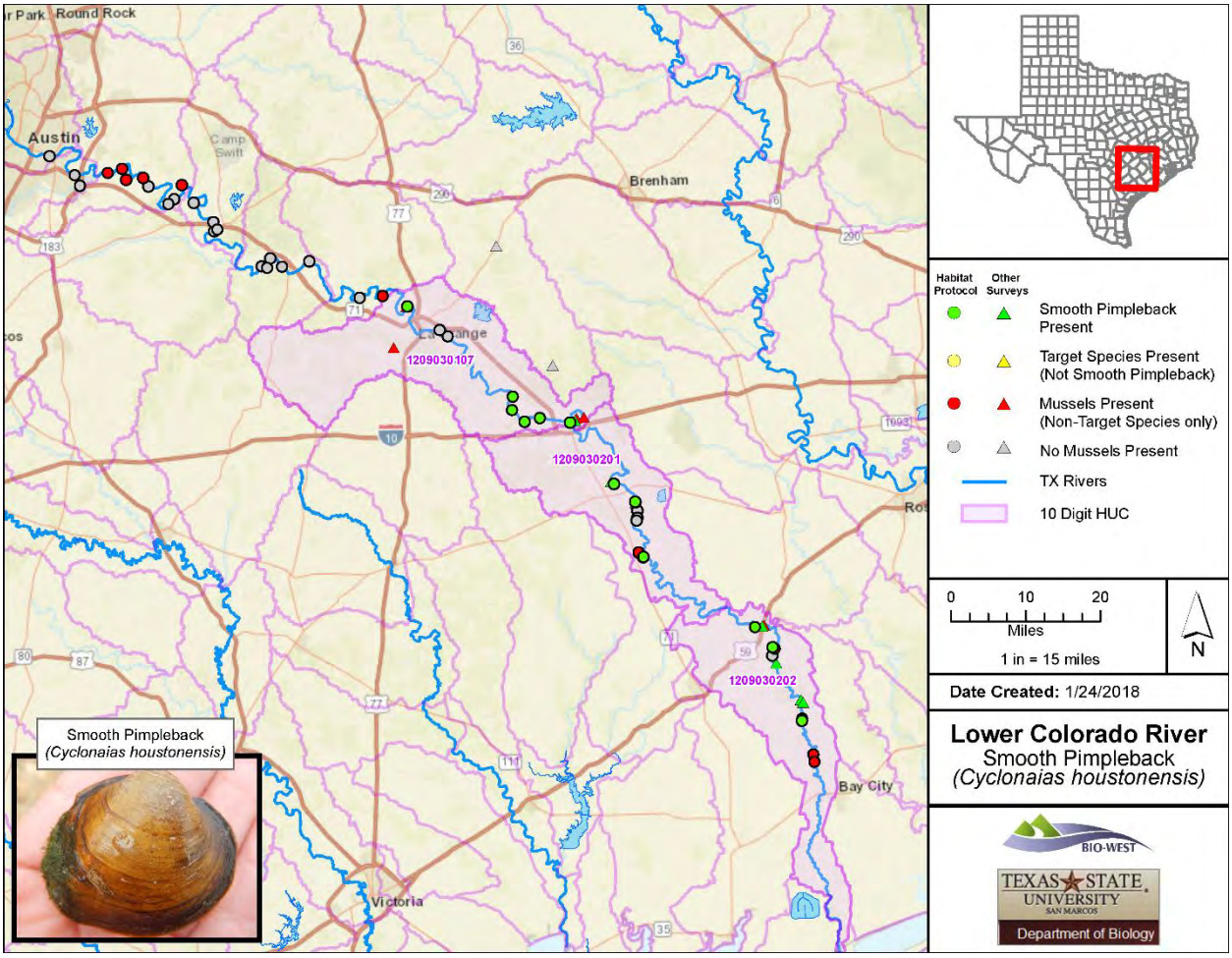

Figure 13. Map of *C. houstonensis* occurrence in the Lower Colorado River basin.

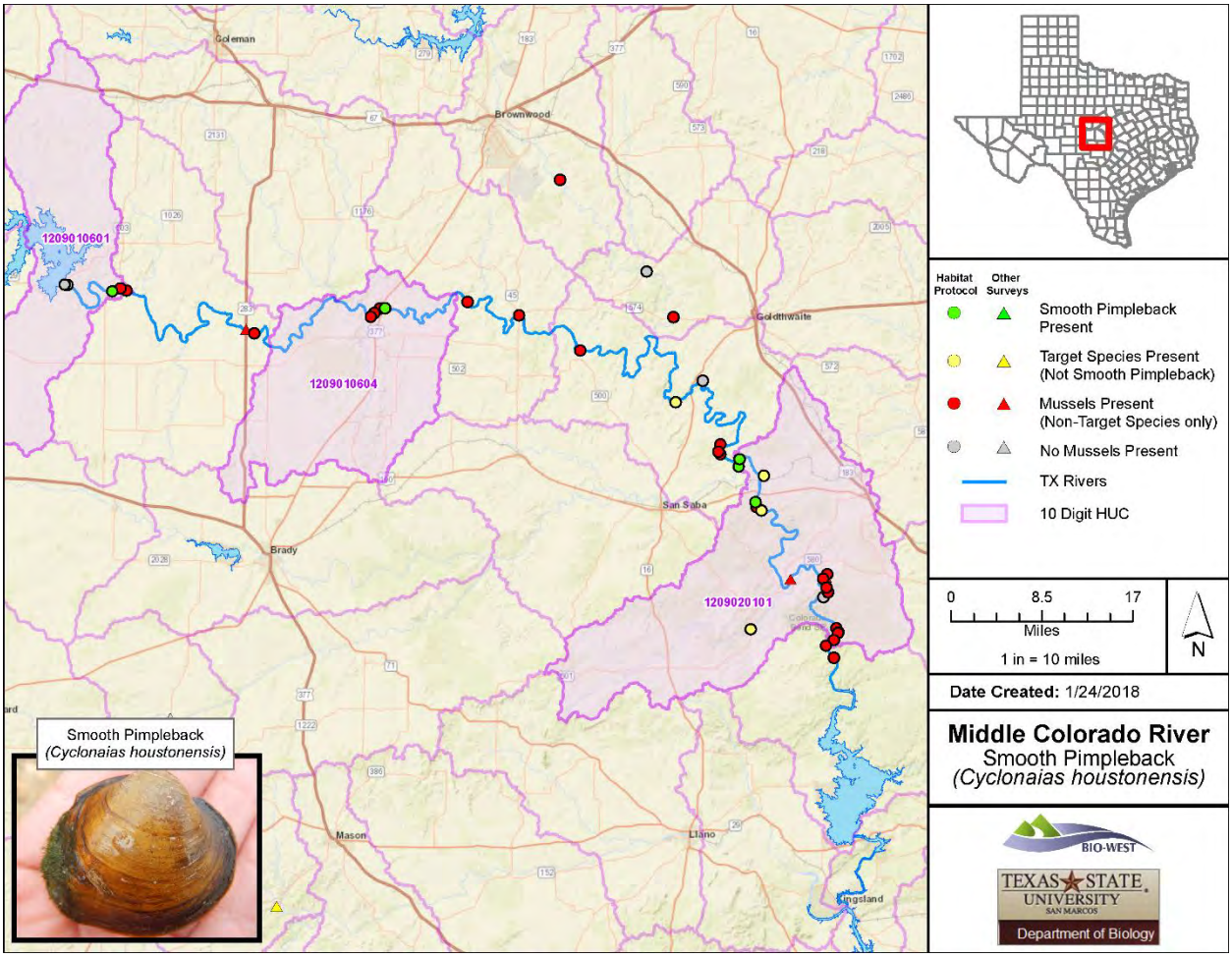

Figure 14. Map of *C. houstonensis* occurrence in the Middle Colorado River basin.

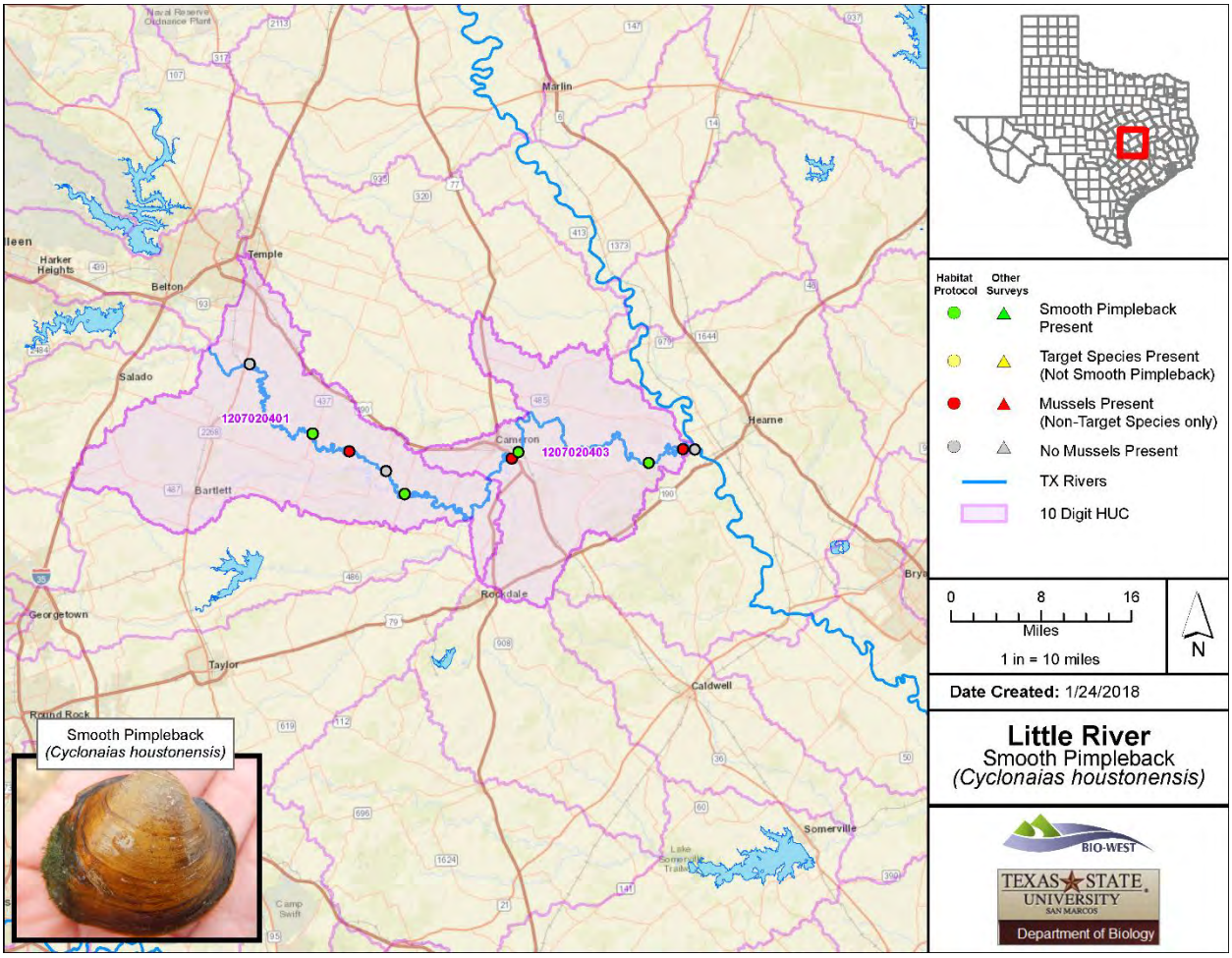

Figure 15. Map of *C. houstonensis* occurrence in the Little River basin.

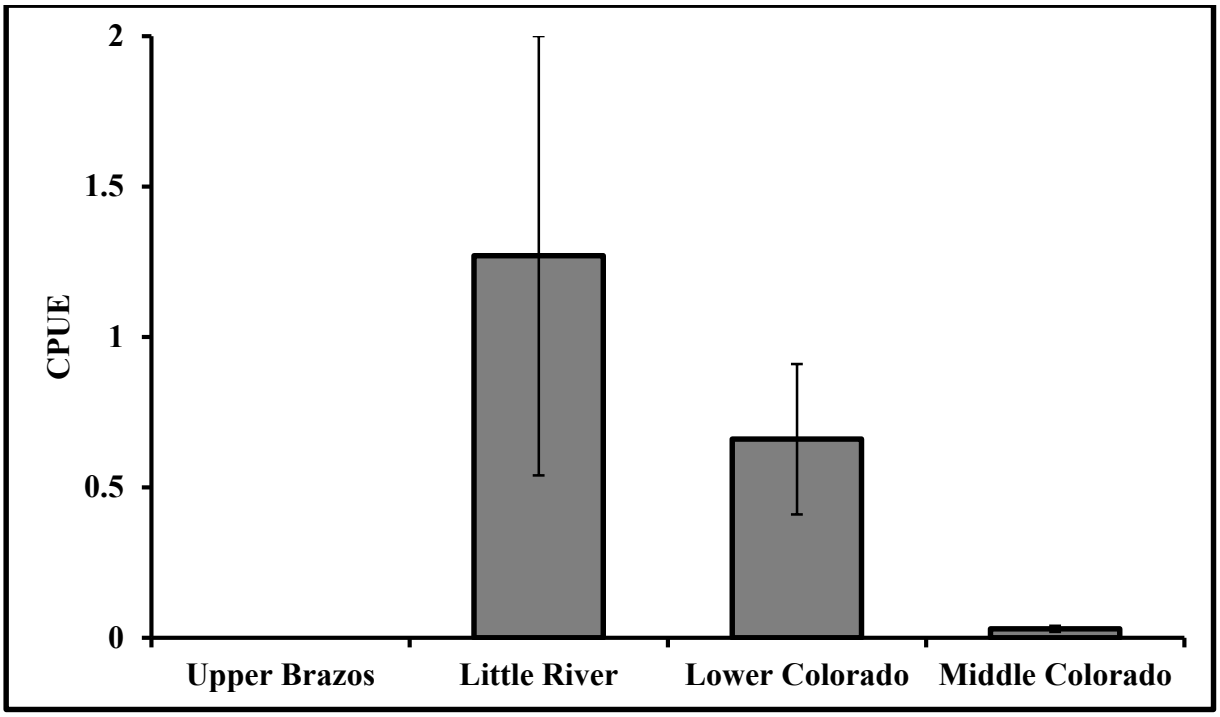

Figure 16. Catch per unit effort (CPUE; mussels/p-h.) of *C. houstonensis* among drainages.

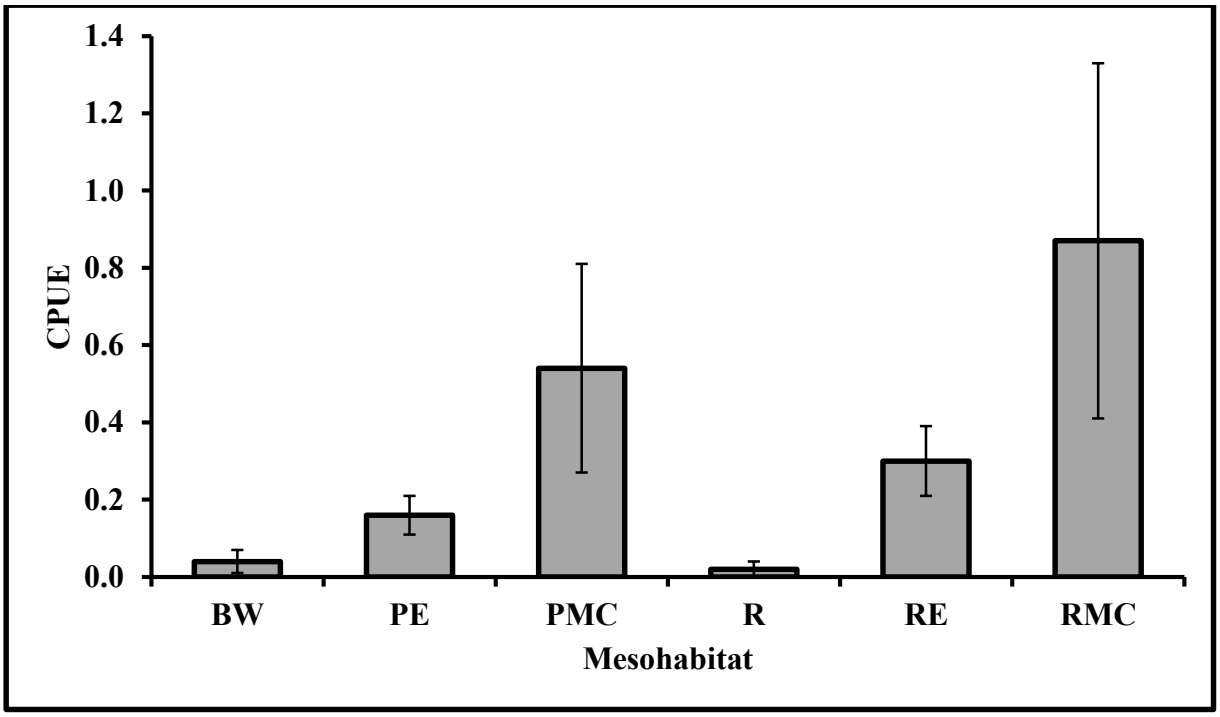

Figure 17. Catch-per-unit effort (CPUE; mussels/p-h.) of *C. houstonensis* by mesohabitat among all survey basins. BW = backwater, PE = pool edge, PMC = pool mid-channel, R = riffle, RE = run edge, RMC = run mid-channel.

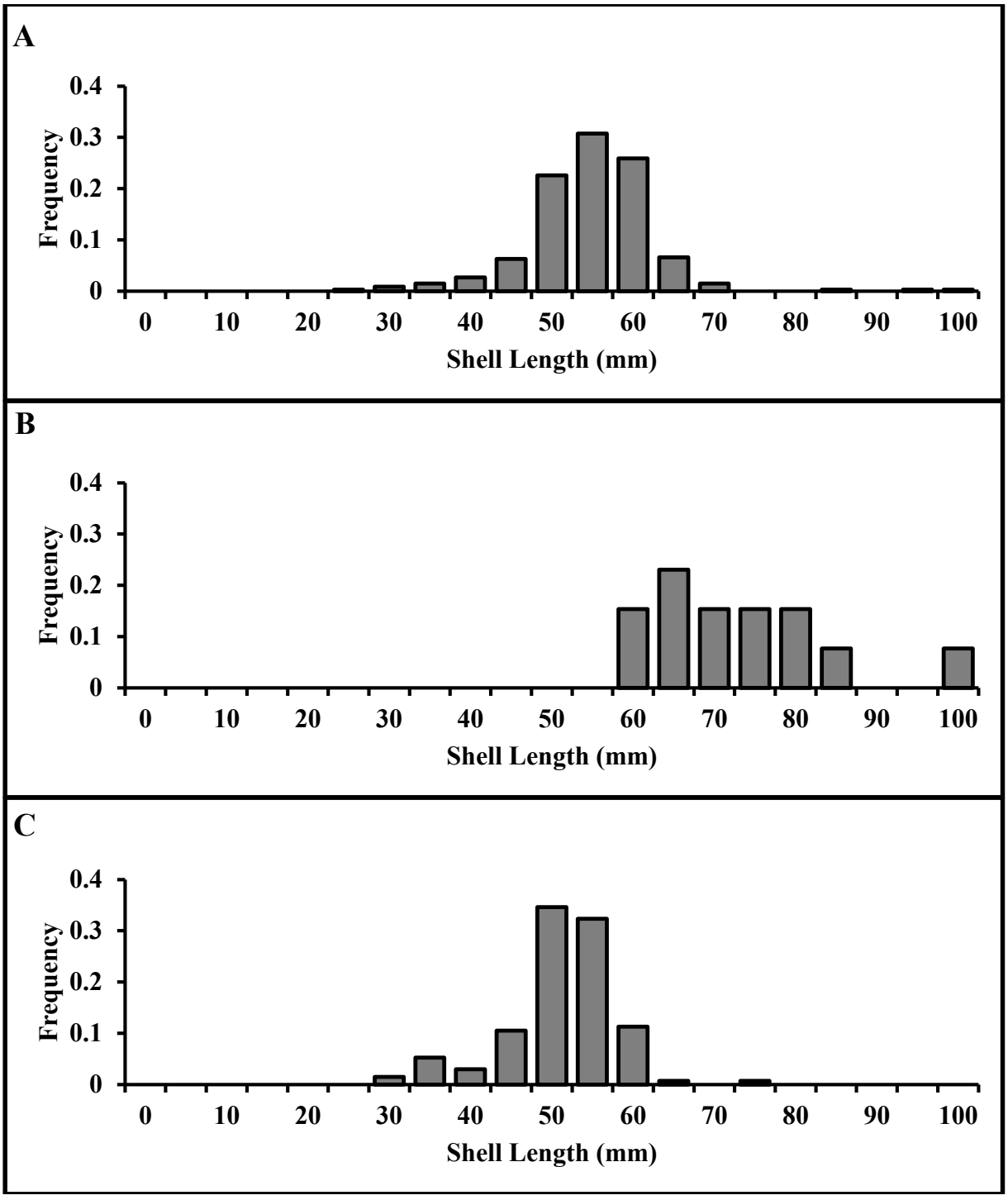

Figure 18. Proportional size structure of *C. houstonensis* within all basins of occurrence. A = Lower Colorado (N = 387), B = Middle Colorado (N = 13), C = Little River (N = 133).

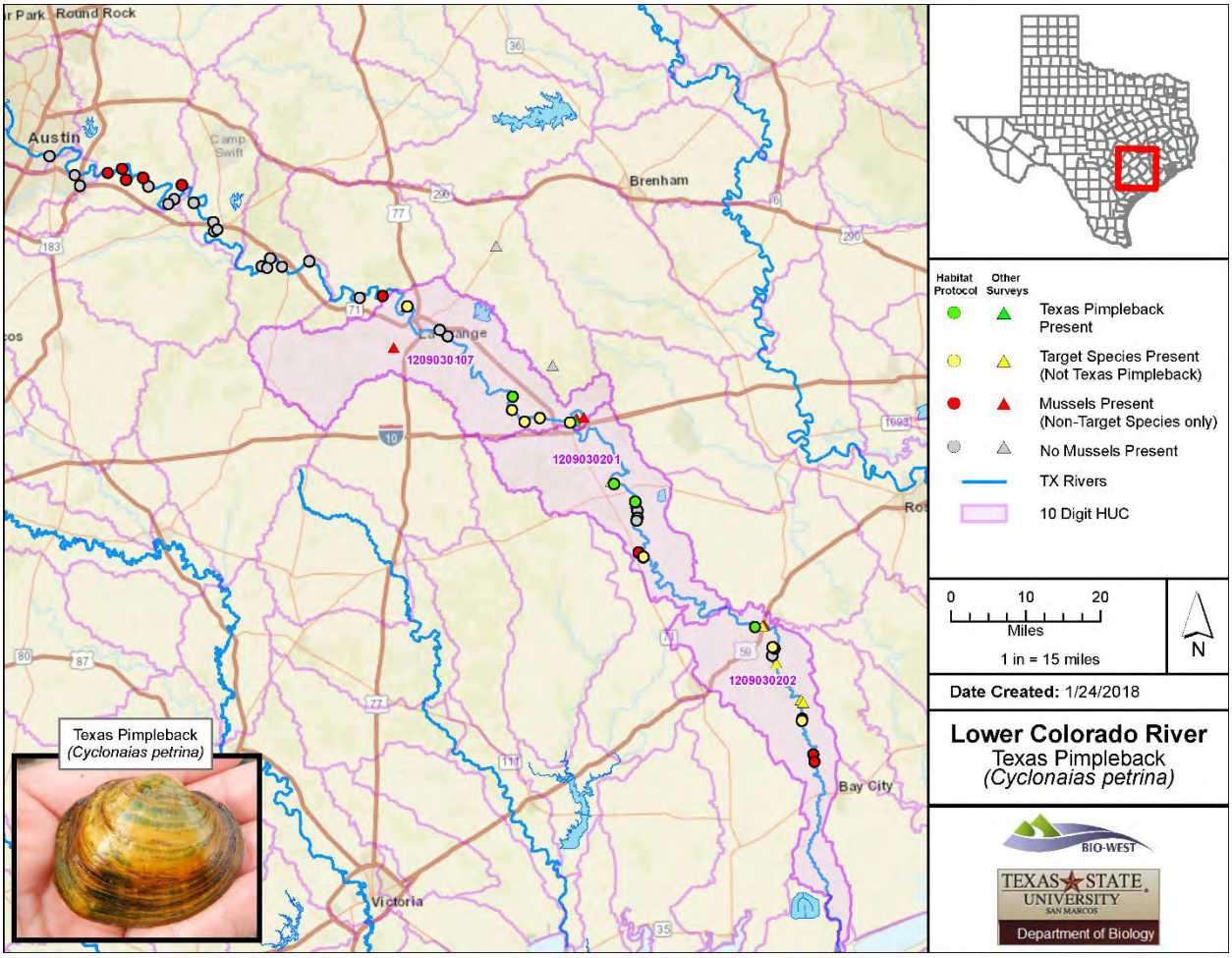

Figure 19. Map of *C. petrina* occurrence in the Lower Colorado River basin.

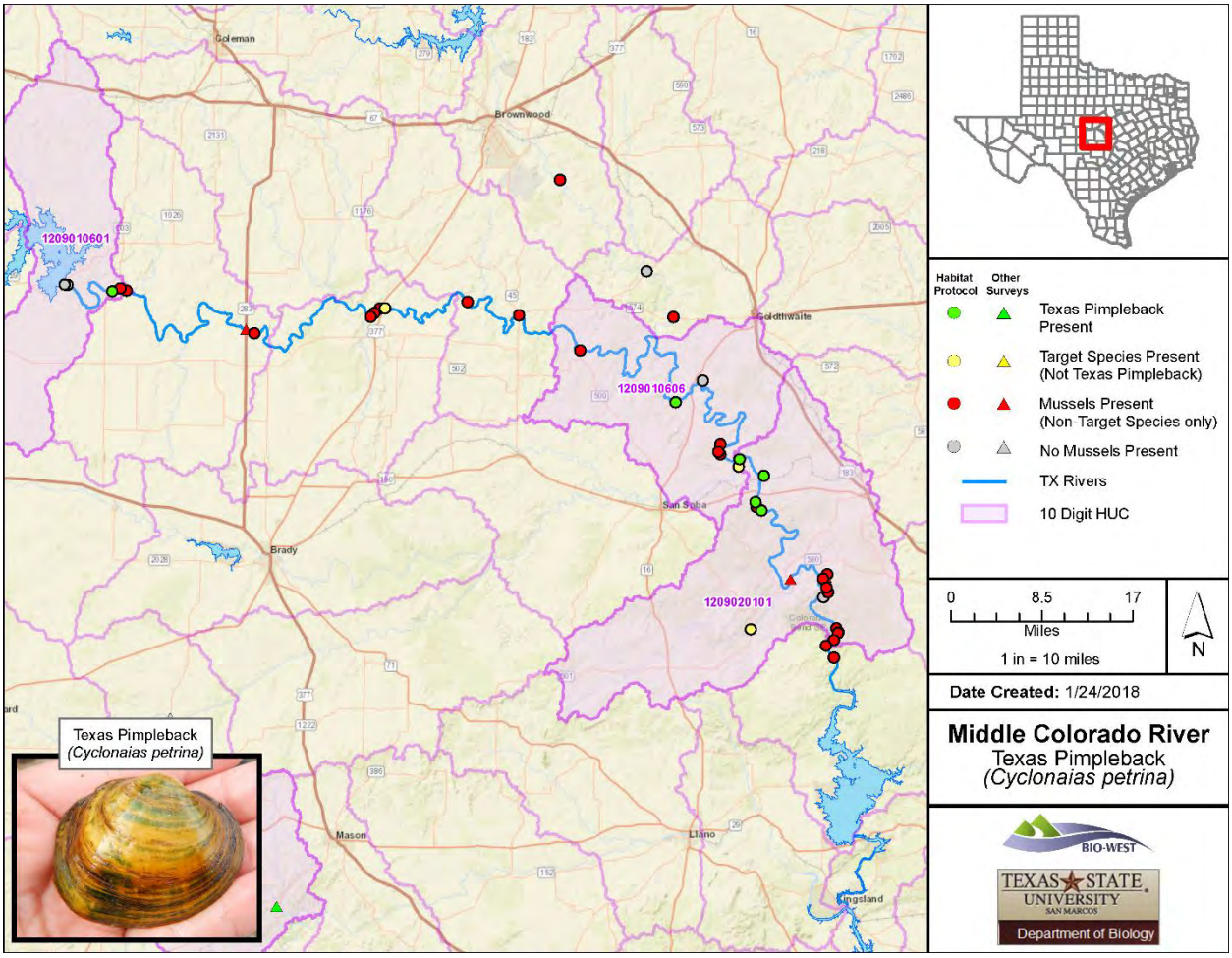

Figure 20. Map of *C. petrina* occurrence in the Middle Colorado River basin.

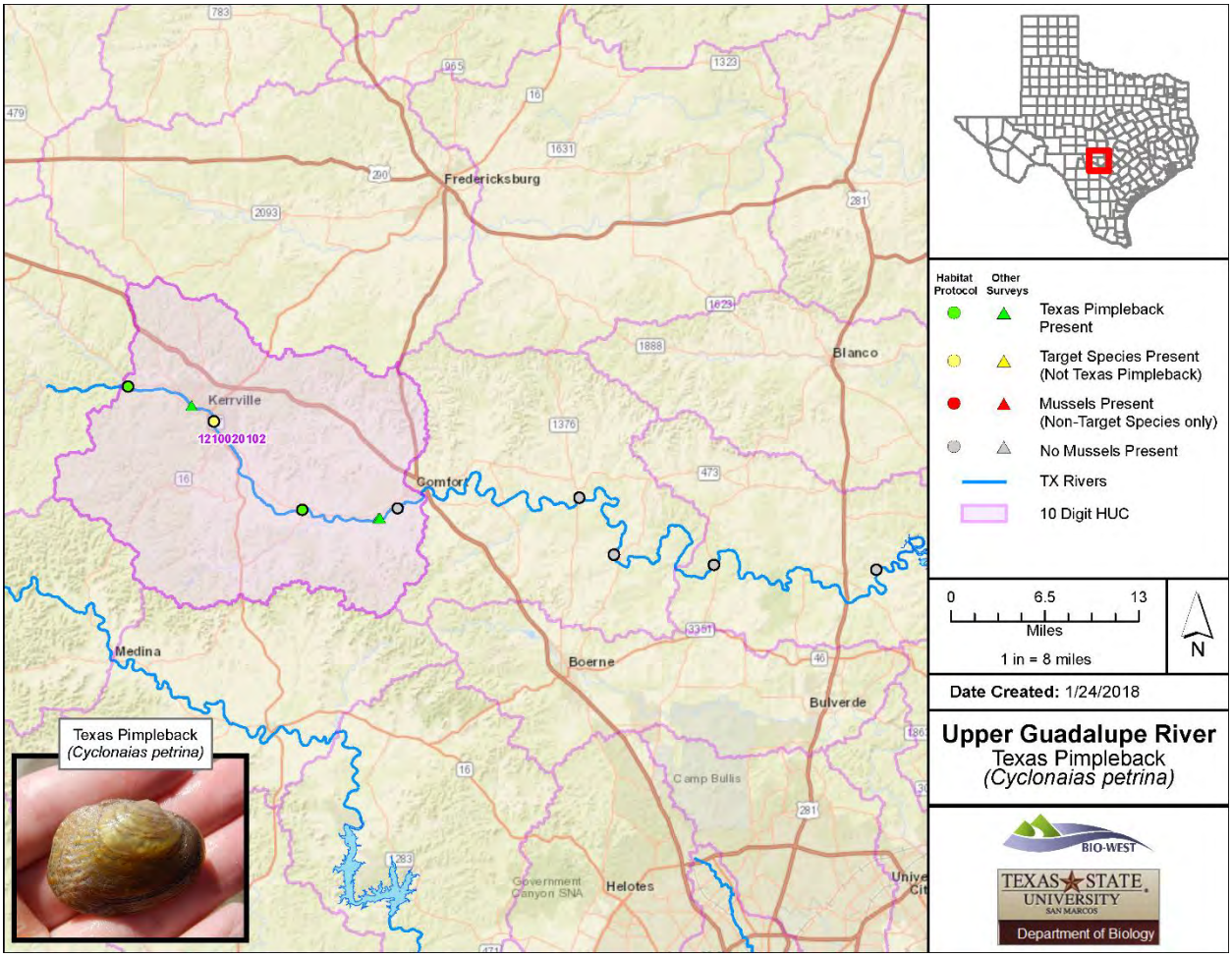

Figure 21. Map of *C. petrina* occurrence in Upper Guadalupe River basin.

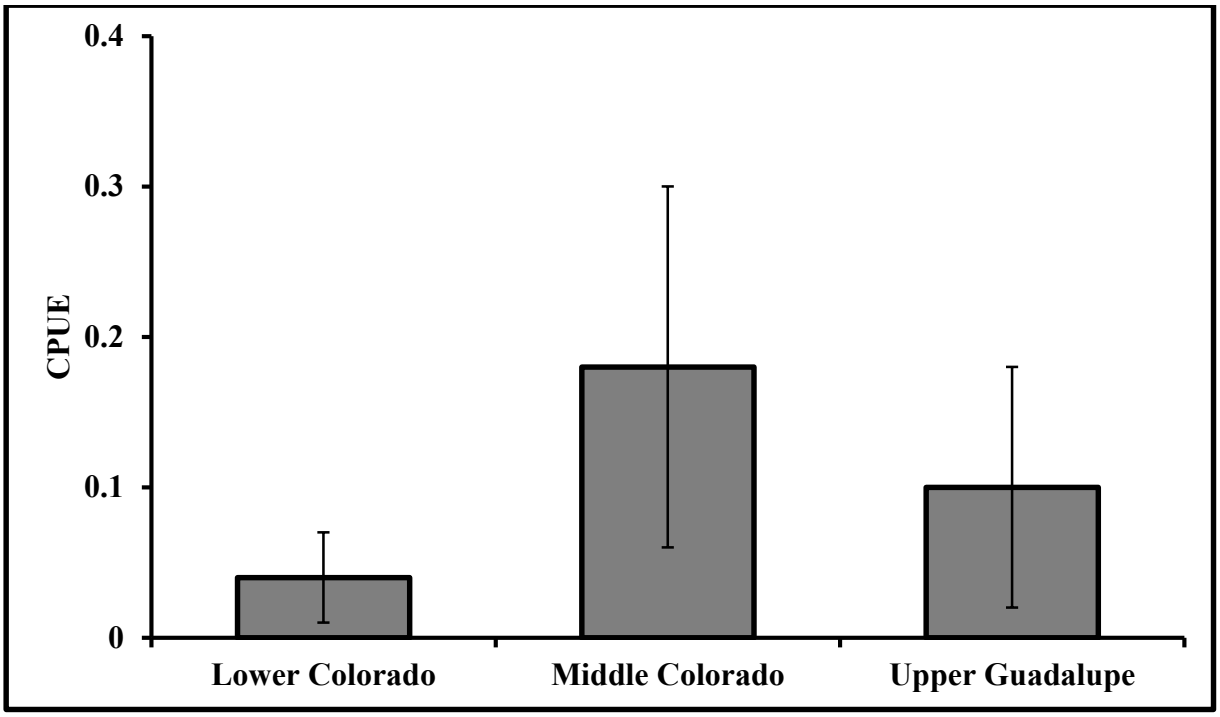

Figure 22. Catch-per-unit effort (CPUE; mussels/p-h.) of *C. petrina* among drainages.

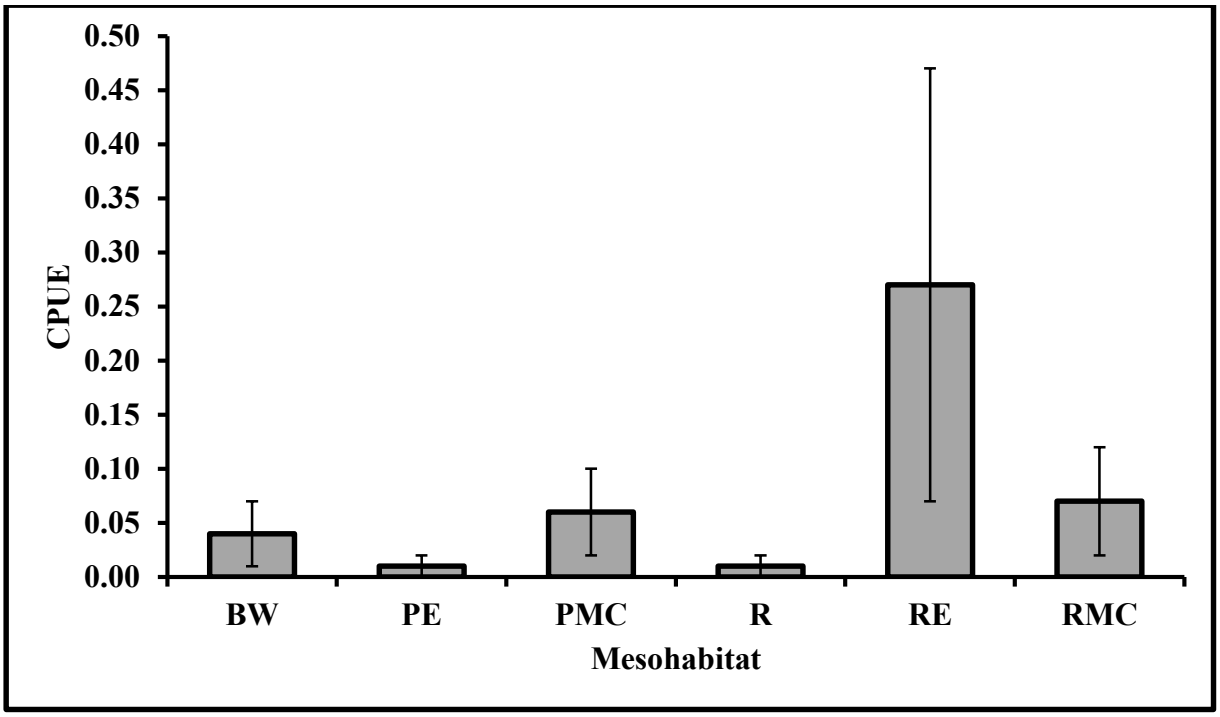

Figure 23. Catch-per-unit effort (CPUE; mussels/p-h.) of *C. petrina* by mesohabitat among all survey basins. BW = backwater, PE = pool edge, PMC = pool mid-channel, R = riffle, RE = run edge, RMC = run mid-channel

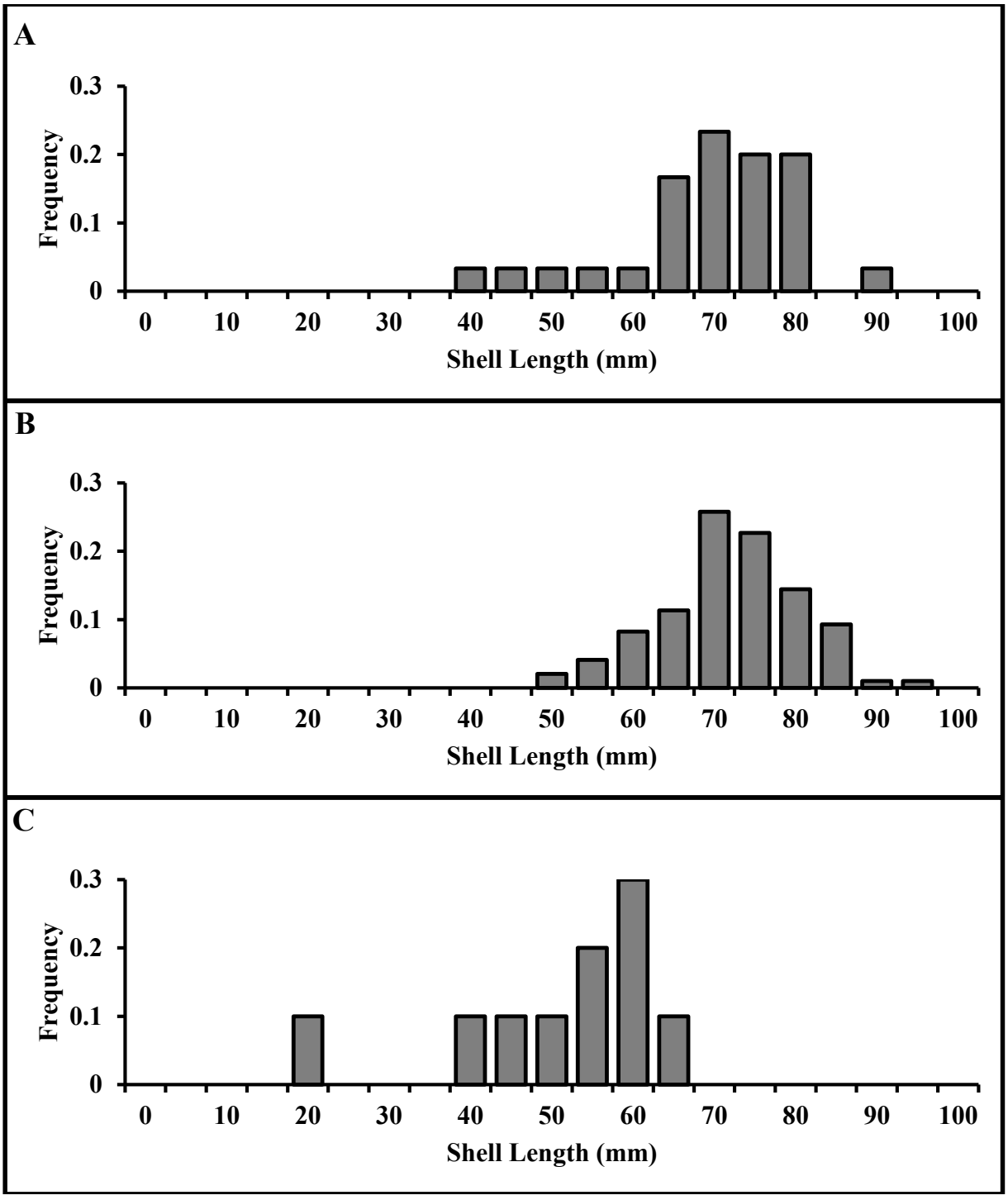

Figure 24. Proportional size structure of *C. petrina* within all basins of occurrence.
A = Lower Colorado (N = 30), B = Middle Colorado (N = 97), C = Upper Guadalupe (N = 10).

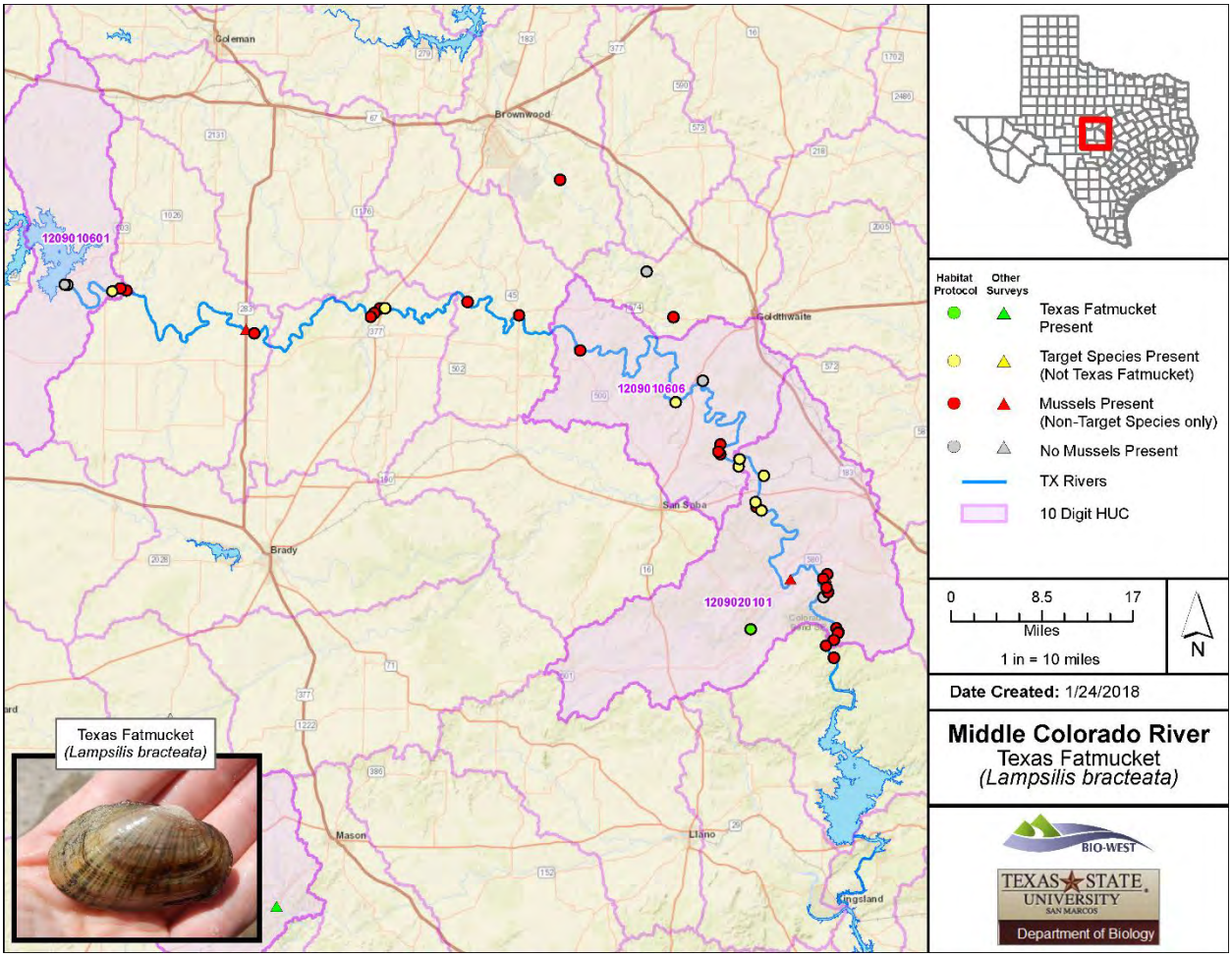

Figure 25. Map of *L. bracteata* occurrence in the Middle Colorado River basin.

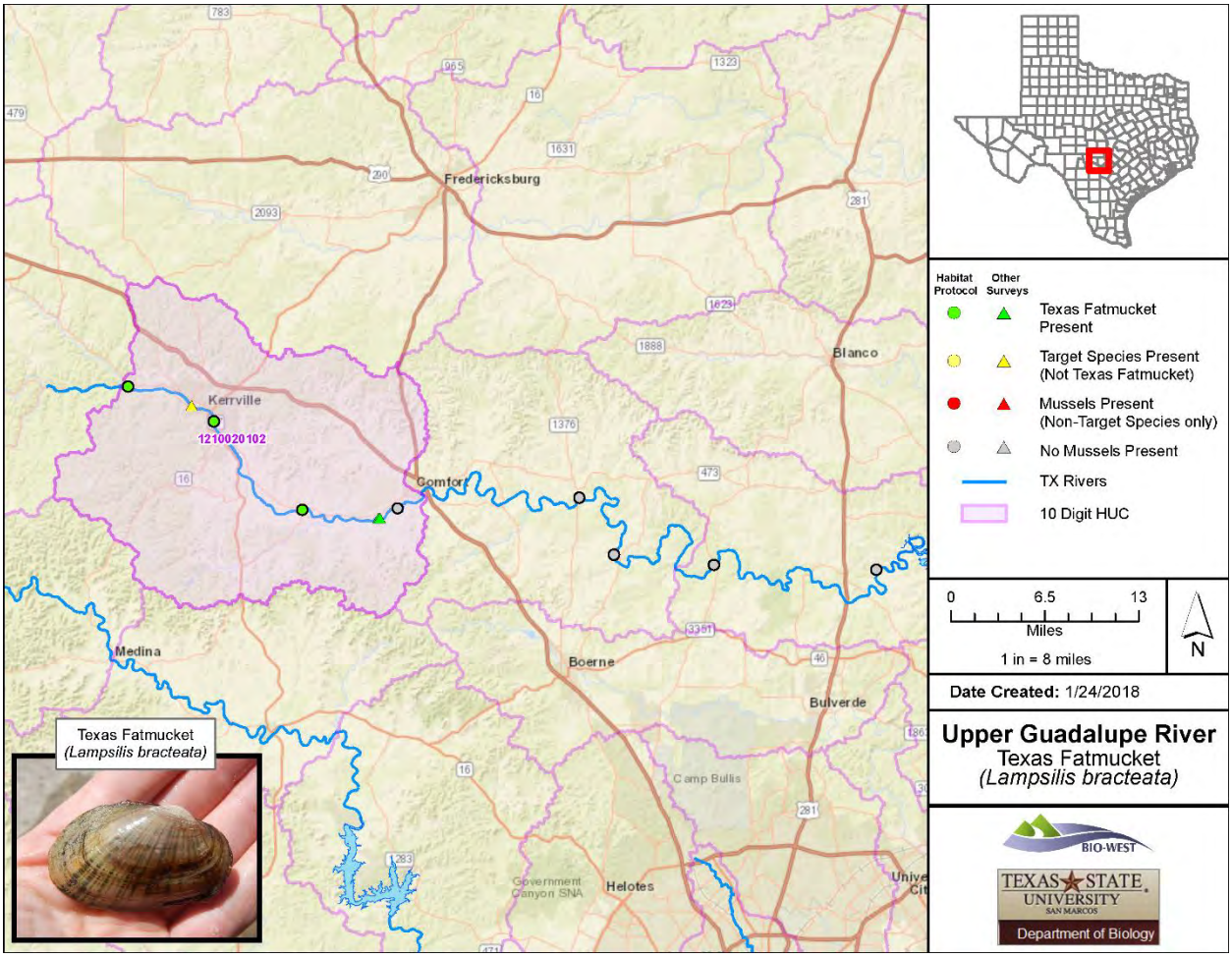

Figure 26. Map of *L. bracteata* occurrence in the Upper Guadalupe River basin.

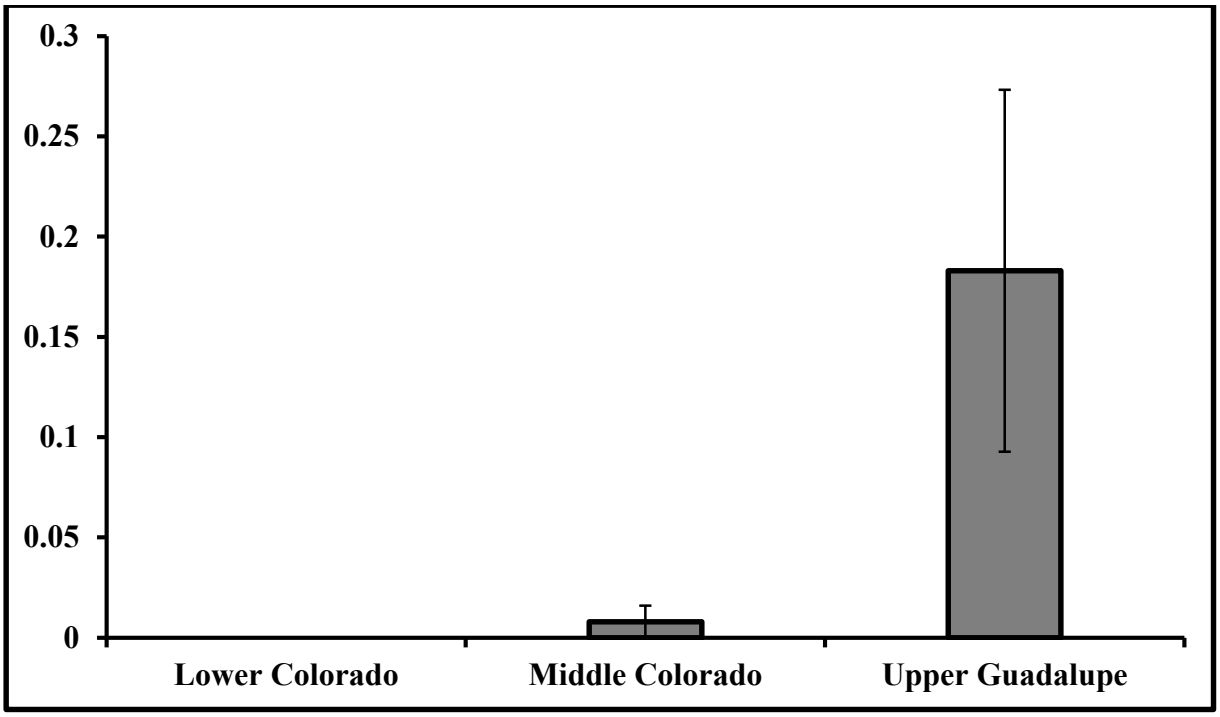

Figure 27. Catch-per-unit effort (CPUE; mussels/p-h.) of *L. bracteata* among drainages.

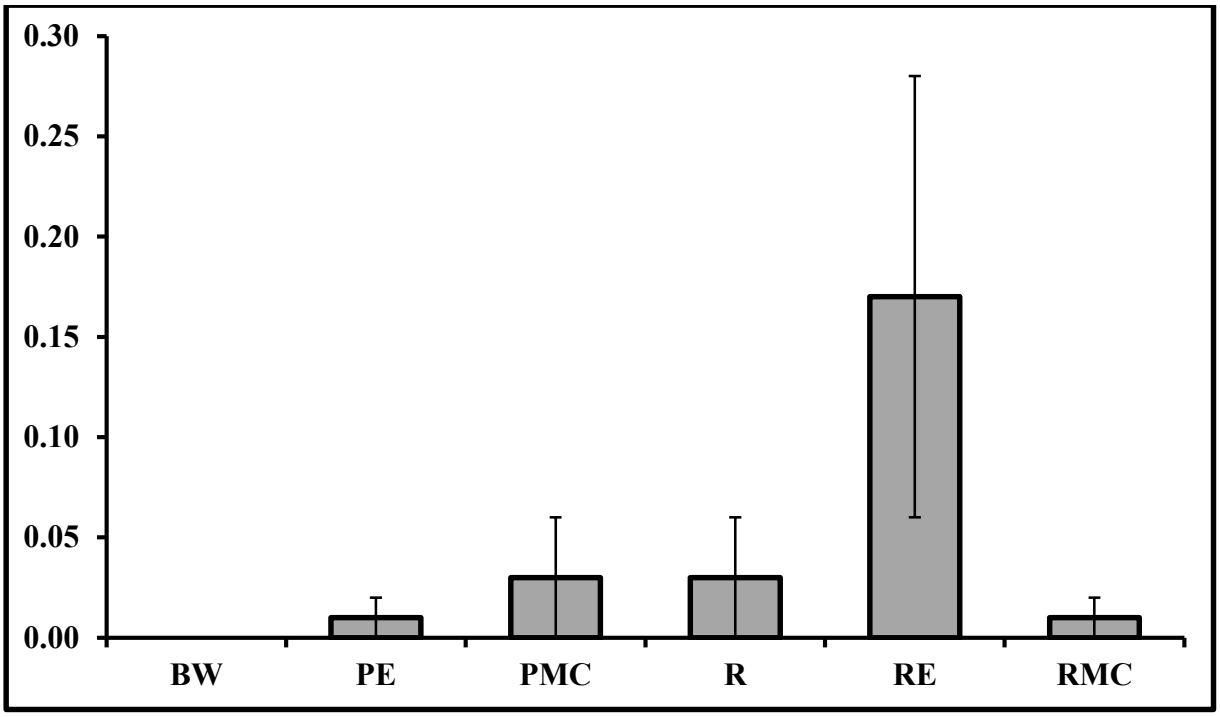

Figure 28. Catch-per-unit effort (CPUE; mussels/p-h.) of *L. bracteata* by mesohabitat among all survey basins. BW = backwater, PE = pool edge, PMC = pool mid-channel, R = riffle, RE = run edge, RMC = run mid-channel.

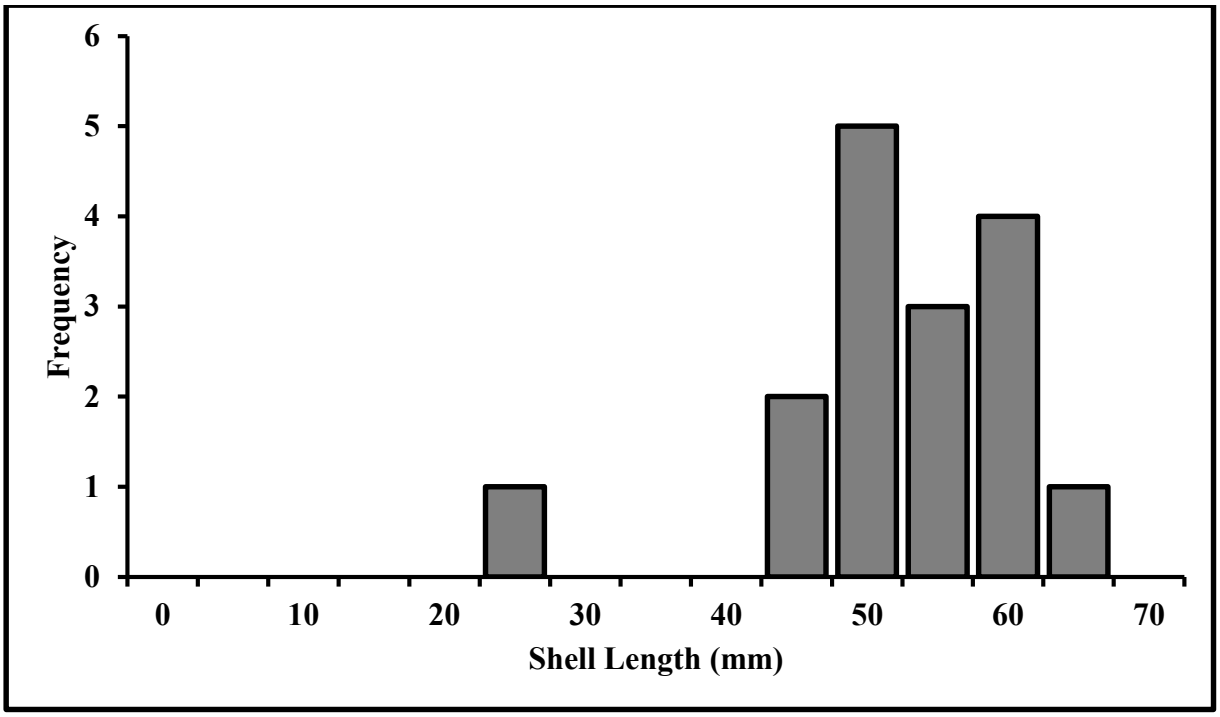

Figure 29. Size structure of *L. bracteata* within the Upper Guadalupe River.

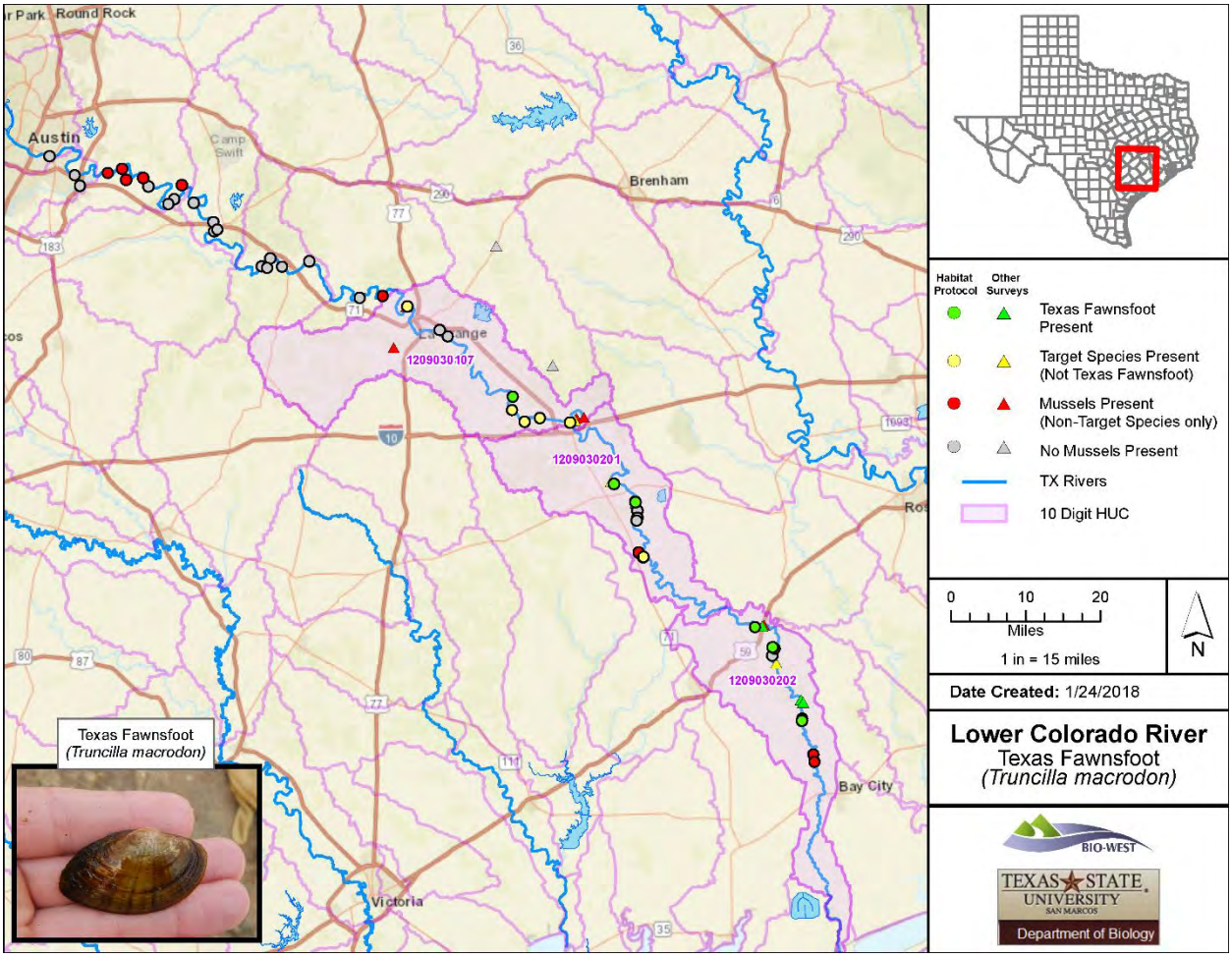

Figure 30. Map of *T. macrodon* occurrence within the Lower Colorado River basin.

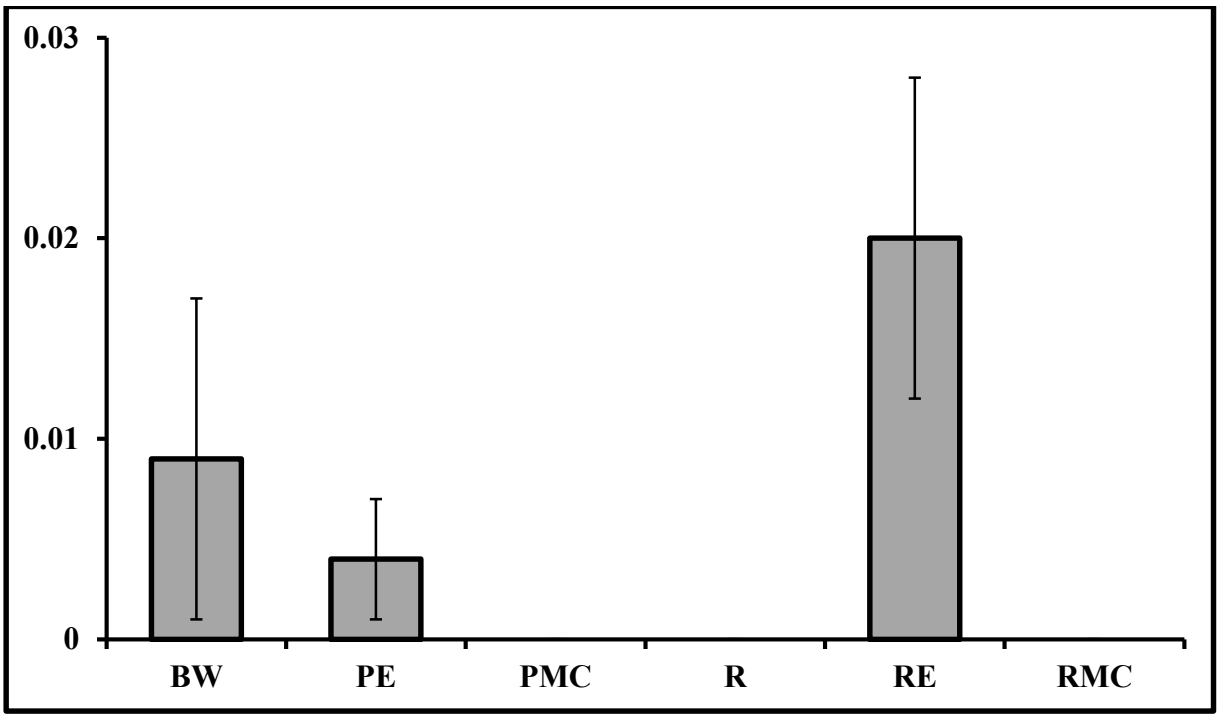

Figure 31. Catch-per-unit effort (CPUE; mussels/p-h.) of *T. macrodon* by mesohabitat among all survey basins. BW = backwater, PE = pool edge, PMC = pool mid-channel, R = riffle, RE = run edge, RMC = run mid-channel.

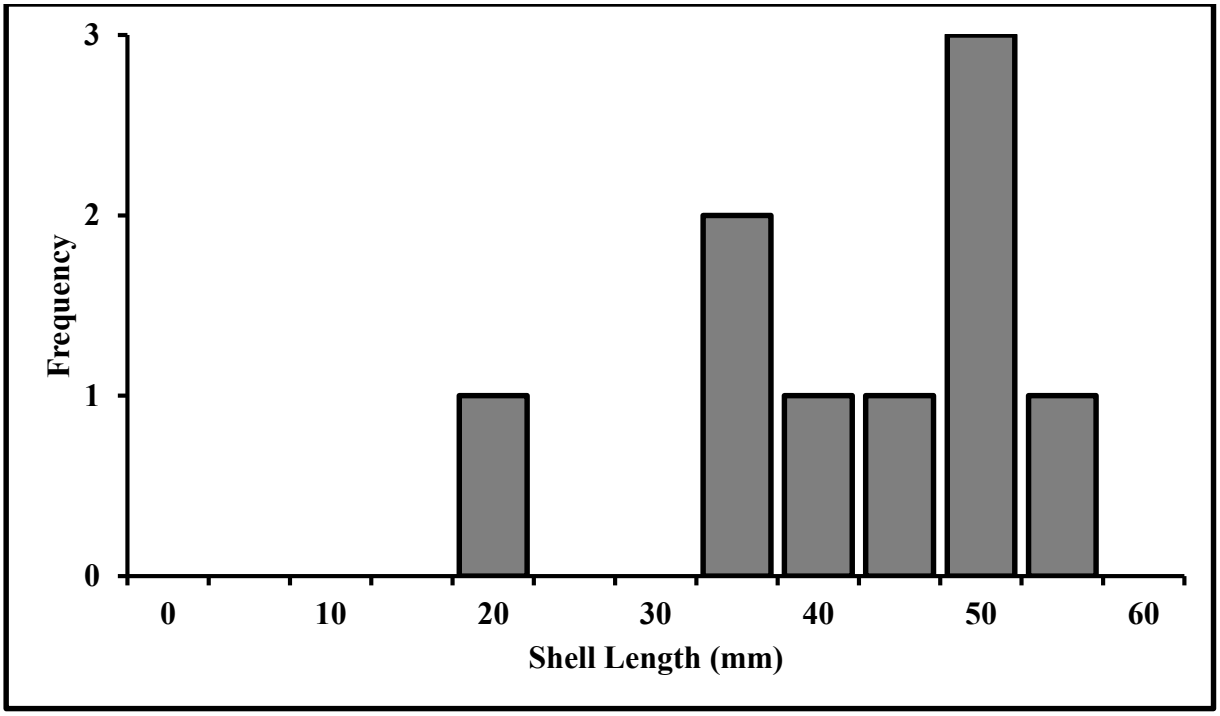

Figure 32. Size structure of *T. macrodon* within the Lower Colorado River.

Part II: Study Objectives

Objectives for Part II were to assess occurrences and abundances of mussels among habitat parameters (e.g., mesohabitat, current velocity, depth, substrates) within reaches and georegions of the Brazos River, Colorado River, and Guadalupe River basins. Univariate habitat associations were assessed only for candidate mussel species, when present, within a reach or basin.

Part II Methods

Information was taken from study areas and surveying techniques described in Part I methods. For Part II assessment, Colorado River basin was assessed by georegion instead of Middle Colorado River and Lower Colorado River. Middle Colorado River was divided among Georegion 1 (Prairie) and Georegion 3 (Llano Uplift). Lower Colorado River was divided among Georegion 4 (Balcones) and Georegion 5 (Lowland). Georegion 2 (Edwards Plateau) is described herein but was not sampled as part of this study. Georegions were developed for exploring correspondence between mussel communities and surface geology (Strayer 1983). Colorado River basin has a diverse geology from headwater reaches to terminus with Gulf of Mexico, along with diverse climate gradient that contains arid climate in the headwater reaches to a sub-humid climate near its terminus. Surface geology and climate interact to form unique georegional aquatic habitats with respect to groundwater quality and quantity, surface water quality and quantity, stream gradient, stream substrates, and stream morphology (Table 1).

Perennial flows of the Colorado River mainstem begin on the western edge of the Llano Estacado (deposits during Tertiary Period). In a general southeast direction, the perennial flowing portion of the Colorado River main stem and tributaries bisects Carboniferous, Permian,

and Triassic strata layers (Georegion 1), forming low gradient prairie streams with predominately silt substrates, although sandstones and limestones form a limited amount of rocky outcroppings and gravel to boulder substrates. Streams, common to this strata layer in nearby upper Brazos River and Red River, tend to be dominated by shallow runs, braided channels, and highly turbid, and of moderate to high salinity. The Colorado River then enters the Llano Uplift area with Precambrian and Cambrian strata (Georegion 3; Latitude: 31.090572, Longitude: -98.463806; upstream from Colorado Bend State Park, San Saba County) consisting primarily of granite but interspersed with some limestones, dolomites, and sandstones. The river and tributaries have less silt substrate and more gravel to boulder substrates and diversity in mesohabitats (e.g., run, riffle, pools), and are also characterized by their higher gradient, lower turbidity, and less saline waters. From the west, the Edwards Plateau with its Cretaceous limestone and karst aquifers (Georegion 2) contribute substantial spring flows to the Georegion 1 (via Concho River) and Georegion 3 (via San Saba River, Llano River, and Pedernales River). From the Llano Uplift, the Colorado River enters another section of the Edwards Plateau and the Balcones Escarpment (Georegion 4; Lake Travis area, Travis County) before bisecting the gulf coastal plains of Tertiary deposits (Georegion 5; Latitude: 30.200572, Longitude: -97.525748; upstream from Webberville Park, Travis County). Tertiary deposits and stream substrates of Georegion 5 are dominated by sands and silts, but various sandstone strata layers occur in the lower Colorado River main stem.

Principal component analysis (PCA; Canoco 4.5, Microcomputer Power 2002) was used to assess linear combinations of habitat parameters. Mesohabitats were coded as dummy variables and quantitative data (e.g., current velocity column, current velocity bottom, depth) were z-transformed. Parameters with diel fluctuations (e.g., water temperature) were omitted

from the analysis. The resulting PCA loadings were plotted and grouped to assess habitat variability within and among basins and georegions. Canonical correspondence analysis (CCA; Canoco 4.5) was used to assess patterns in habitat associations among Brazos River, Colorado River, and Colorado River mussel community. Initial plot was informative, but highlighted differences among basins (e.g., specific conductance, substrate types) and not mussel-habitat associations within basin. A subsequent CCA model was used to assess within basin mussel-habitat associations for the Colorado River basin. Brazos River and the Guadalupe River lacked sufficient samples to perform a CCA analyses with the same variables as used with the Colorado River basin. As such, CCA was not used on the Brazos River and Guadalupe River data. For univariate assessments, habitat observed was calculated for each habitat parameter and each candidate species using occurrence data. Habitat available was calculated for each habitat parameter by basin. A second habitat observed versus habitat available assessment was conducted on all mussels across basins using relative abundances (i.e., weighted occurrences) to compare similarities and differences in habitat variables among all mussels.

Part II Results

Qualitative surveys were conducted at 707 mesohabitats within 114 sites and among the three river drainages between March 15, 2017 and October 11, 2017. Exploratory surveys were conducted at an additional 12 sites in the Upper Colorado River (near Colorado City, Texas, one site, no mussels), tributary of the Middle Colorado River (upper reach of San Saba River, two sites, one Southern Mapleleaf), tributaries of the Lower Colorado River (Buckner's Creek, one site, one Giant Floater; Cummins Creek, two sites, no mussels), and Clear Fork Brazos River (6 sites, one Yellow Sandshell, two Fragile Papershell). The additional 12 sites were not sampled

with qualitative survey methodologies because lack of candidate mussel species observed during exploratory surveys.

Among the five basin or reach mesohabitats from qualitative surveys, principal component axis I explained 32% of the habitat variation and described a substrate and current velocity gradient (Figure 1). Principal component axis II explained 18% of the habitat variation and described primarily a substrate gradient. Central tendencies of mesohabitats within the Upper Brazos River and Little River were associated positively with PC I (i.e., greater amounts of silt, large woody debris, and detritus) and negatively associated with PC II (i.e., greater amounts of sand substrates). Central tendencies of mesohabitats within Colorado River Georegions 4 and 5 were associated negatively with PC I (i.e., greater amounts of gravel substrates, swifter water) and PC II. Upper Guadalupe River, and Colorado River Georegions 1 and 3 were positively associated with PC II (i.e., greater amounts of cobble substrates).

Within the Brazos River basin, 120 mesohabitats from 20 sites consisted of riffle, run, pool, and backwater habitats with predominately clay, silt, sand, and gravel substrates (Table 2). Habitats ranged from slack to swift waters in shallow depths and from fresh to brackish waters. Minimum water temperature was 16.6°C during surveys (Table 3). Only one mussel (Pondhorn) was taken from the Upper Brazos River (Table 4) occurring in 1.7% of total habitats sampled (Table 5). Six species, including non-native zebra mussel, and 358 individuals were taken from the Little River. Most abundant mussels were Smooth Pimpleback (37% in relative abundance) followed by Threeridge (21%) and Tampico Pearlymussel (18%). Most wide spread mussels were Tampico Pearlymussel (occurred in 25% of total habitats sampled) followed by Threeridge (18%) and Smooth Pimpleback (18%). For the one candidate species, Smooth Pimpleback occurrences were associated with slack and shallow waters and at low to moderate minimum

bottom shear stress and FST hemispheres (Figure 2). Smooth Pimpleback occurrences were in pool edges (45%), pool main channel (18%), run edge (18%), and run main channel (18%) and habitats having predominantly silt (57%), sand (21%), and gravel (13%) substrates. Smooth Pimpleback had a positive association with pool edge habitats and silt substrates.

Within the upper Guadalupe River, 60 mesohabitats from 10 sites consisted of riffle, run, pool, and backwater habitats with predominately silt, gravel, cobble, and bedrock substrates. Minimum water temperature was 17.7°C during surveys. Five species and 47 individuals were taken from the upper Guadalupe River. Most abundant mussels were Texas Fatmucket (34% in relative abundance) followed by Texas Lilliput (28%) and Texas Pimpleback (21%). Most wide spread mussels were Texas Fatmucket (occurred in 10% of total habitats sampled) followed by Texas Pimpleback (6.7%) and Texas Lilliput (6.7%). Texas Fatmucket and Texas Pimpleback occurrences were associated with flowing waters at shallower than average depths and low to moderate minimum bottom shear stress and FST hemispheres (Figures 3, 4, 5). Texas Fatmucket occurrences were in run edges (50%), riffles (17%), run main channel (17%), and pool edges (17%) and habitats having predominately gravel (31%) and bedrock (29%) substrates. Texas Fatmucket had a positive association with run edge habitats and bedrock substrates (Figure 6). Texas Pimpleback occurrences were in run edges (50%), riffle (25%), and pool edges (25%) and habitats having predominately bedrock (35%), gravel (25%), and cobble (13%) substrates. Texas Pimpleback had a positive association with run edge habitats and bedrock substrates.

Within the Colorado River basin, 527 mesohabitats from 84 sites consisted of riffle, run, pool, and backwater habitats with predominately silt, sand, gravel, cobble, boulder, and bedrock substrates (Table 6). Minimum water temperature was 22.3°C during surveys (Table 7). Sixteen species and 2,819 individuals were taken from the Colorado River (Table 8) with mussels

occurring in 25 to 87% of the habitats sampled by georegion (Table 9). Habitats explained 31% ($P < 0.01$) of the mussel community variation (Figure 7). Physical parameters and mesohabitats with strong loadings were specific conductance (bi-plot score: 0.80), pool channel (0.39), gravel (0.38), bottom current velocity (-0.36), run edge (-0.44), and sand (-0.50) on CCA axis I and gravel (0.61), cobble (0.53), minimum bottom shear stress (0.50), pool edge (-0.44), and silt (-0.65) on CCA axis II. Among candidate mussels associated with CCA I and II, Smooth Pimpleback (N = 400) was associated with lower specific conductance and run habitats with sandy substrates and swifter current velocities. Texas Pimpleback (N = 127) was associated with run habitats, swifter current velocities, and gravel and cobble substrates. Texas Fawnsfoot (N = 9) was associated with run edges with clay, silt, and sandy substrates.

Abundances and occurrences of mussels differed among georegions. Georegion 1 consisted of 10 species with Fragile Papershell (24% in relative abundance), Southern Mapleleaf (22%), and Tampico Pearlymussel (16%) being most abundant and Southern Mapleleaf (9.8% occurrence among habitats sampled), Yellow Sandshell (9.0%), Bleufer (6.8%), and Paper Pondshell (6.8%) being most widespread. Relative abundances of candidate mussels were 2.4% for Texas Pimpleback (ranked 8th most abundant) and 1.2% for Smooth Pimpleback (ranked 9th). Both were taken in 1.5% of total habitats sampled. Georegion 3 consisted of 11 species with Texas Pimpleback (37% in relative abundance), Pistolgrip (21%), and Southern Mapleleaf (6.5%) being most abundant and Texas Pimpleback (7.1% occurrence among habitats sampled), Tampico Pearlymussel (6.2%), and Southern Mapleleaf (6.2%) being most widespread. Relative abundances of other candidate mussels were 2.7% for Smooth Pimpleback (ranked 6th) and 0.9% for Texas Fatmucket (ranked 11th). Georegion 4 consisted of seven species with Yellow Sandshell (33% in relative abundance), Giant Floater (33%), and Paper Pondshell (15%) being

most abundant and Tampico Pearlymussel (5.6% occurrence among habitats sampled) and Yellow Sandshell (5.6%) being more widespread. Candidate mussels were not taken from Georegion 4. Georegion 5 consisted of 14 species with Threeridge (58% in relative abundance), Smooth Pimpleback (17%), and Yellow Sandshell (17%) being most abundant and Threeridge (18% occurrence among habitats sampled), Yellow Sandshell (18%), and Smooth Pimpleback (15%) being most widespread. Relative abundances of candidate mussels were 1.3% for Texas Pimpleback (ranked 7th) and 0.4% for Texas Fawnsfoot (ranked 9th).

Univariate associations were assessed for candidate mussels across Colorado River basin georegions. Smooth Pimpleback, Texas Pimpleback, and Texas Fawnsfoot were taken from column and bottom current velocities at about the same current velocities available (Figure 8). Smooth Pimpleback, Texas Pimpleback, and Texas Fawnsfoot occurred proportionally less at shallowest depths (<0.5 m) than available and occurred at the lower range of substrate compaction (Figure 9). Smooth Pimpleback and Texas Pimpleback generally occurred in proportion to available minimum bottom shear stress and FST hemispheres, although low occurrence were observed at the greater ends of minimum bottom shear stress (>5 dyn/cm^2) and FST hemispheres (>10) (Figure 10). Smooth Pimpleback occurrences were in run edges (37%), pool edges (22%), pool main channel (17%), run main channel (15%), backwater (7.3%), and riffle (2.4%) mesohabitats. Smooth Pimpleback occurred more in run edge mesohabitats than expected (Figure 11), although the largest number of individuals taken (N = 104) was from a run main channel mesohabitat. Texas Pimpleback occurrences were in pool main channel (31%), run main channel (23%), run edge (18%), pool edge (14%), backwater (9.0%), and riffle (4.5%) mesohabitats. Texas Pimpleback occurred more in pool main channel, run main channel, and run edge than expected, with the largest number of individuals taken (N = 54) from a run edge

mesohabitat. Texas Fawnsfoot occurrences were in run edges (63%), pool edge (25%), and backwater (13%) mesohabitats, occurring in more run edge habitats than expected. Dominant substrates (mean percent composition) of habitats were sand (33%), silt (24%), and boulder (12%) boulder for Smooth Pimpleback, gravel (21%), cobble (17%), and boulder (16%) for Texas Pimpleback, and silt (34%), sand (32%), clay (16%), and boulder (9%) for Texas Fawnsfoot. Generally, Smooth Pimpleback occurred in habitats with more sand and boulder than expected, Texas Pimpleback occurred in more boulder and less silt than expected, and Texas Fawnsfoot occurred in more clay, silt, sand, and boulder and in less gravel and cobble than expected.

Univariate estimates across regions and basins

Summaries of habitat parameters across regions and basins are provided for Smooth Pimpleback (Table 10), Texas Pimpleback (Table 11), Texas Fatmucket (Table 12), and Texas Fawnsfoot (Table 13). In addition, weighted mean (i.e., using relative abundances) habitat summaries were calculated for other species within mussel community across regions and basin. Texas Fatmucket, Pistolgrip, and Texas Pimpleback had the swiftest mean current velocities (column and bottom), whereas Tampico Pearlymussel, Bleufer, and Giant Floater had the lowest mean current velocities (Figure 12). Smooth Pimpleback, Threeridge, and Tampico Pearlymussel had the deepest mean depths, whereas Texas Fatmucket, Texas Pimpleback, and Pistolgrip had the shallowest mean depths (Figure 13). Fragile Papershell, Pistolgrip, Paper Pondshell, Bleufer, and Giant Floater had the greater substrate compaction variability, whereas the remaining species had lesser substrate compaction variability. Relative abundances of mussels ranged from absent to abundant among all mesohabitats (Table 14). Most species (S =

15) were taken pool-edge mesohabitats (S=15), ranging in relative abundance scale (Stiers et al. 2011) from occasional to abundant, and fewest species (S=10) were taken from run-channel, ranging in relative abundant scale from rare to frequent. Majority of species (75%) were taken from habitats consisting of all substrate types (Table 15). Mean percent silt was occasional to common for all (S = 16) species. Mean percent sand, gravel, and cobble were rare to frequent for all species. Mean percent boulder and bedrock were rare to frequent for 15 species. Mean percent clay was rare to occasional for 14 species. Mean percent detritus was rare to occasional for 13 species.

Georegion 5 Pre-hurricane community compared to post hurricane community

In August 2017, Hurricane Harvey caused widespread flooding and high flows (>140,000 cfs) in the lower Colorado River. Previous to high flows, 179 mesohabitats were sampled in Georegion 5 (Figure 14). Pre-hurricane community consisted 14 species with Threeridge (59% in relative abundance), Yellow Sandshell (17%), and Smooth Pimpleback (16%) being most abundant. After high flows subsided, 66 mesohabitats were sampled in Georegion 5. Post hurricane community consisted of 11 species with Threeridge (53%), Smooth Pimpleback (21%), and Yellow Sandshell (17%) being most abundant. Changes in relative abundances between pre- and post-hurricane ranged from -5.9% for Threeridge to 4.7% for Smooth Pimpleback.

Part II. Tables

Table 1. Surface geology, groundwater sources, stream gradient, and water quality and quantity estimates among georegions of the Colorado River basin.

	Georegions				
	1	2	3	4	5
Descriptive name	Prairie	Edwards Plateau	Llano Uplift	Balcones	Lowland
Period[1]	Carboniferous, Permian, Triassic	Cretaceous	Pre-Cambrian, Cambrian	Cretaceous	Tertiary
Surface strata[1]	clay, sand, shale, sandstone, siltstone, mudstone, limestone, dolomite, gypsum, colluvium	limestone, colluvium, dolomite, chalk, marl, mudstone	Granite, gneiss, schist, limestone, colluvium, dolomite	limestone, chalk, marl, dolomite, mudstone, clay, alluvial shale	clay, silt, sand, sandstone
Ecoregions[2]	Southwest Tablelands, Central Great Plains, Cross Timbers	Semiarid Edwards Plateau, Edwards Plateau Woodland	Llano Uplift, Edwards Plateau Woodland	Balcones Canyonlands, Texas Blackland Prairie	Texas Blackland Prairie, Central Texas Plains, Western Gulf Coast Plains
Aquifer type[3]	alluvium	karst	karst	karst	alluvium
Aquifers[3]	Ogallala, Dockum, Lipan	Edwards-Trinity	Marble Falls, Ellenburger-San Saba	Edwards-Trinity	Carrizo-Wilcox, Gulf Coast
Groundwater type[3]	fresh to saline	fresh, some brackish	fresh, some brackish	fresh	fresh
Dominant substrates	sand and silt	gravel to bedrock	silt to boulder	silt to gravel in mainstem, limestone in tributaries	silt and sand with some boulders and bedrock
Mean stream gradient (m/km)	0.56	1.70	1.60	1.00	0.27

Table 1. Continued

	Georegions				
	1	2	3	4	5
Descriptive name	Prairie	Edwards Plateau	Llano Uplift	Balcones	Lowland
Water quantity[4]:					
N of stations	9	8	3	5	4
Average flow (cfs)	103	59	274	366	2,297
Coefficient of variation	5.6	7.5	5.5	4.6	2.1
% zero flow days	4.7	15.9	1.4	19.9	0.0
% of stations with zero flow days	56	44	33	20	0
Base flow index	0.08	0.23	0.16	0.04	0.23
Water quality[5]:					
Mean dissolved oxygen (mg/l)	9.0	7.9	8.3	8.7	8.5
1 SD	3.55	1.98	2.33	2.27	1.90
Median pH	8.0	8.0	8.2	8.0	8.1
range of pH	3.89	2.40	3.25	2.78	2.90
Mean specific conductance (µS/cm)	4,030	741	653	556	588
1 SD	4,369.8	390.8	348.9	111.4	199.7
Mean water temperature (°C)	19.5	19.9	20.3	21.1	21.9
1 SD	7.95	6.78	6.90	6.33	6.68
Mean turbidity (NTU)	55.5	19.4	22.1	10.9	50.5
1 SD	49.00	75.43	28.71	22.15	73.55

[1] Source: USGS Texas Geology https://txpub.usgs.gov/dss/texasgeology/
[2] Source: Griffith et al. 2007. Ecoregions of Texas.
[3] Source: Texas Aquifers; https://www.twdb.texas.gov/groundwater/aquifer/
[4] Source: USGS Stations-Colorado River basin; https://waterdata.usgs.gov/tx/nwis/current/?type=flow
[5] Source: LCRA Water Quality Data; waterquality.lcra.org; period of record: 1980 – 2016.

Table 2. Total number, percent, and physical characterizations of habitats sampled in the Brazos River and Guadalupe River basins from March through October 2017.

	Brazos River				Guadalupe River	
	Upper		Little River		Upper	
N of habitats	60		60		60	
Habitat types (%)						
Riffle	5		17		17	
Run-channel	16		23		15	
Run-edge	21		13		17	
Pool-channel	18		12		17	
Pool-edge	34		32		22	
Backwater	5		3		13	
	Mean	1 SD	Mean	1 SD	Mean	1 SD
Depth (m)	0.94	0.59	0.76	0.52	0.83	0.55
Current velocity column (m/s)	0.14	0.19	0.25	0.32	0.32	0.36
Current velocity bottom (m/s)	0.07	0.14	0.12	0.17	0.13	0.17
Penetrometer (kg/cm^2)	0.24	0.22	0.27	0.98	0.43	1.12
FST hemispheres	1.67	2.26	3.37	4.54	4.68	5.26
Minimum bottom shear stress (dyn/cm^2)	1.14	0.91	3.29	6.64	6.57	15.04
Specific conductance (uS/cm)	2,747	1,461	631	143	479	56
Substrate (%)						
Clay	15	21	14	28	1	5
Silt	24	32	32	37	22	23
Sand	34	33	25	23	7	12
Gravel	15	20	23	26	24	20
Cobble	6	15	5	11	22	24
Boulder	4	15	0.3	1	4	9
Bedrock	2	7			18	25
Detritus	1	3	1	3	1	3
Large woody debris (%)	5	12	8	15	3	9
Undercut bank (%)	0.2	1	5	15	3	11
Root wad (%)	0.2	1			11	23

Table 2 continued

	Brazos River		Guadalupe River	
	Upper	Little River	Upper	
Vegetation (%)	0	0	4	14
Chara				
Ceratophyllum			0.2	1
Filamentous Algae			2	10
Hydrilla				
Justicia			1	2
Nuphar			0.2	1
Potamogeton			1	6
Heteranthera				

Table 3. Water quality parameters (mean for temperature, dissolved oxygen, and turbidity, median for pH) for mesohabitats sampled in the Brazos River and Guadalupe River basins from March through October 2017.

		Temperature (°C)	Dissolved oxygen (mg/L)	pH	Turbidity (NTU)
Brazos River	Central tendency	29.7	8.6	8.2	44.7
Upper	1 SD	1.63	1.96		25.54
	Minimum	25.8	4.8	7.2	3.8
	Maximum	32.2	13.4	9.6	110.4
Little River	Central tendency	29.0	9.2	8.1	54.7
	1 SD	5.21	1.90		49.83
	Minimum	16.6	2.2	7.5	24.7
	Maximum	32.8	12.3	9.4	200.2
Guadalupe River	Central tendency	23.0	8.5	8.3	
Upper	1 SD	4.06	0.91		
	Minimum	17.7	5.0	7.2	
	Maximum	30.2	10.1	11.0	

Table 4. Mussel species and relative abundances (% of total N) taken from the Brazos River and Guadalupe River basins from March through October 2017.

		Abundance (%)		
		Brazos River		Guadalupe River
Scientific Name	Common Name	Upper	Little River	Upper
Amblema plicata	Threeridge		21	
Cyclonaias houstonensis	Smooth Pimpleback		37	
Cyclonaias petrina	Texas Pimpleback			21
Cyrtonaias tampicoensis	Tampico Pearlymussel		18	
Dreissena polymorpha	Zebra Mussel		11	
Lampsilis bracteata	Texas Fatmucket			34
Lampsilis teres	Yellow Sandshell		11	
Leptodea fragilis	Fragile Papershell		1.7	
Toxolasma parvum	Lilliput			2.1
Toxolasma texasiense	Texas Lilliput			28
Uniomerus tetralasmus	Pondhorn	100		15
	Total N	1	358	47

Table 5. Mussel species and occurrences (% of total habitats sampled) taken from the Brazos River and Guadalupe River basins from March through October 2017.

		Occurrence (%)		
		Brazos River		Guadalupe River
Scientific Name	Common Name	Upper	Little River	Upper
Amblema plicata	Threeridge		18	
Cyclonaias houstonensis	Smooth Pimpleback		18	
Cyclonaias petrina	Texas Pimpleback			6.7
Cyrtonaias tampicoensis	Tampico Pearlymussel		25	
Dreissena polymorpha	Zebra Mussel		6.7	
Lampsilis bracteata	Texas Fatmucket			10
Lampsilis teres	Yellow Sandshell		12	
Leptodea fragilis	Fragile Papershell		5.0	
Toxolasma parvum	Lilliput			1.7
Toxolasma texasiense	Texas Lilliput			6.7
Uniomerus tetralasmus	Pondhorn	1.7		3.3
	Total N of habitats	60	60	60
	Total % of habitats	1.7	78	28

Table 6. Total number, percent, and physical characterizations of habitats sampled within georegions of the Colorado River basin March through October 2017.

	Colorado River							
	Georegion 1		Georegion 3		Georegion 4		Georegion 5	
N of habitats	132		114		36		245	
Habitat types (%)								
Riffle	11		15		19		11	
Run-channel	12		12		28		20	
Run-edge	6		12		19		22	
Pool-channel	25		26		6		15	
Pool-edge	37		27		22		22	
Backwater	10		8		6		11	
	Mean	1 SD	Mean	1 SD	Mean	1 SD	Mean	1 SD
Depth (m)	0.47	0.30	0.48	0.37	0.47	0.25	0.64	0.46
Current velocity column (m/s)	0.10	0.18	0.14	0.25	0.33	0.32	0.23	0.27
Current velocity bottom (m/s)	0.04	0.08	0.07	0.12	0.19	0.21	0.12	0.15
Penetrometer (kg/cm^2)	0.36	1.07	0.63	1.42	0.14	0.15	0.12	0.33
FST hemispheres	1.54	2.62	1.98	3.22	4.25	4.05	2.86	3.33
Minimum bottom shear stress (dyn/cm^2)	1.24	1.47	1.62	2.64	2.65	2.68	1.82	2.77
Specific conductance (uS/cm)	992	365	600	101	561	64	597	45
Substrate (%)								
Clay	3	10	7	17	3	12	5	15
Silt	26	28	23	27	16	30	21	28
Sand	9	15	6	11	30	23	38	30
Gravel	23	24	16	20	37	28	19	22
Cobble	26	25	23	27	14	25	9	18
Boulder	7	20	5	14			3	14
Bedrock	3	14	15	28			3	12
Detritus	3	9	5	13			1	5
Large woody debris (%)	3	10	4	11	1	2	3	7
Undercut bank (%)	1	5	1	4			1	5
Root wad (%)	<0.1	0.1	<0.1	0.2			0.4	2

Table 6 continued

	Georegion 1		Georegion 3		Georegion 4		Georegion 5	
Vegetation (%)	5	19	1	5	3	9	1	4
Chara	2	12						
Ceratophyllum								
Filamentous Algae	2	11	0.5	5				3
Hydrilla						1	0.1	1
Justicia								
Nuphar								
Potamogeton								
Heteranthera	1	10			3	9	0.4	3

Table 7. Water quality parameters (mean for temperature, dissolved oxygen, and turbidity, median for pH) for mesohabitats sampled within georegions of the Colorado River basin March through October 2017.

		Temperature (°C)	Dissolved oxygen (mg/L)	pH	Turbidity (NTU)
Georegion 1	Central tendency	28.7	8.0	8.3	96.2
	1 SD	2.52	2.01		51.67
	Minimum	24.3	3.6	7.2	19.5
	Maximum	34.5	14.1	10.9	152.2
Georegion 3	Central tendency	28.0	8.5	8.3	76.4
	1 SD	2.52	1.57		44.56
	Minimum	22.3	5.4	6.9	20.6
	Maximum	32.5	12.8	10.2	152.2
Georegion 4	Central tendency	26.9	8.8	7.8	11.7*
	1 SD	2.65	11.04		25.78
	Minimum	23.4	5.2	7.6	0.49
	Maximum	34.4	73.1	7.9	339
Georegion 5	Central tendency	28.8	9.0	8.1	33.9
	1 SD	2.75	3.14		40.60
	Minimum	22.7	5.7	6.9	1.3
	Maximum	35.1	41.0	11.4	309.3

*Estimates obtained from waterquality.lcra.org, Site 12474 and Site 12466 (downstream of Lady Bird Lake to Webberville; period of record: 1998 – 2016).

Table 8. Mussel species and relative abundances (% of total N) taken from georegions within the Colorado River basin from March through October 2017.

		Abundance (%)			
Scientific Name	Common Name	Georegion 1	Georegion 3	Georegion 4	Georegion 5
Amblema plicata	Threeridge		2.0		58
Cyclonaias houstonensis	Smooth Pimpleback	1.2	4.0		17
Cyclonaias petrina	Texas Pimpleback	2.4	37		1.3
Cyrtonaias tampicoensis	Tampico Pearlymussel	16	4.5	7.4	1.5
Lampsilis bracteata	Texas Fatmucket		0.8		
Lampsilis teres	Yellow Sandshell	11		33	17
Leptodea fragilis	Fragile Papershell	24	15	3.7	2.7
Potamilus purpuratus	Bleufer	4.5	3.6		0.7
Pyganodon grandis	Giant Floater	11	2.8	33	0.3
Quadrula apiculata	Southern Mapleleaf	22	6.5	3.7	0.2
Toxolasma parvum	Lilliput			3.7	0.1
Toxolasma texasiense	Texas Lilliput				1.5
Tritogonia verrucosa	Pistolgrip	0.8	21		
Truncilla macrodon	Texas Fawnsfoot				0.4
Uniomerus tetralasmus	Pondhorn				0.04
Utterbackia imbecillis	Paper Pondshell	7.8	2.8	15	0.1
	Total N	245	247	27	2,300

Table 9. Mussel species and occurrences (% of total habitats sampled) taken from georegions within the Colorado River basin from March through October 2017.

		Occurrence (%)			
Scientific Name	Common Name	Georegion 1	Georegion 3	Georegion 4	Georegion 5
Amblema plicata	Threeridge		1.8		18
Cyclonaias houstonensis	Smooth Pimpleback	1.5	2.7		15
Cyclonaias petrina	Texas Pimpleback	1.5	7.1		4.9
Cyrtonaias tampicoensis	Tampico Pearlymussel	6.0	6.2	5.6	4.9
Lampsilis bracteata	Texas Fatmucket		0.9		
Lampsilis teres	Yellow Sandshell	9.0		5.6	18
Leptodea fragilis	Fragile Papershell	13	21	2.8	11
Potamilus purpuratus	Bleufer	6.8	4.4		2.4
Pyganodon grandis	Giant Floater	12	4.4	2.8	1.6
Quadrula apiculata	Southern Mapleleaf	9.8	6.2	2.8	1.6
Toxolasma parvum	Lilliput			2.8	0.8
Toxolasma texasiense	Texas Lilliput				2.9
Tritogonia verrucosa	Pistolgrip	1.5	15		
Truncilla macrodon	Texas Fawnsfoot				3.3
Uniomerus tetralasmus	Pondhorn				0.4
Utterbackia imbecillis	Paper Pondshell	6.8	5.3	2.8	1.2
	Total N of habitats	132	114	36	245
	Total % of habitats	68	75	25	87

Table 10. Summary of parameters in habitats with Smooth Pimpleback.

		Little River	Colorado River			
			Overall	Georegion 1	Georegion 3	Georegion 5
N of habitats		11	41	2	3	36
N of individuals		133	400	3	10	387
Current velocity column (m/s)	Mean	0.15	0.13	0.02	0.26	0.13
	SD	0.30	0.17	0.03	0.06	0.18
Current velocity bottom (m/s)	Mean	0.09	0.08	0.01	0.15	0.08
	SD	0.19	0.11	0.01	0.09	0.12
Depth (m)	Mean	0.74	0.73	0.99	0.74	0.71
	SD	0.70	0.67	0.75	0.94	0.66
Penetrometer (kg/cm^2)	Mean	0.02	0.06	0.07	0.29	0.04
	SD	0.01	0.11	0.01	0.31	0.06
Shear stress (dyn/cm^2)	Mean	1.15	1.28	0.77	2.35	1.22
	SD	0.95	0.82	0.00	1.50	0.73
FST hemispheres	Mean	1.40	2.27	0.00	5.33	2.14
	SD	2.60	2.61	0.00	3.06	2.47
Substrate (%)	Clay	4	7	5		7
	Silt	57	24	30		26
	Sand	21	33	10	13	36
	Gravel	13	10	35	20	8
	Cobble	2	8	15	60	3
	Boulder	1	12		7	13
	Bedrock		5			6
	Detritus	2	1			1
Habitat types (%)	Riffle		2			3
	Run-channel	18	15		67	11
	Run-edge	18	37		33	39
	Pool-channel	18	17	100		14
	Pool-edge	45	22			25
	Backwater		7			8

Table 11. Summary of parameters in habitats with Texas Pimpleback.

		Guadalupe River	Colorado River			
			Overall	Georegion 1	Georegion 3	Georegion 5
N of habitats		4	22	2	8	12
N of individuals		10	127	6	91	30
Current velocity column (m/s)	Mean	0.17	0.17	0.04	0.19	0.17
	SD	0.07	0.20	0.01	0.14	0.25
Current velocity bottom (m/s)	Mean	0.09	0.09	0.01	0.12	0.09
	SD	0.07	0.13	0.01	0.09	0.15
Depth (m)	Mean	0.40	0.76	0.91	0.34	1.02
	SD	0.15	0.82	0.65	0.16	1.01
Penetrometer (kg/cm^2)	Mean	0.08	0.08	0.16	0.11	0.04
	SD	0.04	0.07	0.12	0.08	0.04
Shear stress (dyn/cm^2)	Mean	1.49	1.36	0.77	1.56	1.32
	SD	0.91	0.97	0.00	1.08	0.98
FST hemispheres	Mean	3.30	2.45	0.00	3.25	2.33
	SD	3.30	2.76		2.96	2.71
Substrate (%)	Clay		3			5
	Silt	15	12	20	9	13
	Sand	10	25	20	19	30
	Gravel	25	22	40	33	12
	Cobble	13	18	15	38	6
	Boulder		15	5		28
	Bedrock	35	5		1	9
	Detritus	3				
Habitat types (%)	Riffle	25	5			8
	Run-channel		23		38	17
	Run-edge	50	18		25	17
	Pool-channel		32	100	13	33
	Pool-edge	25	14			25
	Backwater		9		25	

Table 12. Summary of parameters in habitats with Texas Fatmucket.

		Guadalupe River	Colorado River Georegion 3
N of habitats		6	1
N of individuals		16	2
Current velocity column (m/s)	Mean	0.28	0.00
	SD	0.18	
Current velocity bottom (m/s)	Mean	0.15	0.00
	SD	0.14	
Depth (m)	Mean	0.43	0.40
	SD	0.26	
Penetrometer (kg/cm^2)	Mean	0.05	0.00
	SD	0.04	
Shear stress (dyn/cm^2)	Mean	1.65	0.77
	SD	0.89	
FST hemispheres	Mean	3.83	0.00
	SD	2.99	
Substrate (%)	Clay		
	Silt	13	50
	Sand	7	
	Gravel	31	
	Cobble	16	
	Boulder	3	50
	Bedrock	29	
	Detritus	2	
Habitat types (%)	Riffle	17	
	Run-channel	17	
	Run-edge	50	
	Pool-channel		100
	Pool-edge	17	
	Backwater	0	

Table 13. Summary of parameters in habitats with Texas Fawnsfoot.

		Colorado River Georegion 3
N of habitats		8
N of individuals		9
Current velocity column (m/s)	Mean	0.10
	SD	0.15
Current velocity bottom (m/s)	Mean	0.06
	SD	0.11
Depth (m)	Mean	0.52
	SD	0.17
Penetrometer (kg/cm^2)	Mean	0.05
	SD	0.07
Shear stress (dyn/cm^2)	Mean	0.97
	SD	0.49
FST hemispheres	Mean	1.13
	SD	2.03
Substrate (%)	Clay	16
	Silt	34
	Sand	32
	Gravel	8
	Cobble	1
	Boulder	9
	Bedrock	0
	Detritus	
Habitat types (%)	Riffle	0
	Run-channel	0
	Run-edge	63
	Pool-channel	0
	Pool-edge	25
	Backwater	13

Table 14. Mesohabitat associations by species using ACFOR scale (Stiers et al. 2011): Abundant (75 – 100% in a species relative abundance), Common (50 – 74%), Frequent (25 – 49%), Occasional (5 – 24%), and Rare (>0 – 4%). For example, Threeridge were taken rarely from riffle, occasionally from run-channel, pool-edge, and backwater, and frequently taken from run-edge and pool-channel habitats. Blank represents a species was not found in the mesohabitat.

Species	N	Riffle	Run-channel	Run-edge	Pool-channel	Pool-edge	Backwater
Threeridge	1405	rare	occasional	frequent	frequent	occasional	occasional
Smooth Pimpleback	533	rare	frequent	occasional	frequent	occasional	rare
Yellow Sandshell	461	rare	rare	frequent	occasional	frequent	occasional
Fragile Papershell	166	rare	rare	frequent	occasional	frequent	occasional
Tampico Pearlymussel	152	rare	rare	rare	frequent	frequent	occasional
Texas Pimpleback	137	rare	occasional	common	occasional	occasional	occasional
Southern Mapleleaf	75	occasional	occasional	rare	abundant	occasional	rare
Pistolgrip	54	occasional	occasional	frequent	occasional	occasional	occasional
Giant Floater	49			rare	occasional	common	occasional
Texas Lilliput	47	occasional		occasional	occasional	common	occasional
Bleufer	35				frequent	common	occasional
Paper Pondshell	33		occasional	occasional	occasional	frequent	occasional
Texas Fatmucket	18	occasional	occasional	common	occasional	occasional	
Texas Fawnsfoot	9			common		frequent	occasional
Pondhorn	9			abundant			occasional
Lilliput	4	frequent				abundant	

Table 15. Species-substrate associations using ACFOR scale (Stiers et al. 2011): Abundant (75 – 100% mean percent substrate), Common (50 – 74%), Frequent (25 – 49%), Occasional (5 – 24%), and Rare (>0 – 4%). For example, Threeridge were taken from substrates comprised, on average, rarely of cobble and detritus and occasionally of clay, silt, sand, gravel, boulder, and bedrock. Blank represents a substrate type where a species was not found.

Species	N	Clay	Silt	Sand	Gravel	Cobble	Boulder	Bedrock	Detritus
Threeridge	1405	occasional	occasional	occasional	occasional	rare	occasional	occasional	rare
Smooth Pimpleback	533	rare	frequent	frequent	occasional	occasional	occasional	rare	rare
Yellow Sandshell	461	occasional	frequent	frequent	rare	rare	occasional	rare	rare
Fragile Papershell	166	occasional	occasional	occasional	occasional	occasional	occasional	rare	rare
Tampico Pearlymussel	152	rare	frequent	occasional	occasional	occasional	occasional	rare	rare
Texas Pimpleback	137	rare	occasional	frequent	occasional	occasional	occasional	rare	rare
Southern Mapleleaf	75	rare	occasional	occasional	frequent	occasional	occasional	rare	rare
Pistolgrip	54	rare	occasional	occasional	occasional	frequent	occasional	occasional	rare
Giant Floater	49	occasional	common	occasional	occasional	occasional	occasional	rare	occasional
Texas Lilliput	47	rare	frequent	rare	occasional	rare	occasional	occasional	occasional
Bleufer	35	rare	frequent	frequent	occasional	occasional	occasional	rare	rare
Paper Pondshell	33	rare	frequent	rare	occasional	occasional	rare	occasional	occasional
Texas Fatmucket	18		occasional	rare	frequent	occasional	rare	frequent	rare
Texas Fawnsfoot	9	occasional	frequent	frequent	occasional	rare	occasional		
Pondhorn	9	rare	occasional	occasional	frequent	occasional		occasional	
Lilliput	4		common	rare	occasional	occasional	occasional	occasional	

Part II. Figures

Figure 1. Plot of principal components axes I and II for physical characters of mesohabitats taken from the Brazos, Guadalupe, and Colorado River basins taken from March through October 2017. Black circles represent mean and whiskers represent 1 SD of mesohabitat scores grouped by basin, reach, or georegion.

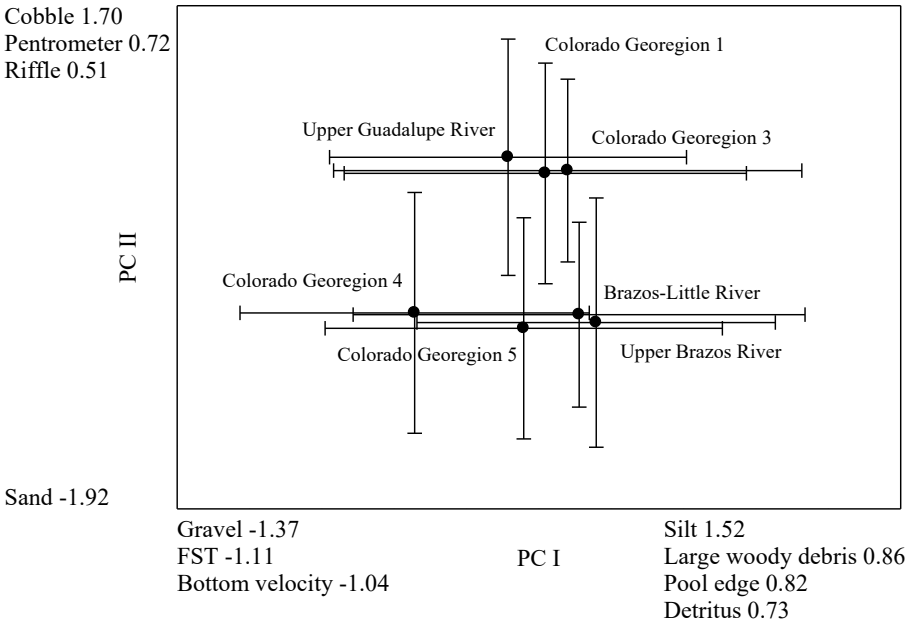

Figure 2. Percent occurrences of Smooth Pimpleback (gray bars) among multiple physical parameters taken from the Little River (Brazos River basin) from March through October 2017. Black line in each graph represents the percent of available parameter. Mesohabitat and substrate graphs plot percent observed minus percent expected to infer a positive or negative association.

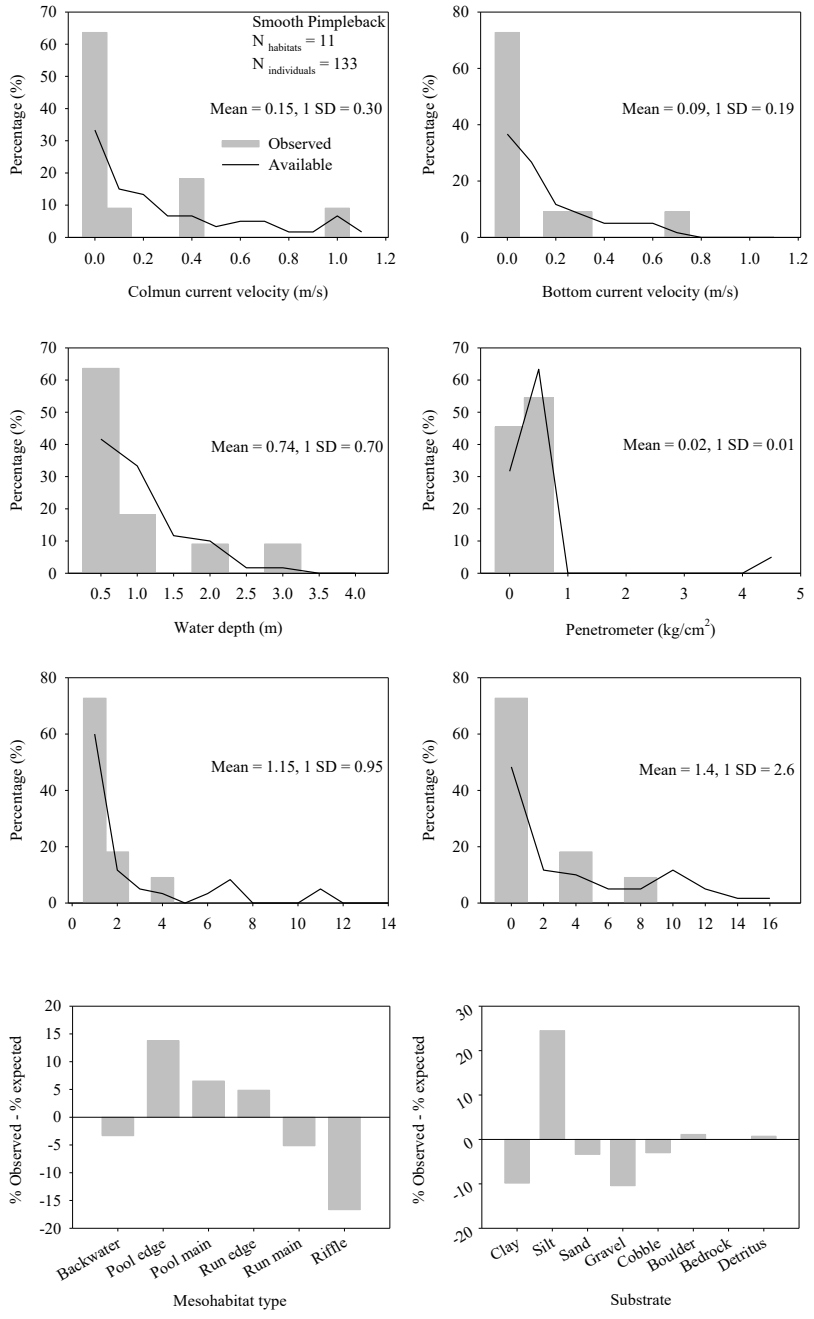

Figure 3. Percent occurrences of Texas Fatmucket and Texas Pimpleback (gray bars) by column current velocity and bottom current velocity taken from upper Guadalupe River from March through October 2017. Black line represents the percent of current velocities available. Bars above line suggest positive association and bars below line (or absent) suggest negative association.

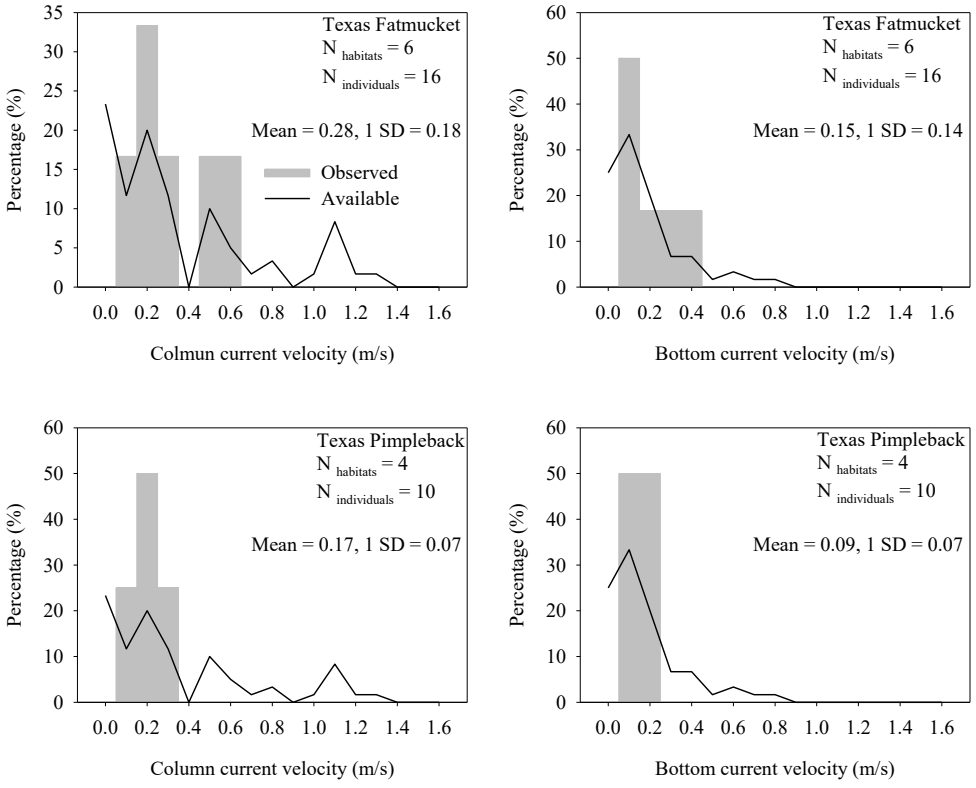

Figure 4. Percent occurrences of Texas Fatmucket and Texas Pimpleback (gray bars) by water depth and substrate penetrometer measurement taken from upper Guadalupe River from March through October 2017. Black line represents the percent of current velocities available. Bars above line suggest positive association and bars below line (or absent) suggest negative association.

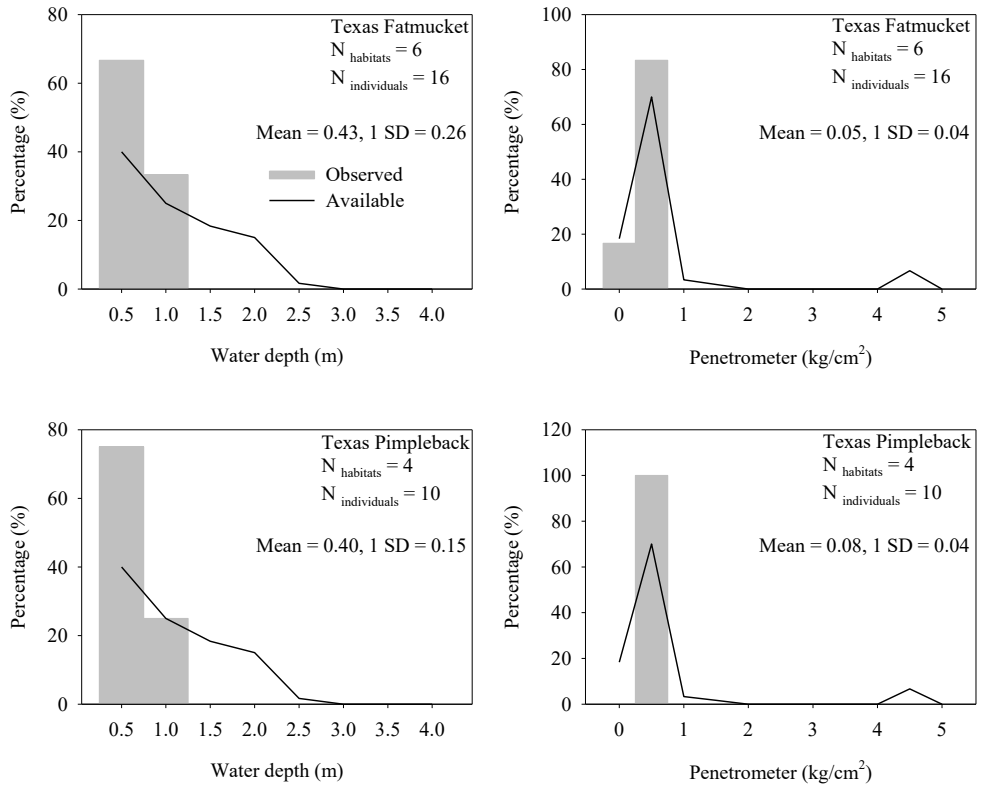

Figure 5. Percent occurrences of Texas Fatmucket and Texas Pimpleback (gray bars) by minimum bottom shear stress and FST hemispheres taken from upper Guadalupe River from March through October 2017. Black line represents the percent of current velocities available. Bars above line suggest positive association and bars below line (or absent) suggest negative association.

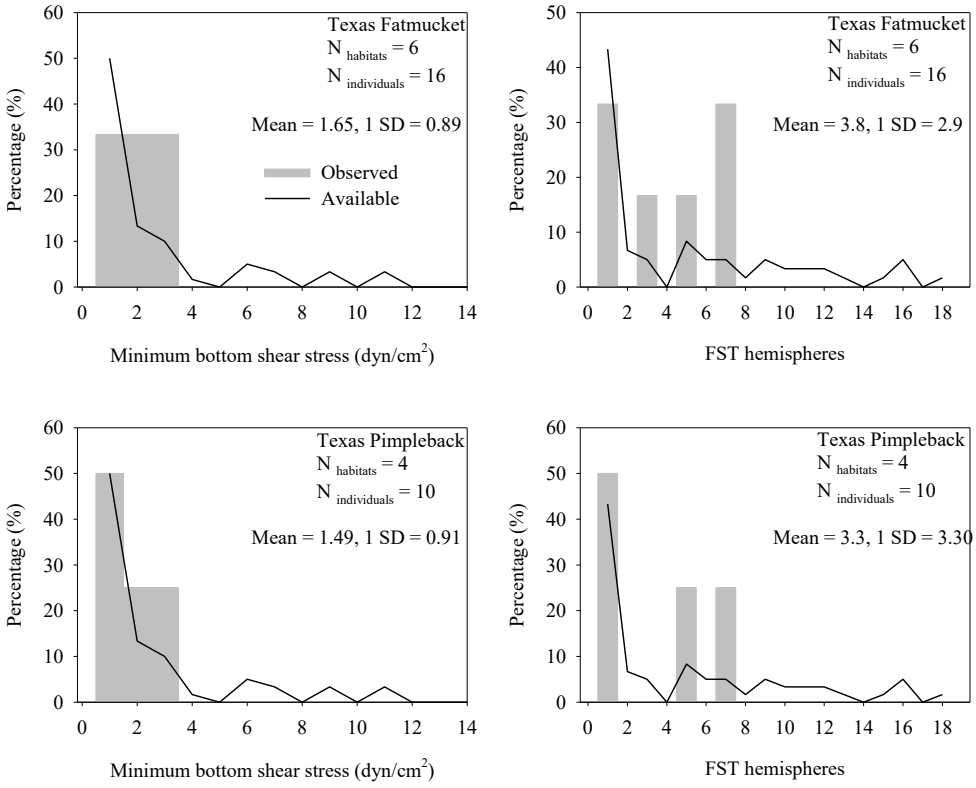

Figure 6. Differences in percent observed occurrences and percent available (i.e., expected) among mesohabitats and substrates for Texas Fatmucket and Texas Pimpleback from upper Guadalupe River from March through October 2017. Positive differences suggest positive association with a mesohabitat or substrate. Negative differences suggest negative association with a mesohabitat or substrate.

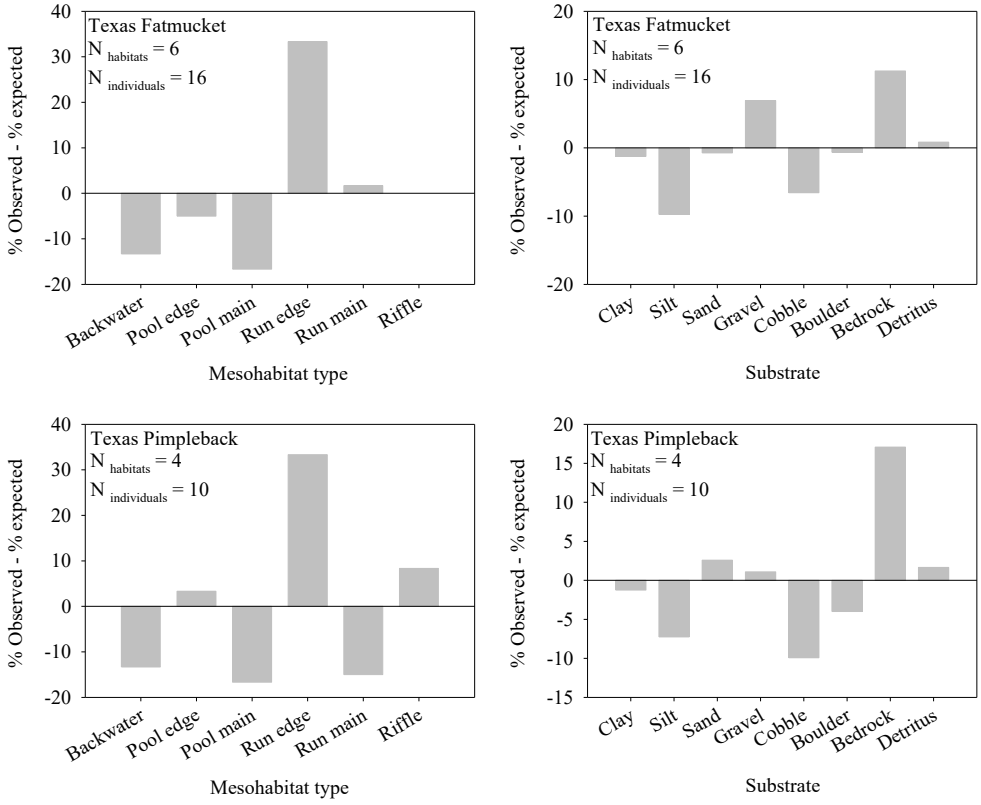

Figure 7. Plot of conical correspondence axes I and II for mesohabitats and their physical characters taken from the Colorado River basin from March through October 2017 (top panel). Arrow lengths indicate weight of mesohabitat and physical parameters along axes I and II. Centroid of species scores are represented by the first three letters of a species generic and specific epithets.

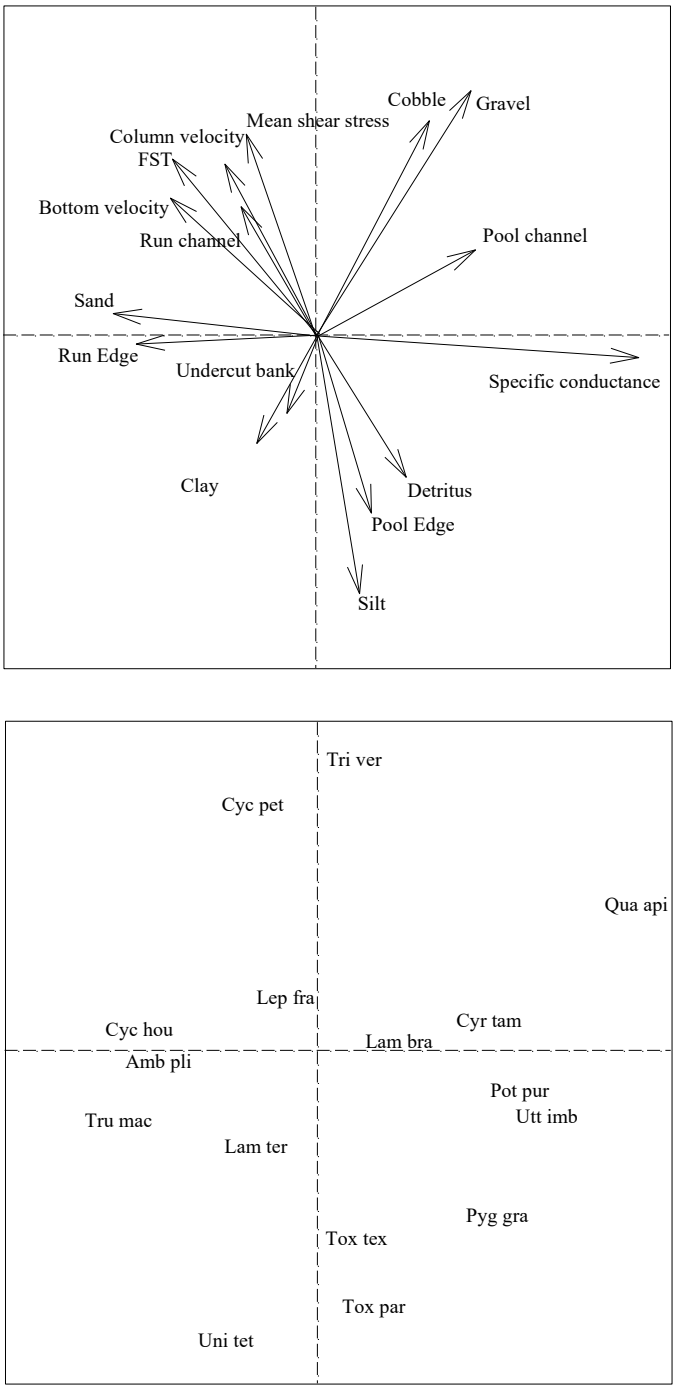

Figure 8. Percent occurrences of Smooth Pimpleback, Texas Pimpleback, and Texas Fawnsfoot (gray bars) by column current velocity and bottom current velocity taken from Colorado River from March through October 2017. Black line represents the percent of current velocities available. Bars above line suggest positive association and bars below line (or absent) suggest negative association.

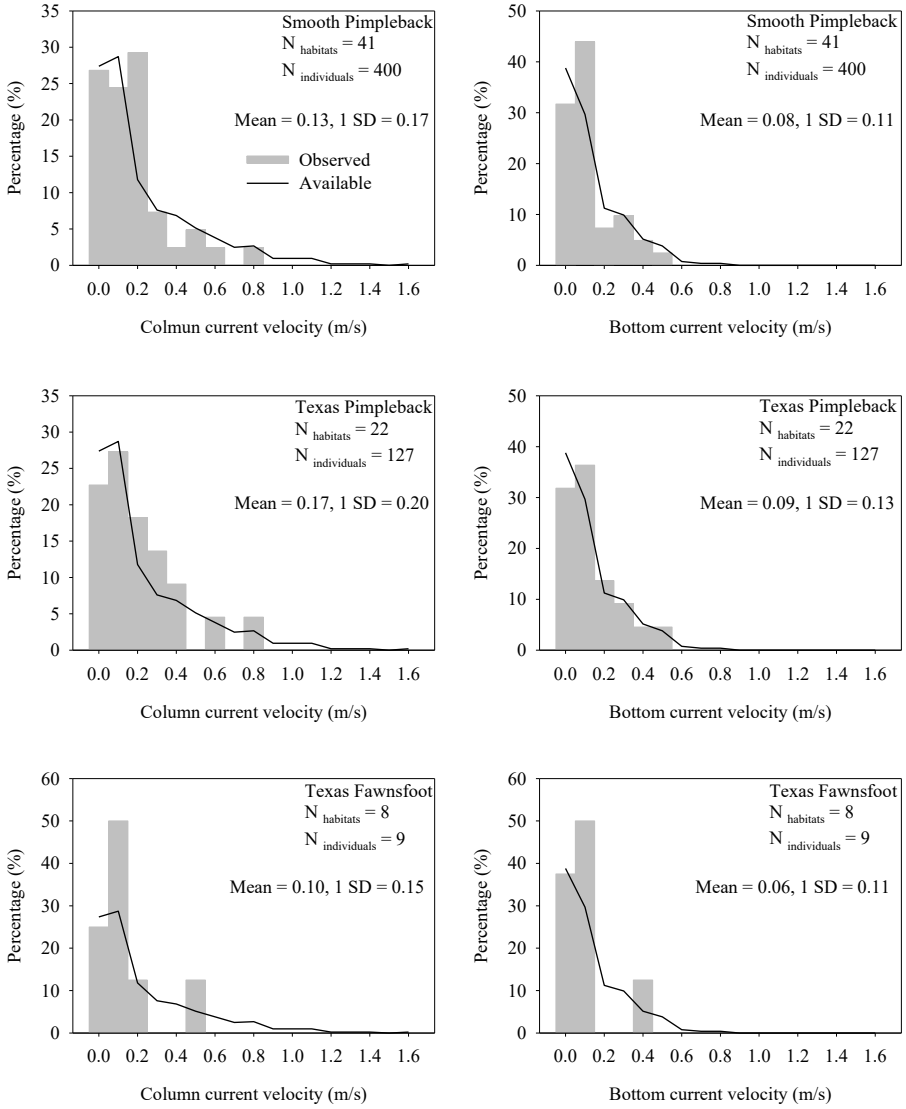

Figure 9. Percent occurrences of Smooth Pimpleback, Texas Pimpleback, and Texas Fawnsfoot (gray bars) by water depth and substrate penetrometer measurement taken from the Colorado River from March through October 2017. Black line represents the percent of current velocities available. Bars above line suggest positive association and bars below line (or absent) suggest negative association.

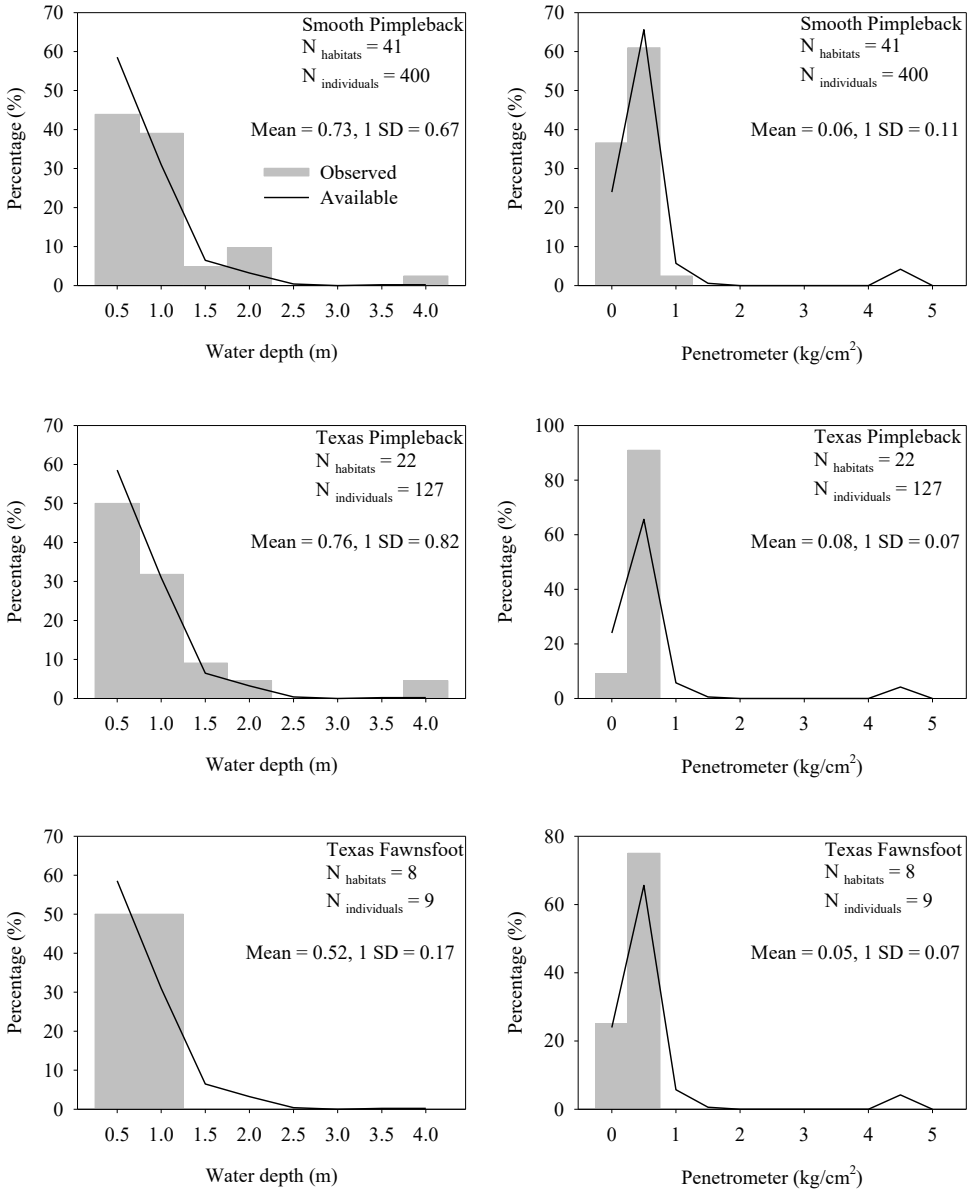

Figure 10. Percent occurrences of Smooth Pimpleback, Texas Pimpleback, and Texas Fawnsfoot (gray bars) by minimum bottom shear stress and FST hemispheres taken from Colorado River from March through October 2017. Black line represents the percent of current velocities available. Bars above line suggest positive association and bars below line (or absent) suggest negative association.

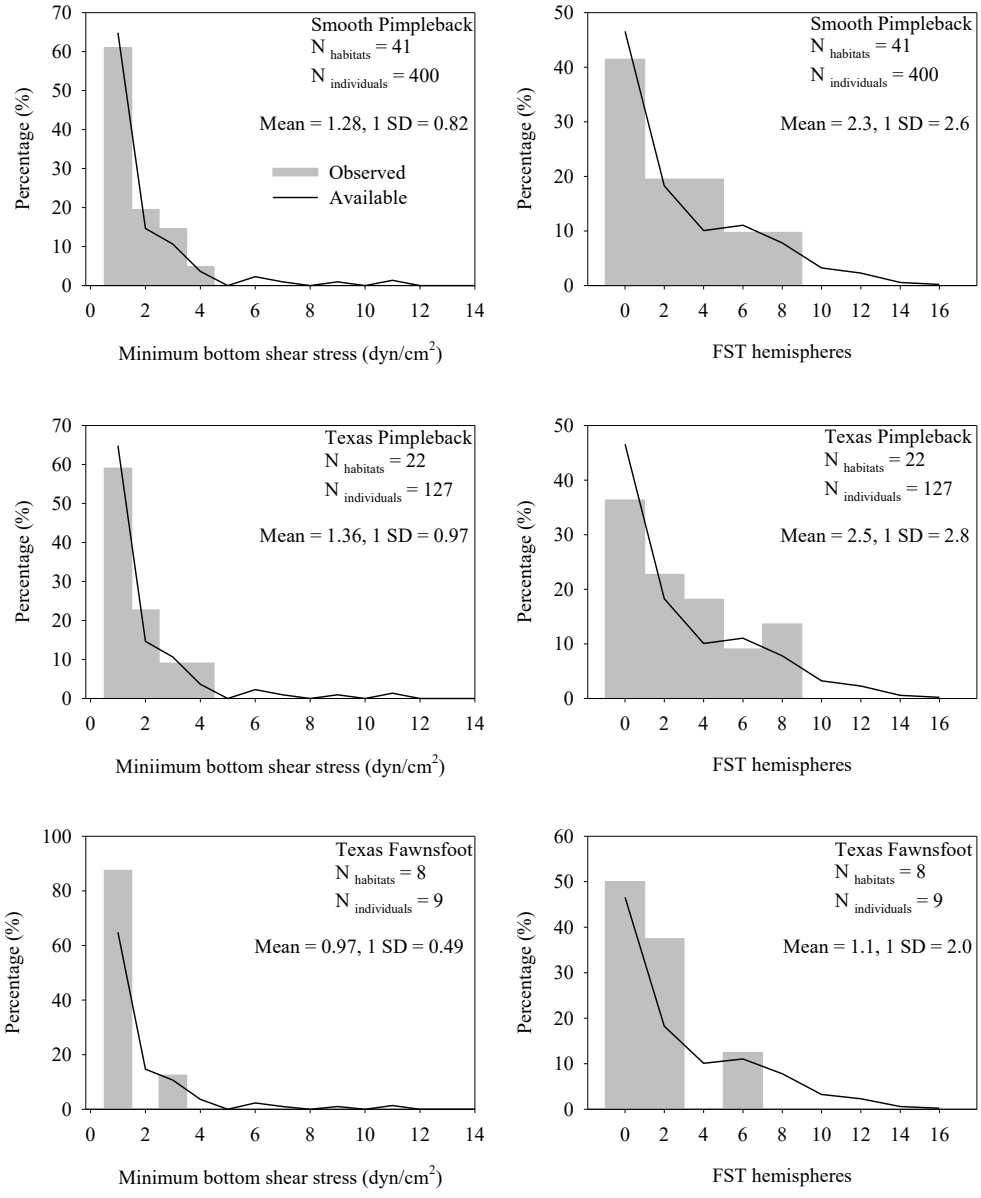

Figure 11. Differences in percent observed occurrences and percent available (i.e., expected) among mesohabitats and substrates for Smooth Pimpleback, Texas Pimpleback, and Texas Fawnsfoot from the Colorado River from March through October 2017. Positive differences suggest positive association with a mesohabitat or substrate. Negative differences suggest negative association with a mesohabitat or substrate.

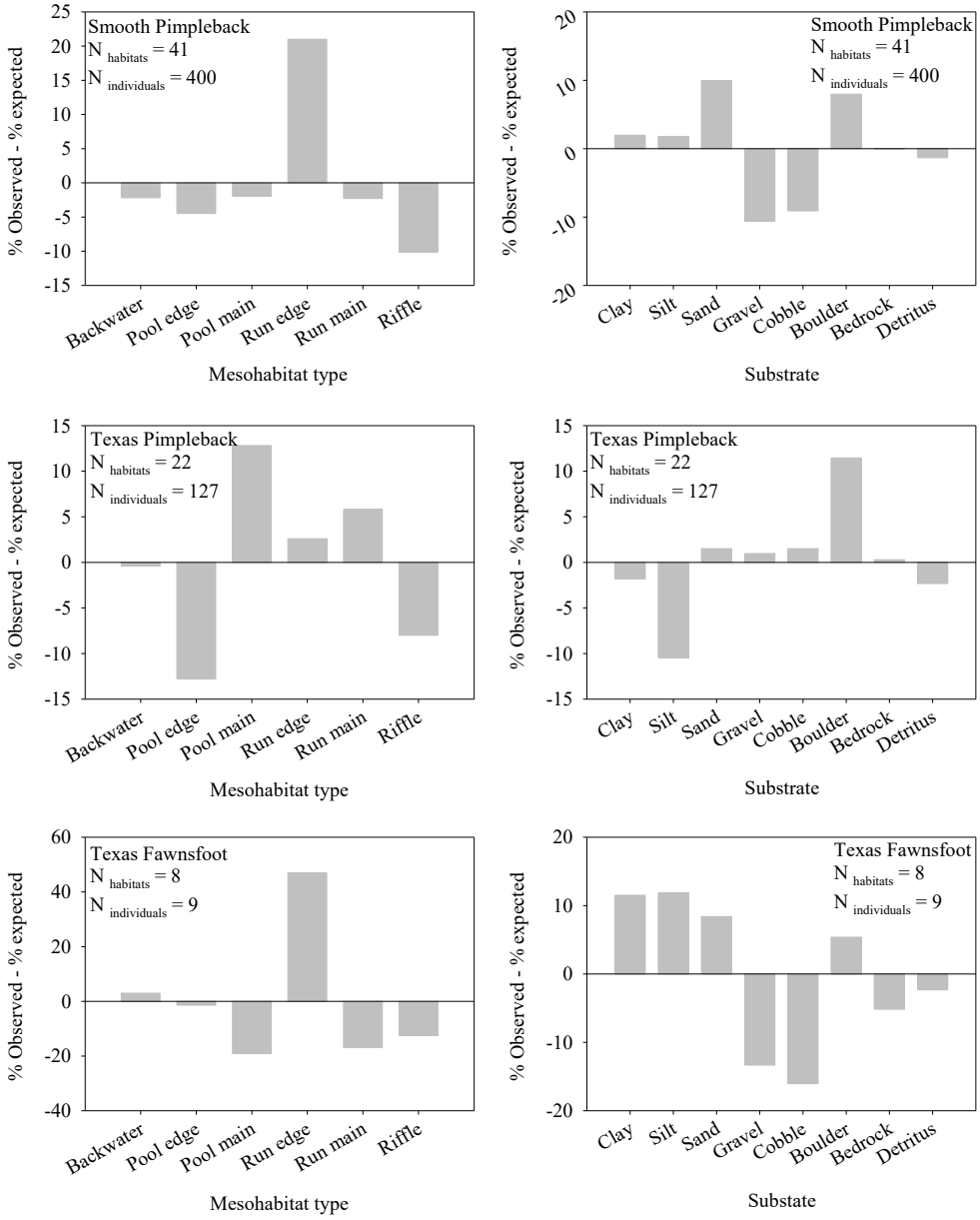

Figure 12. Weighted mean (black circle) and one SD (whiskers) of current velocities (column, top panel; bottom, bottom panel) for mussels taken from Brazos River, Colorado River, and Guadalupe Rivers from March through October 2017. Dashed vertical line represents mean of all available habitats, white area represents within 1 SD of all available habitats, and gray represents >1 SD of all habitats available. Total N for each species is provided in Table 14.

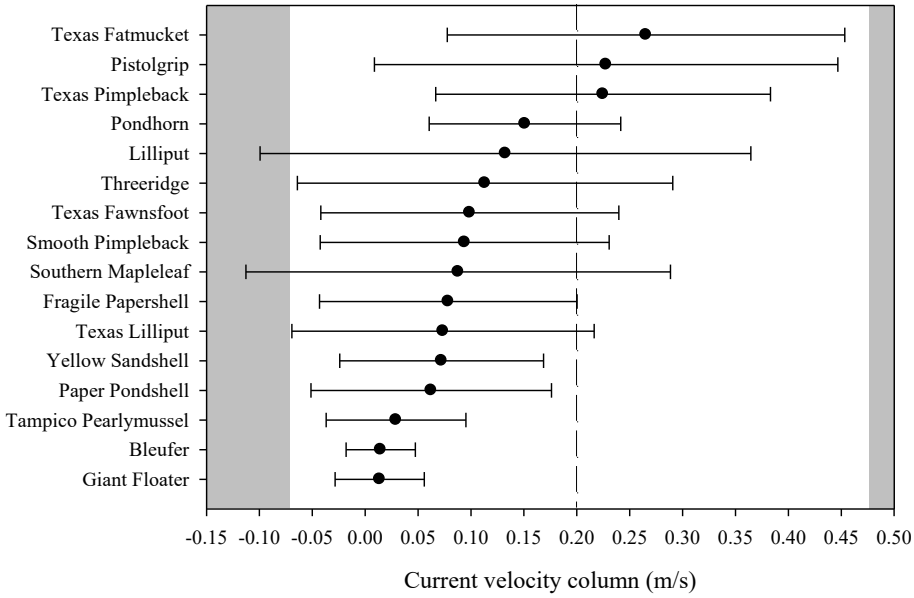

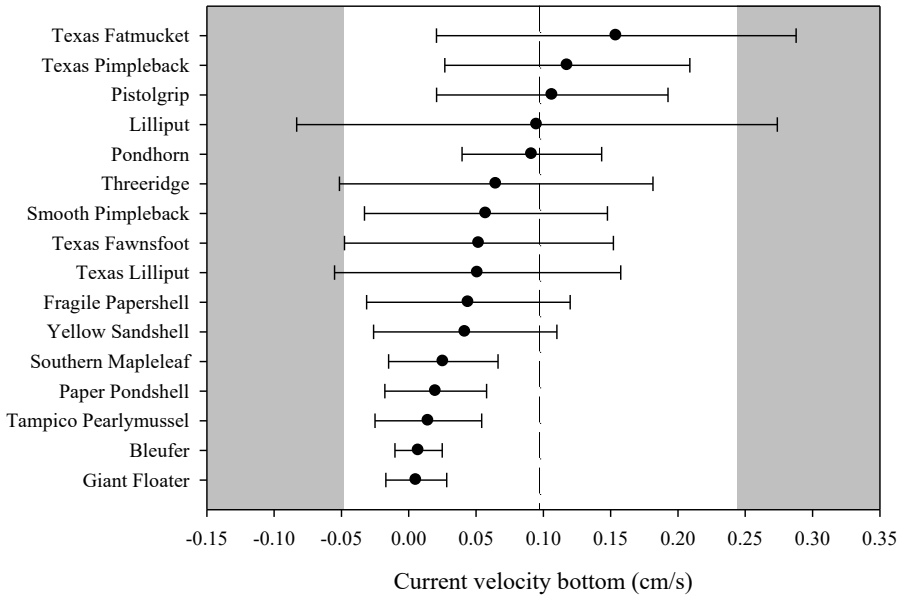

Figure 13. Weighted mean (black circle) and one SD (whiskers) of depth (top panel) and penetrometer (bottom panel) for mussels taken from Brazos River, Colorado River, and Guadalupe Rivers from March through October 2017. Dashed vertical line represents mean of all available habitats, white area represents within 1 SD of all available habitats, and gray represents >1 SD of all habitats available. Total N for each species is provided in Table 14.

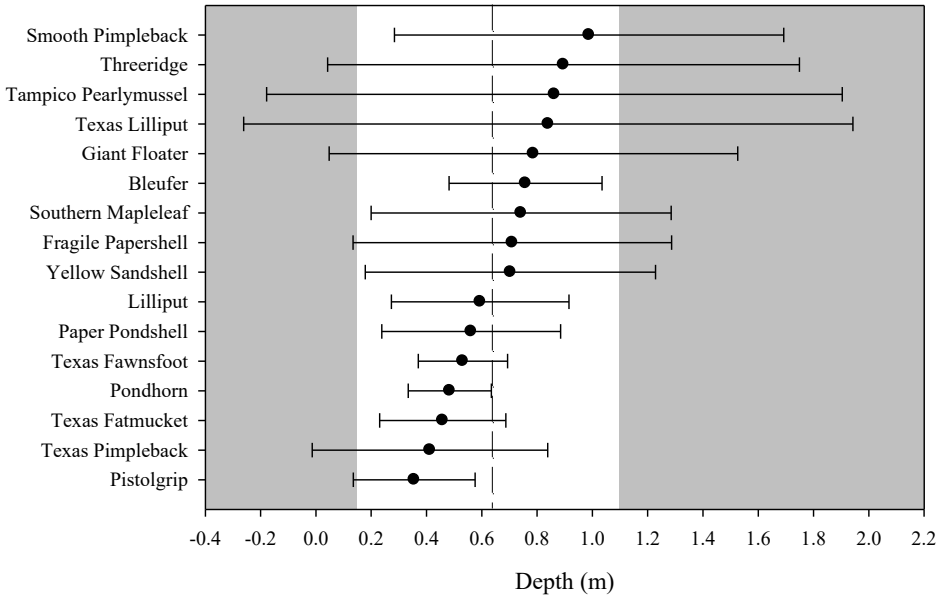

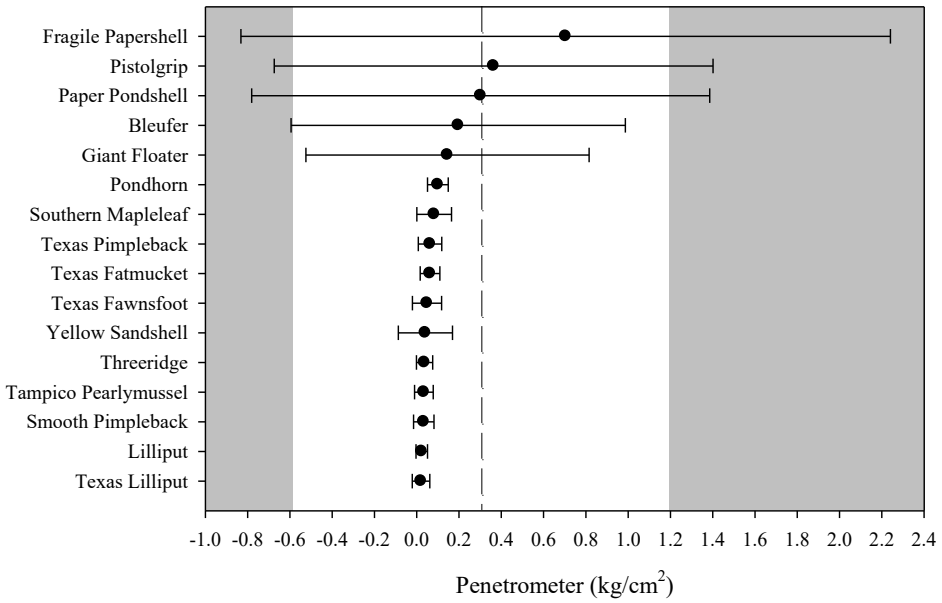

Figure 14. Differences in mussel community relative abundances before and after Hurricane Harvey and >150,000 cfs in the lower Colorado River (Georegion 5; top panel). Relative abundances of mussel species pre and post Harvey, ranked by magnitude of percent change (bottom table). Species names are abbreviated by the first three letters of their generic and specific epithets.

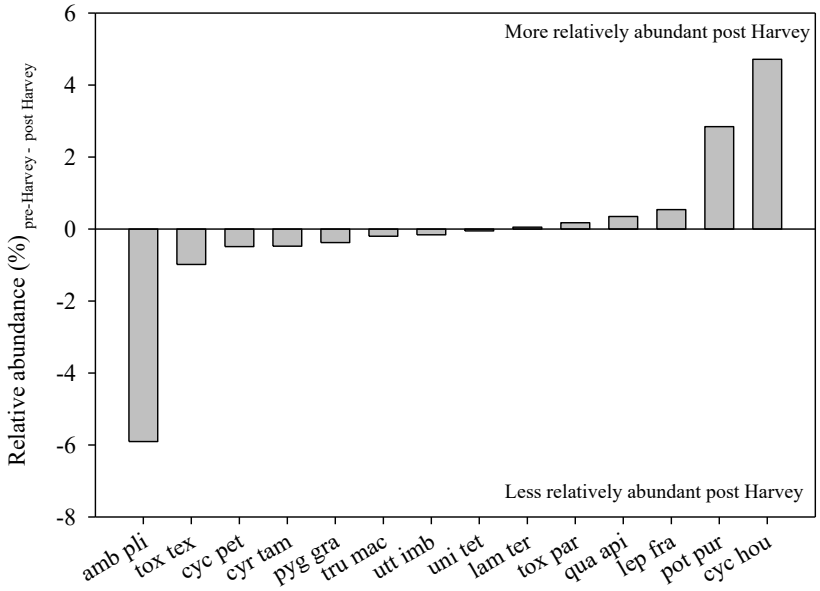

Species	Pre-Harvey	Post Harvey	Change in percent
amb pli	59	53	-5.91
tox tex	1.7	0.68	-0.99
cyc pet	1.4	0.91	-0.49
cyr tam	1.6	1.1	-0.48
pyg gra	0.38		-0.38
tru mac	0.43	0.23	-0.20
utt imb	0.16		-0.16
uni tet	0.05		-0.05
lam ter	17	17	0.05
tox par	0.05	0.23	0.17
qua api	0.11	0.45	0.35
lep fra	2.6	3.2	0.54
pot pur	0.11	2.9	2.84
cyc hou	16	21	4.71
N of mussels	1859	441	
N of habitats	179	66	

Part I & II References

Avery-Gomm, S., J.S. Rosenfeld, J.S. Richardson, and M. Pearson. 2014. Hydrological drought and the role of refugia in an endangered riffle-dwelling fish, Nooksack dace (*Rhinichthys cataractae ssp.*). Canadian Journal of Fisheries and Aquatic Sciences 71:1625-1634.

Baker, S.M., and J.S. Levinton. 2003. Selective feeding by three native North American freshwater mussels implies food competition with zebra mussels. Hydrobiologia 505:97-105.

Brim Box, J., R.M. Dorazio, and W.D. Liddell. 2002. Relationships between streambed substrate Characteristics and freshwater mussels (Bivalvia:Unionidae) in Coastal Plain streams. Journal of North American Benthological Society 21:253-260.

Brown, K.M., and P.D. Banks. 2001. The conservation of unionid mussels in Louisiana rivers: diversity, assemblage composition, and substrate use. Aquatic Conservation: Marine and Freshwater Ecosystems 11:189-191.

Burlakova, L.E., and A.Y. Karatayev. 2010. State-wide Assessment of Unionid Diversity in Texas. Final Performance Report to State Wildlife Grants Program. Federal Aid Grant T-43.

Burlakova, L.E., A.Y. Karatayev, V.A. Karatayev, M.E. May, D.L. Bennett, M.J. Cook. 2011. Endemic species: Contribution to community uniqueness, effect of habitat alteration, and conservation priorities. Biological Conservation 144:155-165.

Burlakova, L.E., B.L. Tulumello, A.Y. Karatayev, R.A. Krebs, D.W. Schloesser, D.T. Zanatta, W.L. Paterson, T.A. Griffith, M.W. Scott, and T. Crail. 2014. Competitive replacement of Invasive congeners may relax impact on native species: interactions among zebra, Quagga, and native unionid mussels. PLoS ONE https://doi.org/10.1371/journal.pone.0114926

Cummings, K. 2011. *Amphinaias pustulosa.* The IUCN Red List of Threatened Species 2011: e.T189523A8743529. http://dx.doi.org/10.2305/IUCN.UK.2011-2.RLTS.T189523A8743529.en

Dahm, C.N., R.J. Edwards, and F.P. Gelwick. 2005. Gulf Cost Rivers of the Southwestern United States. Rivers of North America. Eslevier Academic Press, NY.

Dascher, E.D., L.E. Burlakova, A.Y. Karatayev, D.F. Ford, A.N. Schwalb. 2017. Distribution of unionid freshwater mussels and host fishes in Texas. A study of broad-scale spatial patterns across basins and a strong climate gradient. Hydrobiologia DOI: 10.1007/s10750-017-3168-5

Freshwater Mollusk Conservation Society (FMCS). 2016. A national strategy for the

conservation of native freshwater mollusks. Freshwater Mollusk Biology and Conservation 19:1-21.

Gough, H.M., A.M. Gascho Landis, and J.A. Stoeckel. 2012. Behavior and physiology are linked in the responses of freshwater mussels to drought. Freshwater Biology 57:2356-2366.

Haag, W. R. 2012. Life history variation in mussels. North American Freshwater Mussels: Natural History, Ecology, and Conservation. Cambridge University Press, NY.

Haag, W.R., and J.D. Williams. 2014. Biodiversity on the brink: an assessment of conservation strategies for North American freshwater mussels. Hydrobiologia 735:45-60.

Hakala, J.P., and K.J. Hartman. 2004. Drought effect on stream morphology and brook trout (*Salvelinus fontinalis*) populations in forested headwater streams. Hydrobiologia 515:203-213.

Howells, R.G. 2014. Field Guide to Texas Freshwater Mussels. BioStudies, Kerrville, TX.

Johnson, P.D., and K.M. Brown. 2000. The importance of microhabitat factors and habitat stability to the threatened Louisiana pearl shell, *Margaritifera hembeli* (Conrad). Canadian Journal of Zoology 78:271-277.

Karatayev, A.Y., L.E. Burlakoka, and D.K. Padilla. 2017. Can introduced species replace lost biodiversity? A test with freshwater molluscs. https://doi-org.cmich.idm.oclc.org/10.1007/s10750-017-3135-1

Metcalfe-Smith, J.L., J. Di Maio, S.K. Station, and G.L. Macki. 2000. Effect of sampling effort on the efficiency of the timed search method for sampling freshwater mussel communities. Journal of North American Benthological Society 19:725-732.

Randklev, C.R., B.J. Lundeen, R.G. Howells, and J.H. Kennedy. 2009. First Account of a Living Population of Texas Fawnsfoot, *Truncilla macrodon* (Bivalvia: Unionidae), in the Brazos River, Texas. The Southwestern Naturalist 55:297-298.

Randklev, C.R., M.S. Johnson, E.T. Tsakiris, S. Rogers-Oetker, K.J. Roe, S. McMurray, C. Robertson, J. Groce, and N. Wilkins. 2012. False Spike, *Quadrula mitchelli* (Bivalvia: Unionidae) is not extinct: first account of a live population in over 30 years. American Malacological Bulletin 30:327-328.

Randklev, C.R., M.S. Johnson, E.T. Tsakiris, J. Groce, and N. Wilkins. 2013. Status of freshwater mussel (Family: Unionidae) fauna in mainstem of the Leon River, Texas. Aquatic Conservation: Marine and Freshwater Ecosystems 23:390-404.

Randklev, C.R., M. Cordova, J. Groce, E. Tsakiris, and B. Sowards. 2014. Freshwater mussel (Family: Unionidae) data collection in the middle and lower Brazos River. Institute of

Renewable Natural Resources, Texas A&M University. Texas Parks and Wildlife Contract No. 424520.

Randklev, C. R., N. A. Johnson, T. Miller, J. M. Morton, J. Dudding, K. Skow, B. Boseman, M. Hart, E. T. Tsakiris, K. Inoue, and R. R. Lopez. 2017. Freshwater Mussels (Unionidae): Central and West Texas Final Report. Texas A&M Institute of Renewable Natural Resources, College Station, Texas.

Rose, D.R., and A.A. Echelle. 1981. Factor Analysis of Associations of Fishes in Little River, Central Texas, with an Interdrainage Comparison. The American Midland Naturalist 106:379-391.

Sietman, B.E., M.A. Furman, and F.A. Pursell. 1999. Colonization of Bedrock by Freshwater Mussels (Bivalvia: Unionidae). American Midland Naturalist 141:209-211.

Statzner, B., F. Kohmann, and A.G. Hildrew. 1991. Calibration of FST-hemispheres against bottom shear stress in a laboratory flume. Freshwater Biology 26:227-231.

Strayer, D. 1983. The effects of surface geology and stream size on freshwater mussels (Bivalvia, Unionidae) distribution in southeastern Michigan, U.S.A. Freshwater Biology 12:253-264.

Strayer, D.L. 2008. Freshwater Mussel Ecology: Multifactor Approach to Distribution and Abundance. University of California Press, CA.

Strayer, D.L. and D.R. Smith. 2003. A Guide to Sampling Freshwater Mussel Populations. Bethesda, Maryland.

Stiers, I., N. Crohain, G. Josens, L. Triest. 2011. Impact of three aquatic invasive species on native plants and macroinvertebrates in temperate ponds. Biological Invasions 13:2715-2726.

Texas Parks and Wildlife (TPWD). 2010. Threatened and Endangered Nongame Species. Texas Register 35:249-251.

Texas Parks and Wildlife (TPWD). 2014. 2014 Fisheries Management Survey Report: Belton Reservoir. Inalnd Fisheries Division Monitoring and Management Program.

Tsakiris, E.T., and C.R. Randklev. 2016. Distribution and habitat associations of freshwater mussels (Bivalvia: Unionidae) in the lower Guadalupe River, Texas. Texas A&M Institute of Renewable Natural Resources, College Station, Texas.

Tsakiris, E.T., and C.R. Randklev. 2016. Structural changes in freshwater mussel (Bivalve: Unionidae) assemblages downstream of Lake Somerville, Texas. American Midland Naturalist 175:120-127.

U.S. Fish and Wildlife Service (USFWS). 2011. Endangered and threatened wildlife and plants: 90-day finding on petitions to list nine species of mussels from Texas as threatened or

endangered with critical habitat. Federal Register. 2011 74:66260–66271.

U.S. Fish and Wildlife Service (USFWS). 2016. U.S. Fish and Wildlife Service Species Assessment and Listing Assignment Form. https://ecos.fws.gov/docs/candidate/assessments/2016/r2/F04G_I01.pdf

Vaughn, C.C., M. Taylor, and K.J. Eberhard. 1997. A comparison of the effectiveness of timed Searches vs. quadrat surveys. Conservation and Management of Freshwater Mussels II: Proceedings of a UMRCC Symposium 157-162.

Vaughn, C.C. 2017. Ecosystem services provided by freshwater mussels. https://doi.org/10.1007/s10750-017-3139-x

Wentworth, C.K. 1922. A scale grade and class terms for clatic sediments. Journal of Geology 30:377-392.

Williams, J.D., A.E. Bogan, R.S. Butler, K.S. Cummings, J.T. Garner, J.L. Harris, N.A. Johnson, and G.T. Watters. 2017. A Revised List of Freshwater Mussels (Mollusca: Bivalvia: Unionida) of the United States and Canada. Freshwater Mollusk Biology and Conservation 20:33-58.

Task 2: Potential Factors Limiting Growth, Survival, and Reproduction of Freshwater Mussel Species of Interest

Contributing authors: Austin Haney[1], Ryan Fluharty[1], Hisham Abdelrahman[1], Rebecca Tucker[1], Kaelyn Fogelman[1], Brian Helms[2], and James Stoeckel[1]

Addresses: [1]203 Swingle Hall, School of Fisheries, Aquaculture, and Aquatic Sciences, Auburn University, Auburn, Alabama 36849

[2]Department of Biological & Environmental Science, Troy University, Troy, AL 36082

Principle Investigators: James Stoeckel and Brian Helms

Email: jimstoeckel@auburn.edu, helmsb@troy.edu

Task 2. Objectives: The overall objective of this study was to conduct applied research experiments on up to three mussel species of interest to investigate impacts of the following stressors: temperature, hypoxia, suspended solids, salinity, and nitrogenous compounds. Specific objectives are listed under each sub-task.

Task 2.1 Sublethal effects of thermal and hypoxia stress

Task 2.1.A. Test microplate respirometry using early stage *Ligumia subrostrata*

2.1.A. Goal: The goal of this objective was to use a surrogate species to develop protocols for conducting microplate respirometry on early stage (glochidia and/or juveniles) mussels.

2.1.A. Methods: During the course of developing microrespirometry protocols, it became apparent that software needed to be updated in order to calibrate each individual microplate chamber rather than a general calibration for the microplate as a whole. Loligo Inc. made this software update available in December 2017. We are currently modifying our methodology to

incorporate the updated software and will provide a full description of updated methodology in the August 2018 addendum to this report.

2.1.A. Results: Despite the limitations of the original software, we were able to conduct initial trials and measure respiration rates of glochidia of *Ligumia subrostrata* (Fig. 1). Results were very promising and indicated that respiration patterns of glochidia subjected to hypoxia stress (declining dissolved oxygen) were similar to adults.

Task 2.1.B. Collection of focal species to be used in trials

Mussels for experiments were collected by BIO-WEST, Texas State University, and Auburn University personnel during surveys (see Table 1 for species list and collection information). Mussels were placed in coolers between moist cotton towels. Sufficient ice-packs were added above and below the toweling to try to maintain a shipping temperature intermediate between collection temperature in Texas and holding temperature (18ºC) at Auburn. All coolers were shipped overnight via FedEx. Upon arrival, mussels were tagged, measured (length), and placed in upwellers containing ~80 L of hard artificial freshwater (HAFW: 0.192 g $NaHCO_3$, 0.10 g $CaSO_4$*H20, 0.10 g $CaCl_2$, 0.06 g $MgSO_4$, and 0.008 g KCl per liter of reverse osmosis/deionized water; modified from Smith et al. 1997) at 18ºC. Biofilters in each upweller were allowed to establish for > 2 weeks prior to arrival of experimental mussels. Mussels in each upweller were fed 2 mL Shellfish Diet 1800 (Reed Mariculture Inc, Campbell, CA) in the morning and 1 mL in the afternoon on a daily basis. Water quality (ammonia, nitrites, nitrates) was measured 3 times/week using either Tetra 6-in-1 and Ammonia Aquarium Test Strips or API 5 in 1 and Ammonia Test Strips. Ammonia and nitrites remained at undetectable levels (< 0.5

mg/L) throughout the study. Nitrates were consistently detected and water changes were triggered when nitrate concentrations reached or exceeded 20-40 mg/L.

Newly arrived mussels were allowed to acclimate to HAFW and laboratory holding conditions for > 2 weeks. Following the lab acclimation, mussels were randomly assigned to one of six temperature treatments (13, 17, 23, 28, 32, and 36ºC). However, the lowest temperature was changed to 15°C after we found respiration rates at 13ºC were too low to reliably assess metabolic patterns. Mussels were acclimated in insulated upwellers (~70 L) equipped with chillers and/or heaters with temperature control (4 mussels/species/cooler, 2 coolers per temperature treatment). During acclimation, temperature was adjusted up or down at a rate of 1ºC/day until the target temperature was reached. Mussels were then acclimated to the temperature treatment for > 1 week. During the acclimation period, mussels were fed Shellfish Diet 1800 twice daily (2 mL morning, 1 mL afternoon per ~70 L upweller) and held at a 12h light: 12h dark cycle.

Task 2.1.C1. Thermal and hypoxia tolerance of adult mussels: Effects on metabolic patterns.

2.1.C1. Goals:

Following acclimation, we used closed respirometry to estimate resting metabolic rates (RMR) of freshwater mussels at different temperatures as dissolved oxygen (DO) decreased from near 100% saturation to anoxic conditions. RMR represents the oxygen demand of organisms while at rest and approximates the metabolic rate required for basic maintenance. We then used the relationship between RMR and DO to calculate a regulation index (RI) for each mussel. The regulation index provides an assessment of the ability of an organism to maintain a constant

respiration rate (i.e. meet its basic metabolic requirements) as oxygen declines. The closer the RI is to 1, the better an organism is able to continue to meet its energetic demands as DO declines (Fig. 2a,c). The closer the RI is to zero, the less an organism is able to meet its energetic demands as DO declines (Fig. 2b,c). We also used the relationship between RMR and DO to calculate critical dissolved oxygen levels (DO_{crit}). The DO_{crit} indicates the DO threshold below which an organism switches from aerobic to anaerobic respiration and thus is experiencing severe respiratory stress (Fig. 2a,b).

2.1.C1. Methods:

Respirometry experiments were conducted in 8-chamber fiber optic respirometry systems using AutoResp™ 2.3.0 software (Loligo, Inc.). Chambers were made of acrylic and ranged in volume from ~200 – 700 mL. Each chamber was connected to two Eheim submersible 300 L/h pumps: one circulated fresh oxygenated water through the chamber during acclimation, and the other circulated water through the chamber during experiments. A fiber-optic sensor was inserted in the closed recirculation line of each chamber. Respirometry chambers and associated pumps and sensors were submerged in a ~300 L tub filled with HAFW. Temperature was controlled by means of a TECO 1/3 hp chiller/heater unit. Chambers, tubing, and gravel associated with the respirometry setup were chlorinated (5 ml bleach/gallon tap water) to reduce bacteria and then rinsed thoroughly before each trial.

We measured respiration rates of 8 randomly selected individuals per temperature for *Cyclonaias houstonensis* and *C. petrina* (4 individuals per species/run * 2 runs per temperature). Acclimated individuals were removed from temperature-controlled upwellers, scrubbed lightly with a brush to remove any algae, and weighed (gWW). Mussels were then set in PVC cups

filled with gravel within the respirometry tub, and held without food for ~24 hours to prevent feeding and digestion from affecting estimates of RMR.

Following the 24 hr starvation period, mussels were assigned to an appropriately sized respirometry chamber (chamber that accommodated a mussel's shell without touching sides or lid). A PVC cup (1.5" H) half full of pea gravel was placed in each chamber to provide substrate for the mussels to burrow into. Cups had 4-mm mesh screening on the bottom to allow for water recirculation and reduce the chance of 'dead zones'. Flush pumps associated with each chamber were turned on and mussels allowed to acclimate to respirometry chambers for 5 hrs – a period of time which equaled or exceeded the amount of time required for mussels to reach a stable RMR as determined by previous experiments (Haney and Stoeckel, unpublished data). During this time, DO levels were near 100% saturation levels. Respirometry rooms were held at a 12h light: 12h dark cycle.

Acclimation periods were always initiated in late afternoon/early evening, and respirometry initiated before midnight. Following acclimation, the flush pumps were turned off and closed pumps turned on – creating a closed system where the volume of water recirculating within each chamber and associated tubing was constant, and no new, oxygenated water entered the system. Pumps were controlled remotely using TeamViewer software to minimize any disturbance to the mussels within the respirometry rooms. Mussels were allowed to respire until dissolved oxygen levels fell below ~0.2 mgO_2/L in the chambers or until mussels exhibited valve closure (abrupt cessation of respiration). Valve closure rendered respiration data unusable for RI or DO_{crit} analyses. At the end of each experimental run, mussels were removed from their testing chambers and then returned to upwellers to recover. Duration of each run was temperature dependent. At the coldest temperature, it generally took > 8 hrs for DO to fall below 0.2 mgO_2/L

whereas at the warmest temperature, DO typically declined to < 0.2 mgO_2/L within 8 hours or less.

Additional respiration experiments were conducted for *Amblema plicata, Fusconaia mitchelli,* and *Lampsilis teres* at a single temperature of 21°C using the methodology described above. Results will be included in a later draft of this report as an addendum.

Correction for background (bacterial) oxygen demand

Chlorination, followed by rinsing, was used to reduce/eliminate bacteria in chambers and associated tubing prior to each respiration run. However, bacteria populations tend to grow quickly and may have accounted for a significant portion of chamber oxygen demand by the end of a given run (i.e. background respiration). To account for this, we measured background respiration rate of each chamber before and after each run, under normoxic conditions (DO ≥ 5 mgO_2/L), for ~1.5 hrs without mussels present. The mean background oxygen demand was then divided by the mean observed respiration rate under normoxic conditions with mussels present in order to determine the proportion of total chamber respiration that was due to background respiration. This proportion was referred to as the correction factor. We assumed that this proportion remained constant as dissolved oxygen declined below normoxia and corrected our respirometry data in each chamber by multiplying the observed respiration rate by 1 minus the correction factor.

Regulation Index and DO_{crit}

Regulation indexes (RI's) were calculated using the methodology of Mueller and

Seymour (2011). Corrected RMR ($mgO_2/g/hr$) values were plotted against DO (mgO_2/L) for each respirometry run. The upper limit of the DO range for which RI was calculated was held constant at 6 mg O_2/L to avoid bias in colder temperature runs where initial DO could be much higher than warmer runs (Mueller and Seymour 2011). Data were fitted with the curve (3-parameter exponential rise to maximum, 2-parameter hyperbola, or 2-segment piecewise regression) that showed the lowest Akaike information criterion adjusted for small sample size (AICc: SigmaPlot 13.0). We then used the Sigma Plot area under the curve (AUC) macro to calculate AUC for 1) the observed data, 2) a horizontal line that represented perfect regulation, and 3) a linear decrease that represented perfect conformation (see Fig. 2c). RI was calculated as (Observed AUC-Conformation AUC)/(Regulation AUC-Conformation AUC). The RI provided a quantitative measure of the degree to which mussels were able to regulate oxygen consumption as ambient DO declined from 6 to < 0.2 mg O_2/L. DO_{crit} was calculated as the dissolved oxygen concentration showing the greatest distance between the observed RMR and the perfect conformation line (Mueller and Seymour 2011).

2.1.C1: Results:

Resting metabolic rate increased linearly with increasing temperature for *Cyclonaias houstonensis* from the Colorado (RMR = 0.0007*temp – 0.0053; $R^2 = 0.9744$, $P = 0.0002$) and Navasota rivers (RMR = 0.0004*temp – 0.0046; $R^2 = 0.9423$, $P = 0.0013$). The regulation index did not show a significant linear relationship with temperature for *C. houstonensis* from the Colorado ($R^2 = 0.6328$, $P = 0.0584$) or Navasota ($R^2 = 0.0164$, $P = 0.8088$) rivers. Similarly, DO_{crit} did not show a significant linear relationship with temperature for *C. houstonensis* from the Colorado ($R^2 = 0.1166$, $P = 0.5078$) or Navasota ($R^2 < 0.01$, $P = 0.9922$) rivers (Fig. 3).

Cyclonaias petrina exhibited similar patterns. Resting metabolic rate increased linearly with increasing temperature for *C. petrina* from the Colorado (RMR = 0.0004*temp – 0.0038; R^2 = 0.9757, P = 0.0002) and Guadalupe (RMR = 0.0005*temp – 0.0070) rivers. The regulation index did not show a significant linear relationship with temperature for *C. petrina* from the Colorado (R^2 = 0.4592, P = 0.2088) or Guadalupe (R^2 = 0.4574, P = 0.2100) rivers. DO_{crit} did not show a significant linear relationship with temperature for *C. petrina* from the Colorado (R^2 = 0.6336, P = 0.1072) or Guadalupe (R^2 = 0.5517, P = 0.1504) rivers (Fig. 4).

There was no significant difference in mean RI (calculated across all temperatures) among species and locations (ANOVA, P = 0.079). There were significant differences in DO_{crit} among species and locations (ANOVA, P = 0.025) with *C. houstonensis* from the Navasota River exhibiting a significantly lower DO_{crit} than *C. houstonensis* from the Colorado River (Tukey's, P = 0.026). DO_{crit} of *C. petrina* did not differ between locations or from *C. houstonensis* collected from either location (Tukey's, P > 0.05) (Fig. 5).

The proportion of animals exhibiting at least one episode of valve closure, as evidenced by a sudden drop of RMR to 0, increased at high temperatures. *C. petrina* tended to show higher proportions of valve closure than did *C. houstonensis* (Fig. 6).

2.1.C1 Conclusions:

Results suggest that the main impact of increasing temperatures to a maximum of 36°C is to increase metabolic demand for basic maintenance. Thus, mussels of both species require more food, and are likely to become more susceptible to food limitation, at warm temperatures. *C. houstonensis* from the Colorado River is likely the most sensitive to food limitation as its RMR increased at a faster rate with increasing temperature than did *C. houstonensis* from the Navasota

River or *C. petrina* from either location. This result emphasizes the importance of understanding mussel food resource availability, particularly during the warm summer months.

Valve closure results further support the potential for food limitation at high temperatures. Previous studies have shown bivalves exhibit valve closure in response to stressful temperatures (e.g. Anestis et al. 2007). In our study, all species/location combinations showed a trend of increasing episodes of valve closure as temperatures increased, with 40-87% of all mussels exhibiting at least one episode of closure when temperatures reached 36ºC. Because increased frequency of valve closure would reduce feeding and aerobic respiration activities while demand for energy is increasing, mussels would become increasingly susceptible to growth limitation as temperatures approach and exceed 36ºC. However, mussels appeared to exhibit tradeoffs to potentially offset this effect. *C. houstonensis* (Colorado River) exhibited the greatest increase in energy demand as temperatures increased, but kept valves open until temperatures reached 36ºC. *C. petrina* exhibited a greater frequency of closed valves than *C. houstonensis* as temperatures approached 36ºC, but exhibited a lower energy demand. Studies examining the effects of intermittent valve closure on mussel energy budgets at high temperatures would help determine which species is more strongly affected by food limitation at high temperatueres.

Surprisingly, there was little evidence that increasing temperatures up to 36ºC increased sensitivity to hypoxia for any species/location tested. Although some weak trends in RI and DO_{crit} with increasing temperature were apparent, none were significant. The ability of mussels to obtain oxygen from the water column (RI) remained fairly constant as temperatures increased, with a switch from aerobic to anaerobic respiration (DO_{crit}) only becoming apparent when DO levels fell below ~2.0 mgO_2/L. Short term tolerance of low DO, even at high temperatures, is

further supported by the lack of mortality when mussels remained in respirometry chambers at 36ºC at DO concentrations < 1 mgO_2/L for several hours prior to termination of trials.

2.1.C1. Ongoing work

Respirometry results for *Lampsilis bracteata* will be added to this report by the end of April 2018.

Task 2.1.C2. Thermal tolerance of adult mussels: Effects on respiratory enzymes.

2.1.C2. Objectives:

The electron transport system (ETS) assay measures the activity of enzymatic complexes I and III of the respiratory chain within the mitochondria. It provides excess substrate (NADH and NADPH) for the enzyme complexes to act upon and utilizes INT dye as the electron acceptor. Originally developed by Packard (1971) it has since been used as a proxy for in-situ respiration rates of marine and freshwater organisms (Owens and King 1975, Madon et al. 1998, Elderkin et al. 1998). It yields an estimate of the potential oxygen consumption rate of an organism if all enzymes function maximally by quantifying ETS activity in the presence of excess substrates (Fanslow et al. 2001). Recently, Simcic et al. (2014) showed that the relationship between ETS enzyme activity and temperature can be used to estimate optimal thermal temperatures for organisms at the cellular level. They also showed that ETS activity shows a high degree of correlation with scope for growth at the organismal level, with optimal temperatures for organism growth being a few degrees cooler than optimal temperature for ETS enzymes. We used the ETS assay to determine optimal enzymatic temperatures for acclimated

and non-acclimated mussels and to compare intra and interspecific variation in optimal temperatures among species and locations.

2.1.C2. Methods:

We used two different approaches to examine the relationships between ETS activity and temperature. In the first approach, mussels were acclimated for >1 week to each of nine experimental temperatures (see *Acclimated Approach* below). ETS activity at each temperature was measured as the mean of four acclimated mussels, and tissue sampling was non-lethal. This approach yielded a single, composite, thermal performance curve for a given species and was limited to a non-lethal temperature range because it requires acclimation of mussels to each temperature for > 1 week with minimal mortality. It also required a large number of mussels (e.g. ≥ 4 mussels/temperature x 9 temperatures = ≥ 36 mussels).

In the second approach (non-acclimated), mussels were acclimated to only a single temperature (21ºC), and tissue sampling was lethal. However, this approach required fewer mussels because the enzymes extracted from a single mussel were tested across all temperatures, yielding a separate thermal performance curve for each individual mussel. The temperature range tested could include and exceed the lethal range for mussels because only the extracted enzymes, not the mussels themselves, are exposed to each temperature. Methods for the two approaches are described in detail below.

Acclimated Mussels

Within 24 hours of respirometry measurements (see 2.1.C1), we randomly selected four mussels from each of the original six temperature treatments, gently pried their shells open, and

collected two, ~10 mg tissue plugs from the foot of each mussel using a nasal biopsy tool (Karl Storz nasal biopsy tool #453733) (Fritts et al. 2015). Tissue plugs were placed in cryovials and immediately frozen at -80ºC. An additional two mussels were randomly selected from each temperature, placed in a temperature-controlled upweller, and assigned to a new temperature of 20, 25, or 30ºC. Temperatures were raised or lowered at a rate of 1ºC/day until the target temperature was reached. Mussels were then acclimated for >1 week at the new target temperature and tissue plugs collected and stored in the same manner as described previously. Thus, we collected tissue plugs from four mussels/species acclimated for >1 week to each of 9 temperatures (15, 17, 20, 23, 25, 28, 30, 32, 36ºC). After tissue collection, all mussels were cooled back down to 18ºC at a rate of 1ºC/day and transferred back to the original upwellers to allow them to recover.

ETS activity of acclimated mussels was measured using standard methodologies adapted from Packard (1971) and Simcic et al. (2014). Frozen tissue plugs collected from a single mussel were weighed and placed in a 5 mL vial (note: vial could actually hold up to 7 mL) (self-standing sample tube, 5 mL, Globe Scientific via VWR, number 89497-730) filled to the 4 mL mark with 1.0 mm diameter glass beads (Biospec Products, Cat. No. 11079110) and containing 4 mL of homogenization buffer (0.1 M sodium phosphate buffer pH=8.4; 75 uM $MgSO_4$; 0.15% (w/v) polyvinyl pyrrolidone; 0.2% (v/v) Triton-X-100). Tissue was then homogenized with a BeadBeater (MiniBeadBeater-24; BioSpec Products, Inc., Bartlesville, OK) for 1 min and chilled for 1-2 min in a freezer. The beadbeating/chilling cycle was repeated for 3-4 cycles until tissue was thoroughly homogenized. The vial was then centrifuged for 4 min, at 10,000 rpm, at 0ºC in a refrigerated centrifuge (Allegra X-30R, Beckman Coulter, Brea, CA). Homogenate generated from a given mussel was placed in a flask, diluted to 2.5 mg tissue/mL using reagent grade DI

water (Ricca, cat# 9150-1), mixed with a stir bar, distributed amongst ~ 2 mL vials (Eppendorf$^{(R)}$ Safe-Lock microcentrifuge tubes (MCT), polypropylene) and frozen at -80^{o}C. Homogenate was stored for ≤ 6 weeks prior to measurement of ETS activity.

To measure ETS activity, two, replicate, 0.5 mL subsamples of thawed homogenate were each incubated in 1.5 mL substrate solution (0.1M sodium phosphate buffer pH = 8.4; 1.7mM NADH; 0.25 mM NADPH; 0.2% (v/v) Triton-X-100) with 0.5 mL INT solution (2.5mM 2-(p-iodophenyl)-3-(p-nitrophenyl)-5-phenyl tetrazolium chloride) for 30 minutes, in the dark, at the temperature to which the mussel had been acclimated. The reaction was then stopped by adding 0.5 mL of stopping solution (Formalin: H_3PO_4 = 1:1). A blank for the replicate samples was made by combining 1.5 mL substrate solution with 0.5 mL INT solution, and incubated and stopped along with the samples. Following addition of stopping solution, 0.5 mL of the corresponding homogenate was added to the blank. Absorbance (490 nm) of the replicate samples was measured with a spectrophotometer (Genesys 10S UV-VIS, ThermoScientific, Waltham, MA) and corrected for absorbance of the blank. ETS activity was calculated according to the following formula (Kenner and Ahmed, 1975):

$$\text{ETS activity } (\mu l\ O_2\ g^{-1}\ WW\ h^{-1}) = (ABS^{490nm} * V_h * V_r * 60)/(V_a * S * t * 1.42)$$

where ABS^{490nm} is the absorption of the sample corrected for blank; V_h is the volume of the homogenate (4 mL) prior to removal of subsamples; V_r is the volume of the reaction mixture (homogenate subsample + substrate solution + INT solution + stopping solution = 3mL); V_a is the volume of the homogenate subsample (0.5 mL); S is the mass of the tissue sample (g); t is the incubation time (min); 60 is a correction factor to convert the rate to hours, and 1.42 is the factor for conversion to volume O_2.

The mean ETS activity was then calculated for each acclimation temperature (~4 mussels per temperature), graphed against temperature, and fitted with a four-parameter Gaussian curve (SigmaPlot 13.0; Systat Software, Inc., San Jose, CA). Optimal temperature was defined as the temperature which exhibited the highest ETS activity. Optimal temperature range was defined as the temperature range within which ETS activity was within 10% of the maximum value.

Non-acclimated mussels

Following respiration measurements (see 2.1.C1), two mussels were randomly selected from each of six experimental temperatures, placed in temperature controlled upwellers, and brought to 21ºC at a rate of 1ºC / day. All mussels were held at 21ºC for at least 1 week. Following the > 1 week holding period, each mussel was sacrificed by severing the adductor mussels with a scalpel and opening the shell. Approximately 100 mg of foot tissue was immediately collected from each mussel using the nasal biopsy tool, and frozen at -80ºC. Tissue from each mussel was subsequently removed from the freezer and homogenized using the previously described beadbeater technique. Homogenate generated from a given mussel was combined in a flask, diluted to 2.5 mg tissue/mL using reagent grade DI water (Ricca, cat# 9150-1), mixed with a stir bar, distributed amongst ~ 1.8 mL vials and refrozen at -80ºC. ETS activity was subsequently measured following the same methodology as described above.

For each mussel, two replicate enzyme samples were incubated for 30 minutes at each temperature of interest, yielding a complete thermal performance curve (ETS activity vs temperature) for each individual. Initially, incubation temperatures were 12, 15, 17, 20, 23, 25, 28, 30, 32, and 36°C. Optimal temperatures for each individual was calculated using a four parameter Gaussian regression. Because optimal temperature data was not normally distributed,

we used a Kruskal-Wallis ANOVA on rank-transformed data to test for significant differences among species/location combinations (SigmaPlot 13.0, Systat Software, Inc., San Jose, CA, USA). Pairwise comparisons were conducted using Dunn's Method (SigmaPlot 13.0).

While analyzing samples for optimal temperature, we conducted some exploratory runs at temperatures >36ºC and found ETS activity did not decline symmetrically with increasing temperatures as would be described by a Gaussian curve. We hypothesized that the post-peak decline pattern might yield additional information regarding thermal stress. We therefore added temperatures of 39, 42, 45, 48, 51, 54, and 57ºC to the non-acclimated assay for remaining species and populations. We also added a cooler temperature (9ºC). We then used a 5-segment piecewise regression (SigmaPlot 13.0) to characterize the relationship between ETS activity and temperature during the decline following peak activity.

2.1.C2. Results

Acclimated Mussels

Optimal temperatures for ETS enzyme activity were higher for *C. petrina* from the Colorado (35.3ºC) and Guadalupe (34.6ºC) rivers than for *C. houstonensis* from the Colorado (31.6ºC) and Navasota (27.6ºC) rivers. Optimal range estimates predicted mussels would begin to experience enzymatic thermal stress at some point >36ºC for Colorado and Guadalupe River *C. petrina*, >35.8ºC for Colorado River *C. houstonensis*, and > 30.6ºC for Navasota River *C. houstonensis* (Fig. 7).

Because the acclimated approach generates only a single, composite, thermal performance curve for each species/location, we were not able to test for significant differences in optimal temperature between species or locations, nor were we able to assess variability in

optimal temperature among individuals within the same species/location group. To address these issues, we analyzed thermal performance curves for individual mussels using the non-acclimated approach.

Non-acclimated Mussels

ETS activity was strongly correlated with temperature for individual, non-acclimated mussels, with four parameter Gaussian regressions typically yielding an $R^2 > 0.90$ (see Fig. 8 for example; full set of graphs for other species/location combinations available upon request). Summary graphs (Fig. 9) show variation in curve height and optimal temperature (temperature at which curve peaks) within and among each species/location combination. Intraspecific variation in optimal temperature was highest for *C. petrina* from the Colorado River and lowest for *L. bracteata* (Llano River) and *C. houstonensis* (Navasota River) (Fig. 10). We expect curves for Llano Lake *Lampsilis bracteata* to be available prior to April 30, 2018.

There were significant differences in mean optimal temperature among the four candidate species tested (Kruskal-Wallis ANOVA: H=18.836, d.f.= 4, $P < 0.001$). Optimal temperature for *C. houstonensis* from the Colorado River was significantly higher than *C. houstonensis* (Navasota River), *C. petrina* (Guadalupe River), *L. bracteata* (Llano River), and *F. mitchelli* (Guadalupe River) (Dunn's Method, $P < 0.05$; Fig. 11). *Fusconaia mitchelli* (Guadalupe River) and *L. bracteata* had significantly lower optimal temperatures than *C. houstonensis* or *C. petrina* from the Colorado River (Dunn's Method, $P < 0.05$; Fig. 11). However, their optimal temperatures did not differ significantly from *C. houstonensis* from the Navaota River or C. *petrina* from the Guadalupe River (Dunn's Method, $P > 0.05$; Fig. 11).

There was evidence of differences in thermal optima between subpopulations of *C.*

houstonensis, but not between subpopulations of *C. petrina*. Optimal temperature of *C. houstonensis* from the Colorado River was significantly higher than that of *C. houstonensis* from the Navasota River (Dunn's Method, $P < 0.05$; Fig. 11), but optimal temperature of *C. petrina* from the Colorado River was not higher than that of *C. petrina* from the Guadalupe River (Dunn's Method, $P > 0.05$; Fig. 11).

There was no evidence that the four candidate species had lower thermal optima than two common species tested. *Amblema plicata* (Colorado River) had an intermediate optimal temperature, and *Lampsilis teres* (Colorado River) had a low optimal temperature relative to the four candidate species (Tables 3 and 4).

We measured activity of ETS enzymes from non-acclimated adult mussels at temperatures expected to exceed 24-hr lethal temperature (LT_{50}) thresholds for five species (Fig. 12). As temperatures increased above the thermal optimum, ETS activity did not decline in a linear fashion. Rather, each species exhibited a "shoulder" pattern where enzyme activity initially declined, then leveled off, then declined again. In a previous study, Marshall et al. (2011) showed that a bimodal pattern of snail respiration with increasing temperature was correlated with the onset of heat shock protein production and 24-hr LT_{50} thresholds. Because ETS activity represents the maximum potential respiration rate of an organism (Fanslow 2001), it is likely that similar endpoints are correlated with ETS activity patterns. We hypothesize that the point at which the decline in ETS activity begins to level off represents the activation of heat shock proteins – signaling the onset of major thermal stress and the transition from sublethal to lethal thermal stress. Preliminary comparison of independent LT_{05} (temperature at which 5% of animals die) data from the lab of Dr. Charles Randklev (Texas A&M University) is providing support for this hypothesis. We plan to continue this line of inquiry with Dr. Randklev in 2018.

The hypothesized breakpoint between sublethal and lethal effects was 38.9ºC for *C. petrina* from the Guadalupe River, 37.1ºC for *C. houstonensis* from the Navasota River, 29.4ºC for *L. teres* from the Colorado River, 31.0ºC for *F. mitchelli* from the Guadalupe River, and 36.0ºC for *A. plicata* from the Colorado River (Fig. 12).

2.1.C2. Conclusions:

Mussels acclimated to warm temperatures generally exhibited higher optimal temperatures than non-acclimated mussels (Table 4). However, optimal temperatures of non-acclimated mussels still fell within the optimal range of acclimated mussels – usually near the lower end of the range (Fig. 13, Table 4). The primary effect of acclimation appeared to be an increase in the upper portion of the optimal range rather than shifting the entire range. This suggests that in natural populations, a given mussel species will enter its optimal thermal range at approximately the same temperature threshold regardless of previous thermal history. However, mussels subjected to rapid, flashy increases in temperature will leave their thermal optima and start to experience thermal stress at lower temperatures than mussels subjected to gradual, stable increases in temperature. Intraspecific variation in non-acclimated optimal temperature (Fig. 10) was highest for *C. petrina* from the Colorado River, suggesting they may have a greater capacity to adapt to future fluctuations in temperature than species such as *L. bracteata* (Llano River) and *C. houstonensis* (Navasota River), which exhibited relatively low variation in optimal temperatures.

A summary of the estimated optimal and stressful temperatures for ETS enzymes of acclimated and non-acclimated mussels can be found in Table 4. While the ETS assay estimates optimal temperatures at the enzymatic level, corresponding estimates of optimal temperature

measured at the more complex organismal level (e.g. optimal scope for growth) may be cooler by 2-3º C (Simcic et al. 2014). Therefore, temperature ranges that are optimal or stressful to the organism as a whole are likely to be a few degrees lower than temperatures optimal or stressful to the organism's ETS enzymes.

Task 2.1.D. Effect of temperature on respiration of glochidia and juveniles.

Preliminary respirometry runs on *Ligumia subrostrata* glochidia have been conducted (see 2.1.A). Respirometry data from target species will be added as an addendum to this report by Aug. 31 2018 if glochidia and/or juveniles are available before that deadline.

Task 2.3 Effect of turbidity/suspended solids on valve closure of adult mussels

2.3 Objectives:

Mussels must keep their shells open to obtain food and oxygen from the surrounding waters. However, they often respond to stressors by closing their shells. Electromagnetic sensors attached to each valve can be used to monitor gaping and closing behavior and set off alarms when behavior indicates the presence of stressful toxicants in the water (Manley and Davenport 1979, Kramer et al. 1989, Gnyubkin 2009). Systems such as the MosselMonitor (www.mosselmonitor.nl; Kramer et al. 1989) and the Dreissena Monitor (Envicontrol Köln Germany; Borcherding, 1994) have been used to monitor stressors in fresh and saltwater environments in Europe. In this study, we used a MosselMonitor to determine whether mussels fully or partially close their valves in response to high turbidity/suspended solids – indicating negative impacts on feeding and respiration.

2.3. Methods:

Sediments

Sediments were obtained from a drained, 0.1 ha, earthen pond at the South Auburn Fisheries Research Station of Auburn University, Alabama. The top two inches of sediment were collected, mixed in a 5 gallon bucket, distributed into baking pans, and dried for 24 hrs at 105ºC. Dried sediment was passed through a #60 (250 μm) Fisher Scientific Company sieve and stored in an air tight 5-gallon bucket. This process was repeated until we had obtained enough sieved sediments to complete all trials. Stored sediment was mixed thoroughly via rolling and shaking in a closed container to ensure even distribution of particles immediately prior to each use. Soil analysis (T. Knappenberger, Auburn University) showed the sediments were composed of 53.5% sand (63 – 2000 μm), 46.6% silt (2.0-63 μm) and 0.0% clay (< 2.0 μm).

Experimental animals

Following respirometry experiments (see previous section), mussels were allowed to recover for > 4 weeks at 18ºC. Water temperature was then raised by 1ºC/day to the experimental temperature of 28ºC. Mussels were acclimated to this temperature for ≥ 1 week prior to initiation of experiments. During this time mussels were fed Shellfish Diet 1800 twice daily (2 mL morning, 1 mL afternoon per ~70 L upweller) and held at a 12h light: 12h dark cycle.

Experimental protocol

To monitor valve movements, mussels were held in individual, mesh bottom, plastic baskets (8 X 5 X 4 cm) screwed to the walls of a MosselMonitor (Flow through version,

AquaDect B. V.Brouwershaven, Netherlands). MosselMonitor settings, data downloads, and data display were controlled via PresentIT^{TM} 3.0 software on a connected desktop computer. The MosselMonitor was filled with HAFW and held at 28ºC. One valve of each mussel was glued (Unifast Trad Methylmethacrylate two part Resin GC America Inc. Alsip IL) to the plastic basket wall parallel to the side of the MosselMonitor. This ensured the mussel remained at a fixed distance from an electromagnetic sensor in the MosselMonitor wall. A second sensor was glued directly to the other valve of the mussel. Aquarium pea gravel was then added to the basket until half of the mussel was embedded in the substrate. Throughout the subsequent experiment, mussels were fed Shellfish Diet 1800 at the same rate as during the acclimation period. The Light:Dark cycle was held constant at 12:12.

Mussels were acclimated to the system for three days, during which time the MosselMonitor monitored distance between sensors and assessed the baseline maximum and minimum valve opening exhibited by each mussel. During the subsequent portions of the experiment, distance between valves (sensors) was reported as percent gape, based on the baseline maximum and minimum distances calculated during the acclimation period. Percent gape was calculated and recorded every 10 seconds for the remainder of the experiment. The first 24 hours following acclimation (Day 4) served as a control period, during which time food, but no sediment, was added to the MosselMonitor. The experimental period began on day 5. Sediment was added to a belt feeder located above a cone tank that was connected to the MosselMonitor. The belt feeder dropped sediment into the cone tank at a constant rate over a period of 10 hours. Sediment was suspended in the cone tank via a submersible Resun King-2 pump (1000 L/hr) and multiple air stones. A second submersible Resun King-2 pump transferred water and suspended sediments to the MosselMonitor at a constant rate of 360 L/hr.

Flexible tubing returned water at the same rate to the cone tank via ambient head pressure. A LaMotte 2020we turbidimeter was used to measure turbidity in replicate 10 mL samples collected immediately after mussel attachment (0 h), at the start of the control period (72 h), every hour for the first 12 hours of the experimental period (hrs 96-108), and at the end of the experimental period (hr 120). Supplemental samples were periodically collected to quantify TSS concentrations. A ~250 mL sample was siphoned from the center of the MosselMonitor. The siphon tube was attached to the MusselMonitor prior to the experiment so that subsequent samples could be collected without disturbing mussels. Sample water was filtered through a pre-ashed (1 hr at 550ºC) 1.2 µm Whatman 47 mm glass microfiber filter to collect sediments. Filters were then dried overnight at 105ºC and weighed. Filter weight was subtracted from total weight and then divided by sample volume to calculate TSS in mg dry weight/liter.

This protocol resulted in an initial ~6-hour ramping period (9:00 – 15:00 hrs) on Day 5 during which suspended solid concentration in the MosselMonitor increased with time as the rate at which sediment was added to the system exceeded the rate at which sediment settled within the system. Equilibrium between sediment addition and settlement was reached within 5-6 hrs, after which time total suspended solids (TSS) concentrations remained relatively stable for the remaining four hours (15:00 – 19:00 hrs) of the run (Fig. 14 bottom panels). Mussels were exposed to one of two treatments, with two runs per treatment. Different mussels were used for each run. Within each run, sufficient sediment was added to the belt feeder to allow turbidity to ramp up to the target level. During our first three runs, we set a high turbidity target of ~25 NTU (~70 mg TSS/L), intending to reduce turbidity in subsequent runs. However, due to the lack of obvious effects on valve closure even under high turbidity conditions (see results), we changed

our subsequent runs to target excessive turbidity levels of ~70 NTU (~ 250 mg TSS/L) for the two final runs (Fig. 14).

2.3. Results

Individuals of both species exhibited highly variable relationships between percent gape and turbidity during the ramping periods when turbidity increased from 0 to 25 or 65-75 NTU's over a 6-hr period (Figs. 15-18). During the excessive turbidity ramping period, mean percent gape of all *C. petrina* combined exhibited a negative linear relationship with turbidity (Figure 19 top panel: $R^2 = 0.53$, $P < 0.0001$, mean percent gape = 59.3214 – 0.1478*NTU). Mean percent gape during the high turbidity ramping period showed a similar negative relationship with turbidity, albeit with a steeper slope (Fig 19 top panel: $R^2 = 0.83$, $P < 0.0001$, mean percent gape = 62.7746 – 0.4654*NTU).

During the excessive turbidity ramping period, mean percent gape of all *C. houstonensis* combined exhibited a significant positive linear relationship with turbidity, but turbidity explained very little of the variation in valve gape (Figure 19 bottom panel: $R^2 = 0.064$, $P < 0.0001$, mean percent gape = 45.8459 + 0.0451*NTU). Mean percent gape during the high turbidity ramping period showed a significant, negative linear relationship with turbidity, but, again, turbidity explained very little of the variation in gape (Fig. 19 bottom panel: $R^2 = 0.040$, $P < 0.0001$, mean percent gape = 63.9433 - 0.1675*NTU).

During the constant turbidity period of the high treatment (~25 NTU), there was little to no evidence that turbidity resulted in decreased gape for either species. Exposed *C. petrina* exhibited less frequent gape values exceeding 65% than control mussels but percent gape peaked

at 65% in both groups. Gape of exposed *C. houstonensis* peaked at a higher value (75%) than control *C. houstonensis* (55%) (Fig. 20).

During the constant turbidity period of the excessive treatment (60-75 NTU), there was evidence that gape decreased slightly for both species. Gape peaked at 65% in exposed *C. petrina* compared to 75% for control mussels. Gape peaked at 65% in exposed and control *C. houstonensis*, but very few exposed mussels gaped more than 65% compared to control mussels (Fig. 21).

2.3. Conclusions:

Because mussels obtain food and oxygen from surrounding water, there was concern that high concentrations of suspended solids may trigger valve closure by mussels, with subsequent, negative effects on feeding and respiration. However, we found little to no evidence that exposure to suspended solids, even at high (turbidity ~25 NTU; TSS ~70 mg/L) or excessive (turbidity ~75 NTU, TSS ~250 mg/L) concentrations resulted in valve closure. As turbidity increased, *C. petrina* exhibited only a small reduction in mean percent gape. Increasing turbidity explained very little of the variation in percent gape for *C. houstonensis*. Under conditions of excessive turbidity, mussels appeared to close valves slightly, but the peak in percent gape remained high at 65% as compared to a peak of 65-75% during the preceding control period. If high suspended solids have a negative effect on mussel feeding rates or ability to obtain oxygen, the mechanism behind negative effects is not likely to be valve closure.

2.2 Sublethal effects of nitrogenous compounds and salinity on adult mussels

2.2A. Effect of Ammonia on Respiration.

2.2A. Objectives:

In 2013, the U.S.EPA updated its Aquatic Life Ambient Water Quality Criteria for Ammonia – Freshwater in order to take into account data for highly sensitive unionid mussel and non-pulmonate snail species that had not previously been tested (USEPA 2013). Because ammonia toxicity issues are fairly complex, a brief explanation is provided here.

Ammonia in surface waters is typically reported as total ammonia nitrogen (TAN). This refers to the combined concentration of nitrogen (mg/L) occurring in two co-existing forms of ammonia – ionized (NH_4^+) and un-ionized (NH_3). Un-ionized ammonia is the most toxic form. The proportion of un-ionized to unionized (NH_3: NH_4^+) ammonia increases with increasing pH and temperature. Thus ammonia becomes more toxic with increases in temperature and/or pH even if the concentration of ammonia, measured as TAN, remains the same. The U.S.EPA 2013 ammonia benchmark is 17 mg TAN/L for acute (1 hour average) exposure and 1.9 mg TAN/L for chronic (30-d rolling average) exposure. These benchmarks are referred to as "criterion maximum concentrations" (CMC) and represent a concentration that is expected to be lethal to <50% of individuals in sensitive species. They specifically apply to a pH of 7 and a temperature of 20ºC. In many Texas rivers, pH is typically ≥8 and temperatures rise well above 20ºC during the summer months. The toxicity of 17 (acute) and 1.9 (chronic) mg TAN/L benchmark concentrations would therefore increase and may no longer be sufficiently protective of unionid mussels. The USEPA is cognizant of this issue and provides tables to adjust benchmark concentrations for specific temperature and pH values (see tables 5b, 6 in USEPA 2013).

Unionized ammonia can affect organisms such as mussels via multiple mechanisms that include increased ventilation rates (volume of water passing through gills per unit time), gill damage, and a reduction in the ability of blood (hemolymph) to carry oxygen. Thus it is

reasonable to expect that metabolic and respiration patterns would be sensitive to ammonia. The objectives of this study were to determine whether ammonia affected metabolic patterns of mussels by 1) reducing their ability to regulate oxygen consumption, 2) increasing their DO_{crit}, and 3) altering their resting metabolic rate. Note that this task was completed last due to the high probability of significant sublethal and lethal effects on experimental mussels when exposed to ammonia.

2.2A. Methods:

Following turbidity assays described in previous sections, *C. petrina* and *C. houstonensis* from the Colorado River were allowed to recover for ≥ 2 weeks at 28ºC prior to initiation of ammonia experiments. During this time, they were fed Shellfish Diet 1800 according to the standard feeding regime (2 mL morning, 1 mL afternoon, per 70 L upweller). Due to a limited number of mussels remaining from the original collections, we were only able to test 5-6 individuals of *C. petrina*, and 6 individuals of *C. houstonensis* per ammonia treatment, prior to preparation of this report. Each mussel was exposed to only a single ammonia treatment. Thus we tested a total of 16 *C. petrina* and 18 *C. houstonensis*.

Resting metabolic rates (RMR) were measured at 28ºC using the same respirometry system described in section B of this chapter. Mussels were starved for 24 hrs prior to experiments to prevent feeding and digesting from affecting metabolism. Following the starvation period, sufficient ammonia from a stock solution (Hach ammonia standard, 1,000 mg TAN/L) was added to the respirometry trough to bring it to the target concentration of 0.5 or 2.0 mg TAN/L. No ammonia was added to the trough for the control runs. Ammonia concentrations in the respirometry trough were measured using a YSI 9300 Photometer (YSI Inc. 2017) at the

beginning and end of each experiment to ensure the target concentration had been reached and remained stable throughout the duration of each trial. The moderate concentration, (0.5 mg TAN/L) was selected to represent the average concentration that we observed in our respirometry chambers following a standard, closed respirometry experiment (section B). The higher concentration represents the 2013 USEPA CCC chronic criteria of 1.9 mg TAN / L at pH 7, 20ºC. Note that in our experiments temperature was 28ºC, and pH was ~8.5. Under these conditions, the recommended acute and chronic benchmarks (CMC; Tables 5b and 6 in USEPA 2013) are adjusted downward to 0.77 (acute) and 0.21 (chronic) mg TAN/L. Thus the highest TAN concentration in our study exceeded both the acute and chronic benchmarks adjusted for pH and temperature.

Mussels were acclimated to respiration chambers for ≥ 5 hrs. During this time both the flush and closed pumps were turned on to ensure oxygenated water containing the appropriate ammonia concentration circulated through chambers and tubing. Following acclimation, flush pumps were turned off, and only the closed pumps remained on - creating a closed system where the volume of water recirculating within each chamber and associated tubing was constant, and no new, oxygenated, water entered the system.

Because mussels excrete ammonia as a waste product, and this ammonia can build up in closed respirometry chambers over time, we periodically flushed chambers during a respirometry run to ensure that ammonia levels remained fairly constant during each trial. The modified respirometry protocol was as follows: After allowing closed respirometry to run for 50 minutes, nitrogen gas was bubbled into the trough water (external to the submerged respirometry chambers) using DO-SET software (Loligo Inc.), until DO had fallen from 7 to 5 mg O_2/L. Previous closed respirometry trials at 28ºC (section 2.1.C1) using the same two mussel species

yielded a decrease of approximately 2 mg O_2 per hour within the respiration chambers. At 60 minutes, the flush pumps were turned on and chambers flushed for 5 minutes with ~5 mg O_2/L water from the trough in order to flush out any ammonia excreted by the mussels that would otherwise increase ammonia levels above the targeted trial concentration. Flush pumps were then turned off to once more create a closed system at the target ammonia concentration. After 50 minutes DO in the trough was reduced from 5 to 3 mg O_2/L, and ten minutes later chambers were flushed again for 5 minutes. Flush pumps were then turned off and mussels allowed to draw DO down from 3 to < 0.2 mg O_2/L at which time the trial was terminated. This technique yielded a relationship between resting metabolic rate (RMR) and dissolved oxygen (e.g. Fig. 22) that could be analyzed for regulation index and DO_{crit} using the same methodology as described in task 2.1.C1, while at the same time avoiding problems associated with accumulating ammonia in closed respiration chambers.

2.2A Results:

TAN of the respirometry water matched the nominal treatment TAN concentrations fairly well and remained stable throughout the experiment. Background levels within the control treatment ranged from 0.04 to 0.1 mg TAN / L. Respirometry water pH ranged from 8.4 to 8.6 (Table 5).

The proportion of individuals exhibiting valve closure (cessation of respiration) increased with increasing TAN for both species, and was more frequent in *C. petrina* than *C. houstonensis* (Fig. 23). Because accurate RMR, RI, and DO_{crit} values could not be calculated for individuals that closed during respirometry, we did not have enough usable respiration curves to test for effects of TAN on these endpoints for *C. petrina*. For *C. houstonensis*, valve closure eliminated

only four individuals from the experiment, yielding 4-5 replicate estimates of these endpoints for each TAN treatment. There was no significant effect of TAN on RMR (ANOVA: $F = 2.528$, df = 2, 11; $P = 0.125$), RI (ANOVA: $F = 1.988$; df = 2, 11; $P = 0.183$), or DO_{crit} (ANOVA: $F = 1.178$, df = 2, 11; $P = 0.344$) (Fig. 24).

2.2A Conclusions:

At a pH of 8.5 and temperature of 18 C, the USEPA ammonia benchmarks are revised downward from 17 to 0.77 mg TAN/L for acute (1 hour average) exposure and from 1.9 to 0.21 mg TAN/L for chronic (30 day rolling average) exposure (see Tables 5b and 6 in USEPA 2013). In our study, mussels were exposed to treatment TAN concentrations exceeding both of these benchmarks for ~10 hours. Results suggest that the revised benchmarks are sufficient to protect *C. houstonensis* from short term effects of ammonia on metabolic rate (RMR) and ability to extract oxygen even under low oxygen conditions (RI and DO_{crit}). However it remains to be tested whether chronic (30 day) exposure would affect metabolism. Also, the revised benchmarks may not be sufficient to protect mussels from increased frequency of valve closure (see Fig. 23) which could affect respiration, filtration, and fertilization efficiency during long term exposure. Future studies examining effects of chronic exposure to TAN concentrations matching and exceeding the revised chronic benchmarks on metabolism and valve closure are warranted.

A major challenge of working with rare species is having a sufficient sample size to be able to detect significant differences between treatments. In the case of the ammonia studies, the sample sizes were low, increasing the chances of us not finding an effect of ammonia when one existed. We performed a power analysis (G*Power 3.1.9.2; Faul et al. 2007) to determine 1) the

difference between treatments that we had a ≥ 80% chance of detecting with the current sample size, and 2) the minimum number of samples (mussels) required to have a ≥ 80% chance of detecting a specific difference between treatments. Given our sample size of 5 individuals/treatment and the observed variance among individuals, we had a ≥ 80% chance of detecting a change of 0.004 mgO_2/gWW/hr in RMR, a change of 0.15 in RI, and a change of 1.0 mg O_2/L in DO_{crit} among treatments. In future studies, if we want to double the sensitivity of our assays (i.e. reduce the detectable difference by half) and thus have a ≥ 80% chance of detecting a change of 0.002 mgO_2/gWW/hr in RMR, 0.075 in RI, and 0.5 mg O2/L in DO_{crit}, we would need sample sizes of at least 17, 10, and 18 mussels/treatment respectively. We are currently evaluating our remaining mussel stocks and may be able to conduct additional ammonia trials with *C. petrina* and *houstonensis*. If so, data will be included in a future addendum, no later than August 2018.

A legitimate concern regarding closed respirometry techniques, such as those employed in task 2.1.C1 (thermal tolerance), is that a buildup of metabolic wastes might affect respiration rates and patterns measured in the chambers. However, these potential effects are not well understood and have not been previously tested for freshwater mussels. In our closed respirometry experiments, accumulation of metabolic-waste ammonia in closed chambers rarely exceeded 0.5 mg TAN/L and never reached 2mg TAN/L. The lack of a significant effect of 0.5-2 mg TAN/L on respiration rates, RI, or DO_{crit} in of *C. houstonensis* in the current experiment (Task 2.2A) suggests that accumulation of metabolic wastes did not affect our estimates of these parameters in the thermal tolerance experiments (Task 2.2.C1).

2.2B. Effect of salinity on adult mussel valve closure

Mussels must keep their shells open to obtain food and oxygen from the surrounding waters. However, they often respond to stressors by closing their shells. Electromagnetic sensors attached to each valve can be used to monitor gaping and closing behavior, setting off alarms when behavior indicates the presence of stressful toxicants in the water (Manley and Davenport 1979, Kramer et al. 1989, Gnyubkin 2009). Systems such as the MosselMonitor (www.mosselmonitor.nl; Kramer et al. 1989) and the Dreissena Monitor (Envicontrol Köln Germany; Borcherding, 1994) have been used to monitor stressors in fresh and saltwater environments in Europe. Valve movements have been recommended as a sublethal, behavioral endpoint for stressors such as chloride (Hartmann et al. 2016). In this experiment, we use a MosselMonitor to determine whether mussels fully or partially close their valves in response to increasing salinity – indicating negative impacts on feeding and respiration.

Experimental animals

Following respirometry experiments (see section 2.1.C1), *C. petrina* (Guadalupe River) and *C. houstonensis* (Navasota River) were allowed to recover for > 4 weeks at 18ºC. Water temperature was then raised by 1ºC/day to the experimental temperature of 28ºC. Mussels were acclimated to this temperature for ≥ 1 week prior to initiation of experiments. During this time mussels were fed Shellfish Diet 1800 twice daily (2 mL morning, 1 mL afternoon per ~70 L upweller) and held at a 12h light: 12h dark cycle.

Experimental protocol

To monitor valve movements, four mussels of each species (eight mussels total) were placed in the MosselMonitor and sensors attached to their valves following the same methodology as described for the suspended solids experiment (section 2.3). Mussels were acclimated to the system for three days, during which time the MosselMonitor assessed distance between sensors and calculated the baseline maximum and minimum valve opening exhibited by each mussel. During the subsequent portions of the experiment, distance between valves (sensors) was reported as percent gape, based on the baseline maximum and minimum distances calculated during the acclimation period. Percent gape was calculated and recorded every 10 seconds for the remainder of the experiment.

The first 24 hours following acclimation (Day 4) served as a control period, during which time food, but no salt, was added to the MosselMonitor. The experimental period began on Day 5. A belt feeder dropped salt (Diamond Crystal pool salt; Cargill Inc., Minneapolis, MN) into the cone tank at a constant rate of 27.3 g/hr over a period of 11 hours. Salt was mixed in the cone tank via a submersible Resun King-2 pump (1000 L/hr) and multiple air stones. A second submersible Resun King-2 pump transferred saltwater to the MosselMonitor at a constant rate of 360 L/hr. Flexible tubing returned water at the same rate to the cone tank via ambient head pressure. A PinPoint Salinity Monitor (American Marine Inc., Ridgefield, CT) was used to measure salinity at the time of attachment, start of the control period, and every hour during the beginning of the experimental period. The salinity meter's probe was held in the cone tank to make sure the mussels were not disturbed. Previous trials determined that the salinity in the cone tank and the MosselMonitor were equivalent due to constant flow between the two units. This protocol resulted in an 11-hour ramping period (9:00 – 20:00) during which salinity rose linearly with time from a low of <1 ppt to a high of ~4ppt at a rate of ~0.3ppt/h (Fig. 25).

2.2B Results

Six of the eight *C. petrina* (Guadalupe River) were >50% open at the beginning of the experimental period. Each exhibited a period of steady decline in percent gape with increasing salinity until valves were completely closed or nearly so. One individual subsequently re-opened to 50%, but quickly closed again (Fig. 26). Similarly, six of the eight *C. houstonensis* (Guadalupe River) were >50% open at the beginning of the experimental period. Each exhibited a subsequent period of steady decline in percent gape with increasing salinity, but degree of closure was more variable than for *C. petrina*, with more individuals exhibiting >10% gape at high salinities (Fig. 27). On average, *C. petrina* exhibited a steady decline in percent gape as salinity levels increased beyond 2.0 ppt, with a final mean gape of < 5% whereas *C. houstonensis* exhibited a steady decline in percent gape as salinity increased beyond 2.5 ppt and mean gape subsequently leveling out at ~35% as salinity increased from 3.0 to 4.0 ppt (Fig. 28).

2.2B Conclusions:

Previous studies have shown that adult mussels (*Elliptio complanata*) exposed to 6 and 4 ppt exhibited 50% mortality by day 3 and 4 respectively, while mussels exposed to 2 ppt exhibited reduced metabolic rates but no mortality after 28 days (Blakeslee et al. 2013). Our results suggest that a reduction in gape and/or complete closure, and resultant reduction and/or cessation of water flowing past the gills is a likely mechanism driving reduced metabolic rates (i.e. respiration) as salinity increases. Valve closure would also be expected to interfere with feeding and fertilization success. These sublethal impacts of salinity >2 ppt are likely greater for *C. petrina* than *C. houstonensis* as they exhibited an earlier and steeper decline in gape.

In our study, mussels were exposed to salinities ≥2 ppt for less than 6 hours and exhibited zero mortality during the experiment or within 7 days of being transferred back to freshwater. However, if high salinity conditions were sustained over a long period of time, lethal effects of high salinity might occur more quickly for *C. houstonensis* due to increased exposure. They did not close valves as tightly and appeared to reopen to a greater degree than *C. petrina* as salinity approached LC_{50} (4ppt, 7d) concentrations reported by Blakeslee et al (2013).

We are currently analyzing results of a similar salinity experiment run on *L. bracteata* (Llano Lake). Results will be included in an addendum to this report prior to August 2018.

References

Anestis, A., A. Lazou, H.O. Portner, and B. Michaelidis. 2007. Behavioral, metabolic, and molecular stress responses of marine bivalve *Mytilus galloprovincialis* during long-term acclimation at increasing ambient temperature. Comparative and Evolutionary Physiology. 293(2):R911-R921.

Blakeslee, C.J., H.S. Galbraith, L.S. Robertson, and B. St. John White. 2013. The effects of salinity exposure on multiple life stages of a common freshwater mussel, *Elliptio complanata*. Environmental Toxicology and Chemistry 32(12):2849-2854.

Elderkin, C.L., D.W. Schneider, J.A. Stoeckel, and D.K. Padilla. 1998. A method for measuring in situ oxygen consumption rates of freshwater gastropods. Journal of the North American Benthological Society 17(3):338-347.

Fanslow, D.L., T.F. Nalepa, and T.H. Johengen. 2001. Seasonal changes in the respiratory electron transport system (ETS) and respiration of the zebra mussel, *Dreissena polymorpha* in Saginaw Bay, Lake Huron. Hydrobiologia 448:61-70.

Faul, F., E. Erdfelder, A.G. Lang, and A. Buchner. 2007. G*Power 3: A flexible statistical power analysis program for the social, behavioral, and biomedical sciences. Behavior research methods 39(2):175-191.

Fritts, A.K., J.T. Peterson, P.D. Hazelton and R.B. Bringolf. 2015. Evaluation of methods for assessing physiological biomarkers of stress in freshwater mussels. Canadian Journal of Fisheries and Aquatic Sciences 72:1450-1459.

Gnyubkin, V. F. 2009. An early warning system for aquatic environment state monitoring based on an analysis of mussel valve movements. Russian Journal of Marine Biology 35: 431436.

Hartmann, J.T., S.B. Beggel, K. Auerswald, and B.C. Stoeckle. 2016. Establishing mussel behavior as a biomarker in ecotoxicology. Aquatic Toxicology. 170:279-288.

Kenner, R.A. and S.I. Ahmed. 1975. Measurements of electron transport activities in marine phytoplankton. Marine Biology 33:119-127.

Kramer, K. J. M., H. A. Jenner, and D. Dezwart. 1989. The Valve Movement Response of Mussels - A Tool In Biological Monitoring. Hydrobiologia 188: 433-443.

Madon S.P., D.W. Schneider, and J.A. Stoeckel. 1998. In situ estimation of zebra mussel metabolic rates using the electron transport system (ETS) assay. Journal of Shellfish Research 17(1):195-203.

Manley, A. R., and J. Davenport. 1979. Behavioral-Responses of Some Marine Bivalves to Heightened Seawater Copper Concentrations. Bull. Environ. Contam. Toxicol. 22: 739744.

Marshall, D.J., Y. Dong, C.D. McQuaid, and G.A. Williams. 2011. Thermal adaptation in the intertidal snail *Echinolittorina malaccana* contradicts current theory by revealing the crucial roles of resting metabolism. Journal of Experimental Biology 3649-3657.

Mueller, C.A. and R.S. Seymour. 2011. The regulation index: A new method for assessing the relationship between oxygen consumption and environmental oxygen. Physiological and Biochemical Zoology 84(5):522-532.

Packard, T.T., M.L. Healy, and F.A. Richards. 1971. Vertical distribution of the activity of the respiratory electron transport system in marine plankton. Limnology and Oceanography 16(1):60-70.

Owens, T.G. and F.D. King 1975. The measurement of respiratory electron-transport-system activity in marine zooplankton. Marine Biology 30:27-36.

Simcic T., F. Pajk, M. Jaklic, A. Brancelj and A. Vrezec. 2014. The thermal tolerance of crayfish could be estimated from respiratory electron transport system activity. Journal of Thermal Biology 41:21-30.

Smith, M.E., J. M. Lazorchak, L.E. Herrin, S. Brewer-Swartz, and W.T. Thoeny. 1997. A reformulated, reconstituted water for testing the freshwater amphipod, Hyallela azteca. Environmental Toxicology and Chemistry 16(6):1229-1233.

USEPA. 2013. Aquatic Life Ambient Water Criteria for Ammonia – Freshwater. United States Environmental Protection Agency, Office of Water. EPA 822-R-13-001.

Table 1. Species, collection sites, and shipping information for mussels used in thermal and hypoxia tolerance experiments at Auburn University.

Species	Drainage	Site	Collection Date	# shipped	Collection Temp. (°C)	Receiving Temp. (°C)
Cyclonaias petrina	Colorado River	Altair	4/28/2017	6		*NT*
			5/17/2017	33		16.2
		Lometa	6/1/2017	11	26.6	22.0
	Gauadalupe River	Gonzales	11/01/2017	14	18	16.9
		Gonzales	8/17/2017	32	30.9	23.5
Cyclonaias houstonensis	Colorado River	Altair	4/27/2017	6		*NT*
			5/17/2017	50		16.4
	Navasota River	Easterly	7/17/2017	50		22.6
Lampsilis bracteata	Llano River	Mason	5/31/2017	20	23	15.3
		Llano Park Lake	11/01/2017	50	Stranded, 13.7	15.1, 14.4
Fusconaia mitchelli	Guadalupe River	Gonzales	8/17/2017	6	30.9	23.5
			11/01/2017	4	18	16.9
Truncilla macrodon	Brazos River	Highbank	12/4/2017	7	19	*NT*
Amblema plicata	Colorado River	Altair	4/27/2017	12		*NT*
			8/4/2017	20	31	21.7
Lampsilis teres	Colorado River	Altair	11/02/2017	12	18	*NT*

Table 2. Optimum temperature and optimum range for acclimated ETS activity. Prior to ETS measurement, individuals were acclimated for >1 week to each of 10 temperatures from 15 – 36ºC.

Species	**Drainage**	**Optimum**	**Range**
Cyclonaias petrina	Colorado River	35.3	28.2 - >36
	Gauadalupe River	34.6	26.5 - >36
Cyclonaias houstonensis	Colorado River	31.6	27.5 – 35.8
	Navasota River	27.6	24.8 – 30.6

Table 3. Optimal temperature data for non-acclimated mussels. Individuals were all acclimated for >1 week to 21ºC. Enzymes were then extracted from foot tissue of each individual and incubated at each of 9 temperatures ranging from 12 – 36ºC, generating a separate thermal performance curve for each individual (see Fig. 9). Min and max refer to the minimum and maximum optimal temperatures among all individuals within each species X drainage combination.

Species	**Drainage**	**Mean**	**Min**	**Max**	**Stdev**	**CV**	**n**
Cyclonaias petrina	Colorado River	30.2	28.6	34.8	1.7	5.7	12
	Gauadalupe River	28.5	27.6	29.5	0.7	2.6	6
Cyclonaias houstonensis	Colorado River	30.5	28.3	32.1	1.1	3.7	11
	Navasota River	28.8	27.7	29.8	0.6	2.0	12
Lampsilis bracteata	Llano River	28.4	27.6	29.1	0.6	2.1	11
	Llano Lake	*April 2018*					
Fusconaia mitchelli	Guadalupe River	27.8	26.5	28.8	0.9	3.3	6
Amblema plicata	Colorado River	28.4	27.5	29.0	0.5	1.6	10
Lampsilis teres	Colorado River	27.1	27.9	26.2	0.6	2.1	12

Table 4. Summary of ETS enzyme thermal tolerance endpoints from acclimated and non-acclimated experiments. Optimal Range for acclimated mussels represents the temperature range where ETS activity was within 10% of the observed maximum rate, whereas for non-acclimated mussels it represents the range in optimal temperatures estimated for individual mussels. The upper end of the acclimated range indicates the temperature threshold above which we predict the initiation of thermal stress at the enzymatic level for at least some individuals in the population. The upper end of the non-acclimated range represents the maximum optimal temperature observed for enzymes subjected to a sudden increase in temperature. Onset of lethal effects indicates the temperature threshold beyond which we predict the onset of mortality due to thermal stress. Months indicate when we expect additional information will be available. Blank cells indicate no results due to a lack of samples and/or animals. All temperatures are ºC.

Species	**Drainage**	**Optimal Temp.**	**Optimal Range**	**Estimated onset of lethal effects**	**Assay Type**
Cyclonaias petrina	Colorado River	35.3	28.2 - >36		Acclimated
		30.2	28.6-34.8		Non-acclimated
	Gauadalupe River	34.6	26.5 - >36		Acclimated mussels
		28.5	27.6-29.5	38.9	Non-acclimated
Cyclonaias houstonensis	Colorado River	31.6	27.5 – 35.8		Acclimated mussels
		30.5	28.3-32.1		Non-acclimated
	Navasota River	27.6	24.8 – 30.6		Acclimated mussels
		28.8	27.7-29.8	37.1	Non-acclimated
Lampsilis bracteata	Llano River	28.4	27.6-29.1		Non-acclimated
	Llano Lake				Acclimated mussels
		May	***May***	***May***	Non-acclimated
Fusconaia mitchelli	Guadalupe River	27.8	26.5-28.8	31.0	Non-acclimated
Amblema plicata	Colorado River	28.4	27.5-29.0	36.0	Non-acclimated
Lampsilis teres	Colorado River	27.1	26.2-27.9	29.4	Non-acclimated

Table 5. Total ammonia nitrogen (TAN) and pH measurements in respirometry water for individual runs within ammonia treatments.

		TAN (mg/L)		**pH**	
Run	*Treatment*	*Initial*	*Final*	*Initial*	*Final*
1	0	0.05	0.4	8.6	8.6
2	0	0.1	0.1	8.6	8.6
1	0.5	0.60	0.43		8.4
2	0.5	0.66	0.30	8.6	8.5
1	2.0	2.40	2.08	8.6	8.4
2	2.0	2.16	1.76	8.5	8.4

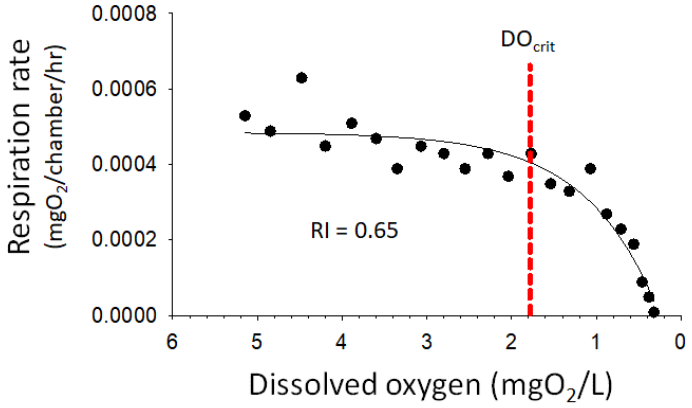

Figure 1. Example of preliminary data showing respiration pattern of *L. subrostrata* glochidia subjected to declining dissolved oxygen. Regulation index (RI) and DO_{crit} values could be calculated for glochidia and were similar to that observed for adult mussels.

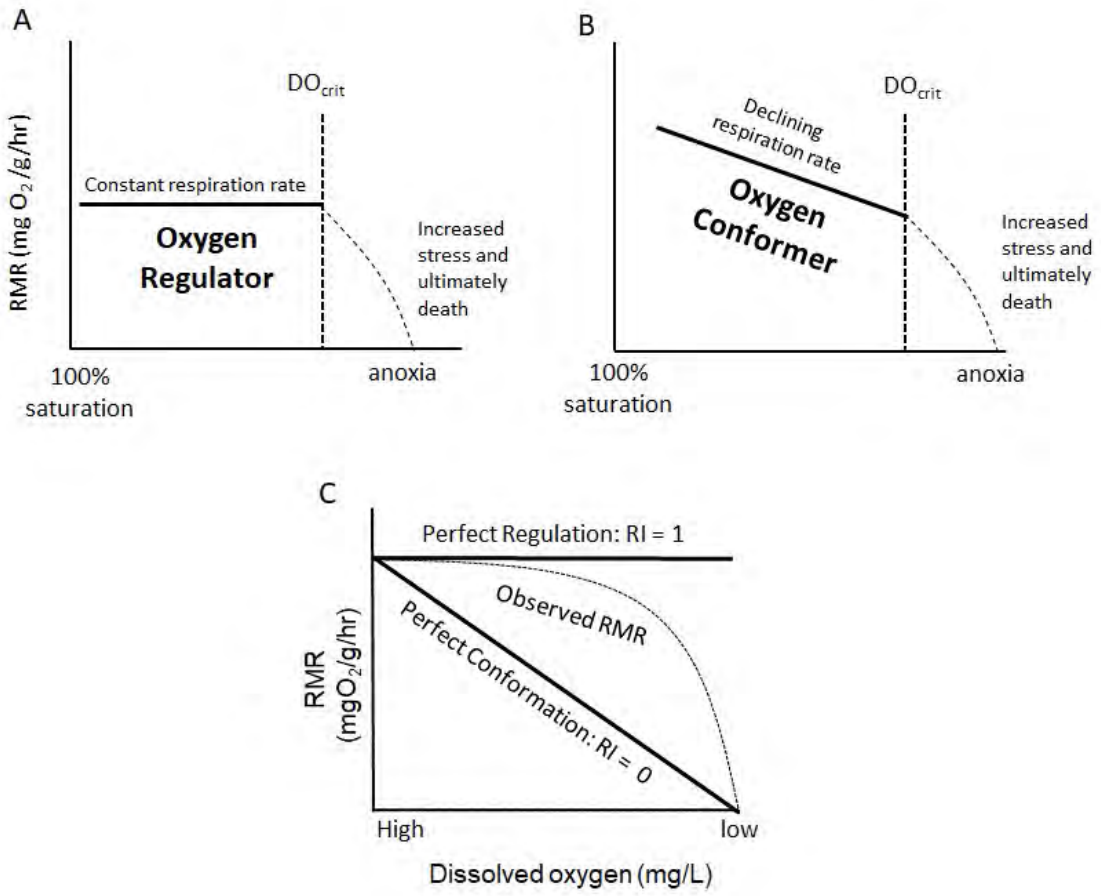

Figure 2. Resting metabolic rates (RMR) graphed as a function of declining dissolved oxygen showing A) an oxyregulator and B) an oxyconformer. DO_{crit} is the DO threshold below which respiration rates show a marked decrease or increase, indicating the switch from aerobic to anaerobic respiration. C) RMR graphed as a function of DO indicating the range of values of the Regulation Index (RI; Mueller and Seymour 2011). Solid lines indicating either perfect regulation (RI = 1) or perfect conformation (RI = 0) and dashed line indicates an intermediate, typically observed pattern that falls between perfect regulation and perfect conformation.

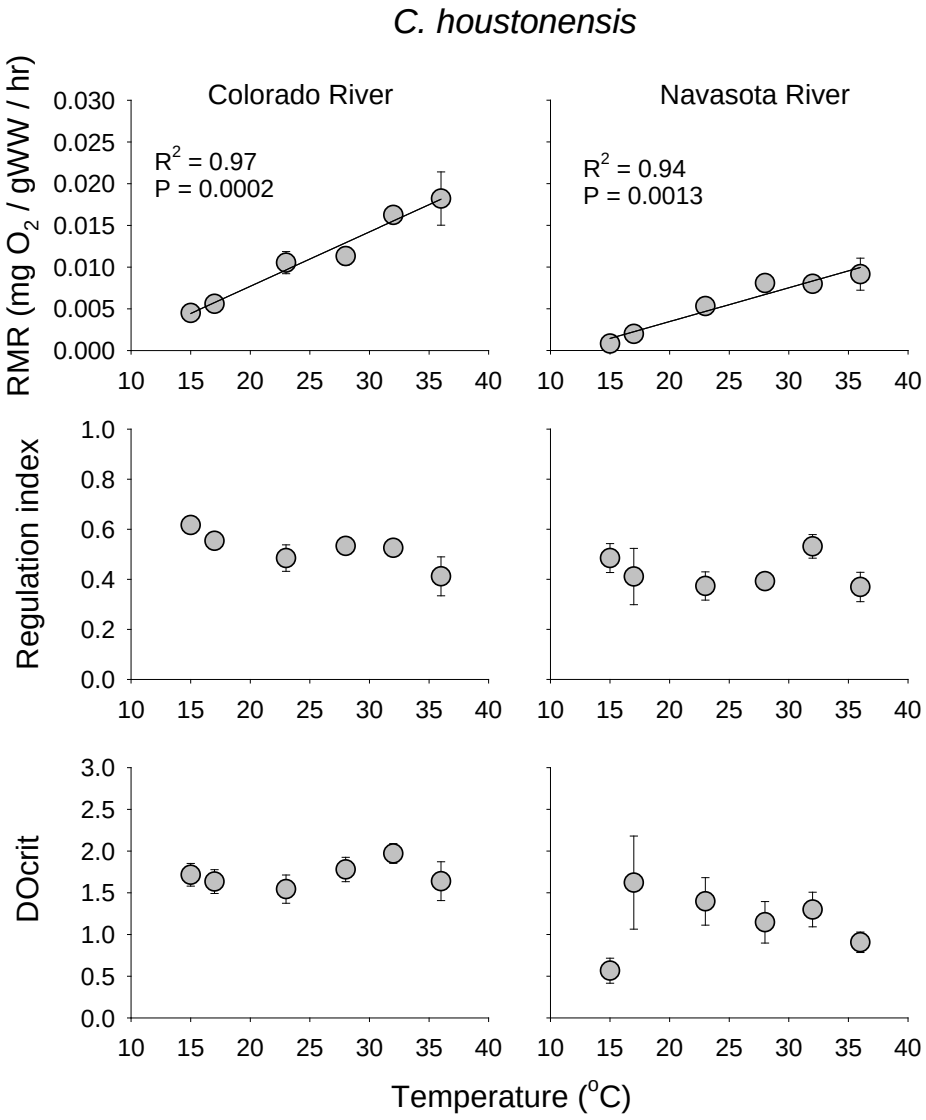

Figure 3. Relationships between resting metabolic rate (RMR), regulation index, DO_{crit} and temperature for *C. houstonensis* collected from two drainage basins. Neither regulation index nor DO_{crit} yielded a significant linear relationship with temperature.

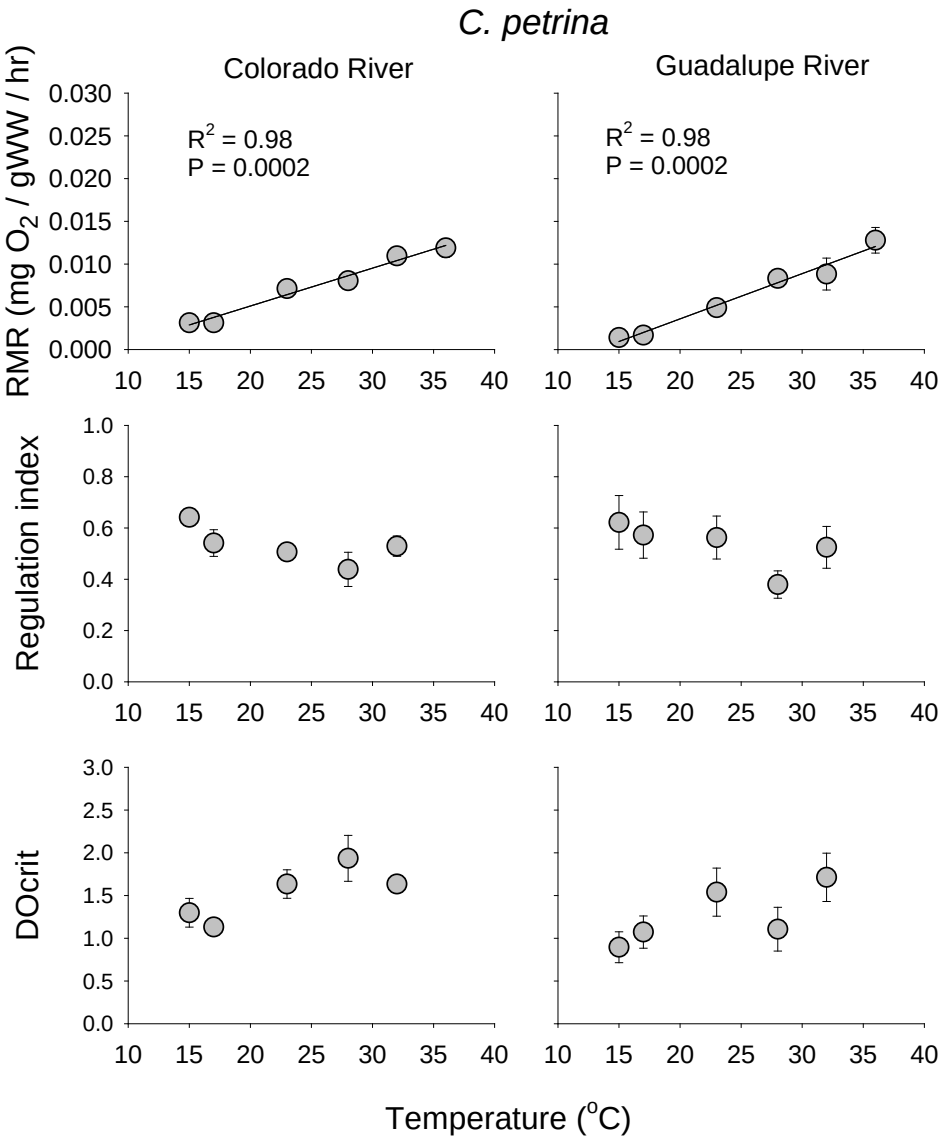

Figure 4. Relationships between resting metabolic rate (RMR), regulation index, DO_{crit} and temperature for *C. petrina* collected from two drainage basins. Neither regulation index nor DO_{crit} yielded a significant linear relationship with temperature.

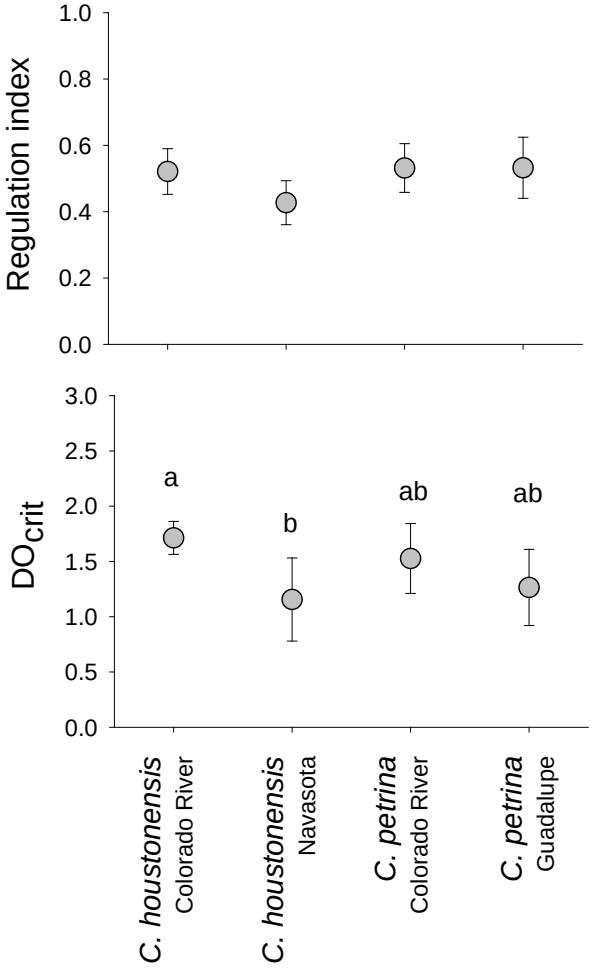

Figure 5. Mean regulation index and DO_{crit} across all temperatures for *C. houstonensis* and *C. petrina* collected from different drainage basins. No significant differences among mussel groups were found for mean regulation index. Letters indicate significant differences in DO_{crit} among mussel groups. Error bars represent ± 1 standard deviation.

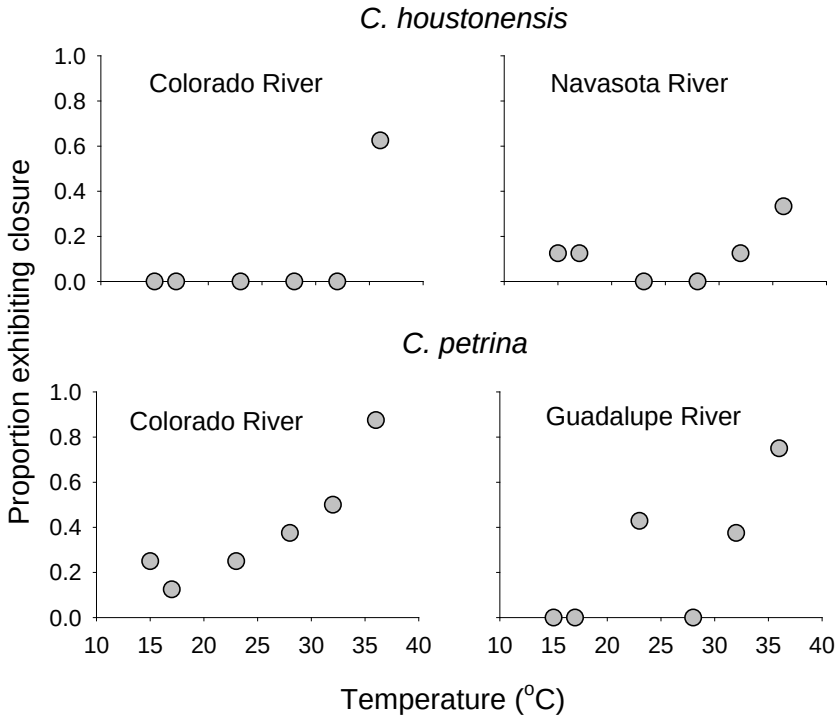

Figure 6. Proportion of individuals exhibiting at least one closure event during respirometry runs at six temperatures.

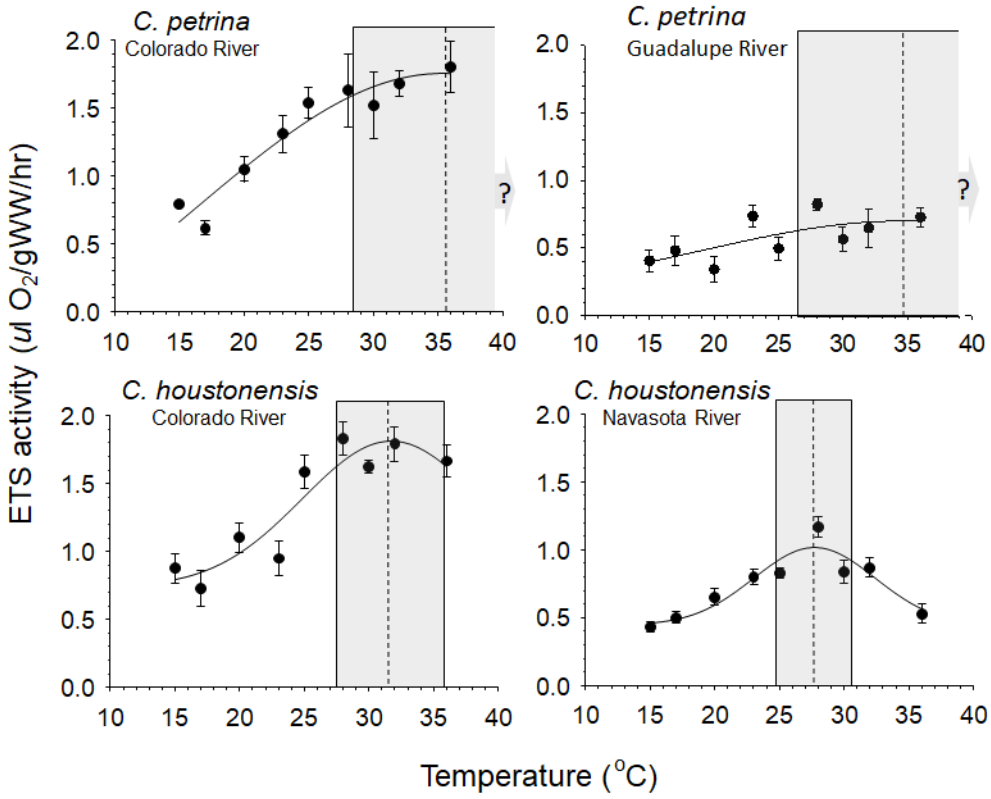

Figure 7. Relationship between ETS activity and temperature for acclimated mussels. Each data point represents the mean ETS activity of all mussels acclimated to that particular temperature. Mussel groups at each temperature were unique. ETS activity of a given mussel was measured only for the temperature to which it had been acclimated. Dashed lines indicate the optimal temperature for enzymatic activity. Grey rectangles represent the optimal temperature range within which ETS activity is within 10% of the maximum.

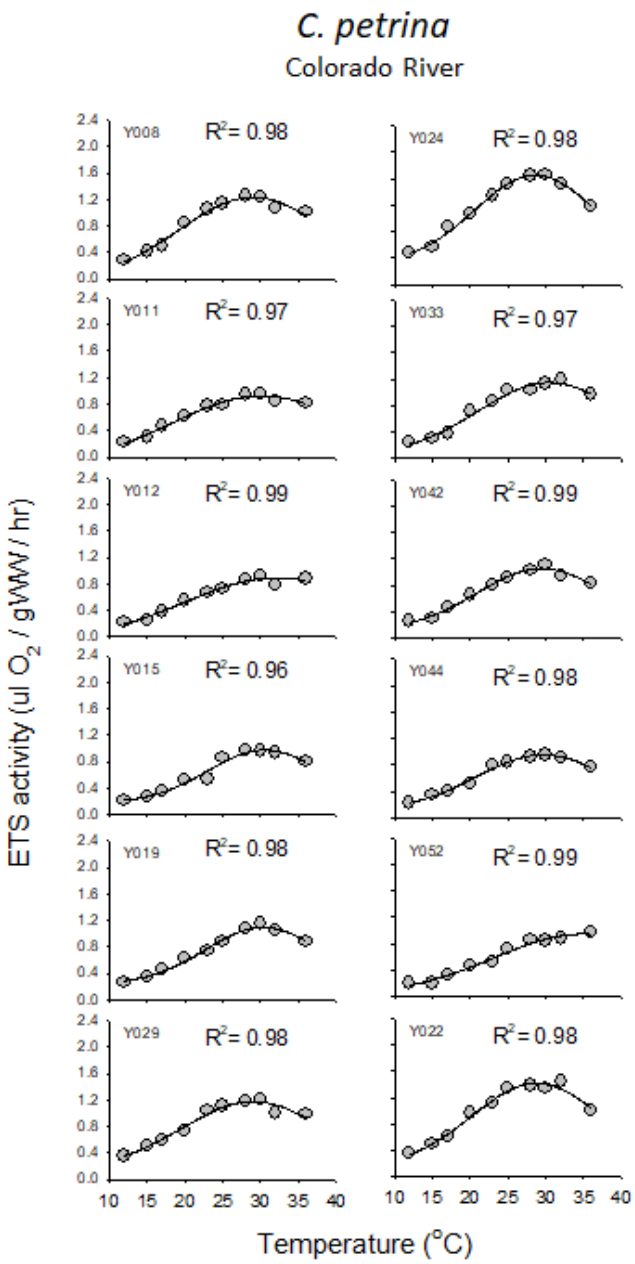

Figure 8. Relationship between ETS activity and temperature for non-acclimated *C. petrina* from the Colorado River. The tag number identifying each mussel is given in the upper left corner of each graph. Each data point represents ETS activity of enzymes collected from the same individual and incubated for 30 minutes at each temperature. Solid lines represent a four parameter Gaussian curve fitted through the data points. Optimal temperature for each individual was calculated as the temperature at the peak of each Gaussian curve.

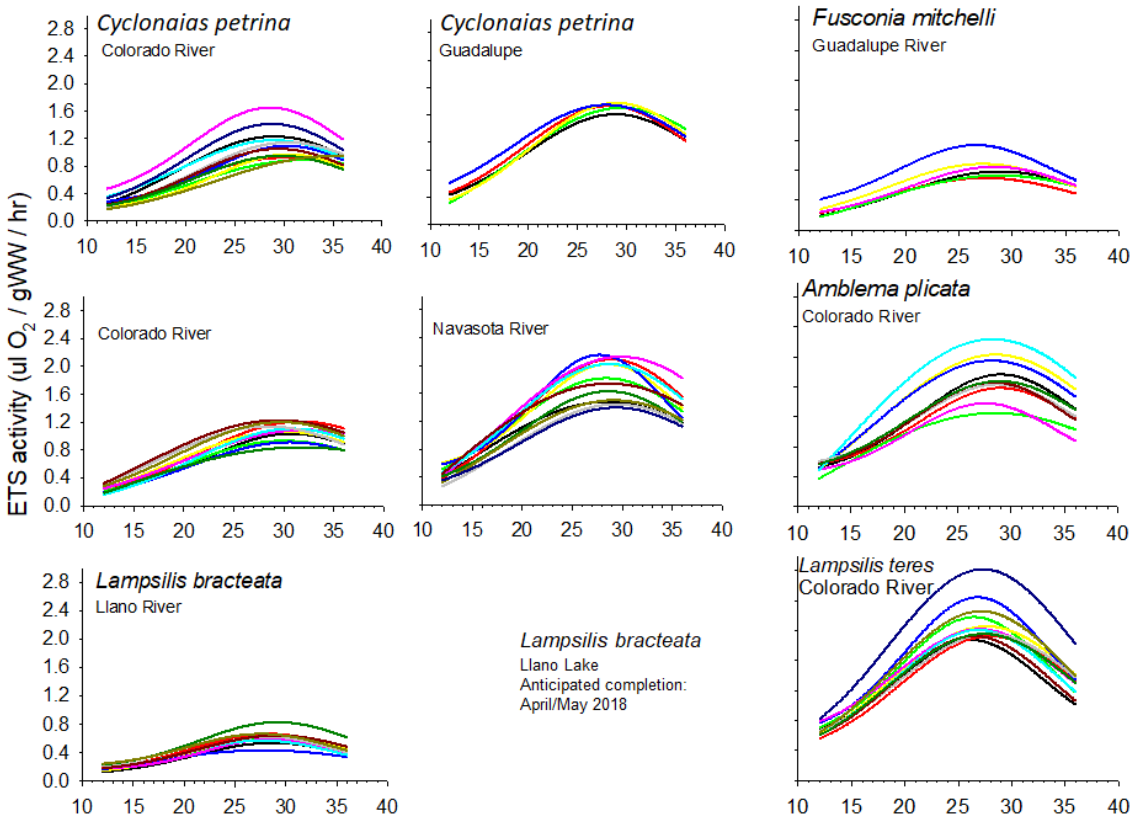

Figure 9. Summary graphs of relationship between ETS enzyme activity and temperature for non-acclimated mussels. Each curve represents a single mussel. ETS enzymes were extracted from each mussel and incubated at nine temperatures to which the mussel had not been acclimated. Colored lines represent a four parameter Gaussian curve fitted through the data for each individual mussel.

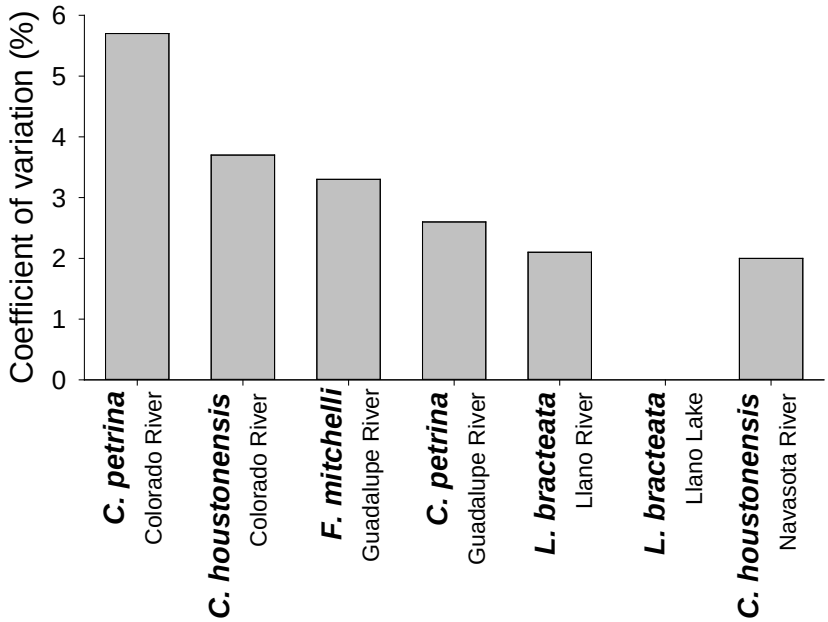

Figure 10. Coefficient of variation for optimal ETS temperatures of non-acclimated mussels from a given species and drainage, arranged in order from highest to lowest. Data for Llano Lake *L. bracteata* are expected to be available by May 2018.

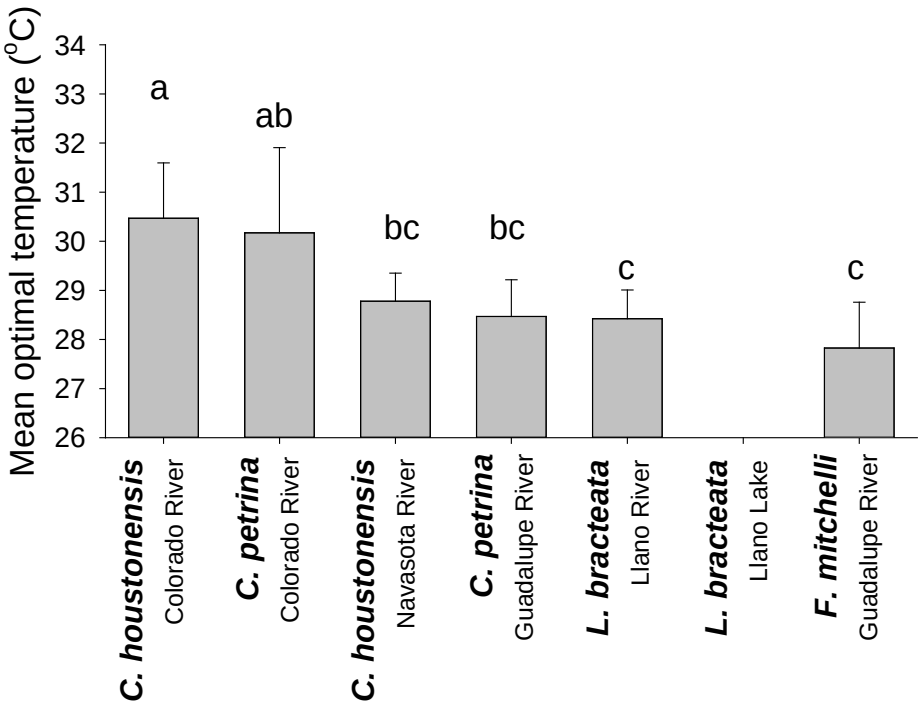

Figure 11. Mean optimal ETS temperatures of non-acclimated mussels determined from individual curves shown in Figure 2, arranged from highest to lowest. Error bars represent ± 1 SD. Letters indicate significant differences. Data for Llano Lake *L. bracteata* is expected to be available by May 2018

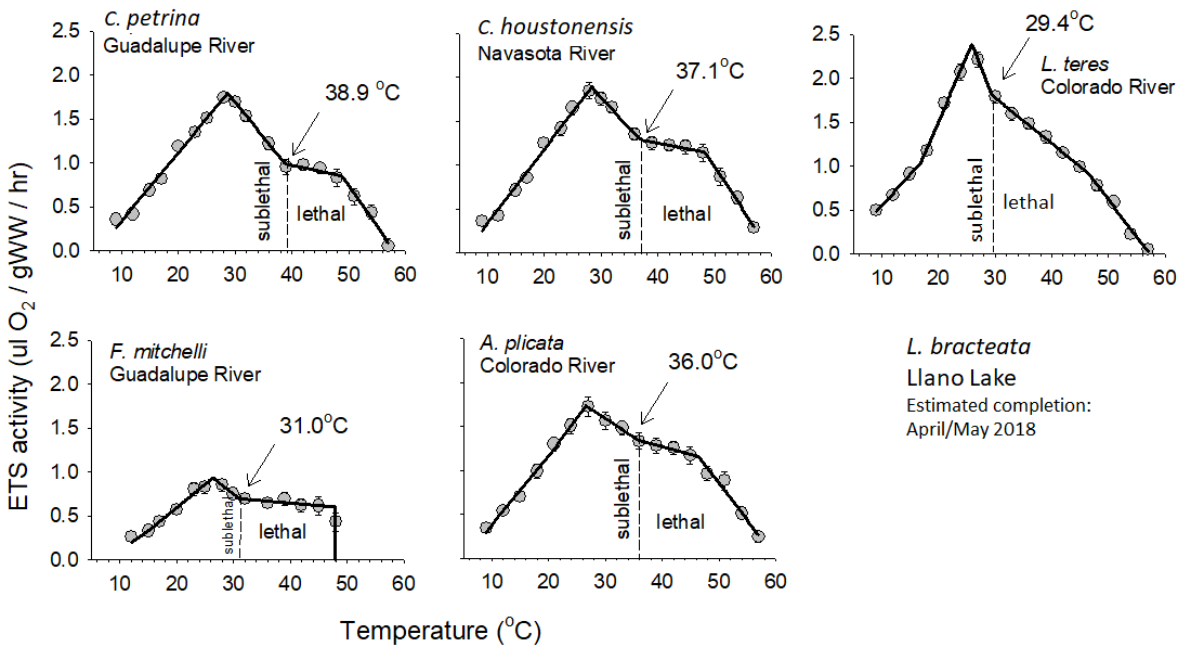

Figure 12. Relationship between ETS activity and temperature for non-acclimated mussels across the full range of experimental temperatures. Each data point within a panel represents the mean activity of enzymes extracted from the same group of 6-12 mussels. Error bars represent ± 1 standard error. Solid lines represent 5-segment piecewise regressions. Dotted lines indicate temperature at which we hypothesize sublethal effects transition to lethal effects.

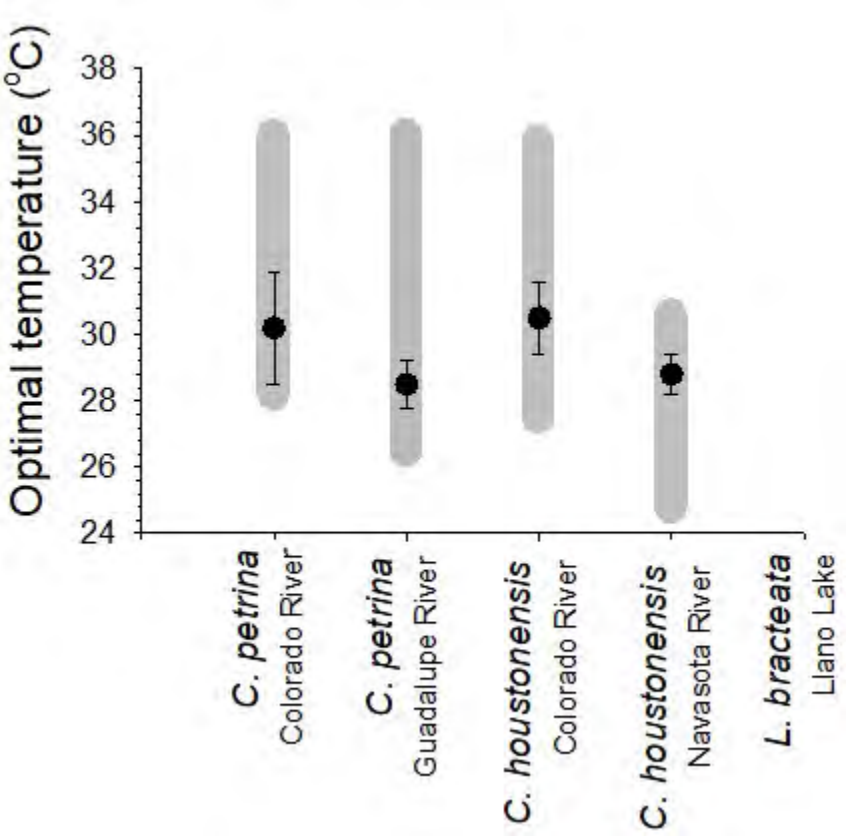

Figure 13. Comparison of optimal temperature range (grey bars) obtained from acclimated mussels and mean optimal temperature (black circles) obtained from non-acclimated mussels. Error bars represent ± 1 SD. Data for *L. bracteata* is expected to be available by May 2018.

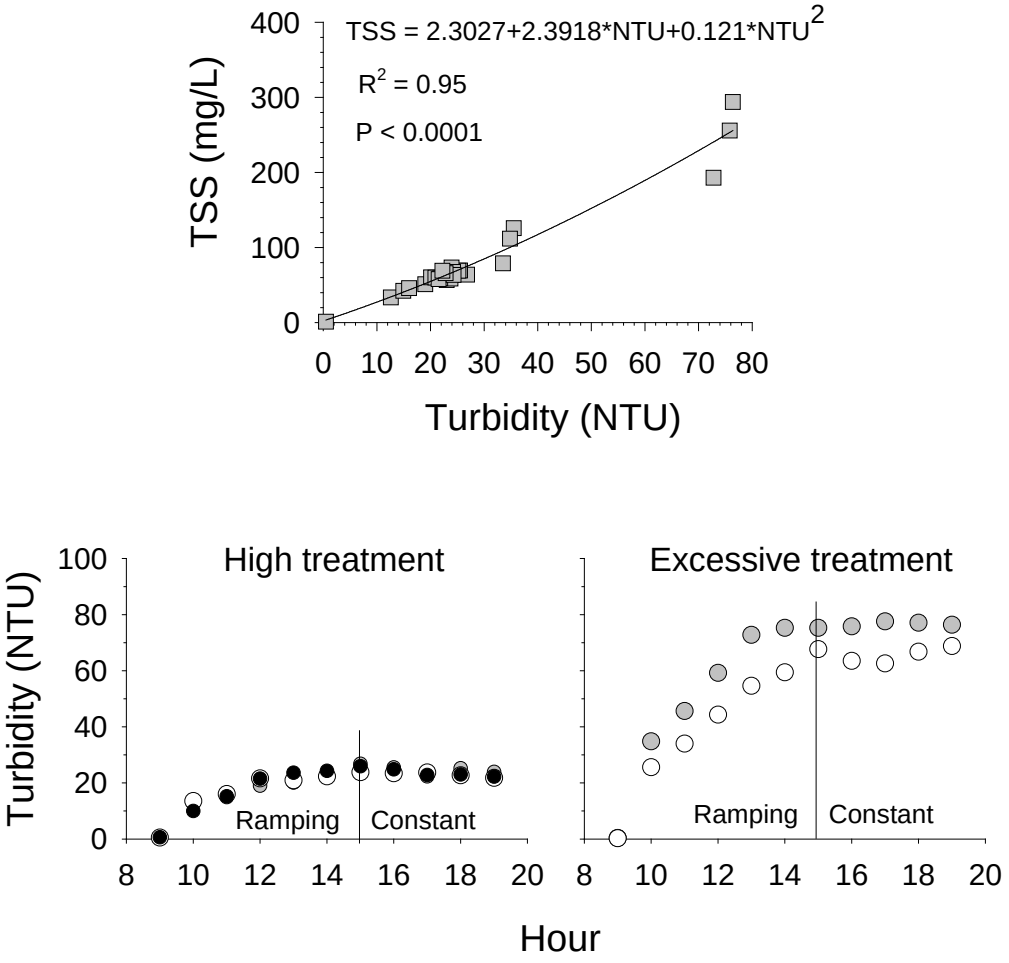

Figure 14. Top panel: Predictive relationship between turbidity (NTU) and total suspended solids (TSS mg/L). Bottom panel: Changes in turbidity through time in the High and Excessive turbidity treatments. Solid vertical line indicates the break between the ramping turbidity and the constant turbidity periods.

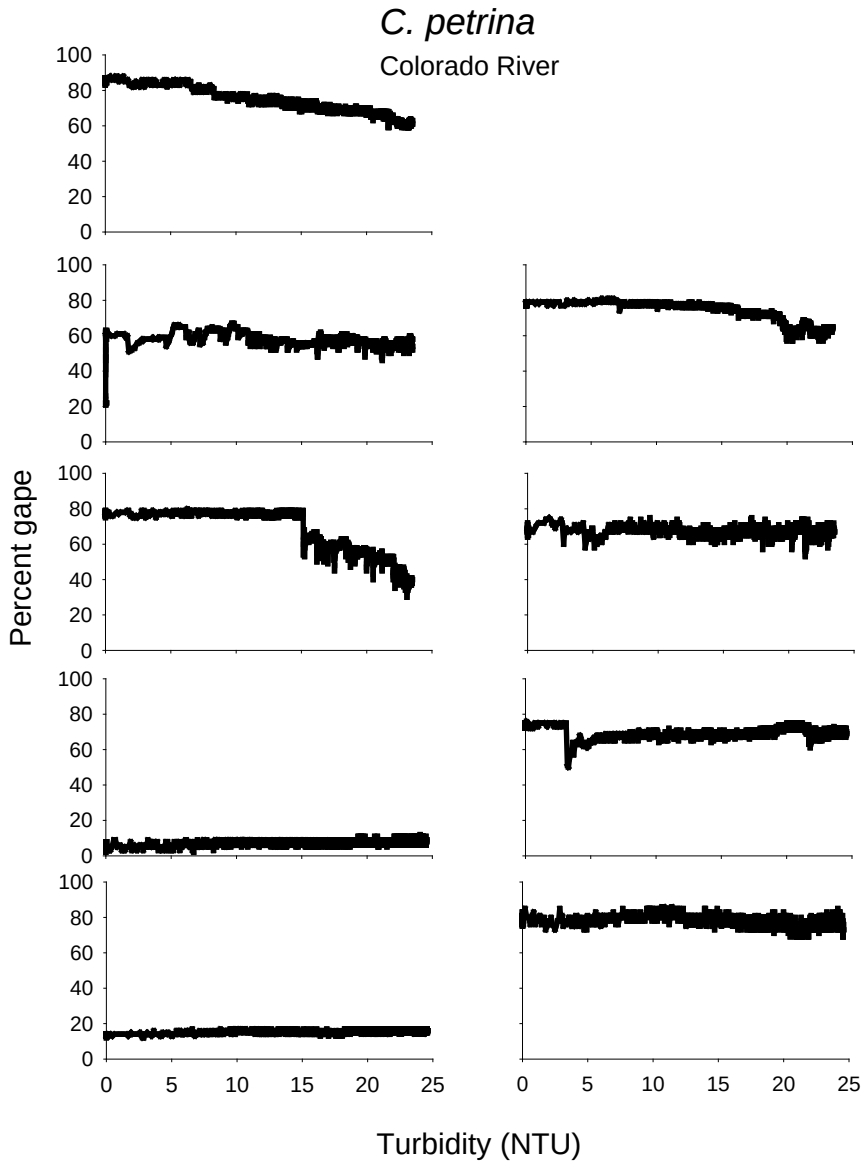

Figure 15. Percent gape for *C. petrina* from the Colorado River as turbidity increased over a ~6-hr period to a maximum of ~25 NTU. Each graph represents a unique individual.

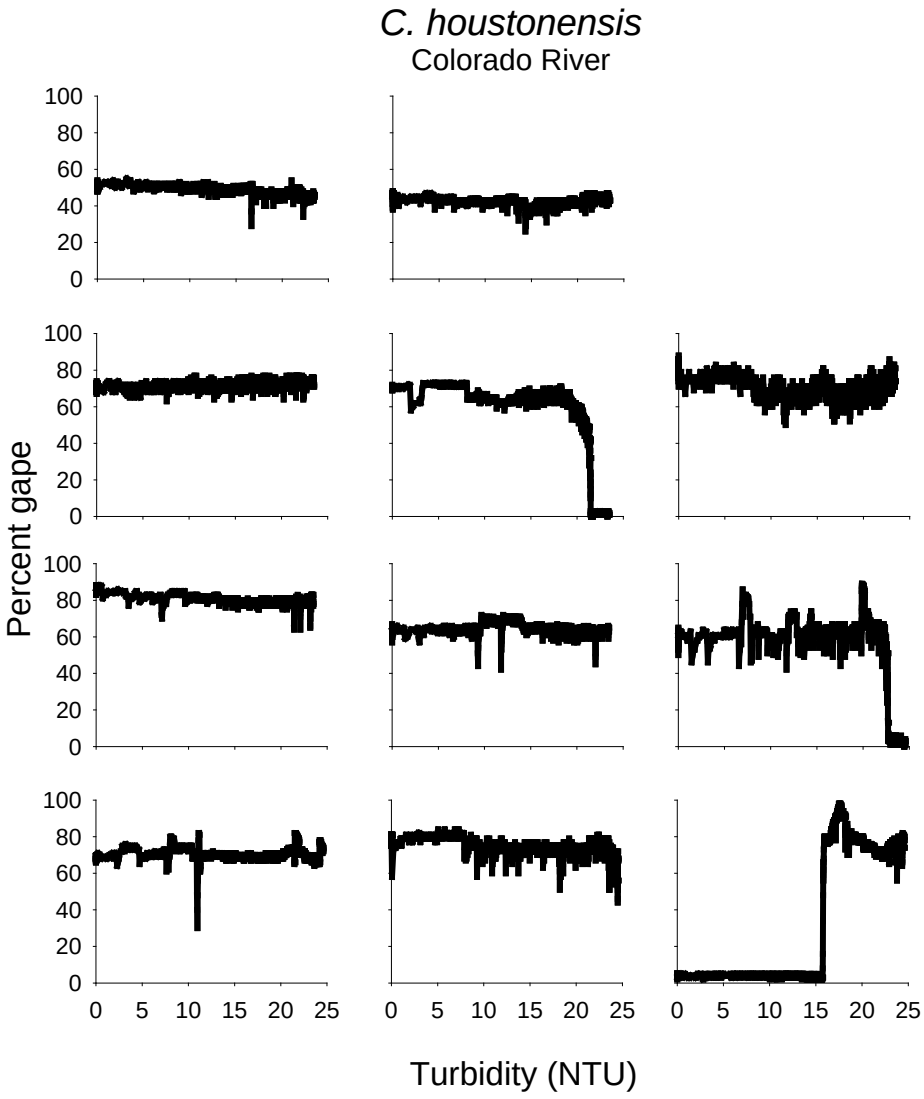

Figure 16. Percent gape for *C. houstonensis* from the Colorado River as turbidity increased over a ~6-hr period to a maximum of ~25 NTU. Each graph represents a unique individual.

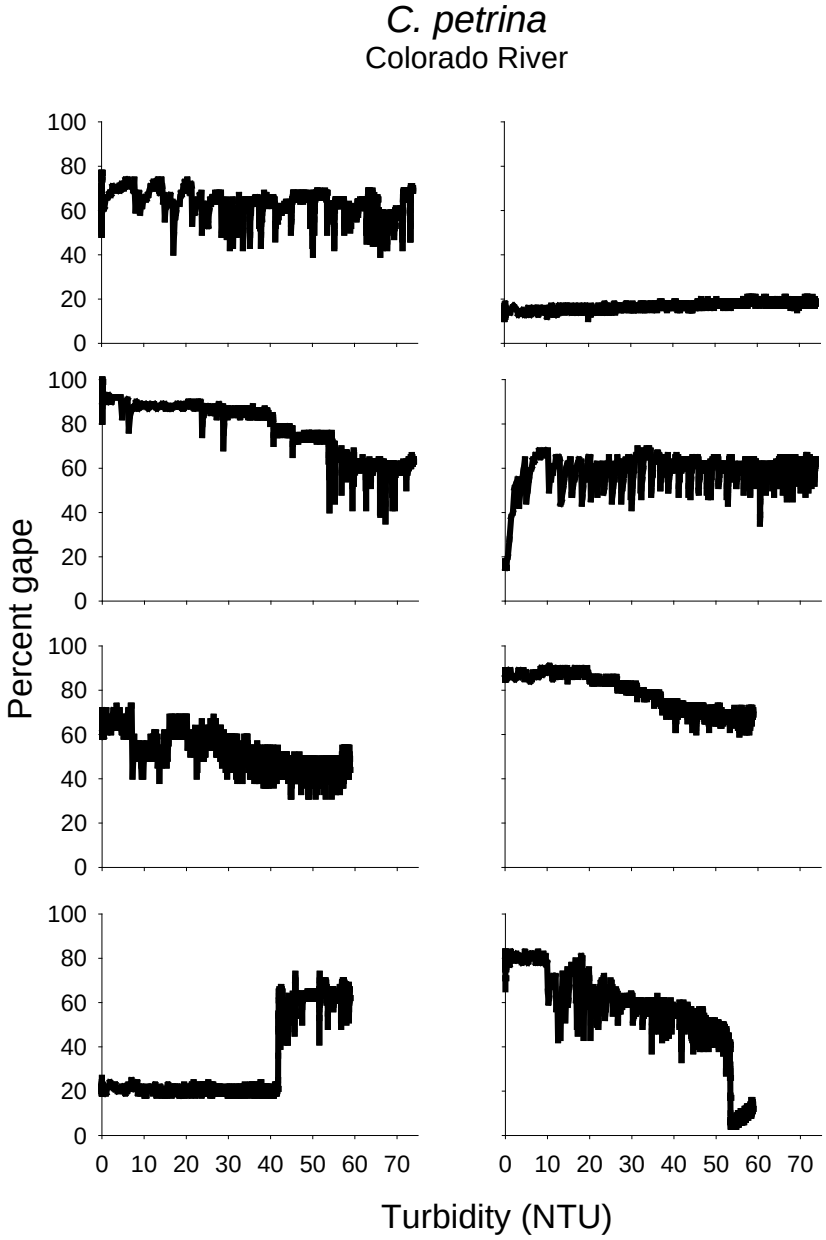

Figure 17. Percent gape for *C. petrina* from the Colorado River as turbidity increased over a ~6-hr period to a maximum of 60-75 NTU. Each graph represents a unique individual.

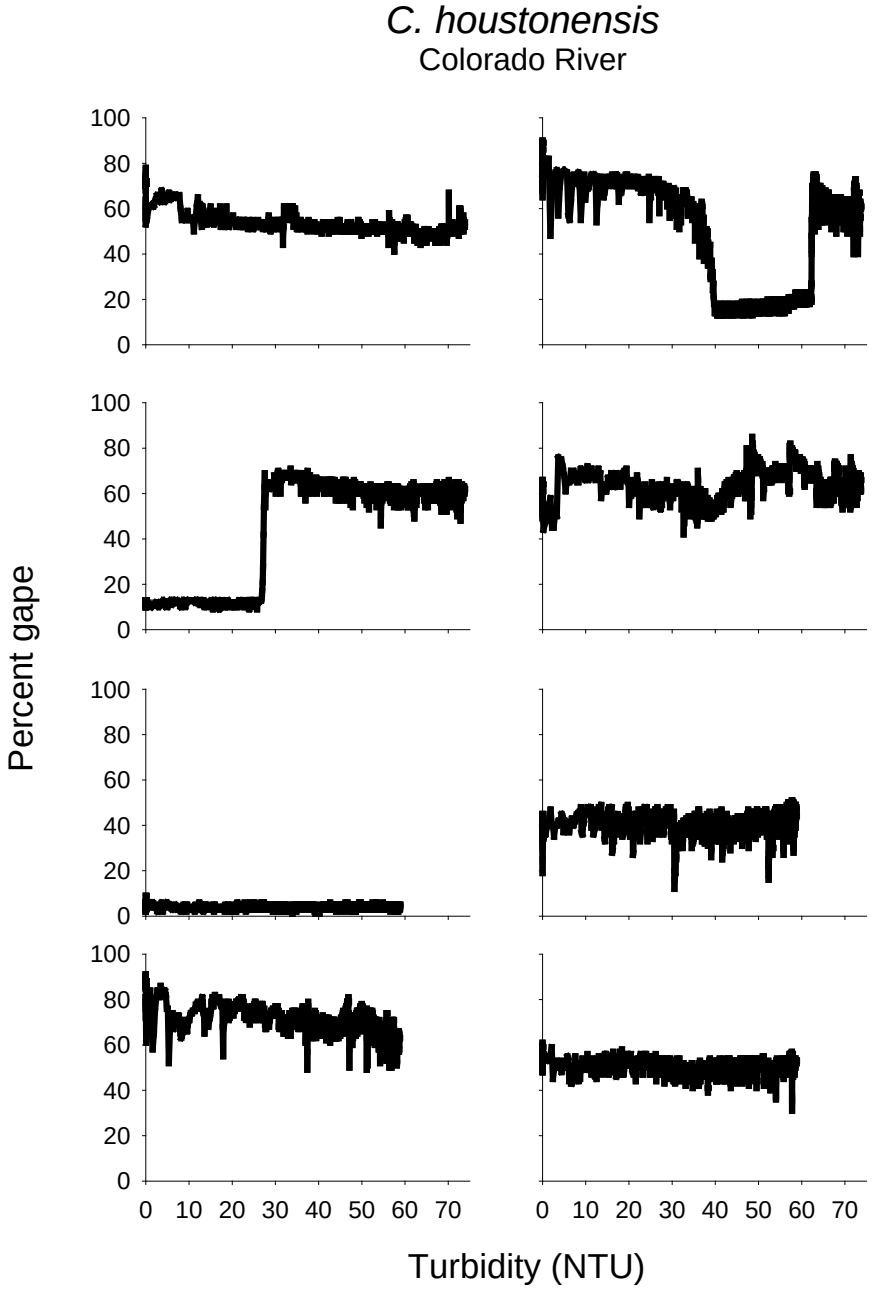

Figure 18. Mean percent gape for *C. houstonensis* from the Colorado River as turbidity increased over a ~6-hr period to a maximum of 60-75 NTU. Each graph represents a unique individual.

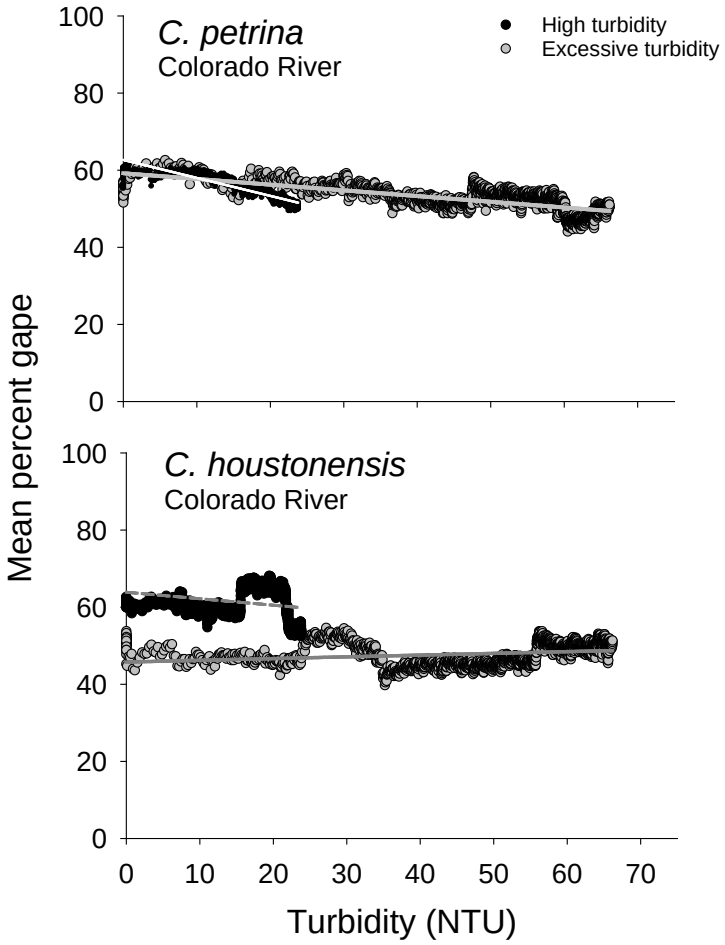

Figure 19. Mean percent gape for all individuals within each species as turbidity increased over a ~6-hr period to a high (25 NTU) or excessive (60-75 NTU) turbidity level. Solid grey lines represent linear regressions through the excessive turbidity dataset. Solid white line and dashed grey line represent linear regressions through the high turbidity datasets for top and bottom panels respectively.

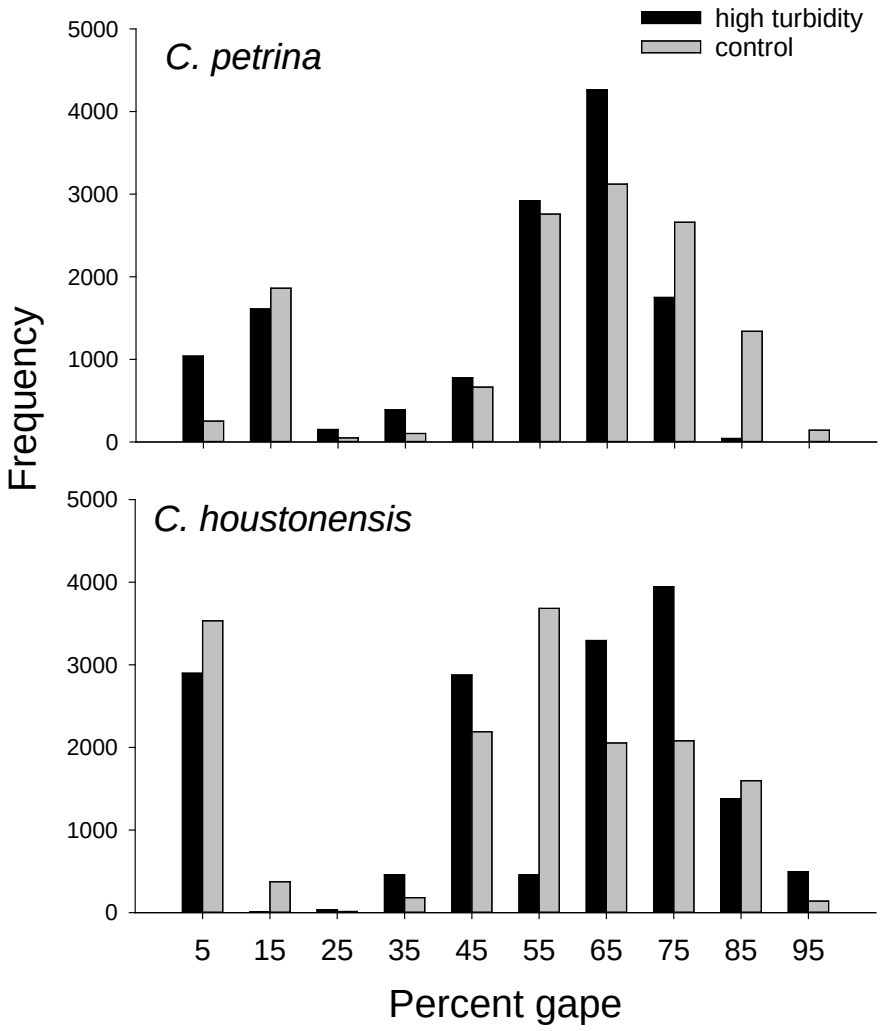

Figure 20. Frequency (# of occurrences) of a range of percent gape measurements for mussels during an initial, pre-exposure period (control: < 1 NTU) and subsequent constant turbidity period (treatment: High ~25 NTU). Only data from the same time frame (15:00 – 19:00 h) were compared between control and constant periods.

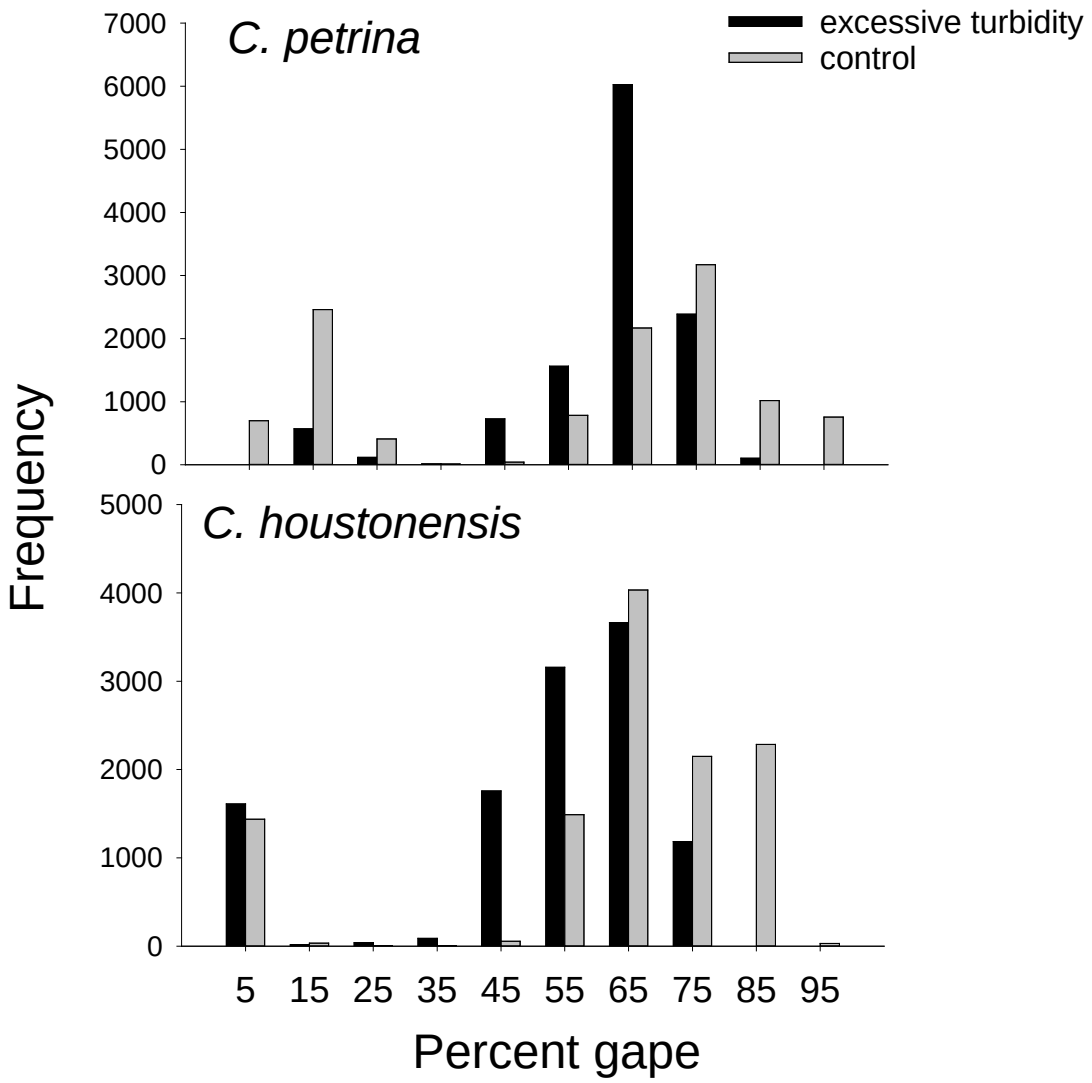

Figure 21. Frequency (# of occurrences) of a range of percent gape measurements for mussels during an initial, pre-exposure, control period (< 1 NTU) and subsequent constant turbidity period (Treatment: excessive 60-75 NTU). Only data from the same time frame (15:00 – 19:00 hrs) were compared between control and constant periods.

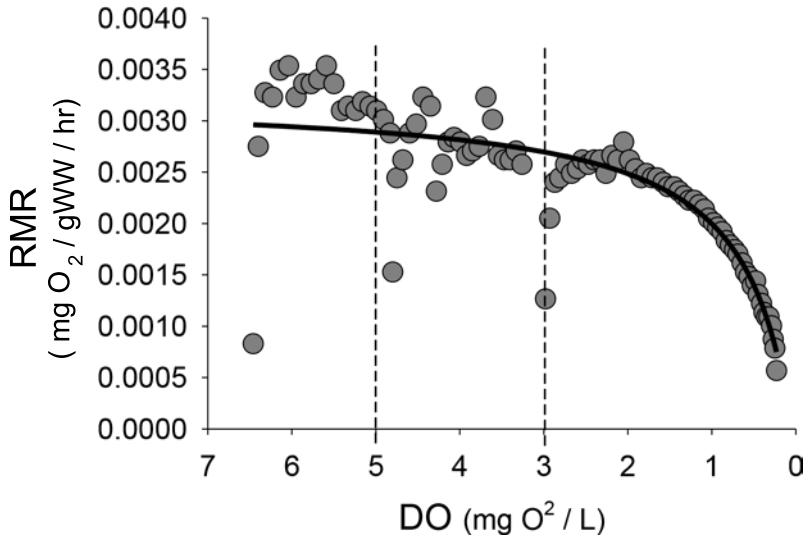

Figure 22. Typical pattern of RMR changing with declining DO when using periodic flushes to prevent excreted ammonia from accumulating in chambers. Dotted lines show when flushing occurred.

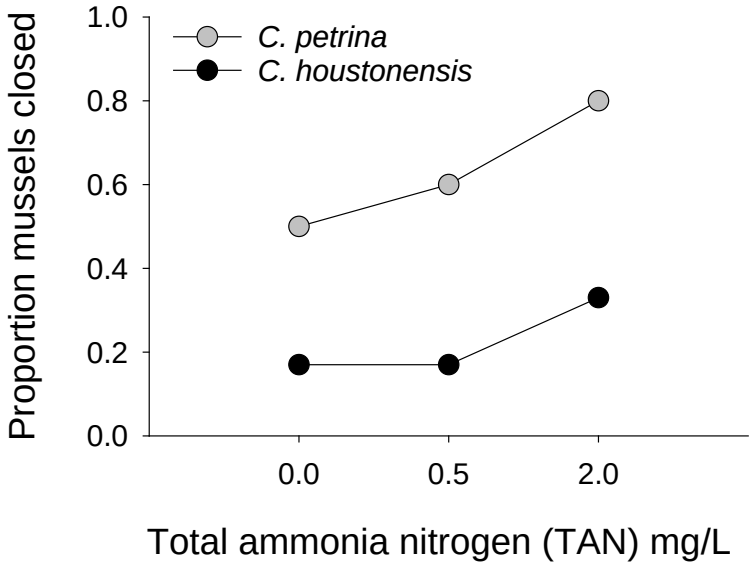

Figure 23. Proportion of mussels that exhibited at least one valve closure during respirometry at each of three TAN concentrations.

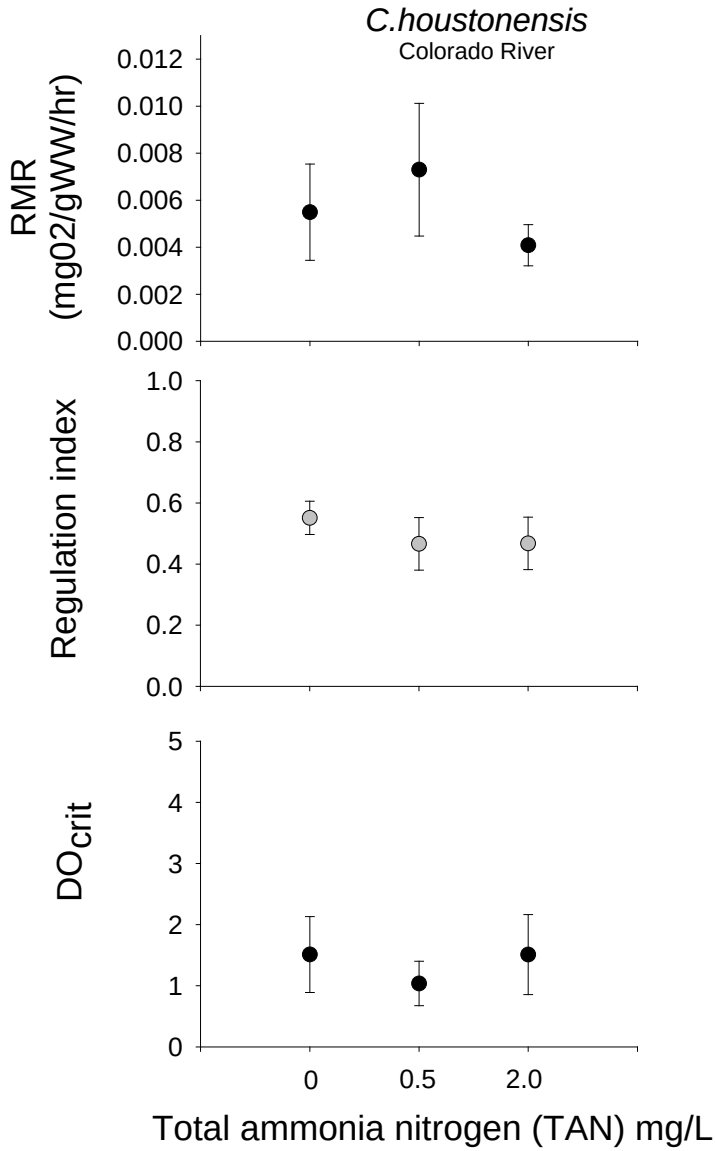

Figure 24. Mean resting metabolic rate (RMR), regulation index, and critical oxygen concentration (DO_{crit}) at three total ammonia nitrogen (TAN) concentrations. No significant differences in any response variable was found among different TAN concentrations.

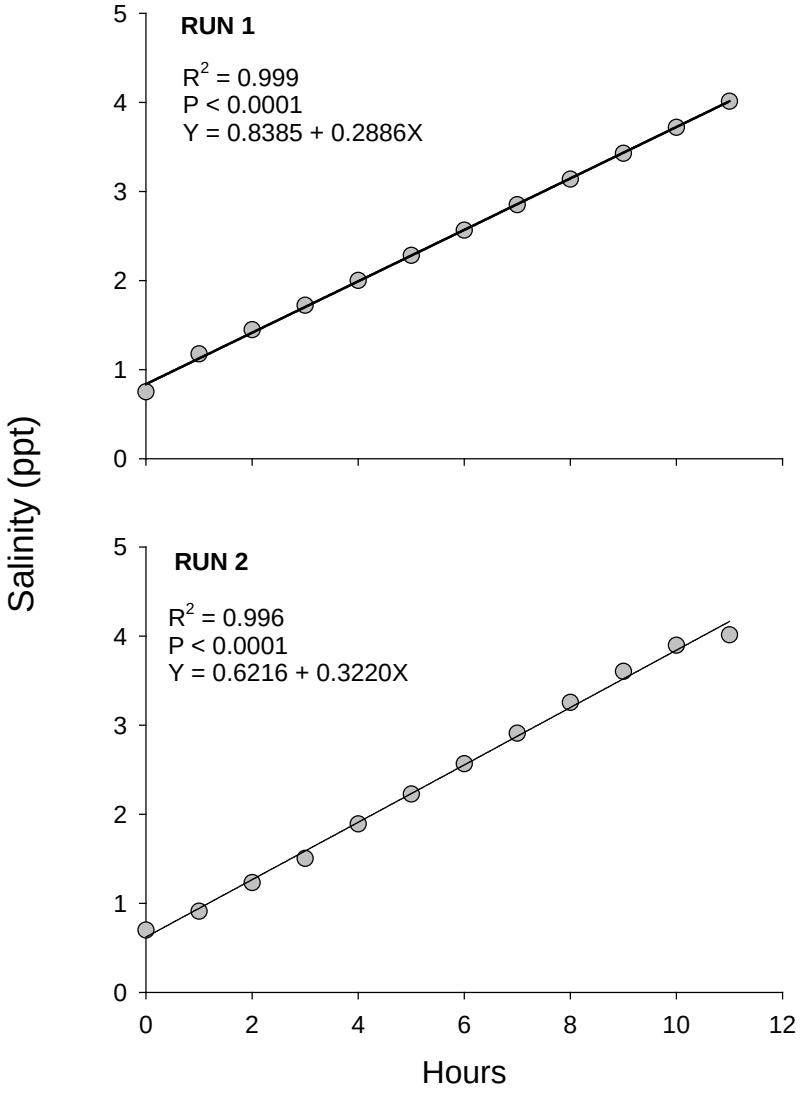

Figure 25. Increase in salinity over time for runs 1,2 of salinity experiments for *C. petrina* and *C. houstonensis*

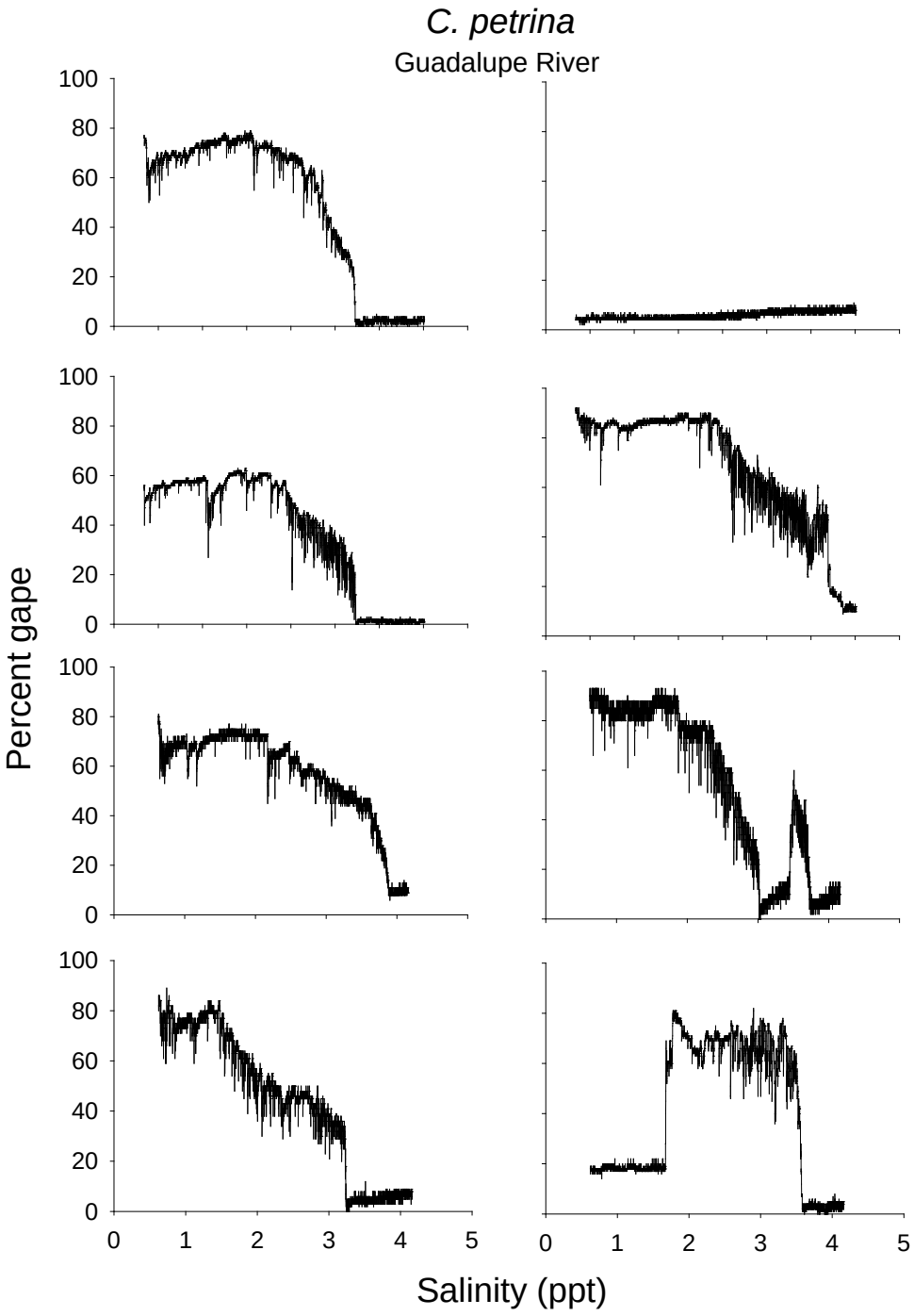

Figure 26. Change in percent gape with increasing salinity for C. petrina collected from the Guadalupe River. Each graph represents an individual mussel.

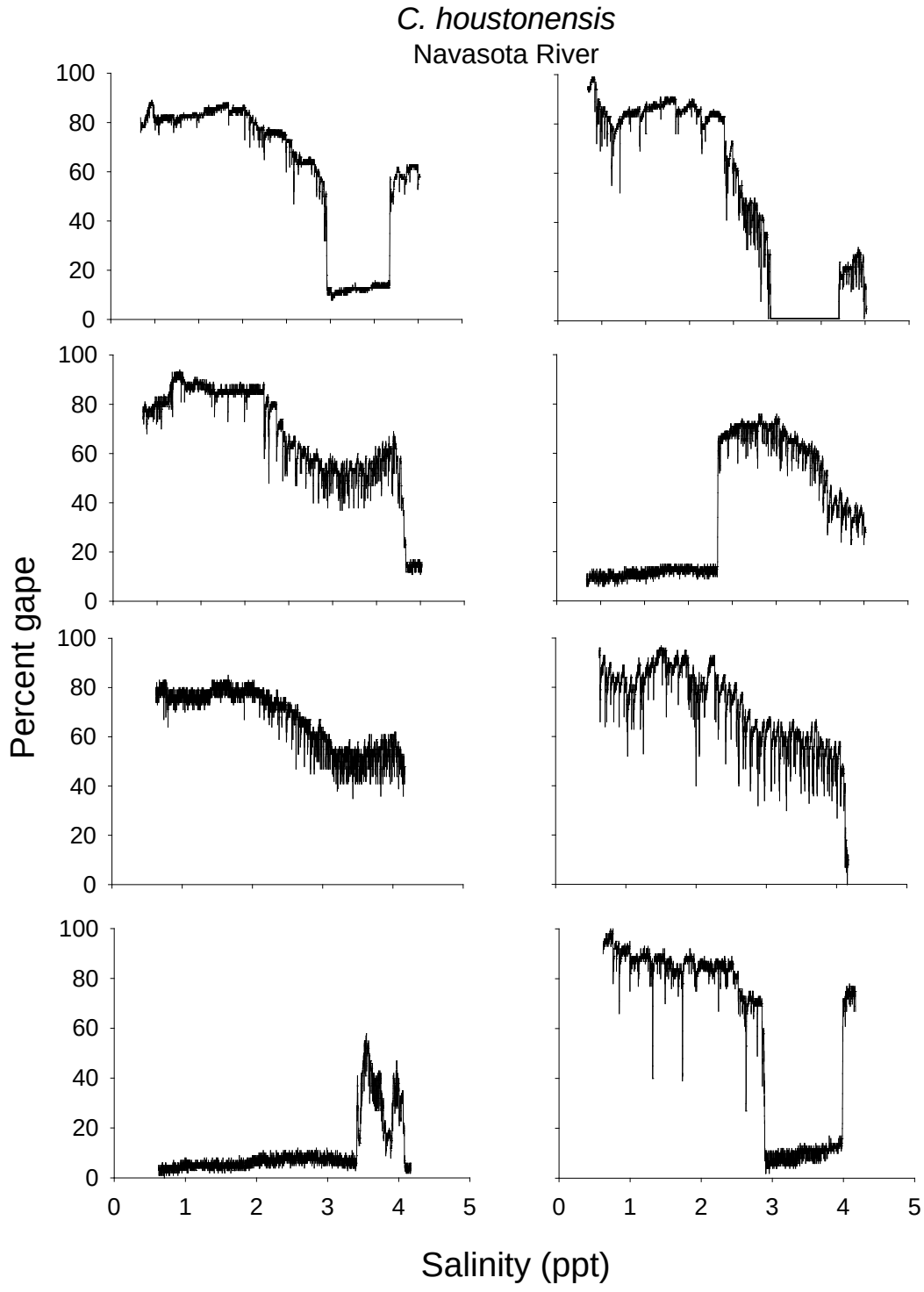

Figure 27. Change in percent gape with increasing salinity for C. houstonensis collected from the Colorado River. Each graph represents an individual mussel.

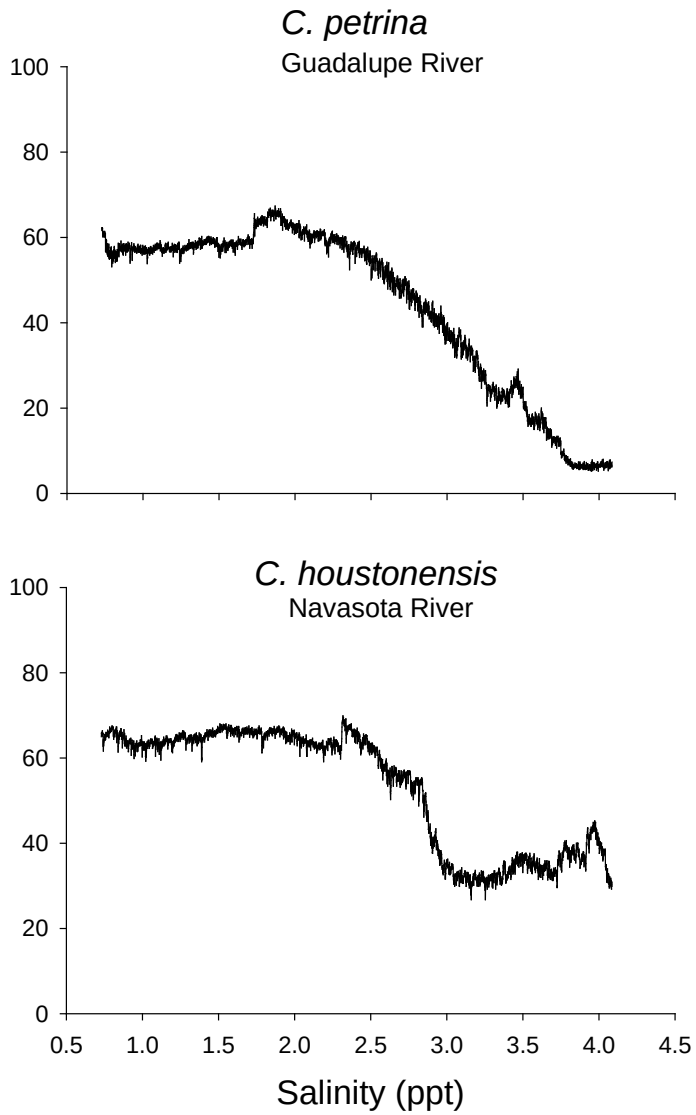

Figure 28. Change in mean percent gape (averaged across all mussels) with increasing salinity for *C. petrina* and *C. houstonensis*.

Task 2.4: Desiccation Tolerances and Behavioral Responses to Dewatering of Central Texas Endemic Mussels

Contributing authors: Joshua Abel, Jennifer Morton, Randy Gibson, Kenneth Ostrand

Addresses:
U.S. Fish and Wildlife Service, San Marcos Aquatic Resources Center, 500 E. McCarty Lane, San Marcos TX 78666.

Principal Investigators: Kenneth Ostrand

Email: Kenneth_Ostrand@fws.gov

Freshwater mussels are a highly imperiled fauna that provide important ecosystem services (Vaughn and Hakenkamp 2001). Most species of mussel are largely sessile, and have limited ability to escape threats. Some species will exhibit varying degrees of vertical and horizontal movement in response to environmental and reproductive cues (Amyot and Downing 1997, Watters et al. 2001, Perles et al. 2003, Schwalb and Pusch 2007). Drought conditions can have severe negative consequences for mussels (Galbraith et al. 2010); extreme low flow events expose mussels to high temperatures, low dissolved oxygen, and often high ammonia levels, which can result in sublethal affects such as reduction in growth and cessation of reproduction, and in severe cases, high mussel mortality (Gagnon et al. 2004, Golladay et al. 2004, Haag and Warren 2008). In worst-case scenarios, extreme low flows can lead to stream dewatering, which results in mussel emersion, and, if prolonged, can lead to mortality. Therefore, the objectives of this study are to determine the desiccation tolerances of three mussel species endemic to Central Texas, and to study the behavioral responses to dewatering.

Methods

<u>Laboratory desiccation trail</u>

Species Collection and Holding

Three endemic Central Texas mussel species were examined for desiccation tolerances: *Lampsilis bracteata, Cyclonaias houstonensis,* and *Cyclonaias petrina.* Both *Cyclonaias* species were collected from the Colorado River near Altair, Texas, and the *L. bracteata* were collected from the Llano River near Mason, Texas. At the time of collection, all mussels were wrapped in towels saturated with source water within an insulated cooler and transported to San Marcos, Texas. Upon arrival to the San Marcos Aquatic Resources Center (SMARC), all mussels were placed in a coarse sand mixture within recirculating indoor raceways. Mussels were acclimated to 25 °C slowly, over a four week period, and held at this temperature for at least two weeks prior to testing. During this acclimation period, all mussels were fed daily a 2:1 mixture of Shellfish Diet 1800 and Nannochloropsis 3600 (Reed Mariculture, Campbell, California) targeting a final concentration of ca. 300,000 cells/mL.

Laboratory Desiccation

Laboratory desiccation trials were conducted at the SMARC during July through September 2017. Fifteen adult mussels of each species were placed in an environmental chamber (Powers Scientific; Pipersville, PA) maintained at 25 °C on a 16:8 hour light-dark cycle. Prior to entering the environmental chamber, all mussels were blotted dry to remove excess moisture and placed in separate 14 x 14 cm plastic weigh dishes. We assessed mussel condition daily by manually stimulating abductor mussel retraction via probing. Once mortality occurred, we measured shell length to the nearest 0.01 mm and extracted gonadal fluid to determine gender. Gender was determined by the presence of sperm or eggs (Galbraith and Vaughn 2009). Gills were also visually inspected to determine gravidity.

Statistical Analysis

Lethal time to desiccation (LT_{50}) was calculated (in days) for each species using probit analysis. A one-way analysis of variance (ANOVA) was used to examine differences in survival time between species. All statistical analysis was performed in R (version 3.4.1; R Project for Statistical Computing, Vienna, Austria) and Excel (Microsoft Corporation, Redmond, Washington) software.

Simulated field dewatering trial

Study Species

Twenty-three *L. bracteata* were collected from the San Saba River (n=11) and the Llano River (n=12) in September 2017. Twenty-four *Q. petrina* were collected from the Llano River in September 2017. All mussels were transferred to the SMARC wrapped in source-water saturated towels inside coolers. All mussels were then held in quarantine systems and acclimated to the hatchery water temperature of 19 °C not exceeding more than 1 °C temperature change per day. After a two week quarantine and acclimation period, all mussels were held under hatchery conditions for 6 weeks. All mussels were fed daily a 2:1 mixture of Shellfish Diet 1800 and Nannochloropsis 3600 (Reed Mariculture Inc. Campbell, CA) with a target dilution of 300,000 cells/mL. Prior to beginning experiment, all mussels were weighed, measured and tagged with Passive Integrative Transponders (PIT) (Biomark®, Boise, ID). PIT tags were affixed with dental cement to the left valve of each mussel, directly posterior to the medial axis. A 15 cm length of nylon fishing line was also affixed to the posterior tip of left valve of each mussel. A duct tape flag was attached to the free end of fishing line with the last 3 digits of the corresponding mussels PIT tag identification number.

Dewatering Methodology

To examine the differences in behavior between *L. bracteata* and *Q. petrina*, a simulated field-dewatering trial was conducted in November and December 2017 following the modified methods of Galbraith et al. (2015). The trials were conducted in two outdoor concrete raceways (5 m x 2 m x1 m) filled with coarse sand to simulate a small stream (Figure 2). Each raceway was filled with water to a depth of 1 m. Four gallons per minute of fresh well water were continuously added to each raceway. Twenty animals of each species were assigned without bias to one treatment and one control raceway. All mussels were evenly spaced at the top of each simulated bank. Mussel position was marked for each individual using surveying flags labeled with the last three digits of the corresponding mussel's PIT tag identification number. Water was removed from the treatment raceway via submersible pump at a rate of 0.044 m per day. Water was not removed from the control raceway. Horizontal movement was assessed twice weekly and totaled for each individual upon reaching experimental endpoint. Vertical movement was also recorded by measuring the length of fishing line above the sediment surface.

Statistical Analysis

To determine the effects of dewatering on mussel behavior, t-tests were used to test for differences in horizontal and vertical movements compared between the control and treatment groups of each species. A one-way Analysis of Variance (ANOVA) was used to test differences in lengths and weights between treatment groups. All statistical analyses were conducted using Excel (Microsoft, Redmond, WA) software.

Results

Lethal times to desiccation (LT_{50}) were 2.86 days, 18.39 days, and 32.04 days for *Lampsilis bracteata, Cyclonaias houstonensis,* and *Cyclonaias petrina* respectively. Survival times differed significantly between species (F=98.1, p<0.001) (Figure 1). Of the other factors measured which could affect survival times, shell length (Table 1) was the only one which could be recorded among species and did not have a significant interaction with survival times. Gender determination was not possible with the *Cyclonaias* species because little to no fluid was extracted from the desiccated mussels. No gravid females were found in the *L. bracteata* test organisms.

Vertical movement did not significantly differ between control and treatment groups of either species. Horizontal movement did not differ between control and treatment groups of *L. bracteata,* but did differ significantly between control and treatment groups of *Q. petrina* (t(11)=2.90, p =.007) (Figure 3). There were no significant differences in lengths and weights of mussels between treatment groups (Table 2).

Discussion

Based on the results of the laboratory desiccation trials, *L. bracteata* was predicted to display more horizontal movement than *Cyclonaias petrina.* With a greater than ten-fold time to mortality, when removed from water, it was hypothesized that *Q. petrina* would be more likely to remain stationary when exposed to dewatering. Despite these predictions, the opposite was observed. *Q. petrina,* within the dewatered group, displayed an almost four times greater average horizontal movement (2,237 mm) than that of their control counterparts (572 mm). At the

experimental endpoint, no *Q. petrina* were considered stranded, defined as an individual mussel remaining stationary out of water for greater than 48 hours. In contrast, horizontal movement of *L. bracteata* was not significantly different between treatment groups, and 30% of mussels in the dewatered group where considered stranded. These data help further elucidate the habitat niches of these two species.

Lampsilis bracteata have been found in the upper reaches of the Colorado and Guadalupe River basins and their tributaries (Morton et al. 2016, Howells 2010). Recent surveys have shown that *L. bracteata* is most commonly found in bedrock substrates with high water permanency (Burlakova and Karatayev 2010; Figure 4). Occupying habitat with low water capacity coupled with a low tolerance to desiccation make dewatering possibly a deleterious event for *L. bracteata* when compared to *Q. petrina.* This point was illustrated in a 2011 survey when a recently dewatered stretch of the San Saba River was found to contain 65 recently dead individuals of *L. bracteata* (Burlakova and Karatayev 2010). Unlike *L. bracteata, Q. petrina's* LT_{50} of 32 days and clear movement response make it likely more tolerant of drought induced dewatering events. *Cyclonaias petrina's* avoidance of stranding, when exposed to dewatering at the rate of 0.044 m per day, illustrates its ability to better likely respond to the conditions found at lower reaches of these systems.

REFERENCES

Amyot, J.-P., and J. A. Downing. 1997. Seasonal variation in vertical and horizontal movement of the freshwater bivalve *Elliptio complanata* (Mollusca: Unionidae). Freshwater Biology 37:345–354.

Burlakova, L. E., and A. Y. Karatayev. 2010. State-Wide Assessment of Unionid Diversity in Texas. Final Performance Report to State Wildlife Grants Program. Federal Aid Grant T-43.

Burlakova, L.E., A.Y. Karatayev, V.A. Karatayev, M.E. May, D.L. Bennett, M.J. Cook. 2011. Endemic species: Contribution to community uniqueness, effect of habitat alteration, and conservation priorities. Biological Conservation 144:155-165.

Gagnon, P. M., S. W. Golladay, W. K. Michener, and M. C. Freeman. 2004. Drought responses of freshwater mussels (Unionidae) in coastal plain tributaries of the Flint River basin, Georgia. Journal of Freshwater Ecology 19:667–679.

Galbraith, H. S., and Vaughn, C. C. 2009. Temperature and food interact to influence gamete development in freshwater mussels. *Hydrobiologia*, 636(1): 35-47.

Galbraith, H. S., D. E. Spooner, and C. C. Vaughn. 2010. Synergistic effects of regional climate patterns and local water management on freshwater mussel communities. Biological Conservation 143:1175–1183.

Galbraith, H. S., C. J. Blakeslee, and W. A. Lellis. 2015. Behavioral responses of freshwater mussels to experimental dewatering. Freshwater Science 34:42–52.

Golladay, S. W., P. Gagnon, M. Kearns, J. M. Battle, and D. W. Hicks. 2004. Response of freshwater mussel assemblages (Bivalvia: Unionidae) to a record drought in the Gulf Coastal Plain of southwestern Georgia. Journal of the North American Benthological Society 23:494–506.

Haag, W. R., and M. L. Warren. 2008. Effects of Severe Drought on Freshwater Mussel Assemblages. Transactions of the American Fisheries Society 137:1165–1178.

Hernandez, B.A. 2016. *Movement behavior of unionid mussels in Central Texas.* (Master of Science Thesis). Texas State University, San Marcos.

Morton, J., B. Bosman, L. Martindale, K. Skow, R. Lopez, C. Randklev. 2016. Survey results and habitat use for *Lampsilis bracteata* (Texas fatmucket) in the Colorado River drainage, Texas. Interagency Task Force on Economic Growth and Endangered Species, Texas.

Perles, S. J., A. D. Christian, and D. J. Berg. 2003. Vertical migration, orientation, aggregation and fecundity of the freshwater mussel *Lampsilis siliquoidea*. Ohio J. Sci. Vol. 102:73–78.

Schwalb, A. N., and M. T. Pusch. 2007. Horizontal and vertical movements of unionid mussels in a lowland river. Journal of the North American Benthological Society 26:261–272.

Vaughn, C. C., and C. C. Hakenkamp. 2001. The functional role of burrowing bivalves in freshwater ecosystems. Freshwater Biology 46:1431–1446.

Watters, G. T., S. H. O'Dee, and S. Chordas. 2001. Patterns of vertical migration in freshwater mussels (Bivalvia: Unionoida). Journal of Freshwater Ecology 16:541–549.

Table 1: Average lengths of mussels used in laboratory desiccation trial.

Species	**Average (mm)**	**Standard Deviation**
Q. petrina	69.86	4.73
Q. houstonensis	52.51	4.91
L. bracteata	49.05	6.49

Table 2: Average lengths and weights of mussels used in field dewatering trial.

	Lengths (mm)	Weights (g)
L. bracteata		
Treatment	61.64 (± 4.03)	37.19 (± 6.85)
Control	58.68 (± 3.67)	31.71 (± 5.97)
Q. petrina		
Treatment	45.75 (± 1.65)	20.69 (± 2.07)
Control	44.33 (± 2.23)	20.11 (± 2.85)

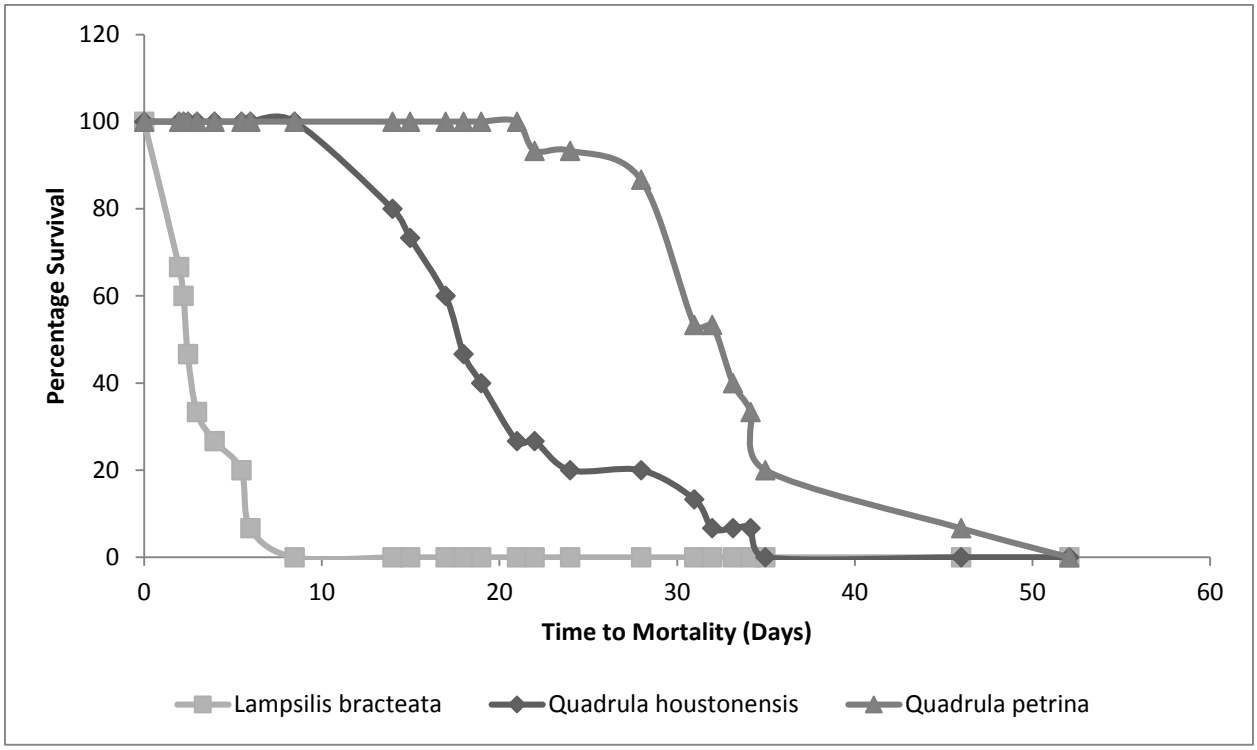

Figure 1: Percentage survival over time in laboratory desiccation trial.

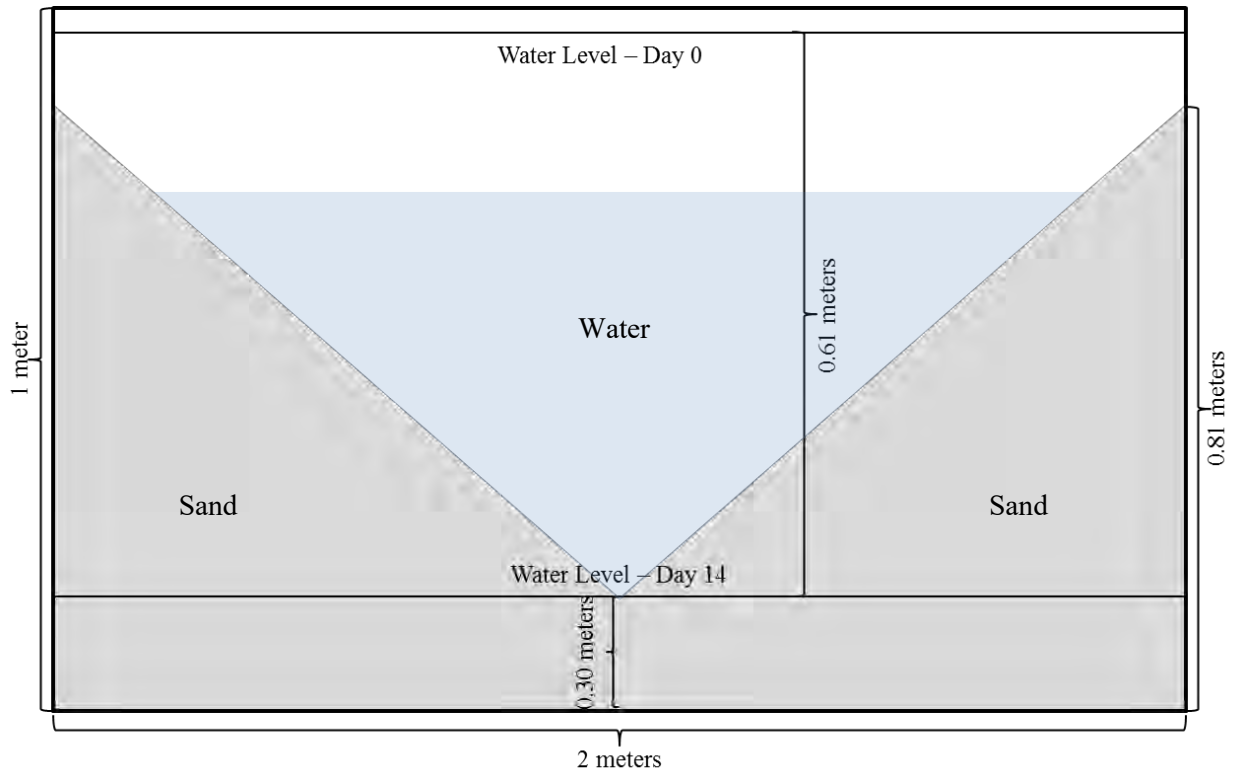

Figure 2: Cross-section view of raceway design used in simulated field dewatering trials.

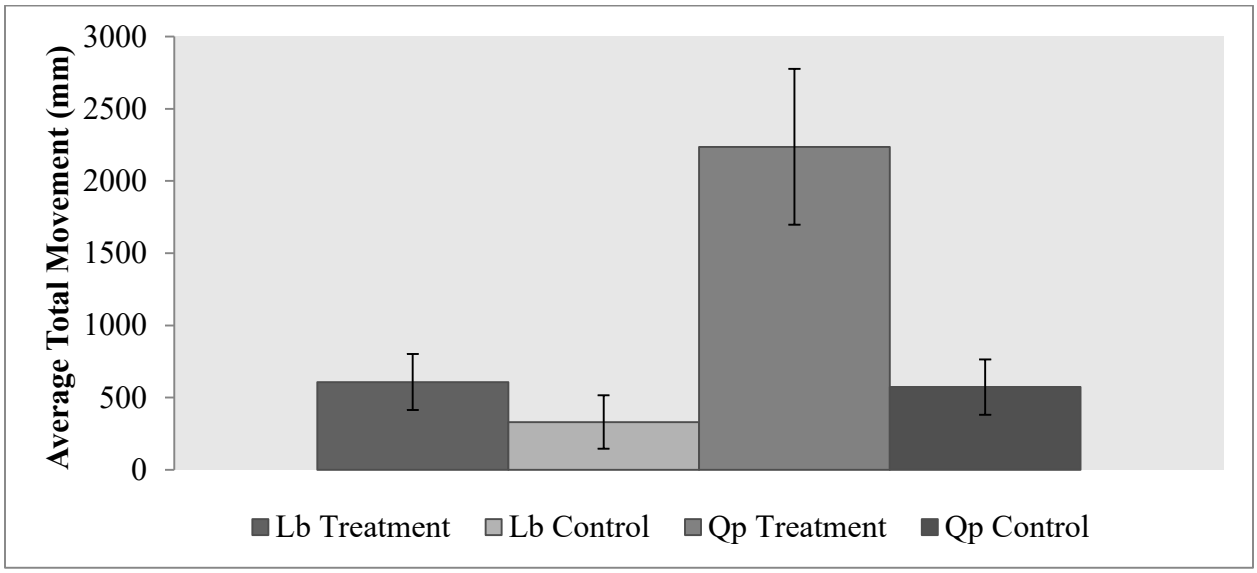

Figure 3: Average total horizontal movement of all test groups in simulated field dewatering trials. Lb = *Lampsilis bracteata*, Qp = *Cyclonaias petrina*.

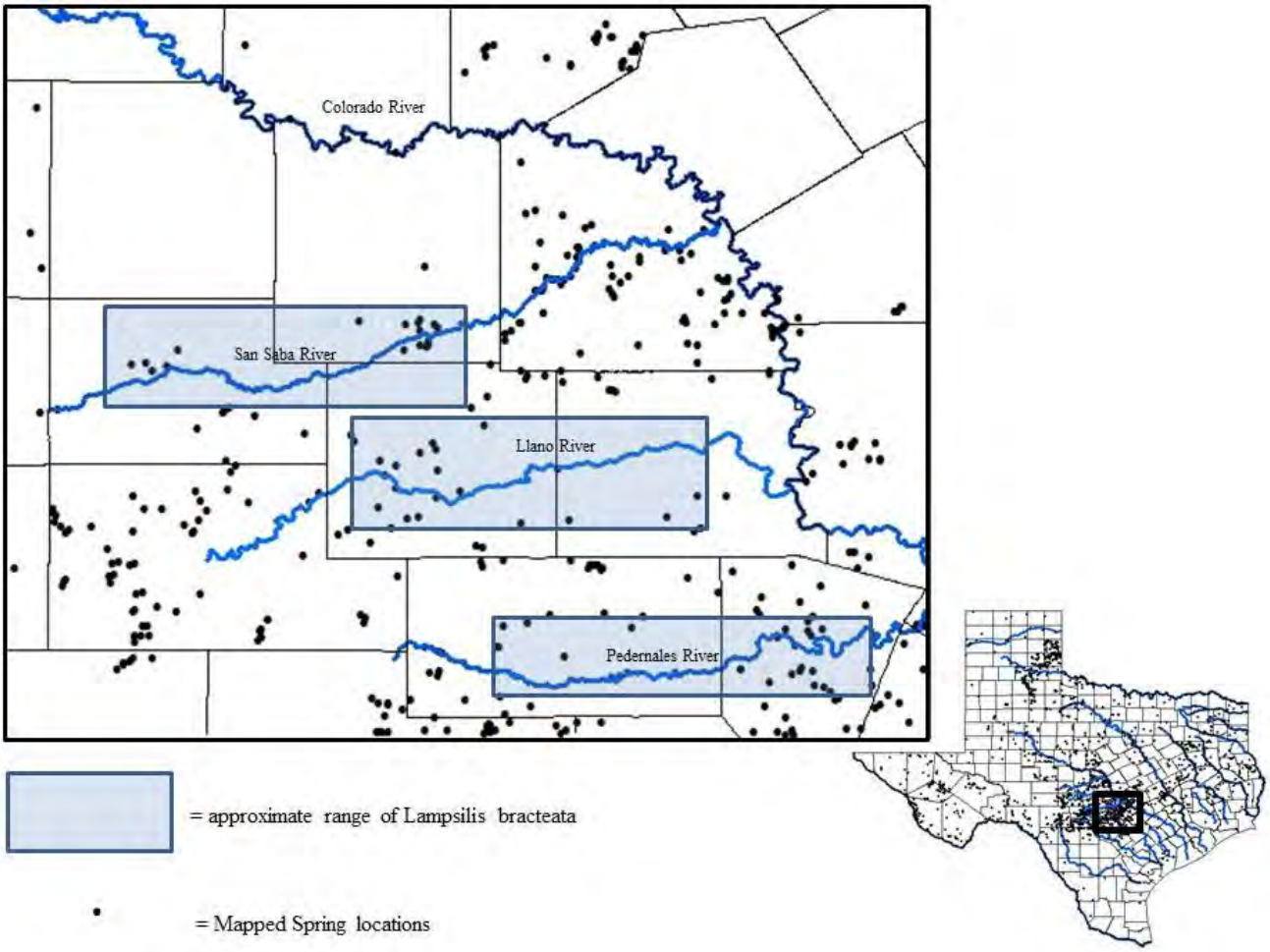

Figure 4: Map shows approximate *Lampsilis bracteata* range found in surveys by Morton et al. (2016), in relation to mapped spring locations in survey area.

Task 2.5. Stable isotope analysis to determine relative mussel food sources

Contributing authors: Brian Helms, Kaelyn Fogelman, Jim Stoeckel

Addresses: Department of Biological & Environmental Science, Troy University
Troy, AL 36082 (BH)
School of Fisheries, Aquaculture, and Aquatic Sciences, Auburn University, Auburn, AL 36804 (KF, JS)

Principal Investigators: Brian Helms, Jim Stoeckel

Email: helmsb@troy.edu, kjf0021@tigermail.auburn.edu, jimstoeckel@auburn.edu,

Mussels have long been considered to be suspension feeders (i.e., feeding on material suspended in the water column), with a diet comprised of phytoplankton, protozoans, detritus, bacteria, and dissolved organic carbon (Strayer et al. 2008). Previous studies using stable isotope analysis, fatty acid analysis and biochemical markers have elucidated the more prevalent components of suspended particulate organic matter (SPOM) that mussels use for food. Bacteria (Nichols & Garling 2000; Christian & Smith 2004), algae and phytoplankton (Weber et al. 2017; Raikow and Hamilton 2001) have been identified as important contributors to the freshwater mussel diet. While individual components of the mussel diet have become clearer, what they are actually assimilating from their food resources is poorly understood. Although mussels are largely considered suspension feeders, burrowing habits and associated pedal feeding (sweeping their ciliated foot through sediments) allow access to benthic food sources such as sediment-based organisms and detritus (Yeager et al. 1994; Nichols et al. 2005; Raikow and Hamilton 2001). While evidence shows that juveniles can consume benthic organic matter (Yeager et al. 1994; Haag 2012), the extent to which adult mussels utilize non-suspended food sources through pedal feeding is not fully understood.

A highly efficient method of determining mussel feeding ecology is stable isotope analysis. This approach is effective in inferring both ultimate energy sources and trophic position in organisms and can help elucidate the relative assimilation of suspended or benthic food sources (Cabana and Rasmussen 1996; Raikow and Hamilton 2001; Post 2002; Christian et al. 2004; Vuorio et al. 2007; Vaughn et al. 2008; Weber et al. 2017). Ultimate energy source is determined through carbon stable isotope ratios ($^{13}C/^{12}C$, or $\delta^{13}C$) and trophic position is determined through nitrogen stable isotope signatures ($^{15}N/^{14}N$, or $\delta^{15}N$) (Cabana & Rasmussen 1996; Vuorio et al. 2008; Newton et al. 2013). Although ^{13}C of many primary producers vary, the stable C isotope ratios of consumers are similar to that of their food reflecting the ultimate carbon source (DeNiro and Epstein 1978). However, the N pools of animals are enriched with ^{15}N relative to their food and this enrichment is on average +3.4 $^{O}/_{OO}$, i.e. 3.4 $^{O}/_{OO}$ difference in trophic levels (Deniro and Epstein 1981, Minagawa and Wada 1984). Sulfur ($^{34}S/^{32}S$) stable isotope ratios have also been useful in marine bivalve food web studies, and can potentially separate producers when stable C and N cannot (Connolly et al. 2004). Analysis of the stable isotope signatures of potential food resources for freshwater mussels in an aquatic system, including suspended organic matter, benthic sediment containing detritus, algae, bacteria and fungi mixed with sand, detritus (decaying organic leaf material), and primary producing plants, can ultimately identify the major contributors to the mussel diet in a specific system or season.

Several drivers for population decline of endemic mussels in Texas include habitat loss and destruction through impoundments, sedimentation, dewatering, and pollution (Howells et al. 1996; Randklev et al. 2013a; Randklev et al. 2013b). The status of three Texas endemics, *Cyclonaias petrina*, *Cyclonaias houstonensis* and *Lampsilis bracteata* is currently being assessed to identify conservation needs and inform management efforts. Incomplete knowledge of mussel

food resources can inhibit successful conservation and a better understanding of mussel feeding ecology can help elucidate causes of their imperilment and inform management efforts such as propagation and relocation. Thus the objectives of this study are to 1) determine the potential food resources of focal taxa through stable isotope analysis and, 2) assess spatial and temporal variations in feeding.

Methodology

Study Sites

Study sites were chosen from previously identified sites containing beds of target mussel species (*C. houstonensis*, *C. petrina* and *L bracteata*). Sites in the Colorado River watershed were located on the lower Colorado (LC; 29.556197N, -96.402160W) near Altair, Texas and on the Llano River, a tributary of the middle Colorado River (MC; 30.39267N, -99.19214W), located near Mason, Texas. The Guadalupe River drainage was sampled on the upper Guadalupe (UG; 29.93953N, -98.94846W) in Comfort, Texas and the Brazos River was sampled on the Navasota River, a tributary of the Lower Brazos (LB, 31.15155N, -96.19501W), near Easterly, Texas.

Mussel Sampling

Each mussel species (and its respective potential food resources) was sampled from two different basins each. *C. petrina* was sampled in the lower Colorado and upper Guadalupe Rivers, *C. houstenensis* was sampled in the lower Colorado and Navasota Rivers and *L. bracteata* was sampled in the upper Guadalupe and Llano Rivers. Ten individuals were collected per species at the site by snorkeling and searching benthic sediments by hand. Individual mussels were collected and measured for length, width, height and weight. Mussels were opened using

reverse action pliers and two sublethal tissue samples were taken from the foot using a 1.5 x 4.5 mm biopsy punch (Karl Storz 453733) (Fritts et al. 2015). Mussels were subsequently returned to the streambed where they were collected and tissue samples were transported on ice from the field and subsequently frozen and transported to Auburn University. Tissue samples were dried at 80°C to a constant mass, ground using a mortar and pestle, weighed (nearest 10^{-5} g) and placed in 4 x 6 mm tin capsules and sent to Washington State University (WSU) Stable Isotope Core Laboratory for $\delta^{13}C$, $\delta^{15}N$, and $\delta^{34}S$ stable isotope analysis (see below).

Potential Food Source Sampling

Hypothesized food sources were suspended particulate organic matter (SPOM), fine particulate organic matter associated with benthic sediments (FPOM), and coarse particulate organic matter (CPOM). Five 1-2 L water column samples were collected in spring (April 2017), summer (July 2017) and fall (October 2017) at all four sites to sample for SPOM. To isolate the particulate organic matter (primarily phytoplankton and detritus) in the water column that mussels could utilize as a food source, sample water was passed through 55 µm mesh to remove larger particles, as mussels utilize items <55 µm for food (Newton et al. 2013). The filtered water was then filtered again through a precombusted 47 cm Whatman GF/F filter (nominal pore size = 0.7 µm) using vacuum filtration. This procedure isolates suspended solids between 55 and 0.7 µm, which reflects the size fraction of identified potential food sources for mussels (Christian et al. 2004; Post 2002; Newton et al. 2013). Filters were then frozen for transportation back to Auburn University where they were dried at 80°C to a constant mass. The filters were fumigated in 3N H_3PO_4 for 8 hours to remove carbonates (Harris et al. 2000). Whole filters were sent to WSU Stable Isotope Core for analysis of stable C, N and S (see below).

Ten mid-channel benthic sediment samples for FPOM (which includes detritus, algae, bacteria and fungi mixed with sand) were collected in spring and summer in the same habitats where mussels were collected to reflect the available food resources mussels could access through pedal feeding. Five mid-channel, five bank and five bedrock surface sediment samples were taken from each site during fall sampling to further differentiate between benthic food sources being utilized. Sediment FPOM samples were prefiltered through an 80 and 55 □m sieve to remove gravel and debris larger than the previously established size fraction for potential mussel food resources. Samples were filtered through Whatman GF/F filters using vacuum filtration, frozen and transported to Auburn University as above with the SPOM filters. Samples were dried to a constant mass at 80°C and the sediment layer was then removed from the filter. Sediment was fumigated in 3N H_3PO_4 for 8 hours to remove carbonates and was then ground to a fine powder using a mortar and pestle, weighed (nearest 10^{-5} g) and encapsulated in 4 x 6 mm tin capsules and sent to WSU Stable Isotope Core for analysis of $\delta^{13}C$, $\delta^{15}N$, and $\delta^{34}S$ (see below).

Coarse particulate organic matter (CPOM, a mixture of decaying terrestrial leaf litter and organic aquatic material, i.e. "detritus") was collected from each site seasonally. Previous studies confirm that mussels produce the necessary enzymes to digest detrital food resources (Christian et al. 2004; Newton et al. 2013), and CPOM may be an important carbon source for bacteria production (Besemer et al. 2009). Additionally, filamentous algae and representative emergent (*Justicia*), submerged (*Myriophyllum*), and riparian ("grass") vascular plants were collected when present as further potential basal food resources and to provide primary producer context. Vascular algae and vascular plant samples were identified and separated in the field and all samples were frozen for transportation to Auburn University. Samples were dried at 80°C to a constant dry mass, ground to a fine powder using a mortar and pestle, weighed (nearest 10^{-5} g)

and placed in 4 x 6 mm tin capsules and sent for analysis of stable $\delta^{13}C$, $\delta^{15}N$, and $\delta^{34}S$. Water temperature, conductivity and pH were measured and discharge from the nearest USGS gauge was recorded at the time of sample collection for each site to inform any potential patterns identified in feeding ecology.

Stable Isotope Analysis

Stable carbon, nitrogen and sulfur isotopic analyses were conducted at Washington State University Stable Isotope Core Laboratory. Samples for carbon and nitrogen isotopic analysis are converted to N_2 and CO_2 with an elemental analyzer (ECS 4010, Costech Analytical) and the two gases are separated with a 3m GC column and analyzed with a continuous flow isotope ratio mass spectrometer (Delta PlusXP, Thermofinnigan, Bremen). Isotopic reference materials are interspersed with samples for calibration. Isotope ratios are reported in parts per thousand (‰) relative to standards (Vienna Peedee belemnite (VPDB) for carbon, atmospheric N for nitrogen and Vienna-Canyon Diablo Troilite (VCDT) for sulfur), defined in delta notation as:

$$\delta_{13}C \text{ or } \delta_{15}N \text{ or } \delta_{34}S = (R_{sample} / R_{standard} - 1) \times 10^3$$

where $R = {}^{13}C / {}^{12}C$ or ${}^{15}N / {}^{14}N$ or ${}^{34}S/{}^{32}S$ (Craig 1957, Jepsen and Winemiller 2002).

Statistical Analysis

Size data for species collected were averaged across all three seasons and compared across basins (Tables 1-3). Mean ($\bar{X}$) and standard deviation (σ) were calculated for each species across all seasons. Two-tailed *t*-tests were performed to compare length, width, height and length of species across basins. $\delta^{13}C$ and $\delta^{15}N$ data was averaged for each species for spring and summer seasons across basins and a two-tailed *t*-test was performed to determine within species

variation between seasons. We compared mussel length and stable isotope ratios with Pearson Product-Moment correlations.

To estimate feeding patterns, data initially were visually inspected using biplots. We then applied linear mixing models following the IsoSource procedure (Phillips and Greg 2003) to model the contribution of potential source materials to mussels. Since isotopic ratios of baseline resources are often different across systems, we analyzed each basin independently. We only used potential sources that were represented across all basins in IsoSource models for comparative purposes. These sources were SPOM, CPOM, and FPOM. Due to difficulties in the laboratory analysis of $\delta^{34}S$ and as a conservative measure until all seasonal isotope data are received from the analytical lab (see below), we constrained modeling to $\delta^{13}C$ for this report. Thus a 3 source single-isotope model was run for each mussel species for each site with a source increment set at 1% and tolerance initially set at 0.1‰ and increased incrementally (up to 2‰) until a solution was obtained. This model effectively assesses the relative contribution of CPOM, SPOM and FPOM to the basal carbon source(s) of mussel diet (i.e., this model may or may not reflect *direct* feeding). Reflecting this approach, and as a conservative measure, we did not correct consumer $\delta^{13}C$ in these models due to lack of information on the true trophic position of these species.

Results

Mussel Size

C. petrina was significantly larger in length, width, height and weight in the lower Colorado River compared to the upper Guadalupe River with mean length difference of 17.78 mm, width difference of 19.03 mm, height difference of 14.63 mm and weight difference of

70.31 g (two-tailed *t*-test; p = 1.23E-08 for length, p = 1.74E-12 for width, p = 1.69E-14 for height, p = 1.66E-07 for weight) (Table 1).

C. houstonensis was significantly longer and wider in the lower Colorado River compared to the lower Brazos River basin. Mean length difference was 6.12 mm and mean width difference was 5.88 mm (two-tailed t-test; p = 0.00094 for length; p = 0.00034 for width). There was no difference found in height and weight across basins (two-tailed *t*-test; p = 0.79 for height, p = 0.16 for weight) (Table 2).

L. bracteata was significantly larger in length, width, height and weight in the upper Guadalupe compared to the middle Colorado River basin with mean length difference of 5.11 mm, width difference of 2.46 mm, height difference of 1.46 mm and weight difference of 2.77 g (two-tailed *t*-test; p = 0.0047 for length, p = 0.019 for width, p = 0.018 for height, p = 0.022 for weight) (Table 3).

Environmental Sampling

The upper Guadalupe consistently had lower water temperatures due to being spring-fed. pH had low variability across seasons and sites. Conductivity and discharge were greatest in the lower Colorado River and lowest in the lower Brazos River basin during all seasons sampled (Table 4).

Stable Isotope Analysis

Stable isotope $\delta^{13}C$ and $\delta^{15}N$ analysis was completed for mussel foot tissue, SPOM, FPOM, CPOM and primary producing plants for samples collected in April 2017. Stable isotope $\delta^{13}C$ and $\delta^{15}N$ analysis also was completed for mussel foot tissue, SPOM, FPOM, CPOM, and primary producing plants for samples collected in July 2017. Laboratory analysis of $\delta^{34}S$ from

April samples was unsuccessful due to low sample volume causing sulfur detachment. This was corrected in sampling protocol for future seasons, yet summer and fall data have not been returned from the WSU Stable Isotope Core Laboratory and thus are not available for statistical analysis at this time. For samples collected in October 2017, $\delta^{13}C$, $\delta^{15}N$, and $\delta^{34}S$ isotope data has not been returned from WSU at this date. Presumably due to the impacts of Hurricane Harvey on the lower Colorado River, only three *C. petrina* and four *C. houstonensis* were located for fall sampling, compared to the standard sampling protocol for this study of 10 individuals per species per site.

Average isotopic signatures (± SD) and C:N ratios for all sampled sources and potential resources are presented (Table 5). In general, mussels exhibited $\delta^{15}N$ enrichment and $\delta^{13}C$ depletion relative to their respective environments with minimal intraspecific variation in both $\delta^{13}C$ and $\delta^{15}N$ (Table 6, Figures 1-4). Despite this, mussel size and $\delta^{13}C$ were positively correlated for mussels in the Upper Guadalupe and Lower Colorado and $\delta^{15}N$ and size was positively correlated for *C. houstonensis* in the Upper Guadalupe (Figure 5-7). An enrichment of $\delta^{13}C$ as mussels increase in size may reflect ontogenetic feeding shifts. For the spring, average $\delta^{13}C$ signatures for mussels ranged from -29.91‰ – -26.63‰ and average $\delta^{15}N$ ranged from 7.38‰ – 13.41‰ (Table 6). For the summer, average $\delta^{13}C$ signatures for mussels ranged from -26.45‰ – -28.83‰ and average $\delta^{15}N$ ranged from 7.28‰ – 13.38‰ (Table 6). Across seasons, mussels were more $\delta^{13}C$ enriched in the Middle Colorado basin and more $\delta^{15}N$ enriched in the Lower Colorado (Table 6). Also, where multiple species were sampled at a given site (Upper Guadalupe and Lower Colorado), all mussels had nearly identical isotopic signatures for both $\delta^{13}C$ and $\delta^{15}N$ (Table 6, Figure 1 and 2).

We observed seasonal changes in mussel isotopic signature, indicative of potential shifts in feeding and/or assimilation. There were significant changes in $\delta^{13}C$ signatures of *C. petrina*

between spring and summer with a mean enrichment of 0.90 ‰ from spring to summer in the upper Guadalupe (two-tailed *t*-test; $p = 0.0015$) and a mean enrichment of 1.18 ‰ in the lower Colorado (two-tailed *t*-test; $p = 3.43E-06$). *C. houstonensis* also had significant changes of $\delta^{13}C$ between spring and summer with a mean enrichment of 1.54 ‰ in the lower Colorado (twotailed *t*-test; $p = 0.0021$) and a mean enrichment of 0.84 ‰ in the lower Brazos basin (two-tailed *t*-test; $p = 0.0021$). There were no seasonal differences in $\delta^{13}C$ of *L. bracteata* in the Upper Guadalupe (two-tailed *t*-test; $p = 0.58$) or in the middle Colorado basin (two-tailed *t*-test; $p = 0.35$). There were no seasonal differences in the $\delta^{15}N$ signatures of any species in any basin (two-tailed *t*-test; $p > 0.05$).

Linear Mixing Models

Linear mixing models revealed that food resources are comprised primarily of materials with a carbon base of CPOM (i.e., benthic detritus) and to a lesser extent SPOM (i.e., seston) and FPOM (i.e., sediment deposits). All mussels and all seasons had high proportions of CPOM contributions, with the exception of *L. bracteata* in the Middle Colorado basin during spring. In general, there was little seasonal variation in dietary contributions of basal C resources, with the exception of *C. houstonensis* in the Lower Brazos basin, which showed a decreased reliance on CPOM in the summer, and *L. bracteata* in the Middle Colorado, which showed a shift from SPOM to CPOM contributions (Table 8, Figure 8). It should be noted that mussel stable isotope ratios remained largely consistent throughout both seasons within a given system, but basal resource signatures were often variable between seasons. Thus linear mixing models likely reflect less of a feeding shift in mussels and more of a changing food base offering insight on the timing of assimilation. Also, several models were only attainable after increasing tolerance

above reliable levels (up to 2‰). These included *C. petrina* in the Upper Guadalupe during the summer and *L. bracteata* in the Upper Guadalupe in the spring and summer. These models should be interpreted with extreme caution. Other models had tolerance levels set at 0.1‰.

For *C. houstonensis*, the mean dietary contribution of CPOM ranged from a low of 62.5% in the Lower Brazos basin during the summer to 96%, also in the Lower Brazos basin during the summer (Table 8). FPOM-based food sources represented a slightly higher proportion of total during the spring in the Lower Brazos basin whereas SPOM had a higher representation in Summer. In the Lower Colorado, *C. houstonensis* had somewhat higher contributions of SPOM than FPOM in the spring and summer, but this was still <5% on average of total dietary contribution (Table 8, Figure 8).

For *C. petrina*, the mean dietary contribution of CPOM ranged from a low of 93.9% during the spring in the Lower Colorado to 99% in the Upper Guadalupe, also in the spring (Table 8). FPOM-based food sources contributed near 1% in the Lower Colorado in both seasons and less than 1% in the Upper Guadalupe in both seasons. In the Lower Colorado, SPOM contributed on average 3 - 4.9% to total *C. petrina* diet but only 1 - 1.7% to total diet in the Upper Guadalupe (Table 8, Figure 8).

The contribution of CPOM based carbon for *L. bracteata* was more variable than for the other mussel species, with a high of 100% in the Upper Guadalupe in the summer to 2% in the Middle Colorado basin during the spring. The contribution of FPOM was similarly low for *L. bracteata* in both seasons and both systems, with averages ranging from 0 in the Upper Guadalupe to 5.4% in the Middle Colorado basin during the summer. The dietary contribution of SPOM based sources ranged from 0 in the Upper Guadalupe in the summer to 97.8% in the Middle Colorado basin during the spring (Table 8, Figure 8).

Brief Interpretation

These data reflect samples from spring 2017 ($\delta^{13}C$ and $\delta^{15}N$, no sulfur) and summer 2017 (carbon and nitrogen, no sulfur). Sulfur results from summer and the entire fall field season have not been returned from WSU analytical lab at the time of writing. Further, based on preliminary analysis, additional food sources were captured/isolated in fall (e.g., periphyton on hard surfaces, additional primary producers, and additional size fractions in FPOM). Any interpretation based on these data presented should be considered *preliminary* and undoubtedly more insight will be available once all data are received and full analyses can be complete. Several preliminary conclusions however seem to be arising. First, all three species appear to feed similarly. This is evidenced by the consistent stable C and N signatures across systems, and particularly the nearly identical signatures of *L. bracteata* and *C. petrina* in the Upper Guadalupe, and *C. petrina* and *C. houstonensis* in the Lower Colorado. The only deviation from this similarity is *L. bracteata* in the Middle Colorado, which displayed a relatively less-enriched $\delta^{15}N$ pattern. This characterization was from the Llano River, and whether this reflects differential feeding or simply is a system artifact is unclear at this point. Also, all three species showed a general trend to become carbon-enriched with increasing body size. This could reflect the inherent shift in diet from the parasitic glochidial stage thru adulthood. However, these trends were found in mussels in the Upper Guadalupe and Lower Colorado, but not the Middle Colorado basin and Lower Brazos basin, so that, again, a system artifact cannot be ruled out at this time.

From the data presented, with the exception of *L. bracteata* in the Middle Colorado basin during the summer, a major interpretation is that a majority of the carbon assimilated by all species is derived from CPOM. Whether this is direct feeding on CPOM particles or associated bacteria and fungi is not clear. Further, the role of SPOM (i.e, suspended producers and other

associated organics) and FPOM (benthic diatoms, algae, and organic matter associated with sediment) seem to play a much more minor role in contribution to dietary C as compared to CPOM. This could be interpreted as a reduced dietary reliance on filter-feeding phytoplankton and pedal feeding in sediments. However, it should be noted that mussels in general showed minimal (albeit statistically significant) seasonal variation, while food sources often showed considerable variation. This could indicate mussels assimilate food resources that are produced seasonally, or that we have yet to capture the C sources for their food. Full analysis of the complete dataset ($\delta^{13}C$, $\delta^{15}N$, and $\delta^{34}S$), including updated mixing models with additional food sources and size fractions, should elucidate these trends.

References

Besemer, K, I Hodl, G Singer, and TJ Battin. 2009. Architectural differentiation reflects bacterial community structure in stream biofilms. The ISME Journal 3: 1318-1324

Cabana, G, and JB Rasmussen. 1996. Comparison of aquatic food chains using nitrogen isotopes. Proceedings of the National Academy of Science. 93: 10844-10847.

Christian, AD, BN Smith, DJ Berg, JC Smoot, and RH Findlay. 2004. Trophic position and potential food sources of 2 species of unionid bivalves (Mollusca:Unionidae) in 2 small Ohio streams. Journal of the North American Benthological Society. 23(1): 101-113.

Craig, H. 1957. Isotopic Standards for Carbon and Oxygen and Correction Factors for MassSpectrometric Analysis of Carbon Dioxide. Geochimica et Cosmochimica Acta. 12: 133-149.

Connolly, RM, MA Guest, AJ Melville, and JM Oakes. 2004. Sulfur stable isotopes separate producers in marine food-web analysis. Oceologia. 138(2): 161-167.

DeNiro, MJ, and S Epstein. 1978. Influence of diet on the distribution of carbon isotopes in animals. Geochemica et Cosmochimica Acta. 42: 495-506.

Deniro, MJ, and S Epstein. 1981. Influence of diet on the distribution of nitrogen isotopes in animals. Geochimica et Cosmochimica Acta. 45: 341-351.

Fritts, AK, JT Peterson, PD Hazelton, and RB Bringolf. 2015. Evaluation of methods for assessing physiological biomarkers of stress in freshwater mussels. Canadian Journal of Fisheries and Aquatic Sciences. 72(10): 1450-1459.

Gangloff, MM, and JW Feminella. 2007. Stream channel geomorphology influences mussel abundance in southern Appalachian streams, USA. Freshwater Biology. 52: 64-74.

Haag, WR. 2012. North American Freshwater Mussels. New York, NY: Cambridge University Press.

Harris, D, RH Williams, and C van Kessel. 2000. Acid fumigation of soils to remove carbonates prior to total organic carbon or CARBON-13 isotopic analysis. Soil Science of America Journal. 65(6): 1853-1856.

Howard, JK, and KM Cuffey. 2006. The functional role of native freshwater mussels in the fluvial benthic environment. Freshwater Biology. 51: 460-474.

Howells, RG, RW Neck, and HD Murray. 1996. Freshwater mussels of Texas. Austin, TX: Texas Parks and Wildlife Press.

Jepsen, DB, and KO Winemiller. 2002. Structure of tropical river food webs revealed by stable isotope ratios. Oikos. 96: 46-55.

Minagawa, M, and E Wada. 1984. Stepwise enrichment of ^{15}N along food chains: Further evidence and the relation between $d^{15}N$ and animal age. Geochemica et Cosmochimica Acta. 48: 1135-1140.

Nichols, SJ, and D Garling. 2000. Food-web dynamics and trophic-level interactions in a multi-species community of freshwater unionids. Canadian Journal of Zoology. 78: 871-882.

Nichols, SJ, H Silverman, TH Dietz, JW Lynn, and DL Garling. 2005. Pathways of food uptake in native (Unionidae) and introduced (Corbiculidae and Dreissenidae) freshwater bivalves. Journal of Great Lakes Research. 31: 87-96.

Newton, TJ, CC Vaughn, DE Spooner, J Nichols, and MT Arts. 2013. Profiles of Biochemical Tracers in Unionid Mussels Across a Broad Geographical Range. Journal of Shellfish Research. 32(2): 497-507.

Phillips, DL, and JW Gregg. 2003. Source partitioning using stable isotopes: coping with too many sources. Oecologia. 136: 261-269.

Post, DM. 2002. Using stable isotopes to estimate trophic position: models, methods and assumptions. Ecology. 83(3): 703-718.

Raikow, DF, and SK Hamilton. 2001. Bivalve diets in a Midwestern U.S. stream: A stable isotope enrichment study. Limnology and Oceanography. 46(3): 514-522.

Randklev, CR, MS Johnson, ET Tsakiris, J Groce, and N Wilkins. 2013a. Status of the freshwater mussel (Unionidae) communities of the mainstem of the Leon River, Texas. Aquatic Conservation: Marine and Freshwater Ecosystems. 23: 390-404.

Randklev, CR, ET Tsakiris, MS Johnson, JA Skorupski, LE Burlakova, J Groce, and N Wilkins. 2013b. Is False spike, *Quadrula mitchelli* (Bivalvia: Unionidae), extinct? First account of a very recently deceased individual in over thirty years. Southwestern Naturalist. 58(2): 247-249.

Silverman, H, SJ Nichols, JS Cherry, E Archberger, JW Lynn, and TH Dietz, 1997. Clearance of laboratory-cultured bacteria by freshwater bivalves: differences between lentic and lotic unionids. Canadian Journal of Zoology. 75: 1857-1866.

Strayer, DL. 2008. Freshwater Mussel Ecology. Berkeley, CA: University of California Press.

Strayer, DL, NF Caraco, JJ Cole, S Findley, and ML Pace. 1999. Transformation of freshwater ecosystems by bivalves. BioScience. 49: 19-27.

Strayer, DL, JA Downing, WR Haag, TL King, JB Layzer, TJ Newton, and S Nichols. 2004. Changing perspectives on pearly mussels, North America's most imperiled animals. BioScience. 54: 429-439.

Spooner, DE, and CC Vaughn. 2006. Context-dependent effects of freshwater mussels on the benthic community. Freshwater Biology. 51: 1016-1024.

Vaughn, CC, KB Gido, and DE Spooner. 2004. Ecosystem processes performed by unionid mussels in stream mecocosms: species roles and effects of abundance.

Hydrobiologia. 527: 35-47.

Vaughn, CC and CC Hakenkamp. 2001. The functional role of burrowing bivalves in freshwater ecosystems. Freshwater Biology. 46: 1431-1446.

Vaughn, CC, SJ Nichols, and DE Spooner. 2008. Community and foodweb ecology of freshwater mussels. Journal of the North American Benthological Society. 27(2): 409-423.

Vuorio, K, M Tarvainen, and J Sarvala. 2008. Unionid mussels as stable isotope baseline indicators for long-lived secondary consumers in pelagic food web comparisons. Fundamental and Applied Limnology. 169(3): 237-245.

Weber, AM, JE Bauer, and GT Watter. 2017. Assessment of nutritional subsidies to freshwater mussels using a multiple natural abundance isotope approach. Freshwater Biology. 62: 615-629.

Williams, JD, AE Bogan, JT Garner. 2008. Freshwater Mussels of Alabama & the Mobile Basin. Tuscaloosa, AL: University of Alabama Press.

Winemiller, K, NK Lujan, RN Wilkins, RT Snelgrove, AM Dube, KL Skow, and AG Snelgrove. 2010. Status of Freshwater Mussels in Texas. College Station, TX: Texas A&M Department of Wildlife and Fisheries Sciences and Texas A&M Institute of Renewable Natural Resources.

Yeager, MM, DS Cherry, and RJ Neves. 1994. Burrowing behaviors of juvenile rainbow mussels, *Villosa iris* (Bivalvia: Unionidae). Journal of the North American Benthological Society. 13(2): 217-222.

Table 1. Size data for *C. petrina* sampled in the upper Guadalupe River and the lower Colorado River. Note significant p-values in bold (two-tailed t-test with unequal variance).

	Upper Guadalupe		**Lower Colorado**		
C. petrina	$\bar{X}$	σ	$\bar{X}$	σ	*p*
Length (mm)	48.12	5.19	65.90	10.12	**1.23E-08**
Width (mm)	33.46	4.55	52.49	7.41	**1.74E-12**
Height (mm)	18.83	2.75	33.46	4.84	**1.69E-14**
Weight (g)	18.40	7.02	88.71	41.61	**1.66E-07**

Table 2. Size data for *C. houstonensis* sampled in the lower Colorado River and the lower Brazos River basin. Note significant p-values in bold (two-tailed t-test with unequal variance).

	Lower Colorado		**Lower Brazos**		
C. houstonensis	$\bar{X}$	σ	$\bar{X}$	σ	*p*
Length (mm)	50.34	7.07	44.22	4.97	**0.00094**
Width (mm)	44.46	5.88	38.58	5.14	**0.00034**
Height (mm)	28.10	3.54	27.83	3.86	0.79
Weight (g)	44.61	18.9	37.52	14.16	0.16

Table 3. Size data for *L. bracteata* sampled in the upper Guadalupe River and the middle Colorado River basin. Note significant p-values in bold (two-tailed t-test with unequal variance).

	Upper Guadalupe		**Middle Colorado**		
L. bracteata	$\bar{X}$	σ	$\bar{X}$	σ	*p*
Length (mm)	50.69	4.53	45.58	8.39	**0.0047**
Width (mm)	32.13	3.21	29.67	4.50	**0.019**
Height (mm)	19.26	1.83	17.80	2.70	**0.018**
Weight (g)	15.12	4.40	12.33	4.56	**0.022**

Table 4. Seasonal environmental data collected at sites in spring, summer and fall of 2017 during mussel and food source sampling.

Season	Site	Temp (°C)	pH	Conductivity (µS/cm)	Discharge (cfs)
Spring	UG	22.6	8.3	471	125
	LC	24.5	8.5	500	1310
	MC	24.1	7.9	329	138
	LB	21.7	7.5	340	38
Summer	UG	26.5	8.4	497	55
	LC	32.7	9.2	584	1225
	MC	31.5	8.7	354	88.7
	LB	27.7	7.9	283	23
Fall	UG	16	8.7	510	56
	LC	20.6	8.4	765	1230
	MC	19.7	8.5	388	60
	LB	12.7	8.3	248	11

Table 5. Stable isotope values for all consumers and potential food source samples.

		Spring							Summer				
	Source	**$\delta^{13}C$**	**σ**	**$\delta^{15}N$**	**σ**	**C:N**	**$\delta^{34}\Sigma$**	**σ**	**$\delta^{13}C$**	**σ**	**$\delta^{15}N$**	**σ**	**C:N**
Upper Guadalupe	*C. petrina*	-29.21	0.48	11.15	0.45	3.76	1.03	0.2	-28.3	0.36	10.96	0.16	3.66
	L. bracteata	-28.95	0.55	11.06	0.3	3.89	0.85	0.46	-28.78	0.67	10.75	0.68	7.81
	Seston	-24.84	0.41	2.75	0	8.94			-17.3	0.3	6.34	2.84	14.71
	CPOM	-29.26	0.54	1.85	1.46	42.99			-28.14	0	3	0	15.33
	Sediment	-9.53	0.56	4.86	0.28	38.01			-10.86	0.14	8.48	0.25	33.17
	Grass								-30.36	0	5.47	0	25.48
	Justicia	-25.79	0.46	8.41	0.55	11.05			-26.26	0	8.32	0	14.4
	Myriophyllum	-29.16	0.27	10.29	0.82	16.47							
Lower Colorado	*C. petrina*	-29.86	0.37	13.41	0.46	3.91	-0.13	0.2	-28.68	0.43	13.38	0.92	9.77
	C. houstonensis	-29.91	0.8	13.1	0.87	3.97	-0.14	0.2	-28.83	0.39	12.71	0.4	8.61
	Seston	-24.49	2.21	2.35	0.52	9.56			-22.3	0.29	8.47	0.49	8.15
	CPOM	-29.58	0.78	4.7	1.54	29.57			-29.1	0	10.97	0	16.16
	Sediment	-12.63	0.75	3.86	0.56	21.51			-13.95	0.25	7.79	0.37	29.51
	Grass	-30.54	0.06	10.92	0.27	20.16			-13.78	0	8.68	0	9.82
	Justicia												
	Myriophyllum								-27.97	2.88	10.25	4.44	12.16
	Algae								-19.7	0	2.17	0	21.75

Table 5 (continued).

		Spring							Summer				
	Source	**$\delta^{13}C$**	**σ**	**$\delta^{15}N$**	**σ**	**C:N**	**$\delta^{34}\Sigma$**	**σ**	**$\delta^{13}C$**	**σ**	**$\delta^{15}N$**	**σ**	**C:N**
Middle Colorado	*L. bracteata*	-26.63	0.55	7.38	0.55	3.75	4.5	0.19	-26.45	0.33	7.28	0.26	9.47
	Seston	-22.92	0.77	0.24	0.92	10.26			-19.02	0.7	2.88	1.49	15.26
	CPOM	-20.85	2.99	5.67	2.09	23.61			-28.26	0	0.48	0	16.16
	Sediment	-11.11	0.16	3.34	0.36	36.43			-11.01	0.19	5.3	0.22	38.75
	Grass	-28.81	0.58	4.97	0.31	22.1			-26.5	0	1.17	0	9.77
	Justicia	-15.74	0.59	6.06	0.28	22.13			-22.97	0	5.57	0	8.71
	Myriophyllum	-25	0.65	3.4	0.46	16.1			-18.89	6.5	2.68	4.12	11.19
	Algae								-17.68	0	10.1	0	9.09
Lower Brazos	*C. houstonensis*	-28.37	0.18	11.81	0.45	3.76	-0.93	0.4	-27.99	0.2	12.22	0.52	10.63
	Seston	-22.3	2.02	2.76	0.22	9.09			-25.89	0.23	4.06	1.31	9.59
	CPOM	-29.16	1.49	5.36	1	33.7			-29.97	0	3.98	0	30.46
	Sediment	-23.08	0.63	3.02	0.48	9.14			-22.85	0.62	-0.76	2.65	10.37
	Grass	-30.38	0.07	9.56	0.22	14.42							
	Justicia								-31.75	0	9.98	0	14.42
	Myriophyllum								-32.37	0	7.35	0	17.67

Table 6. Mean $\delta^{13}C$ and $\delta^{15}N$ signatures of tissue from focal taxa in spring and summer 2017.

Source	Season	Site	n	$\delta^{13}C$	$\delta^{15}N$
C. petrina	Spring	UG	7	-29.21	11.15
		LC	10	-29.86	13.41
	Summer	UG	11	-28.31	10.40
		LC	10	-28.68	13.38
C. houstonensis	Spring	LC	10	-29.91	13.10
		LB	12	-28.37	11.81
	Summer	LC	10	-28.83	12.71
		LB	10	-27.99	12.21
L. bracteata	Spring	UG	6	-28.95	11.06
		MC	12	-26.38	7.38
	Summer	UG	13	-28.78	10.75
		MC	10	-26.45	7.23

Table 7. Pearson product-moment coefficients and associated p-values for correlations between mussel size and $\delta^{13}C$ and mussel size and $\delta^{15}N$. Data were pooled across seasons for each species and each site. Bold values are statistically significant.

		$\delta_{13}C$		**$\delta^{15}N$**	
Site	*Species*	*r*	*p*	*r*	*p*
Upper Guadalupe	*C. petrina*	**0.47**	**0.05**	0.01	0.98
	L. bracteata	**0.46**	**0.05**	0.45	0.06
Lower Colorado	*C. houstonensis*	**0.58**	**0.01**	**0.48**	**0.03**
	C. petrina	**0.57**	**0.01**	0.22	0.36
Middle Colorado basin	*L. bracteata*	0.36	0.10	0.34	0.12
Lower Brazos basin	*C. houstonensis*	0.26	0.24	0.39	0.08

Table 8. IsoSource model estimates for the 3 mussel species for Spring and Summer.'C: N' is average carbon:nitrogen ratio, CPOM is coarse particulate organic matter, FPOM is fine particulate organic matter, SPOM is suspended particulate organic matter, and values are mean, minimum, maximum, and standard deviation estimated proportional composition of each C source.

Species	Site	C:N		Spring 2017				Summer 2017			
			C source	Mean	Min	Max	SD	Mean	Min	Max	SD
Cyclonais houstensis	LB	3.62	CPOM	0.876	0.87	0.88	0.005	0.625	0.53	0.72	0.062
			FPOM	0.074	0.03	0.13	0.047	0.145	0.02	0.27	0.083
			SPOM	0.05	0	0.09	0.042	0.23	0.01	0.45	0.146
	LC	3.89	CPOM	0.943	0.87	1	0.033	0.96	0.94	0.98	0.012
			FPOM	0.01	0	0.03	0.01	0.01	0	0.02	0.009
			SPOM	0.047	0	0.13	0.036	0.03	0	0.06	0.019
Cyclonais petrina	LC	3.86	CPOM	0.939	0.86	1	0.035	0.96	0.94	0.98	0.012
			FPOM	0.012	0	0.04	0.011	0.01	0	0.02	0.009
			SPOM	0.049	0	0.14	0.039	0.03	0	0.06	0.019
	UG	3.79	CPOM	0.99	0.99	0.99	0	0.974	0.95	1	0.014
			FPOM	0	0	0	0	0.009	0	0.03	0.01
			SPOM	0.01	0.01	0.01	0	0.017	0	0.05	0.016
	MC	3.82	CPOM	0.02	0	0.05	0.019	0.85	0.8	0.9	0.03
			FPOM	0.003	0	0.01	0.005	0.054	0	0.11	0.034
			SPOM	0.978	0.95	1	0.017	0.096	0	0.2	0.063
Lampsilis bracteata	UG	3.83	CPOM	0.93	0.93	0.93	0	1	1	1	0
			FPOM	0	0	0	0	0	0	0	0
			SPOM	0.07	0.07	0.07	0	0	0	0	0

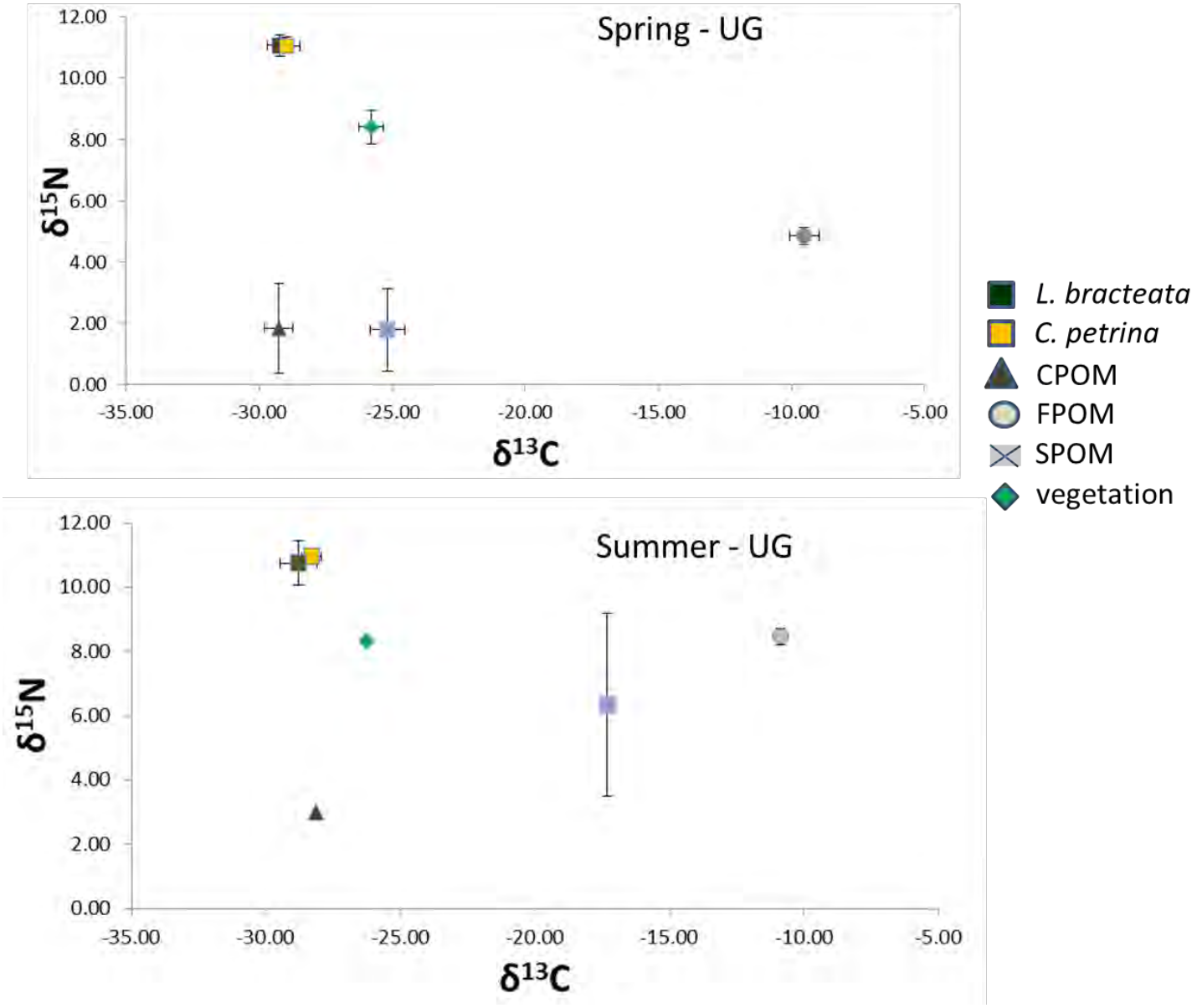

Figure 1. Stable CN isotope biplots for the Upper Guadalupe River site in April (Spring) and July (Summer) 2017. CPOM is coarse particulate organic matter (benthic detritus), FPOM is fine particulate organic matter from benthic sediments, SPOM is suspended particulate organic matter (seston), and 'vegetation' is *Justicia*.

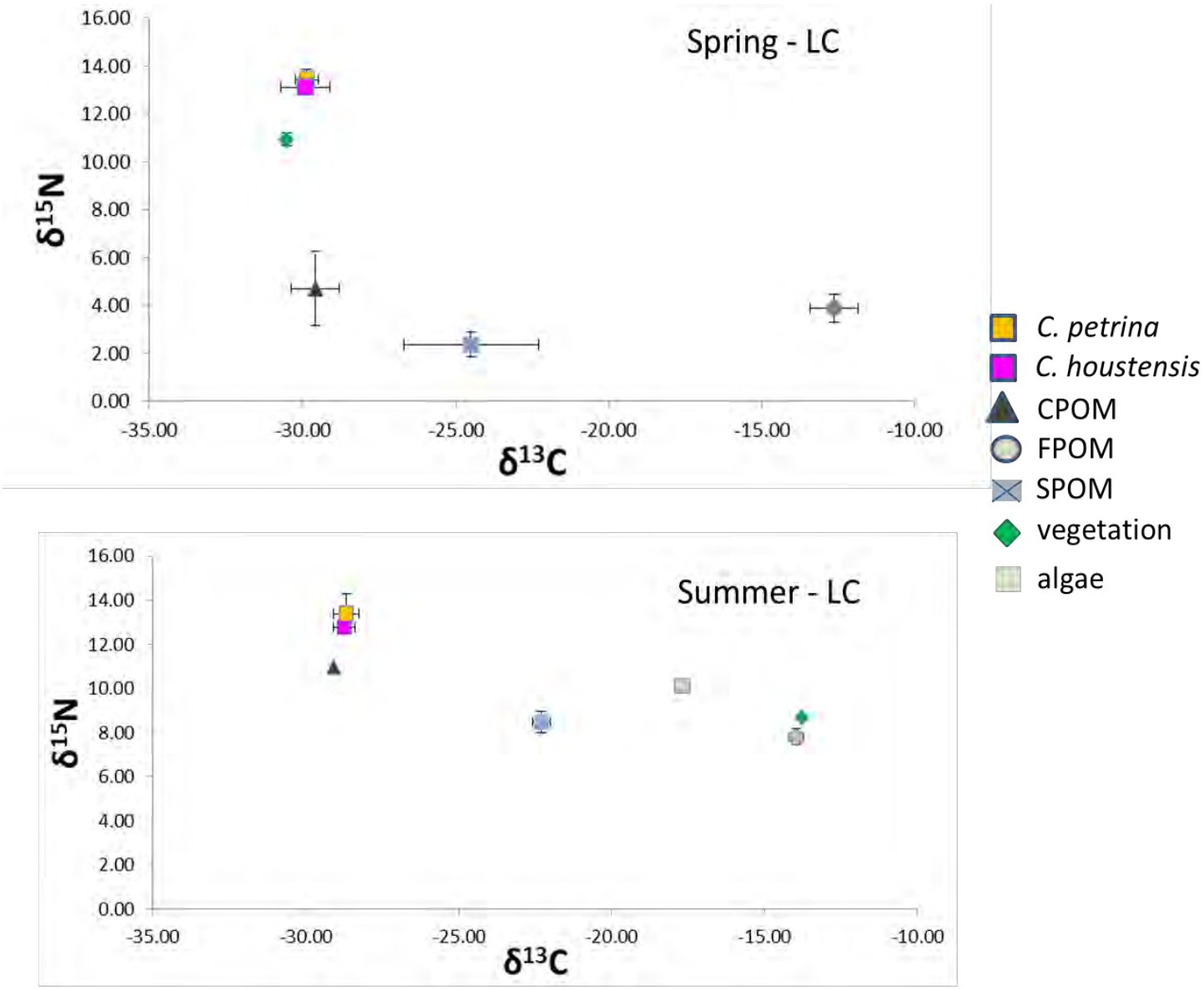

Figure 2. Stable CN isotope biplots for the Lower Colorado River site in April (Spring) and July (Summer) 2017. CPOM is coarse particulate organic matter (benthic detritus), FPOM is fine particulate organic matter from benthic sediments, SPOM is suspended particulate organic matter (seston), 'vegetation' is *Justicia* in the spring, riparian grass in the summer, and 'algae' is benthic filamentous algae

.

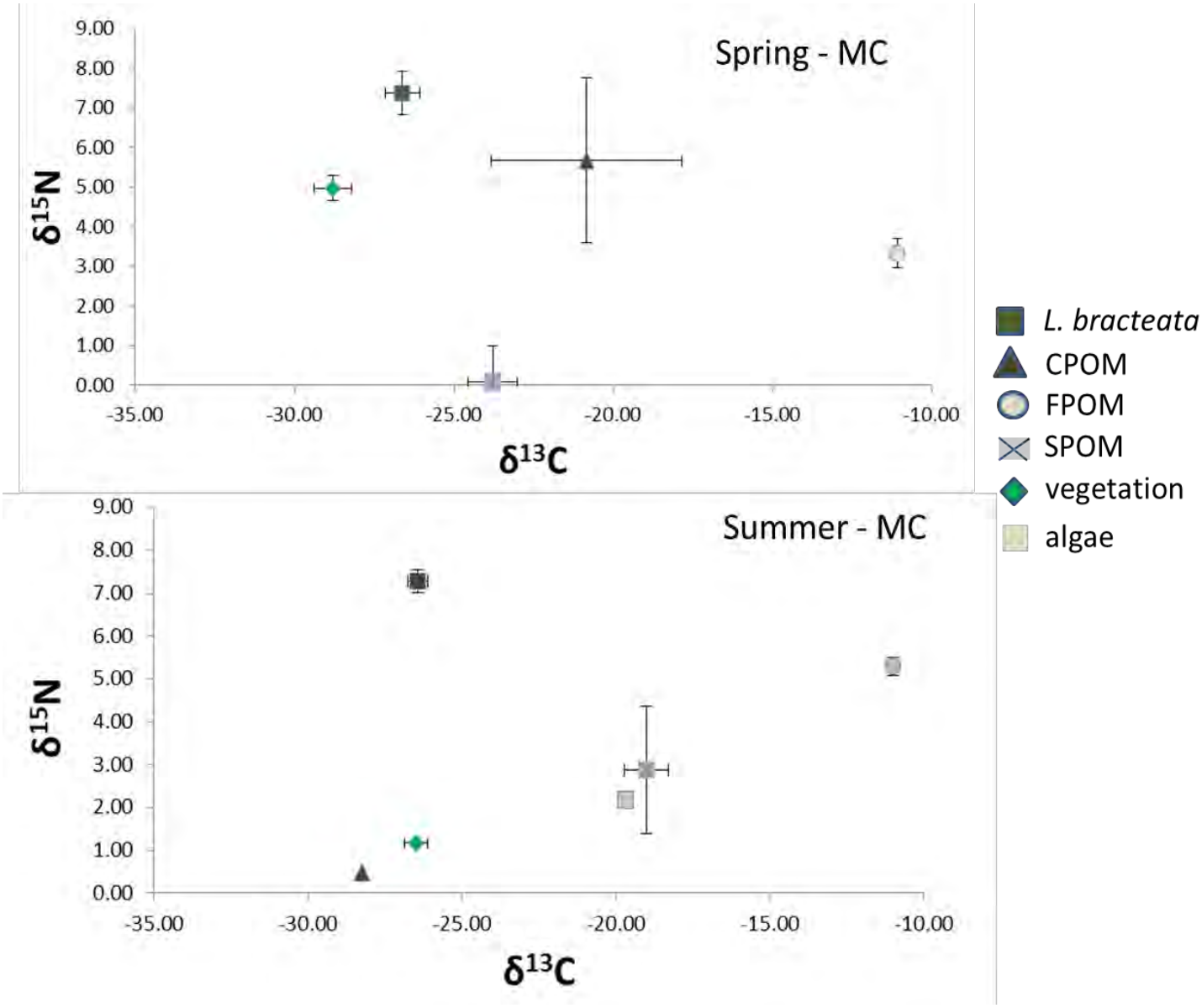

Figure 3. Stable CN isotope biplots for the Middle Colorado River basin site in April (Spring) and July (Summer) 2017. CPOM is coarse particulate organic matter (benthic detritus), FPOM is fine particulate organic matter from benthic sediments, SPOM is suspended particulate organic matter (seston), 'vegetation' is *Justicia*, and 'algae' is benthic filamentous algae.

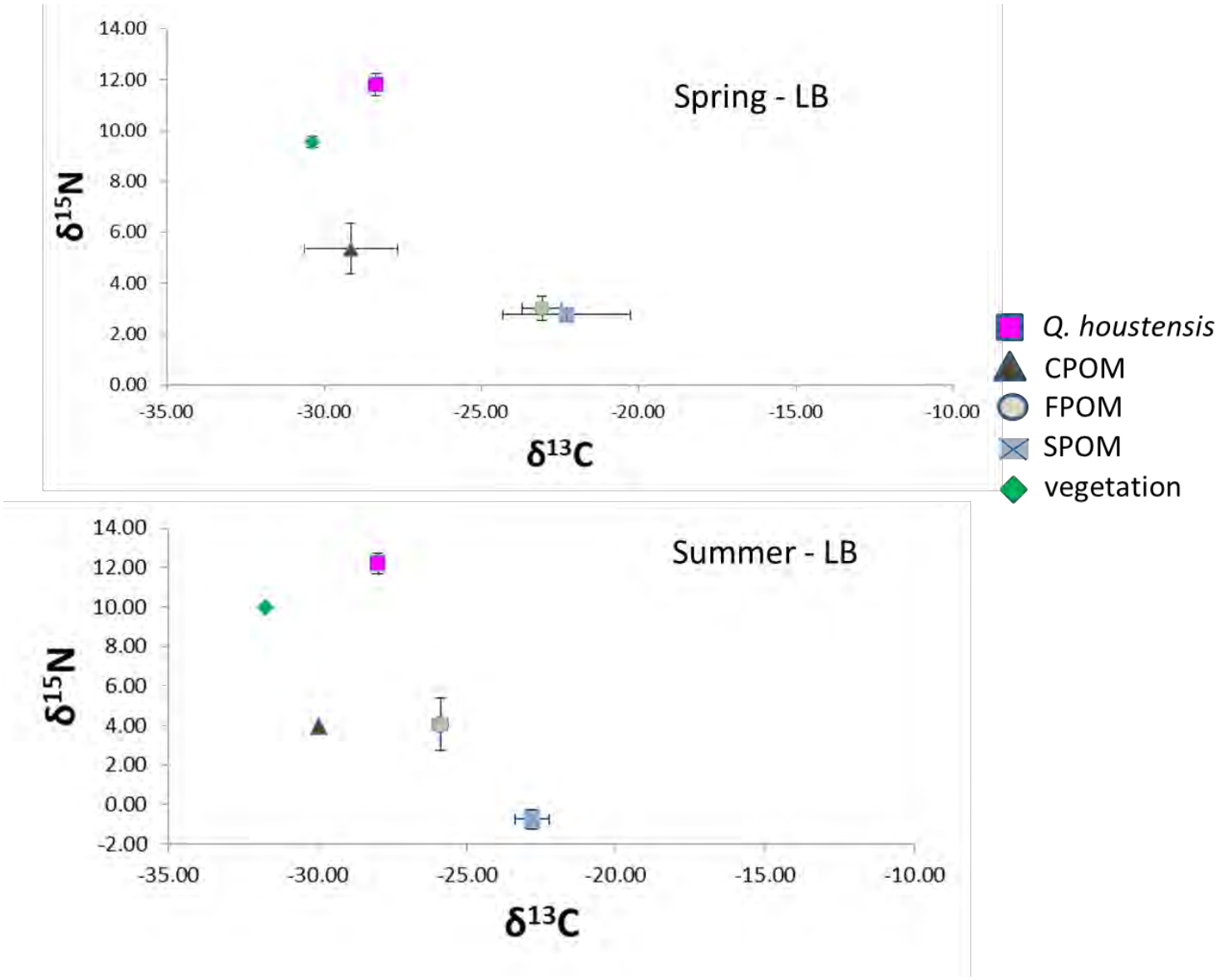

Figure 4. . Stable CN isotope biplots for the Lower Brazos River basin site in April (Spring) and July (Summer) 2017. CPOM is coarse particulate organic matter (benthic detritus), FPOM is fine particulate organic matter from benthic sediments, SPOM is suspended particulate organic matter (seston), and 'vegetation' is *Justicia*.

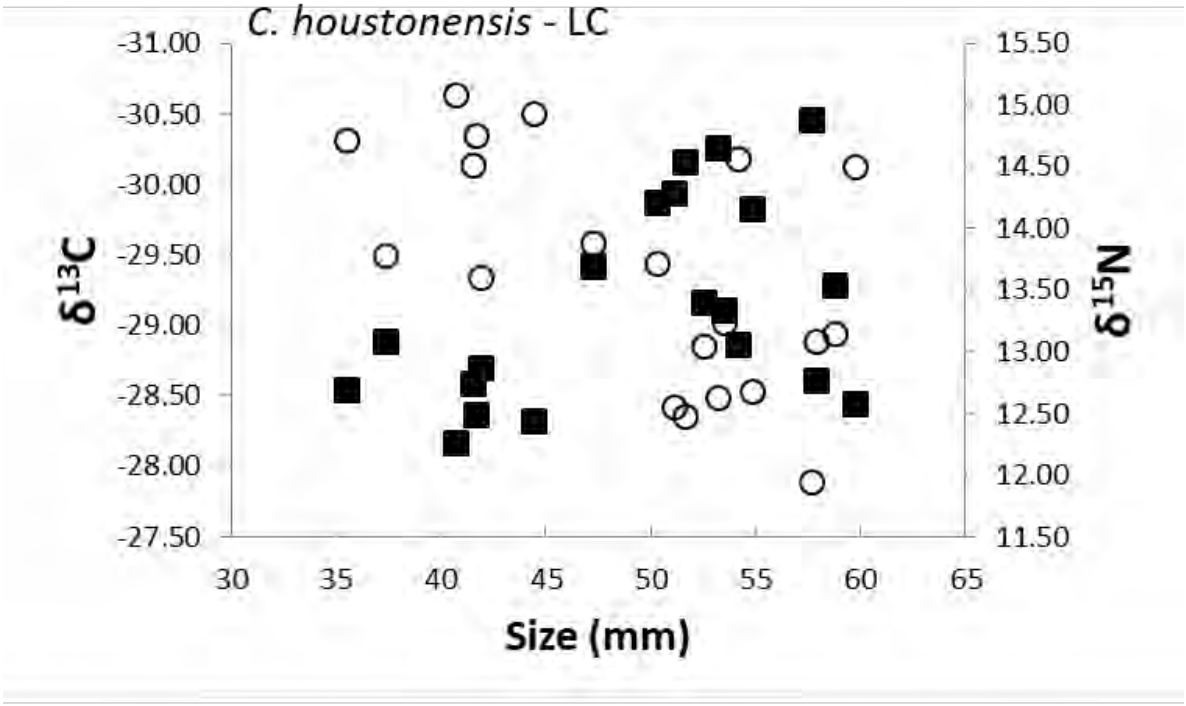

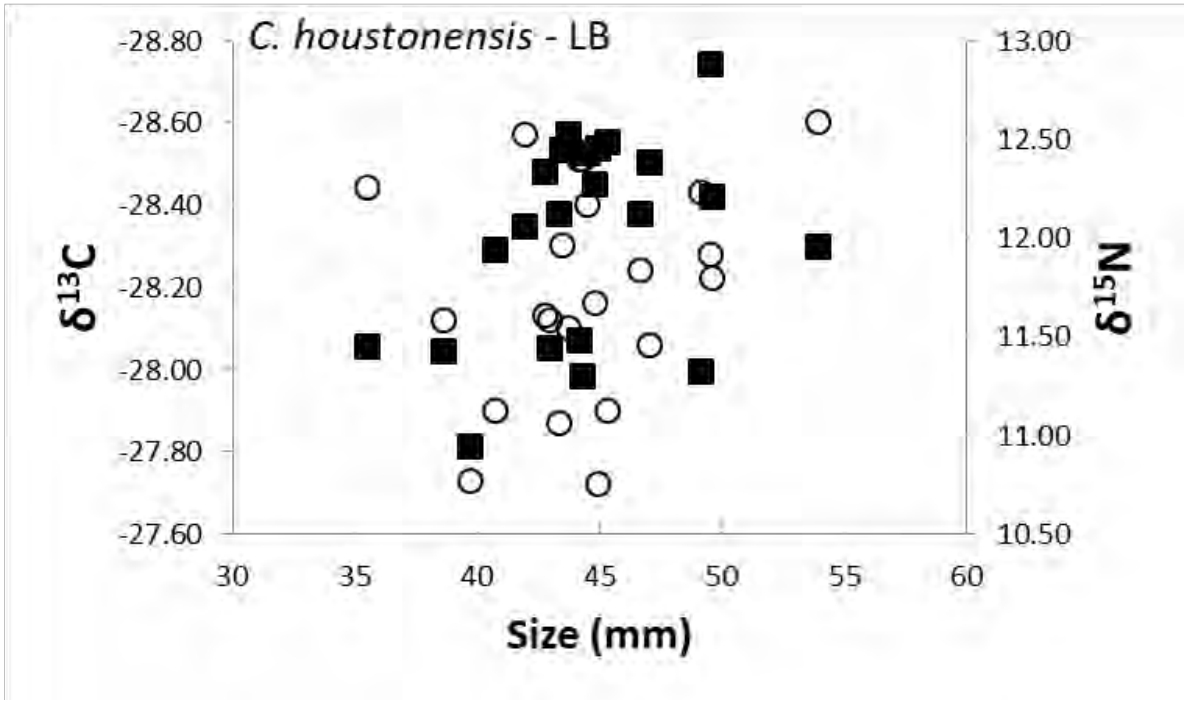

Figure 5. Relationships between stable isotope ratios ($\delta^{13}C$ and $\delta^{15}N$) and *C. houstonensis* size (length) in the Lower Colorado (LC) and Lower Brazos basin (LB). Open circles are $\delta^{13}C$ and filled squares are $\delta^{15}N$. Note $\delta^{13}C$ axis is inverted. See Table 7 for statistics.

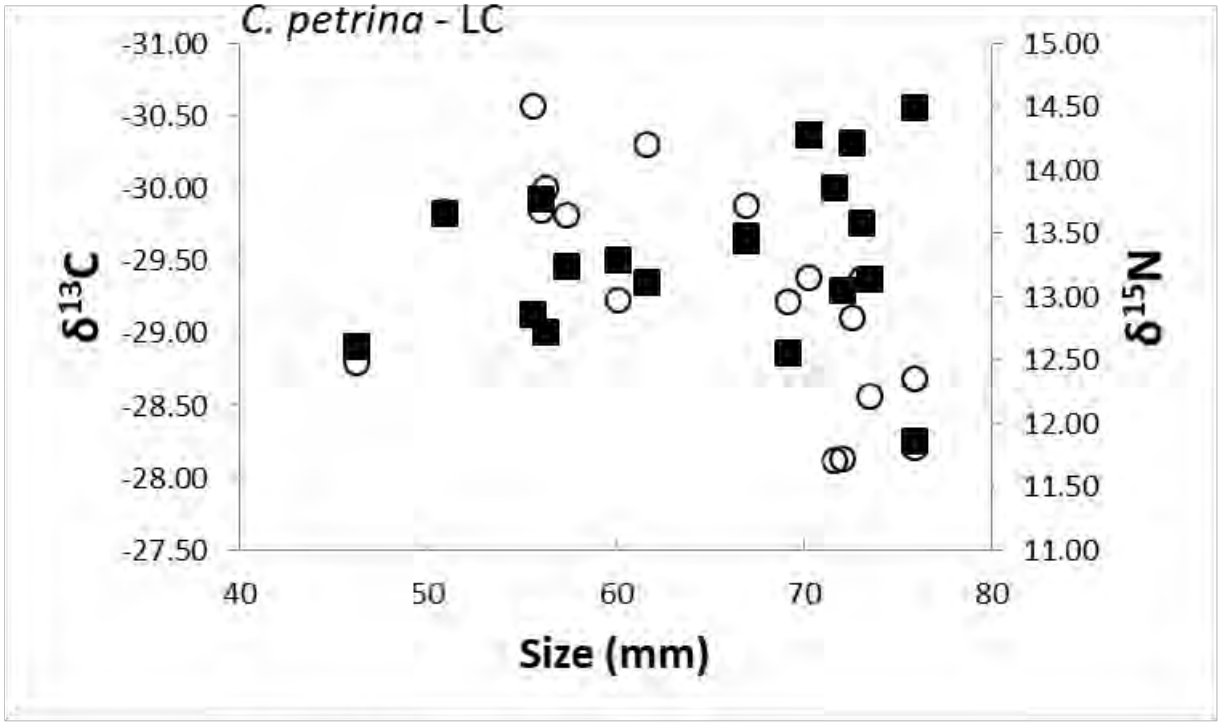

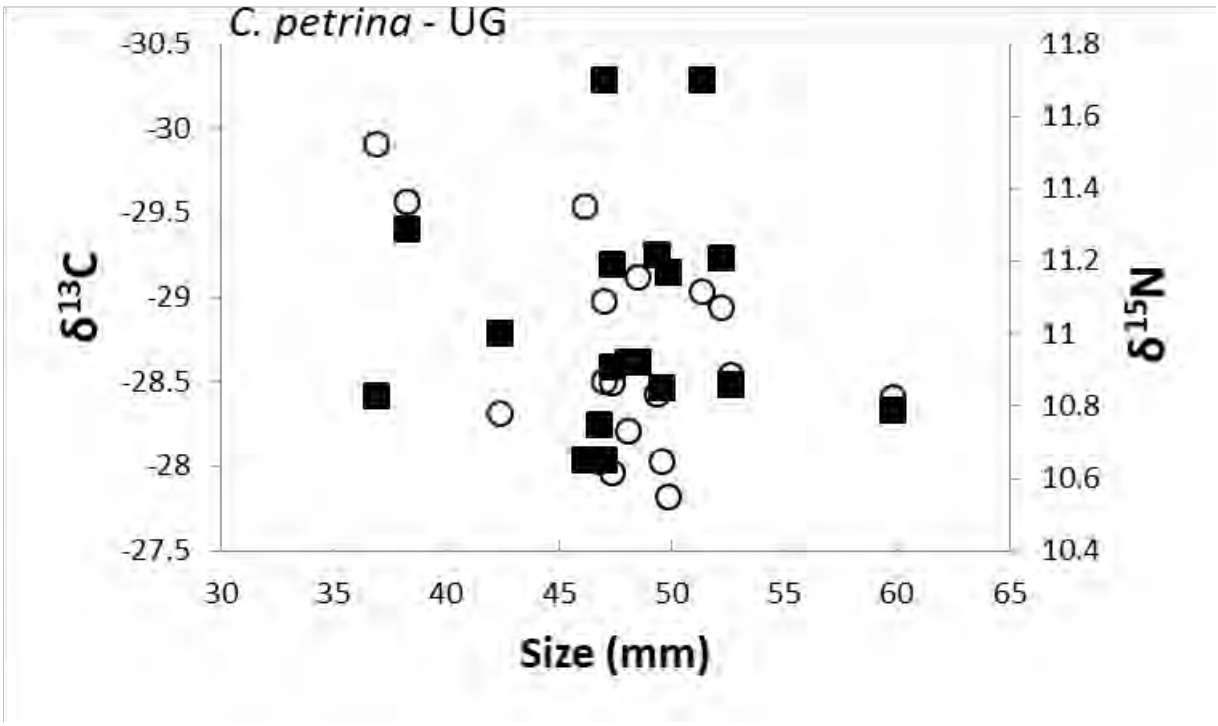

Figure 6. Relationships between stable isotope ratios ($\delta^{13}C$ and $\delta^{15}N$) and *C. petrina* size (length) in the Middle Colorado basin (MC) and Upper Guadalupe (UG). Open circles are $\delta^{13}C$ and filled squares are $\delta^{15}N$. Note $\delta^{13}C$ axis is inverted. See Table 7 for statistics.

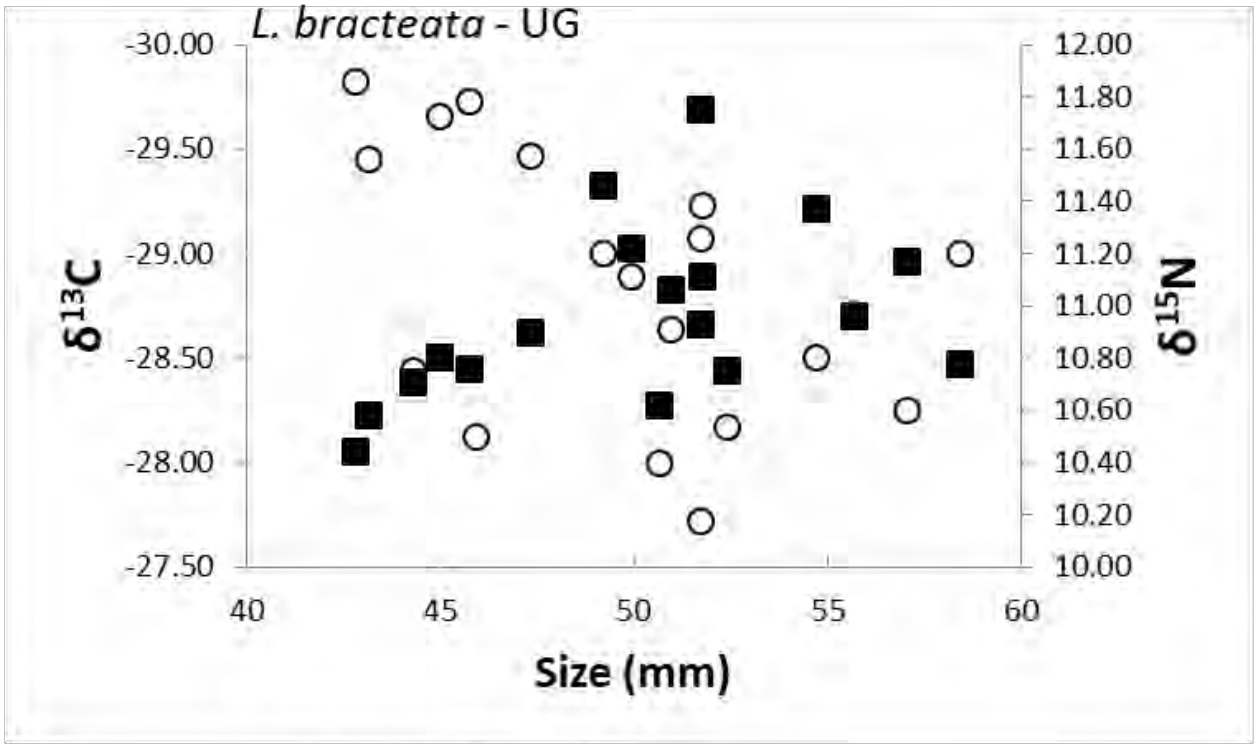

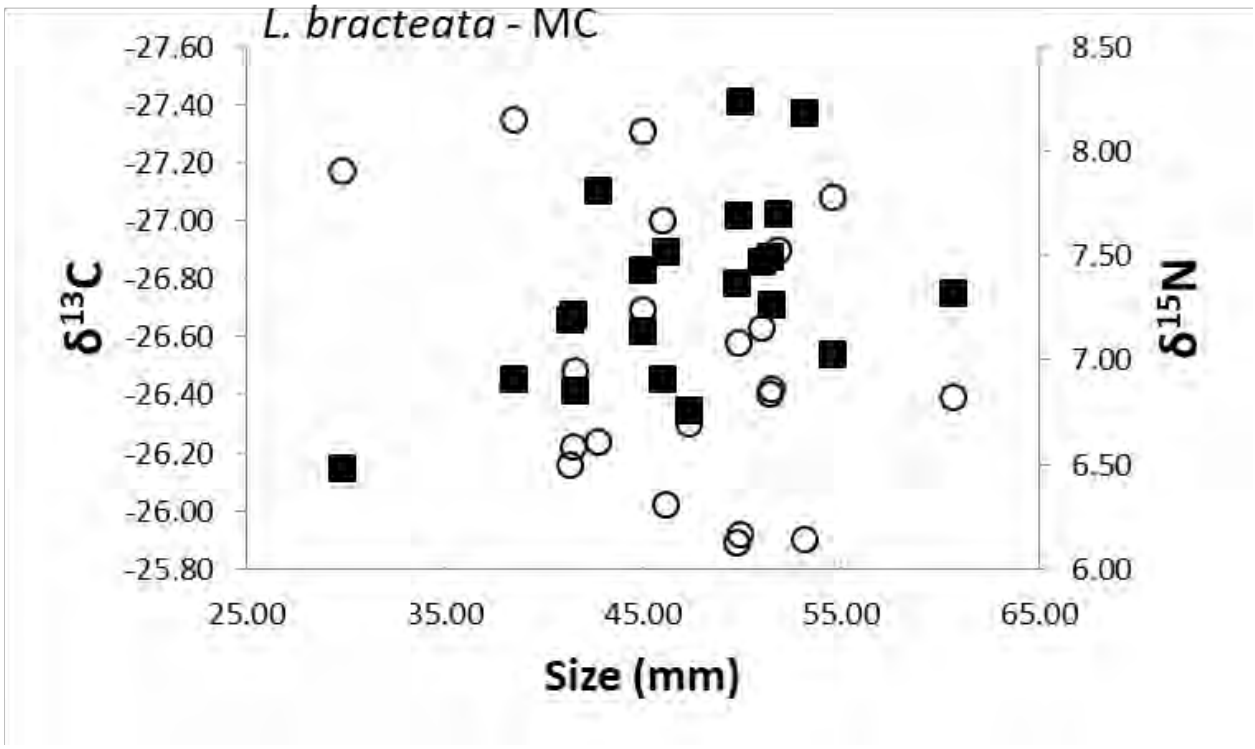

Figure 7. Relationships between stable isotope ratios ($\delta^{13}C$ and $\delta^{15}N$) and *L. bracteata* size (length) in the Upper Guadalupe (UG) and Middle Colorado basin (MC). Open circles are $\delta^{13}C$ and filled squares are $\delta^{15}N$. Note $\delta^{13}C$ axis is inverted. See Table 7 for statistics.

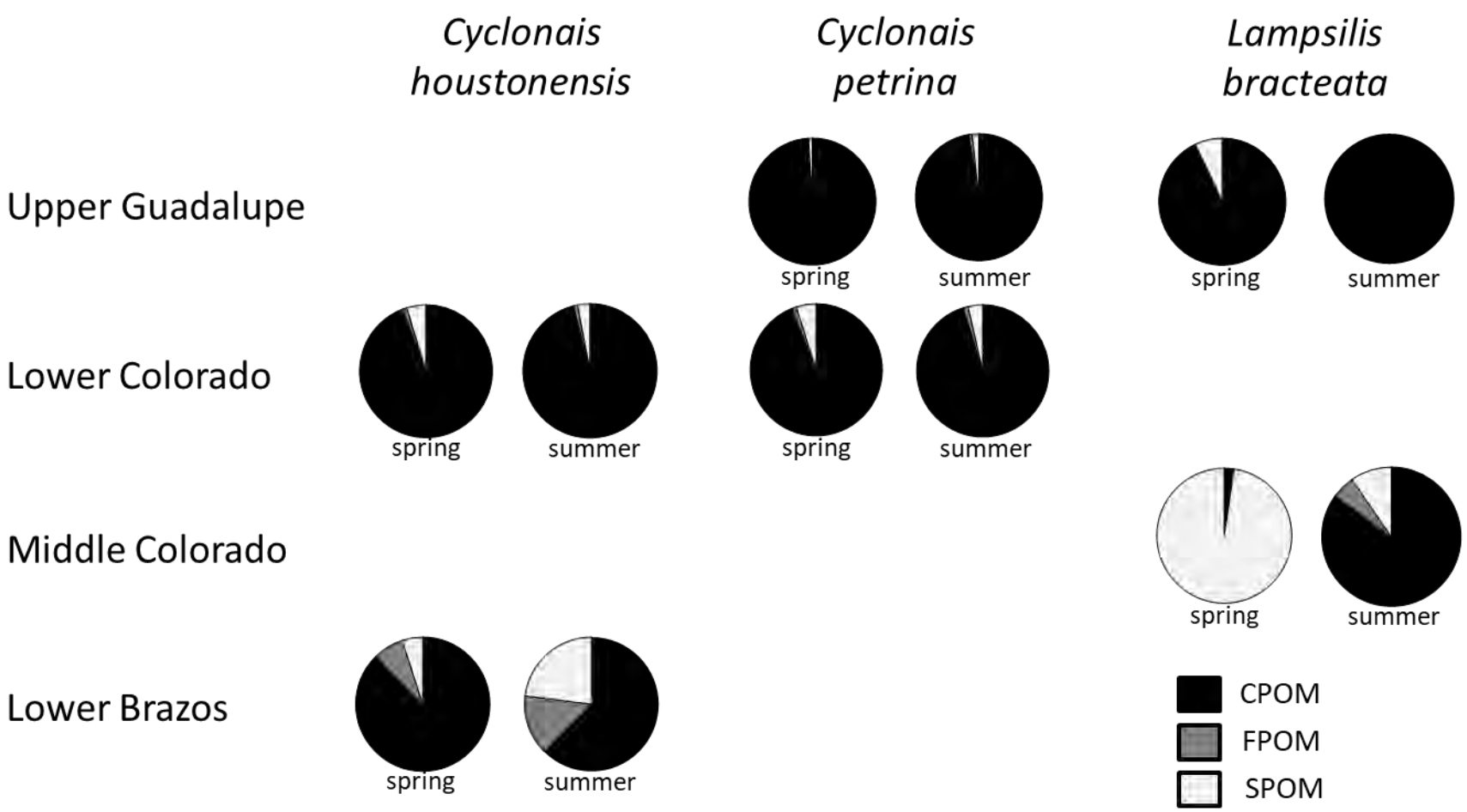

Figure 8. Estimated carbon source of *C. houstonensis, C. petrina,* and *L. bracteata* across the Upper Guadalupe, Lower Colorado, Middle Colorado, and Lower Brazos basin. Charts reflect mean estimate values of potential C sources from linear mixing models derived from IsoSource

Task 3 Environmental Flow Analysis and Modeling Update and Evaluation

Contributing authors: Brad Littrell, Kyle Sullivan, Ed Oborny

Address:
BIO-WEST, Inc. San Marcos, Texas 78666 (BL, KS, EO)

Principal Investigators: Brad Littrell and Ed Oborny

Email: blittrell@bio-west.com, eoborny@bio-west.com

Traditional instream flow studies model changes in simple hydraulic parameters, such as depth and velocity, under varying stream discharge levels and how they influence habitat availability for target organisms, usually fishes (BIO-WEST 2008). The underlying assumptions are that target organisms select their habitat based on these parameters, and that they have the ability to move to new habitats when discharge conditions change. Freshwater mussels challenge these assumptions due to their slow locomotion and sessile nature. Compared to fishes, mussels tend to move little and occupy small habitat patches for long periods. Therefore, for a mussel to persist at a location, suitable habitat must occur across a range of flow conditions. As a result, some have suggested that modeling simple hydraulic variables such as depth and velocity are of little use in determining conservation flows for mussels, but that complex hydraulic parameters such as shear stress are better predictors of mussel abundance (Layzer and Madison 1995, Maloney et al. 2012). However, some of the same authors recognized that mussels did show a preference for particular hydraulic conditions and that depth and velocity were important factors limiting their distribution under base flow conditions (Layzer and Madison 1995). Due to the variety of factors influencing suitable mussel habitat, others have suggested that environmental flow recommendations for mussels should focus more on the

biological traits of species guilds (Gates et al. 2015), although such biological information is lacking for many species.

Previous environmental flow studies conducted on the lower Colorado River as part of the Lower Colorado River Authority (LCRA) – San Antonio Water System (SAWS) Water Project (LSWP) established 10 intensive study sites with detailed hydraulic models (Figure 1) (BIO-WEST 2008). These models were used to generate instream flow recommendations for the lower Colorado River based on fish habitat modeling and other flow dependent ecological variables. However, freshwater mussels were not considered as part of this previous instream flow assessment. Therefore, the overall goal of the current study was to evaluate availability and persistence of freshwater mussel habitat within the lower Colorado River using a variety of both traditional (depth, velocity) and complex (shear stress) hydraulic variables at existing hydraulic model sites used previously for fish habitat modeling.

To do this, the first specific objective of Task 3 was to conduct mussel surveys at previously established hydraulic model sites on the lower Colorado River to determine which sites support significant mussel populations. These sites were included in Task 1 survey work to assess the occurrence and abundance of freshwater mussels at each location. Based on the results of these surveys, sites were chosen to focus additional habitat modeling efforts, as described in the results below.

The second specific objective was to develop habitat suitability criteria for freshwater mussels within the lower Colorado River. Detailed habitat information collected as part of Task 1 survey work was summarized and used to develop initial habitat suitability criteria. Additional site-specific data collection is planned in 2018 to characterize mussel habitat associations at a finer spatial scale and refine suitability criteria.

The third specific objective of this task was to collect additional physical and hydraulic data to validate and/or update existing hydraulic models. Initially, it appeared that hydraulic model sites had changed little since development of the models and only some minor validation data would be necessary. However, a large flood event occurred in the lower Colorado River following heavy rains from Hurricane Harvey in August 2017. A visit to one of the selected model sites shortly afterwards revealed extensive changes to channel bathymetry. Therefore, current bathymetric and hydraulic data at multiple flow ranges will be necessary to update existing models to incorporate these changes. Collection of this additional physical and hydraulic data is planned in 2018, after which habitat suitability information will be combined with revised model output to evaluate the effects of varying flows on freshwater mussel habitat within the selected study sites. This complete analysis will be provided in a final report in August 2018. The analysis and results below summarize initial environmental flow work conducted in 2017 pertaining to site selection and development of initial habitat suitability criteria.

Methods

Freshwater mussel data was collected using the methodology described in detail under Task 1 surveys. Surveys were conducted at several of the previously established hydraulic model sites to evaluate the mussel communities present and choose sites for further habitat modeling. Habitat utilization data from the lower Colorado River were used to develop Habitat Suitability Criteria (HSC) for all freshwater mussels, as well as for each of the candidate species inhabiting the lower Colorado River (i.e., *Cyclonaias houstonensis*, *Cyclonaias petrina*, and *Truncilla macrodon*). For each species or combination of species, HSC were developed for depth, mean column velocity, Froude number, Reynolds number, mean substrate compaction,

FST hemisphere number, minimum bottom shear stress (MBSS; inferred from FSTs using Statzner et al. 1991), and dominant substrate. Data for depth, mean column velocity, mean substrate compaction, FST hemisphere number, and minimum bottom shear stress (inferred from FSTs using Statzner et al. 1991) were measured during surveys as describe in the Task 1 methods. Percent substrate composition taken from survey data was converted to dominant substrate for development of suitability criteria. Froude number and Reynolds number are hydraulic parameters used to evaluate turbulence. Froude number represents a ratio of inertial to gravitational forces. Reynolds number represents a ratio of inertial force to viscous force. These parameters were calculated from survey data using the following equations:

Reynolds number *(Re):* $Re = Ud/v$

where U = benthic velocity (m/s), d = water depth (m), v = kinematic viscosity of water (1.0×10^{-6} m^2/s)

Froude number *(Fn):* $Fn = U/\sqrt{gd}$

where U = benthic velocity (m/s), g = acceleration of gravity (9.8 m/s^2), d = water depth (m)

Suitability criteria for continuous variables were created using nonparametric tolerance limits (NPTL) (Bovee 1986). The tolerance limits representing the central 50% of the data were used to represent the highest utilization and given a suitability value of 1.0. The tolerance limits for the central 75% were assigned a suitability of 0.5. The tolerance limits for the central 90% of the data were given a suitability of 0.2. Lastly, the tolerance limits representing the central 95% of the data were given a suitability value of 0.1. Anything outside of the central 95% tolerance limit was considered unsuitable, and given a suitability value of 0.0. For the categorical variable of dominant substrate, suitability values were established using the Strauss Linear Index (Strauss

1979, Persinger et al. 2011). Values of this index range from -1 to 1, with larger positive values indicating selection and negative values indicating avoidance. Significant positive values were given a suitability of 1.0, non-significant positive values were given a suitability of 0.5, non-significant negative values were given a suitability of 0.2, and significant negative values were assigned a suitability of 0.0.

Results

Study Site Selection

A total of 85 person-hours (p-h) of search time was conducted at the ten intensive model sites resulting in collection of 862 mussels for an overall catch-per-unit-effort (CPUE) of 10.1 mussel/p-h (Table 1). Site-specific CPUE ranged from 0.0 – 2.5 mussels/p-h at sites between Longhorn Dam and Smithville, and from 3.2 – 47.6 mussels/p-h from La Grange downstream to Lane City. Maximum site-specific CPUE (47.6 mussels/p-h) was observed at the Altair intensive study site. Candidate species were present from La Grange downstream, with all three candidate species (i.e., *C. houstonensis*, *C. petrina*, and *T. macrodon*) being present at the Altair and Wharton study sites.

Initial Habitat Suitability Criteria

Initial HSC generated from survey data for all unionids in aggregate demonstrated highest habitat suitability at depths of 0.6 – 0.9 meters (m), mean column velocity below 0.2 m/s, Froude number below 0.05, and Reynolds numbers below 50,000 (Figure 2). Mussels were most commonly found in habitats with mean substrate compaction less than 0.075 kg/cm^2, and showed highest suitability when MBSS < 2 dyn/cm^2 and in silt and boulder substrates (Figure 3).

For *C. houstonensis*, suitability was highest at depths of 0.9 – 1.2 m, mean column velocities of 0.1 – 0.2 m/s, Froude numbers near 0.05, and Reynolds numbers of approximately

50,000 (Figure 4). They were most commonly found in habitats with mean substrate compaction from 0.025 – 0.05 kg/cm^2, in habitats with MBSS < 2 dyn/cm^2, and exhibited highest suitability in boulder substrates (Figure 5).

For *C. petrina*, suitability was highest at depths from 0.6 – 0.9 m, mean column velocities below 0.2 m/s, Froude numbers below 0.05, and at Reynolds numbers below 150,000 (Figure 6). They were most commonly found where mean substrate compaction ranged from 0.025 - 0.075 kg/cm^2, at MBSS < 2 dyn/cm^2, and showed moderate suitability (0.5) in sand, boulder, and bedrock substrates (Figure 7).

Due to insufficient sample size (n = 9), HSC were not generated for *T. macrodon*. However, data suggests highest utilization in depths of 0.6 – 0.9 m, in relatively low velocities, and in habitats with relatively low Froude and Reynolds numbers (Figure 8). They were most commonly found where substrate compaction and MBSS were relatively low, and Strauss Linear Index values for substrate were highest in silt (0.25), clay (0.09), and boulder (0.08) (Figure 9).

Discussion

Based on survey results, the Altair and La Grange study sites were chosen as the focus for additional data collection and modeling. The Altair study site exhibited the highest mussel abundance, and contained all three candidate species. Therefore, it was chosen to represent high-quality habitat conditions within the lower Colorado River. The La Grange study site was the upstream-most site that contained a candidate species (*C. houstonensis*), and it ranked third in overall CPUE. Understanding differences in hydraulic and habitat conditions between these two sites may elucidate patterns in freshwater mussel occurrence and abundance within the lower Colorado River. Additional physical and hydraulic data collection to update hydraulic models at these two sites is planned in 2018.

Initial habitat suitability criteria developed from survey data suggest that freshwater mussels in the lower Colorado River are most commonly utilizing moderate-depth low-energy habitats with silt and boulder substrates. Compared to all mussels in aggregate, *C. houstonensis* showed lower suitability in areas with 0 velocity, 0 turbulence, and 0 substrate compaction. In contrast, *C. petrina* showed broader curves for mean column velocity, Froude number, Reynolds number, and MBSS, suggesting increased utilization of high-energy environments compared to all mussels in aggregate.

Although the HSC described above provide a good starting point for evaluating habitat utilization, they are based on data collected under relatively low base flow conditions during mussel surveys, and should therefore be interpreted with caution. Given that freshwater mussels are rather sessile organisms they must occupy habitat that is acceptable at base flows, as well as high flows, in order to persist. Additional mussel habitat data collection is planned in 2018 under varying flow conditions. Once additional habitat data is available, it will be combined with updated hydraulic model output to evaluate the influence of varying flow conditions on the availability and persistence of habitat within the selected model sites.

Table 1. Results of mussel surveys at ten previously established LSWP intensive study sites on the Lower Colorado River.

LSWP Site	Search Time (person-hours)	Mussel Abundance	CPUE (mussels/p-h)	Number of Candidate Species Present
Longhorn Dam	6	0	0.0	0
Utley	11	28	2.5	0
Bastrop	6	0	0.0	0
Smithville - US	6	0	0.0	0
Smithville - DS	6	0	0.0	0
La Grange	11	74	6.7	1
Columbus	10	88	8.8	2
Altair	13	619	47.6	3
Wharton	11	35	3.2	3
Lane City	5	18	3.6	2
	85	862	10.1	

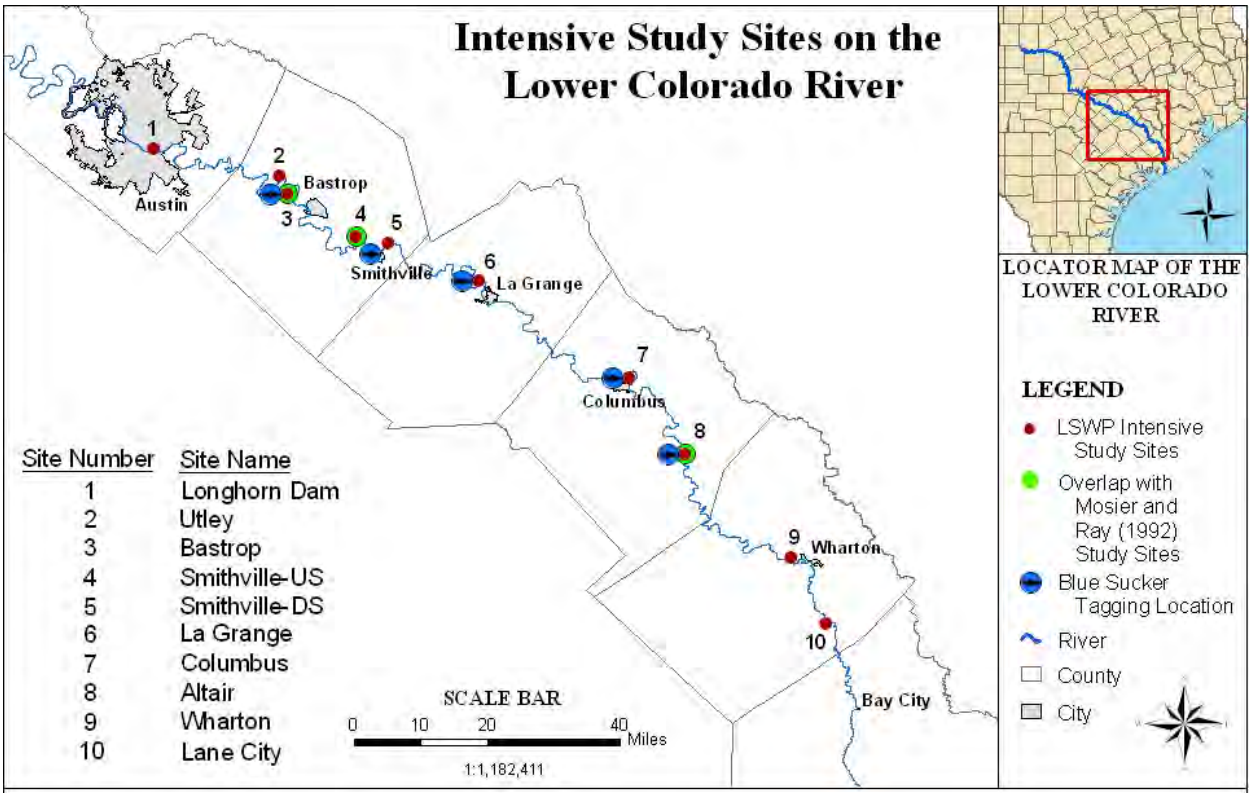

Figure 1. LSWP intensive study sites with existing hydraulic models.

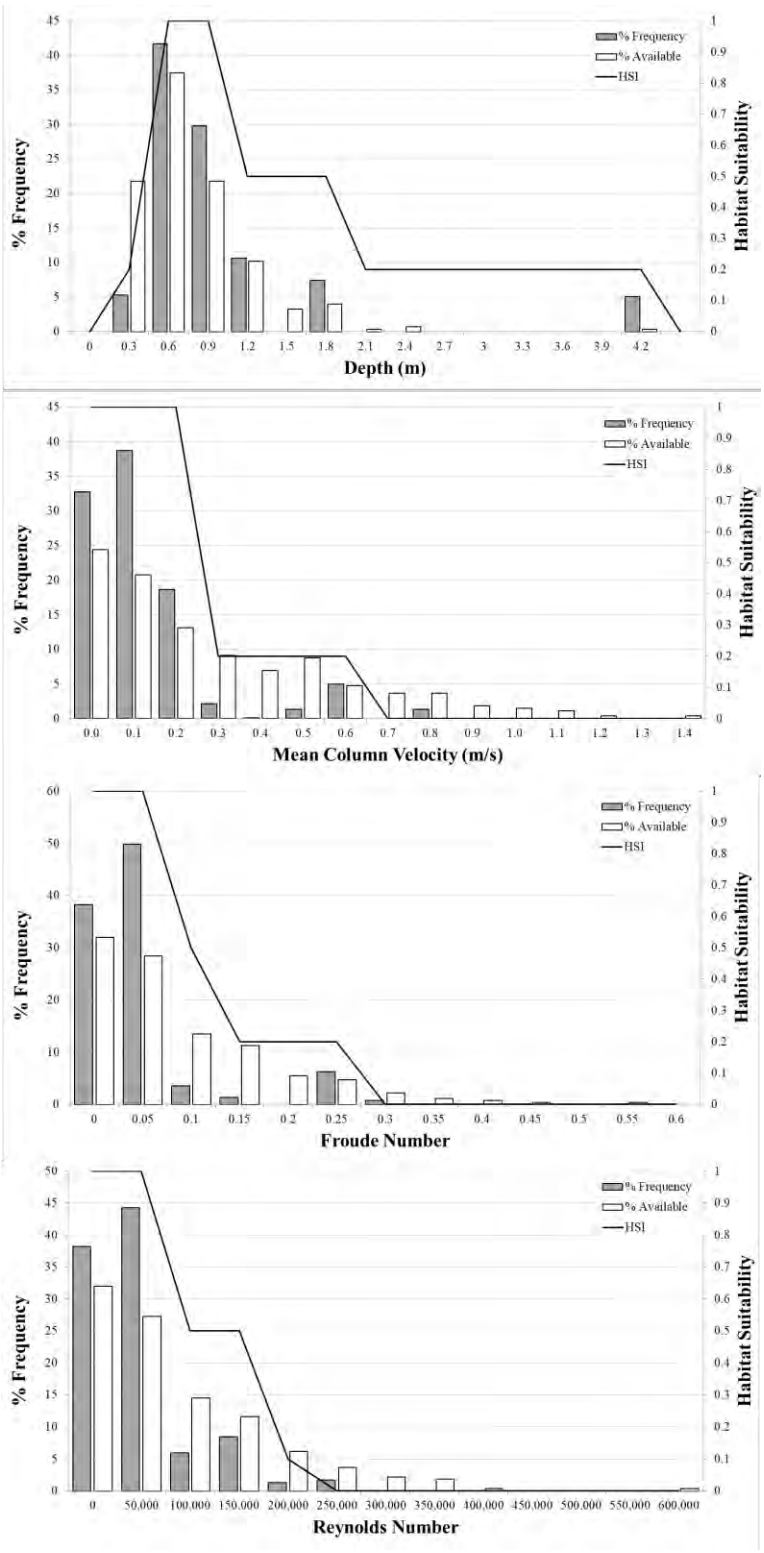

Figure 2. Percent frequency of occurrence (gray bars), percent frequency of habitats sampled (white bars), and habitat suitability values (black line) for lower Colorado River unionids (n = 2327) in relation to depth (m), mean column velocity (m/s), Froude number, and Reynolds number.

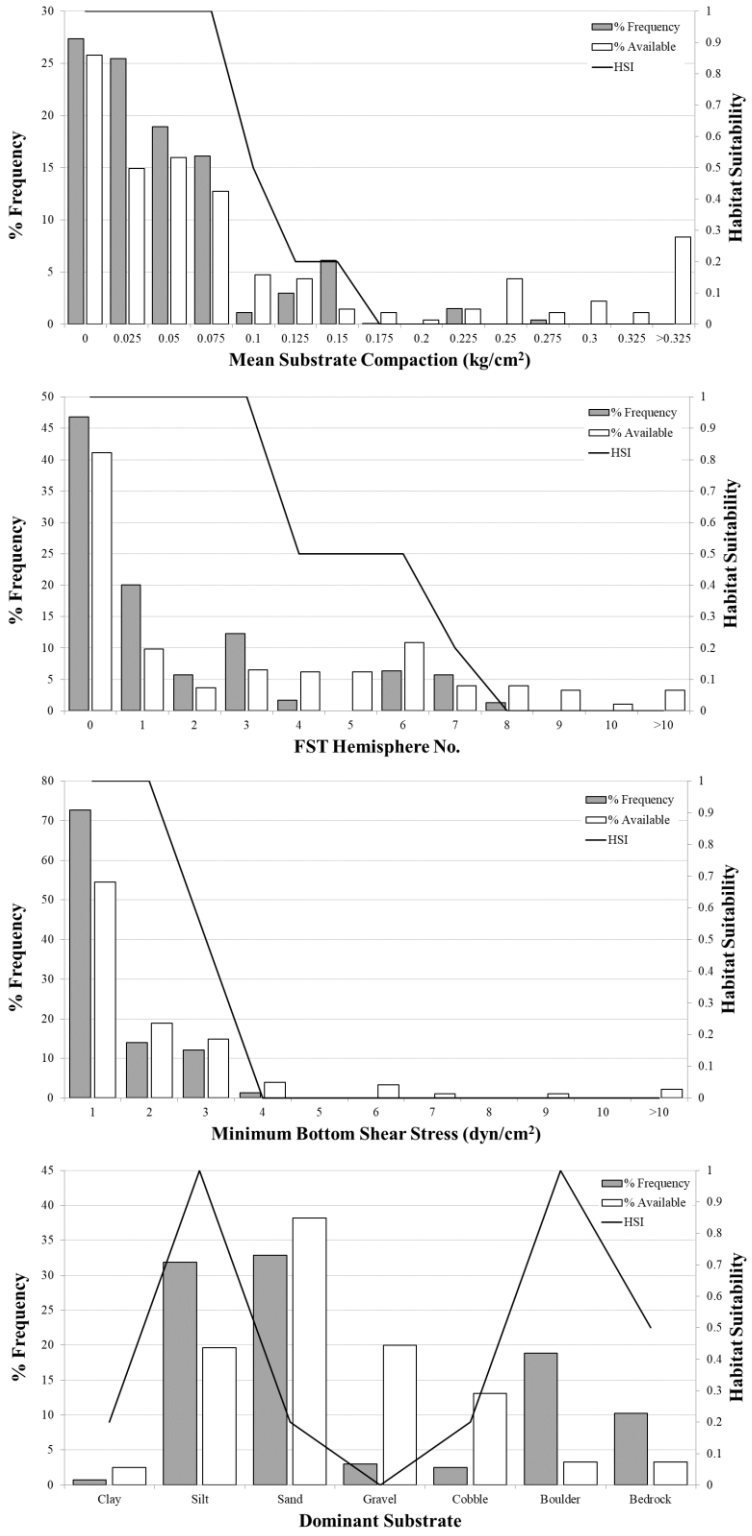

Figure 3. Percent frequency of occurrence (gray bars), percent frequency of habitats sampled (white bars), and habitat suitability values (black line) for lower Colorado River unionids (n = 2327) in relation to mean substrate compaction (kg/cm^2), FST hemisphere number, minimum bottom shear stress (dyn/cm^2), and dominant substrate.

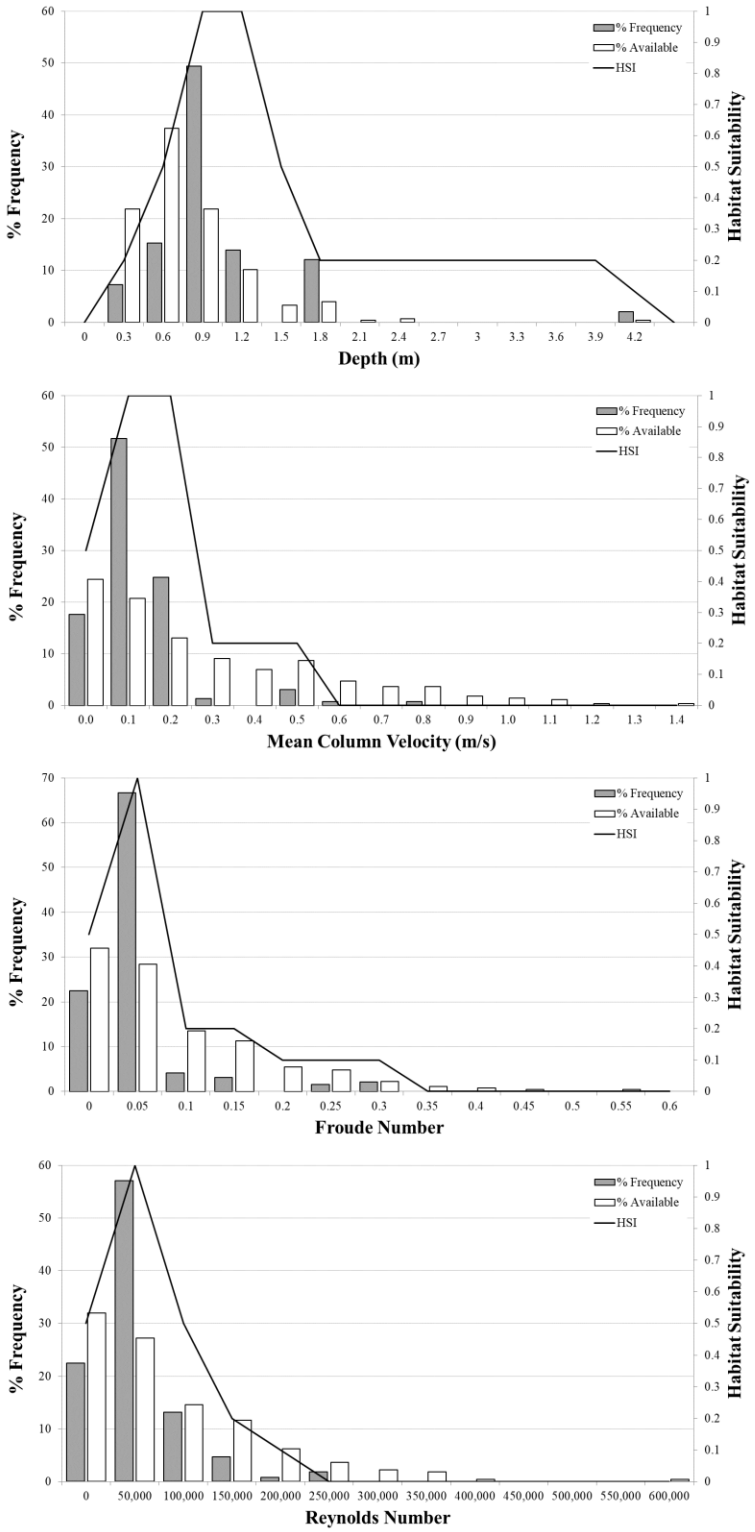

Figure 4. Percent frequency of occurrence (gray bars), percent frequency of habitats sampled (white bars), and habitat suitability values (black line) for lower Colorado River *C. houstonensis* (n = 387) in relation to depth (m), mean column velocity (m/s), Froude number, and Reynolds number.

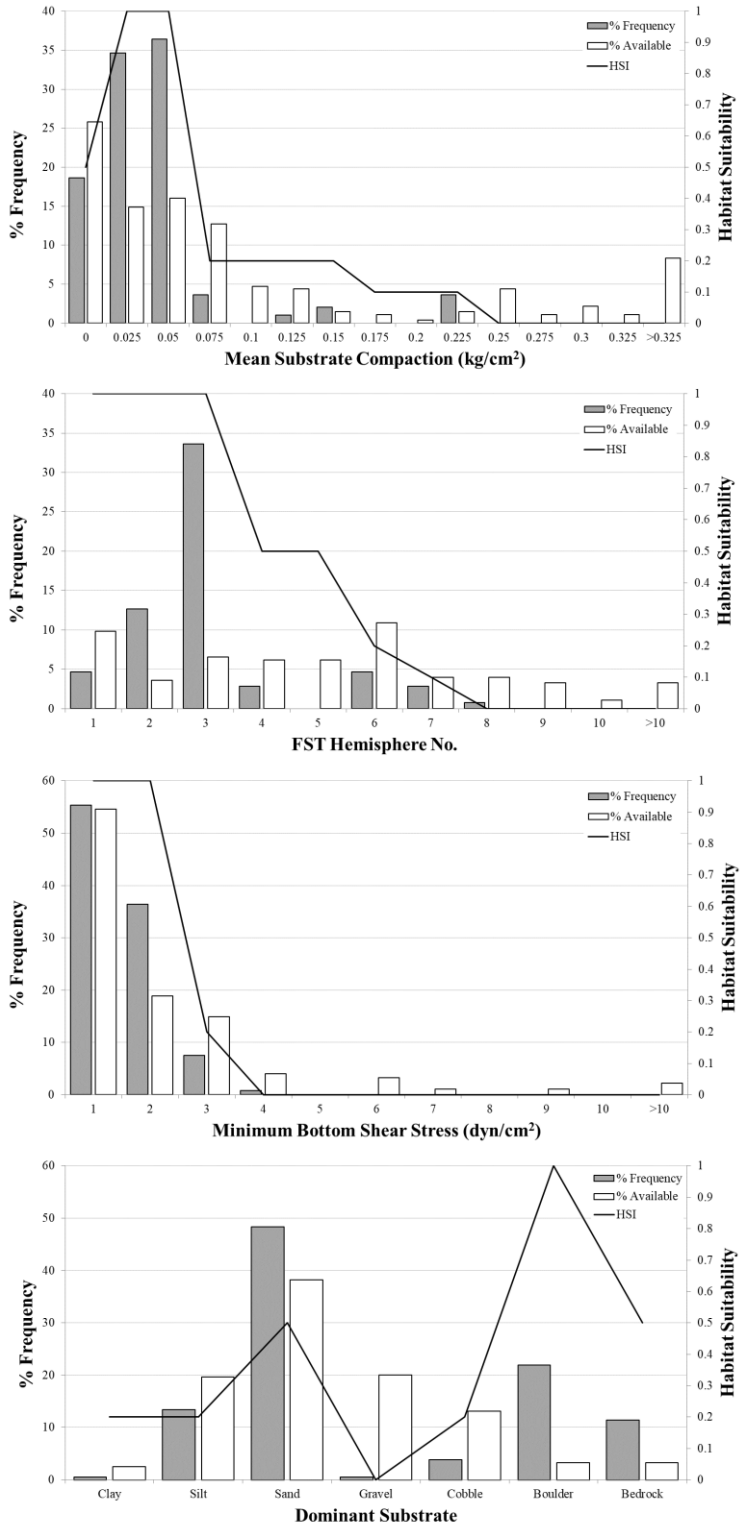

Figure 5. Percent frequency of occurrence (gray bars), percent frequency of habitats sampled (white bars), and habitat suitability values (black line) for lower Colorado River *C. houstonensis* (n = 387) in relation to mean substrate compaction (kg/cm^2), FST hemisphere number, minimum bottom shear stress (dyn/cm^2), and dominant substrate.

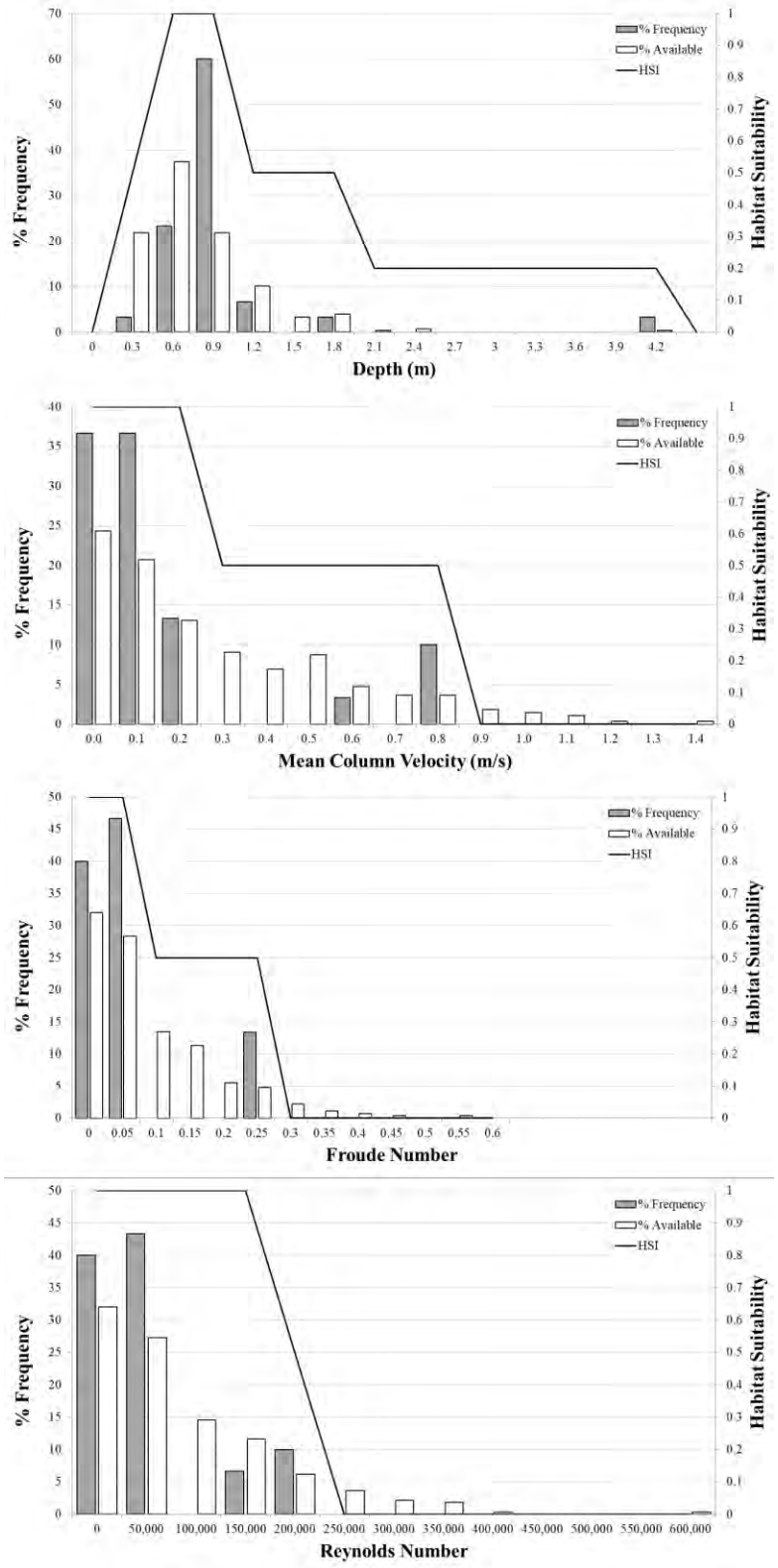

Figure 6. Percent frequency of occurrence (gray bars), percent frequency of habitats sampled (white bars), and habitat suitability values (black line) for lower Colorado River *C. petrina* (n = 30) in relation to depth (m), mean column velocity (m/s), Froude number, and Reynolds number.

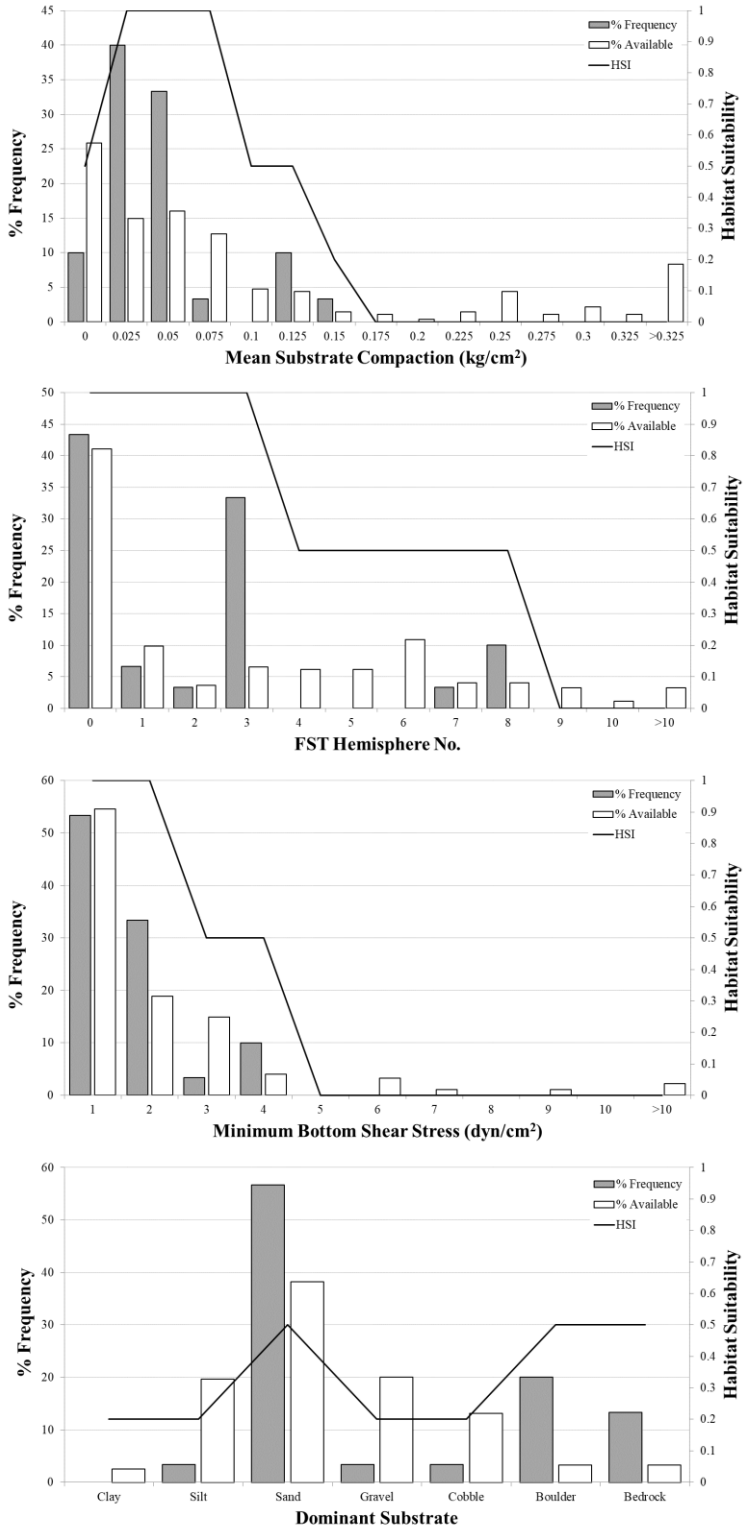

Figure 7. Percent frequency of occurrence (gray bars), percent frequency of habitats sampled (white bars), and habitat suitability values (black line) for lower Colorado River *C. petrina* (n = 30) in relation to mean substrate compaction (kg/cm^2), FST hemisphere number, minimum bottom shear stress (dyn/cm^2), and dominant substrate.

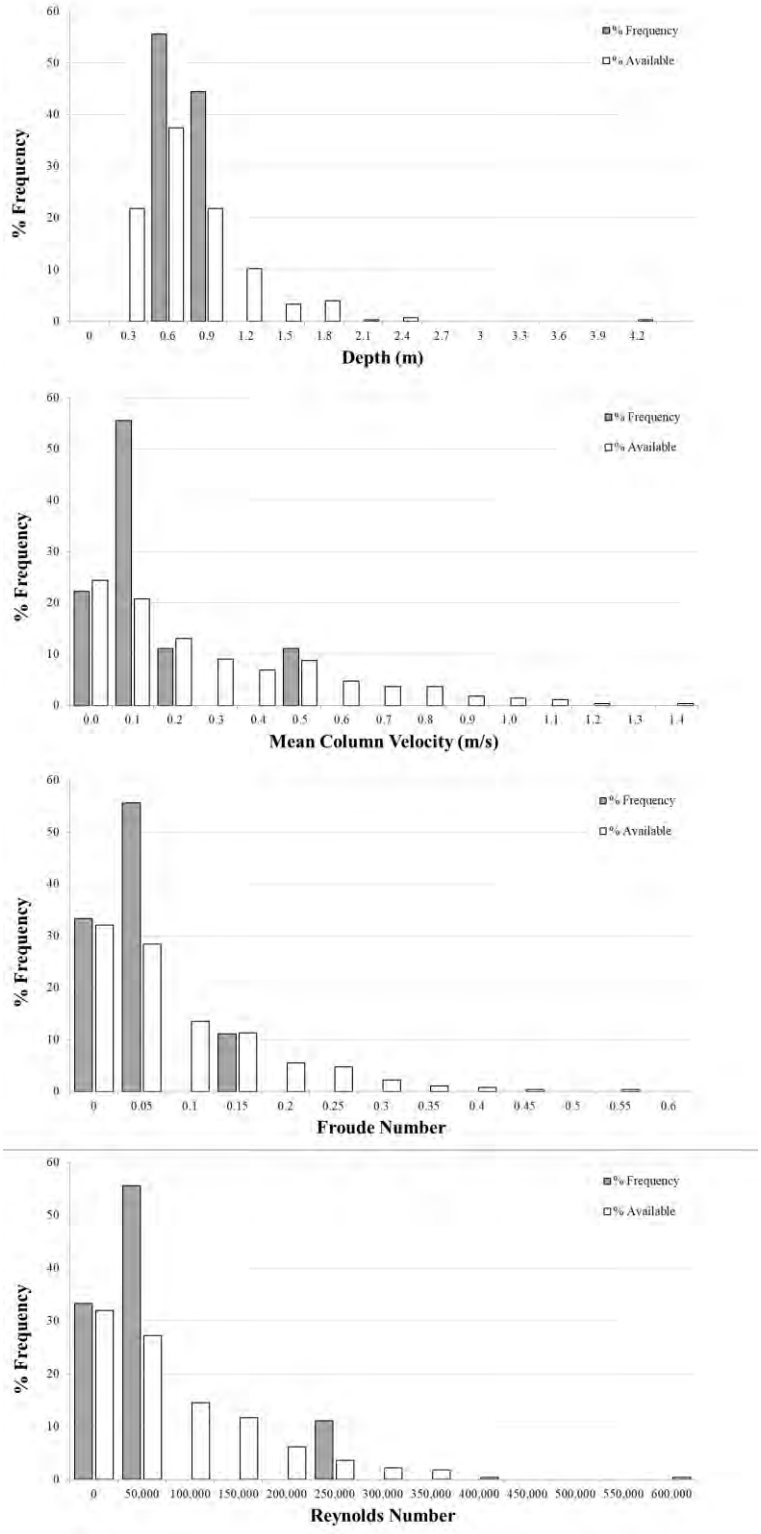

Figure 8. Percent frequency of occurrence (gray bars) and percent frequency of habitats sampled (white bars) for lower Colorado River *T. macrodon* (n = 9) in relation to depth (m), mean column velocity (m/s), Froude number, and Reynolds number. HSC were not generated for *T. macrodon* due to insufficient sample size.

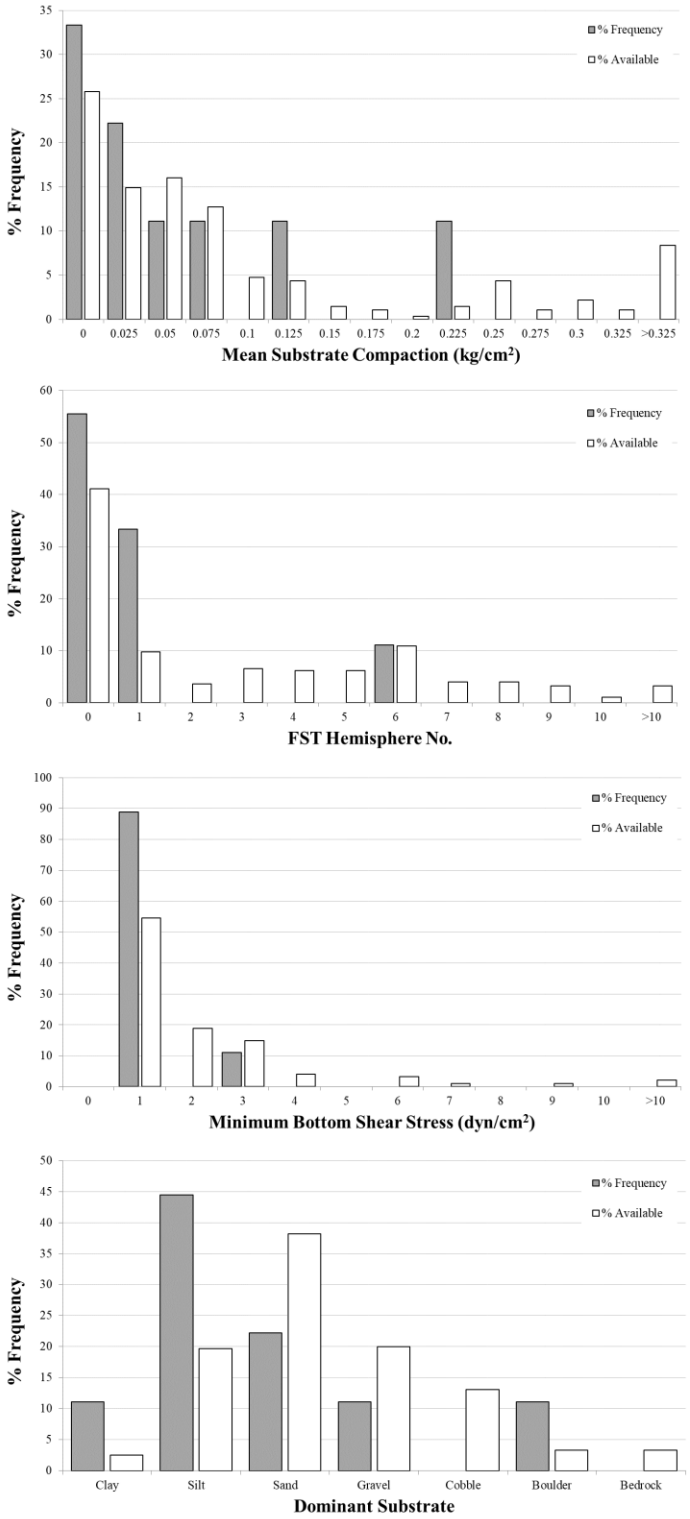

Figure 9. Percent frequency of occurrence (gray bars) and percent frequency of habitats sampled (white bars) for lower Colorado River *T. macrodon* (n = 9) in relation to mean substrate compaction (kg/cm^2), FST hemisphere number, minimum bottom shear stress (dyn/cm^2), and dominant substrate. HSC were not generated for *T. macrodon* due to insufficient sample size.

References

BIO-WEST, Inc. 2008. Lower Colorado River, Texas Instream Flow Guidelines. Colorado River Flow Relationships to Aquatic Habitat and State Threatened Species: Blue Sucker. Report prepared for Lower Colorado River Authority (LCRA) and San Antonio Water System (SAWS) Water Project.

Gates, K. K., C. C. Vaughn, and J. P. Julian. 2015. Developing environmental flow recommendations for freshwater mussels using the biological traits of species guilds. Freshwater Biology (2015) 60:620-635.

Layzer, J. B., and L. M. Madison. 1995. Microhabitat use by freshwater mussels and recommendations for determining their instream flow needs. Regulated Rivers: Research and Management 10:329-345.

Maloney, K. O., W. A. Lewis, R. M. Bennett, and T. J. Waddle. 2012. Habitat persistence for sedentary organisms in managed rivers: the case for the federally endangered dwarf wedgemussel (Alasmidonta heterodon) in the Delaware River. Freshwater Biology 57:1315-1327.

Task 4: Freshwater mussel mark-capture assessment

Contributing authors: David Ruppel, Cody Craig, Brad Littrell, Kyle Sullivan, Tim Bonner

Addresses:
BIO-WEST, Inc. San Marcos, Texas 78666 (BL, KS)
Texas State University, Department of Biology/Aquatic Station, San Marcos Texas 78666 (DR, CC, TB)

Principal Investigators: Brad Littrell and Tim Bonner

Email: blittrell@bio-west.com, TBonner@txstate.edu

When surveying freshwater mussels with conventional methods, certain factors have the potential to affect sampling efficiency such as habitat, substrate particle size, water temperature, turbidity, and shell length (Strayer & Smith 2003; Wisniewski et al. 2013). Freshwater mussels can also remain endobenthic for extended periods of time, resulting in reduced capture efficiency (Strayer & Smith 2003). Decreased sampling efficiency may result in incomplete detection, which could bias survey results (Wisniewski et al. 2013). This is particularly problematic when trying to estimate population parameters. To account for incomplete detection and improve population demographic calculations, recent studies have utilized mark-recapture methodologies which survey the same location multiple times (Strayer & Smith 2003; Meador et al. 2013; Wisniewski et al. 2013; Inoue et al. 2014).

Robust mark-recapture study designs are considered beneficial to prevent biased population estimates, including population size, capture rates, and survival (Strayer & Smith 2003). A robust design incorporates two types of sampling intervals, primary and secondary. The primary sampling period is associated with open-population models (e.g., annual, seasonal), wherein the assumptions of recruitment, mortality, immigration, and emigration are relaxed. The secondary sampling period is associated with closed-population models, and are conducted as

multiple sampling events occurring within the primary sampling period. These secondary sampling periods operate under the assumption that recruitment, mortality, immigration, and emigration are not occurring during these relatively shorter time periods. The number of secondary sampling events and the intervals between them vary depending on the goals of the study (Meador et al. 2011, Inoue et al. 2014).

In addition to the estimation of population demographics, mark-recapture study designs can also be useful for the assessment of ancillary life history characteristics. The comprehensive individual monitoring involved during field studies can provide valuable data on both mussel movement and rates of growth.

A variety of methods have been used to tag mussels during mark-recapture studies, most commonly numbered shellfish tags. Compared to the use of traditional shellfish tags, Passive Integrated Transponder (PIT) tags can greatly increase recapture success. Kurth et al. (2007) found that PIT tagged mussel recapture rates ranged from 72% - 80%, while recapture rates for visual searches ranged 30% - 47%. In addition, currently available PIT tag readers that record GPS coordinates along with each detection (BioMark HPR Plus) enhance the ability to monitor the horizontal movement of freshwater mussels at an individual level.

As outlined above, mark-recapture studies in combination with PIT tagging can provide considerable data on population parameters, growth, and movement of freshwater mussels. This information is generally lacking for most mussel species, particularly rare species, and is beneficial for accurate conservation assessments. In the Colorado River basin of Texas, five species of freshwater mussels (i.e., *Cyclonaias houstonensis*, *Cyclonaias petrina*, *Lampsilis bracteata*, *Truncilla macrodon*, and *Fusconaia mitchelli*) are currently being evaluated for endangered species listing by the United States Fish and Wildlife Service (USFWS). The goals

of this study were to use mark-recapture methodologies in combination with PIT tag technology to gain insight into population parameters and movement of these species, and how they relate to river discharge. Specific objectives were to: (1) quantify population demographics (i.e., abundance, survival, immigration) of candidate mussels in relation to river discharge and flow events, (2) assess candidate mussel movement and its relationship to flow, and (3) to evaluate baseline growth rates for candidate species. Although additional data collection is planned to fully evaluate these objectives, this report presents a summary of 2017 results and analysis conducted to date.

Methods

Site Selection

We selected a site within both the Lower Colorado River (Colorado County) and Middle Colorado River (San Saba County) based on results of Task 1 survey work and where candidate species were known to occur within the Colorado River basin (Figure 1). We delineated each site into 300 m^2 areas and used a GPS unit to mark the boundaries of each area so that we could accurately return to the same location. The Middle Colorado River Site had an average depth of 0.31 m, mean column velocity of 0.25 m/s, mean benthic velocity of 0.03 m/s, and substrate consisted of silt (8%), sand (12%), gravel (25%), cobble (35%), and boulder (20%). The Lower Colorado River Site had an average depth of 0.43 m, a mean column velocity of 0.17 m/s, a mean benthic velocity of 0.33 m/s, and substrate at this site consisted of sand (15%), gravel (10%), cobble (5%), and bedrock (70%).

Study Design

We implemented a robust mark-recapture design to account for temporal variation in population dynamics and imperfect detection among sampling events, with primary periods separated by season. In the Lower Colorado River, we initially tagged mussels in March 2017 and conducted three primary period recapture surveys (i.e, Spring [April], Summer [August], Fall [November]). In the Middle Colorado, we initially tagged mussels in June 2017, and conducted two primary period recapture surveys (i.e, Summer [August-September], Fall [November]). Within each primary period, we conducted three secondary period surveys. Each secondary period survey was separated by at least 24 hours but not more than 72 hours to allow for individual mussels to reacclimate following handling but not violate closed population model assumptions.

During the initial tagging event at each site, mussels were collected via visual and tactile surveys using a two-pass depletion method within the 300 m^2 sampling area. All live mussels collected were tagged with laminated vinyl shellfish tags (Floy®), and all live candidate species collected also received a Passive Integrated Transponder (PIT) tag (Biomark®). For adhesion of shellfish and PIT tags, we used a cyanoacrylic glue (Loctite Gel Control Super Glue). The PIT tags were encapsulated with this adhesive to prevent tag damage and increase retention. After glue application, all tag types were sprayed with non-toxic accelerant to expedite curing time and decrease mussels' time out of water. The use of cyanoacrylate adhesives is beneficial when PIT tagging a high volume of mussels, due to the decrease in handling time. Furthermore, tag retention with cyanoacrylates has not been shown to differ compared to other adhesive types (e.g., epoxy, dental cement; Ashton et al. 2017).

During each sample event, we conducted a minimum of two survey passes at each site. We performed the first pass using the Biomark reader to locate PIT tagged individuals. The

second pass was conducted using visual and tactile methods to capture mussels. Unmarked individuals collected were identified to species, measured (length, width, height), sexed (if applicable), and tagged. In addition, water quality (i.e., temperature, DO, conductivity, pH), water depth, and current velocity were measured during each sampling event. Percent substrate composition was visually estimated based on the standard Wentworth scale for particle size.

Mark-Recapture Data Analysis

To investigate changes in population dynamics of the candidate species at both sites, we conducted all data analyses in R 3.3.2, package 'Rcapture', a program that utilizes loglinear models to estimate demographic parameters for mark-recapture study designs, including closed population, open population, and robust design models. Package 'Rcapture' is beneficial for these types of analyses because it offers multiple options for modeling capture probabilities to best account for potential capture heterogeneity for closed population models or within primary periods of a robust design. Having the ability to select the model of best fit for each primary period improves the demographic parameter estimates for robust design models (Baillargeon & Rivest 2007).

Prior to fitting a robust design model, closed population models were conducted separately to identify which model type was most appropriate for each primary period. In addition, an open population model was performed to identify if it was appropriate for the robust design model. After the selected models were deemed appropriate, we ran robust design models for each candidate species where sufficient data were available. The model of best fit for closed, open, and robust design models were selected based on Rivest and Daigle (2004) and Baillargeon and Rivest (2007).

Candidate Species Growth Evaluation

As part of the mark-recapture study, mussel size data was recorded for all native unionids captured. Shell length (mm) at recapture from multiple recapture events was used to evaluate growth of candidate species. Lower Colorado River Site growth estimates are based on four sampling events occurring in March, April, August, and November, respectively. Middle Colorado River Site growth estimates are based on three sampling events occurring in June, August-September, and November. For some species and time intervals, the repeated individual length measurements required for growth estimates were not available. For both sites and all candidate species, growth rate estimates from all seasons were standardized by month (i.e., mm/month).

Movement Analysis

Movements of *C. houstonensis*, *C. petrina*, and *T. macrodon* were assessed using mark-recapture data collected from primary and secondary sampling using the Biomark reader. Movement calculations were derived from the final known location of species of concern from previous primary sampling event and the first known location from the subsequent primary sampling event. Last known location was subtracted from first known location and converted to meters using a formula derived from the Law of Cosines. Average (± SD) movement was calculated between all primary periods. In the lower Colorado River, movement was calculated for the periods of March to April, April to August, and August to November. In the middle Colorado River, movement was calculated for the periods of June to August and August to November.

Results

Lower Colorado River Site: Colorado County

During initial sampling in March, a total of 160 candidate species were captured: 103 *C. houstonensis* (64%), 48 *C. petrina* (30%), and 9 *T. macrodon* (5.6%). Across all subsequent primary and secondary sampling periods there were a total of 380 recaptures, of which, 259 were *C. houstonensis* (68%), 119 were *C. petrina* (31%), and 2 were *T. macrodon* (0.5%). Recaptures varied between primary sampling periods, with 177 recaptures in April, 132 recaptures in August, and 12 recaptures in November (Table 1). Numbers of *T. macrodon* collected (N=16) were insufficient for mark-recapture modeling. Preliminary modeling results of 2017 data are presented below for *C. houstonensis* and *C. petrina*.

Cyclonaias houstonensis

Capture probability of *C. houstonensis* in the lower Colorado River site using visual and tactile searches ranged from 0.47 ± 0.06 (SE) in Period 2 to 0.52 ± 0.19 in Period 3 (Table 3). We observed a decline in survivorship between periods, which decreased from 0.88 ± 0.13 (SE) between Period 1 and 2, to 0.04 ± 0.03 (SE) between Periods 3 and 4. Abundance estimates were 401.9 ± 22.10 (SE) within Period 1, 351.6 ± 47.60 (SE) within Period 2, and decreased sharply to 19.9 ± 7.40 (SE) within Period 3. Number of new arrivals (immigrants) ranged from 0.0 ± 0.00 between Period 1 and Period 2 to 6.2 ± 4.80 between Period 2 and Period 3.

Capture probability of *C. houstonensis* in the lower Colorado River was much higher with the PIT reader, and ranged from 0.87 ± .13 (SE) to 0.95 ± 0.01 (SE) (Table 3). PIT tag information was valuable in monitoring movement of individual mussels between primary periods. However, each mussel detected with the PIT reader was not collected to confirm if the

individual was alive, and therefore, abundance and survival estimates from this data have less confidence until PIT tag individuals are confirmed alive via tactile searches.

Cyclonaias petrina

Capture probability of *C. petrina* at the lower Colorado River site ranged from 0.54 ± 0.33 (SE) in Period 3 to 0.58 ± 0.09 in Period 1 (Table 3). We observed a substantial decline in survivorship between periods, which decreased from 0.79 ± 0.15 (SE) between Period 1 and 2, to 0.04 ± 0.04 (SE) between Periods 3 and 4. Abundance estimates were 127.4. ± 21.30 within Period 1, 127.8 ± 21.10 in Period 2, and decreased sharply to 7.5 ± 5.30 (SE) within Period 3. Number of new arrivals (immigrants) ranged from 26.7 ± 20.70 (SE) between Period 1 and 2, to 2.5 ± 3.20 between Period 2 and 3.

Capture probability of *C. petrina* in the lower Colorado River was much higher with the PIT reader, and ranged from 0.82 ± 0.14 (SE) to 0.94 ± 0.02 (SE) (Table 3). However, each mussel detected with the PIT reader was not collected to confirm if the individual was alive, and therefore, abundance and survival estimates from this data have less confidence until PIT tag individuals are confirmed alive via tactile searches.

Movement

A total of 386 individual movements were calculated for *C. houstonensis* (N = 259), *C. petrina* (N = 113), and *T. macrodon* (N = 14). Movements ranged between 0 m and 20 m for *C. houstonensis* and *C. petrina* and between 1 m and 20 m for *T. macrodon* (Figure 4). Between primary sampling periods, *C. houstonensis* average movement (± 1 SD) ranged from 3.9 (± 2.9) m between March and April (N = 88) to 12.4 (± 5) m between August and November (N = 6), *C.*

petrina average movement ranged from 3.9 (± 2.9) m between March and April (N = 42) to 7.6 (± 5.4) m between April and August (N = 64), and *T. macrodon* average movement ranged from 6.6 (± 5) m between March and April (N = 7) to 10.2 (± 6.2) m between August and November (N = 7).

Middle Colorado River Site: San Saba County

During initial sampling in June, a total of 123 candidate species were captured: 9 *C. houstonensis* (7.3%) and 114 *C. petrina* (92.7%). Across both subsequent primary and secondary sampling periods, there was a total of 255 recaptures, of which, 238 were *C. petrina* (93.3%) and 17 were *C. houstonensis* (6.7%). Recaptures did not vary much between primary sampling events with 128 recaptures in August, and 127 recaptures in November (Table 2). Numbers of *T. macrodon* collected (N = 1) were insufficient for mark-recapture modeling and growth analysis. Preliminary modeling results of 2017 data are presented below for *C. houstonensis* and *C. petrina*.

Robust design models require data from three or more primary periods, and only two recapture events were conducted at the Middle Colorado River Site in 2017. Therefore, for the Middle Colorado River Site, we estimated abundance within primary periods using closed population models based on recapture data from visual/tactile searches. Robust-design mark-recapture models will be conducted after additional sampling events occur.

Estimated abundance of *C. houstonensis* ranged from 7.0 ± 0.00 (SE) within Period 1 to 4.90 ± 1.60 (SE) within Period 2 (Table 4). Estimated abundance of *C. petrina* ranged from 490.2 ± 47.50 (SE) within Period 1 to 254.8 ± 4.2 (SE) within Period 2.

Movement

A total of 265 individual movements were calculated for *C. houstonensis* (N = 11) and *C. petrina* (N = 254), and movements ranged between 0 m and 24 m for both species (Figure 5). Between primary sampling periods, *C. houstonensis* average movement ranged from 5 (± 0.8) m between August and November (N = 4) to 9.4 (± 6.4) m between June and August (N = 7), and *C. petrina* average movement ranged from 4.2 (± 2.6) m between August and November (N = 151) to 7.8 (± 3.9) m between June and August (N = 103).

Mussel Growth Rates

Lower Colorado River

At the Lower Colorado River Site, lengths for *C. houstonensis* ranged from 24 – 79 mm, lengths of *C. petrina* ranged from 32 – 85 mm, and lengths of *T. macrodon* ranged from 32 – 58 mm. Across all candidate species, observed monthly growth ranged from 0 to 12 mm. The highest mean monthly growth rate observed was for *C. petrina* between April and August (2.250 mm/month) (Table 5). The lowest mean monthly growth rate observed was for *C. houstonensis* during the same time period (1.289 mm/month).

Middle Colorado River

At the Middle Colorado River Site, lengths for *C. houstonensis* ranged from 36 – 84 mm, lengths of *C. petrina* ranged from 30– 94 mm, and only one *T. macrodon* (14 mm) was collected. Across all candidate species, observed monthly growth ranged from 0.400 to 0.754 mm. The highest mean monthly growth rate observed was for *C. petrina* between April and August (0.754

mm/month) (Table 6). The lowest mean monthly growth rate observed was for *C. houstonensis* between June and August (0.400 mm/month).

Discussion

Preliminary results of robust design mark-recapture models at the Lower Colorado River Site suggest population sizes of approximately 350 – 400 *C. houstonensis* and approximately 127 *C. petrina* from within our 300 m^2 sampling area during April and August sampling events. A large flood event occurred in the lower Colorado River resulting from intense rains from Hurricane Harvey in late August and September 2017 (Figure 2). The study site was extensively scoured and large bathymetric changes were noted in the river following this event. Population estimates for both species at the Lower Colorado River Site decreased sharply. Mark-recapture models estimated approximately 20 *C. houstonensis* and 7.5 *C. petrina* during the November sampling event. Additional sampling to evaluate recovery following this event will be important in understanding the impacts of such flood events on mussel communities in the Lower Colorado River.

As expected, PIT reader capture probabilities were relatively high (0.82 – 0.95) when compared to capture probabilities from visual/tactile surveys (0.47 – 0.58). However, not every individual detected by the PIT reader was captured and removed from the substrate to assess survival, so data from visual and tactile surveys were more appropriate for estimating population parameters. Georeferenced detections from the PIT reader were used to evaluate movement of candidate species. Target species moved between 0 and 20 meters in the lower Colorado River and between 0 and 24 meters in the middle Colorado River among all primary sampling events.

Preliminary results of mark-recapture analysis at the Middle Colorado River Site suggest population sizes of approximately 5 – 7 *C. houstonensis* and 254 – 490 *C. petrina* within our 300 m^2 sampling area. Although insufficient data exists to run robust design models and analyze changes among primary periods, no substantial changes in mussel abundance were observed by surveyors in 2017. The Middle Colorado River was influenced less by flooding in 2017 (Figure 3), and overall abundance of mussels appeared to be relatively stable between events based on field observations. As more data becomes available from additional sampling, robust design models will be analyzed to evaluate changes among primary periods.

Preliminary estimates of mean monthly growth of candidate species were generally higher for *C. petrina* than *C. houstonensis*, although limited data is available for *C. houstonensis* from the Middle Colorado River Site. Observed mean monthly growth rates were lower at the Middle Colorado River Site than at the Lower Colorado River Site. This may be influenced by a wide variety of environmental factors that have yet to be evaluated. Additionally, this may be a result of differences in size structure of the population. The Middle Colorado River Site was dominated by large individuals, which are assumed to have slower growth rates, than smaller individuals.

Table 1. Results of mark-recapture primary sampling periods at the Lower Colorado River Site.

	March	April		August		November	
Species	**Initial Captures**	**New Captures**	**Recaptures**	**New Captures**	**Recaptures**	**New Captures**	**Recaptures**
C. houstonensis	103	128	115	62	135	6	9
C. petrina	48	39	61	31	55	2	3
T. macrodon	9	6	1	1	1	0	0
Total	160	173	177	94	191	8	12

Table 2. Results of mark-recapture primary sampling periods at the Middle Colorado River Site.

	June	August		November	
Species	**Initial Captures**	**New Captures**	**Recaptures**	**New Captures**	**Recaptures**
C. houstonensis	9	2	10	1	7
C. petrina	114	212	118	68	120
T. macrodon	0	1	0	0	0
Total	123	215	128	69	127

Table 3. Results of Rcapture robust design model in the Lower Colorado River.

	Visual/Tactile Search Efforts		PIT Tag Reader	
Model Fit	*C. houstonensis*	*C. petrina*	*C. houstonensis*	*C. petrina*
Deviance	124.87	76.76	157.80	107.68
Df	496	496	494	495
AIC	298.09	196.48	353.76	247.48
Model Parameters				
Capture Probabilities				
Period 1	0.49 ± 0.03	0.58 ± 0.09	0.90 ± 0.03	0.91 ± 0.06
Period 2	0.47 ± 0.06	0.54 ± 0.08	0.95 ± 0.01	0.94 ± 0.02
Period 3	0.52 ± 0.19	0.54 ± 0.33	0.87 ± 0.13	0.82 ± 0.14
Survival Probabilities				
Period 1 - Period 2	0.88 ± 0.13	0.79 ± 0.15	0.99 ± 0.02	0.87 ± 0.05
Period 2 - Period 3	0.04 ± 0.03	0.04 ± 0.04	0.03 ± 0.01	0.08 ± 0.03
Abundance Estimates				
Period 1	401.9 ± 22.10	127.4 ± 21.30	204.4 ± 7.60	88.3 ± 4.90
Period 2	351.6 ± 47.60	127.8 ± 21.10	292.1 ± 5.50	108.3 ± 3.60
Period 3	19.9 ± 7.40	7.5 ± 5.30	11.4 ± 2.10	9.8 ± 2.20
Number of New Arrivals Estimates				
Period 1 - Period 2	0.0 ± 0.00	26.7 ± 20.70	91.5 ± 12.50	31.0 ± 7.30
Period 2 - Period 3	6.2 ± 4.80	2.5 ± 3.20	3.3 ± 2.00	1.0 ± 1.20

Table 4. Results of Rcapture closed population models for each primary period in the Middle Colorado River.

	Visual/Tactile Search Efforts	
Model Fit	*C. houstonensis*	*C. petrina*
Period 1		
Deviance	2.96	0.77
Df	2	2
AIC	24.19	46.95
Period 2		
Deviance	5.14	3.77
Df	3	2
AIC	19.75	50.12
Abundance Estimates		
Period 1	7.0 ± 0.00	490.2 ± 47.50
Period 2	4.9 ± 1.60	254.8 ± 4.20

Table 5. Candidate species average monthly growth rate estimates for the Lower Colorado River mark-recapture study site.

	Average Monthly Growth (mm ± SE)		
Species	**March – April (n)**	**April – August (n)**	**Total**
Cyclonaias houstonensis	1.429±0.235 (98)	1.289±0.438 (45)	1.359
Cyclonaias petrina	1.878±0.474 (41)	2.250± 0.396 (16)	2.064
Truncilla macrodon	1.500±1.147 (6)	N/A	1.500
Total	1.602	1.770	**1.641**

Average growth estimated between mark-recapture periods was standardized on a monthly rate.

Table 6. Candidate species average monthly growth rate estimates for the Middle Colorado River mark-recapture study site.

	Average Monthly Growth (mm ± SE)		
Species	**June – August (n)**	**August – November (n)**	**Total**
Cyclonaias houstonensis	0.400±0.125 (5)	N/A	0.400
Cyclonaias petrina	0.643±0.133 (43)	0.754±0.121 (61)	0.609
Truncilla macrodon	N/A	N/A	N/A
Total	0.522	0.754	**0.405**

Average growth estimated between mark-recapture periods was standardized on a monthly rate.

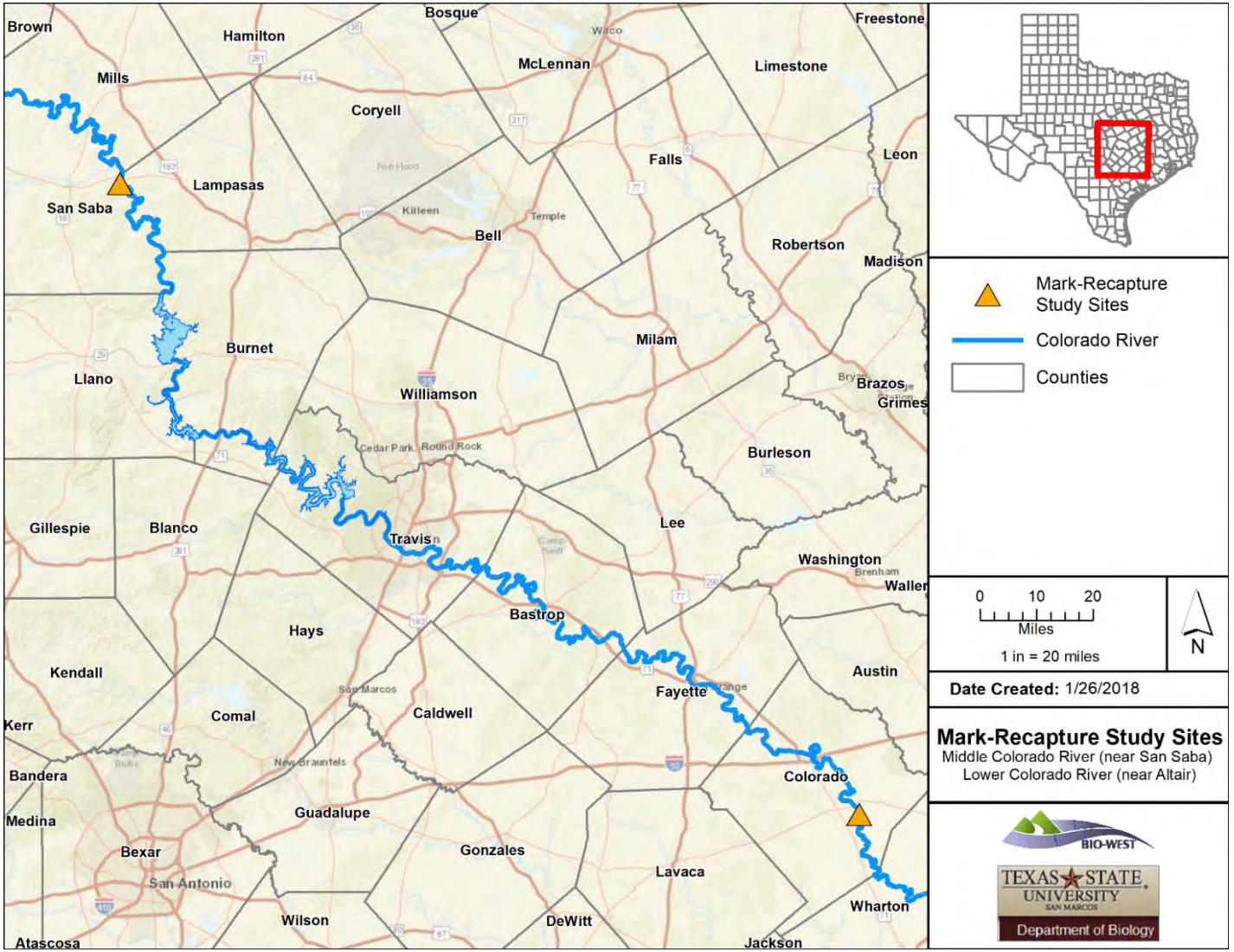

Figure 1. Map of mark-recapture study sites in the Colorado River basin, Texas.

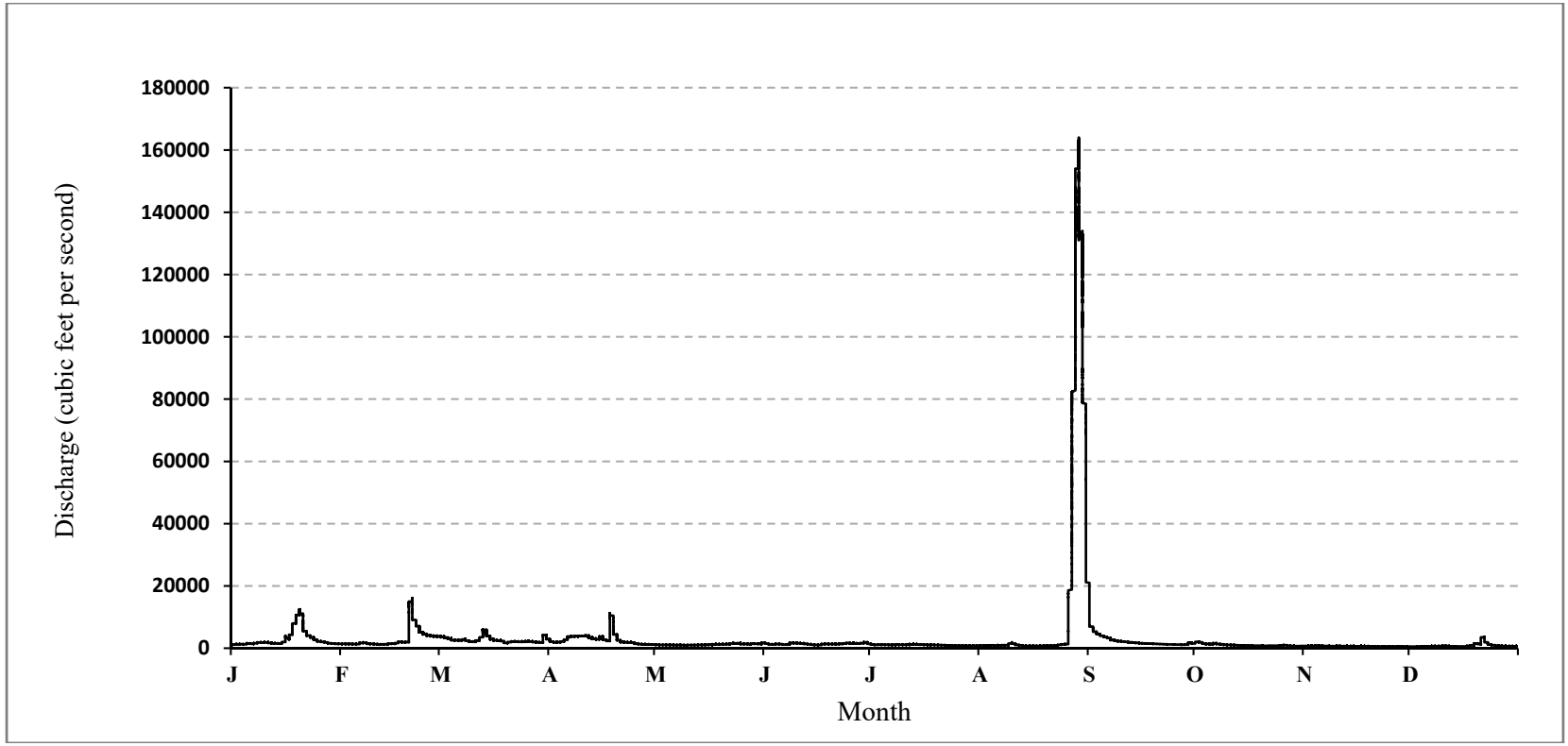

Figure 2. Discharge from the USGS gage on the Lower Colorado River at Columbus (USGS gage# 08161000) during 2017.

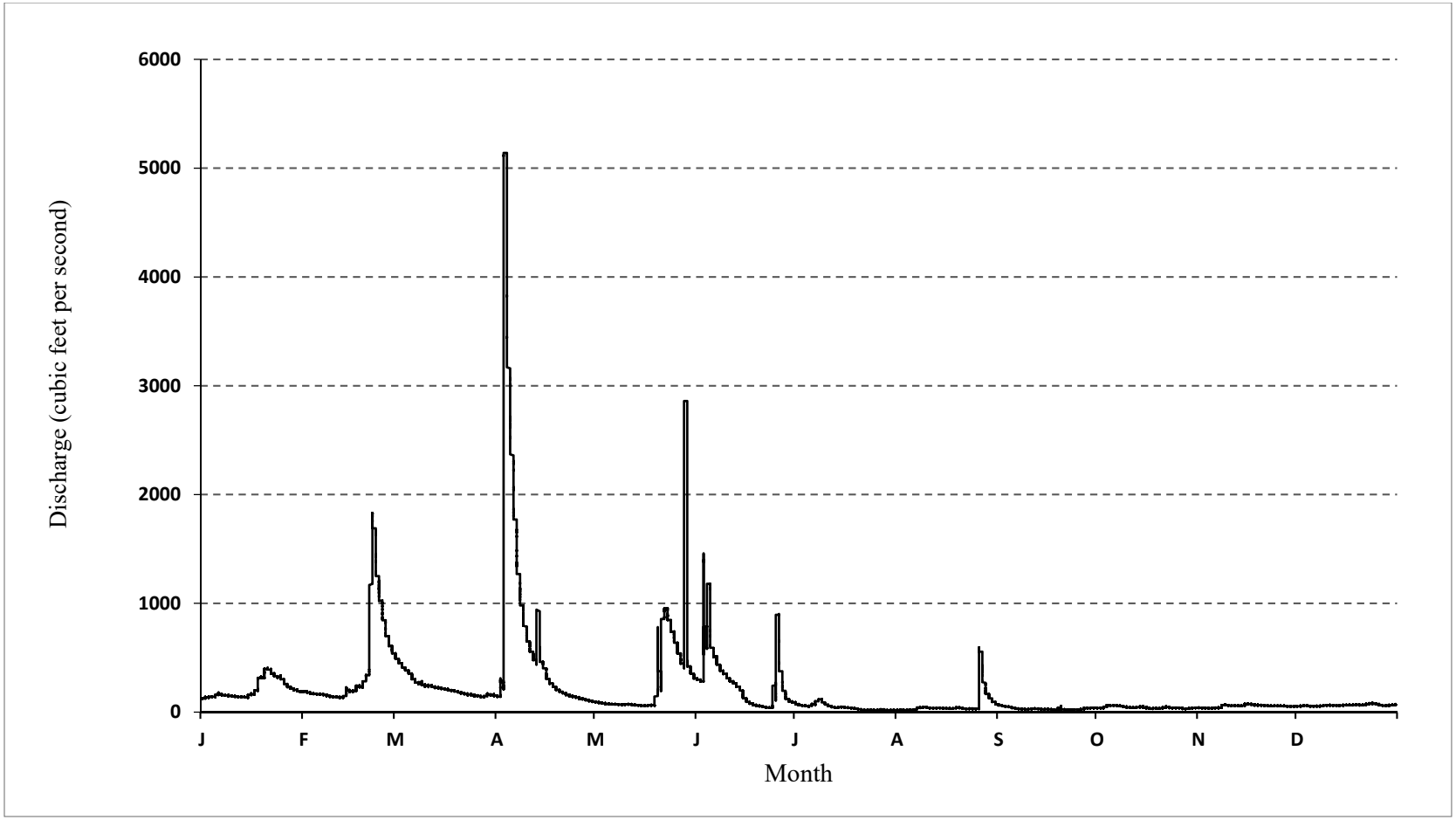

Figure 3. Discharge at the USGS gage on the Colorado River near San Saba (USGS gage# 08147000) during 2017.

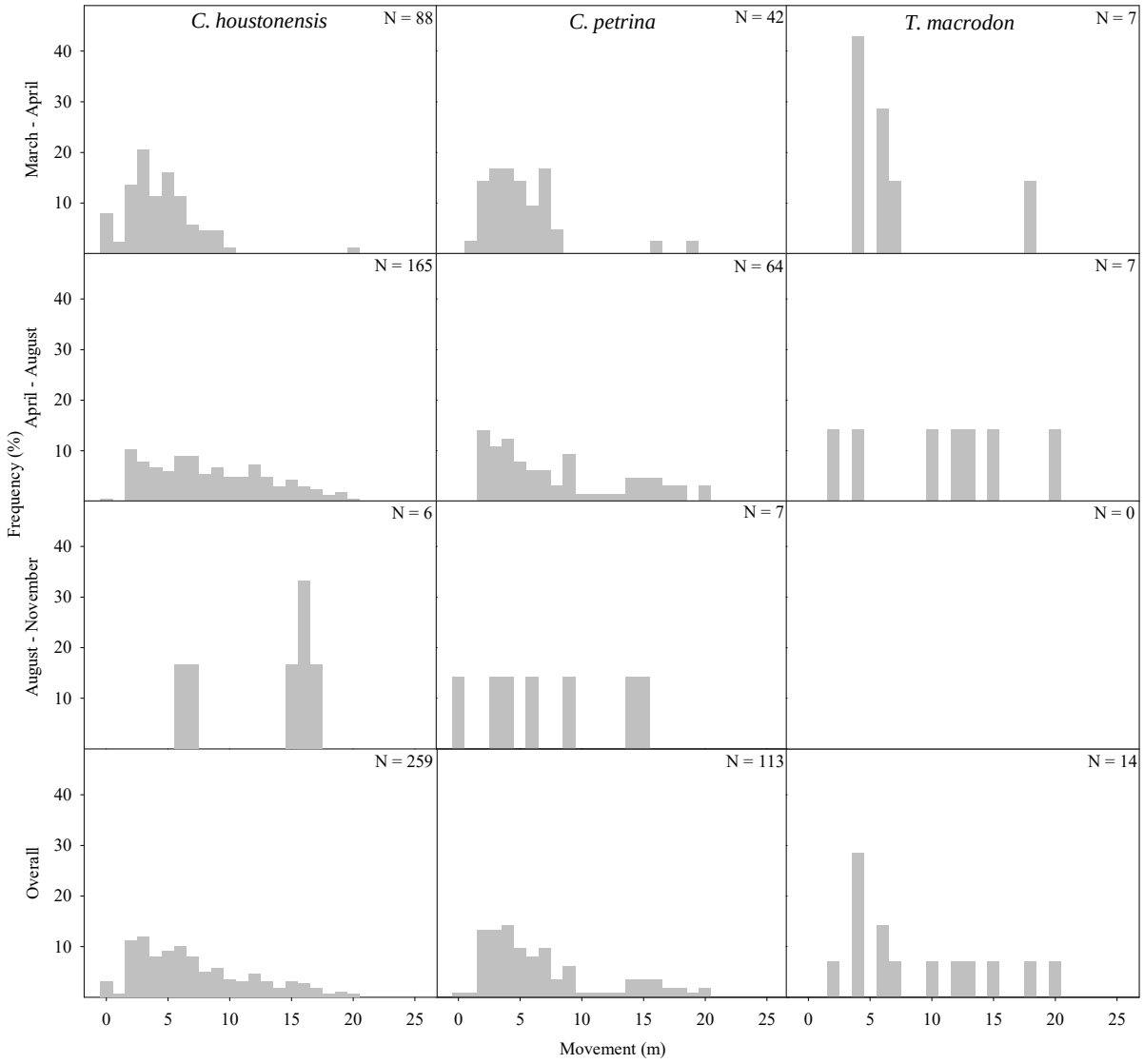

Figure 4. Percent frequency of mussels by distance (m) by time period and overall by species from the Lower Colorado River site in 2017.

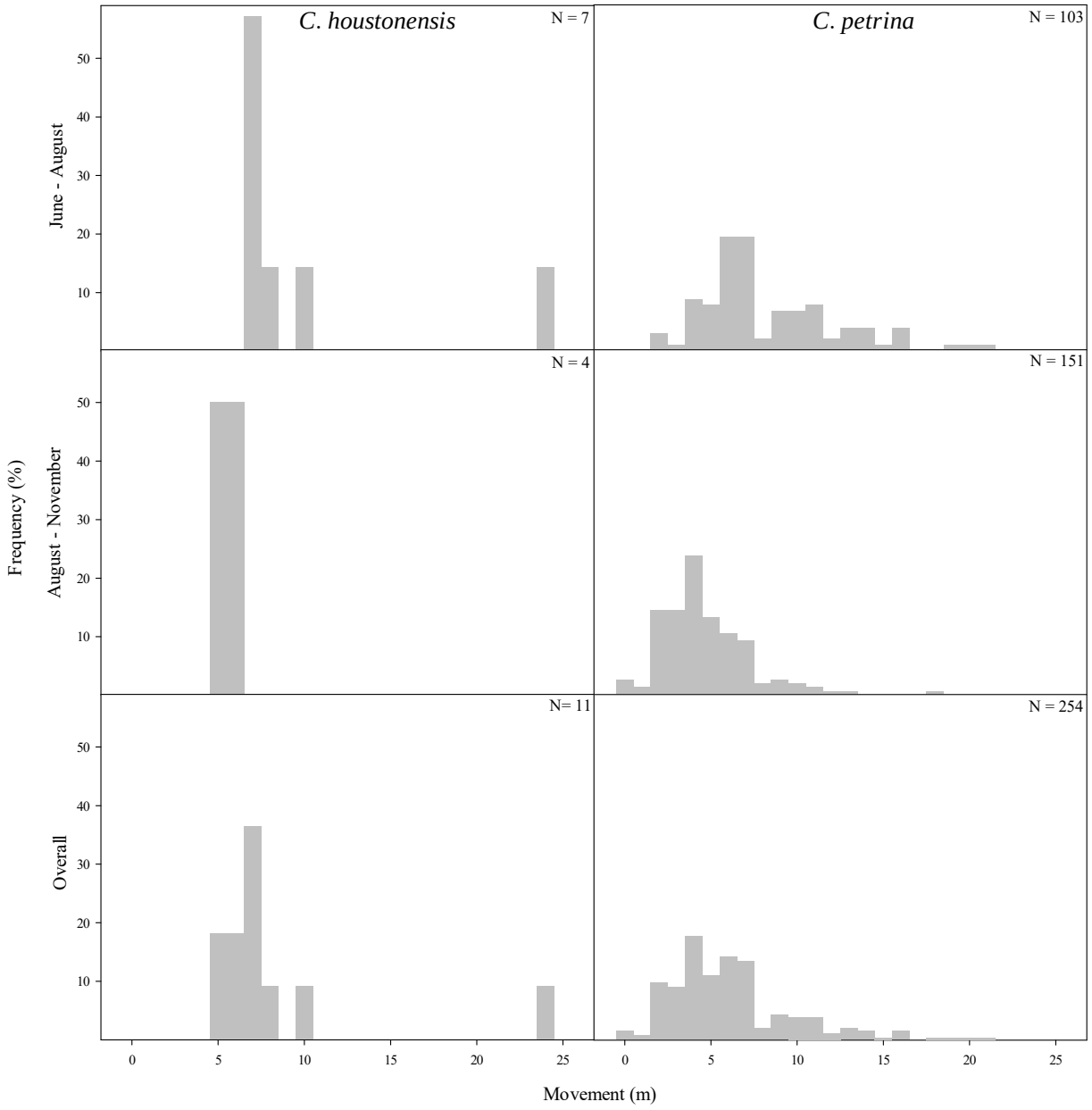

Figure 5. Percent frequency of mussels by distance (m) by time period and overall by species from the middle Colorado River site in 2017.

References

Ashton, M.J., J.S. Tiemann, and D. Hua. 2017. Evaluation of Costs Associated with Externally Affixing PIT Tags to Freshwater Mussels Using Three Commonly Employed Adhesives. Freshwater Mollusk Biology and Conservation 20:114-122.

Baillargeon, S. and L.P. Rivest. 2007. Rcapture: Loglinear Models for Capture-Recapture in R. Journal of Statistical Software 19:1-31.

Inoue, K., T.D. Levine, B.K. Lang, and D.J. Berg. 2014. Long-term mark-and-recapture study of a freshwater mussel reveals patterns of habitat use and am association between survival and river discharge. Freshwater Biology 59:1872-1883.

Haag, Wendell R. 2012. North American freshwater mussels: natural history, ecology, and conservation. Cambridge University Press, Cambridge, England.

Kurth, J., C. Loftin, J. Zydlewski, and J. Rhymer. 2007. PIT tags increase effectiveness of freshwater mussel recaptures. The North American Benthological Society 26(2):253-260.

Meador, J.R., J.T. Peterson, and J.M. Wisniewski. 2011. An evaluation of the factors influencing freshwater mussel capture probability, survival, and temporary emigration in a large lowland river. The North American Benthological Society 30(2):507-521.

Strayer, D.L. and D.R. Smith. 2003. A Guide to Sampling Freshwater Mussel Populations. Bethesda, Maryland.

Rivest, L.P. and G. Daigle. 2004. Loglinear Models for the Robust Design in Mark-Recapture Experiments. Biometrics 60:100-107.

Wisniewski, J.M., C.P. Shea, S. Abbot, and R.C. Stringfellow. 2013. Imperfect Recapture: A Potential Source of Bias in Freshwater Mussel Studies. The American Midland Naturalist 170(2):229-247.

Task 5: Captive Propagation
Task 6: Captive Rearing

Principal Investigators: Ken Ostrand, Patricia Duncan, Jeff Conway

Addresses:
U.S. Fish and Wildlife Service, San Marcos Aquatic Resources Center, 500 E. McCarty Lane, San Marcos TX 78666 (KO)

U.S. Fish and Wildlife Service, Uvalde National Fish Hatchery, 754 County Road 203 Uvalde, TX 78801 (PD)

U.S. Fish and Wildlife Service, Inks Dam National Fish Hatchery, 345 Clay Young Road Burnet, Texas 78611 (JC)

Email: Kenneth_Ostrand@fws.gov, patricia_duncan@fws.gov, jeff_conway@fws.gov

We thank B. Gaines, S. Walker, G. Cottingham, V. Cantu, R. Gibson, J. Abel and J. Morton for their significant contributions.

San Marcos Aquatic Resources Center

Task 5: Captive Propagation

Collection

In March 2017, San Marcos Aquatic Resources Center (SMARC) staff collected two gravid Texas fatmucket mussels as part of collection efforts for desiccation and long-term holding of adults. These mussels were brought to the SMARC and held in recirculating systems containing coarse sand substrate (Figure 1). These mussels were fed a 2:1 mixture of Shellfish Diet 1800 and Nannochloropsis 3600 (Reed Mariculture Inc. Campbell, CA) daily at a target concentration of 300,000 cells/mL. Feeding concentrations were verified using a Beckman Coulter Multisizer 4e (Figure 2).

Captive Propagation of Juveniles

SMARC staff inoculated Green sunfish (*Lepomis cyanellus*), Bluegill (*Lepomis macrochirus*), and Blacktail shiner (*Cyprinella venusta*) with glochidia from two gill water tubes of a gravid Texas fatmucket (*Lampsilis bracteata*) to determine the most efficient host fish. After 28 days, 21 juveniles transformed on Green sunfish, seven juveniles transformed on Bluegill, and zero juveniles transformed on

Blacktail shiner. Based on these results, 25 Green Sunfish were inoculated with the remaining glochidia from the previous trial and an additional gravid Texas fatmucket. All host fish were held in a modified flow-through Aquatic Habitats (AHAB) system at 21°C (Figure 3). After 35 days, 1533 live glochidia transformed into juveniles. All juveniles were then held in a pulsed flow-through system equipped with an automatic feeder (Figure 4). A 2:1 mixture of Shellfish Diet 1800 and Nannochloropsis 3600 (Reed Mariculture Inc. Campbell, CA) was delivered to each individual holding container hourly with a target concentration of 30,000 cells/mL. Substrate was changed weekly in beakers and growth rates were assessed. All juveniles measured approximately 300 µm upon transformation. Three weeks post transformation, juveniles averaged 450 µm (Figure 5) in length. However, within six weeks, growth rates stopped and an effective mortality rate of 100% was observed. Based on these results, several changes will be implemented before propagation efforts in 2018 begin. Among these are using filtered pond water instead of well water, increasing holding temperatures to 25°C, and modifying the delivery system of feed in pulsed flow-through systems.

Task 6: Long-term Captive Rearing and Holding

Mussels collected in March and April 2017 were housed in indoor recirculating systems containing coarse sand substrate (Figure 6). Survival rates of both Texas pimpleback and Smooth pimpleback have been 100%. These mussels are fed daily, the same mixture listed above. Beginning in Spring 2018, all long term holding will be moved to floating baskets, filled with coarse sand substrate, in outdoor ponds. All Texas fatmuckets collected for long-term rearing in this task were used as organisms in the lethal desiccation trials.

Inks Dam National Fish Hatchery

Increasing concern over the status of native freshwater mussels in the Lower Colorado River watershed has prompted efforts to evaluate the viability of freshwater mussel propagation in a hatchery setting. Inks Dan National Fish Hatchery (IDNFH) is currently holding on station Texas pimpleback (*Cyclonaias petrina*), Smooth pimpleback (*Cyclonaias houstonensis*) and Texas fatmucket (*Lampsilis bracteata*) for research and development of a propagation program (Figure 7). In early 2017 IDNFH staff completed an outdoor flow-through aquaculture system with six independent 5-ft. circular tanks for holding adult fresh water mussels (Figure 8). Since that time, multiple indoor and outdoor systems have been planned and brought into operation.

Task 5: Captive Propagation

Collection

IDNFH collection efforts of adult mussels for captive propagation began in April, 2017 with a trip to the Llano River at FM1871 with San Marcos Aquatic Resource Center (SMARC) staff. Texas pimpleback and Texas fatmucket were collected in sufficient numbers for compliance with state collection permits. Four mussels of each species were collected and brought to IDNFH for holding in the outdoor flow-through system. The functionality of the system had previously been tested using locally abundant Giant floaters (*Pyganodon grandis*). IDNFH and SMARC staff next accompanied BIO-WEST, Inc. staff for collection on the Lower Colorado River Hwy 90 crossing near Altair, TX. This trip yielded plentiful numbers of Texas pimpleback and Smooth pimpleback. Twelve of each species were brought on station, separated by species and held in the outdoor flow-through system. Additional collection trips to multiple sites on the Llano River were made but yielded low numbers for collection. IDNFH staff returned to the Llano River at FM1871 for two additional collections and sampled different reaches of the river during each trip. During these collection trips, only Texas pimplebacks were brought back to the

hatchery. Most recently, five gravid Texas fatmucket females were brought on station from a dewatering operation on a reservoir of the Llano River near Llano, TX.

Captive Propagation of Juveniles

IDNFH hatchery staff, with the assistance of SMARC staff, infested Bluegill sunfish (*Lepomis macrochirus*) and Green sunfish (*Lepomis cyanellus*) using glochidia from two gravid Texas fatmuckets on June 20, 2017. After infestation, host-fish were held in Z-Habitat type rearing units until metamorphosis and drop-off occurred 10-14 days post infestation (Figure 9). Staff estimated 2,300 metamorphosed juveniles were collected. Due to the time consuming nature of microscopic enumeration of newly metamorphosed juveniles, an additional Nikon microscope was purchased to increase future propagation efficiency.

Juvenile mussels were placed into a staff designed flow-through rearing system with sand substrate (Figure 10). The rearing system utilized water from Inks Lake filtered to 50 µm by the facilities filtration system. No supplemental feed was offered. The juvenile mussels experienced good growth over the first month, increasing in size from approximately 250 µm to 1000 µm. Anoxic influent water (dissolved oxygen < 0.5 mg/L) from the hatchery water source (Inks Lake) was experienced in early August, 2017 and led to near total mortality of the juvenile mussels.

One survivor was found in the system on September 27, 2017 and measured 2.8 mm in length (Figure 11). Since September, 2017, this individual has shown steady growth (over 8 mm by November, 2017) and is presumably meeting nutritional requirements for survival on filtered lake water.

Additionally, in mid-December, 2017, while modifying the juvenile rearing system, a second juvenile Texas fatmucket from the June, 2017 infestation was discovered on the filter screen of the system. This individual may have been living on the filter screen before anoxic conditions led to the mortality event for the June, 2017 cohort. If this was the case, its larger size may have been the result of more favorable environmental conditions during the anoxic event. The continued growth and survival of

these mussels lends credence to the belief that freshwater mussels can be cultured at IDNFH without the addition of supplemental feed (Figure 12). To mitigate the impact of future anoxic events, IDNFH staff are currently modifying the original juvenile rearing system. The new system(s) will have increased rearing capacity and features that allow for supplemental aeration should the need arise.

As previously mentioned, five gravid female Texas fatmuckets were brought to IDNFH from a de-watered reservoir near Llano, TX. The mussels were placed in newly constructed indoor raceway style tanks with flow-through lake water (Figure 13). Mussels from prior collection trips had already been brought indoors and placed in the new holding system. While in the indoor system, the five newly collected females began to actively display their lures. Two females were transferred to the Z-habitat system where water temperature could be controlled via an in-line heater. Water temperature was gradually increased from 18ºC to 24ºC which resulted in an increase in lure display frequency. Because a December infestation was not planned, only 26 Green sunfish were available on station, most of which had previously been infested in June of that year. All 26 host-fish were infested on December 8, 2017 with glochidia from a single gravid female. The glochidia were found to be 99% viable with an estimated number of 117,400 (Figure 14). After infestation of all 26 Green sunfish, unattached glochidia were enumerated and estimated at 59,200. Assuming equal distribution among host-fish, this yielded an attachment rate of approximately 2,200 glochidia per fish. Recovery of metamorphosed juveniles was low compared to the June, 2017 host-fish infestation. Staff believe the low number of metamorphosed juveniles was due to the reuse of the Green sunfish, which may have developed immunity to infestation. Only 550 juveniles were recovered from the December, 2017 host-fish infestation. Furthermore, survival of the metamorphosed juveniles has been low. Because host-fish infestation occurred during a winter month when primary production in the facilities source water would be relatively low, and juvenile mussels were maintained at a temperature (24ºC) indicative of spring or summer, metabolic requirements for growth and survival may have out-paced available food supply.

Task 6: Long-term Captive Rearing and Holding

The new indoor raceway system is functionally similar to the outdoor system in that they both utilize flow-through design and supplemental aeration. However, the new system is much shallower and allows for observation without handling. This system will be especially useful for observation of short term brooders (*Cyclonaias petrina* and *C. houstonensis*) and collection of glochidia if conglutinates from gravid females are released. The outdoor circular tank system will be utilized for holding different fish species in quarantine for future host-fish identification studies.

Once juvenile mussels reach a size to be contained in floating baskets, they will be moved to ponds for grow-out. In November, 2017, two floating docks were installed at IDNFH to assist with the investigation of pond mussel culture (Figure 15). Floating baskets fitted with wire mesh and sand substrate will be tethered to the floating docks. After the spring 2018 collection of glochidia from captive wild caught adult mussels, juvenile mussels will be moved to floating baskets as individual size and circumstances allow.

Mussel Inventory at IDNFH

Freshwater mussel inventory at IDNFH is shown in Table 1.

Table 1. January, 2018 freshwater mussel inventory at IDNFH.

Species	Scientific name	Adults held on station	Drop-offs produced	Juveniles held alive on station
Texas Fatmucket	*Lampsilis bracteata*	12	2850	2
Texas Pimpleback	*Cyclonaias petrina*	23	-	-
Smooth Pimpleback	*Cyclonaias houstonensis*	9	-	-

UVALDE NATIONAL FISH HATCHERY

Construction

In May, as an effort to assist in mussel conservation and conduct future studies (e.g. on propagation and rearing techniques) on the Central Texas federal candidate and petitioned fresh water mussel species, a Beckman Multisizer 4E Coulter Particle Analyzer was purchased. The Multisizer would be used to automatically count algal densities for feeding studies and the culture of the federal candidate freshwater mussels that are currently on station. The particle analyzer will save personnel on labor and time in measuring algal densities fed to both young and adult mussels. The analyzer is also capable of quantifying, mammalian cells, bacteria, yeast, spheroids, and large protein and cell aggregates. This instrument has data overlay capability for detecting and analyzing complex samples over a wide variety of particle sizes from 0.2 µm-1600 µm in diameter from sample volumes as small as 5 ml. On July 10th, a Beckman Coulter technician trained staff members from the UNFH how to measure samples and use some of the standard operating procedures (SOPs).

In July, Pat Duncan guided Lead Fish Biologist Valentin Cantu and Fish Biologist Greg Cottingham in constructing a flow-through system for mussels held in separate containers by species and number at the facility's existing Quarantine Building (Figure 16). All effluents from the system's holding mussels flow through a chlorinated sand filter and then on dry ground (Figure 17) to guard against the release of organisms into outside waters. During FY 2017, staff members maintained and monitored the chlorine levels and sand in the system to maximize the efficacy and efficiency of the system.

In August, Pat Duncan had made plans and guided lead Fish Biologists Valentin Cantu and Fish Biologist Greg Cottingham to begin to construct an algal feeding system that is driven by a peristaltic pump. By September 19th, the mussel systems were equipped with peristaltic pumps to provide continuous feeding of concentrated algal solutions. A Tecniplast stand-alone Zeb-Hab rack system with a complete recirculating system was installed on September 11th at UNFH (Figure 18). The system will provide additional facilities for holding mussels and host fish for future glochidia production and later

juvenile rearing and culture trials. The Z-Hab is a computerized tank system capable of automatically monitoring temperature, pH, and specific conductivity and setting off alarms if water parameters exceed upper or lower limits. A Z-Hab technician trained UNFH staff members on how to use and maintain the Z-Hab system on September 12th. Data may be uploaded from the system for data analysis. The system is designed with specialized containers for holding aquatic species and a drum filter that automatically removes debris from the system. The system will be used for mussels in refugia and for propagation. Tecniplast personnel are scheduled to install a chiller for system completion.

On October 31st, UNFH staff worked with USFWS IT personnel to authorize software to begin installing a state of the art microscope that will be used to conduct mussel research. The microscope is an Olympus BX43 Phase Contrast Upright Custom System uses unique software (Cellsens) that will save personnel on labor and time on live acquisition, live measuring, annotation, time lapse, and fluorescence overlay. The unique software has a process manager for several types of experiments and images that can be readily shared with other Cellsens users without having to convert the image format or lose all functionality on the analysis side. An Olympus representative installed the microscope in the laboratory of the UNFH and trained staff members on microscope operation.

Collection

Freshwater mussel collection near Comfort, Texas was scheduled on April 12th, but was cancelled due to inclement weather.

On August 3rd, Lead Biologist Valentin Cantu, Fish Biologist Greg Cottingham, and Student Intern Brittany Germain met BIO-WEST, Inc. at the Colorado River, Columbus, Texas (Figure 19) to collect the candidate species for the UNFH refugia. UNFH team members were transported to shallow collection sites by boat. Mussels were collected from the Colorado River with the assistance of BIO-WEST, Inc. staff members.

The river water from the Colorado River was warm (31.40ºC) and turbid (visibility < 1 inch). Most mussels were collected by hand from substrates rich in mud, sand, and detritus over coble and bedrock. A total of 30 Smooth Pimpleback (*Cyclonaias houstonensis*), 15 Texas Pimpleback (*C. petrina*), and two Texas Fawnsfoot (*Truncilla macrodon*) mussels were collected. Mussels were carefully packed into 40-quart ice coolers with ice packs and burlap bags and transported to the UNFH (Figure 20). Standard hatchery protocols were followed to prevent the transfer of aquatic nuisance species and disease. Upon arrival to the UNFH Quarantine Building, mussels were carefully acclimated to their tank systems and specimens were monitored daily.

Culture

In August, the Project Leader Pat Duncan began training the Lead biologist Valentin Cantu and Fish Biologist Greg Cottingham the art of feeding a special algal diet to three species of federal candidate and petitioned freshwater mussels including the Texas Fawnsfoot (*Truncilla macrodon*), smooth pimpleback (*Cyclonaias houstonensis*), and Texas pimpleback (*C. petrina*) that were brought on station in early August. After the freshwater mussels were brought on station, staff members routinely fed mussels, maintained water flows, cleaned screens of debris, replaced air stones, and checked for mortalities. Mussels were maintained in flow-through systems throughout culture period.

Figure 1: Texas fatmuckets held in indoor recirculating system.

Figure 2: Beckman Coulter Multisizer 4e used to size and quantify particle levels in water.

Figure 3: Flow-through AHAB system used to house host fish.

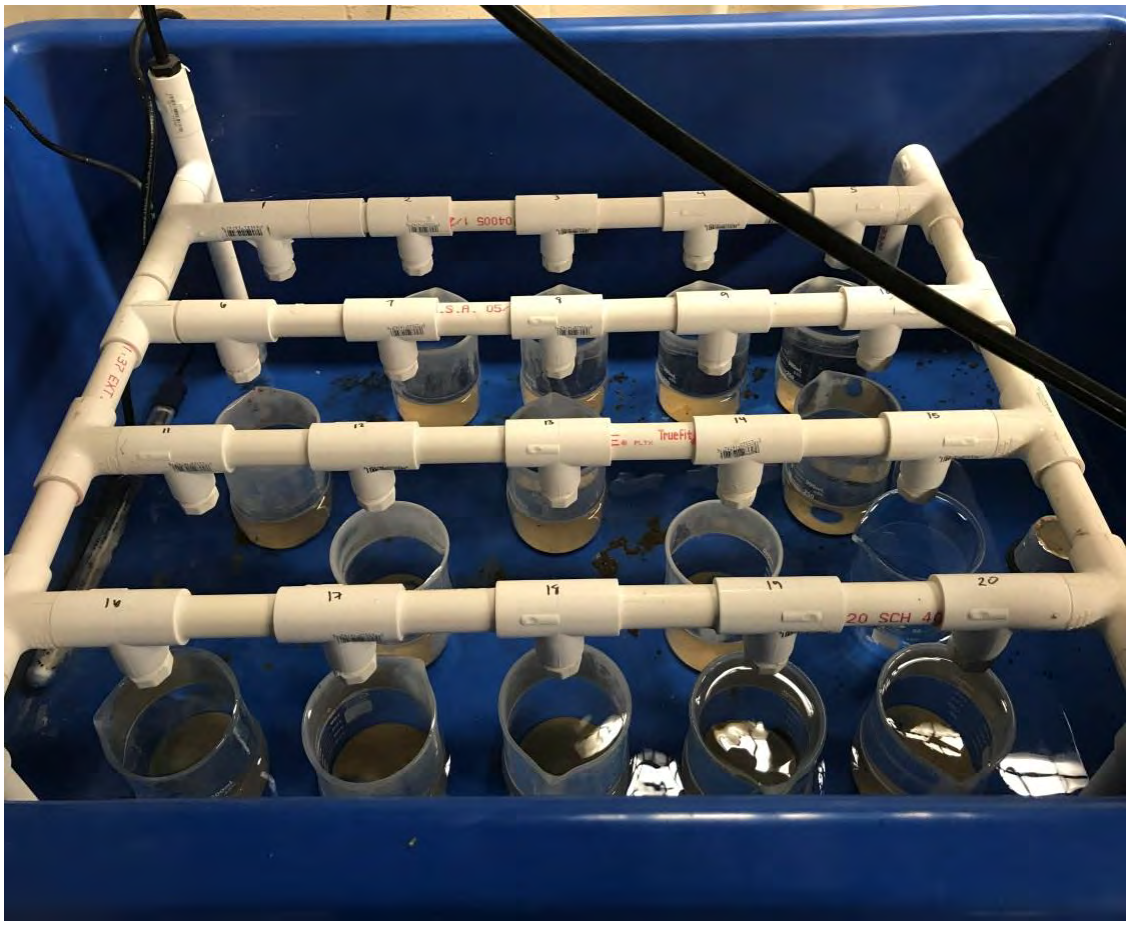

Figure 4: Pulsed flow-through system used to house juveniles. Each beaker is capable of housing approximately 100 juveniles.

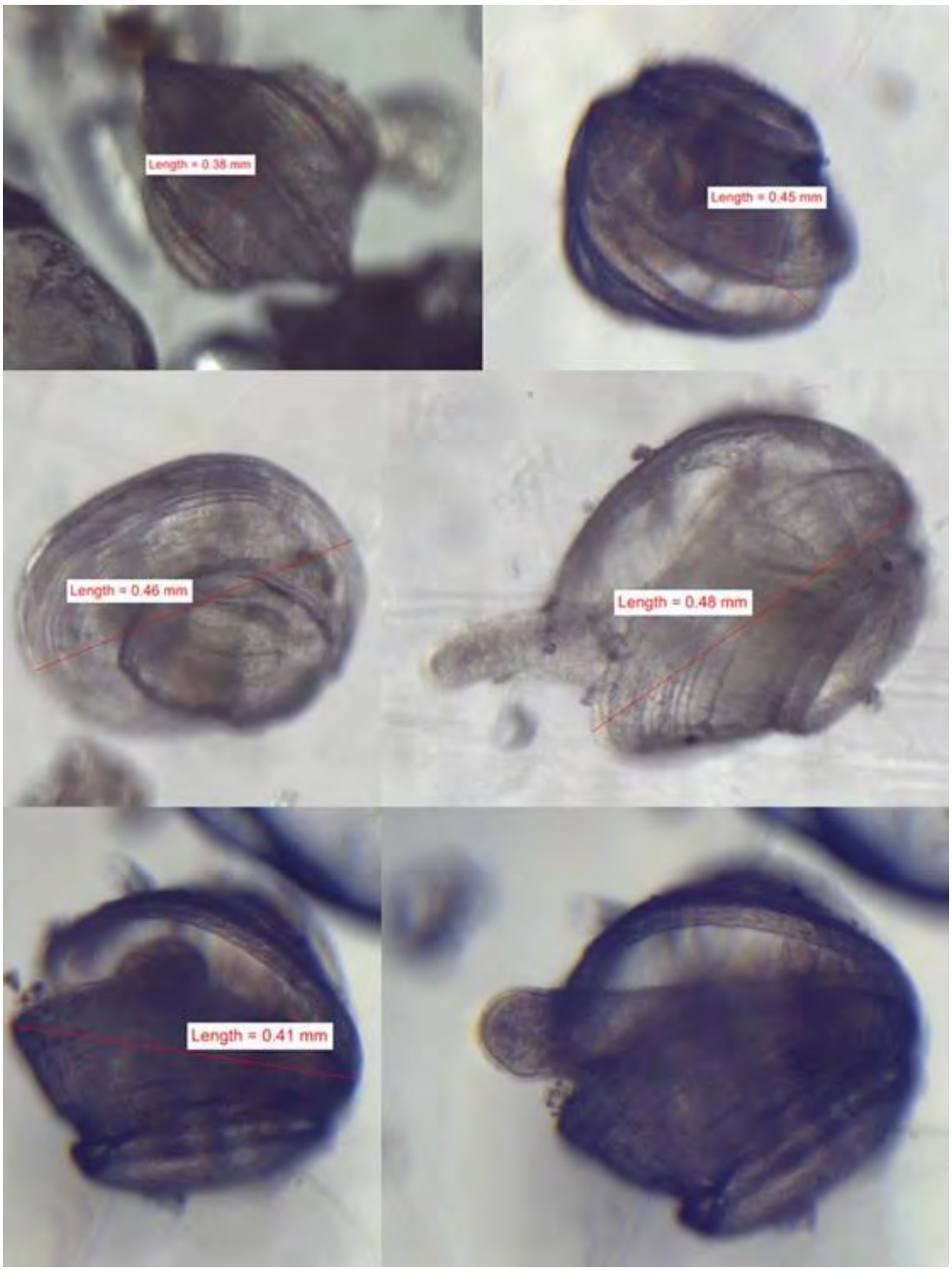

Figure 5: Juvenile Texas fatmuckets cultured at the SMARC.

Figure 6: Indoor recirculating systems used for long term holding of adult mussels in 2017.

Figure 7. Freshwater mussels collected from the Colorado River watershed for use in propagation at IDNFH. From left to right: Texas fatmucket (*Lampsilis bracteata*), Texas pimpleback (*Cyclonaias petrina*) and Smooth pimpleback (*Cyclonaias houstonensis*).

Figure 8. Outdoor flow-through freshwater mussel holding tanks at IDNFH.

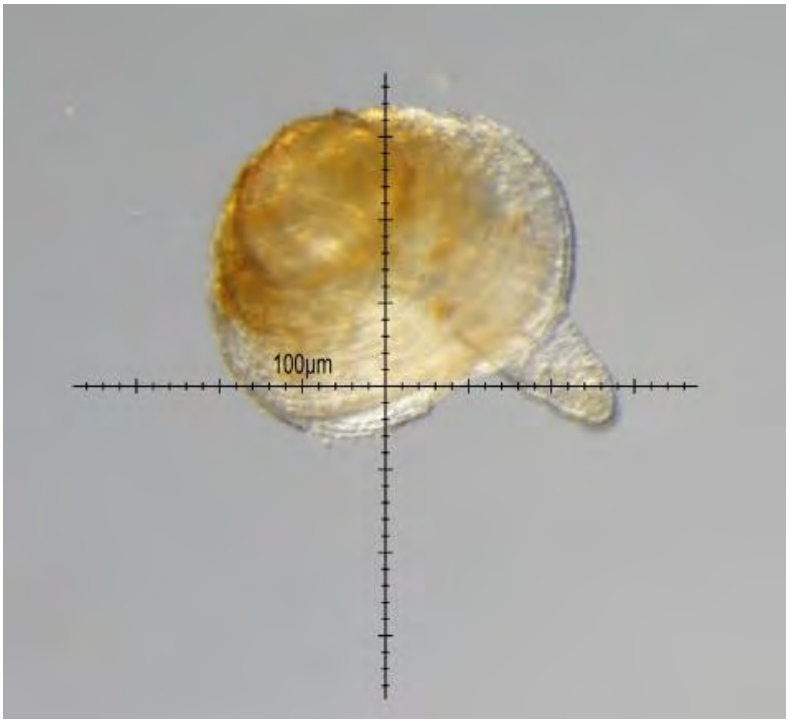

Figure 9. Newly metamorphosed juvenile Texas fatmucket (*Lampsilis bracteata*) at IDNFH.

Figure 10. Flow-through juvenile mussel rearing system at IDNFH.

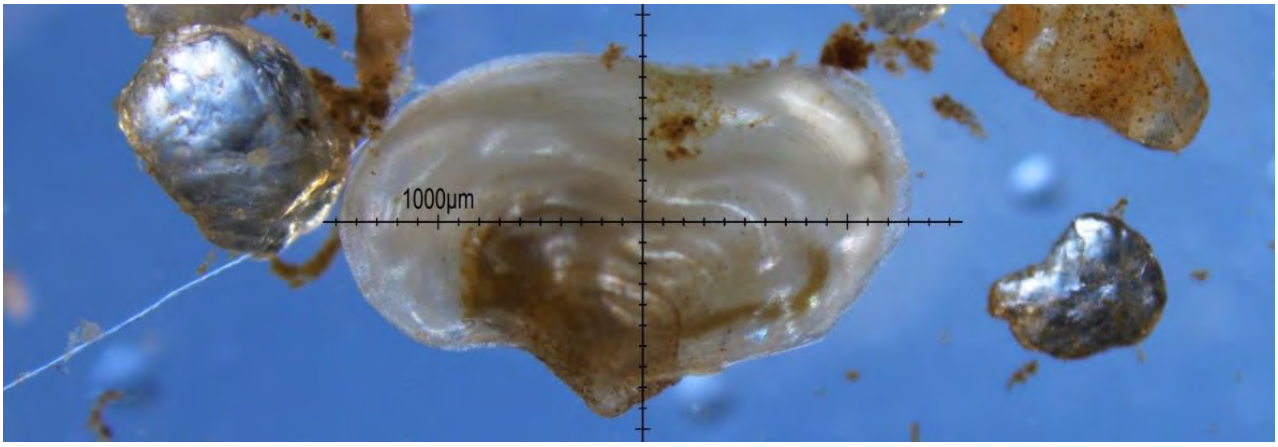

Figure 11. Juvenile Texas fatmucket at IDNFH 100-d post metamorphosis.

Figure 12. Juvenile Texas fatmuckets (*Lampsilis bracteata*) six months post metamorphosis.

Figure 13. Indoor flow-through raceway system for holding adult freshwater mussels at Inks Dam National Fish Hatchery

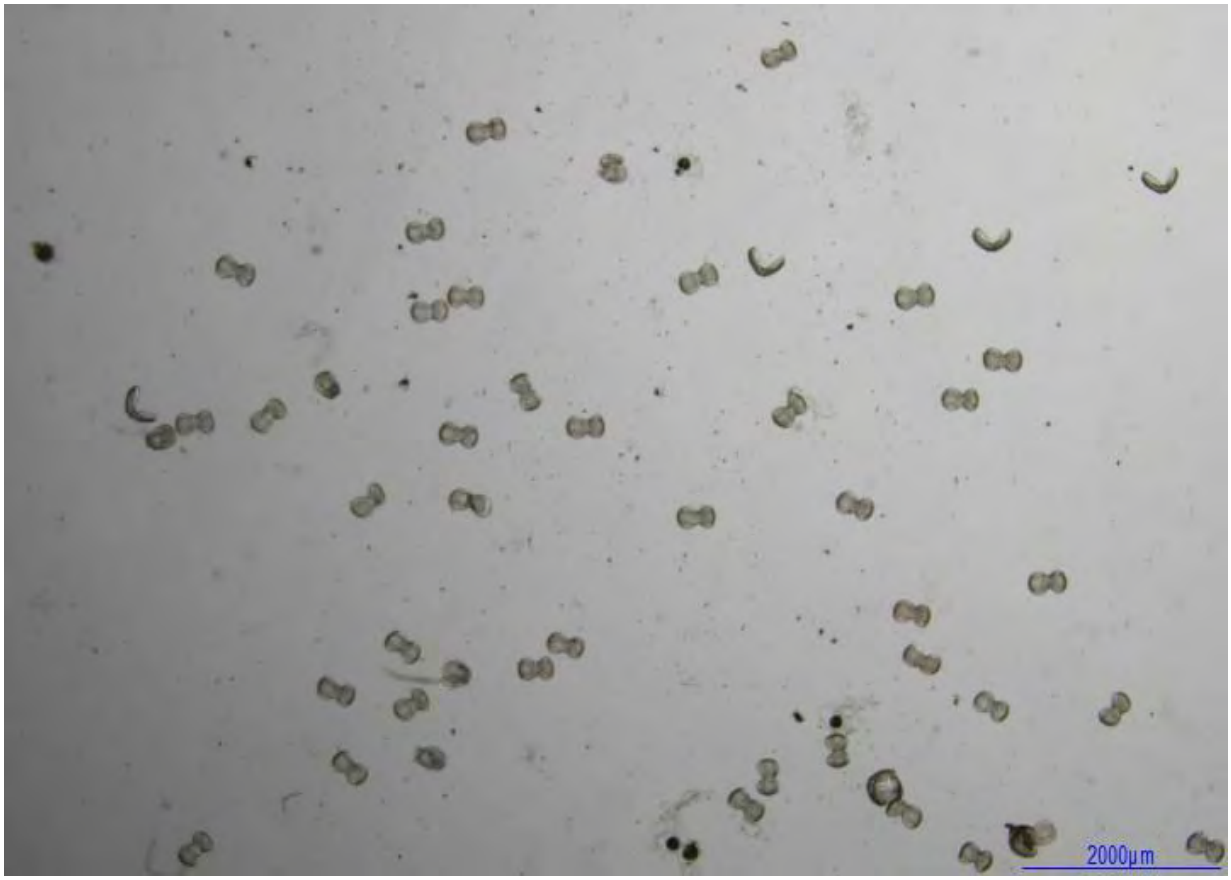

Figure 14. Glochidia extracted from Texas fatmucket (*Lampsilis bracteata*) on December 8, 2017 at Inks Dam National Fish Hatchery

Figure 15. Floating dock at Inks Dam National Fish Hatchery

Figure 16. The freshwater mussel tank system that holds Central Texas federal candidate and petitioned freshwater mussel species at the Uvalde National Fish Hatchery. Photo credit: USFWS.

Figure 17. A chlorinated sand filter system at The Uvalde National Fish Hatchery Quarantine Building. Photo credit: USFWS.

Figure 18. A Z-Hab technician training Uvalde National Fish Hatchery staff members how to use and maintain a state of the art Z-Hab system. Photo credit: USFWS.

Figure 19. The Colorado River in Columbus, Texas near where mussels were collected (photograph above). Uvalde National Fish Hatchery's Lead Biologist Valentin Cantu and Fish Biologist Greg Cottingham searching for freshwater mussels at the Colorado River (photograph below).

Figure 20. Adult mussels collected from the Colorado River packed in an ice cooler with wetted burlap bags for transport to the Uvalde National Fish Hatchery.

Multiple freshwater mussel species of the Brazos River, Colorado River, and Guadalupe River basins

CMD 1—6233CS

Supplemental Report

August 31, 2018

Principal investigators:

Timothy H. Bonner, Texas State University, Department of Biology
Edmund L. Oborny and Bradley M. Littrell, BIO-WEST, Inc.
James A. Stoeckel, Auburn University, School of Fisheries, Aquaculture, and Aquatic Sciences
Brian S. Helms, Troy University, Department of Biology & Environmental Sciences
Kenneth G. Ostrand, USFWS San Marcos Aquatic Resources Center
Patricia L. Duncan, USFWS Uvalde National Fish Hatchery
Jeff Conway, USFWS Inks Dam National Fish Hatchery

Table of Contents

The Texas Comptroller of Public Accounts office provided financial assistance for this study. We thank R. Gulley, M. Hope, and K. Horndeski of the Texas Comptroller of Public Accounts office for their support and coordination of our research activities. We also thank staff from Austin Ecological Field Office, Texas Parks and Wildlife, Lower Colorado River Authority, and Brazos River Authority for their assistance and coordination among our partners.

The findings and conclusions in this report presented by U.S. Fish and Wildlife Service project team members do not necessarily represent the views of the U.S. Fish and Wildlife Service.

Task 2: Potential Factors Limiting Growth, Survival, and Reproduction of Freshwater Mussel Species of Interest

Contributing authors: Austin Haney[1], Ryan Fluharty[1], Hisham Abdelrahman[1], Rebecca Tucker[1], Kaelyn Fogelman[1], Brian Helms[2], and James Stoeckel[1]

Addresses: [1]203 Swingle Hall, School of Fisheries, Aquaculture, and Aquatic Sciences, Auburn University, Auburn, Alabama 36849

[2]Department of Biological & Environmental Science, Troy University, Troy, AL 36082

Principle Investigators: James Stoeckel and Brian Helms

Email: jimstoeckel@auburn.edu, helmsb@troy.edu

Task 2. Objectives: The overall objective of this study was to conduct applied research experiments on up to three mussel species of interest to investigate impacts of the following stressors: temperature, hypoxia, suspended solids, salinity, and nitrogenous compounds. Specific objectives are listed under each sub-task.

Task 2.1 Sublethal effects of thermal and hypoxia stress

Task 2.1.A. Test microplate respirometry using early stage *Ligumia subrostrata*

2.1.A. Goal: The goals of this task were to:

1) Use a surrogate species to develop protocols for conducting microplate respirometry on early stage (glochidia and/or juveniles) mussels.

2) Determine the relationship between respiration rate, regulation index, DOcrit, and brood viability.

Based on initial observations described in previous Final Report(s) we hypothesized that respiration rate would increase, ability to regulate oxygen consumption would decrease, and DO_{crit} would increase as brood viability decreased (Fig. 1).

2.1.A. Methods: Gravid *Ligumia subrostra* were collected from an earthen pond at the South Auburn Fisheries Research Station of Auburn University, and held in the laboratory in the same manner as mussels shipped from Texas (see subsequent sections). All females were held at a cool temperature (18ºC) in order to maximize glochidia retention until used in experiments. During this time they were fed 2 mL Shellfish Diet 1800 (Reed Mariculture Inc, Campbell, CA) in the morning and 1 mL in the afternoon on a daily basis.

Prior to experimental runs, glochidia were flushed from gills of gravid mussels using a syringe and 18ºC AFW into separate beakers. Viability of each brood was calculated using methodology of Fritts et al. (2014). Respiration rates of glochidia were measured using an optical microrespirometry system (Loligo Inc.). Two thousand glochidia were loaded into a single 1 ml respirometry well containing 1 ml AFW at 18ºC. Three replicate wells were loaded per brood. Control wells contained no glochidia. The twenty-four well microrespirometry tray was then sealed with a silicone gasket and PVC block, placed in a waterbath, and gently rocked on a hula-type shaker table to keep water mixed within each well. Dissolved oxygen in each well was measured every 15 seconds. Glochidia remained in wells until dissolved oxygen in each well was drawn down to <0.5 mg O_2/L. Respiration rates were calculated using the following formula:

Respiration (mg O_2 / 2,000 glochidia / hr) = $([O_2]t_0 – [O_2]t_1)*V/t$

Where:

$[O_2]t_0$ = oxygen concentration at t_0 (mg O_2/liter)

$[O_2]t_1$ = oxygen concentration at t_1 ((mg O_2/liter)

V = respirometer volume (liter)

$T = t_1 – t_0$ (hour)

Correction for background (bacterial) oxygen demand

Chlorination, followed by rinsing, was used to reduce/eliminate bacteria in plate wells and associated tubing prior to each respiration run. However, bacteria populations tend to grow quickly and may have accounted for a significant portion of chamber oxygen demand by the end of a given run (i.e. background respiration). To account for this, we measured the respiration rates of control wells (no glochidia) during each run. The mean control oxygen demand was then divided by the mean observed respiration rate under normoxic conditions with glochidia present in order to determine the proportion of total well respiration that was due to background respiration. This proportion was referred to as the correction factor. We assumed that this proportion remained constant as dissolved oxygen declined below normoxia and corrected our respirometry data in each chamber by multiplying the observed respiration rate by 1 minus the correction factor.

Regulation indexes (RI's) were calculated using the methodology of Mueller and Seymour (2011). Corrected RMR ($mgO_2/g/hr$) values were plotted against DO (mgO_2/L) for each respirometry run. Data were fitted with the curve (3-parameter exponential rise to maximum, 2-parameter hyperbola, or 2-segment piecewise regression) that showed the lowest Akaike information criterion adjusted for small sample size (AICc: SigmaPlot 13.0). We then used the Sigma Plot area under the curve (AUC) macro to calculate AUC for 1) the observed data, 2) a horizontal line that represented perfect regulation, and 3) a linear decrease that represented perfect conformation (see Fig. 3c). RI was calculated as (Observed AUC-Conformation AUC)/(Regulation AUC-Conformation AUC). The RI provided a quantitative measure of the degree to which mussels were able to regulate oxygen consumption as ambient DO declined from 6 to < 0.2 mg O_2/L. DO_{crit} was calculated as the dissolved oxygen

concentration showing the greatest distance between the observed RMR and the perfect conformation line (Mueller and Seymour 2011).

2.1.A. Results:

Brood viability of the 14 gravid females tested ranged from 46.5% to 94%. Contrary to our hypothesis, we found no significant linear relationship between respiration rate ($p = 0.2765$), RI ($p = 0.5583$), or DO_{crit} ($p = 0.1006$) and % viability of glochidia (Fig. 2).

2.1.A. Conclusions:

We successfully developed protocols to measure respiratory patterns of mussel glochidia. Due to the low respiration rate of an individual glochidium, the methodology required use of 2,000 glochidia per well in order to obtain usable results. We can apply this methodology to glochidia of focal species in this study, if/when they become available.

Contrary to our hypotheses, respiration rate, regulation index, and DOcrit did not appear to be consistently affected by brood viability of our surrogate species – *Ligumia subrostrata*. Regulation index was as high or higher than adult mussels of focal species in this study and DO_{crit} remained below 2 mg O2/L. These results suggest that glochidia are not more sensitive to declining dissolved oxygen levels than adult mussels. Using different methodologies, Tankersley and Dimock (1993) also found no evidence that response of glochidia to reduced oxygen availability differed from adult mussels. Because respiration rates could not be measured for individual glochidia and we were not able to obtain reliable mass estimates for glochidia, we cannot directly compare mass-specific respiration rates between glochidia and adult mussels at this time.

Task 2.1.B. Collection of focal species to be used in trials

Mussels for experiments were collected by BIO-WEST, Texas State University, and Auburn University personnel during surveys (see Table 1 for species list and collection information). Mussels were placed in coolers between moist cotton towels. Sufficient ice-packs were added above and below the toweling to try to maintain a shipping temperature intermediate between collection temperature in Texas and holding temperature (18ºC) at Auburn. All coolers were shipped overnight via FedEx. Upon arrival, mussels were tagged, measured (length), and placed in upwellers containing ~80 L of hard artificial freshwater (HAFW: 0.192 g $NaHCO_3$, 0.10 g $CaSO_4$*H20, 0.10 g $CaCl_2$, 0.06 g $MgSO_4$, and 0.008 g KCl per liter of reverse osmosis/deionized water; modified from Smith et al. 1997) at 18ºC. Biofilters in each upweller were allowed to establish for > 2 weeks prior to arrival of experimental mussels. Mussels in each upweller were fed 2 mL Shellfish Diet 1800 (Reed Mariculture Inc, Campbell, CA) in the morning and 1 mL in the afternoon on a daily basis. Water quality (ammonia, nitrites, nitrates) was measured 3 times/week using either Tetra 6-in-1 and Ammonia Aquarium Test Strips or API 5 in 1 and Ammonia Test Strips. Ammonia and nitrites remained at undetectable levels (< 0.5 mg/L) throughout the study. Nitrates were consistently detected and water changes were triggered when nitrate concentrations reached or exceeded 20-40 mg/L.

Newly arrived mussels were allowed to acclimate to HAFW and laboratory holding conditions for > 2 weeks. Following the lab acclimation, mussels were randomly assigned to one of six temperature treatments (13, 17, 23, 28, 32, and 36ºC). However, the lowest temperature was changed to 15°C after we found respiration rates at 13ºC were too low to reliably assess metabolic patterns. Mussels were acclimated in insulated upwellers (~70 L) equipped with chillers and/or heaters with temperature control (4 mussels/species/cooler, 2 coolers per

temperature treatment). During acclimation, temperature was adjusted up or down at a rate of 1ºC/day until the target temperature was reached. Mussels were then acclimated to the temperature treatment for > 1 week. During the acclimation period, mussels were fed Shellfish Diet 1800 twice daily (2 mL morning, 1 mL afternoon per ~70 L upweller) and held at a 12h light: 12h dark cycle.

Task 2.1.C1a. Thermal and hypoxia tolerance of adult *C. houstonensis* and *C. petrina*: Effects on metabolic patterns.

2.1.C1a. Goals

Following acclimation, we used closed respirometry to estimate resting metabolic rates (RMR) of freshwater mussels at different temperatures as dissolved oxygen (DO) decreased from near 100% saturation to anoxic conditions. RMR represents the oxygen demand of organisms while at rest and approximates the metabolic rate required for basic maintenance. We then used the relationship between RMR and DO to calculate a regulation index (RI) for each mussel. The regulation index provides an assessment of the ability of an organism to maintain a constant respiration rate (i.e. meet its basic metabolic requirements) as oxygen declines. The closer the RI is to 1, the better an organism is able to continue to meet its energetic demands as DO declines (Fig. 3a,c). The closer the RI is to zero, the less an organism is able to meet its energetic demands as DO declines (Fig. 3b,c). We also used the relationship between RMR and DO to calculate critical dissolved oxygen levels (DO_{crit}). The DO_{crit} indicates the DO threshold below which an organism switches from aerobic to anaerobic respiration and thus is experiencing severe respiratory stress (Fig. 3a,b).

2.1.C1a. Methods:

Respirometry experiments were conducted in 8-chamber fiber optic respirometry systems using AutoResp™ 2.3.0 software (Loligo, Inc.). Chambers were made of acrylic and ranged in volume from ~200 – 700 mL. Each chamber was connected to two Eheim submersible 300 L/h pumps: one circulated fresh oxygenated water through the chamber during acclimation, and the other circulated water through the chamber during experiments. A fiber-optic sensor was inserted in the closed recirculation line of each chamber. Respirometry chambers and associated pumps and sensors were submerged in a ~300 L tub filled with HAFW. Temperature was controlled by means of a TECO 1/3 hp chiller/heater unit. Chambers, tubing, and gravel associated with the respirometry setup were chlorinated (5 ml bleach/gallon tap water) to reduce bacteria and then rinsed thoroughly before each trial.

We measured respiration rates of 8 randomly selected individuals per temperature for *Cyclonaias houstonensis* and *C. petrina* (4 individuals per species/run * 2 runs per temperature). Acclimated individuals were removed from temperature-controlled upwellers, scrubbed lightly with a brush to remove any algae, and weighed (gWW). Mussels were then set in PVC cups filled with gravel within the respirometry tub, and held without food for ~24 hours to prevent feeding and digestion from affecting estimates of RMR.

Following the 24 hr starvation period, mussels were assigned to an appropriately sized respirometry chamber (chamber that accommodated a mussel's shell without touching sides or lid). A PVC cup (1.5" H) half full of pea gravel was placed in each chamber to provide substrate for the mussels to burrow into. Cups had 4-mm mesh screening on the bottom to allow for water recirculation and reduce the chance of 'dead zones'. Flush pumps associated with each chamber were turned on and mussels allowed to acclimate to respirometry chambers for 5 hrs – a period

of time which equaled or exceeded the amount of time required for mussels to reach a stable RMR as determined by previous experiments (Haney and Stoeckel, unpublished data). During this time, DO levels were near 100% saturation levels. Respirometry rooms were held at a 12h light: 12h dark cycle.

Acclimation periods were always initiated in late afternoon/early evening, and respirometry initiated before midnight. Following acclimation, the flush pumps were turned off and closed pumps turned on – creating a closed system where the volume of water recirculating within each chamber and associated tubing was constant, and no new, oxygenated water entered the system. Pumps were controlled remotely using TeamViewer software to minimize any disturbance to the mussels within the respirometry rooms. Mussels were allowed to respire until dissolved oxygen levels fell below ~0.2 mgO_2/L in the chambers or until mussels exhibited valve closure (abrupt cessation of respiration). Valve closure rendered respiration data unusable for RI or DO_{crit} analyses. At the end of each experimental run, mussels were removed from their testing chambers and then returned to upwellers to recover. Duration of each run was temperature dependent. At the coldest temperature, it generally took > 8 hrs for DO to fall below 0.2 mgO_2/L whereas at the warmest temperature, DO typically declined to < 0.2 mgO_2/L within 8 hours or less.

Correction for background (bacterial) oxygen demand

Chlorination, followed by rinsing, was used to reduce/eliminate bacteria in chambers and associated tubing prior to each respiration run. However, bacteria populations tend to grow quickly and may have accounted for a significant portion of chamber oxygen demand by the end of a given run (i.e. background respiration). To account for this, we measured background respiration rate of each chamber before and after each run, under normoxic conditions (DO ≥ 5

mgO_2/L), for ~1.5 hrs without mussels present. The mean background oxygen demand was then divided by the mean observed respiration rate under normoxic conditions with mussels present in order to determine the proportion of total chamber respiration that was due to background respiration. This proportion was referred to as the correction factor. We assumed that this proportion remained constant as dissolved oxygen declined below normoxia and corrected our respirometry data in each chamber by multiplying the observed respiration rate by 1 minus the correction factor.

Regulation Index and DO_{crit}

Regulation indexes (RI's) were calculated using the methodology of Mueller and Seymour (2011). Corrected RMR ($mgO_2/g/hr$) values were plotted against DO (mgO_2/L) for each respirometry run. The upper limit of the DO range for which RI was calculated was held constant at 6 mg O_2/L to avoid bias in colder temperature runs where initial DO could be much higher than warmer runs (Mueller and Seymour 2011). Data were fitted with the curve (3-parameter exponential rise to maximum, 2-parameter hyperbola, or 2-segment piecewise regression) that showed the lowest Akaike information criterion adjusted for small sample size (AICc: SigmaPlot 13.0). We then used the Sigma Plot area under the curve (AUC) macro to calculate AUC for 1) the observed data, 2) a horizontal line that represented perfect regulation, and 3) a linear decrease that represented perfect conformation (see Fig. 3c). RI was calculated as (Observed AUC-Conformation AUC)/(Regulation AUC-Conformation AUC). The RI provided a quantitative measure of the degree to which mussels were able to regulate oxygen consumption as ambient DO declined from 6 to < 0.2 mg O_2/L. DO_{crit} was calculated as the dissolved oxygen

concentration showing the greatest distance between the observed RMR and the perfect conformation line (Mueller and Seymour 2011).

2.1.C1a: Results:

Resting metabolic rate increased linearly with increasing temperature for *Cyclonaias houstonensis* from the Colorado (RMR = 0.0007*temp – 0.0053; R^2 = 0.9744, P = 0.0002) and Navasota rivers (RMR = 0.0004*temp – 0.0046; R^2 = 0.9423, P = 0.0013). The regulation index did not show a significant linear relationship with temperature for *C. houstonensis* from the Colorado (R^2 = 0.6328, P = 0.0584) or Navasota (R^2 = 0.0164, P = 0.8088) rivers. Similarly, DO_{crit} did not show a significant linear relationship with temperature for *C. houstonensis* from the Colorado (R^2 = 0.1166, P = 0.5078) or Navasota (R^2 < 0.01, P = 0.9922) rivers (Fig. 4).

Cyclonaias petrina exhibited similar patterns. Resting metabolic rate increased linearly with increasing temperature for *C. petrina* from the Colorado (RMR = 0.0004*temp – 0.0038; R^2 = 0.9757, P = 0.0002) and Guadalupe (RMR = 0.0005*temp – 0.0070) rivers. The regulation index did not show a significant linear relationship with temperature for *C. petrina* from the Colorado (R^2 = 0.4592, P = 0.2088) or Guadalupe (R^2 = 0.4574, P = 0.2100) rivers. DO_{crit} did not show a significant linear relationship with temperature for *C. petrina* from the Colorado (R^2 = 0.6336, P = 0.1072) or Guadalupe (R^2 = 0.5517, P = 0.1504) rivers (Fig. 5).

There was no significant difference in mean RI (calculated across all temperatures) among species and locations (ANOVA, P = 0.079). There were significant differences in DO_{crit} among species and locations (ANOVA, P = 0.025) with *C. houstonensis* from the Navasota River exhibiting a significantly lower DO_{crit} than *C. houstonensis* from the Colorado River (Tukey's, P = 0.026). DO_{crit} of *C. petrina* did not differ between locations or from *C.*

houstonensis collected from either location (Tukey's, $P > 0.05$) (Fig. 6).

The proportion of animals exhibiting at least one episode of valve closure, as evidenced by a sudden drop of RMR to 0, increased at high temperatures. *C. petrina* tended to show higher proportions of valve closure than did *C. houstonensis* (Fig. 7).

2.1.C1a Conclusions:

Results suggest that the main impact of increasing temperatures to a maximum of 36ºC is to increase metabolic demand for basic maintenance. Thus, mussels of both species require more food, and are likely to become more susceptible to food limitation, at warm temperatures. *C. houstonensis* from the Colorado River is likely the most sensitive to food limitation as its RMR increased at a faster rate with increasing temperature than did *C. houstonensis* from the Navasota River or *C. petrina* from either location. For example, we used temperature data from the San Saba gage in the Colorado River in 2009 as an example of a "warm" (maximum temeratures ≥ 36ºC) temperature regime. The relationships between respiration rate and temperature for each mussel population was used to determine resting metabolic rate for each temperature measurement and the result converted to metabolic energy requirement (Joules/gWW/hr; Gnaiger 1983). Results show that under this temperature regime, maximum energy requirements of *C. houstonensis* from the Colorado River increased by 2-3x between March and July and were approximately twice as high as *C. houstonensis* from the Navasota River, or *C. petrina* from either site (Fig. 8). This result emphasizes the importance of understanding mussel food resource availability, particularly during the warm summer months, as well as differences in energetic requirements among species and subpopulations.

Valve closure results further support the potential for food limitation at high temperatures. Previous studies have shown bivalves exhibit valve closure in response to stressful temperatures (e.g. Anestis et al. 2007). In our study, all species/location combinations showed a trend of increasing episodes of valve closure as temperatures increased, with 40-87% of all mussels exhibiting at least one episode of closure when temperatures reached 36ºC. Because increased frequency of valve closure would reduce feeding and aerobic respiration activities while demand for energy is increasing, mussels would become increasingly susceptible to growth limitation as temperatures approach and exceed 36ºC. However, mussels appeared to exhibit tradeoffs to potentially offset this effect. *C. houstonensis* (Colorado River) exhibited the greatest increase in energy demand as temperatures increased, but kept valves open until temperatures reached 36ºC. *C. petrina* exhibited a greater frequency of closed valves than *C. houstonensis* as temperatures approached 36ºC, but exhibited a lower energy demand. Studies examining the effects of intermittent valve closure on mussel energy budgets at high temperatures would help determine which species is more strongly affected by food limitation at high temperatures.

Surprisingly, there was little evidence that increasing temperatures up to 36ºC increased sensitivity to hypoxia for any species/location tested. Although some weak trends in RI and DO_{crit} with increasing temperature were apparent, none were significant. The ability of mussels to obtain oxygen from the water column (RI) remained fairly constant as temperatures increased, with a switch from aerobic to anaerobic respiration (DO_{crit}) only becoming apparent when DO levels fell below ~2.0 mgO_2/L. Short term tolerance of low DO, even at high temperatures, is further supported by the lack of mortality when mussels remained in respirometry chambers at 36ºC at DO concentrations < 1 mgO_2/L for several hours prior to termination of trials.

Task 2.1.C1b. Thermal and hypoxia tolerance of adult *L. bracteata*: Effects on metabolic patterns and brood retention.

Forty nine adult *L. bracteata* were collected from the dewatered Llano Park Lake shoreline on November 1, 2017 and shipped to Auburn University following previously described methodology. Upon arrival mussels were placed in upwellers containing hard AFW at 18ºC and fed Reed Mariculture Shellfish Diet as described previously. After several days of acclimation, mussels were examined for gender (shell morhpology) and gravidity (swollen gills), revealing 25 males, 14 gravid females, and 10 non-gravid females. Because the presence of embryos was likely to affect metabolic patterns, and based on previous research (Gascho Landis et al. 2012) it was likely that females would expel broods as temperatures increased, we could not simply repeat the full suite of metabolic experiments described previously (2.1.C1a) for *C. houstonensis* and *C. petrina*. Objectives were modified accordingly.

2.1.C1b Objectives:

Objectives of this task were to

1) Determine the relationship between brood expulsion and temperature for gravid *L. bracteata*.
2) Compare metabolic patterns between males, gravid females, and non-gravid females at 28ºC.
3) Determine relationship between temperature and metabolic patterns for male *L. bracteata*.

2.1.C1b. Methods:

After acclimating to laboratory conditions for ≥2 weeks at 18ºC, temperature for 8 males, 7 gravid females, and 5 non-gravid females was reduced to 17ºC. Temperature for an additional 8 males, 7 females, and 5 gravid females was increased by 1ºC/day until temperatures reached 28ºC. Temperature for the remaining 9 males was increased by 1ºC/day until reaching 36ºC. Mussels were subsequently held at each experimental temperature (17, 28, 36ºC) for ≥2 weeks, after which metabolic patterns were measured for each individual following the previously described respirometry protocols (see 2.1.C1a Methods). After respirometry experiments had been conducted, temperatures for gravid females were again raised by 1ºC/day to 36ºC, at which time surviving females were sacrificed and gills removed in order to count # glochidia remaining in gills.

During temperature adjustment and acclimation phases, all gravid females were held in individual cups with screened sides to allow water to flow through while preventing released glochidia from leaving cups. Every 2 days, water from each cup was poured through a 105 μm sieve to retain glochidia. Glochidia were then preserved in 75% ethanol and subsequently enumerated under a compound microscope using cross-polarized lighting. Total brood size of each gravid female was calculated by summing the number of glochidia collected on each sampling date plus the number of glochidia remaining in gills when the mussel died prior to reaching 36ºC, or when it was sacrificed after reaching 36ºC. Proportion of brood released was subsequently calculated for each sampling day by dividing the cumulative number of glochidia released prior to that day by the total brood size calculated for that individual.

2.1.C1b. Results:

Respiration:

Resting metabolic rate (RMR) of male *L. bracteata* was significantly higher at 28 and 36 than 17ºC, but there was no significant difference in RMR between 28 and 36ºC (ANOVA: $F_{2,16} = 17.161$, $p<0.001$; Tukey's p<0.001, p=0.719 respectively). There was no significant difference in either RI (ANOVA: $F_{2,16} = 0.288$, $p=0.753$) or DO_{crit} (ANOVA: $F_{2,14} = 0.239$, $p=0.791$) among temperatures (Fig. 9).

At 28ºC, there was no significant difference in the ability to regulate oxygen consumption among males, non-gravid females, and gravid females (ANOVA: $F_{2,17} = 0.5$, $p = 0.615$). Similarly there was no significant difference in the DO_{crit} (ANOVA: $F_{2,17} = 1.12$, $p = 0.352$) (Fig. 10).

Resting metabolic rate (RMR) data were not normally distributed (K-S: $D = 0.09$, $P < 0.01$). Results of ANCOVA on rank-transformed data revealed a significant effect of gender/gravid status on RMR (ANCOVA: $F_{3, 3799} = 330.16$, $P < 0.0001$). As a covariate, DO showed a significant effect on RMR (ANCOVA: $F_{1, 3799} = 5079.25$, $P < 0.0001$).

Results indicated a significant interaction effect between DO and gender/gravid status (ANCOVA: $F_{2, 3799} = 10.04$, $P < 0.0001$). The homogeneity-of-slopes asumption was violated, which means regression lines for these groups had unequal slopes. The Johnson-Neyman (J-N) technique was used to determine differences among slopes within the range of DO values. At all DO values (0.5 to 7.3 ppm), RMR of males was higher than that of gravid and nongravid females. The J-N technique revealed no significant difference in RMR between gravid and nongravid females when DO values were 2.1 ppm (T-test: $t_{3799} = 2.27$, $P = 0.0602$) or lower. At DO values of 2.2 ppm (T-test: $t_{3799} = 2.43$, $P = 0.0406$) or higher –up to 7.3 ppm (T-test: $t_{3799} = 4.15$, $P = 0.0001$) - RMR of gravid females was significantly higher than that of non-gravid females (Fig. 11).

Brood expulsion: Total brood size of *L. bracteata* scored as "gravid" ranged from 825 to 105,568 glochidia/female. There was no significant difference in total brood size between females in the 17ºC (Mean = 54,509, SD = 3,2081) and warming (Mean = 47,520, SD = 34,087) treatments; t(11)=0.381, $p = 0.355$. During the 50 day trial, there was zero mortality in the cool (17ºC) treatment, whereas five of seven mussels in the warming treatment died before reaching 36ºC. Each mussel that died still retained >50% of its total brood size upon death. There was no significant relationship between total brood size and day of death (Fig. 12a; linear regression, p = 0.4533), nor was there a significant relationship between proportion brood released and day of death (Fig. 12b; linear regression, p = 0.2829). On average, the proportion of brood released by surviving mussels through time was higher in the warming mussel treatment than in the cool mussel treatment (Fig. 13).

2.1.C1b. Conclusions

Similar to the *Cyclonaias* species and subpopulations tested, there was little evidence that sensitivity of *L. bracteata* to hypoxia increased with warming temperatures. RI did not decline, nor did DOcrit increase as temperatures rose from 17 to 36ºC. However, energetic demands, as represented by RMR, showed a faster increase with temperature than even *C. houstonensis* from the Colorado River. This suggests that *L. bracteata* are more sensitive to food limitation at high temperatures than even the most sensitive *Cyclonaias* species/population. Interestingly, RMR of *L. bracteata* did not increase further as temperatures rose from 28 to 36ºC. This leveling off of RMR with increasing temperature was not observed for any of the previously tested *Cyclonaias* species * location combinations. In fishes and some invertebrates, attainment a maximum metabolic rate, followed by metabolic depression as temperatures rise, is considered an indicator

of thermal stress (Brown 1989, Walsh et al. 1997, Anestis et al. 2007). Our results suggest temperatures between 28 and 36ºC begin to cause respiratory stress in *L. bracteata* and this species is more sensitive to thermal stress than *C. houstonensis* or *C. petrina*.

Tankersley and Dimock (1993) found that gravid *Pyganodon cataracta* had reduced respiration rates relative to males, and interpreted this as an indication of stress and declining physiological condition. In our study, gravid females at 28ºC had a lower respiration rate than males at DO concentrations ranging from 0.5 to 7.3 mgO_2/L. This reduction in respiration rate is presumably due to impairment of the ability of brooding females to obtain oxygen from surrounding waters and suggests that brooding *L. bracteata* may be more sensitive to thermal stress than males.

Previous studies have shown that *Ligumia subrostrata* release broods in response to rising temperatures (Gascho Landis et al. 2012). We expected *L. bracteata* to exhibit brood expulsion as temperature rose to 28ºC and mussels showed signs of respiratory stress as well as increased mortality. Females exposed to warming temperatures did release more glochidia than females held at a constant, cool temperature (17ºC). However, the proportion of glochidia released never exceeded 50% even when stress was high enough to result in mussel mortality, nor did mussels release >50% of their brood when temperatures were further elevated to 36ºC. These results show that mussel species have different strategies regarding brood expulsion in response to severe thermal stress. Warming temperatures are less likely to cause complete brood expulsion in *L. bracteata* stress than some other species such as *L. subrostrata*. However, partial brood expulsion in response to rising temperatures is a risk for *L. bracteata*.

Task 2.1.C2. Thermal tolerance of adult mussels: Effects on respiratory enzymes.

2.1.C2. Objectives:

The electron transport system (ETS) assay measures the activity of enzymatic complexes I and III of the respiratory chain within the mitochondria. It provides excess substrate (NADH and NADPH) for the enzyme complexes to act upon and utilizes INT dye as the electron acceptor. Originally developed by Packard (1971) it has since been used as a proxy for in-situ respiration rates of marine and freshwater organisms (Owens and King 1975, Madon et al. 1998, Elderkin et al. 1998). It yields an estimate of the potential oxygen consumption rate of an organism if all enzymes function maximally by quantifying ETS activity in the presence of excess substrates (Fanslow et al. 2001). Recently, Simcic et al. (2014) showed that the relationship between ETS enzyme activity and temperature can be used to estimate optimal thermal temperatures for organisms at the cellular level. They also showed that ETS activity shows a high degree of correlation with scope for growth at the organismal level, with optimal temperatures for organism growth being a few degrees cooler than optimal temperature for ETS enzymes. We used the ETS assay to determine optimal enzymatic temperatures for acclimated and non-acclimated mussels and to compare intra and interspecific variation in optimal temperatures among species and locations.

2.1.C2. Methods:

We used two different approaches to examine the relationships between ETS activity and temperature. In the first approach, mussels were acclimated for >1 week to each of nine experimental temperatures (see *Acclimated Approach* below). ETS activity at each temperature was measured as the mean of four acclimated mussels, and tissue sampling was non-lethal. This

approach yielded a single, composite, thermal performance curve for a given species and was limited to a non-lethal temperature range because it requires acclimation of mussels to each temperature for > 1 week with minimal mortality. It also required a large number of mussels (e.g. ≥ 4 mussels/temperature x 9 temperatures = ≥ 36 mussels).

In the second approach (non-acclimated), mussels were acclimated to only a single temperature (21ºC), and tissue sampling was lethal. However, this approach required fewer mussels because the enzymes extracted from a single mussel were tested across all temperatures, yielding a separate thermal performance curve for each individual mussel. The temperature range tested could include and exceed the lethal range for mussels because only the extracted enzymes, not the mussels themselves, are exposed to each temperature. Methods for the two approaches are described in detail below.

Acclimated Mussels

Within 24 hours of respirometry measurements (see 2.1.C1), we randomly selected four mussels from each of the original six temperature treatments, gently pried their shells open, and collected two, ~10 mg tissue plugs from the foot of each mussel using a nasal biopsy tool (Karl Storz nasal biopsy tool #453733) (Fritts et al. 2015). Tissue plugs were placed in cryovials and immediately frozen at -80ºC. An additional two mussels were randomly selected from each temperature, placed in a temperature-controlled upweller, and assigned to a new temperature of 20, 25, or 30ºC. Temperatures were raised or lowered at a rate of 1ºC/day until the target temperature was reached. Mussels were then acclimated for >1 week at the new target temperature and tissue plugs collected and stored in the same manner as described previously. Thus, we collected tissue plugs from four mussels/species acclimated for >1 week to each of 9

temperatures (15, 17, 20, 23, 25, 28, 30, 32, 36ºC). After tissue collection, all mussels were cooled back down to 18ºC at a rate of 1ºC/day and transferred back to the original upwellers to allow them to recover.

ETS activity of acclimated mussels was measured using standard methodologies adapted from Packard (1971) and Simcic et al. (2014). Frozen tissue plugs collected from a single mussel were weighed and placed in a 5 mL vial (note: vial could actually hold up to 7 mL) (self-standing sample tube, 5 mL, Globe Scientific via VWR, number 89497-730) filled to the 4 mL mark with 1.0 mm diameter glass beads (Biospec Products, Cat. No. 11079110) and containing 4 mL of homogenization buffer (0.1 M sodium phosphate buffer pH=8.4; 75 uM $MgSO_4$; 0.15% (w/v) polyvinyl pyrrolidone; 0.2% (v/v) Triton-X-100). Tissue was then homogenized with a BeadBeater (MiniBeadBeater-24; BioSpec Products, Inc., Bartlesville, OK) for 1 min and chilled for 1-2 min in a freezer. The beadbeating/chilling cycle was repeated for 3-4 cycles until tissue was thoroughly homogenized. The vial was then centrifuged for 4 min, at 10,000 rpm, at 0ºC in a refrigerated centrifuge (Allegra X-30R, Beckman Coulter, Brea, CA). Homogenate generated from a given mussel was placed in a flask, diluted to 2.5 mg tissue/mL using reagent grade DI water (Ricca, cat# 9150-1), mixed with a stir bar, distributed amongst ~ 2 mL vials (Eppendorf$^{(R)}$ Safe-Lock microcentrifuge tubes (MCT), polypropylene) and frozen at -80ºC. Homogenate was stored for ≤ 6 weeks prior to measurement of ETS activity.

To measure ETS activity, two, replicate, 0.5 mL subsamples of thawed homogenate were each incubated in 1.5 mL substrate solution (0.1M sodium phosphate buffer pH = 8.4; 1.7mM NADH; 0.25 mM NADPH; 0.2% (v/v) Triton-X-100) with 0.5 mL INT solution (2.5mM 2-(p-iodophenyl)-3-(p-nitrophenyl)-5-phenyl tetrazolium chloride) for 30 minutes, in the dark, at the temperature to which the mussel had been acclimated. The reaction was then stopped by adding

0.5 mL of stopping solution (Formalin: H_3PO_4 = 1:1). A blank for the replicate samples was made by combining 1.5 mL substrate solution with 0.5 mL INT solution, and incubated and stopped along with the samples. Following addition of stopping solution, 0.5 mL of the corresponding homogenate was added to the blank. Absorbance (490 nm) of the replicate samples was measured with a spectrophotometer (Genesys 10S UV-VIS, ThermoScientific, Waltham, MA) and corrected for absorbance of the blank. ETS activity was calculated according to the following formula (Kenner and Ahmed, 1975):

$$\text{ETS activity } (\mu l\ O_2\ g^{-1}\ WW\ h^{-1}) = (ABS^{490nm} * V_h * V_r * 60)/(V_a * S * t * 1.42)$$

where ABS^{490nm} is the absorption of the sample corrected for blank; V_h is the volume of the homogenate (4 mL) prior to removal of subsamples; V_r is the volume of the reaction mixture (homogenate subsample + substrate solution + INT solution + stopping solution = 3mL); V_a is the volume of the homogenate subsample (0.5 mL); S is the mass of the tissue sample (g); t is the incubation time (min); 60 is a correction factor to convert the rate to hours, and 1.42 is the factor for conversion to volume O_2.

The mean ETS activity was then calculated for each acclimation temperature (~4 mussels per temperature), graphed against temperature, and fitted with a four-parameter Gaussian curve (SigmaPlot 13.0; Systat Software, Inc., San Jose, CA). Optimal temperature was defined as the temperature which exhibited the highest ETS activity. Optimal temperature range was defined as the temperature range within which ETS activity was within 10% of the maximum value.

Non-acclimated mussels

Following respiration measurements (see 2.1.C1), two mussels were randomly selected from each of six experimental temperatures, placed in temperature controlled upwellers, and brought to 21ºC at a rate of 1ºC / day. All mussels were held at 21ºC for at least 1 week. Following the > 1 week holding period, each mussel was sacrificed by severing the adductor mussels with a scalpel and opening the shell. Approximately 100 mg of foot tissue was immediately collected from each mussel using the nasal biopsy tool, and frozen at -80ºC. Tissue from each mussel was subsequently removed from the freezer and homogenized using the previously described beadbeater technique. Homogenate generated from a given mussel was combined in a flask, diluted to 2.5 mg tissue/mL using reagent grade DI water (Ricca, cat# 9150-1), mixed with a stir bar, distributed amongst ~ 1.8 mL vials and refrozen at -80ºC. ETS activity was subsequently measured following the same methodology as described above.

For each mussel, two replicate enzyme samples were incubated for 30 minutes at each temperature of interest, yielding a complete thermal performance curve (ETS activity vs temperature) for each individual. Initially, incubation temperatures were 12, 15, 17, 20, 23, 25, 28, 30, 32, and 36°C. Optimal temperatures for each individual was calculated using a four parameter Gaussian regression. Because optimal temperature data was not normally distributed, we used a Kruskal-Wallis ANOVA on rank-transformed data to test for significant differences among species/location combinations (SigmaPlot 13.0, Systat Software, Inc., San Jose, CA, USA). Pairwise comparisons were conducted using Dunn's Method (SigmaPlot 13.0).

While analyzing samples for optimal temperature, we conducted some exploratory runs at temperatures >36ºC and found ETS activity did not decline symmetrically with increasing temperatures as would be described by a Gaussian curve. We hypothesized that the post-peak

decline pattern might yield additional information regarding thermal stress. We therefore added temperatures of 39, 42, 45, 48, 51, 54, and 57ºC to the non-acclimated assay for remaining species and populations. We also added a cooler temperature (9ºC). We then used a 5-segment piecewise regression (SigmaPlot 13.0) to characterize the relationship between ETS activity and temperature during the decline following peak activity.

2.1.C2. Results

Acclimated Mussels

Optimal temperatures for ETS enzyme activity were higher for *C. petrina* from the Colorado (35.3ºC) and Guadalupe (34.6ºC) rivers than for *C. houstonensis* from the Colorado (31.6ºC) and Navasota (27.6ºC) rivers. Optimal range estimates predicted mussels would begin to experience enzymatic thermal stress at some point >36ºC for Colorado and Guadalupe River *C. petrina*, >35.8ºC for Colorado River *C. houstonensis*, and > 30.6ºC for Navasota River *C. houstonensis* (Fig. 14).

Because the acclimated approach generates only a single, composite, thermal performance curve for each species/location, we were not able to test for significant differences in optimal temperature between species or locations, nor were we able to assess variability in optimal temperature among individuals within the same species/location group. To address these issues, we analyzed thermal performance curves for individual mussels using the non-acclimated approach.

Non-acclimated Mussels

ETS activity was strongly correlated with temperature for individual, non-acclimated mussels, with four parameter Gaussian regressions typically yielding an $R^2 > 0.90$ (see Fig. 15 for example; full set of graphs for other species/location combinations available upon request). Summary graphs (Fig. 16) show variation in curve height and optimal temperature (temperature at which curve peaks) within and among each species/location combination. Intraspecific variation in optimal temperature was highest for *C. petrina* from the Colorado River and lowest for *L. bracteata* (Llano Lake) and *C. houstonensis* (Navasota River) (Fig. 17).

There were significant differences in mean optimal temperature among the nine species x location combinations of rare and common species tested (Kruskal-Wallis ANOVA: H=56.422, d.f.= 8, $P < 0.001$). Optimal temperature for *C. houstonensis* (Colorado River) and *C. petrina* (Colorado River), were significantly higher than *L. teres* (Colorado River) and *L. bracteata* (Llano Lake) (Dunn's Method, $P < 0.05$). Optimal temperature of *C. houstonensis* (Navasota River) was significantly higher than *L. teres* Colorado River) (Dunn's Method, $P = 0.018$) and marginally higher than *L. bracteata* (Llano Lake) (Dunn's Method, $P = 0.057$). Optimal temperatures of *F. mitchelli* (Guadalupe River), *C. petrina* (Guadalupe River), *A. plicata* (Colorado River) and *L. bracteata* (Llano River) were intermediate (Figure 18).

There was no evidence of intraspecific differences in thermal optima between subpopulations of three candidate species. *C. houstonensis* (Colorado River) did not significantly differ from *C. houstonensis* (Navasota River) (Dunn's Method, $P = 0.7$). *C. petrina* (Colorado River) did not significantly differ from *C. petrina* (Guadalupe River) (Dunn's Method, $P = 1.0$). L. bracteata (Llano River) did not significantly differ from L. bracteata (Llano Lake) (Dunn's Method, $P = 0.791$) (Figure 18).

There was no evidence that two common species tested had a higher thermal optima than the four candidate species. *Amblema plicata* (Colorado River) had an intermediate optimal temperature, and *Lampsilis teres* (Colorado River) had a low optimal temperature relative to the four candidate species (Figure 18).

We measured activity of ETS enzymes from non-acclimated adult mussels at temperatures expected to exceed 24-hr lethal temperature (LT_{50}) thresholds for five species (Fig. 19). As temperatures increased above the thermal optimum, ETS activity did not decline in a linear fashion. Rather, each species exhibited a "shoulder" pattern where enzyme activity initially declined, then leveled off, then declined again. In a previous study, Marshall et al. (2011) showed that a bimodal pattern of snail respiration with increasing temperature was correlated with the onset of heat shock protein production and 24-hr LT_{50} thresholds. Because ETS activity represents the maximum potential respiration rate of an organism (Fanslow 2001), it is likely that similar endpoints are correlated with ETS activity patterns. We hypothesize that the point at which the decline in ETS activity begins to level off represents the activation of heat shock proteins – signaling the onset of major thermal stress and the transition from sublethal to lethal thermal stress. Preliminary comparison of independent LT_{05} (temperature at which 5% of animals die) data from the lab of Dr. Charles Randklev (Texas A&M University) is providing support for this hypothesis. We plan to continue this line of inquiry with Dr. Randklev in 2018. The hypothesized breakpoint between sublethal and lethal effects was 38.9ºC for *C. petrina* (Guadalupe River), 37.1ºC for *C. houstonensis* (Navasota River), 36.0ºC for *A. plicata* (Colorado River), 32.7ºC for L. bracteata (Llano Lake), 32.6ºC for *F. mitchelli* (Guadalupe River) collected in November, 31.0ºC for *F. mitchelli* collected from the same site in August, and 29.4ºC for *L. teres* (Colorado River) (Fig. 19). Season of collection did not appear to have a large impact on

these estimates. *F. mitchelli* collected in summer (August) and fall (November) differed by only 1.6ºC in terms of estimated breakpoint between sublethal and lethal effects.

2.1.C2. Conclusions:

There were significant differences in optimal enzymatic temperatures among specific species x location combinations. However there was no evidence for differences in optimal temperatures between subpopulations within the same species. Optimal temperatures for common species were intermediate to low compared to the rare, candidate species. There was some evidence that optimal temperatures were linked to taxonomic status as *Cyclonais spp*. generally exhibited higher thermal optima than *Lampsilis spp*.

Mussels acclimated to warm temperatures generally exhibited higher optimal temperatures than non-acclimated mussels (Table 4). However, optimal temperatures of non-acclimated mussels still fell within the optimal range of acclimated mussels – usually near the lower end of the range (Fig. 20, Table 4). The primary effect of acclimation appeared to be an increase in the upper portion of the optimal range rather than shifting the entire range. This suggests that in natural populations, a given mussel species will enter its optimal thermal range at approximately the same temperature threshold regardless of previous thermal history. However, mussels subjected to rapid, flashy increases in temperature will leave their thermal optima and start to experience thermal stress at lower temperatures than mussels subjected to gradual, stable increases in temperature. Intraspecific variation in non-acclimated optimal temperature (Fig. 17) was highest for *C. petrina* from the Colorado River, suggesting they may have a greater capacity to adapt to future fluctuations in temperature than species such as *L. bracteata* (Llano River/Lake) and *C. houstonensis* (Navasota River), which exhibited relatively low variation in

optimal temperatures. A summary of the estimated optimal and stressful temperatures for ETS enzymes of acclimated and non-acclimated mussels can be found in Table 4.

While the ETS assay estimates optimal temperatures at the enzymatic level, corresponding estimates of optimal temperature measured at the more complex organismal level (e.g. optimal scope for growth) may be cooler by 2-3^{o} C (Simcic et al. 2014). Therefore, temperature ranges that are optimal or stressful to the organism as a whole are likely to be a few degrees lower than temperatures optimal or stressful to the organism's ETS enzymes. One way to explain this is using the concept of Aerobic Scope - the difference between an organisms resting metabolism (energy required to meet basic metabolic needs) and its metabolic potential (maximum metabolic rate). The greater the aerobic scope, the more energy can be used for growth and reproduction (e.g Clark et al. 2011, Simcic et al. 2017). In the context of this project, ETS activity is an estimate of metabolic potential whereas respiration rates of mussels starved for 24 hrs provide an estimate of resting metabolic rate. As temperatures increased, metabolic potential increased, leveled off, and then declined whereas resting metabolic rate continued to increase (Fig 21A). For *C. houstonensis* (Colorado River), aerobic scope was greatest at ~28^{o}C (Fig. 21 A,B) which suggests that the optimal temperature at the organismal level was ~ 3.6^{o}C lower than the enzymatic optimal temperature of 31.6^{o}C (Table 4, acclimated).

Task 2.1.D. Effect of temperature on respiration of glochidia and juveniles.

2.1.D. Objectives: The objectives of this task were to:

1) Refine methodology for conducting microrespirometry on early stage juveniles.

2) Determine the differences in metabolic rate, regulation index, and DO_{crit} between juvenile and adult mussels at one or more temperatures.

3) Determine the relationship between metabolic rate, regulation index, DO_{crit} and temperature for juveniles of one or more candidate mussel species.

2.1.D. Methods:

Approximately 150 *C. petrina* early juveniles (< 1mm length) were shipped to Auburn University from the Inks Dam hatchery. Shipping temperature upon arrival was 20.4ºC. Mussels were placed in AFW, gradually brought up to 25ºC and held overnight in a beaker without food. The following day they were distributed among the microrespirometry wells at 50, 20, and 10 individuals per well, with temperature remaining at 25ºC. Methodology followed that previously described for glochidia (2.1.A).

After determining that ≥ 50 individuals/well were required to conduct respirometry on early (<1mm length) juveniles (see results), we obtained older, juvenile *L. cardium* from the Center for Mollusk Conservation in Frankfort, Kentucky as part of an ongoing collaborative project with W.R. Haag (USDA Forest Service). Juveniles ranged from ~6 – 12 mm in length and were shipped and acclimated in the same manner as the *C. petrina*. However, in contrast to the smaller *C. petrina* juveniles, only a single *L. cardium* individual was placed in each respirometry well. Respirometry was conducted following the same procedures as described previously.

2.1.A. Results

C. petrina early juveniles

Wells with 10-20 early juveniles were deemed insufficient to obtain reliable respiration curves due to 1) background oxygen demand comprising a large proportion of the overall respiration rates, and 2) >24 hrs required to bring oxygen down to < 0.5 mg O_2/L. However, the

well containing 50 individuals yielded usable results, showing that, on average, early juveniles were good at regulating oxygen consumption (respiration rates remained stable as dissolved oxygen declined to low levels) and DO_{crit} did not occur until oxygen had declined below 1 mg/L (Figure 22).

L. cardium juveniles

Wells containing single *L. cardium* juveniles, ranging from 6 to 12 mm in length, yielded usable respiration curves allowing us to calculate respiration rates, regulation indices, and DO_{crit} for individual mussels. There was no significant linear relationship between RMR ($p = 0.550$) or RI ($p = 0.263$) and juvenile length. However, there was a significant linear increase in DO_{crit} with increasing juvenile length ($R^2 = 0.65$, $p = 0.029$) (Fig. 23). On average, respiration rates of this size range were approximately 10x those observed for adult mussels of other species in this study (e.g. see Figures 4, 5) and in previous studies (Chen et al. 2001).

2.1.A. Conclusions

After discussion with personnel heading the propagation portion of the overall mussel project, it was decided that the demand for large numbers of early juvenile mussels (≥ 50 individuals per well) was too high to allow for thermal tolerance experiments with the focal species juveniles. Based on the *L. cardium* microrespirometry runs, we are recommending that we resume thermal tolerance experiments when focal species juveniles in the 6-12mm size range are available from the production facilities as this will greatly reduce the numbers of animals needed and also yield mass specific respiration rates (mg O2/gWW/hr) of individuals – which are more useful than combined (mg O_2 / x individuals/hr).

Preliminary data suggests that energy demands of juvenile mussels are much higher than adults – this is supported by anecdotal evidence from hatchery managers that juveniles have much greater food requirements for good survivorship and growth than do adult mussels. Estimates of resting metabolic rates will be of great use in developing energy budgets and determining optimal temperatures for growth for early juveniles. The ability to strongly regulate oxygen consumption, and the low DO_{crit} exhibited by the early juvenile *C. petrina* suggests that they are not more sensitive to hypoxia than adults. This makes sense in that juvenile mussels typically burrow into the sediments where dissolved oxygen is lower than overlying waters. However, these are preliminary results based on a single well containing 50 individuals. Additional runs will be required to confirm these patterns. Results from the larger juvenile *L. cardium* suggest that DO*crit* may increase as juveniles grow, making them more susceptible to low DO conditions over time. However, similar to *C. petrina*, these results are based on a small sample size and additional runs will be required to confirm patterns.

Task 2.3 Effect of turbidity/suspended solids on valve closure of adult mussels

2.3 Objectives:

Mussels must keep their shells open to obtain food and oxygen from the surrounding waters. However, they often respond to stressors by closing their shells. Electromagnetic sensors attached to each valve can be used to monitor gaping and closing behavior and set off alarms when behavior indicates the presence of stressful toxicants in the water (Manley and Davenport 1979, Kramer et al. 1989, Gnyubkin 2009). Systems such as the MosselMonitor (www.mosselmonitor.nl; Kramer et al. 1989) and the Dreissena Monitor (Envicontrol Köln Germany; Borcherding, 1994) have been used to monitor stressors in fresh and saltwater

environments in Europe. In this study, we used a MosselMonitor to determine whether mussels fully or partially close their valves in response to high turbidity/suspended solids – indicating negative impacts on feeding and respiration.

2.3. Methods:

Sediments

Sediments were obtained from a drained, 0.1 ha, earthen pond at the South Auburn Fisheries Research Station of Auburn University, Alabama. The top two inches of sediment were collected, mixed in a 5 gallon bucket, distributed into baking pans, and dried for 24 hrs at 105^{o}C. Dried sediment was passed through a #60 (250 μm) Fisher Scientific Company sieve and stored in an air tight 5-gallon bucket. This process was repeated until we had obtained enough sieved sediments to complete all trials. Stored sediment was mixed thoroughly via rolling and shaking in a closed container to ensure even distribution of particles immediately prior to each use. Soil analysis (T. Knappenberger, Auburn University) showed the sediments were composed of 53.5% sand (63 – 2000 μm), 46.6% silt (2.0-63 μm) and 0.0% clay (< 2.0 μm).

Experimental animals

Following respirometry experiments (see previous section), mussels were allowed to recover for > 4 weeks at 18^{o}C. Water temperature was then raised by 1^{o}C/day to the experimental temperature of 28^{o}C. Mussels were acclimated to this temperature for ≥ 1 week prior to initiation of experiments. During this time mussels were fed Shellfish Diet 1800 twice daily (2 mL morning, 1 mL afternoon per ~70 L upweller) and held at a 12h light: 12h dark cycle.

Experimental protocol

To monitor valve movements, mussels were held in individual, mesh bottom, plastic baskets (8 X 5 X 4 cm) screwed to the walls of a MosselMonitor (Flow through version, AquaDect B. V.Brouwershaven, Netherlands). MosselMonitor settings, data downloads, and data display were controlled via PresentIT^{TM} 3.0 software on a connected desktop computer. The MosselMonitor was filled with HAFW and held at 28ºC. One valve of each mussel was glued (Unifast Trad Methylmethacrylate two part Resin GC America Inc. Alsip IL) to the plastic basket wall parallel to the side of the MosselMonitor. This ensured the mussel remained at a fixed distance from an electromagnetic sensor in the MosselMonitor wall. A second sensor was glued directly to the other valve of the mussel. Aquarium pea gravel was then added to the basket until half of the mussel was embedded in the substrate. Throughout the subsequent experiment, mussels were fed Shellfish Diet 1800 at the same rate as during the acclimation period. The Light:Dark cycle was held constant at 12:12.

Mussels were acclimated to the system for three days, during which time the MosselMonitor monitored distance between sensors and assessed the baseline maximum and minimum valve opening exhibited by each mussel. During the subsequent portions of the experiment, distance between valves (sensors) was reported as percent gape, based on the baseline maximum and minimum distances calculated during the acclimation period. Percent gape was calculated and recorded every 10 seconds for the remainder of the experiment. The first 24 hours following acclimation (Day 4) served as a control period, during which time food, but no sediment, was added to the MosselMonitor. The experimental period began on day 5. Sediment was added to a belt feeder located above a cone tank that was connected to the

MosselMonitor. The belt feeder dropped sediment into the cone tank at a constant rate over a period of 10 hours. Sediment was suspended in the cone tank via a submersible Resun King-2 pump (1000 L/hr) and multiple air stones. A second submersible Resun King-2 pump transferred water and suspended sediments to the MosselMonitor at a constant rate of 360 L/hr. Flexible tubing returned water at the same rate to the cone tank via ambient head pressure. A LaMotte 2020we turbidimeter was used to measure turbidity in replicate 10 mL samples collected immediately after mussel attachment (0 h), at the start of the control period (72 h), every hour for the first 12 hours of the experimental period (hrs 96-108), and at the end of the experimental period (hr 120). Supplemental samples were periodically collected to quantify TSS concentrations. A ~250 mL sample was siphoned from the center of the MosselMonitor. The siphon tube was attached to the MusselMonitor prior to the experiment so that subsequent samples could be collected without disturbing mussels. Sample water was filtered through a pre-ashed (1 hr at 550ºC) 1.2 µm Whatman 47 mm glass microfiber filter to collect sediments. Filters were then dried overnight at 105ºC and weighed. Filter weight was subtracted from total weight and then divided by sample volume to calculate TSS in mg dry weight/liter.

This protocol resulted in an initial ~6-hour ramping period (9:00 – 15:00 hrs) on Day 5 during which suspended solid concentration in the MosselMonitor increased with time as the rate at which sediment was added to the system exceeded the rate at which sediment settled within the system. Equilibrium between sediment addition and settlement was reached within 5-6 hrs, after which time total suspended solids (TSS) concentrations remained relatively stable for the remaining four hours (15:00 – 19:00 hrs) of the run (Fig. 24 bottom panels). Mussels were exposed to one of two treatments, with two runs per treatment. Different mussels were used for each run. Within each run, sufficient sediment was added to the belt feeder to allow turbidity to

ramp up to the target level. During our first three runs, we set a high turbidity target of ~25 NTU (~70 mg TSS/L), intending to reduce turbidity in subsequent runs. However, due to the lack of obvious effects on valve closure even under high turbidity conditions (see results), we changed our subsequent runs to target excessive turbidity levels of ~70 NTU (~ 250 mg TSS/L) for the two final runs (Fig. 24).

2.3. Results

Individuals of both species exhibited highly variable relationships between percent gape and turbidity during the ramping periods when turbidity increased from 0 to 25 or 65-75 NTU's over a 6-hr period (Figs. 25-28). During the excessive turbidity ramping period, mean percent gape of all *C. petrina* combined exhibited a negative linear relationship with turbidity (Figure 29 top panel: $R^2 = 0.53$, $P < 0.0001$, mean percent gape = 59.3214 – 0.1478*NTU). Mean percent gape during the high turbidity ramping period showed a similar negative relationship with turbidity, albeit with a steeper slope (Fig 29 top panel: $R^2 = 0.83$, $P < 0.0001$, mean percent gape = 62.7746 – 0.4654*NTU).

During the excessive turbidity ramping period, mean percent gape of all *C. houstonensis* combined exhibited a significant positive linear relationship with turbidity, but turbidity explained very little of the variation in valve gape (Figure 29 bottom panel: $R^2 = 0.064$, $P < 0.0001$, mean percent gape = 45.8459 + 0.0451*NTU). Mean percent gape during the high turbidity ramping period showed a significant, negative linear relationship with turbidity, but, again, turbidity explained very little of the variation in gape (Fig. 29 bottom panel: $R^2 = 0.040$, $P < 0.0001$, mean percent gape = 63.9433 - 0.1675*NTU).

During the constant turbidity period of the high treatment (~25 NTU), there was little to no evidence that turbidity resulted in decreased gape for either species. Exposed *C. petrina* exhibited less frequent gape values exceeding 65% than control mussels but percent gape peaked at 65% in both groups. Gape of exposed *C. houstonensis* peaked at a higher value (75%) than control *C. houstonensis* (55%) (Fig. 30).

During the constant turbidity period of the excessive treatment (60-75 NTU), there was evidence that gape decreased slightly for both species. Gape peaked at 65% in exposed *C. petrina* compared to 75% for control mussels. Gape peaked at 65% in exposed and control *C. houstonensis*, but very few exposed mussels gaped more than 65% compared to control mussels (Fig. 31).

2.3. Conclusions:

Because mussels obtain food and oxygen from surrounding water, there was concern that high concentrations of suspended solids may trigger valve closure by mussels, with subsequent, negative effects on feeding and respiration. However, we found little to no evidence that exposure to suspended solids, even at high (turbidity ~25 NTU; TSS ~70 mg/L) or excessive (turbidity ~75 NTU, TSS ~250 mg/L) concentrations resulted in valve closure. As turbidity increased, *C. petrina* exhibited only a small reduction in mean percent gape. Increasing turbidity explained very little of the variation in percent gape for *C. houstonensis*. Under conditions of excessive turbidity, mussels appeared to close valves slightly, but the peak in percent gape remained high at 65% as compared to a peak of 65-75% during the preceding control period. If high suspended solids have a negative effect on mussel feeding rates or ability to obtain oxygen, the mechanism behind negative effects is not likely to be valve closure.

2.2 Sublethal effects of nitrogenous compounds and salinity on adult mussels

2.2A. Effect of Ammonia on Respiration.

2.2A. Objectives:

In 2013, the U.S.EPA updated its Aquatic Life Ambient Water Quality Criteria for Ammonia – Freshwater in order to take into account data for highly sensitive unionid mussel and non-pulmonate snail species that had not previously been tested (USEPA 2013). Because ammonia toxicity issues are fairly complex, a brief explanation is provided here.

Ammonia in surface waters is typically reported as total ammonia nitrogen (TAN). This refers to the combined concentration of nitrogen (mg/L) occurring in two co-existing forms of ammonia – ionized (NH_4^+) and un-ionized (NH_3). Un-ionized ammonia is the most toxic form. The proportion of un-ionized to unionized (NH_3: NH_4^+) ammonia increases with increasing pH and temperature. Thus ammonia becomes more toxic with increases in temperature and/or pH even if the concentration of ammonia, measured as TAN, remains the same. The U.S.EPA 2013 ammonia benchmark is 17 mg TAN/L for acute (1 hour average) exposure and 1.9 mg TAN/L for chronic (30-d rolling average) exposure. These benchmarks are referred to as "criterion maximum concentrations" (CMC) and represent a concentration that is expected to be lethal to <50% of individuals in sensitive species. They specifically apply to a pH of 7 and a temperature of 20ºC. In many Texas rivers, pH is typically ≥8 and temperatures rise well above 20ºC during the summer months. The toxicity of 17 (acute) and 1.9 (chronic) mg TAN/L benchmark concentrations would therefore increase and may no longer be sufficiently protective of unionid mussels. The USEPA is cognizant of this issue and provides tables to adjust benchmark concentrations for specific temperature and pH values (see tables 5b, 6 in USEPA 2013).

Unionized ammonia can affect organisms such as mussels via multiple mechanisms that include increased ventilation rates (volume of water passing through gills per unit time), gill damage, and a reduction in the ability of blood (hemolymph) to carry oxygen. Thus it is reasonable to expect that metabolic and respiration patterns would be sensitive to ammonia. The objectives of this study were to determine whether ammonia affected metabolic patterns of mussels by 1) reducing their ability to regulate oxygen consumption, 2) increasing their DO_{crit}, and 3) altering their resting metabolic rate. Note that this task was completed last due to the high probability of significant sublethal and lethal effects on experimental mussels when exposed to ammonia.

2.2A. Methods:

Following turbidity assays described in previous sections, *C. petrina* and *C. houstonensis* from the Colorado River were allowed to recover for ≥ 2 weeks at 28ºC prior to initiation of ammonia experiments. During this time, they were fed Shellfish Diet 1800 according to the standard feeding regime (2 mL morning, 1 mL afternoon, per 70 L upweller). Due to a limited number of mussels remaining from the original collections, we were only able to test 5-6 individuals of *C. petrina*, and 6 individuals of *C. houstonensis* per ammonia treatment, prior to preparation of this report. Each mussel was exposed to only a single ammonia treatment. Thus we tested a total of 16 *C. petrina* and 18 *C. houstonensis*.

Resting metabolic rates (RMR) were measured at 28ºC using the same respirometry system described in section B of this chapter. Mussels were starved for 24 hrs prior to experiments to prevent feeding and digesting from affecting metabolism. Following the starvation period, sufficient ammonia from a stock solution (Hach ammonia standard, 1,000 mg

TAN/L) was added to the respirometry trough to bring it to the target concentration of 0.5 or 2.0 mg TAN/L. No ammonia was added to the trough for the control runs. Ammonia concentrations in the respirometry trough were measured using a YSI 9300 Photometer (YSI Inc. 2017) at the beginning and end of each experiment to ensure the target concentration had been reached and remained stable throughout the duration of each trial. The moderate concentration, (0.5 mg TAN/L) was selected to represent the average concentration that we observed in our respirometry chambers following a standard, closed respirometry experiment (section B). The higher concentration represents the 2013 USEPA CCC chronic criteria of 1.9 mg TAN / L at pH 7, 20ºC. Note that in our experiments temperature was 28ºC, and pH was ~8.5. Under these conditions, the recommended acute and chronic benchmarks (CMC; Tables 5b and 6 in USEPA 2013) are adjusted downward to 0.77 (acute) and 0.21 (chronic) mg TAN/L. Thus the highest TAN concentration in our study exceeded both the acute and chronic benchmarks adjusted for pH and temperature.

Mussels were acclimated to respiration chambers for ≥ 5 hrs. During this time both the flush and closed pumps were turned on to ensure oxygenated water containing the appropriate ammonia concentration circulated through chambers and tubing. Following acclimation, flush pumps were turned off, and only the closed pumps remained on - creating a closed system where the volume of water recirculating within each chamber and associated tubing was constant, and no new, oxygenated, water entered the system.

Because mussels excrete ammonia as a waste product, and this ammonia can build up in closed respirometry chambers over time, we periodically flushed chambers during a respirometry run to ensure that ammonia levels remained fairly constant during each trial. The modified respirometry protocol was as follows: After allowing closed respirometry to run for 50 minutes,

nitrogen gas was bubbled into the trough water (external to the submerged respirometry chambers) using DO-SET software (Loligo Inc.), until DO had fallen from 7 to 5 mg O_2/L. Previous closed respirometry trials at 28^{o}C (section 2.1.C1) using the same two mussel species yielded a decrease of approximately 2 mg O_2 per hour within the respiration chambers. At 60 minutes, the flush pumps were turned on and chambers flushed for 5 minutes with ~5 mg O_2/L water from the trough in order to flush out any ammonia excreted by the mussels that would otherwise increase ammonia levels above the targeted trial concentration. Flush pumps were then turned off to once more create a closed system at the target ammonia concentration. After 50 minutes DO in the trough was reduced from 5 to 3 mg O_2/L, and ten minutes later chambers were flushed again for 5 minutes. Flush pumps were then turned off and mussels allowed to draw DO down from 3 to < 0.2 mg O_2/L at which time the trial was terminated. This technique yielded a relationship between resting metabolic rate (RMR) and dissolved oxygen (e.g. Fig. 32) that could be analyzed for regulation index and DO_{crit} using the same methodology as described in task 2.1.C1, while at the same time avoiding problems associated with accumulating ammonia in closed respiration chambers.

2.2A Results:

TAN of the respirometry water matched the nominal treatment TAN concentrations fairly well and remained stable throughout the experiment. Background levels within the control treatment ranged from 0.04 to 0.1 mg TAN / L. Respirometry water pH ranged from 8.4 to 8.6 (Table 5).

The proportion of individuals exhibiting valve closure (cessation of respiration) increased with increasing TAN for both species, and was more frequent in *C. petrina* than *C. houstonensis*

(Fig. 33). Because accurate RMR, RI, and DO_{crit} values could not be calculated for individuals that closed during respirometry, we did not have enough usable respiration curves to test for effects of TAN on these endpoints for *C. petrina*. For *C. houstonensis*, valve closure eliminated only four individuals from the experiment, yielding 4-5 replicate estimates of these endpoints for each TAN treatment. There was no significant effect of TAN on RMR (ANOVA: $F = 2.528$, df = 2, 11; $P = 0.125$), RI (ANOVA: $F = 1.988$; df = 2, 11; $P = 0.183$), or DO_{crit} (ANOVA: $F = 1.178$, df = 2, 11; $P = 0.344$) (Fig. 34).

2.2A Conclusions:

At a pH of 8.5 and temperature of 18 C, the USEPA ammonia benchmarks are revised downward from 17 to 0.77 mg TAN/L for acute (1 hour average) exposure and from 1.9 to 0.21 mg TAN/L for chronic (30 day rolling average) exposure (see Tables 5b and 6 in USEPA 2013). In our study, mussels were exposed to treatment TAN concentrations exceeding both of these benchmarks for ~10 hours. Results suggest that the revised benchmarks are sufficient to protect *C. houstonensis* from short term effects of ammonia on metabolic rate (RMR) and ability to extract oxygen even under low oxygen conditions (RI and DO_{crit}). However it remains to be tested whether chronic (30 day) exposure would affect metabolism. Also, the revised benchmarks may not be sufficient to protect mussels from increased frequency of valve closure (see Fig. 33) which could affect respiration, filtration, and fertilization efficiency during long term exposure. Future studies examining effects of chronic exposure to TAN concentrations matching and exceeding the revised chronic benchmarks on metabolism and valve closure are warranted.

A major challenge of working with rare species is having a sufficient sample size to be able to detect significant differences between treatments. In the case of the ammonia studies, the sample sizes were low, increasing the chances of us not finding an effect of ammonia when one existed. We performed a power analysis (G*Power 3.1.9.2; Faul et al. 2007) to determine 1) the difference between treatments that we had a ≥ 80% chance of detecting with the current sample size, and 2) the minimum number of samples (mussels) required to have a ≥ 80% chance of detecting a specific difference between treatments. Given our sample size of 5 individuals/treatment and the observed variance among individuals, we had a ≥ 80% chance of detecting a change of 0.004 mgO_2/gWW/hr in RMR, a change of 0.15 in RI, and a change of 1.0 mg O_2/L in DO_{crit} among treatments. In future studies, if we want to double the sensitivity of our assays (i.e. reduce the detectable difference by half) and thus have a ≥ 80% chance of detecting a change of 0.002 mgO_2/gWW/hr in RMR, 0.075 in RI, and 0.5 mg O2/L in DO_{crit}, we would need sample sizes of at least 17, 10, and 18 mussels/treatment respectively. We are currently evaluating our remaining mussel stocks and may be able to conduct additional ammonia trials with *C. petrina* and *houstonensis*. If so, data will be included in a future addendum, no later than August 2018.

A legitimate concern regarding closed respirometry techniques, such as those employed in task 2.1.C1 (thermal tolerance), is that a buildup of metabolic wastes might affect respiration rates and patterns measured in the chambers. However, these potential effects are not well understood and have not been previously tested for freshwater mussels. In our closed respirometry experiments, accumulation of metabolic-waste ammonia in closed chambers rarely exceeded 0.5 mg TAN/L and never reached 2mg TAN/L. The lack of a significant effect of 0.5-2 mg TAN/L on respiration rates, RI, or DO_{crit} in of *C. houstonensis* in the current experiment

(Task 2.2A) suggests that accumulation of metabolic wastes did not affect our estimates of these parameters in the thermal tolerance experiments (Task 2.2.C1).

2.2.A2. Effects of TAN on Valve Closure

Additional respirometry trials were conducted to increase the number of replicates in each treatment for *C. houstonensis* and *C. petrina* from the Colorado River. However, >50% of these additional animals closed during control (0 mg/L TAN) respirometry, indicating that they were in poor condition. The additional runs were therefore not integrated into the existing dataset, and results are not changed from the previous report.

Because of the increased incidence of valve closure observed in the original ammonia respirometry trials, we decided to use the MosselMonitor to better quantify these effects. It should be kept in mind that all mussels had been kept in the lab for an extended period by this point and exposed to multiple stressors in previous trials. Results of the MosselMonitor ammonia trials should therefore be interpreted as effects of ammonia on animals that were likely in fair to poor condition.

2.2.A2 Methods:

To monitor valve movements, *C. houstonensis* and *C. petrina* from the Colorado River were placed in the MosselMonitor and sensors attached to their valves following the same methodology as described for the suspended solids experiment (section 2.3). Mussels were acclimated to the system for three days, during which time the MosselMonitor assessed distance between sensors and calculated the baseline maximum and minimum valve opening exhibited by each mussel. During the subsequent portions of the experiment, distance between valves (sensors) was reported as percent gape, based on the baseline maximum and minimum distances

calculated during the acclimation period. Percent gape was then recorded every 10 seconds for the subsequent 48 hrs. This protocol was repeated four times in the following treatment order: Control (0 mg TAN/L), Ammonia (2 mg TAN/L), Control, Ammonia, until all experimental animals had been run. Different individuals were used for each run. Ammonia was added from a stock solution of Nitrogen, Ammonia Standard solution (HACH Company: 1,000 mg/L as NH_3-N) to bring the concentration of water in the MosselMonitor and associated mixing tank to a nominal concentration of 2 mg TAN /L. Actual concentrations of TAN in the MosselMonitor were measured approximately 15 minutes after the ammonia addition using the previously described YSI 9300 Photometer. After 24 hours, TAN was again measured and sufficient stock solution added to the MosselMonitor to bring concentrations back up to 2 mg TAN/L.

2.2.A2 Results:

Mean percent gape was significantly lower in the ammonia treatment (M = 65.1, SD = 16.4) compared to the control (M= 45.1, SD = 8.5) for *C. houstonensis*; t(14) = 3.173, $p = 0.003$). Mean percent gape was also significantly lower in the ammonia treatment (M = 63.1, SD = 14.5) compared to the control (M = 42.5, SD = 8.8) for *C. petrina*; t(7) = 2.652, $p = 0.016$) (Fig. 35).

The percent of time gape exceeded 50% was significantly higher in the control (M = 74.5, SD = 17.2) compared to the ammonia treatment (M = 52.6, SD = 12.3) for *C. houstonensis*; t(14) = 2.976, $p = .005$). Similarly, the duration of time gape exceeded 50% was significantly higher in the control (M = 64.2, SD = 16.9) compared to the ammonia treatment (M = 43.6, SD = 11.8) for *C. houstonensis*; t(7) = 2.161, $p = .034$) (Fig. 36)

The percent of time gape was < 10% did not differ between control (M = 10.0, SD = 6.6) compared to the ammonia treatment (M = 16.1, SD = 17.3) for *C. houstonensis*; t(14) = -0.881, $p = 0.197$). Similarly, the percent of time gape was <10% did not between control (M =

3.2, SD = 5.5) compared to the ammonia treatment (M = 21.5, SD = 24.1) for *C. petrina*; t(7) = -1.472, $p = 0.092$) (Fig. 37). However the variance among individuals was much greater in the ammonia treatment compared to the control for *C. houstonensis* (300.8 vs 44.0) and *C. petrina* (578.7 vs 29.9) (Levene's test for homogeneity of time variance; p = 0.033 and 0.005, respectively)

2.2A2 Conclusions:

For both species, ammonia concentrations of 2.0 mg/L caused a reduction in mean percent gape over a 48 hour period when averaged across all individuals. This was primarily caused by a reduction in the mean percentage of time the mussels remained mostly open (>50% gape) rather than an increase in the percentage of time mussels remained closed (<10% gape). Thus, exposure to 2.0 mg TAN/L ammonia may have reduced feeding and respiratory activity but was not likely to result in a complete cessation of feeding or respiration when averaged across all mussels. However, individual mussels exhibited high variance in their susceptibility to ammonia with some individuals remaining closed for >40% of the experiment duration (i.e. ≥19 hrs) in the TAN treatment whereas this never happened in the control treatment. This is cause for concern in that it suggests exposure to high ammonia concentrations in the natural environment would have a strong, detrimental effect on a sensitive subset of the population even though effects may not be detectable when averaged across the entire population. This is also supported by the observed increased frequency of mussels switching from aerobic to anaerobic respiration (see Fig 33) as TAN rose to 2 mg/L. Although some mussels remained open during the entire respirometry run, an increasing proportion closed their valves and periodically ceased respiring when exposed to high ammonia levels.

2.2B. Effect of salinity on adult mussel valve closure

Mussels must keep their shells open to obtain food and oxygen from the surrounding waters. However, they often respond to stressors by closing their shells. Electromagnetic sensors attached to each valve can be used to monitor gaping and closing behavior, setting off alarms when behavior indicates the presence of stressful toxicants in the water (Manley and Davenport 1979, Kramer et al. 1989, Gnyubkin 2009). Systems such as the MosselMonitor (www.mosselmonitor.nl; Kramer et al. 1989) and the Dreissena Monitor (Envicontrol Köln Germany; Borcherding, 1994) have been used to monitor stressors in fresh and saltwater environments in Europe. Valve movements have been recommended as a sublethal, behavioral endpoint for stressors such as chloride (Hartmann et al. 2016). In this experiment, we use a MosselMonitor to determine whether mussels fully or partially close their valves in response to increasing salinity – indicating negative impacts on feeding and respiration.

Experimental animals

Following respirometry experiments (see section 2.1.C1), *C. petrina* (Colorado and Guadalupe Rivers) and *C. houstonensis* (Colorado and Navasota River) were allowed to recover for > 4 weeks at 18ºC. Water temperature was then raised by 1ºC/day to the experimental temperature of 28ºC. Mussels were acclimated to this temperature for ≥ 1 week prior to

initiation of experiments. During this time mussels were fed Shellfish Diet 1800 twice daily (2 mL morning, 1 mL afternoon per ~70 L upweller) and held at a 12h light: 12h dark cycle.

Experimental protocol

To monitor valve movements, four mussels of each species (eight mussels total) were placed in the MosselMonitor and sensors attached to their valves following the same methodology as described for the suspended solids experiment (section 2.3). Mussels were acclimated to the system for three days, during which time the MosselMonitor assessed distance between sensors and calculated the baseline maximum and minimum valve opening exhibited by each mussel. During the subsequent portions of the experiment, distance between valves (sensors) was reported as percent gape, based on the baseline maximum and minimum distances calculated during the acclimation period. Percent gape was calculated and recorded every 10 seconds for the remainder of the experiment. Valve closure was defined as percent gape ≤ 10%.

The first 24 hours following acclimation (Day 4) served as a control period, during which time food, but no salt, was added to the MosselMonitor. The experimental period began on Day 5. A belt feeder dropped salt (Diamond Crystal pool salt; Cargill Inc., Minneapolis, MN) into the cone tank at a constant rate of 27.3 g/hr over a period of 11 hours. Salt was mixed in the cone tank via a submersible Resun King-2 pump (1000 L/hr) and multiple air stones. A second submersible Resun King-2 pump transferred saltwater to the MosselMonitor at a constant rate of 360 L/hr. Flexible tubing returned water at the same rate to the cone tank via ambient head pressure. A PinPoint Salinity Monitor (American Marine Inc., Ridgefield, CT) was used to measure salinity at the time of attachment, start of the control period, and every hour during the beginning of the experimental period. The salinity meter's probe was held in the cone tank to

make sure the mussels were not disturbed. Previous trials determined that the salinity in the cone tank and the MosselMonitor were equivalent due to constant flow between the two units. This protocol resulted in an 11-hour ramping period (9:00 – 20:00) during which salinity rose linearly with time from a low of <1 ppt to a high of ~4ppt at a rate of ~0.3ppt/h (Fig. 38).

2.2B Results

On average, *C. petrina* from both locations exhibited a steady decline in percent gape as salinity levels increased beyond 2.0 ppt. Both subpopulation exhibited valve closure, with percent gape declining to ≤ 10% at the highest salinities (Figure 39). *C. houstonensis* (Colorado River) showed a slow but steady decline in percent gape as salinity increased above 1.5 ppt whereas *C. houstonensis* (Navasota River) showed an abrupt decline as salinity increased above 2.5 ppt. Neither population exhibited valve closure with percent gape declining to only ~30% at high salinities (Figure 40). *L. bracteata* (Llano Lake) exhibited a rapid decline in percent gape as salinity increased above 3.0 ppt and exhibited valve closure at high salinities (Figure 41).

2.2B Conclusions:

Previous studies have shown that adult mussels (*Elliptio complanata*) exposed to 6 and 4 ppt exhibited 50% mortality by day 3 and 4 respectively, while mussels exposed to 2 ppt exhibited reduced metabolic rates but no mortality after 28 days (Blakeslee et al. 2013). Our results suggest that a reduction in gape and/or complete closure, and resultant reduction and/or cessation of water flowing past the gills is a likely mechanism driving reduced metabolic rates (i.e. respiration) as salinity increases. Valve closure would also be expected to interfere with

feeding and fertilization success. These sublethal impacts of salinity >2 ppt are likely greater for *C. petrina* and *L. bracteata* than *C. houstonensis* as they exhibited steeper declines in gape.

In our study, mussels were exposed to salinities ≥2 ppt for less than 6 hours and exhibited zero mortality during the experiment or within 7 days of being transferred back to freshwater. However, if high salinity conditions were sustained over a long period of time, lethal effects of high salinity might occur more quickly for *C. houstonensis* due to increased exposure. They did not close valves as tightly and appeared to reopen to a greater degree than *C. petrina* and *L. bracteata* as salinity approached LC_{50} (4ppt, 7d) concentrations reported by Blakeslee et al (2013).

References

Anestis, A., A. Lazou, H.O. Portner, and B. Michaelidis. 2007. Behavioral, metabolic, and molecular stress responses of marine bivalve *Mytilus galloprovincialis* during long-term acclimation at increasing ambient temperature. Comparative and Evolutionary Physiology. 293(2):R911-R921.

Blakeslee, C.J., H.S. Galbraith, L.S. Robertson, and B. St. John White. 2013. The effects of salinity exposure on multiple life stages of a common freshwater mussel, *Elliptio complanata*. Environmental Toxicology and Chemistry 32(12):2849-2854.

Brown, L.R. 1989. Temperature preferences and oxygen consumption of three species of sculpin (*Cottus*) from the Pit River drainage, California. Environmental Biology of Fishes. 26:223-236.

Chen, L.Y., A.G. Heath, and R.J. Neves. 2001. Comparison of oxygen consumption in freshwater mussels (Unionidae) from different habitats during declining dissolved oxygen concentration. Hydrobiologia 450:209-214.

Clark T.D., K.M. Jeffries, S.G. Hinch, and A.P. Farrell. 2011. Exceptional aerobic scope and cardiovascular performance of pink salmon (*Oncorhynchus gorbuscha*) may underlie resilience in a warming climate. Experimental Biology 216:2771-2782.

Elderkin, C.L., D.W. Schneider, J.A. Stoeckel, and D.K. Padilla. 1998. A method for measuring in situ oxygen consumption rates of freshwater gastropods. Journal of the North American Benthological Society 17(3):338-347.

Fanslow, D.L., T.F. Nalepa, and T.H. Johengen. 2001. Seasonal changes in the respiratory electron transport system (ETS) and respiration of the zebra mussel, *Dreissena polymorpha* in Saginaw Bay, Lake Huron. Hydrobiologia 448:61-70.

Faul, F., E. Erdfelder, A.G. Lang, and A. Buchner. 2007. G*Power 3: A flexible statistical power analysis program for the social, behavioral, and biomedical sciences. Behavior research methods 39(2):175-191.

Fritts, A.K., M.C. Barnhart, M. Bradley, N. Liu, W.G. Cope, E. Hammer, and R.B. Bringolf. 2014. Assessment of toxicity test endpoints for freshwater mussel larvae (glochidia). Environmental Toxicology and Chemistry. 33(1):199-207).

Fritts, A.K., J.T. Peterson, P.D. Hazelton and R.B. Bringolf. 2015. Evaluation of methods for assessing physiological biomarkers of stress in freshwater mussels. Canadian Journal of Fisheries and Aquatic Sciences 72:1450-1459.

Gascho Landis, A.M., T.L. Mosley, W.R. Haag, and J.A. Stoeckel. 2012. Effects of temperature and photoperiod on lure display and glochidial release in a freshwater mussel. Freshwater Science 31(3):775-786.

Gnyubkin, V. F. 2009. An early warning system for aquatic environment state monitoring based on an analysis of mussel valve movements. Russian Journal of Marine Biology 35: 431436.

Hartmann, J.T., S.B. Beggel, K. Auerswald, and B.C. Stoeckle. 2016. Establishing mussel behavior as a biomarker in ecotoxicology. Aquatic Toxicology. 170:279-288.

Kenner, R.A. and S.I. Ahmed. 1975. Measurements of electron transport activities in marine phytoplankton. Marine Biology 33:119-127.

Kramer, K. J. M., H. A. Jenner, and D. Dezwart. 1989. The Valve Movement Response of Mussels - A Tool In Biological Monitoring. Hydrobiologia 188: 433-443.

Madon S.P., D.W. Schneider, and J.A. Stoeckel. 1998. In situ estimation of zebra mussel metabolic rates using the electron transport system (ETS) assay. Journal of Shellfish Research 17(1):195-203.

Manley, A. R., and J. Davenport. 1979. Behavioral-Responses of Some Marine Bivalves to Heightened Seawater Copper Concentrations. Bull. Environ. Contam. Toxicol. 22: 739744.

Marshall, D.J., Y. Dong, C.D. McQuaid, and G.A. Williams. 2011. Thermal adaptation in the intertidal snail *Echinolittorina malaccana* contradicts current theory by revealing the crucial roles of resting metabolism. Journal of Experimental Biology 3649-3657.

Mueller, C.A. and R.S. Seymour. 2011. The regulation index: A new method for assessing the relationship between oxygen consumption and environmental oxygen. Physiological and Biochemical Zoology 84(5):522-532.

Packard, T.T., M.L. Healy, and F.A. Richards. 1971. Vertical distribution of the activity of the respiratory electron transport system in marine plankton. Limnology and Oceanography 16(1):60-70.

Owens, T.G. and F.D. King 1975. The measurement of respiratory electron-transport-system activity in marine zooplankton. Marine Biology 30:27-36.

Simcic T., F. Pajk, M. Jaklic, A. Brancelj and A. Vrezec. 2014. The thermal tolerance of crayfish could be estimated from respiratory electron transport system activity. Journal of Thermal Biology 41:21-30.

Simcic, T., D. Jesensek, and A. Brancelj. 2017. Metabolic characteristics of early life history stages of native marble trout (*Salmo marmoratus*) and introduced brown trout (*Salmo trutta*) and their hybrids in the Soca River. Ecology of Freshwater Fishes 26:141-149.

Smith, M.E., J. M. Lazorchak, L.E. Herrin, S. Brewer-Swartz, and W.T. Thoeny. 1997. A reformulated, reconstituted water for testing the freshwater amphipod, Hyallela azteca. Environmental Toxicology and Chemistry 16(6):1229-1233.

Tankersley, R.A., and R.V. Dimock. 1993. The effect of larval brooding on the respiratory physiology of the freshwater unionid mussel *Pyganodon cataracta*. The American Midland Naturalist. 130(1):146-163.

USEPA. 2013. Aquatic Life Ambient Water Criteria for Ammonia – Freshwater. United States Environmental Protection Agency, Office of Water. EPA 822-R-13-001.

Walsh, S.J., D.C. Haney, and C.M. Timmerman. 1997. Variation in thermal tolerance and routine metabolism among spring- and stream-dwelling freshwater sculpins (Teleostei: Cottidae) of the southeastern United States. Ecology of Freshwater Fish 6:84-94.

Table 1. Species, collection sites, and shipping information for mussels used in thermal and hypoxia tolerance experiments at Auburn University.

Species	Drainage	Site	Collection Date	# shipped	Collection Temp. (°C)	Receiving Temp. (°C)
Cyclonaias petrina	Colorado River	Altair	4/28/2017	6		*NT*
			5/17/2017	33		16.2
		Lometa	6/1/2017	11	26.6	22.0
	Gauadalupe River	Gonzales	11/01/2017	14	18	16.9
		Gonzales	8/17/2017	32	30.9	23.5
Cyclonaias houstonensis	Colorado River	Altair	4/27/2017	6		*NT*
			5/17/2017	50		16.4
	Navasota River	Easterly	7/17/2017	50		22.6
Lampsilis bracteata	Llano River	Mason	5/31/2017	20	23	15.3
		Llano Park Lake	11/01/2017	50	Stranded, 13.7	15.1, 14.4
Fusconaia mitchelli	Guadalupe River	Gonzales	8/17/2017	6	30.9	23.5
			11/01/2017	4	18	16.9
Truncilla macrodon	Brazos River	Highbank	12/4/2017	7	19	*NT*
Amblema plicata	Colorado River	Altair	4/27/2017	12		*NT*
			8/4/2017	20	31	21.7
Lampsilis teres	Colorado River	Altair	11/02/2017	12	18	*NT*

Table 2. Optimum temperature and optimum range for acclimated ETS activity. Prior to ETS measurement, individuals were acclimated for >1 week to each of 10 temperatures from 15 – 36ºC.

Species	**Drainage**	**Optimum**	**Range**
Cyclonaias petrina	Colorado River	35.3	28.2 - >36
	Gauadalupe River	34.6	26.5 - >36
Cyclonaias houstonensis	Colorado River	31.6	27.5 – 35.8
	Navasota River	27.6	24.8 – 30.6

Table 3. Optimal temperature data for non-acclimated mussels. Individuals were all acclimated for >1 week to 21ºC. Enzymes were then extracted from foot tissue of each individual and incubated at each of 9 temperatures ranging from 12 – 36ºC, generating a separate thermal performance curve for each individual (see Fig. 9). Min and max refer to the minimum and maximum optimal temperatures among all individuals within each species X drainage combination.

Species	**Drainage**	**Mean**	**Min**	**Max**	**Stdev**	**CV**	**n**
Cyclonaias petrina	Colorado River	30.2	28.6	34.8	1.7	5.7	12
	Gauadalupe River	28.5	27.6	29.5	0.7	2.6	6
Cyclonaias houstonensis	Colorado River	30.5	28.3	32.1	1.1	3.7	11
	Navasota River	28.8	27.7	29.8	0.6	2.0	12
Lampsilis bracteata	Llano River	28.4	27.6	29.1	0.6	2.1	11
	Llano Lake	*April 2018*					
Fusconaia mitchelli	Guadalupe River	27.8	26.5	28.8	0.9	3.3	6
Amblema plicata	Colorado River	28.4	27.5	29.0	0.5	1.6	10
Lampsilis teres	Colorado River	27.1	27.9	26.2	0.6	2.1	12

Table 4. Summary of ETS enzyme thermal tolerance endpoints from acclimated and non-acclimated experiments. Optimal Range for acclimated mussels represents the temperature range where ETS activity was within 10% of the observed maximum rate, whereas for non-acclimated mussels it represents the range in optimal temperatures estimated for individual mussels. The upper end of the acclimated range indicates the temperature threshold above which we predict the initiation of thermal stress at the enzymatic level for at least some individuals in the population. The upper end of the non-acclimated range represents the maximum optimal temperature observed for enzymes subjected to a sudden increase in temperature. Onset of lethal effects indicates the temperature threshold beyond which we predict the onset of mortality due to thermal stress. Months indicate when we expect additional information will be available. Blank cells indicate no results due to a lack of samples and/or animals. All temperatures are ºC.

Species	**Drainage**	**Optimal Temp.**	**Optimal Range**	**Estimated onset of lethal effects**	**Assay Type**
Cyclonaias petrina	Colorado River	35.3	28.2 - >36		Acclimated
		30.2	28.6-34.8		Non-acclimated
	Gauadalupe River	34.6	26.5 - >36		Acclimated mussels
		28.5	27.6-29.5	38.9	Non-acclimated
Cyclonaias houstonensis	Colorado River	31.6	27.5 – 35.8		Acclimated mussels
		30.5	28.3-32.1		Non-acclimated
	Navasota River	27.6	24.8 – 30.6		Acclimated mussels
		28.8	27.7-29.8	37.1	Non-acclimated
Lampsilis bracteata	Llano River	28.4	27.6-29.1		Non-acclimated
	Llano Lake				Acclimated mussels
					Non-acclimated
Fusconaia mitchelli	Guadalupe River	27.8	26.5-28.8	31.0	Non-acclimated
Amblema plicata	Colorado River	28.4	27.5-29.0	36.0	Non-acclimated
Lampsilis teres	Colorado River	27.1	26.2-27.9	29.4	Non-acclimated

Table 5. Total ammonia nitrogen (TAN) and pH measurements in respirometry water for individual runs within ammonia treatments.

		TAN (mg/L)		**pH**	
Run	*Treatment*	*Initial*	*Final*	*Initial*	*Final*
1	0	0.05	0.4	8.6	8.6
2	0	0.1	0.1	8.6	8.6
1	0.5	0.60	0.43		8.4
2	0.5	0.66	0.30	8.6	8.5
1	2.0	2.40	2.08	8.6	8.4
2	2.0	2.16	1.76	8.5	8.4

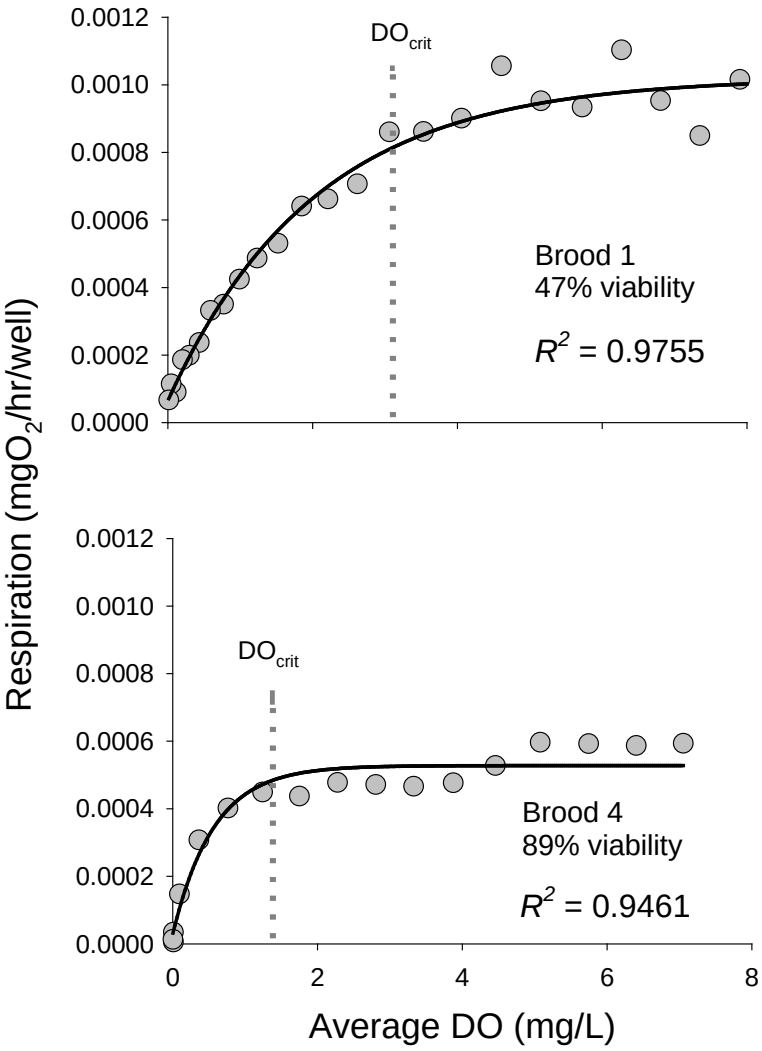

Figure 1. Example of preliminary data showing respiration patterns of *L. subrostrata* broods with low (top panel) and high (bottom panel) viability. The low viability brood had a greater respiration rate, reduced ability to regulate oxygen consumption, and increased DO_{crit} relative to the higher viability brood.

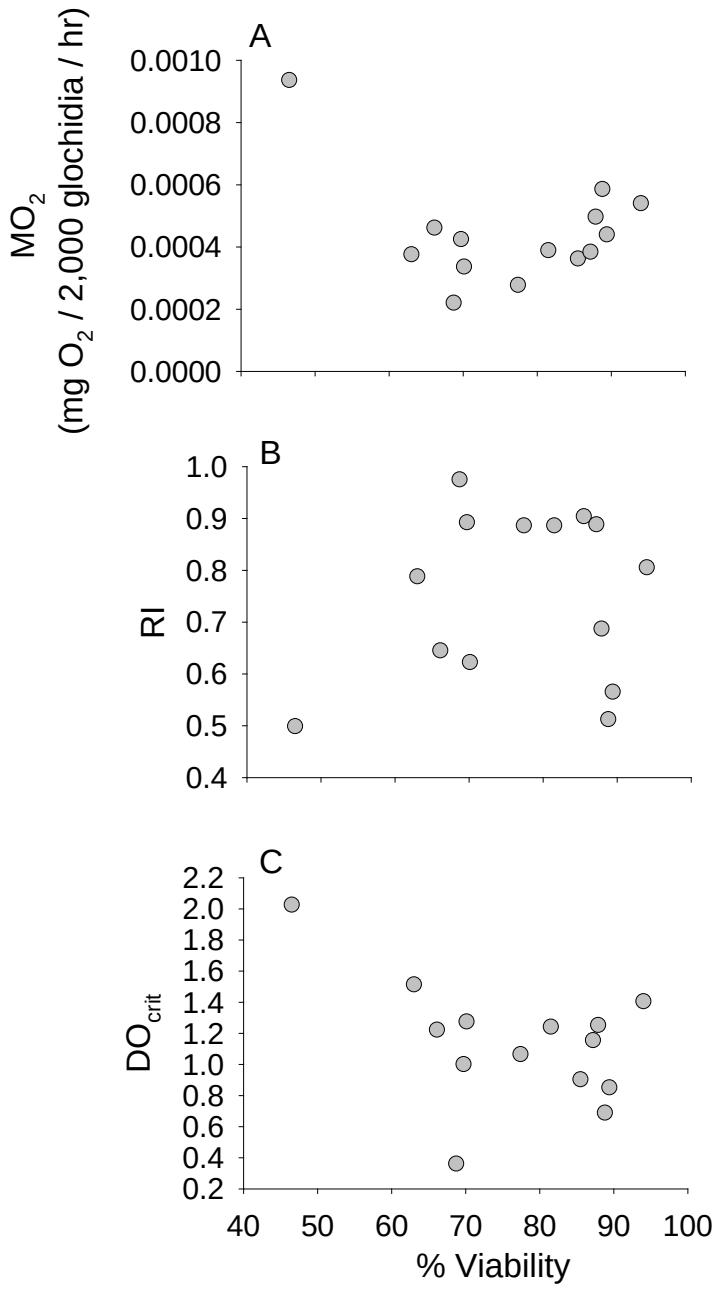

Figure 2. Relationships between (A) respiration rate (MO2), (B) regulation index (RI), and (C) critical dissolved oxygen concentration (DOcrit) and % brood viability for glochidia of *L. subrostrata*. Each data point represents the mean value for 2,000 glochidia from a given brood.

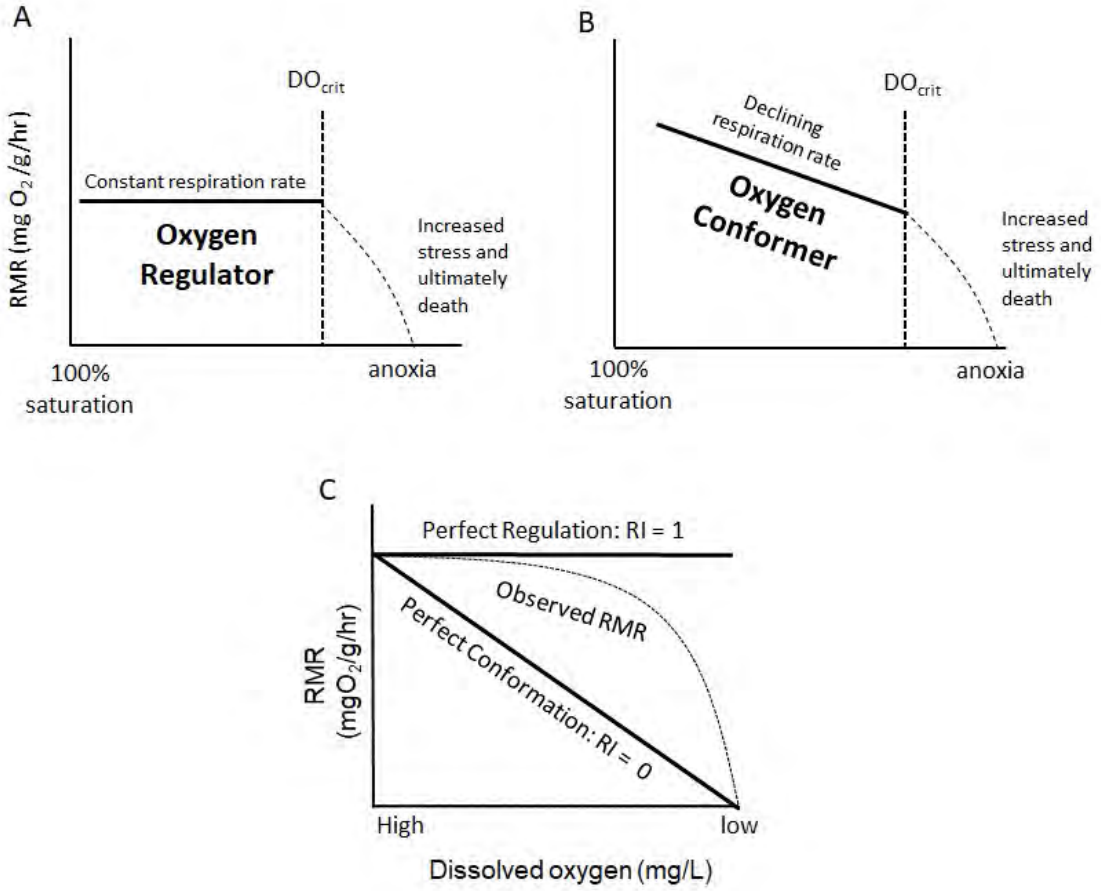

Figure 3. Resting metabolic rates (RMR) graphed as a function of declining dissolved oxygen showing A) an oxyregulator and B) an oxyconformer. DO_{crit} is the DO threshold below which respiration rates show a marked decrease or increase, indicating the switch from aerobic to anaerobic respiration. C) RMR graphed as a function of DO indicating the range of values of the Regulation Index (RI; Mueller and Seymour 2011). Solid lines indicating either perfect regulation (RI = 1) or perfect conformation (RI = 0) and dashed line indicates an intermediate, typically observed pattern that falls between perfect regulation and perfect conformation.

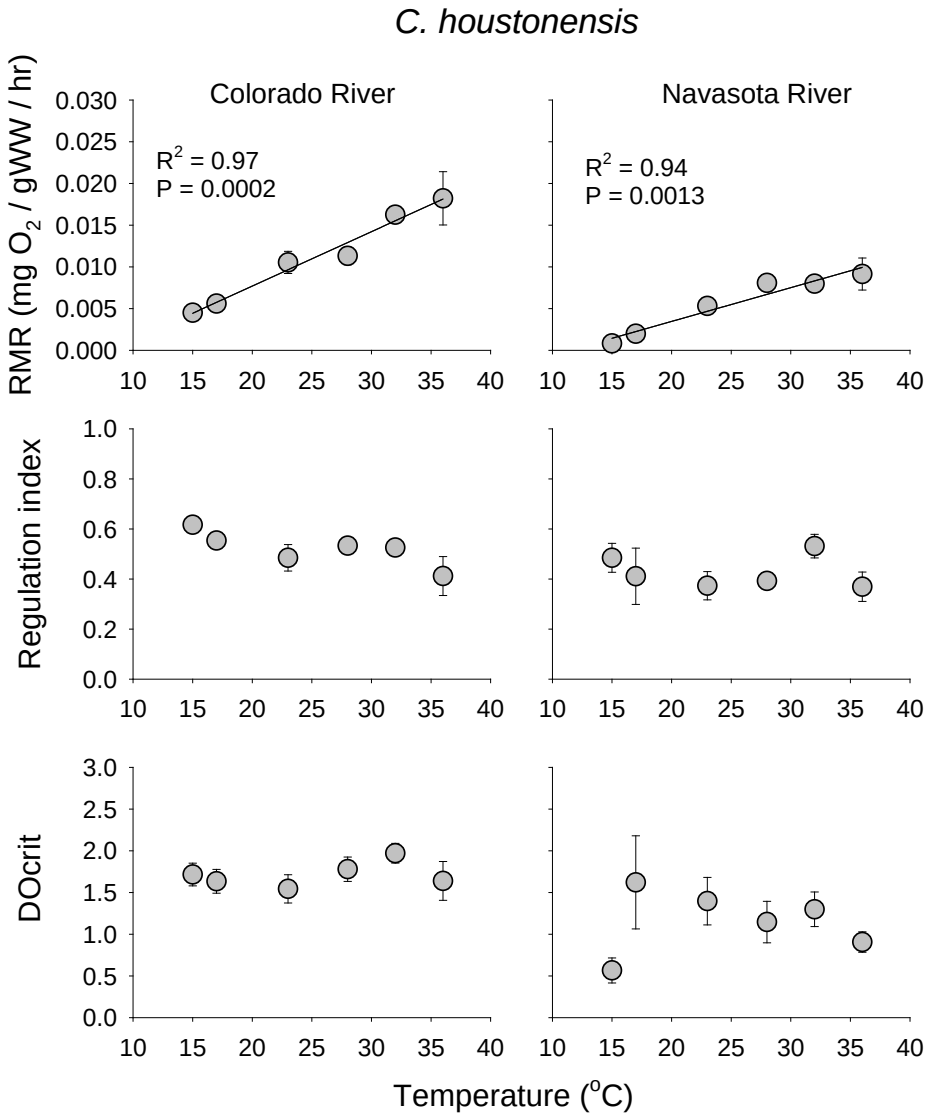

Figure 4. Relationships between resting metabolic rate (RMR), regulation index, DO_{crit} and temperature for *C. houstonensis* collected from two drainage basins. Neither regulation index nor DO_{crit} yielded a significant linear relationship with temperature. Vertical lines represent ± 1 SE.

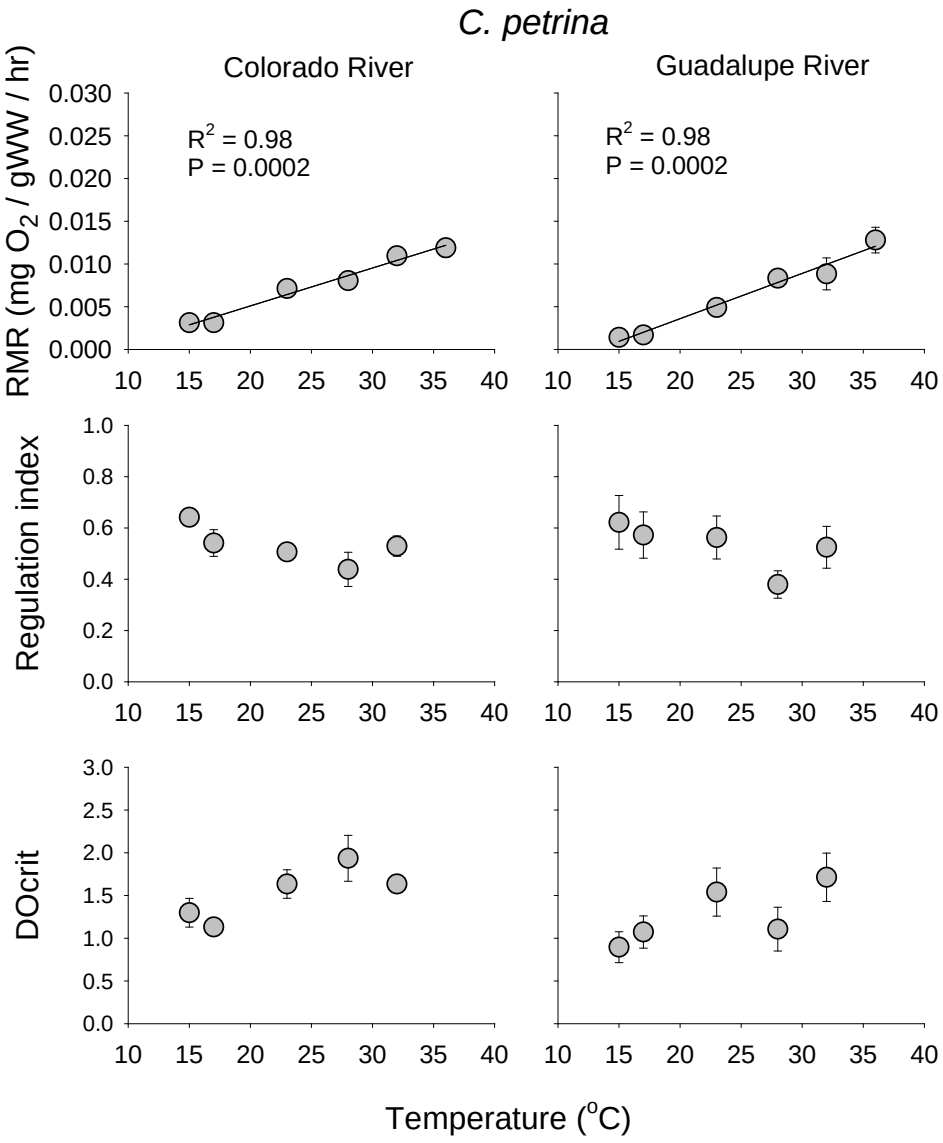

Figure 5. Relationships between resting metabolic rate (RMR), regulation index, DO_{crit} and temperature for *C. petrina* collected from two drainage basins. Neither regulation index nor DO_{crit} yielded a significant linear relationship with temperature. Vertical lines represent ± 1 SE.

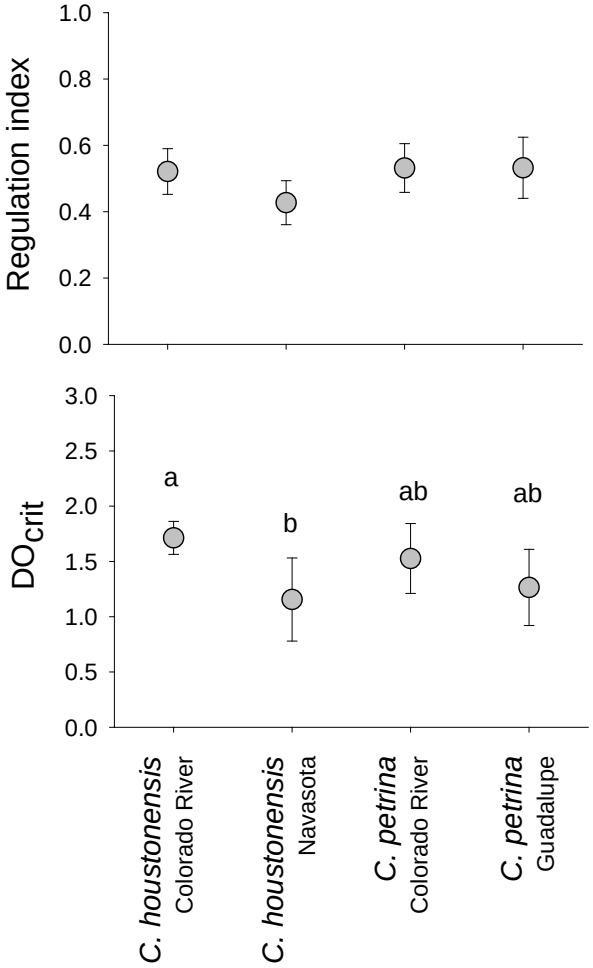

Figure 6. Mean regulation index and DO_{crit} across all temperatures for *C. houstonensis* and *C. petrina* collected from different drainage basins. No significant differences among mussel groups were found for mean regulation index. Letters indicate significant differences in DO_{crit} among mussel groups. Error bars represent ± 1 standard deviation.

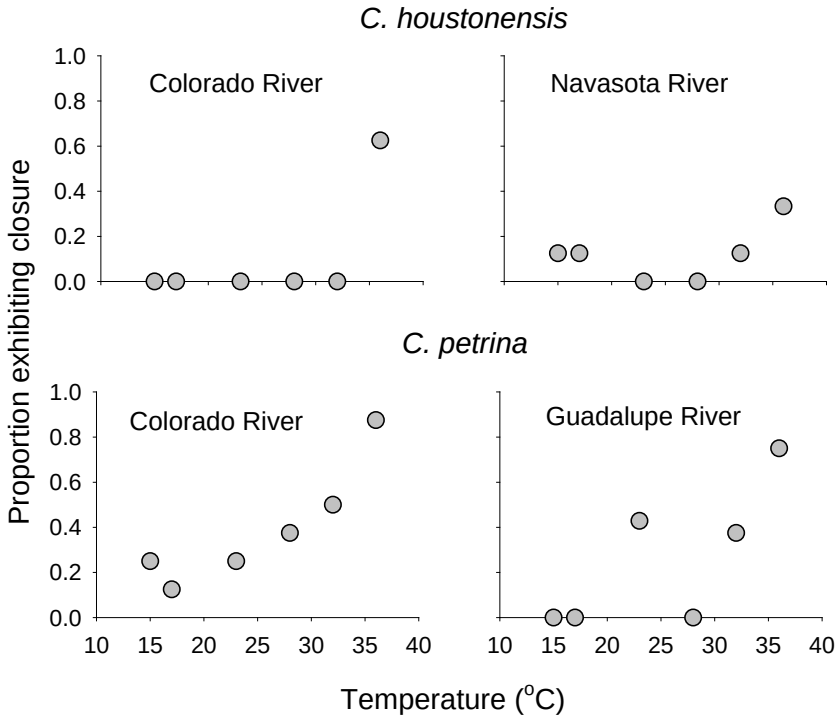

Figure 7. Proportion of individuals exhibiting at least one closure event during respirometry runs at six temperatures.

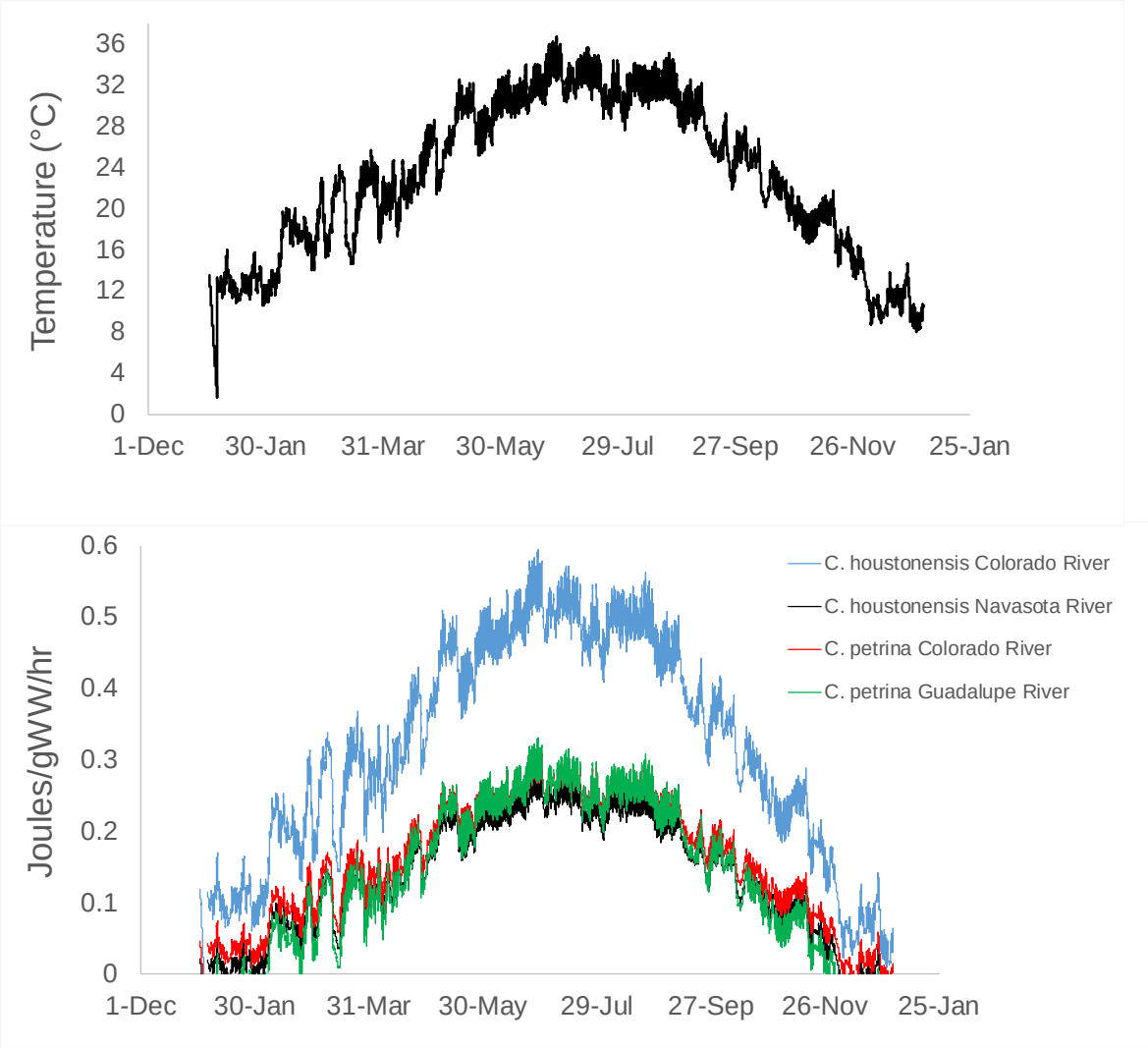

Figure 8. Comparison of estimated energy requirements to meet basic metabolic demands (Joules/gWW/hr) for 4 mussel populations if they were exposed to the same temperature regime. In this case, temperatures were obtained from the San Saba gage of the Colorado River, 2009.

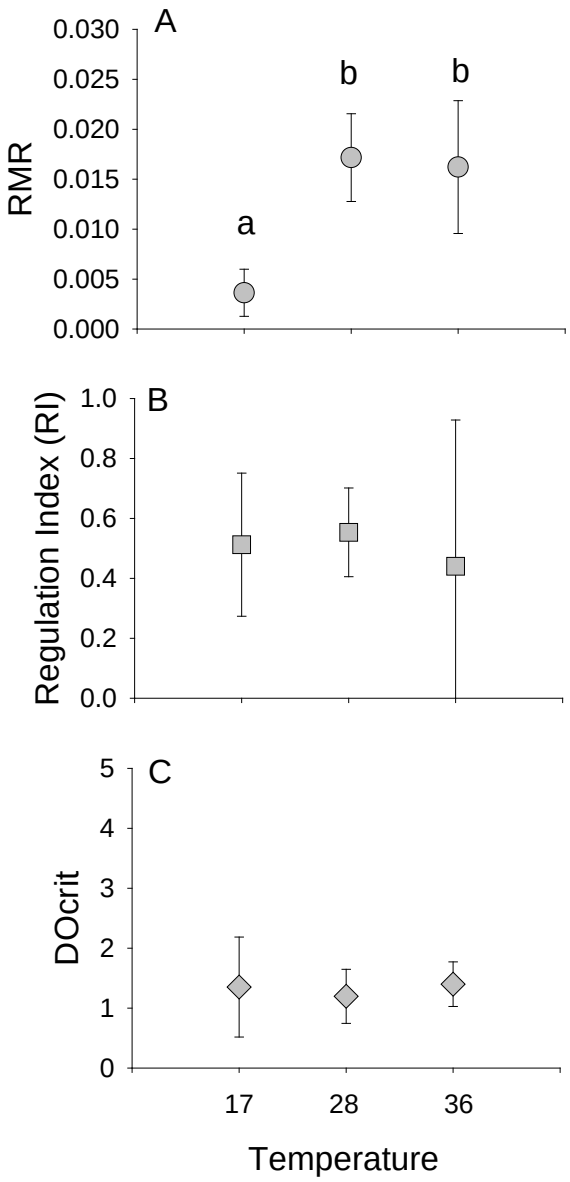

Figure 9. Relationships between (a) resting metabolic rate at 6 mg O_2/L, (b) regulation index, and (c) DO_{crit} and three temperatures for *L. bracteata* males. Vertical lines represent 95% CI. Letters above data points indicate significant differences among temperatures.

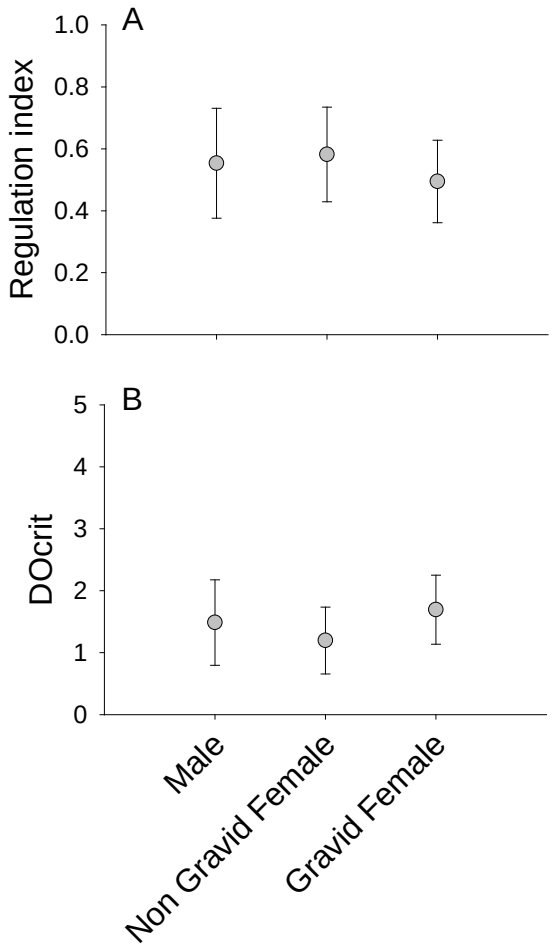

Figure 10. Mean (A) regulation index and (B) DO_{crit} estimates at 28ºC for males, nongravid females, and gravid females. Vertical lines represent ± 1 standard deviation.

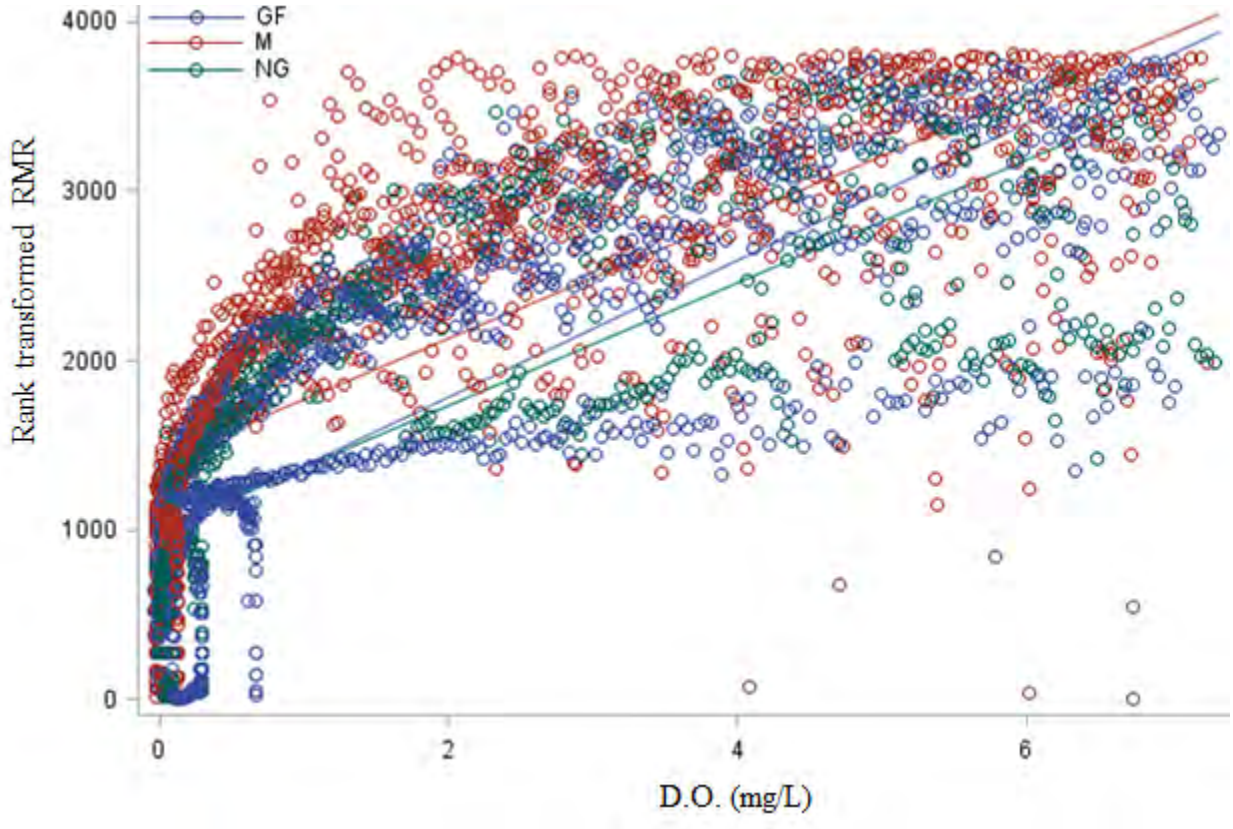

Figure 11. Relationship between resting metabolic rate (RMR) and dissolved oxygen (DO) for gravid females (GF), males (M), and nongravid females (NG) at 28ºC. Each data point represents a rank-transformed respiration rate measurement for an individual mussel. All data are from *L. bracteata* collected from Llano Lake.

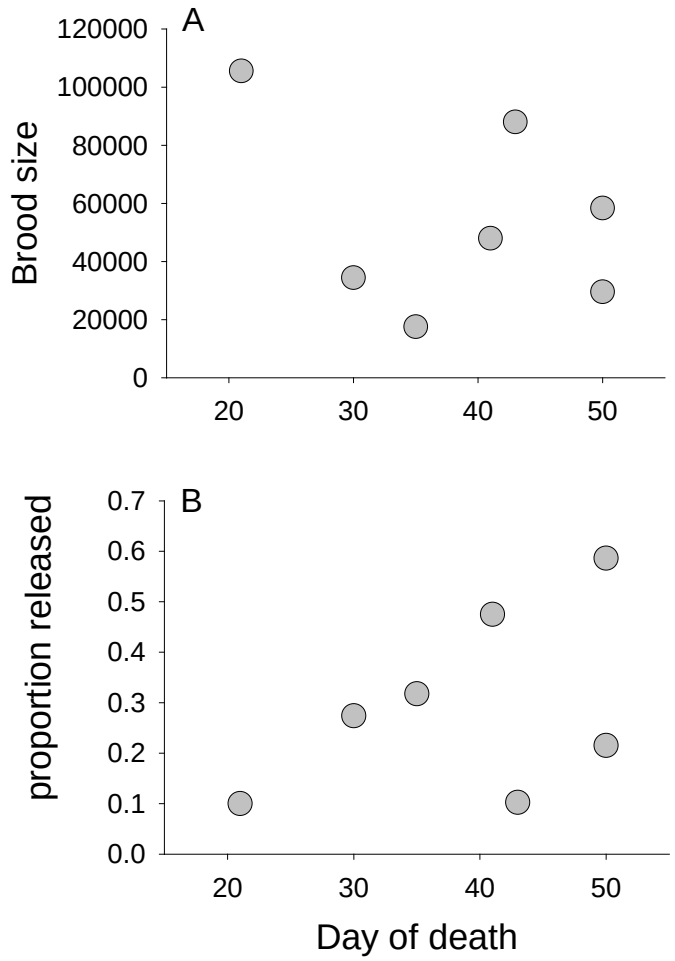

Figure 12. Relationship between (A) brood size and (B) proportion of brood released, and day of death for gravid females in the warming treatment. Each data point represents an individual mussel.

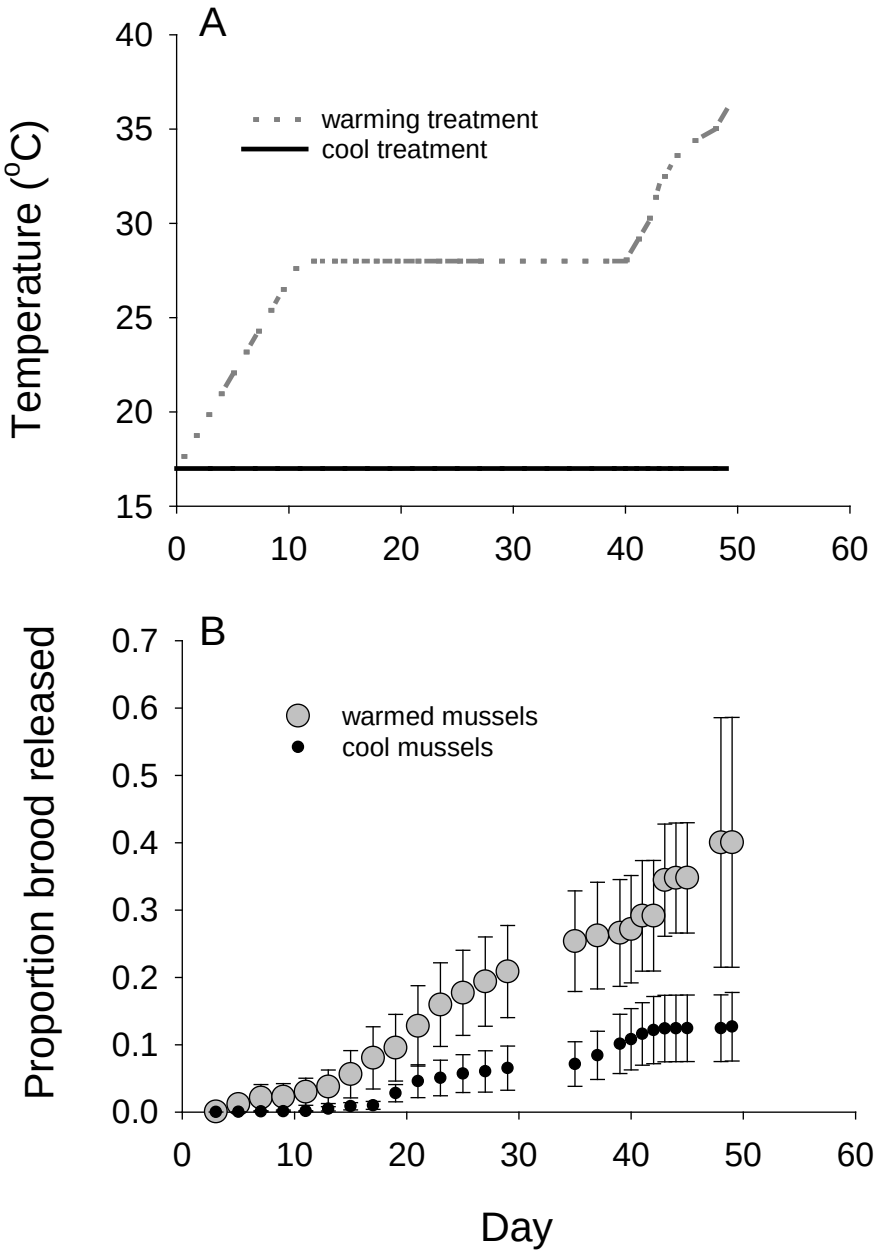

Figure 13. A. Temperature regimes for the cool (control) and warming treatments. B. Proportion of brood released over time for mussels in the cool and warming treatments. Each data point represents the mean of all surviving gravid females on that day. Vertical lines represent ± 1 standard error. Break in data indicates period when respirometry trials were conducted.

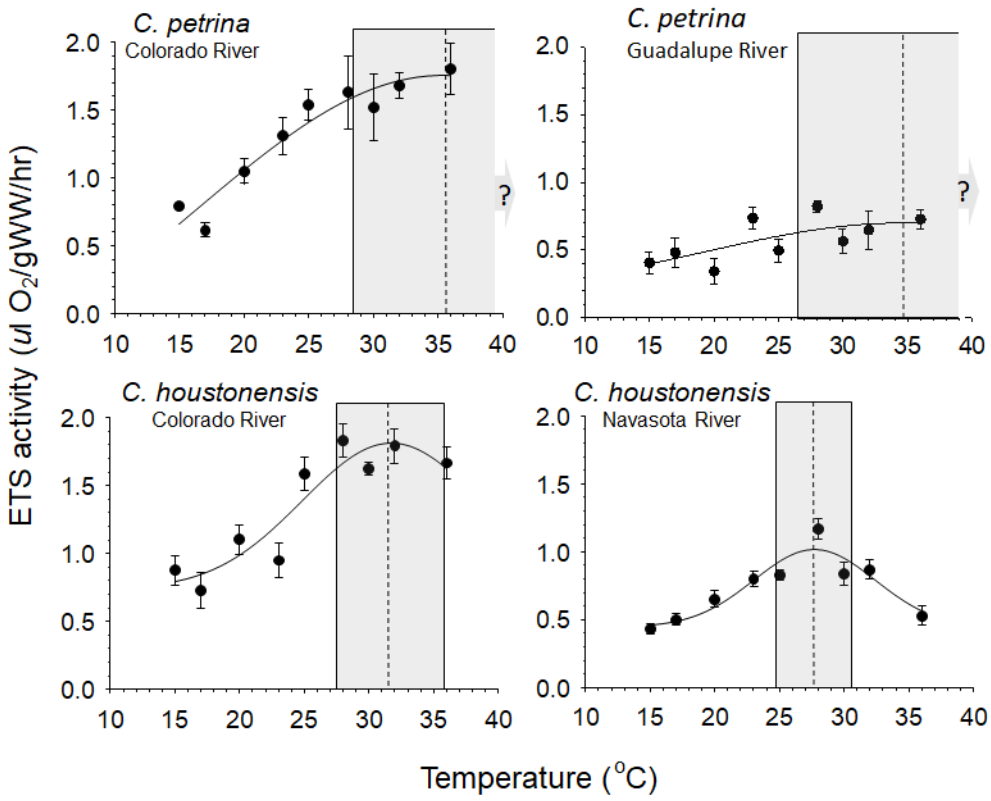

Figure 14. Relationship between ETS activity and temperature for acclimated mussels. Each data point represents the mean ETS activity of all mussels acclimated to that particular temperature. Mussel groups at each temperature were unique. ETS activity of a given mussel was measured only for the temperature to which it had been acclimated. Dashed lines indicate the optimal temperature for enzymatic activity. Grey rectangles represent the optimal temperature range within which ETS activity is within 10% of the maximum.

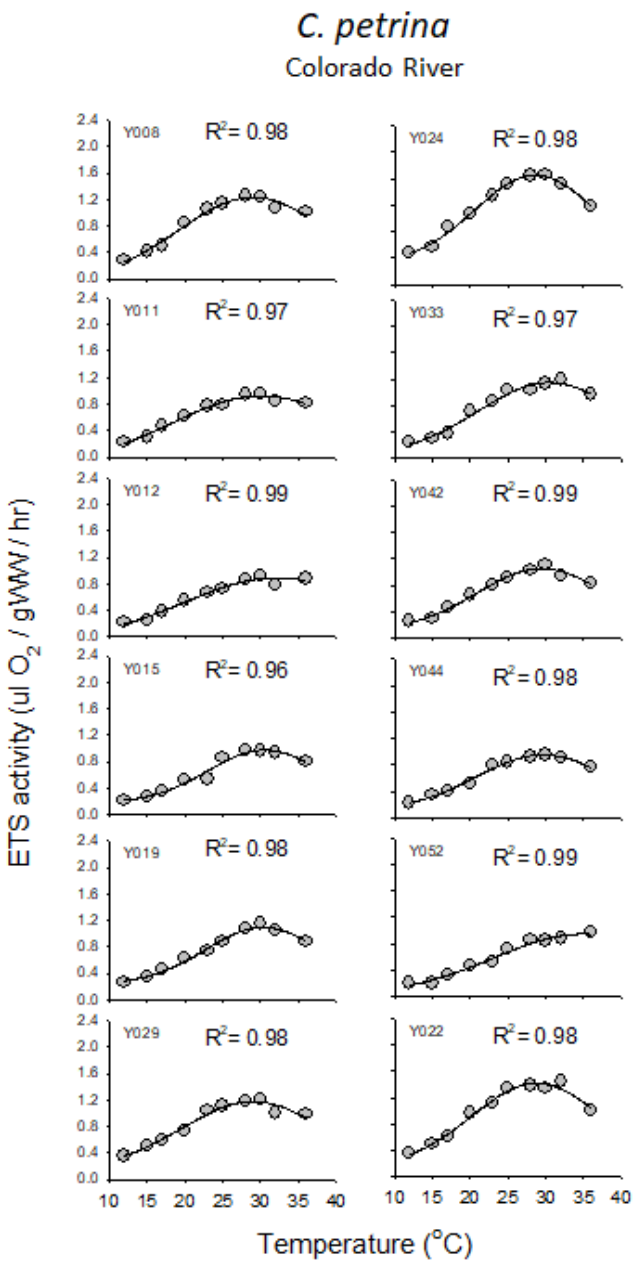

Figure 15. Relationship between ETS activity and temperature for non-acclimated *C. petrina* from the Colorado River. The tag number identifying each mussel is given in the upper left corner of each graph. Each data point represents ETS activity of enzymes collected from the same individual and incubated for 30 minutes at each temperature. Solid lines represent a four parameter Gaussian curve fitted through the data points. Optimal temperature for each individual was calculated as the temperature at the peak of each Gaussian curve.

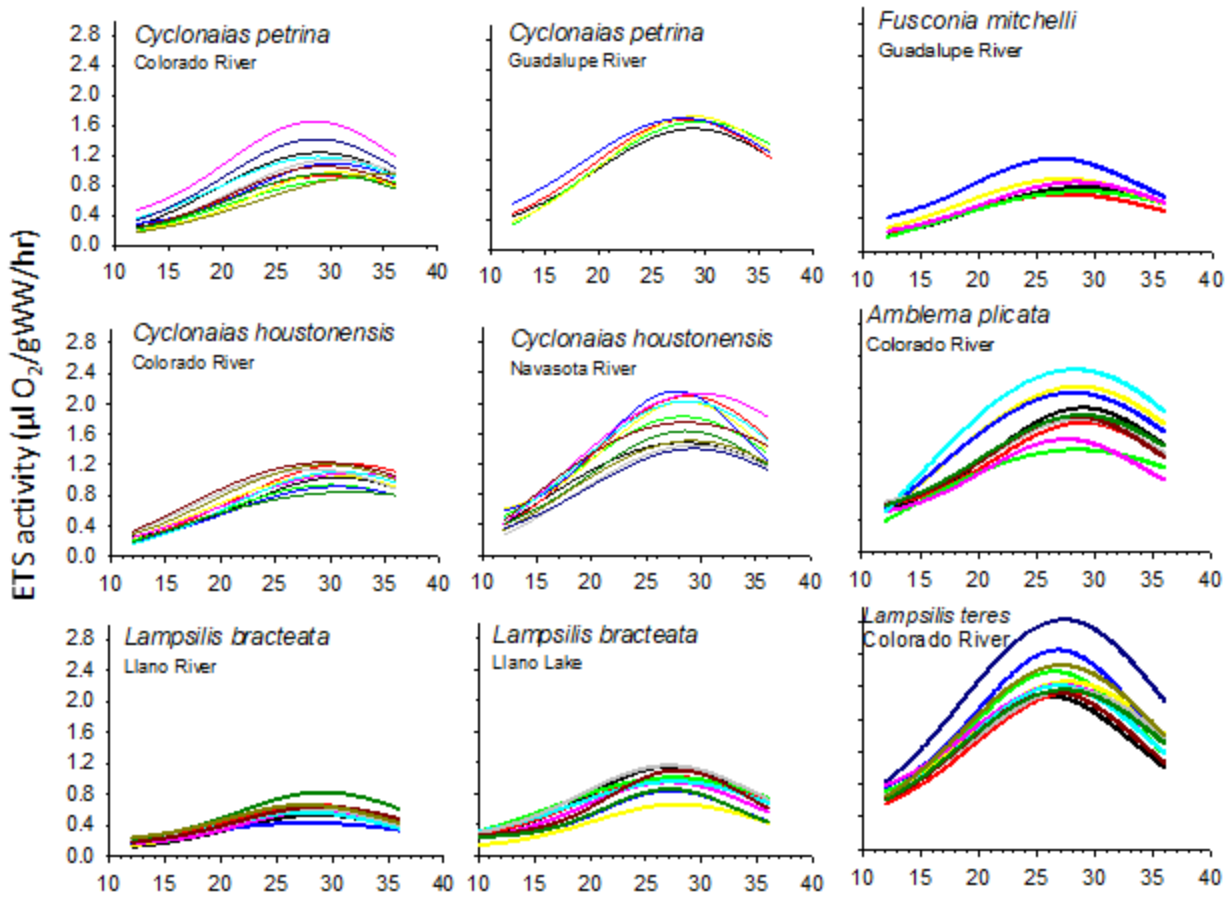

Figure 16. Summary graphs of relationship between ETS enzyme activity and temperature for non-acclimated mussels. Each curve represents a single mussel. ETS enzymes were extracted from each mussel and incubated at nine temperatures to which the mussel had not been acclimated. Colored lines represent a four parameter Gaussian curve fitted through the data for each individual mussel.

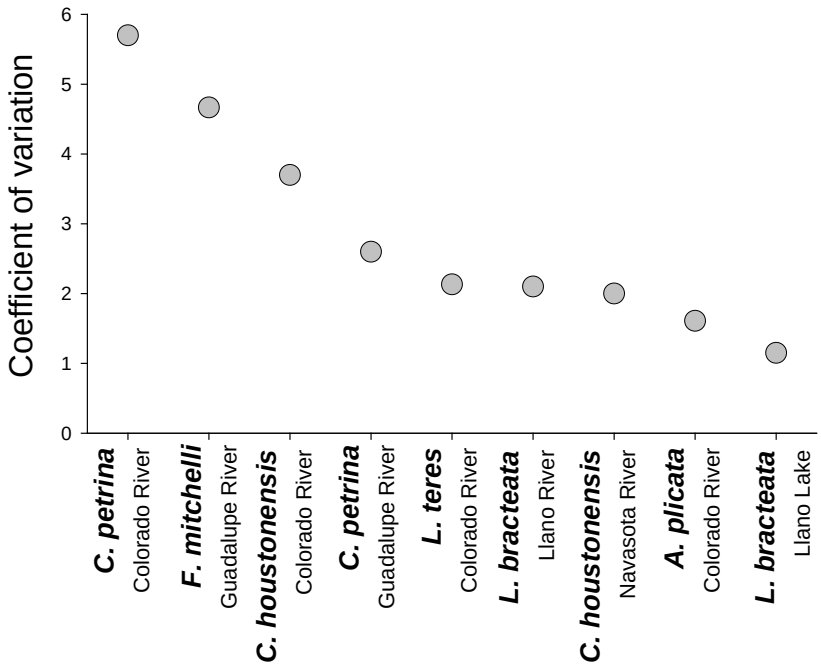

Figure 17. Coefficient of variation for optimal ETS temperatures of non-acclimated mussels from a given species and drainage, arranged in order from highest to lowest.

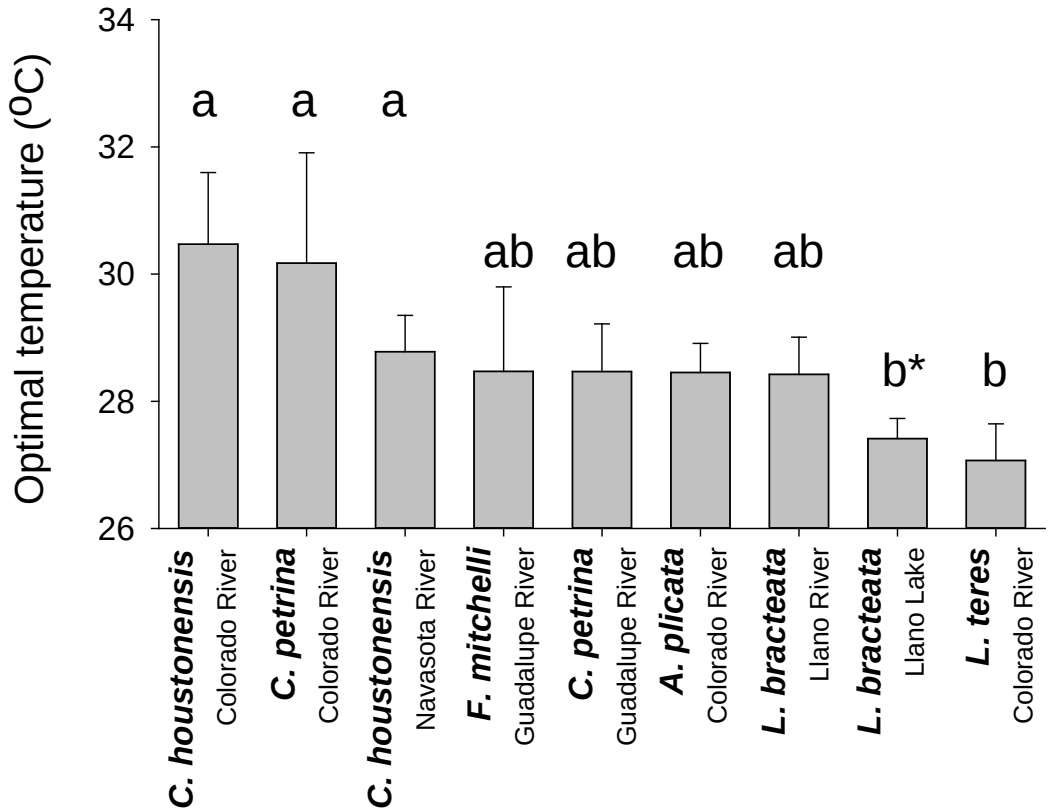

Figure 18. Mean optimal ETS temperatures of non-acclimated mussels determined from individual curves shown in Figure 2, arranged from highest to lowest. Error bars represent ± 1 SD. Letters indicate significant differences.

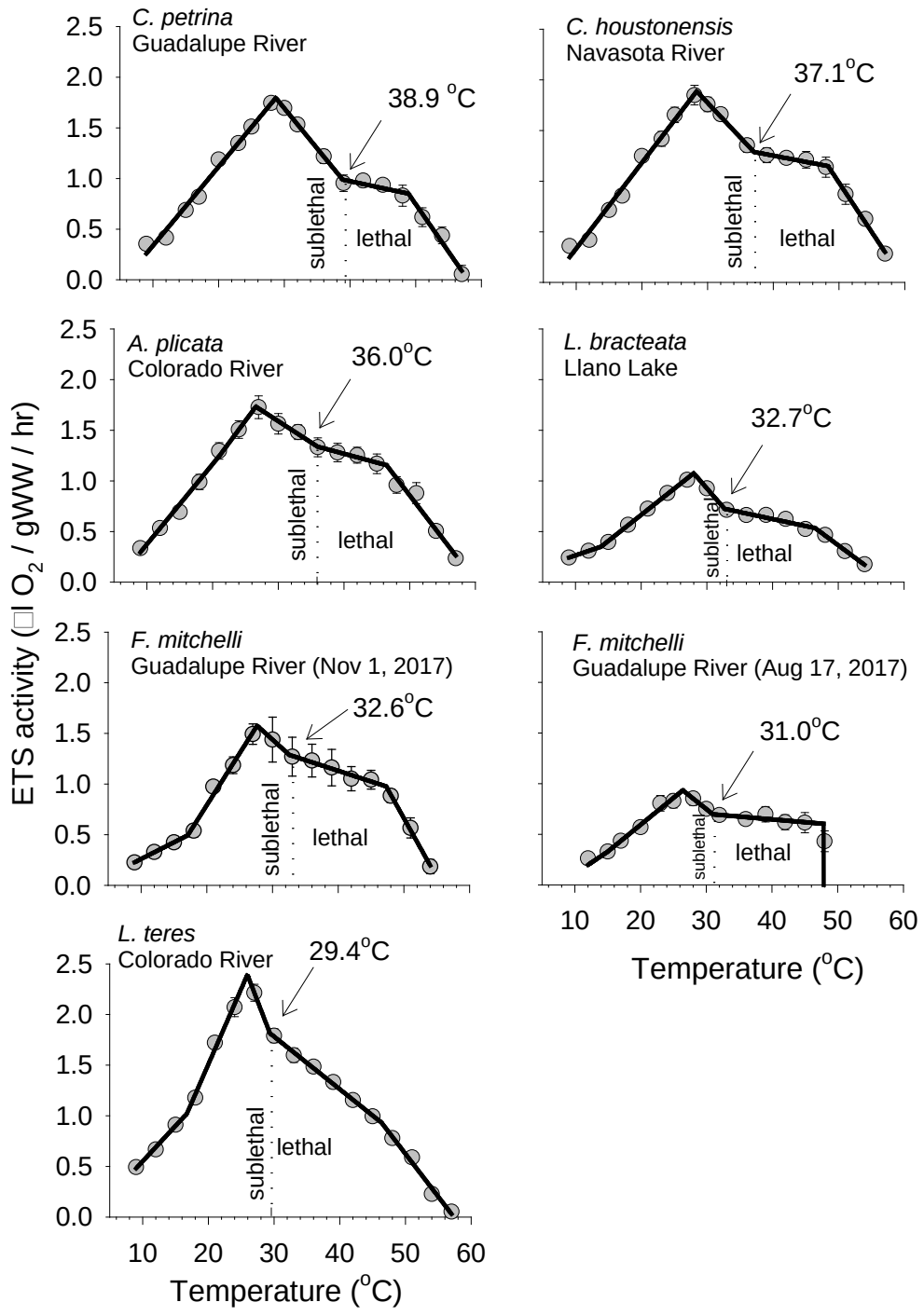

Figure 19. Relationship between ETS activity and temperature for non-acclimated mussels across the full range of experimental temperatures. Each data point within a panel represents the mean activity of enzymes extracted from the same group of mussels. Error bars represent ± 1 standard error. Solid lines represent 5-segment piecewise regressions. Dotted lines indicate temperature at which we hypothesize sublethal effects transition to lethal effects.

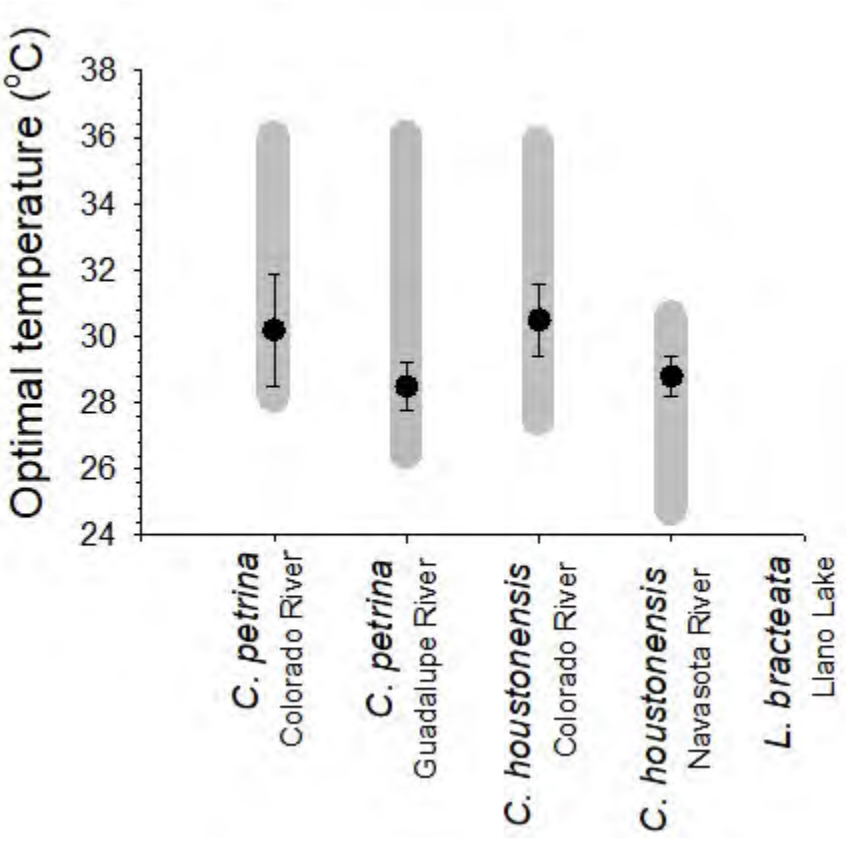

Figure 20. Comparison of optimal temperature range (grey bars) obtained from acclimated mussels and mean optimal temperature (black circles) obtained from non-acclimated mussels. Error bars represent ± 1 SD. Data for *L. bracteata* is expected to be available by May 2018.

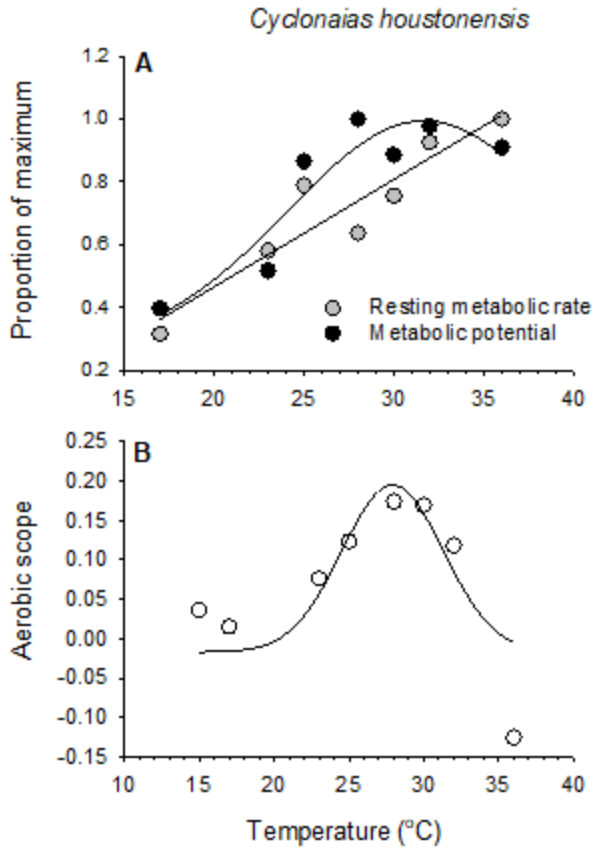

Figure 21. A) Relative changes in resting metabolic rate (RMR) and metabolic potential (ETS activity) with increasing temperature for *C. houstonensis* (Colorado River). B) Aerobic scope calculated as the difference between metabolic potential and RMR – based on this data, the optimal temperature for *C. houstonensis* would be ~28ºC, which, as expected, is lower than the optimal enzymatic temperature (31.6ºC, see Table 4).

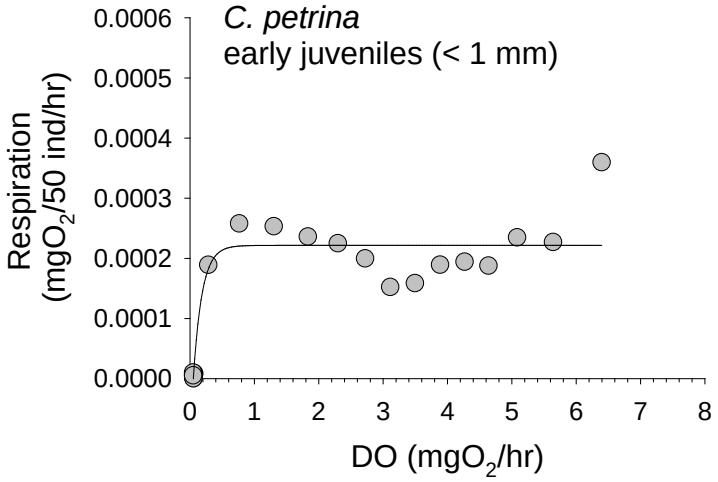

Figure 22. Relationship between respiration rate (per 50 individuals) and dissolved oxygen concentration for early juvenile *C. petrina* (3 parameter exponential rise; $R^2 = 0.8692$; $P < 0.0001$)

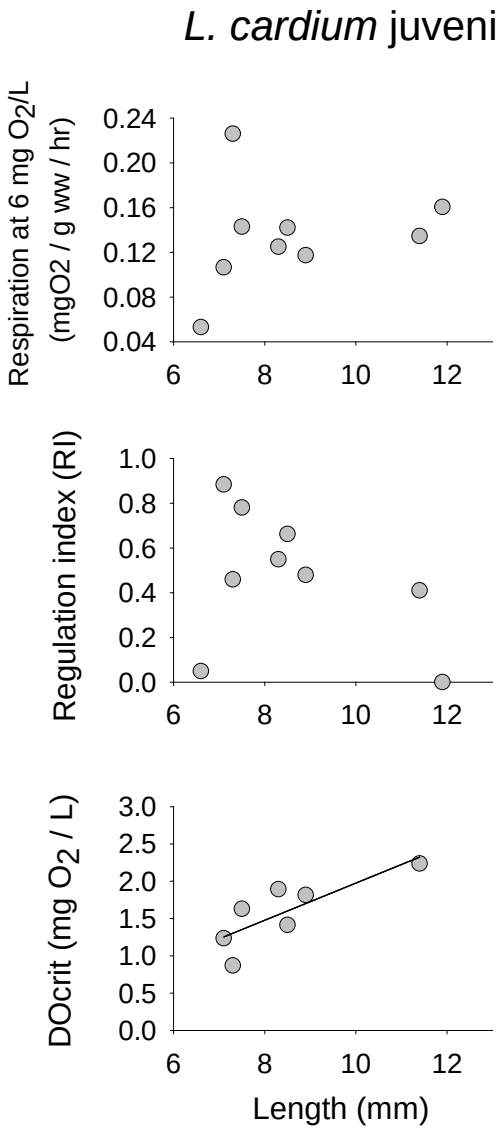

Figure 23. Relationship between respiration rate at 6 mg O_2/L and shell length for *L. cardium* juveniles. Linear regression between DOcrit and shell length was significant ($R^2 = 0.65$, $P = 0.03$).

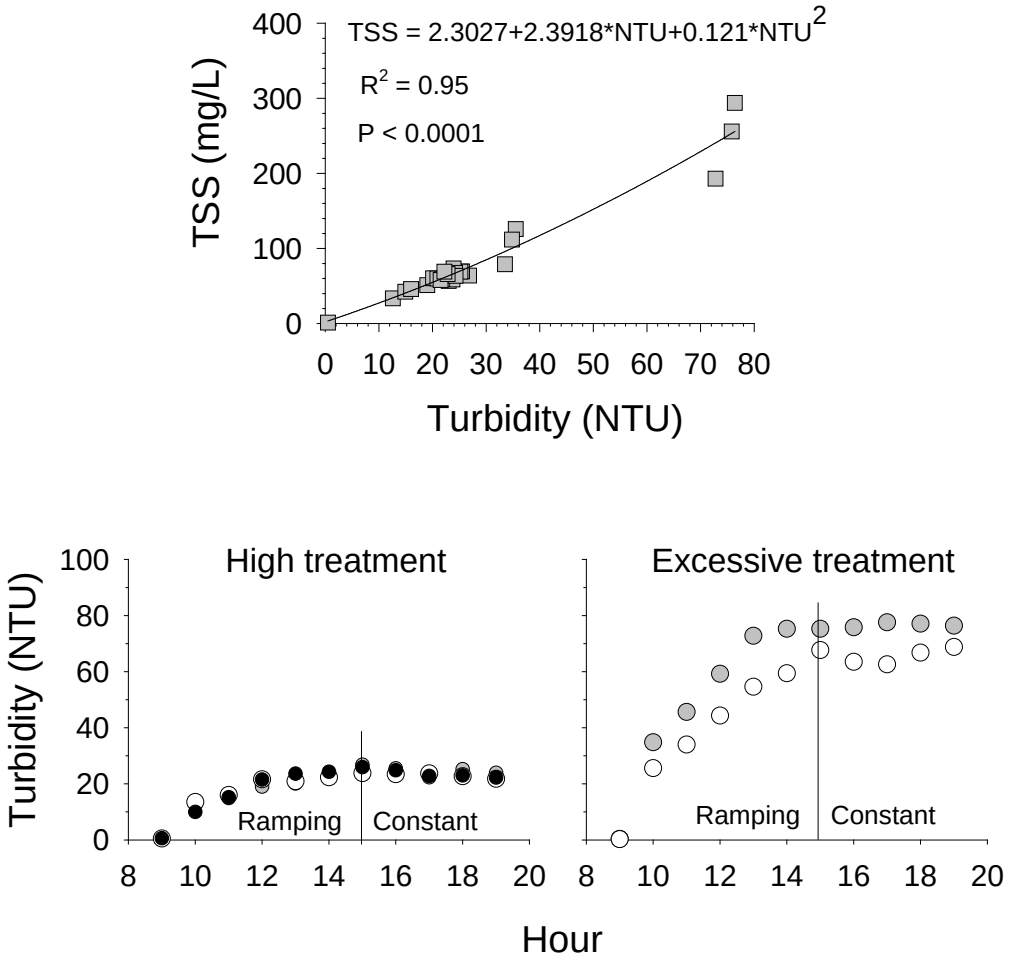

Figure 24. Top panel: Predictive relationship between turbidity (NTU) and total suspended solids (TSS mg/L). Bottom panel: Changes in turbidity through time in the High and Excessive turbidity treatments. Solid vertical line indicates the break between the ramping turbidity and the constant turbidity periods.

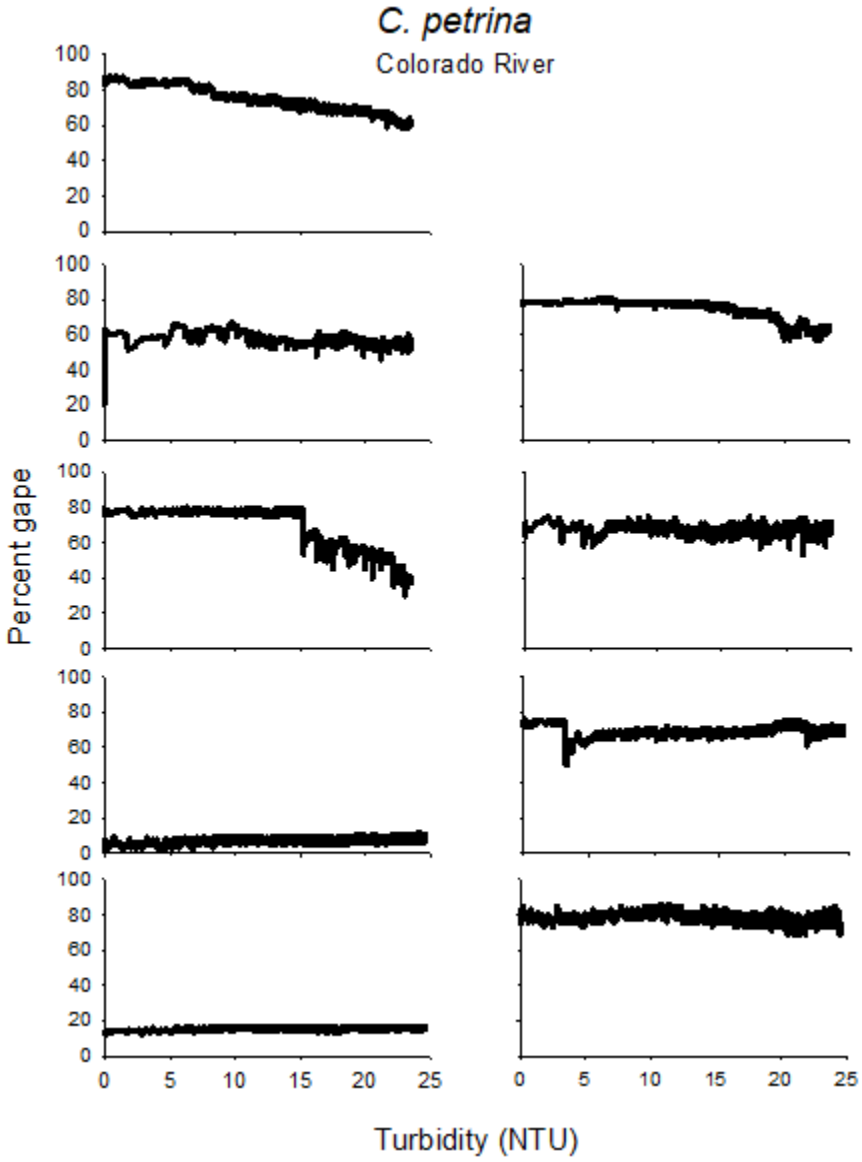

Figure 25. Percent gape for *C. petrina* from the Colorado River as turbidity increased over a ~6-hr period to a maximum of ~25 NTU. Each graph represents a unique individual.

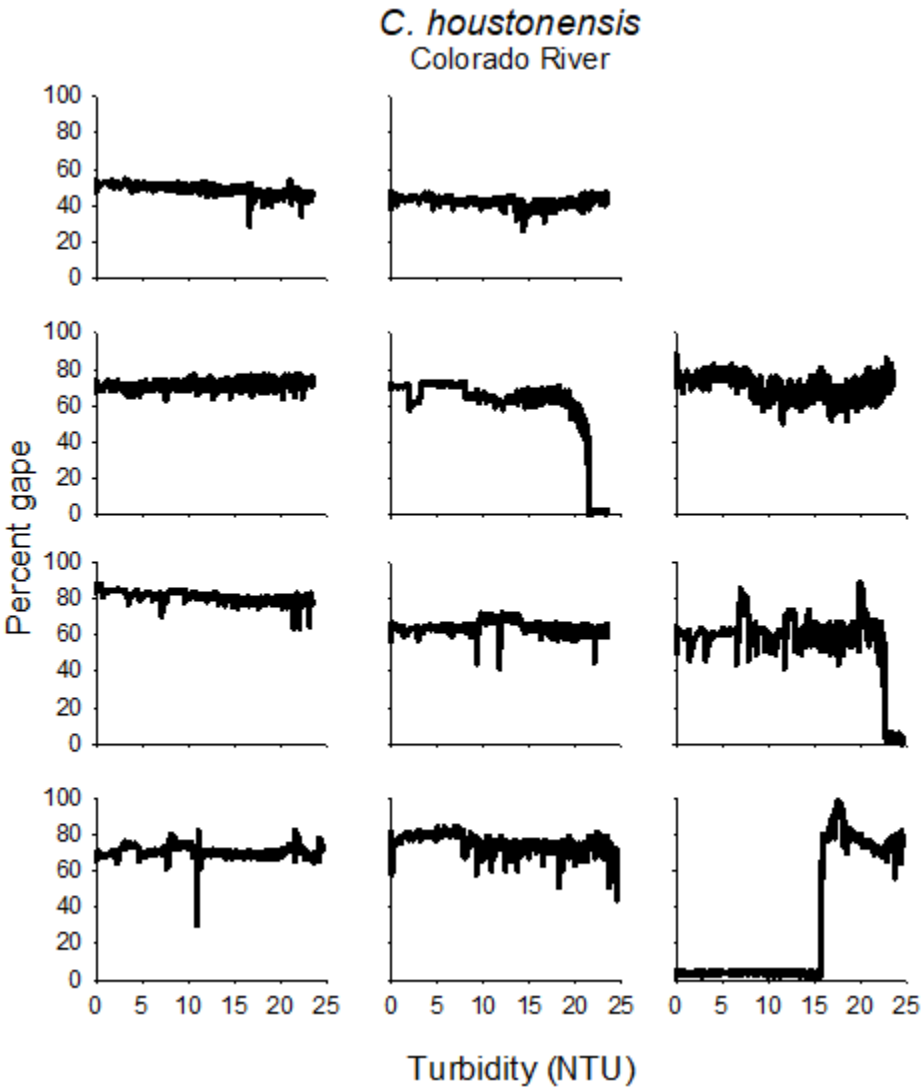

Figure 26. Percent gape for *C. houstonensis* from the Colorado River as turbidity increased over a ~6-hr period to a maximum of ~25 NTU. Each graph represents a unique individual.

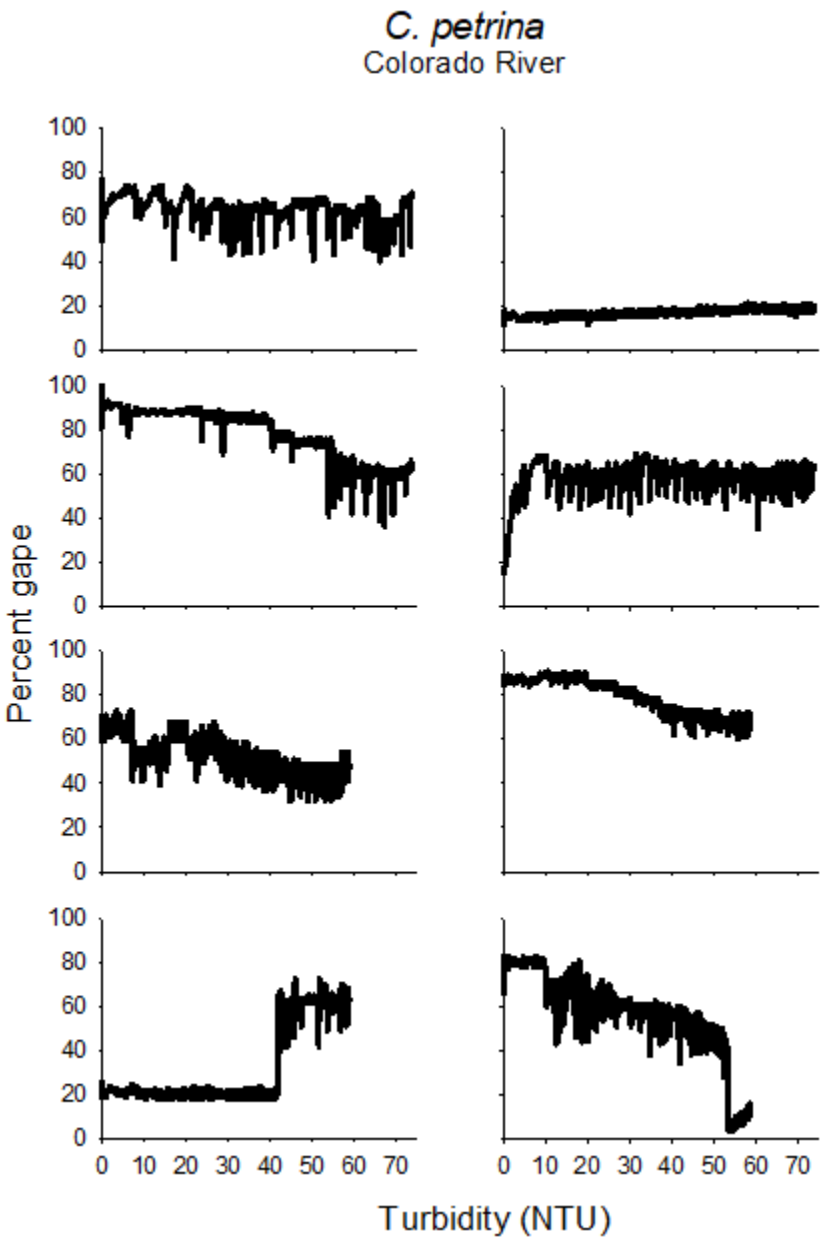

Figure 27. Percent gape for *C. petrina* from the Colorado River as turbidity increased over a ~6-hr period to a maximum of 60-75 NTU. Each graph represents a unique individual.

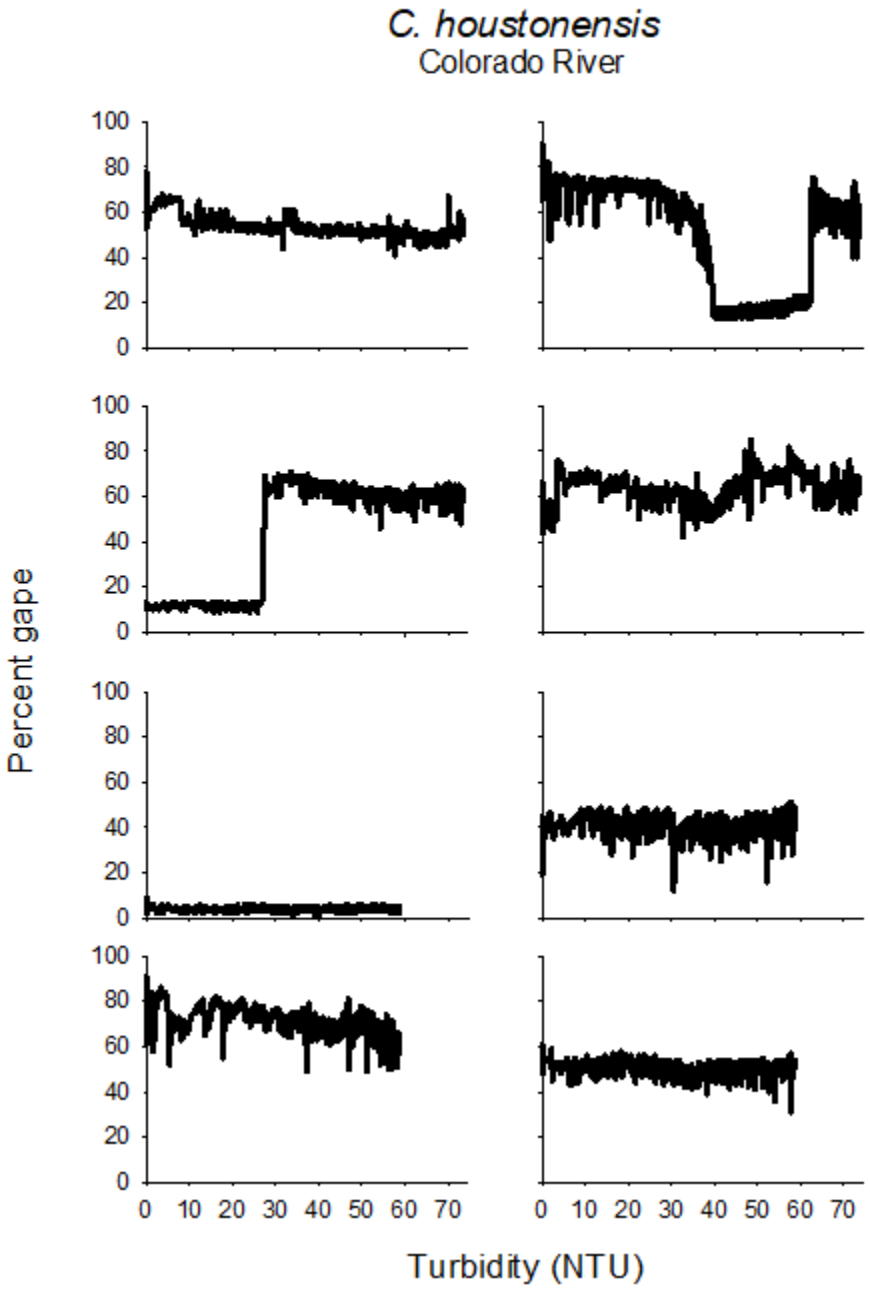

Figure 28. Mean percent gape for *C. houstonensis* from the Colorado River as turbidity increased over a ~6-hr period to a maximum of 60-75 NTU. Each graph represents a unique individual.

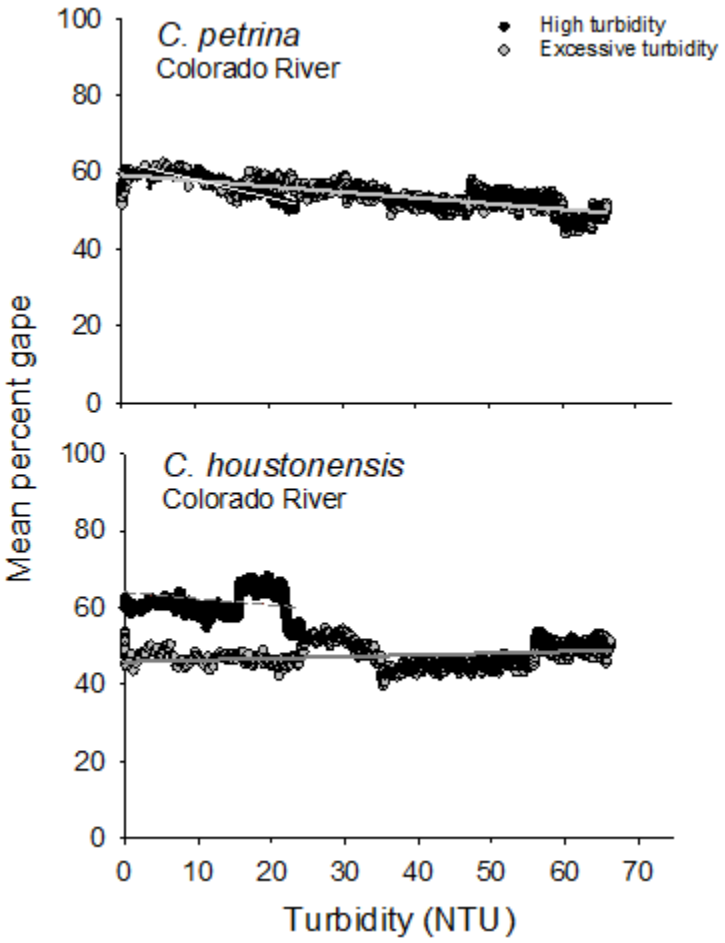

Figure 29. Mean percent gape for all individuals within each species as turbidity increased over a ~6-hr period to a high (25 NTU) or excessive (60-75 NTU) turbidity level. Solid grey lines represent linear regressions through the excessive turbidity dataset. Solid white line and dashed grey line represent linear regressions through the high turbidity datasets for top and bottom panels respectively.

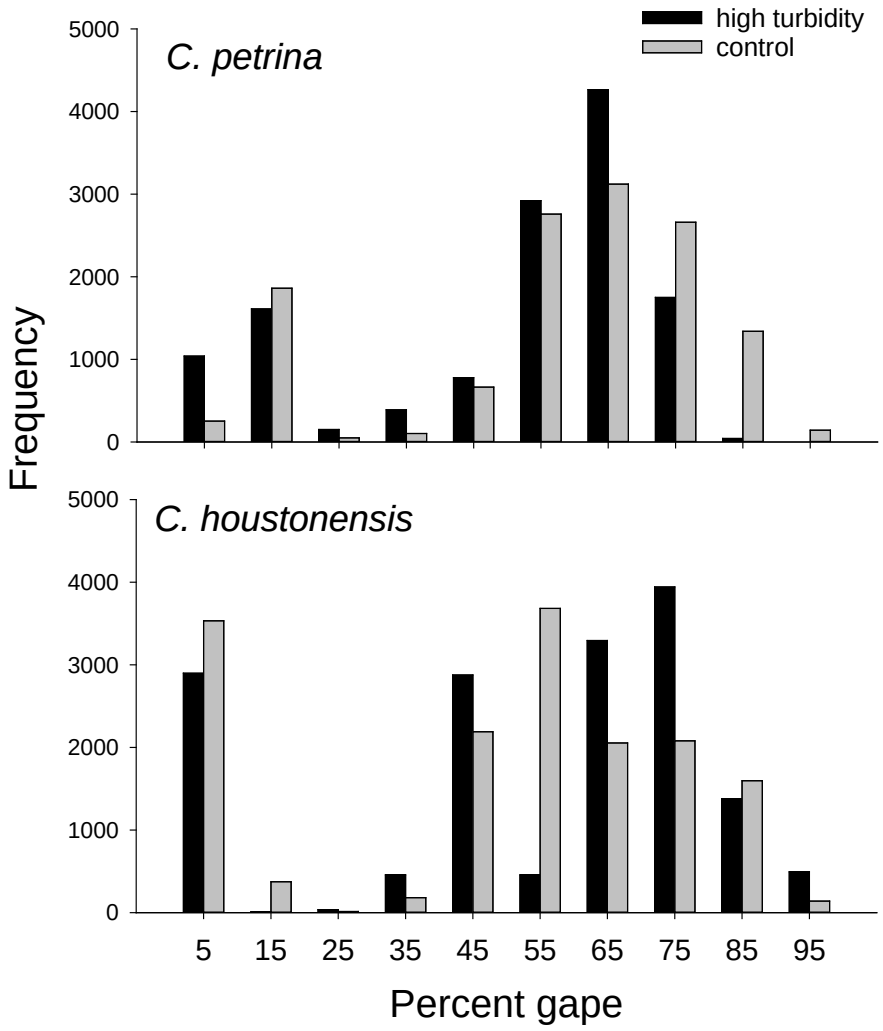

Figure 30. Frequency (# of occurrences) of a range of percent gape measurements for mussels during an initial, pre-exposure period (control: < 1 NTU) and subsequent constant turbidity period (treatment: High ~25 NTU). Only data from the same time frame (15:00 – 19:00 h) were compared between control and constant periods.

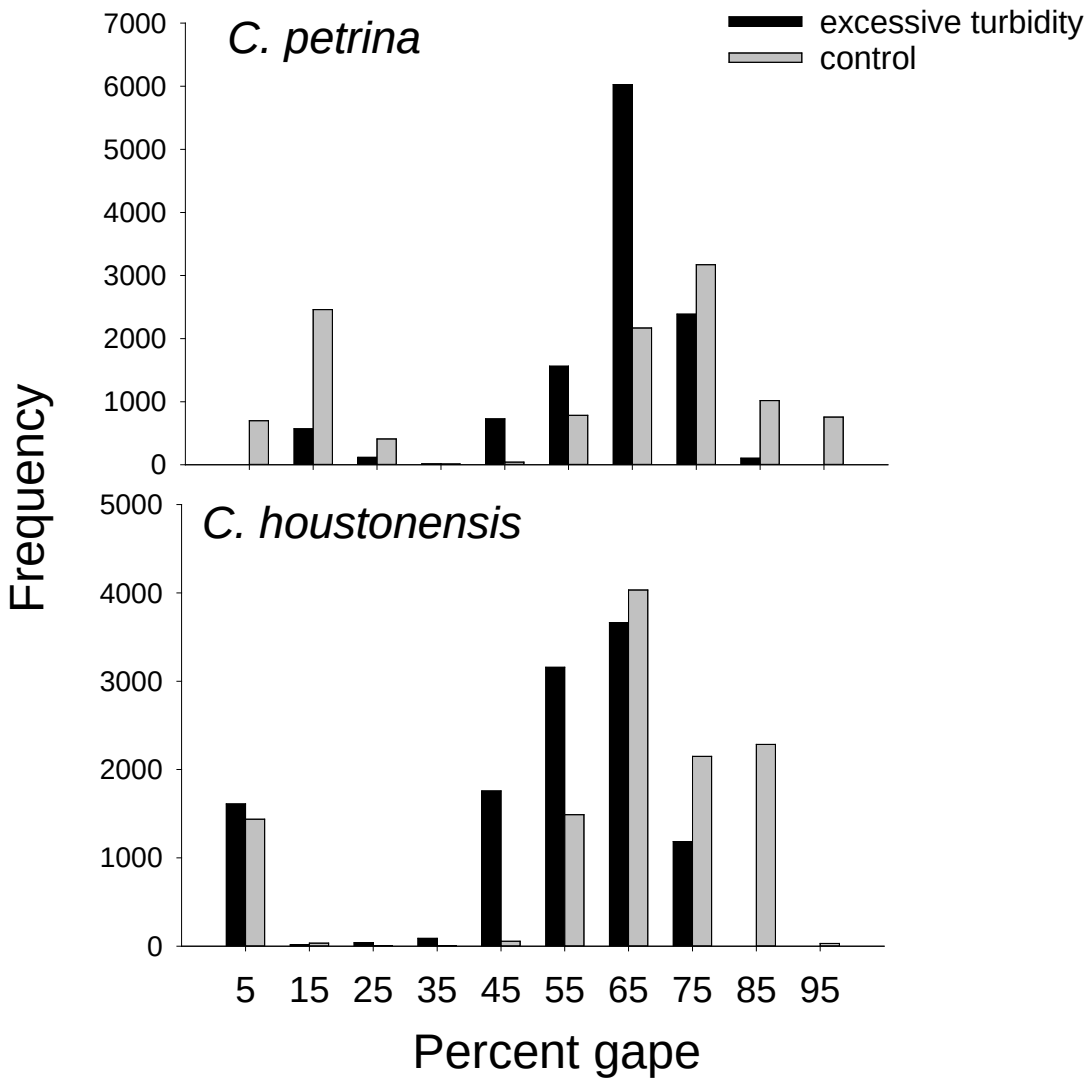

Figure 31. Frequency (# of occurrences) of a range of percent gape measurements for mussels during an initial, pre-exposure, control period (< 1 NTU) and subsequent constant turbidity period (Treatment: excessive 60-75 NTU). Only data from the same time frame (15:00 – 19:00 hrs) were compared between control and constant periods.

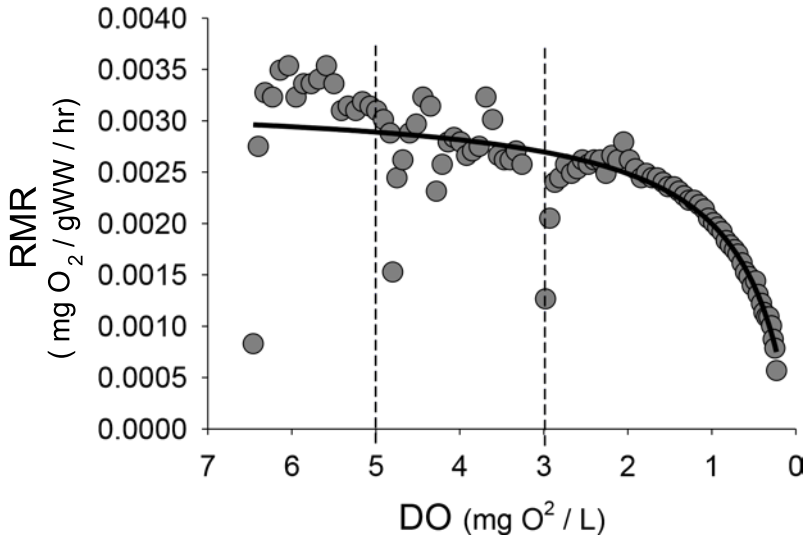

Figure 32. Typical pattern of RMR changing with declining DO when using periodic flushes to prevent excreted ammonia from accumulating in chambers. Dotted lines show when flushing occurred.

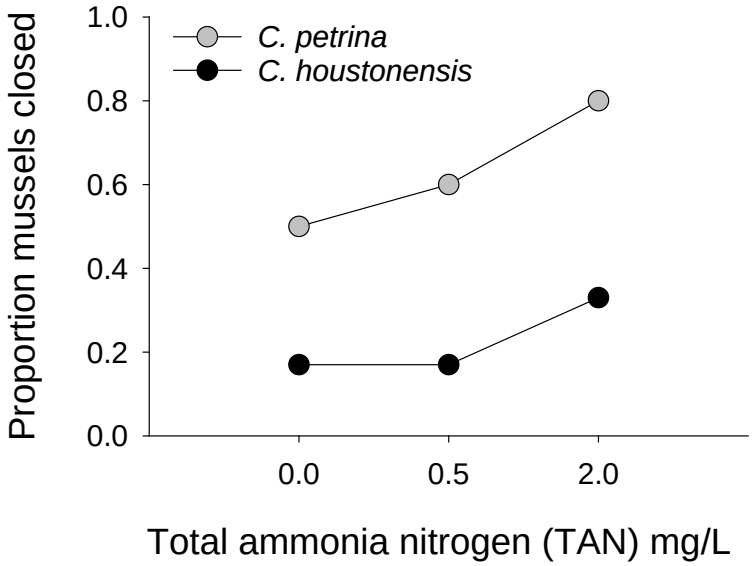

Figure 33. Proportion of mussels that exhibited at least one valve closure during respirometry at each of three TAN concentrations.

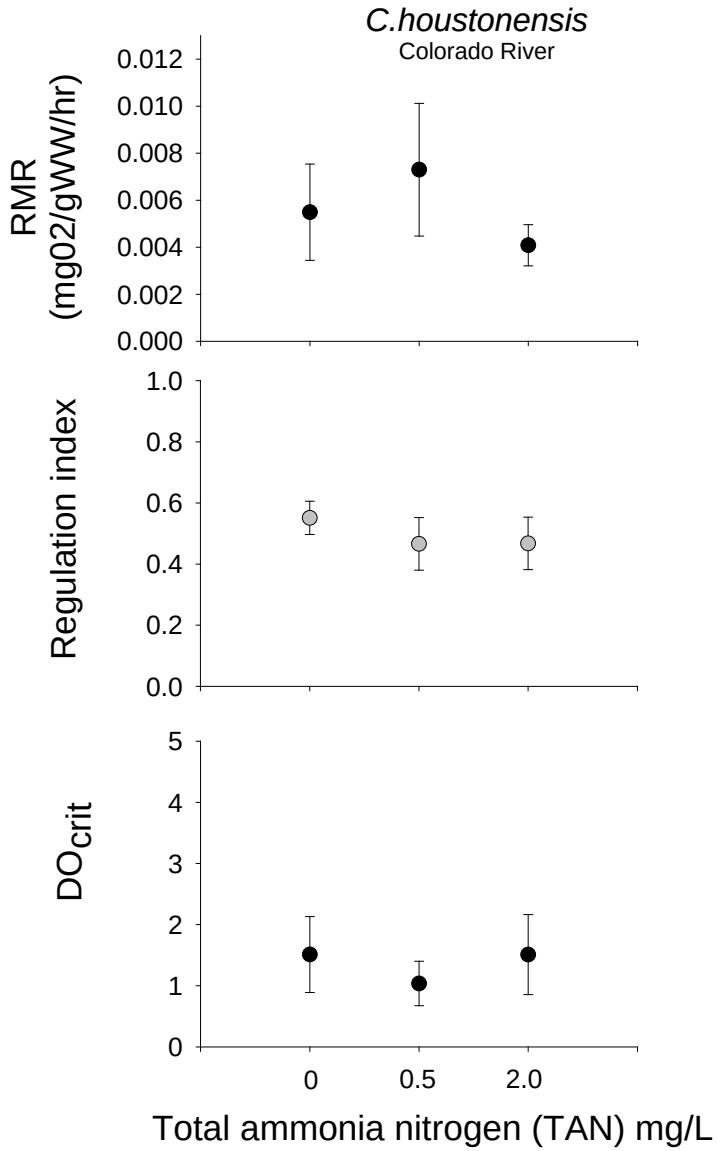

Figure 34. Mean resting metabolic rate (RMR), regulation index, and critical oxygen concentration (DO_{crit}) at three total ammonia nitrogen (TAN) concentrations. No significant differences in any response variable was found among different TAN concentrations.

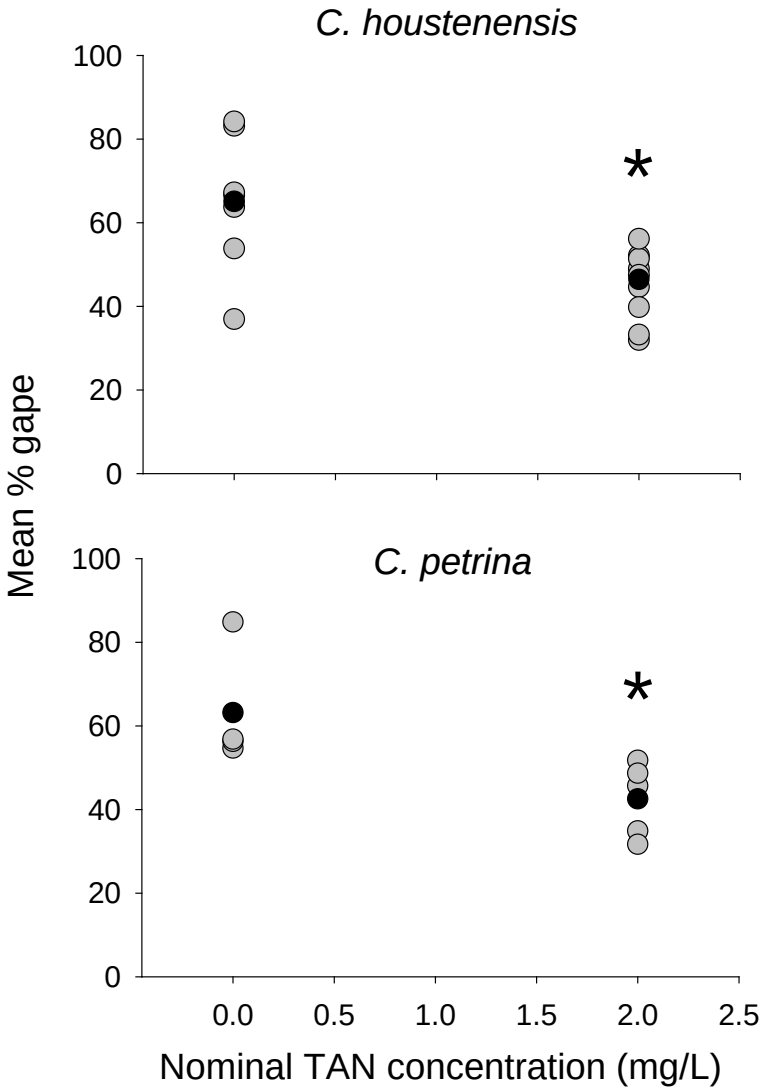

Figure 35. Mean percent gape of *C. houstonensis* and *C. petrina* during 48 hr exposure to 0.0 and 2.0 mg TAN/L. Grey circles indicate mean % gape of individual mussels. Black circles indicate mean % gape of all mussels within that group. Asterix indicates significant difference between control and treatment

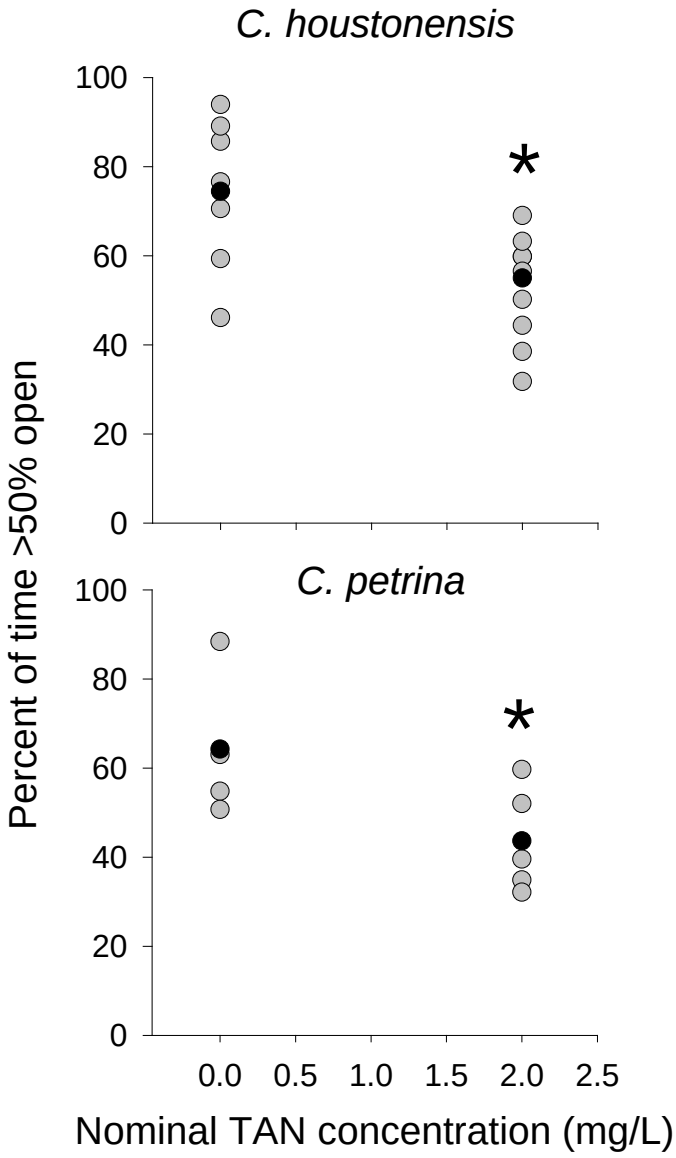

Figure 36. Percent of time mussel gape was >50% under control (0.0 mg TAN/L) and exposed (2.0 mg TAN/L) conditions over 48 hrs. Grey circles indicate percent time for individual mussels. Black circles indicate mean percent time of all mussels within that group. Asterix indicates significant difference between control and treatment.

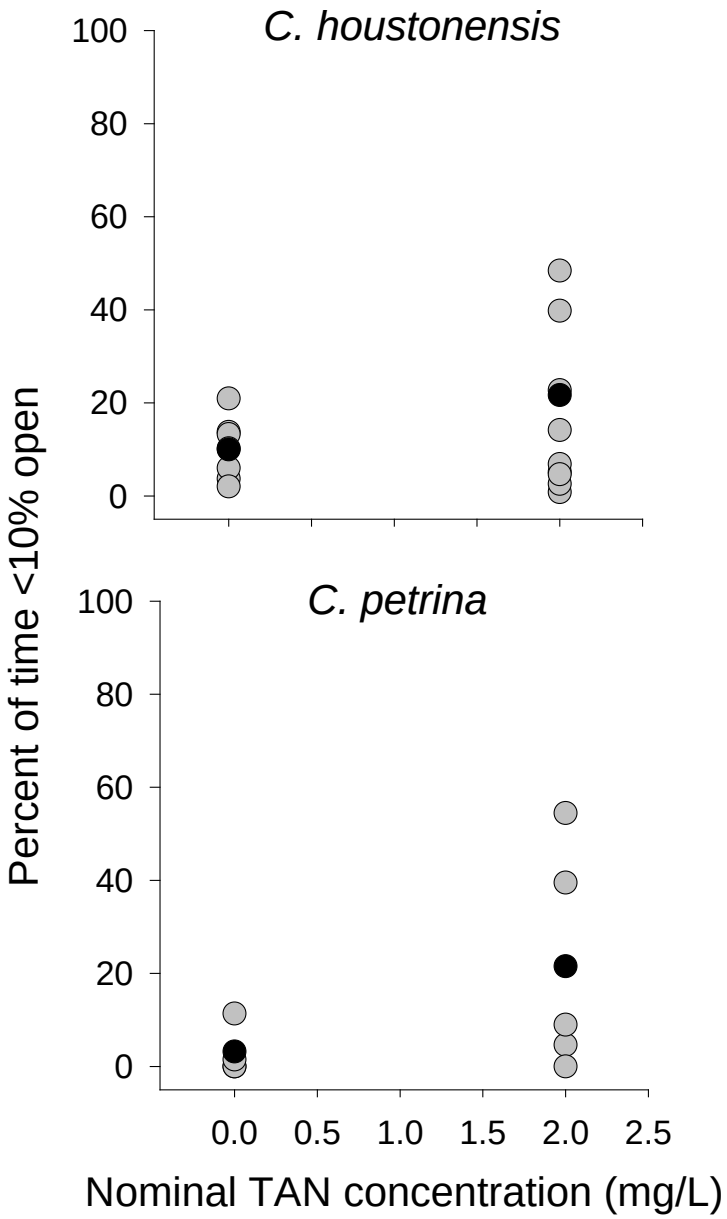

Figure 37. Percent of time mussel gape was less than 10% under control (0.0 mg TAN/L) and exposed (2.0 mg TAN/L) conditions over 48 hrs. Grey circles indicate percent time for individual mussels. Black circles indicate mean percent time of all mussels within that group. There was no significant difference between control and treatment for either species.

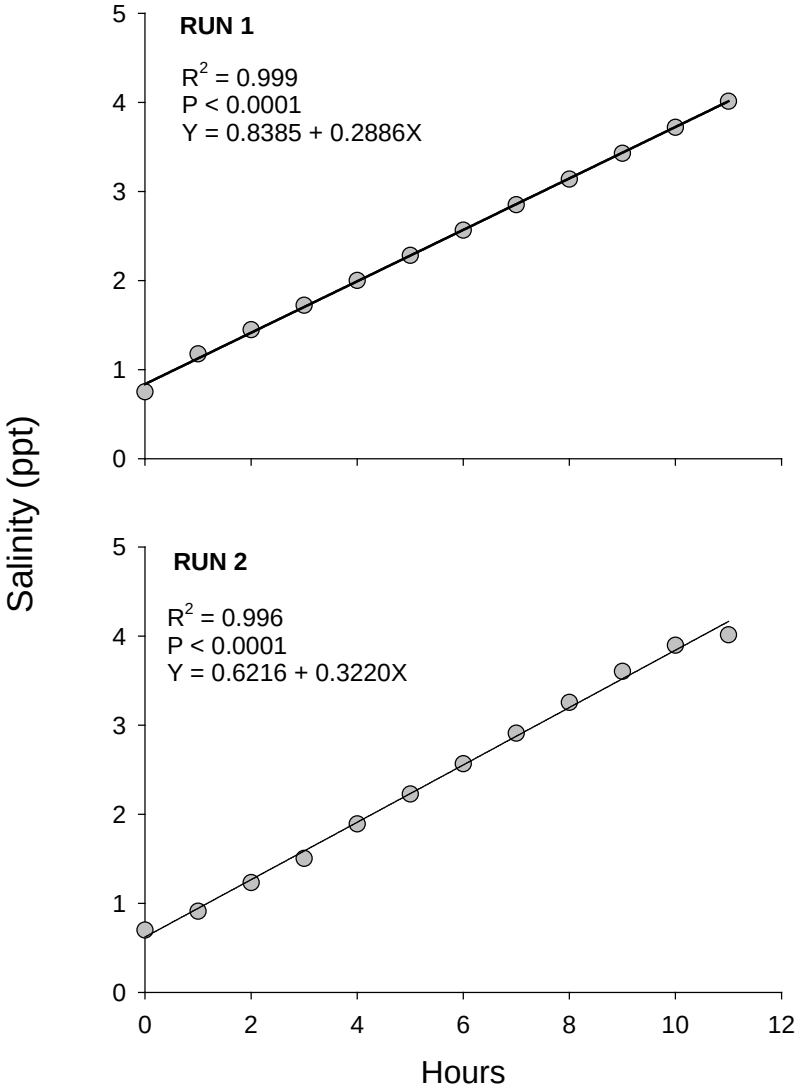

Figure 38. Increase in salinity over time for runs 1,2 of salinity experiments for *C. petrina* and *C. houstonensis* as an example of the rate of increase of salinity over time and the replicability of salinity application among runs.

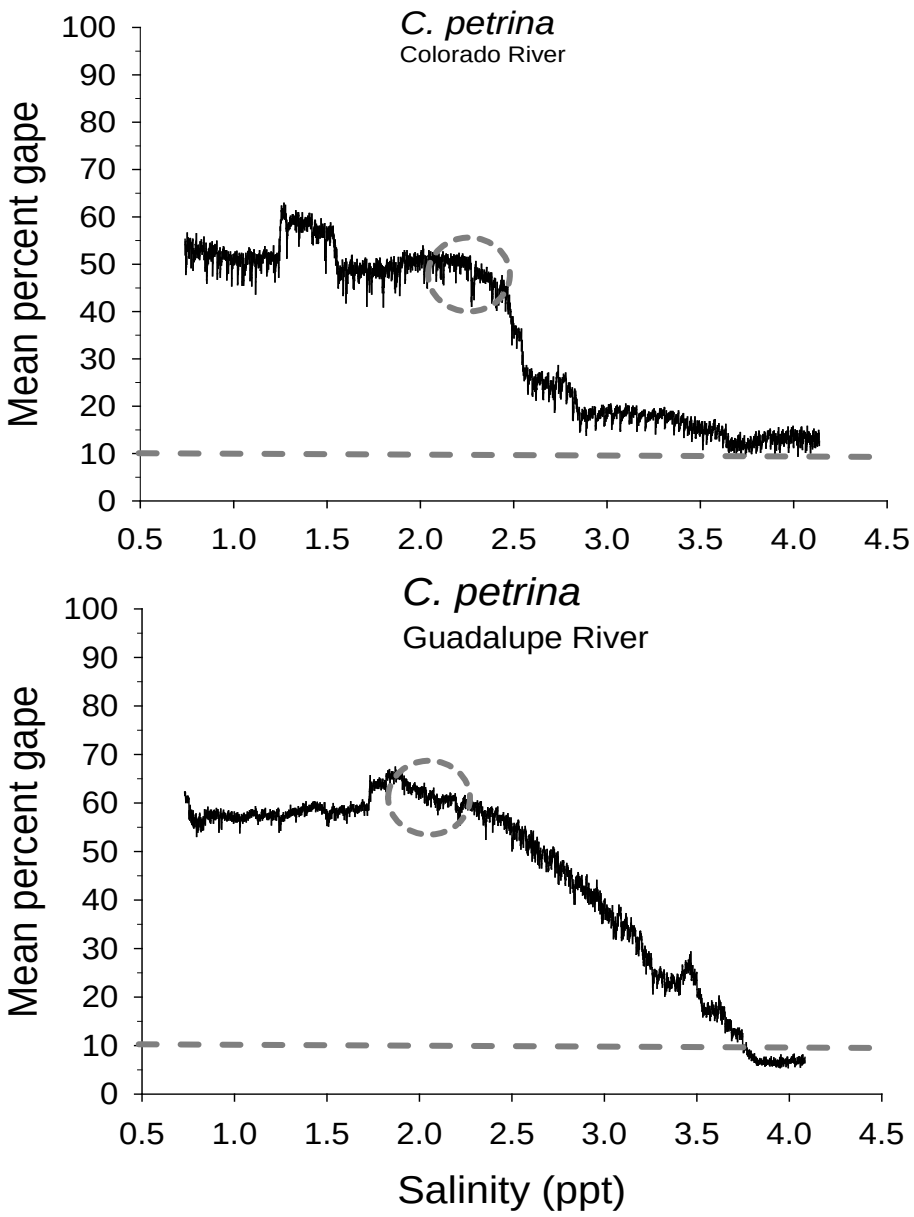

Figure 39. Change in percent gape with increasing salinity for *C. petrina* collected from the Colorado and Guadalupe Rivers. Dotted line represents the threshold for valve closure (≤ 10% gape). Dotted circle indicates the approximate salinity where percent gape begins to decrease.

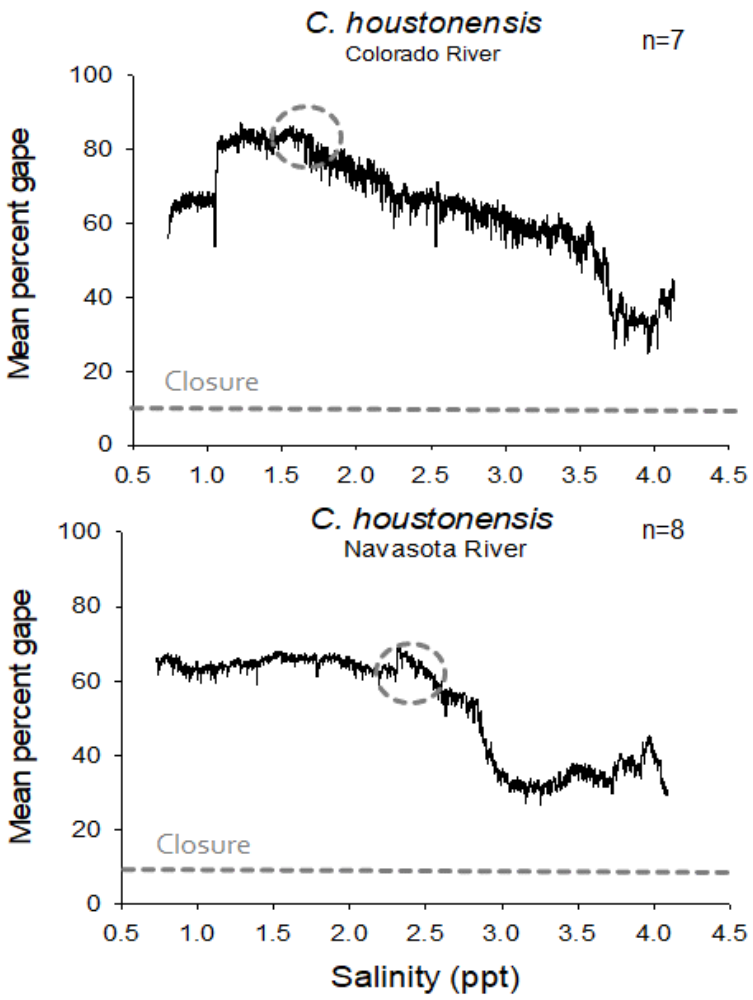

Figure 40. Change in percent gape with increasing salinity for *C. houstonensis* collected from the Colorado and Navasota Rivers. Dotted line represents the threshold for valve closure (≤ 10% gape). Dotted circle indicates the approximate salinity where percent gape begins to decrease.

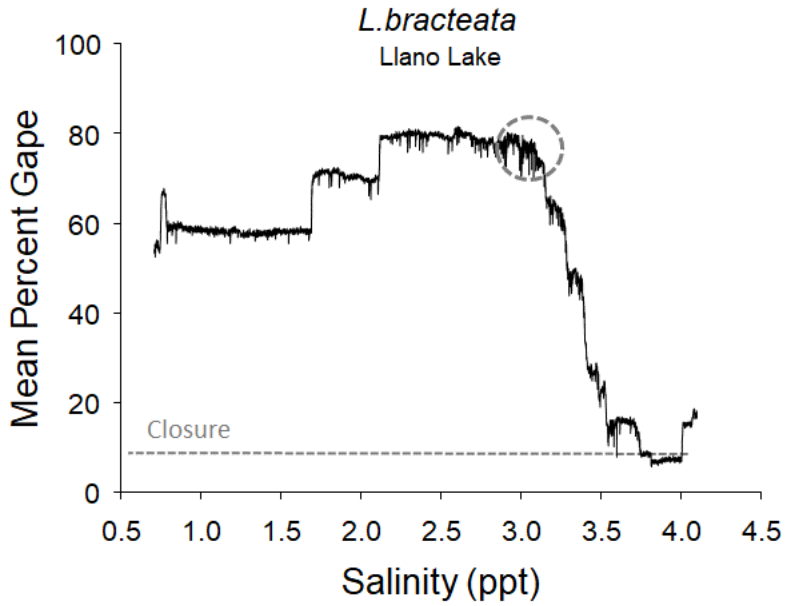

Figure 41. Change in percent gape with increasing salinity for *L. bracteata* collected from Llano Lake. Dotted line represents the threshold for valve closure (≤ 10% gape). Dotted circle indicates the approximate salinity where percent gape begins to decrease.

Task 2.4: Desiccation Tolerances and Behavioral Responses to Dewatering of Central Texas Endemic Mussels

Contributing authors: Joshua Abel, Jennifer Morton, Randy Gibson, Kenneth Ostrand
Addresses:
U.S. Fish and Wildlife Service, San Marcos Aquatic Resources Center, 500 E. McCarty Lane, San Marcos TX 78666.
Principal Investigators: Kenneth Ostrand
Email: Kenneth_Ostrand@fws.gov

During 2017, SMARC conducted desiccation studies on Texas fatmucket, *L. bracteata*, Smooth pimpleback, *C. houstenensis*, and Texas pimpleback, *C. petrina* and dewatering trials for Texas fatmucket and Texas pimpleback. During 2018, no trials were run for Texas fawnsfoot, *P. macrodon*, or false spike *F. mitchelli* due to unsuitable numbers of these rare species encountered during surveys. Surveys for adequate numbers are ongoing to complete the task.

Task 2.5. Stable isotope analysis to determine relative mussel food sources

Contributing authors: Brian Helms, Kaelyn Fogelman, Jim Stoeckel

Addresses: Department of Biological & Environmental Science, Troy University
Troy, AL 36082 (BH)
School of Fisheries, Aquaculture, and Aquatic Sciences, Auburn University, Auburn, AL 36804 (KF, JS)

Principal Investigators: Brian Helms, Jim Stoeckel

Email: helmsb@troy.edu, kjf0021@tigermail.auburn.edu, jimstoeckel@auburn.edu,

Mussels have long been considered to be suspension feeders (i.e., feeding on material suspended in the water column), with a diet comprised of phytoplankton, protozoans, detritus, bacteria, and dissolved organic carbon (Strayer et al. 2008). Suspended particulate organic matter (SPOM) in aquatic systems is a composite matrix, and previous studies using biochemical markers such as stable isotope and fatty acid analysis have elucidated prevalent components of SPOM that mussels use for food. Particularly, bacteria (Nichols & Garling 2000; Christian & Smith 2004), algae and phytoplankton (Weber et al. 2017; Raikow and Hamilton 2001) have been identified as important contributors to the freshwater mussel diet. While individual components of the mussel diet have become clearer, what they are actually assimilating from their food resources is poorly understood. Although mussels are largely considered suspension feeders, burrowing habits and associated pedal feeding (sweeping of ciliated foot through sediments) allow access to benthic food sources such as sediment-based organisms, detritus, and associated biofilms (Yeager et al. 1994; Nichols et al. 2005; Raikow and Hamilton 2001). While evidence shows that juveniles can consume benthic organic matter (Yeager et al. 1994; Haag 2012), the extent to which adult mussels utilize non-suspended food sources through pedal feeding is not fully understood.

A highly efficient method of determining mussel feeding relationships is stable isotope analysis, which compares the heavy-to-light isotopic elemental ratios of consumers to those of their potential food sources. This approach is effective in inferring both ultimate energy sources and trophic position in organisms and can help elucidate the relative assimilation of suspended or benthic food sources (Cabana and Rasmussen 1996; Raikow and Hamilton 2001; Post 2002; Christian et al. 2004; Vuorio et al. 2007; Vaughn et al. 2008; Weber et al. 2017).. Although ^{13}C of many primary producers vary, the stable C isotope ratios of consumers are similar to that of their food, reflecting the ultimate carbon source (DeNiro and Epstein 1978). However, the N pools of animals are enriched with ^{15}N relative to their food and this enrichment is on average +3.4 $^{O}/_{OO}$, i.e. 3.4 $^{O}/_{OO}$ difference in trophic levels (Deniro and Epstein 1981, Minagawa and Wada 1984). Thus ultimate energy source is estimated through carbon stable isotope ratios ($^{13}C/^{12}C$, or $\delta\,^{13}C$) and trophic position is estimated through nitrogen stable isotope signatures ($^{15}N/^{14}N$, or $\delta\,^{15}N$) (Cabana & Rasmussen 1996; Vuorio et al. 2008; Newton et al. 2013). Sulfur ($^{34}S/^{32}S$) stable isotope ratios have also been useful in marine bivalve food web studies, and can potentially separate producers when stable C and N cannot (Connolly et al. 2004). Analysis of the stable isotope signatures of potential food resources for freshwater mussels in an aquatic system, including suspended organic matter, benthic sediment containing detritus, algae, bacteria and fungi mixed with sand, detritus (decaying organic leaf material), and primary producing plants, can ultimately identify the major contributors to the mussel diet in a specific system or season.

Several drivers for population decline of endemic mussels in Texas include habitat loss and destruction through impoundments, sedimentation, dewatering, and pollution (Howells et al. 1996; Randklev et al. 2013a; Randklev et al. 2013b). The status of three Texas endemics, *Cyclonaias petrina*, *Cyclonaias houstonensis* and *Lampsilis bracteata* is currently being assessed to identify conservation needs and inform management efforts. Incomplete knowledge of mussel

food resources can inhibit successful conservation and a better understanding of mussel feeding relationships and requirements can help elucidate causes of their imperilment and inform management efforts such as propagation and relocation. Thus the objectives of this study are to 1) determine the potential food resources of focal taxa through stable isotope analysis and, 2) assess spatial and temporal variations in feeding.

Methodology

Study Sites

Study sites were chosen from previously identified sites containing beds of target mussel species (*C. houstonensis*, *C. petrina* and *L bracteata*). Sites in the Colorado River watershed were located on the lower Colorado (LC; 29.556197N, -96.402160W) near Altair, Texas and on the Llano River, a tributary of the middle Colorado River (MC; 30.39267N, -99.19214W), located near Mason, Texas. The Guadalupe River drainage was sampled on the upper Guadalupe (UG; 29.93953N, -98.94846W) in Comfort, Texas and the Brazos River was sampled on the Navasota River, a tributary of the Lower Brazos (LB, 31.15155N, -96.19501W), near Easterly, Texas.

Mussel Sampling

Each mussel species (and its respective potential food resources) was sampled from two different basins each in spring (April 2017), summer (July 2017) and fall (October 2017). *C. petrina* was sampled in the lower Colorado and upper Guadalupe Rivers, *C. houstonensis* was sampled in the lower Colorado and Navasota Rivers and *L. bracteata* was sampled in the upper Guadalupe and Llano Rivers. Ten individuals were collected per species at the site by snorkeling and searching benthic sediments by hand. Individual mussels were collected and measured for length, width, height and

weight. Mussels were opened using reverse action pliers and two sublethal tissue samples were taken from the foot using a 1.5 x 4.5 mm biopsy punch (Karl Storz 453733) (Fritts et al. 2015). Mussels were subsequently returned to the streambed where they were collected. Tissue samples were transported on ice from the field and subsequently frozen and transported to Auburn University. Tissue samples were dried at 80°C to a constant mass, ground using a mortar and pestle, weighed (nearest 10^{-5} g) and placed in 4 x 6 mm tin capsules and sent to Washington State University (WSU) Stable Isotope Core Laboratory for $\delta^{13}C$, $\delta^{15}N$, and $\delta^{34}S$ stable isotope analysis (see below).

Potential Food Source Sampling

Hypothesized food sources were suspended particulate organic matter (SPOM), fine particulate organic matter associated with benthic sediments (FPOM), and coarse particulate organic matter (CPOM). These sources were collected in spring (April 2017, May 2018), summer (July 2017) and fall (October 2017) at all four sites. To isolate the particulate organic matter (primarily phytoplankton and detritus) in the water column that mussels could utilize as a food source, 1-2 L of sample water was passed through 55 µm mesh to remove larger particles, as mussels utilize items <55 µm for food (Newton et al. 2013). The filtered water was then filtered again through a precombusted 47 cm Whatman GF/F filter (nominal pore size = 0.7 µm) using vacuum filtration. This procedure isolates suspended solids between 55 and 0.7 µm, which reflects the size fraction of identified potential food sources for mussels (Christian et al. 2004; Post 2002; Newton et al. 2013). Filters were then frozen for transportation back to Auburn University where they were dried at 80°C to a constant mass. The filters were fumigated in 3N H_3PO_4 for 8 hours to remove carbonates (Harris et al. 2000). Whole filters were sent to WSU Stable Isotope Core for analysis of stable C, N and S (see below).

Ten mid-channel benthic sediment samples for FPOM (which includes detritus, algae, bacteria and fungi mixed with sand) were collected in spring and summer in the same habitats where mussels were collected to reflect the available food resources mussels could access through pedal feeding. Five mid-channel, five bank and five bedrock surface sediment samples were taken from each site during fall sampling to further differentiate between benthic food sources being utilized. Sediment FPOM samples were prefiltered through an 80 and 55 μm sieve to remove gravel and debris larger than the previously established size fraction for potential mussel food resources. Samples were filtered through Whatman GF/F filters using vacuum filtration, frozen and transported to Auburn University as above with the SPOM filters. Samples were dried to a constant mass at 80°C and the sediment layer was then removed from the filter. Sediment was fumigated in 3N H_3PO_4 for 8 hours to remove carbonates and was then ground to a fine powder using a mortar and pestle, weighed (nearest 10^{-5} g) and encapsulated in 4 x 6 mm tin capsules and sent to WSU Stable Isotope Core for analysis of $\delta^{13}C$, $\delta^{15}N$, and $\delta^{34}S$ (see below).

Coarse particulate organic matter (CPOM, a mixture of decaying terrestrial leaf litter and organic aquatic material, i.e. "detritus") was collected from each site seasonally. Previous studies confirm that mussels produce the necessary enzymes to digest detrital food resources (Christian et al. 2004; Newton et al. 2013), and CPOM may be an important carbon source for bacteria production (Besemer et al. 2009). Additionally, filamentous algae and representative emergent (*Justicia*), submerged (*Myriophyllum*, *Alternanthera* and *Elodea*), and riparian ("grass") vascular plants were collected when present as further potential basal food resources and to provide primary producer context. Vascular algae and vascular plant samples were identified and separated in the field and all samples were frozen for transportation to Auburn University. Additionally, the microbial biofilm associated with detritus was sampled in fall 2017 from the Middle Colorado and Lower Brazos sites. In spring 2018 periphyton, epiphyton and biofilm associated with detritus was sampled. After removing the biofilm from

the associated substrate, the samples were filtered through Whatman GF/F filters using vacuum filtration. Samples were dried at 80°C to a constant dry mass, ground to a fine powder using a mortar and pestle, weighed (nearest 10^{-5} g) and placed in 4 x 6 mm tin capsules and sent for analysis of stable $\delta^{13}C$, $\delta^{15}N$, and $\delta^{34}S$. Water temperature, conductivity and pH were measured and discharge from the nearest USGS gauge was recorded at the time of sample collection for each site to inform any potential patterns identified in feeding ecology.

Stable Isotope Analysis

Stable carbon, nitrogen and sulfur isotopic analyses were conducted at Washington State University Stable Isotope Core Laboratory. Samples for carbon and nitrogen isotopic analysis are converted to N_2 and CO_2 with an elemental analyzer (ECS 4010, Costech Analytical) and the two gases are separated with a 3m GC column and analyzed with a continuous flow isotope ratio mass spectrometer (Delta PlusXP, Thermofinnigan, Bremen). Isotopic reference materials are interspersed with samples for calibration. Isotope ratios are reported in parts per thousand (‰) relative to standards (Vienna Peedee belemnite (VPDB) for carbon, atmospheric N for nitrogen and Vienna-Canyon Diablo Troilite (VCDT) for sulfur), defined in delta notation as:

$$\delta_{13}C \text{ or } \delta_{15}N \text{ or } \delta_{34}S = (R_{sample} / R_{standard} - 1) \times 10^3$$

where $R = {}^{13}C / {}^{12}C$ or ${}^{15}N / {}^{14}N$ or ${}^{34}S/{}^{32}S$ (Craig 1957, Jepsen and Winemiller 2002).

Statistical Analysis

Size data for species collected were averaged across all three seasons and compared across basins (Tables 1-3). Mean ($\bar{X}$) and standard deviation (σ) were calculated for each species across all seasons. Two-tailed *t*-tests were performed to compare length, width, height and length

of species across basins. $\delta^{13}C$ and $\delta^{15}N$ data was averaged for each species for all seasons across basins and a two-tailed *t*-test was performed to determine within species variation between seasons. We compared mussel length and stable isotope ratios with Pearson Product-Moment correlations.

To estimate feeding patterns, data initially were visually inspected using biplots. We then applied linear mixing models (IsoSource, Phillips and Greg 2003) to model the contribution of potential source materials to mussels. Since isotopic ratios of baseline resources are often different across systems, we analyzed each basin independently. We only used potential sources that were represented across all basins in IsoSource models for comparative purposes. These sources were SPOM, CPOM, FPOM and biofilm. Due to difficulties in the laboratory analysis of $\delta^{34}S$ and as a conservative measure, we constrained modeling to $\delta^{13}C$ for this report. Thus a 3 or 4 source single-isotope model was run for each mussel species for each site with a source increment set at 1% and tolerance initially set at 0.1‰ and increased incrementally (up to 2‰) until a solution was obtained. This model effectively assesses the relative contribution of CPOM, SPOM, FPOM, and biofilm to the basal carbon source(s) of mussel diet (i.e., this model may or may not reflect *direct* feeding). Reflecting this approach, and as a conservative measure, we did not correct consumer $\delta^{13}C$ in these models due to lack of information on the true trophic position of these species.

Results

Mussel Size

C. petrina was significantly larger in length, width, height and weight in the lower Colorado River compared to the upper Guadalupe River with mean length difference of 17.78 mm, width difference of 19.03 mm, height difference of 14.63 mm and weight difference of

70.31 g (two-tailed *t*-test; $p < 0.001$ for length, $p < 0.001$ for width, $p < 0.001$ for height, $p =< 0.001$ for weight) (Table 1).

C. houstonensis was significantly longer and wider in the lower Colorado River compared to the lower Brazos River basin. Mean length difference was 6.12 mm and mean width difference was 5.88 mm (two-tailed t-test; $p = 0.00094$ for length; $p = 0.00034$ for width). There was no difference found in height and weight across basins (two-tailed *t*-test; $p = 0.79$ for height, $p = 0.16$ for weight) (Table 2).

L. bracteata was significantly larger in length, width, height and weight in the upper Guadalupe compared to the middle Colorado River basin with mean length difference of 5.11 mm, width difference of 2.46 mm, height difference of 1.46 mm and weight difference of 2.77 g (two-tailed *t*-test; $p = 0.0047$ for length, $p = 0.019$ for width, $p = 0.018$ for height, $p = 0.022$ for weight) (Table 3).

Environmental Sampling

The upper Guadalupe consistently had lower water temperatures, likely due to it being a stenothermal, spring-fed system whereas the other sites are not directly under spring influence. pH had low variability across all sites and seasons. Conductivity and discharge were highest in the lower Colorado River and lowest in the lower Brazos River basin during all seasons sampled (Table 4).

Stable Isotope Analysis

Stable isotope $\delta^{13}C$ and $\delta^{15}N$ analysis was completed for mussel foot tissue, SPOM, FPOM, CPOM and primary producing plants for samples collected in spring, summer, and fall 2017. Stable isotope $\delta^{13}C$ and $\delta^{15}N$ analysis was completed for SPOM, FPOM, CPOM, and biofilm

samples collected in May 2018 (i.e., no mussels were sampled in May 2018). Laboratory analysis of $\delta^{34}S$ from all environmental samples was unsuccessful due to low sample volume causing sulfur detachment. Presumably due to the impacts of Hurricane Harvey on the lower Colorado River, only three *C. petrina* and four *C. houstonensis* were located for fall sampling, compared to the standard sampling protocol for this study of 10 individuals per species per site.

Average isotopic signatures (± SE) and C:N ratios for all sampled sources and potential resources are presented (Table 5). In general, mussels exhibited $\delta^{15}N$ enrichment and $\delta^{13}C$ depletion relative to their respective environments with minimal intraspecific variation in both $\delta^{13}C$ and $\delta^{15}N$ (Table 6, Figures 1-4). Despite this, mussel size and $\delta^{13}C$ were positively correlated for mussels in the Upper Guadalupe and Lower Colorado and $\delta^{15}N$ and size was positively correlated for *C. houstonensis* in the Upper Guadalupe (Table 7, Figure 5-7). An enrichment of $\delta^{13}C$ as mussels increase in size may reflect ontogenetic feeding shifts. For the spring, average $\delta^{13}C$ signatures for mussels ranged from -29.91‰ – -26.63‰ and average $\delta^{15}N$ ranged from 7.38‰ – 13.41‰ (Table 6). For the summer, average $\delta^{13}C$ signatures for mussels ranged from -26.45‰ – -28.83‰ and average $\delta^{15}N$ ranged from 7.28‰ – 13.38‰ (Table 6). Across seasons, mussels were more $\delta^{13}C$ enriched in the Middle Colorado basin and more $\delta^{15}N$ enriched in the Lower Colorado (Table 6). Also, where multiple species were sampled at a given site (Upper Guadalupe and Lower Colorado), all mussels had nearly identical isotopic signatures for both $\delta^{13}C$ and $\delta^{15}N$ (Table 6, Figure 1 and 2).

We observed seasonal changes in mussel isotopic signature, indicative of potential shifts in feeding and/or assimilation. There were significant changes in $\delta^{13}C$ signatures of *C. petrina* between spring and summer with a mean enrichment of 0.90 ‰ from spring to summer in the upper Guadalupe (two-tailed *t*-test; $p = 0.0015$) and a mean enrichment of 1.18‰ in the lower

Colorado (two-tailed *t*-test; $p < 0.001$). *C. houstonensis* also had significant changes of $\delta^{13}C$ between spring and summer with a mean enrichment of 1.54 ‰ in the lower Colorado (two-tailed *t*-test; $p = 0.0021$) and a mean enrichment of 0.84 ‰ in the lower Brazos basin (two-tailed *t*-test; $p = 0.0021$). There were no seasonal differences in $\delta^{13}C$ of *L. bracteata* in the Upper Guadalupe (two-tailed *t*-test; $p = 0.58$) or in the middle Colorado basin (two-tailed *t*-test; $p = 0.35$). There were no seasonal differences in the $\delta^{15}N$ signatures of any species in any basin (two-tailed *t*-test; $p > 0.05$).

Linear Mixing Models

Linear mixing models revealed that food resources are comprised primarily of materials with a carbon base of CPOM (i.e., benthic detritus) and attached biofilm, and to a lesser extent SPOM (i.e., seston) and FPOM (i.e., sediment deposits). All mussels and all seasons had high proportions of CPOM contributions, with the exception of *L. bracteata* in the Middle Colorado basin during spring 2017. In general, there was little seasonal variation in dietary contributions of basal C resources, with the exception of *C. houstonensis* in the Lower Brazos basin, which showed a decreased reliance on CPOM in the summer, and *L. bracteata* in the Middle Colorado, which showed a shift from SPOM to CPOM contributions (Table 8, Figure 8). It should be noted that mussel stable isotope ratios remained largely consistent throughout seasons within a given system, but basal resource signatures were often variable between seasons. Thus linear mixing models likely reflect less of a feeding shift in mussels and more of a changing food base offering insight on the timing of assimilation. Also, several models were only attainable after increasing tolerance above reliable levels (up to 2‰). These included *C. petrina* in the Upper Guadalupe during the summer and *L. bracteata* in the Upper Guadalupe in the spring and summer. These

seasonal models should be interpreted with caution. Other models had tolerance levels set at 0.1‰.

For *C. houstonensis*, the mean dietary contribution of CPOM ranged from a low of 36.8% in the Lower Brazos basin during the Fall to 96% in the Lower Colorado basin during the summer (Table 8). FPOM-based and SPOM-based food sources represented slightly higher proportions of total during the summer in the Lower Brazos. Further, biofilms appear to be an important C course during the Fall, representing 36% of dietary contribution (although it should be noted that these sources were not sampled in the spring and summer). In the Lower Colorado, *C. houstonensis* had somewhat higher contributions of SPOM than FPOM in the spring and summer, but this was still <5% on average of total dietary contribution (Table 8, Figure 8). Biofilm was less than 10% total dietary contribution in spring 2018.

For *C. petrina*, the mean dietary contribution of CPOM ranged from a low of 93% during the spring 2018 in the Lower Colorado to 99% in the Upper Guadalupe, in spring 2017 (Table 8). FPOM-based food sources contributed near 1% in the Lower Colorado in all seasons and less than 1% in the Upper Guadalupe in all seasons. In the Lower Colorado, SPOM contributed on average 3 - 4.9% to total *C. petrina* diet and only 1 – 5.5% to total diet in the Upper Guadalupe (Table 8, Figure 8). Biofilm contributed 2.1% in the Lower Colorado and 6.3% in the Upper Guadalupe.

The contribution of CPOM based carbon for *L. bracteata* was more variable than for the other mussel species, with a high of 100% in the Upper Guadalupe in the summer to 2% in the Middle Colorado basin during spring 2017. The contribution of FPOM was similarly low for *L. bracteata* in all seasons and both systems, with averages ranging from 0 in the Upper Guadalupe to 9.9% in the Middle Colorado basin during the fall. The dietary contribution of SPOM based sources ranged from 0 in the Upper Guadalupe in the summer to 97.8% in the Middle Colorado

basin during the spring (Table 8, Figure 8). The dietary contribution of biofilm was 37% during the fall in the Middle Colorado but only 6.9% during spring 2018.

Brief Interpretation

These data reflect samples from spring 2017, summer 2017, fall 2017, and spring 2018 ($\delta^{13}C$ and $\delta^{15}N$, no sulfur). Sulfur results were unreliable for interpretation due to the low sulfur background levels in these systems. Several conclusions can be drawn from these data. First, all three species appear to feed similarly. This is evidenced by the consistent stable C and N signatures across systems, and particularly the nearly identical signatures of *L. bracteata* and *C. petrina* in the Upper Guadalupe, and *C. petrina* and *C. houstonensis* in the Lower Colorado. The only deviation from this similarity is *L. bracteata* in the Middle Colorado, which displayed a relatively less-enriched $\delta^{15}N$ pattern. This characterization was from the Llano River, and whether this reflects differential feeding or simply is a system artifact is unclear at this point. Also, all three species showed a general trend to become carbon-enriched with increasing body size. This could reflect the inherent shift in diet from the parasitic glochidial stage thru adulthood. However, these trends were found in mussels in the Upper Guadalupe and Lower Colorado, but not the Middle Colorado basin and Lower Brazos basin, so that, again, is a system artifact cannot be ruled.

From the data presented, with the exception of *L. bracteata* in the Middle Colorado basin during the summer, a major interpretation is that a majority of the carbon assimilated by all species is derived from CPOM. Whether this is direct feeding on CPOM particles or associated bacteria and fungi is not clear. The contribution of biofilms, which is typically low but can be as high as 1/3 dietary carbon, as well as the generally elevated $\delta^{15}N$ signature of mussels, further suggests a significant role of bacteria and fungi in assimilated tissue. Further, the role of SPOM

(i.e, suspended producers and other associated organics) and FPOM (benthic diatoms, algae, and organic matter associated with sediment) seem to play a much more minor role in contribution to dietary C as compared to CPOM and biofilm. This could be interpreted as a reduced dietary reliance on filter-feeding phytoplankton and pedal feeding in sediments. However, it should be noted that mussels in general showed minimal (albeit statistically significant) seasonal variation, while food sources often showed considerable variation. Although it cannot be ruled out that we failed to fully capture the true C sources for mussel food, our data indicates these species assimilate food resources that are produced seasonally and that generally are derived from a carbon source corresponding to CPOM.

References

Besemer, K, I Hodl, G Singer, and TJ Battin. 2009. Architectural differentiation reflects bacterial community structure in stream biofilms. The ISME Journal 3: 1318-1324

Cabana, G, and JB Rasmussen. 1996. Comparison of aquatic food chains using nitrogen isotopes. Proceedings of the National Academy of Science. 93: 10844-10847.

Christian, AD, BN Smith, DJ Berg, JC Smoot, and RH Findlay. 2004. Trophic position and potential food sources of 2 species of unionid bivalves (Mollusca:Unionidae) in 2 small Ohio streams. Journal of the North American Benthological Society. 23(1): 101-113.

Craig, H. 1957. Isotopic Standards for Carbon and Oxygen and Correction Factors for MassSpectrometric Analysis of Carbon Dioxide. Geochimica et Cosmochimica Acta. 12: 133-149.

Connolly, RM, MA Guest, AJ Melville, and JM Oakes. 2004. Sulfur stable isotopes separate producers in marine food-web analysis. Oceologia. 138(2): 161-167.

DeNiro, MJ, and S Epstein. 1978. Influence of diet on the distribution of carbon isotopes in animals. Geochemica et Cosmochimica Acta. 42: 495-506.

Deniro, MJ, and S Epstein. 1981. Influence of diet on the distribution of nitrogen isotopes in animals. Geochimica et Cosmochimica Acta. 45: 341-351.

Fritts, AK, JT Peterson, PD Hazelton, and RB Bringolf. 2015. Evaluation of methods for assessing physiological biomarkers of stress in freshwater mussels. Canadian Journal of Fisheries and Aquatic Sciences. 72(10): 1450-1459.

Gangloff, MM, and JW Feminella. 2007. Stream channel geomorphology influences mussel abundance in southern Appalachian streams, USA. Freshwater Biology. 52: 64-74.

Haag, WR. 2012. North American Freshwater Mussels. New York, NY: Cambridge University Press.

Harris, D, RH Williams, and C van Kessel. 2000. Acid fumigation of soils to remove carbonates prior to total organic carbon or CARBON-13 isotopic analysis. Soil Science of America Journal. 65(6): 1853-1856.

Howard, JK, and KM Cuffey. 2006. The functional role of native freshwater mussels in the fluvial benthic environment. Freshwater Biology. 51: 460-474.

Howells, RG, RW Neck, and HD Murray. 1996. Freshwater mussels of Texas. Austin, TX: Texas Parks and Wildlife Press.

Jepsen, DB, and KO Winemiller. 2002. Structure of tropical river food webs revealed by stable isotope ratios. Oikos. 96: 46-55.

Minagawa, M, and E Wada. 1984. Stepwise enrichment of ^{15}N along food chains: Further evidence and the relation between $d^{15}N$ and animal age. Geochemica et Cosmochimica Acta. 48: 1135-1140.

Nichols, SJ, and D Garling. 2000. Food-web dynamics and trophic-level interactions in a multi-species community of freshwater unionids. Canadian Journal of Zoology. 78: 871-882.

Nichols, SJ, H Silverman, TH Dietz, JW Lynn, and DL Garling. 2005. Pathways of food uptake in native (Unionidae) and introduced (Corbiculidae and Dreissenidae) freshwater bivalves. Journal of Great Lakes Research. 31: 87-96.

Newton, TJ, CC Vaughn, DE Spooner, J Nichols, and MT Arts. 2013. Profiles of Biochemical Tracers in Unionid Mussels Across a Broad Geographical Range. Journal of Shellfish Research. 32(2): 497-507.

Phillips, DL, and JW Gregg. 2003. Source partitioning using stable isotopes: coping with too many sources. Oecologia. 136: 261-269.

Post, DM. 2002. Using stable isotopes to estimate trophic position: models, methods and assumptions. Ecology. 83(3): 703-718.

Raikow, DF, and SK Hamilton. 2001. Bivalve diets in a Midwestern U.S. stream: A stable isotope enrichment study. Limnology and Oceanography. 46(3): 514-522.

Randklev, CR, MS Johnson, ET Tsakiris, J Groce, and N Wilkins. 2013a. Status of the freshwater mussel (Unionidae) communities of the mainstem of the Leon River, Texas. Aquatic Conservation: Marine and Freshwater Ecosystems. 23: 390-404.

Randklev, CR, ET Tsakiris, MS Johnson, JA Skorupski, LE Burlakova, J Groce, and N Wilkins. 2013b. Is False spike, *Quadrula mitchelli* (Bivalvia: Unionidae), extinct? First account of a very recently deceased individual in over thirty years. Southwestern Naturalist. 58(2): 247-249.

Silverman, H, SJ Nichols, JS Cherry, E Archberger, JW Lynn, and TH Dietz, 1997. Clearance of laboratory-cultured bacteria by freshwater bivalves: differences between lentic and lotic unionids. Canadian Journal of Zoology. 75: 1857-1866.

Strayer, DL. 2008. Freshwater Mussel Ecology. Berkeley, CA: University of California Press.

Strayer, DL, NF Caraco, JJ Cole, S Findley, and ML Pace. 1999. Transformation of freshwater ecosystems by bivalves. BioScience. 49: 19-27.

Strayer, DL, JA Downing, WR Haag, TL King, JB Layzer, TJ Newton, and S Nichols. 2004. Changing perspectives on pearly mussels, North America's most imperiled animals. BioScience. 54: 429-439.

Spooner, DE, and CC Vaughn. 2006. Context-dependent effects of freshwater mussels on the benthic community. Freshwater Biology. 51: 1016-1024.

Vaughn, CC, KB Gido, and DE Spooner. 2004. Ecosystem processes performed by unionid mussels in stream mecocosms: species roles and effects of abundance.

Hydrobiologia. 527: 35-47.

Vaughn, CC and CC Hakenkamp. 2001. The functional role of burrowing bivalves in freshwater ecosystems. Freshwater Biology. 46: 1431-1446.

Vaughn, CC, SJ Nichols, and DE Spooner. 2008. Community and foodweb ecology of freshwater mussels. Journal of the North American Benthological Society. 27(2): 409-423.

Vuorio, K, M Tarvainen, and J Sarvala. 2008. Unionid mussels as stable isotope baseline indicators for long-lived secondary consumers in pelagic food web comparisons. Fundamental and Applied Limnology. 169(3): 237-245.

Weber, AM, JE Bauer, and GT Watter. 2017. Assessment of nutritional subsidies to freshwater mussels using a multiple natural abundance isotope approach. Freshwater Biology. 62: 615-629.

Williams, JD, AE Bogan, JT Garner. 2008. Freshwater Mussels of Alabama & the Mobile Basin. Tuscaloosa, AL: University of Alabama Press.

Winemiller, K, NK Lujan, RN Wilkins, RT Snelgrove, AM Dube, KL Skow, and AG Snelgrove. 2010. Status of Freshwater Mussels in Texas. College Station, TX: Texas A&M Department of Wildlife and Fisheries Sciences and Texas A&M Institute of Renewable Natural Resources.

Yeager, MM, DS Cherry, and RJ Neves. 1994. Burrowing behaviors of juvenile rainbow mussels, *Villosa iris* (Bivalvia: Unionidae). Journal of the North American Benthological Society. 13(2): 217-222.

Table 1. Size data for *C. petrina* sampled in the upper Guadalupe River and the lower Colorado River. Note significant p-values in bold (two-tailed t-test with unequal variance).

	Upper Guadalupe		**Lower Colorado**		
C. petrina	$\bar{X}$	σ	$\bar{X}$	σ	*p*
Length (mm)	48.12	5.19	65.90	10.12	**<0.001**
Width (mm)	33.46	4.55	52.49	7.41	**<0.001**
Height (mm)	18.83	2.75	33.46	4.84	**<0.001**
Weight (g)	18.40	7.02	88.71	41.61	**<0.001**

Table 2. Size data for *C. houstonensis* sampled in the lower Colorado River and the lower Brazos River basin. Note significant p-values in bold (two-tailed t-test with unequal variance).

	Lower Colorado		**Lower Brazos**		
C. houstonensis	$\bar{X}$	σ	$\bar{X}$	σ	*p*
Length (mm)	50.34	7.07	44.22	4.97	**<0.001**
Width (mm)	44.46	5.88	38.58	5.14	**<0.001**
Height (mm)	28.10	3.54	27.83	3.86	0.79
Weight (g)	44.61	18.9	37.52	14.16	0.16

Table 3. Size data for *L. bracteata* sampled in the upper Guadalupe River and the middle Colorado River basin. Note significant p-values in bold (two-tailed t-test with unequal variance).

	Upper Guadalupe		**Middle Colorado**		
L. bracteata	$\bar{X}$	σ	$\bar{X}$	σ	*p*
Length (mm)	50.69	4.53	45.58	8.39	**0.0047**
Width (mm)	32.13	3.21	29.67	4.50	**0.019**
Height (mm)	19.26	1.83	17.80	2.70	**0.018**
Weight (g)	15.12	4.40	12.33	4.56	**0.022**

Table 4. Seasonal environmental data collected at sites in spring, summer and fall of 2017 and spring 2018 during mussel and food source sampling.

Season	Site	Water Temp (ºC)	pH	Conductivity (*µ*s/cm)	Discharge (cfs)
Upper Guadalupe	Spring '17	22.6	8.3	471	125
	Summer '17	26.5	8.4	497	55
	Fall '17	16	8.7	510	56
	Spring '18	24.5	8.4	454	52.2
Lower Colorado	Spring '17	24.5	8.5	500	1310
	Summer '17	32.7	9.2	584	1225
	Fall '17	20.6	8.4	765	1230
	Spring '18	29.4	8.9	549	1148
Middle Colorado	Spring '17	24.1	7.9	329	138
	Summer '17	31.5	8.7	354	88.7
	Fall '17	19.7	8.5	388	60
	Spring '18	25.2	8.2	198	68.7
Lower Brazos	Spring '17	21.7	7.5	340	38
	Summer '17	27.7	7.9	283	23
	Fall '17	12.7	8.3	248	11
	Spring '18	27.6	7.9	20	15

Table 5. Stable isotope values for all consumers and potential food source samples. Dashes represent unsampled sources at a given location, often due to its absence in the sampling area. Sources are defined in text.

		Spring 2017			Summer 2017			Fall 2017			Spring 2018		
Basin	**Source**	**δ^{13}C ± SE**	**δ^{15}N ± SE**	**C:N**	**δ^{13}C ± SE**	**δ^{15}N ± SE**	**C:N**	**δ^{13}C ± SE**	**δ^{15}N ± SE**	**C:N**	**δ^{13}C ± SE**	**δ^{15}N ± SE**	**C:N**
Upper Guadalupe	*C. petrina*	-29.21 ± 0.18	11.15 ± 0.17	3.76	-28.31 ± 0.11	10.96 ± 0.05	3.66	-28.27 ± 0.18	11.14 ± 0.07	3.79	-	-	-
	L. bracteata	-28.95 ± 0.22	11.06 ± 0.13	3.89	-28.78 ± 0.19	10.75 ± 0.19	7.81	-28.04 ± 0.16	11.12 ± 0.11	3.55	-	-	-
	SPOM	-24.84 ± 0.29	2.75	8.94	-17.30 ± 0.15	6.34 ± 1.42	14.71	-15.17 ± 0.61	3.80 ± 2.87	20.52	-16.85 ± 0.24	8.76 ± 1.41	14.86
	CPOM	-29.26 ± 0.31	1.85 ± 0.85	42.99	-28.14	3.00	15.33	-27.91	3.23	36.48	-29.00 ± 0.42	5.74 ± 0.57	24.50
	FPOM	-9.53 ± 0.19	4.86 ± 0.09	38.01	-10.86 ± 0.16	8.48 ± 0.11	33.17	-10.40 ± 0.08	8.02 ± 0.07	34.25	-11.31 ± 0.11	8.63 ± 0.09	29.63
	Biofilm	-	-	-	-	-	-	-	-	0.05	-18.24 ± 1.87	7.31 ± 0.44	22.08
	Periphyton	-	-	-	-	-	-	-	-	-	-11.41 ± 0.03	9.17 ± 0.13	26.60
	Epiphyton	-	-	-	-	-	-	-	-	-	-14.86 ± 0.22	8.81 ± 0.21	19.37
	Grass	-	-	-	-30.36	5.47	25.48	-	-	-	-	-	-
	Justicia	-25.79 ± 0.26	8.41 ± 0.32	11.05	-26.26	8.32	14.40	-29.22	12.6	10.31	-	-	-
	Myriophyllum	-29.16 ± 0.15	10.29 ± 0.47	16.47	-	-	-	-27.21	10.01	19.07	-	-	-
Lower Colorado	*C. petrina*	-29.86 ± 0.12	13.41 ± 0.14	3.91	-28.68 ± 0.14	13.38 ± 0.29	9.77	-30.34 ± 0.33	11.82 ± 0.56	4.01	-	-	-
	C. houstonensis	-29.91 ± 0.25	13.10 ± 0.28	3.97	-28.83 ± 0.12	12.71 ± 0.13	8.61	-30.01 ± 0.34	12.33 ± 0.59	3.92	-	-	-
	SPOM	-24.49 ± 1.11	2.35 ± 0.26	9.56	-22.30 ± 0.13	8.47 ± 0.22	8.15	-23.37 ± 0.94	8.23 ± 0.49	1.09	-20.81 ± 0.39	5.67 ± 0.99	7.77
	CPOM	-29.58 ± 0.48	4.70 ± 0.89	29.57	-29.10	10.97	16.16	-28.54	6.81	34.57	-27.54 ± 0.13	4.58 ± 0.63	22.41
	FPOM	-12.63 ± 0.24	3.86 ± 0.18	21.51	-13.95 ± 0.11	7.79 ± 0.17	29.51	-13.95 ± 0.83	5.83 ± 0.24	17.06	-12.59 ± 0.25	6.65 ± 0.19	21.47
	Biofilm	-	-	-	-	-	-	-	-	14.52	-16.45 ± 0.75	7.78 ± 0.43	13.27
	Periphyton	-	-	-	-	-	-	-	-	-	-13.16 ± 0.24	8.08 ± 0.42	15.03
	Epiphyton	-	-	-	-	-	-	-	-	-	-16.65 ± 0.29	6.83 ± 0.47	12.60
	Grass	-30.54 ± 0.04	10.92 ± 0.16	20.16	-13.78	8.68	9.82	-29.17	9.73	18.99	-	-	-
	Justicia	-	-	-	-	-	-	-	-	-	-	-	-
	Myriophyllum	-	-	-	-27.97 ± 2.04	10.25 ± 3.14	12.16	-	-	-	-	-	-
	Alternanthera	-	-	-	-	-	-	-28.41	12.88	15.04	-	-	-
	Elodea	-	-	-	-	-	-	-15.09	9.38	32.04	-	-	-
	Algae	-	-	-	-19.70	2.17	21.75	-24.6	9.55	8.16	-	-	-

Table 5. (continued)

		Spring 2017			Summer 2017			Fall 2017			Spring 2018		
Basin	**Source**	**δ^{13}C ± SE**	**δ^{15}N ± SE**	**C:N**	**δ^{13}C ± SE**	**δ^{15}N ± SE**	**C:N**	**δ^{13}C ± SE**	**δ^{15}N ± SE**	**C:N**	**δ^{13}C ± SE**	**δ^{15}N ± SE**	**C:N**
Middle Colorado	*L. bracteata*	-26.63 ± 0.16	7.38 ± 0.16	3.75	-26.45 ± 0.11	7.28 ± 0.08	9.47	-25.60 ± 0.16	7.18 ± 0.11	3.72	-	-	-
	SPOM	-22.92 ± 0.44	0.24 ± 0.52	10.26	-19.02 ± 0.32	2.88 ± 0.67	15.26	-18.09 ± 0.40	0.56 ± 3.08	19.62	-18.61 ± 0.41	2.47 ± 1.44	15.84
	CPOM	-20.85 ± 1.73	5.67 ± 1.20	23.61	-28.26	0.48	16.16	-30.09	3.13	61.37	-26.52 ± 2.26	1.754 ± 1.08	34.89
	FPOM	-11.11 ± 0.05	3.34 ± 0.12	36.43	-11.01 ± 0.08	5.30 ± 0.10	38.75	-11.40 ± 0.27	4.46 ± 0.11	34.28	-10.01 ± 0.12	4.74 ± 0.04	42.47
	Biofilm	-	-	-	-	-	-	-27.96	3.23	31.08	-16.10 ± 1.15	4.93 ± 0.17	24.23
	Periphyton	-	-	-	-	-	-	-	-	-	-11.39 ± 0.36	5.25 ± 0.31	27.08
	Epiphyton	-	-	-	-	-	-	-	-	-	-12.28 ± 0.69	5.32 ± 0.19	27.38
	Grass	-28.81 ± 0.34	4.97 ± 0.18	22.10	-26.50	1.17	9.77	-22.86	5.63	21.13	-	-	-
	Justicia	-15.74 ± 0.34	6.06 ± 0.16	22.13	-22.97	5.57	8.71	-13.98	3.37	22.37	-	-	-
	Myriophyllum	-25.00 ± 0.38	3.40 ± 0.27	16.10	-18.89 ± 4.60	2.68 ± 2.92	11.19	-13.89	-0.95	25	-	-	-
	Algae	-	-	-	-17.68	10.10	9.09	-17.17	3.62	20.81	-	-	-
Lower Brazos	*C. houstonensis*	-28.37 ± 0.05	11.81 ± 0.13	3.76	-27.99 ± 0.06	12.22 ± 0.16	10.63	-27.88 ± 0.06	11.74 ± 0.12	3.62	-	-	-
	SPOM	-22.30 ± 1.01	2.76 ± 0.11	9.09	-25.89 ± 0.10	4.06 ± 0.58	9.59	-26.28 ± 0.72	3.43 ± 1.42	11.58	-27.26 ± 0.04	7.45 ± 0.17	10.81
	CPOM	-29.16 ± 0.86	5.36 ± 0.58	33.70	-29.97	3.98	30.46	-28.47	5.46	28.91	-28.67 ± 0.74	5.64 ± 1.22	27.52
	FPOM	-23.08 ± 0.20	3.02 ± 0.15	9.14	-22.85 ± 0.28	-0.76 ± 1.19	10.37	-23.79 ± 0.66	4.49 ± 0.32	8.55	-24.14 ± 0.21	5.06 ± 0.22	10.34
	Biofilm	-	-	-	-	-	-	-29.09	6.46	15.09	-27.07 ± 0.34	8.26 ± 0.41	9.03
	Periphyton	-	-	-	-	-	-	-	-	-	-25.64 ± 0.31	7.83 ± 0.46	7.14
	Epiphyton	-	-	-	-	-	-	-	-	-	-25.74 ± 0.09	11.29 ± 0.20	5.26
	Grass	-30.38 ± 0.04	9.56 ± 0.13	14.42	-	-	-	-30.79	11.23	17.17	-	-	-
	Justicia	-	-	-	-31.75	9.98	14.42	-32.6	11.49	17.56	-	-	-
	Myriophyllum	-	-	-	-32.37	7.35	17.67	-	-	-	-	-	-
	Algae	-	-	-	-	-	-	-26.48	9.58	11.07	-	-	-

Table 6. Mean $\delta^{13}C$ and $\delta^{15}N$ signatures of tissue from focal taxa in spring, summer, and fall 2017.

Species	Basin	Season	*n*	$\delta^{13}C$	$\delta^{15}N$
		Spring	7	-29.21	11.15
	Upper Guadalupe	Summer	11	-28.31	10.4
		Fall	3	-28.27	11.14
C. petrina					
		Spring	10	-29.86	13.41
	Lower Colorado	Summer	10	-28.68	13.38
		Fall	3	-30.34	11.82
		Spring	10	-29.91	13.1
	Lower Colorado	Summer	10	-28.83	12.71
		Fall	4	-30.01	12.33
C. houstonensis					
		Spring	12	-28.37	11.81
	Lower Brazos	Summer	10	-27.99	12.21
		Fall	10	-27.88	11.74
		Spring	6	-28.95	11.06
	Upper Guadalupe	Summer	13	-28.78	10.75
		Fall	7	-28.04	11.12
L. bracteata					
		Spring	12	-26.38	7.38
	Middle Colorado	Summer	10	-26.45	7.23
		Fall	9	-25.6	7.18

Table 7. Pearson product-moment coefficients and associated p-values for correlations between mussel size and $\delta^{13}C$ and mussel size and $\delta^{15}N$. Data were pooled across seasons for each species and each site. Bold values are statistically significant.

		$\delta^{13}C$		**$\delta^{15}N$**	
Site	*Species*	*r*	*p*	*r*	*p*
Upper Guadalupe	*C. petrina*	**0.47**	**0.05**	0.01	0.98
	L. bracteata	**0.46**	**0.05**	0.45	0.06
Lower Colorado	*C. houstonensis*	**0.58**	**0.01**	**0.48**	**0.03**
	C. petrina	**0.57**	**0.01**	0.22	0.36
Middle Colorado basin	*L. bracteata*	0.36	0.10	0.34	0.12
Lower Brazos basin	*C. houstonensis*	0.26	0.24	0.39	0.08

Table 8. IsoSource model estimates for the 3 mussel species. CPOM is coarse particulate organic matter, FPOM is fine particulate organic matter, SPOM is suspended particulate organic matter, Biofilm is scrubbed CPOM and plants, and values are mean, minimum, maximum, estimated proportional composition of each C source.

Species	Site	C:N	C source	Spring 2017			Summer 2017			Fall 2017		
				Mean	Min	Max	Mean	Min	Max	Mean	Min	Max
C. houstonensis	LB	3.62	CPOM	0.876	0.87	0.88	0.625	0.53	0.72	0.368	0	0.89
			FPOM	0.074	0.03	0.13	0.145	0.02	0.27	0.093	0	0.24
			SPOM	0.05	0	0.09	0.23	0.01	0.45	0.174	0	0.46
			Biofilm	-	-	-	-	-	-	0.364	0	0.79
	LC	3.89	CPOM	0.943	0.87	1	0.96	0.94	0.98	0.955	0.9	1
			FPOM	0.01	0	0.03	0.01	0	0.02	0.036	0	0.1
			SPOM	0.047	0	0.13	0.03	0	0.06	0.009	0	0.03
			Biofilm	-	-	-	-	-	-			
C. petrina	LC	3.86	CPOM	0.939	0.86	1	0.96	0.94	0.98	0.985	0.97	1
			FPOM	0.012	0	0.04	0.01	0	0.02	0.012	0	0.03
			SPOM	0.049	0	0.14	0.03	0	0.06	0.003	0	0.01
			Biofilm	-	-	-	-	-	-			
	UG	3.79	CPOM	0.99	0.99	0.99	0.974	0.95	1	0.984	0.97	1
			FPOM	0	0	0	0.009	0	0.03	0.006	0	0.02
			SPOM	0.01	0.01	0.01	0.017	0	0.05	0.01	0	0.03
			Biofilm	-	-	-	-	-	-			

Table 8. cont.

Species	Site	C:N	C source	Spring 2017			Summer 2017			Fall 2017		
				Mean	Min	Max	Mean	Min	Max	Mean	Min	Max
L. bracteata	MC	3.82	CPOM	0.02	0	0.05	0.85	0.8	0.9	0.373	0	0.76
			FPOM	0.003	0	0.01	0.054	0	0.11	0.099	0	0.24
			SPOM	0.978	0.95	1	0.096	0	0.2	0.153	0	0.38
			Biofilm	-	-	-	-	-	-	0.374	0	0.86
	UG	3.83	CPOM	0.93	0.93	0.93	1	1	1	0.975	0.96	1
			FPOM	0	0	0	0	0	0	0.01	0	0.03
			SPOM	0.07	0.07	0.07	0	0	0	0.015	0	0.04
			Biofilm	-	-	-	-	-	-	-	-	-

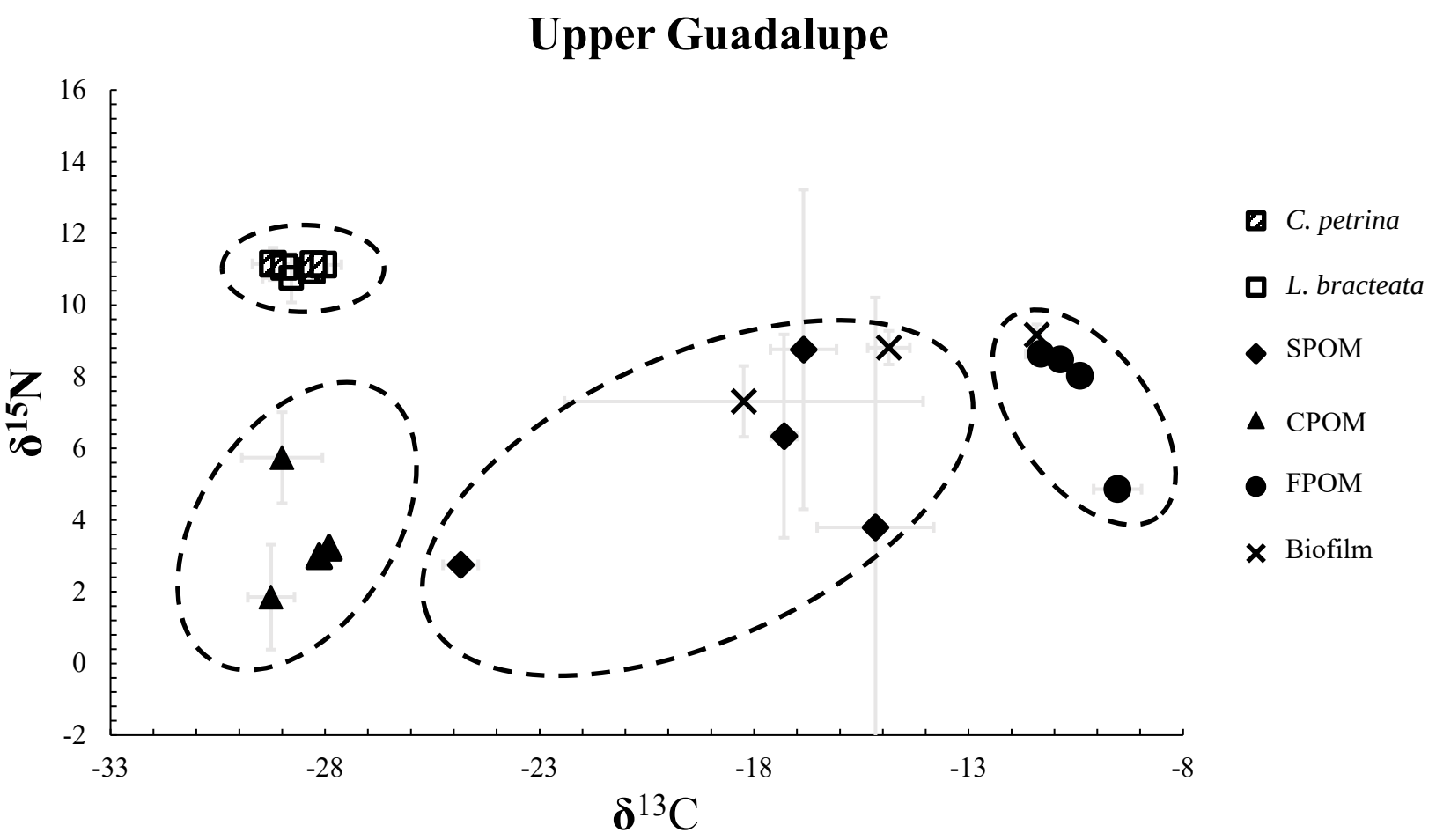

Figure 1. Stable CN isotope biplots for the Upper Guadalupe River site in April (Spring), July (Summer) and October (Fall) 2017 and May (Spring) 2018. Each point is a season average and associated SD. CPOM is coarse particulate organic matter (benthic detritus), FPOM is fine particulate organic matter from benthic sediments, SPOM is suspended particulate organic matter. Biofilm is attached periphyton.

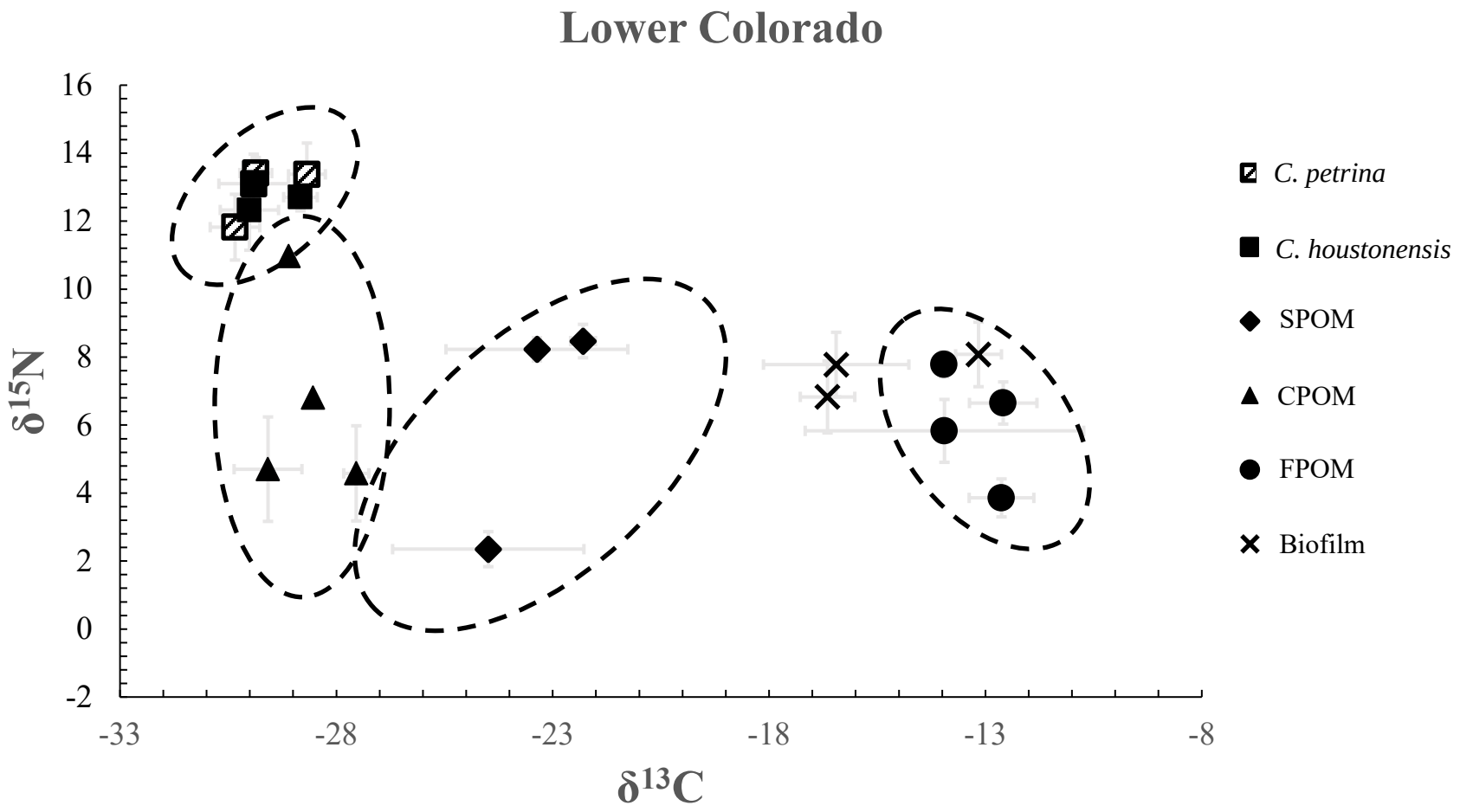

Figure 2. Stable CN isotope biplots for the Lower Colorado River site in April (Spring), July (Summer) and October (Fall) 2017 and May (Spring) 2018. Each point is a season average and associated SD. CPOM is coarse particulate organic matter (benthic detritus), FPOM is fine particulate organic matter from benthic sediments, SPOM is suspended particulate organic matter (seston). Biofilm is attached periphyton.

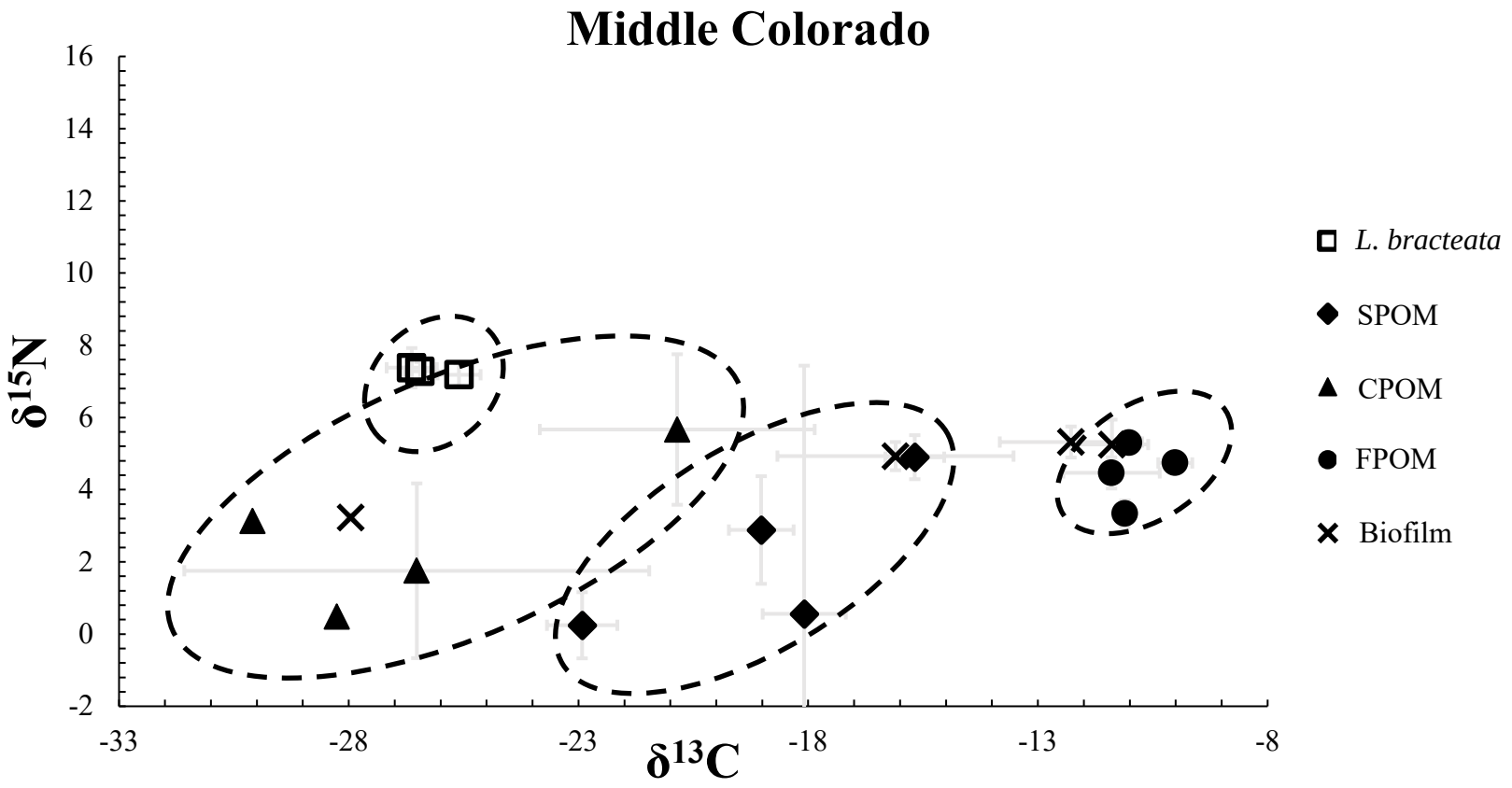

Figure 3. Stable CN isotope biplots for the Middle Colorado River basin site in April (Spring), July (Summer) and October (Fall) 2017 and May (Spring) 2018. Each point is a season average and associated SD. CPOM is coarse particulate organic matter (benthic detritus), FPOM is fine particulate organic matter from benthic sediments, SPOM is suspended particulate organic matter (seston). Biofilm is attached periphyton.

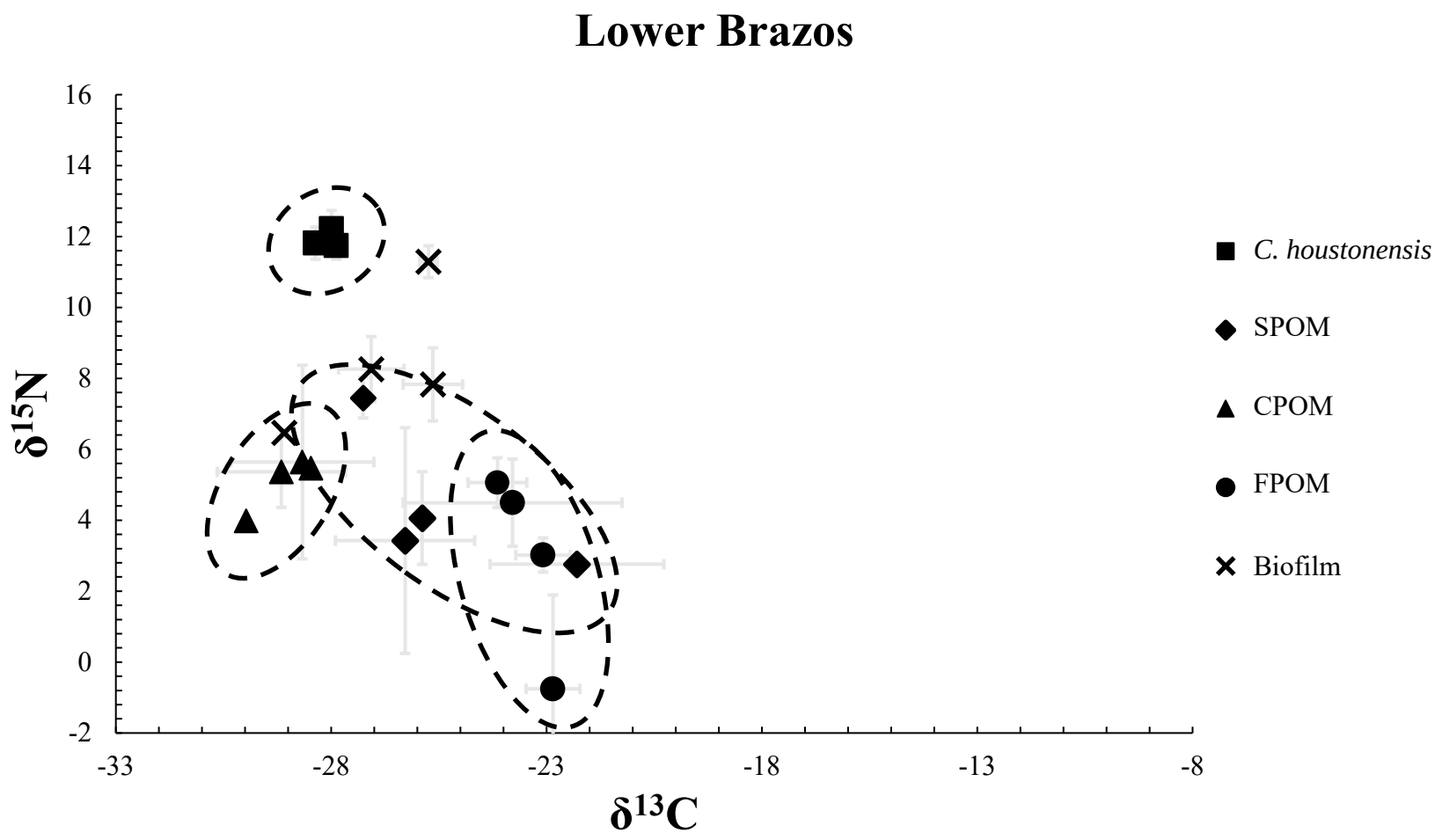

Figure 4. Stable CN isotope biplots for the Lower Brazos River basin site in April (Spring), July (Summer) and October (Fall) 2017 and May (Spring) 2018. Each point is a season average and associated SD. CPOM is coarse particulate organic matter (benthic detritus), FPOM is fine particulate organic matter from benthic sediments, SPOM is suspended particulate organic matter (seston). Biofilm is attached periphyton.

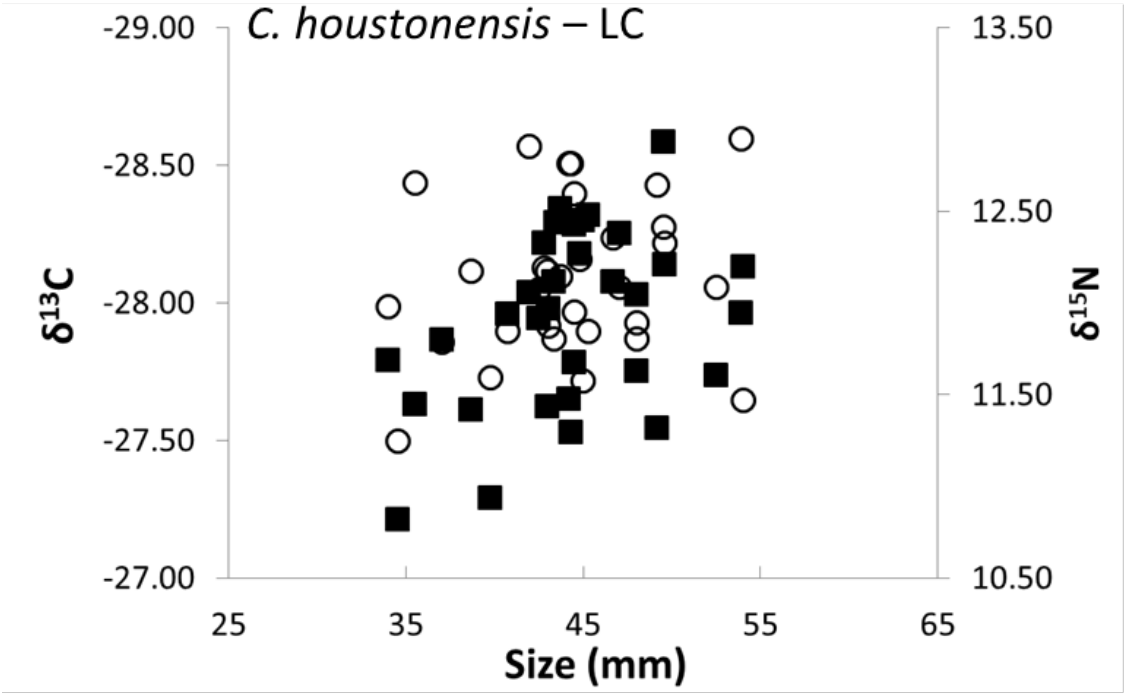

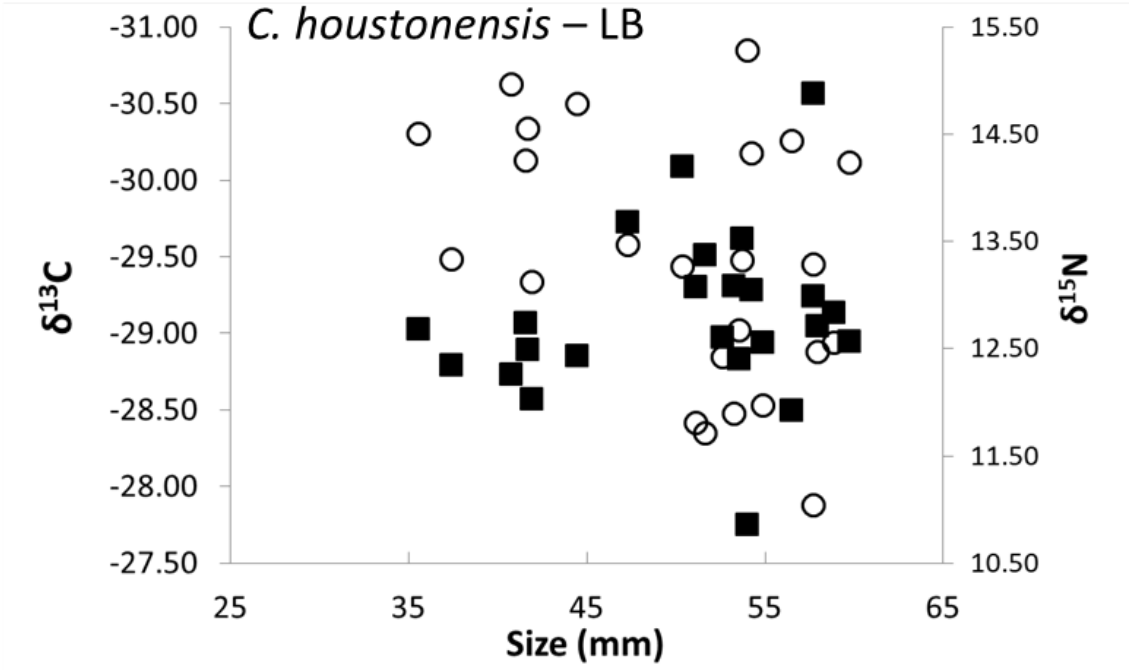

Figure 5. Relationships between stable isotope ratios ($\delta^{13}C$ and $\delta^{15}N$) and *C. houstonensis* size (length) in the Lower Colorado (LC) and Lower Brazos basin (LB). Open circles are $\delta^{13}C$ and filled squares are $\delta^{15}N$. Note $\delta^{13}C$ axis is inverted. See Table 7 for statistics.

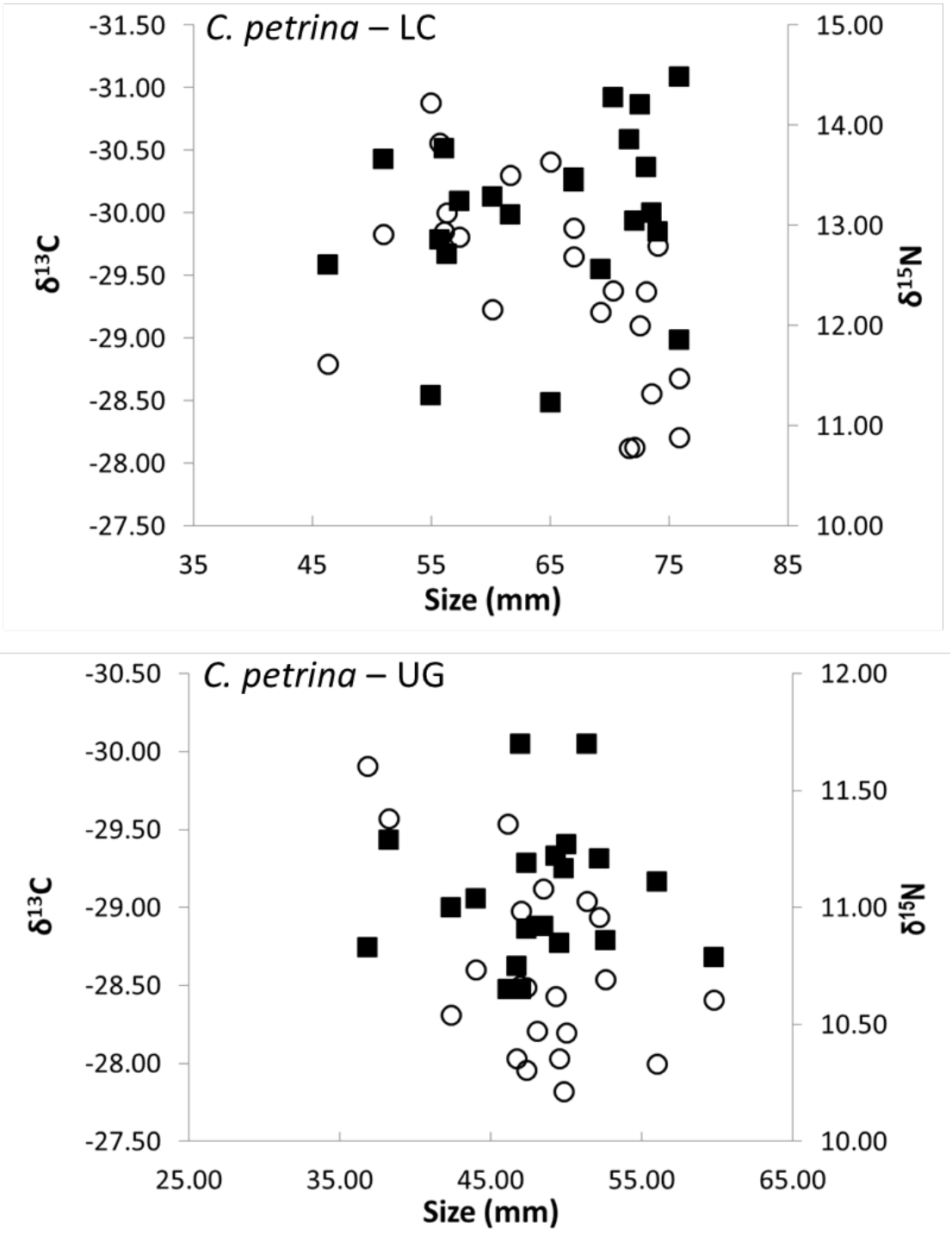

Figure 6. Relationships between stable isotope ratios ($\delta^{13}C$ and $\delta^{15}N$) and *C. petrina* size (length) in the Lower Colorado basin (LC) and Upper Guadalupe (UG). Open circles are $\delta^{13}C$ and filled squares are $\delta^{15}N$. Note $\delta^{13}C$ axis is inverted. See Table 7 for statistics.

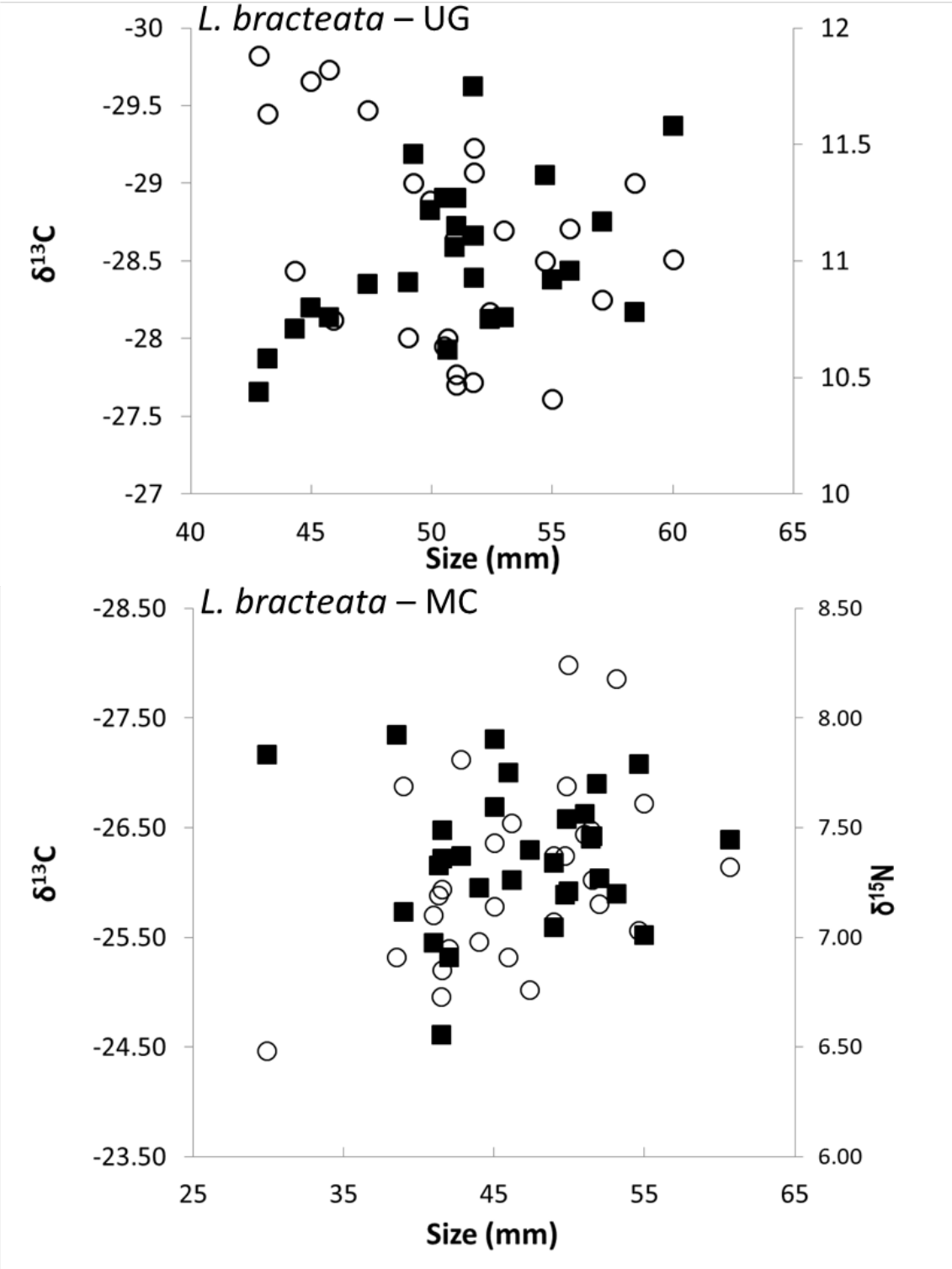

Figure 7. Relationships between stable isotope ratios ($\delta^{13}C$ and $\delta^{15}N$) and *L. bracteata* size (length) in the Upper Guadalupe (UG) and Middle Colorado basin (MC). Open circles are $\delta^{13}C$ and filled squares are $\delta^{15}N$. Note $\delta^{13}C$ axis is inverted. See Table 7 for statistics.

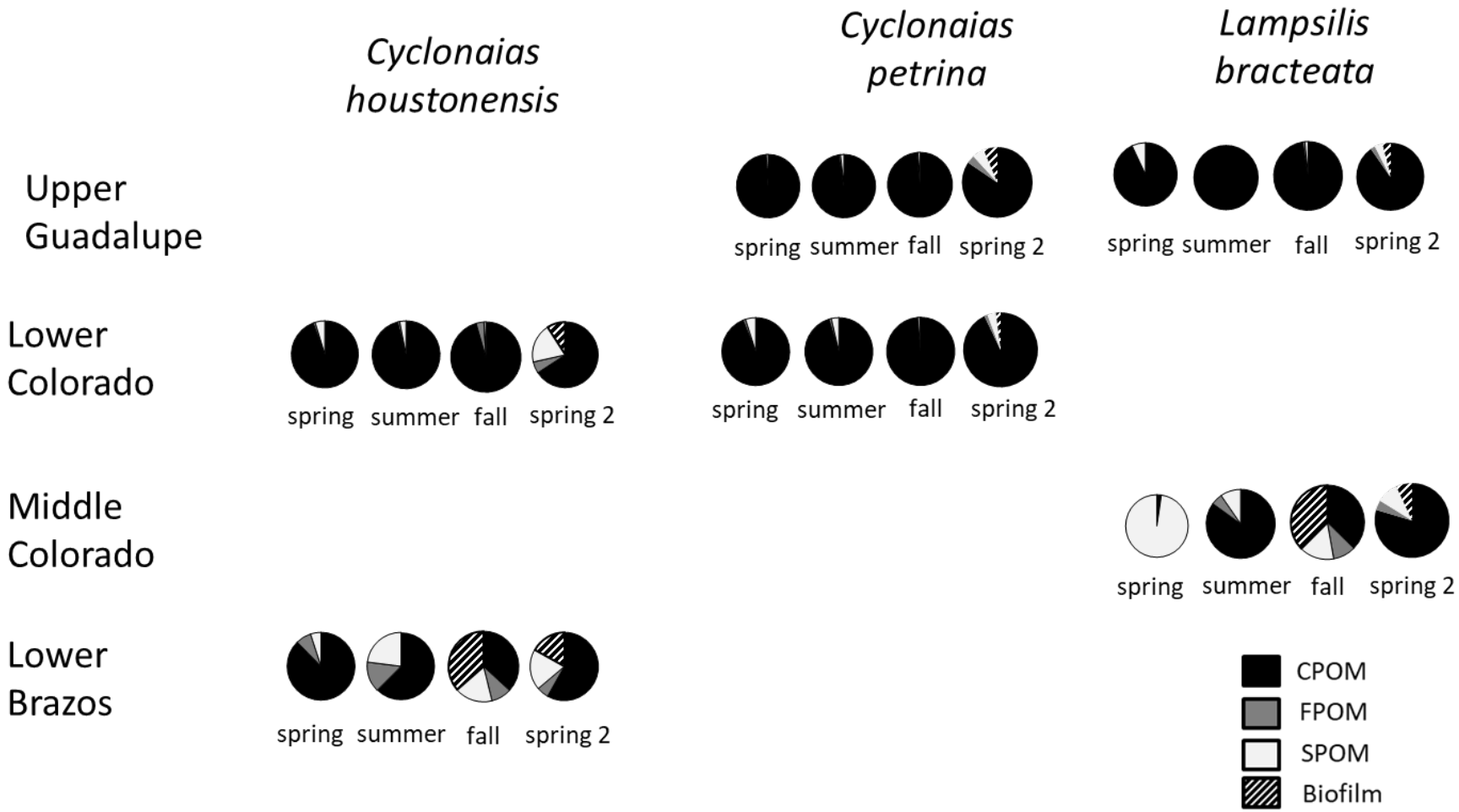

Figure 8. Estimated carbon source of *C. houstonensis, C. petrina,* and *L. bracteata* across the Upper Guadalupe, Lower Colorado, Middle Colorado, and Lower Brazos basin. Charts reflect mean estimate values of potential C sources from linear mixing models derived from IsoSource. Biofilm was only sampled from the Middle Colorado and Lower Brazos in the fall and was not estimated for other seasons and basin.

Task 3 Environmental Flow Analysis

Contributing Authors: Brad Littrell, Kyle Sullivan, Ed Oborny

Address: BIO-WEST, Inc. San Marcos, Texas 78666 (BL, KS, EO)

Principal Investigators: Brad Littrell and Ed Oborny

Email: blittrell@bio-west.com, eoborny@bio-west.com

Introduction and Objectives

Traditional instream flow studies model changes in simple hydraulic parameters such as depth and velocity under varying stream discharge levels and how they influence habitat availability for target organisms, usually fishes (BIO-WEST 2008). The underlying assumptions are that target organisms select their habitat based on these parameters, and that they have the ability to move to new habitats when discharge conditions change. Freshwater mussels challenge these assumptions due to their slow locomotion and sessile nature (Schwalb & Pusch 2007; Gough et al. 2012; Newton et al. 2015). Compared to fishes, mussels tend to move little and occupy small habitat patches for long periods. Therefore, for a mussel to persist at a specific location, suitable habitat must occur across a range of flow conditions. As a result, some have suggested that modeling based on habitat utilization data using simple hydraulic variables such as depth and velocity are of little use in determining conservation flows for mussels, but that complex hydraulic parameters such as shear stress modeled over a range of flow conditions to identify "persistent habitat" are better predictors of mussel abundance (Layzer and Madison 1995, Maloney et al. 2012). However, some of the same authors recognized that mussels did show a preference for particular hydraulic conditions and that depth and velocity were important factors limiting their distribution under base flow conditions (Layzer and Madison 1995). This study uses a combined approach of first evaluating shear stress across a range of flow conditions

to identify persistent habitat patches, followed by modeling with traditional habitat suitability criteria based on hydraulic parameters (i.e., depth, velocity, Froude number, Reynolds number) within those patches at base flow levels. This integrated approach accounts for the requirement of persistent habitat across a broad range of flow conditions, while simultaneously accounting for habitat selectivity of mussels under base flow conditions.

Previous environmental flow studies conducted on the lower Colorado River as part of the Lower Colorado River Authority (LCRA) – San Antonio Water System (SAWS) Water Project (LSWP) established 10 intensive study sites with detailed hydraulic models (Figure 1) (BIO-WEST 2008). These models were used to generate instream flow recommendations for the lower Colorado River based on fish habitat modeling and other flow dependent ecological variables. However, freshwater mussels were not considered as part of this previous instream flow assessment. Therefore, the overall goal of the current study was to evaluate availability and persistence of freshwater mussel habitat under various flow conditions within the lower Colorado River using a variety of both traditional (depth, velocity) and complex (Reynolds number, Froude number, shear stress) hydraulic variables at existing hydraulic model sites used previously for fish habitat modeling.

To do this, the first specific objective of Task 3 was to conduct mussel surveys at previously established hydraulic model sites on the lower Colorado River to determine which sites support significant mussel populations. These sites were included in Task 1 survey work to assess the occurrence and abundance of freshwater mussels at each location. Based on the results of these surveys, two previously-established hydraulic model sites were chosen to focus additional habitat modeling efforts, as described in the results below.

The second specific objective was to develop habitat suitability criteria for freshwater mussels within the lower Colorado River. Detailed habitat information collected as part of Task 1 survey work was summarized and used to develop Habitat Suitability Criteria (HSC). These HSC describe the habitat utilized by freshwater mussels under base flow conditions. Similar criteria were also developed using data from the Little River drainage in the Brazos basin to investigate basin-specific differences in HSC.

The third specific objective of this task was to collect additional physical and hydraulic data to validate and/or update existing hydraulic models. Initially, it appeared that hydraulic model sites had changed little since development of the models and only some minor validation data would be necessary. However, a large flood event occurred in the lower Colorado River following heavy rains from Hurricane Harvey in August 2017. A visit to one of the selected model sites shortly afterwards revealed extensive changes to channel bathymetry. Therefore, additional bathymetric and hydraulic data was collected in 2018 to update existing models to incorporate these changes. Bed topography from updated models were then compared to previous models to investigate changes in river bathymetry between modeling events.

The fourth objective was to incorporate habitat suitability information with revised model output to evaluate the effects of varying flows on freshwater mussel habitat within the selected study sites, and thus inform environmental flow recommendations in the lower Colorado River. Results of this habitat modeling are presented below, along with a discussion of results in the context of current Texas Commission on Environmental Quality (TCEQ) instream flow standards.

Finally, although no hydraulic modeling was done in the Brazos River basin, a desktop analysis of freshwater mussel environmental flow needs in the Brazos basin was conducted based on observations from this study and other available data.

Methods

Study Site Selection

Freshwater mussel data was collected using the methodology described in detail under Task 1 surveys of the previous report (Bonner et al. 2018). Surveys were conducted at several of the previously established hydraulic model sites to evaluate the mussel communities present and choose sites for further habitat modeling. Data was collected to allow for calculation of catch-per-unit-effort (CPUE; mussels/person-hour) at each study site.

Habitat Suitability Criteria

Habitat utilization data from Task 1 surveys on the lower Colorado River were used to develop Habitat Suitability Criteria (HSC) for all freshwater mussels in aggregate, as well as for each of the candidate species inhabiting the lower Colorado River (i.e., *Cyclonaias houstonensis*, *Cyclonaias petrina*, and *Truncilla macrodon*). This data was collected in spring and summer of 2017 at daily average discharges ranging from 507 – 1,870 cfs. Additionally, suitability criteria were developed for all mussels and for *C. houstonensis* from the Little River drainage in the Brazos basin to allow for between-basin comparisons. For each species or combination of species, HSC were developed for depth, mean column velocity, Froude number, Reynolds number, mean substrate compaction, FST hemisphere number, minimum bottom shear stress (MBSS; inferred from FSTs using Statzner et al. 1991), and dominant substrate. Data for depth, mean column velocity, mean substrate compaction, FST hemisphere number, and MBSS were measured during surveys as described in the Task 1 methods from the previous report (Bonner et

al. 2018). Percent substrate composition taken from survey data was converted to dominant substrate for development of suitability criteria. Froude number and Reynolds number are hydraulic parameters used to evaluate turbulence. Froude number represents a ratio of inertial to gravitational forces. Reynolds number represents a ratio of inertial force to viscous force. These parameters were calculated from survey data using the following equations:

Reynolds number *(Re):* $Re = Ud/v$

where U = benthic velocity (m/s), d = water depth (m), v = kinematic viscosity of water (1.0×10^{-6} m^2/s)

Froude number *(Fn):* $Fn = U/\sqrt{gd}$

where U = benthic velocity (m/s), g = acceleration of gravity (9.8 m/s^2), d = water depth (m)

Suitability criteria for continuous variables were created using nonparametric tolerance limits (NPTL) (Bovee 1986). The tolerance limits representing the central 50% of the data were used to represent the highest utilization and given a suitability value of 1.0. The tolerance limits for the central 75% were assigned a suitability of 0.5. The tolerance limits for the central 90% of the data were given a suitability of 0.2. Lastly, the tolerance limits representing the central 95% of the data were given a suitability value of 0.1. Anything outside of the central 95% tolerance limit was considered unsuitable and given a suitability value of 0.0. For the categorical variable of dominant substrate, suitability values were established using the Strauss Linear Index (Strauss 1979, Persinger et al. 2010). Values of this index range from -1 to 1, with larger positive values indicating selection and negative values indicating avoidance. Significant positive values were given a suitability of 1.0, non-significant positive values were given a suitability of 0.5, non-

significant negative values were given a suitability of 0.2, and significant negative values were assigned a suitability of 0.0.

Hydraulic Model Updates

In February and March 2018, target hydraulic model study sites were resurveyed to account for changes in bathymetry following Hurricane Harvey high flow events. Most bathymetric data within the wetted channel was collected using a Son-Tek M9 River Surveyor Acoustic Doppler Current Profiler (ADCP) mounted to a small john boat. This unit simultaneously collects data on water column depth, velocity, and instrument position multiple times per second. By maneuvering the boat in a grid-like fashion across the study sites, a detailed georeferenced depth dataset was generated. This dataset was supplemented by point depth measurements taken with the aid of an incremental wading rod and Trimble GPS unit in wetted areas too shallow for the boat to operate. Additionally, elevation data in dry areas of the river bed was collected with a Trimble R10 VRS rover and data collector. The resulting georeferenced depth data was integrated with water surface elevations collected on the same dates to generate a dataset of georeferenced bed elevation points within each study site for import into River2D hydraulic modeling software (Steffler & Blackburn 2002).

To monitor changes in water surface elevation at the study site over an extended period, and thus generate stage-discharge relationships, water level data loggers (Onset HOBO U20L or Solinst Levelogger Model 3001) were installed at the upstream and downstream boundary of each site. Associated barometric pressure loggers were deployed above-water to account for changes in barometric pressure during the deployment period. On-site water surface elevation data was also collected using a Trimble R10 VRS rover and data collector under multiple flow rates.

Hydraulic modeling was conducted with River2D (Steffler & Blackburn 2002), the same program used in previous modeling efforts as part of the LSWP study. This program predicts water depth and velocity based on several measured inputs including discharge, water surface elevation, and bathymetry. Topographic/bathymetric data were entered into River2D Bed for editing. Based on this data, a triangular finite-element mesh with 5-meter spacing between nodes was generated using River2D Mesh. This mesh represented the final bathymetric input into River2D. Hydraulic data (discharge and water surface elevation) were then entered to generate first-cut models for each site at multiple flow rates. These first-cut models were then calibrated by adjusting model inputs until predictions of water surface elevation, depth, and velocity matched closely with field observations. Bed roughness was the main input adjusted during the calibration process, although minor adjustments to bathymetry and downstream water surface elevation were made sparingly. Final roughness values ranged from 0.1 m to 1.0 m, and were based on substrate conditions, with areas of smooth substrates (silt, sand) receiving lower values, gravel and cobble receiving intermediate values, and overbank areas receiving the highest roughness due to presence of riparian vegetation. To calibrate each modeled flow tier, the observed upstream and downstream water surface elevation from water level loggers or field measurements were compared to model predictions. Calibration within mid-reaches were also performed at flow tiers where water surface elevation data were available. At flow tiers where observed water surface elevation data was not available (extremely low flows), the Depth-Unit Discharge Relationship function in River 2D was used, which does not require the input of a downstream water surface elevation (Steffler & Blackburn 2002).

Habitat Modeling

First, persistent habitat was identified by evaluating shear stress across all modeled flow rates. Shear stress was calculated at each node across all modeled flow rates using the following equation:

Shear stress (τ):

$$\tau = U/5.75log10(\frac{12d}{ks})$$

where U = modeled current velocity (cm/s), d = modeled water depth (cm), and ks = an estimate of bed roughness (cm) based on substrate maps (See Table 2).

Estimates of shear stress from this equation have shown to correspond with field measurements of shear stress from FST hemispheres (Randklev et al. 2014). To evaluate persistent habitat, shear stress HSC were used to identify a maximum shear stress cutoff for mussel occurrence (5.0 dyn/cm^2) which was then applied to model results. Model nodes which exhibited shear stress less than the cutoff for all modeled flow rates were considered "persistent" habitat. If a given model node exhibited a shear stress higher than the cutoff at any modeled flow rate it was labeled "non-persistent". Areas identified as persistent were considered to be potential mussel habitat, and HSC for hydraulic parameters were then applied within these areas, as described below.

Within persistent areas, base flow habitat suitability was evaluated for all unionid mussels in aggregate, as well as for *C. houstonensis*, and *C. petrina*, specifically. To do this, habitat suitability values for depth, velocity, substrate, Froude number, and Reynolds number were calculated for each node in the updated hydraulic model output. Individual habitat suitability values for each category were then combined into a Composite Suitability Index (CSI) for that node. The CSI was calculated by computing the geometric mean of the individual depth

($Depths_{SI}$), velocity ($Velocity_{SI}$), substrate ($Substrate_{SI}$), Froude number ($Froude_{SI}$), and Reynolds number ($Reynolds_{SI}$) suitability, as follows:

$$CSI = (Depths_{SI} * Velocity_{SI} * Substrate_{SI} * Froude_{SI} * Reynolds_{SI})^{1/5}$$

The CSI was then multiplied by the area of each hydraulic model node to generate a Weighted Usable Area (WUA), and these values were summed within persistent habitat to generate a total Persistent Weighted Usable Area (PWUA) for each modeled base/subsistence flow rate. By compiling total PWUA for each mussel category at each flow rate, PWUA to discharge relationships for base and subsistence flow conditions were evaluated.

Habitat Model Validation

Current site-specific mussel distribution and abundance data were collected in summer 2018 to validate habitat modelling results. To do this, mussel survey transects were conducted at random sampling points generated within the model boundaries. Each random sampling point represented the upstream end of a 25-meter lead-core rope transect stretched parallel to streamflow. On each end of the transect the lead-core rope was secured to a cinder block with an attached buoy for easy surface location. Two biologists surveyed each transect with each surveyor maintaining contact with the rope for navigation and surveying one-meter on each side. This resulted in a total survey area of 50 m^2 per transect. Surveyors were equipped with mask and snorkel or surface-supplied-air from a Brownie's Third Lung Hookah System, depending on water depth. All mussels were placed in mesh bags and identified to species, measured, and enumerated following transect completion. Survey time was recorded at each transect and used to calculate CPUE. For each transect, CPUE was calculated for all mussels in aggregate, as well as for *C. houstonensis*, and *C. petrina*, specifically. A total of 85 random points was surveyed at Altair, and 70 random points were surveyed at La Grange.

Using GIS software, transect data were then overlaid with habitat modeling results. Mean CPU for all three categories was compared between non-persistent habitats with low suitability (CSI<0.5), non-persistent habitats with high suitability (CSI>0.5), persistent habitats with low suitability, and persistent habitats with high suitability to provide model validation.

Results

Study Site Selection

A total of 85 person-hours (p-h) of search time was conducted at the 10 intensive model sites during Task 1 surveys, resulting in collection of 862 mussels for an overall catch-per-unit-effort (CPUE) of 10.1 mussel/p-h (Table 1; Bonner et al. 2018). Site-specific CPUE ranged from 0.0 – 2.5 mussels/p-h at sites between Longhorn Dam and Smithville, and from 3.2 – 47.6 mussels/p-h from La Grange downstream to Lane City. Maximum site-specific CPUE (47.6 mussels/p-h) was observed at the Altair intensive study site. Candidate species were present from La Grange downstream, with all three candidate species being present at the Altair and Wharton study sites (Table 1).

Based on the data above, the Altair and La Grange study sites were chosen as the focus for additional data collection and modeling. Based on the high relative abundance observed and the presence of all three-candidate species, Altair was chosen to represent high-quality habitat conditions within the lower Colorado River. The La Grange study site was the upstream-most site that contained a candidate species (*C. houstonensis*), and exhibited a lower relative abundance compared to Altair, ranking third in overall CPUE. Understanding differences in hydraulic and habitat conditions between these two sites may elucidate patterns in freshwater mussel occurrence and abundance within the lower Colorado River.

Habitat Suitability Criteria

Habitat Suitability Criteria generated from survey data for all lower Colorado River unionids in aggregate demonstrated highest habitat suitability at depths of 0.6 – 0.9 meters (m), mean column velocity below 0.2 m/s, Froude number below 0.05, and Reynolds numbers below 50,000 (Figure 2). Mussels were most commonly found in habitats with mean substrate compaction less than 0.075 kg/cm^2 and showed highest suitability when MBSS < 2 dyn/cm^2 and in silt and boulder substrates (Figure 3).

For lower Colorado River *C. houstonensis*, suitability was highest at depths of 0.9 – 1.2 m, mean column velocities of 0.1 – 0.2 m/s, Froude numbers near 0.05, and Reynolds numbers of approximately 50,000 (Figure 4). They were most frequently found in habitats with mean substrate compaction from 0.025 – 0.05 kg/cm^2, in habitats with MBSS < 2 dyn/cm^2, and exhibited highest suitability in boulder substrates (Figure 5).

For lower Colorado River *C. petrina*, suitability was highest at depths from 0.6 – 0.9 m, mean column velocities below 0.2 m/s, Froude numbers below 0.05, and at Reynolds numbers below 150,000 (Figure 6). They were most commonly found where mean substrate compaction ranged from 0.025 - 0.075 kg/cm^2, at MBSS < 2 dyn/cm^2, and showed moderate suitability (0.5) in sand, boulder, and bedrock substrates (Figure 7).

Due to insufficient sample size (n = 9), HSC were not generated for lower Colorado River *T. macrodon*. However, data suggests highest utilization in depths of 0.6 – 0.9 m, in relatively low velocities, and in habitats with relatively low Froude and Reynolds numbers (Figure 8). They were most commonly found where substrate compaction and MBSS were relatively low, and Strauss Linear Index values for substrate were highest in silt (0.25), clay (0.09), and boulder (0.08) (Figure 9).

For Little River unionids in aggregate, HSC demonstrated highest habitat suitability at depths of 0.6 – 1.2 m, mean column velocity below 0.4 m/s, Froude number below 0.05, and Reynolds numbers below 100,000 (Figure 10). Mussels were most commonly found in habitats with mean substrate compaction less than 0.05 kg/cm^2 and showed highest suitability at an MBSS of 1.0 – 1.5 dyn/cm^2 and in silt substrates (Figure 11).

For Little River *C. houstonensis*, suitability was highest at depths of 0.9 – 2.7 m, mean column velocities of less than 0.4 m/s, Froude numbers less than 0.05, and Reynolds numbers below 600,000 (Figure 12). They were most commonly found in habitats with mean substrate compaction less than 0.05 kg/cm^2, in habitats with MBSS between 1.0 – 1.5 dyn/cm^2 and exhibited highest suitability in silt substrates (Figure 13).

Analysis of Bathymetric Change

Updated bathymetric data at each site allowed for analysis of changes in bed elevation between modeling periods. At Altair, comparisons of bed files between the two models showed that approximately 71% of overlapping areas exhibited an elevation change of 0.4 m or less (Figure 14). Maximum deposition of approximately 1.4 m was observed, with areas of considerable deposition occurring near the upstream boundary and near the downstream boundary of the site (Figure 15-16). Scour of over 6.4 m was observed due to the lateral erosion of a high cut bank near the downstream end of the site (Figure 15-16).

At La Grange, approximately 82% of overlapping area exhibited an elevation change of 0.4 m or less (Figure 17). Maximum deposition of 1.6 m was observed, with areas of maximum deposition occurring along the bank on the outside bend (Figure 18-19). Scour was noted along each side of a mid-channel gravel shoal/island near the downstream end of the site (Figure 18-19).

Hydraulic Model Updates

In total across both sites, 14 hydraulic model runs were conducted at flow tiers ranging from 50 cfs to 8,610 cfs (Table 3). For model runs in which field data were available for calibration (n = 9), 82% of the predicted water surface elevations matched observations within 5 cm (2 in) (Table 3). Only 3 upstream water surface elevation predictions were greater than 7 cm (~3 in) from observed water surface elevations (Table 3). For each model, differences between total inflow and total outflow was 0.2% or less.

Habitat Modeling Results

At Altair, node-specific calculations of shear stress ranged from 0 – 102 dyn/cm^2. Although shear stress generally increased with increasing flow rates, some areas experienced maximum shear stress under the lowest flow conditions. Habitat Suitability Criteria from this study suggest that mussels rarely inhabit areas with a shear stress over 5.0 dyn/cm^2 (Figure 3-13). Mussel HSC from the lower Brazos River show a similar trend of low to zero suitability at shear stress values over 5.0 dyn/cm^2 (Randklev 2014). Therefore, nodes with a shear stress of less than 5.0 dyn/cm^2 across all flow rates were labeled "persistent". Much of the Altair study site was labeled as persistent, except for steeper high-energy areas along the eastern edge of the bedrock riffle and an area of constriction around a gravel bar at the downstream end (Figure 20).

At Altair, patterns in PWUA to discharge relationships for all three categories evaluated (aggregate unionids, *C. houstonensis*, *C. petrina*) were relatively consistent. For *C. petrina* and aggregate unionids, maximum PWUA was at the 287 cfs model run, with slight decreases at higher and lower flows (Table 4, Figure 21). PWUA for *C. houstonensis* peaked at the 981 cfs model run. To compare patterns across categories, PWUA was normalized to the percent of maximum in each category (Figure 22). At the lowest modeled flow of 100 cfs, 75-76% of

maximum habitat was available in all categories. Modeled habitat for all categories was greater than 98% of maximum at 287 and decreased to 80% of maximum for all categories at 525 cfs. Increases in PWUA were observed between 525 and 981 cfs, with 93-100% of maximum in each category at 981 cfs. Modeled habitat then dropped sharply to 45-46% of maximum at 1,459 cfs and dipped to 39-41% of maximum by 1,849 cfs.

At La Grange, node-specific calculations of shear stress ranged from 0 – 109 dyn/cm^2. As described above, nodes with a shear stress of less than 5.0 dyn/cm^2 across all flow rates were labeled "persistent". Compared to Altair, persistent habitat was much more limited at La Grange, presumably due to the shallower depths and steeper longitudinal slope at this site. At La Grange, persistent habitat was limited mainly to bank areas and only extended across the channel in a pool below a steep bedrock riffle (Figure 23).

At La Grange, as at Altair, overall patterns in PWUA to discharge for all three categories evaluated (aggregate unionids, *C. houstonensis*, *C. petrina*) were relatively consistent. Model-predicted habitat availability peaked at the 100 cfs model run (Table 5, Figure 24) for all categories, and dropped to 92-99% of maximum at the 50 cfs model run (Figure 25). At the 250 cfs model run PWUA ranged from 93-95% of maximum for all categories. Predicted habitat then dropped to 63-71% of maximum by 738 cfs and reached lows of 49-57% at 2,000 cfs.

Habitat Model Validation

At Altair, CPUE ranged from 0.00-107.14 mussels/p-h (mean CPUE: 7.41 mussels/p-h) for aggregate mussels, 0.00-44.00 mussels/p-h (mean CPUE: 2.17 mussels/p-h) for *C. houstonensis*, and 0.00-3.53 mussels/p-h (mean CPUE: 0.36 mussels/p-h) for *C. petrina*. Model predictions of habitat at 287 cfs compared well to mean CPUE from validation sampling efforts for both *C. houstonensis* and aggregate mussels. For *C. houstonensis*, mean CPUE ranged from

0.18-0.51 mussels/p-h in non-persistent habitat and ranged from 1.22-3.35 mussels/p-h in persistent habitat, with the maximum CPUE observed in high-quality persistent habitat (Figure 26). For aggregate mussels, mean CPUE ranged from 2.64-3.30 mussels/p-h in non-persistent habitat and ranged from 2.01-10.63 in persistent habitat, with the maximum CPUE observed in high-quality persistent habitat. For *C. petrina*, trends in CPUE did not match as well with modeled habitat predictions. Mean CPUE for *C. petrina* ranged from 0.00-1.30 and was actually highest in low-quality non-persistent habitat. Broader HSC for *C. petrina* resulted in large expanses of predicted high-quality habitat in persistent areas and the species was not documented at many of the sites within these areas. Maps demonstrating predicted habitat for all three categories at 287 cfs and CPUE from mussel validation sampling are provided in Figures 27-29.

At La Grange, CPUE ranged from 0.00-18.75 mussels/person-hr (mean CPUE: 0.38 mussels/person-hr) for aggregate mussels and 0.00-17.50 mussels/person-hr (mean CPUE: 0.28 mussels/person-hr) for *C. houstonensis*. Model predictions of habitat at 100 cfs compared well to mean CPUE from validation sampling efforts for all aggregate mussels, as well as for *C. houstonensis*. Only one mussel was collected in non-persistent habitat (mean CPUE range: 0.00-0.06), mean CPUE ranged from 0.00-0.46 mussels/p-h in low-quality persistent habitat, and mean CPUE was highest in high-quality persistent habitat for all aggregate mussels and *C. houstonensis* (mean CPUE range: 2.47-2.61 mussels/p-h) (Figure 30). Maps of predicted habitat at 100 cfs and CPUE from mussel validation sampling are provided in Figures 31-32. Despite considerable predicted habitat, no *C. petrina* were collected from the La Grange site.

Discussion

Habitat Suitability Criteria

Habitat suitability criteria developed from survey data suggest that freshwater mussels in the lower Colorado River are most commonly utilizing moderate-depth low-energy habitats with silt and boulder substrates. Compared to all mussels in aggregate, *C. houstonensis* showed lower suitability in areas with 0 velocity, 0 turbulence, and 0 substrate compaction. *Cyclonaias petrina* showed broader curves for mean column velocity, Froude number, Reynolds number, and MBSS, suggesting increased utilization of high-energy environments compared to all mussels in aggregate.

Bathymetric Changes

As quantified above, substantial bathymetric changes to each of the selected hydraulic model sites were noted between development of the original models in 2008 and the updated models in 2018. Based on observations of the study team, the majority of these changes were due to a large high-flow event following Hurricane Harvey in August-September 2017 in which discharge at the USGS gauge at Columbus (#08161000) peaked at approximately 160,000 cfs. Data from an ongoing mark-recapture study (Bonner et al. 2018) demonstrated that this event impacted mussel densities at the Altair study site. Within the mark-recapture study site, a 300-m^2 area located within the hydraulic model, scouring was observed from about 0.15 m (0.5 ft) to greater than 0.3 m (1 ft) (Figure 15). Post-hurricane monitoring revealed a sharp decrease in overall unionid taxa richness and density within this area (Bonner et al. 2018). These results suggest that unionids resistance to high flows may be related to the magnitude of sediment erosion that occurs within a patch of occupied habitat. However, mussel validation data collected in summer 2018 demonstrates that freshwater mussels (including candidate species)

persist at the hydraulic model site, in high abundance at some locations. Additionally, because this high-flow event likely displaced mussels inhabiting "marginal" habitats, mussel CPUE data from summer 2018 likely represents a good snapshot of high-quality persistent habitat for use in model validation.

Model Validation

Validation data presented above demonstrate that model predictions of persistent habitat were useful in predicting areas of potential mussel habitat and that HSC based on hydraulic parameters were useful in identifying areas of high-quality habitat within these patches. At Altair, areas of highest mussel CPUE occurred within or in close proximity to persistent areas predicted to be highly suitable. However, multiple areas of zero CPUE also occurred in predicted habitats suggesting that criteria could potentially be further refined or that factors other than habitat availability may be important in structuring mussel assemblages at this site. At La Grange, the persistent habitat layer did a better job of excluding poor habitat, and few areas of zero CPUE occurred in persistent habitat patches. Many sites of zero CPUE occurred in mid-channel areas that experience high shear stress under higher flow conditions. Additionally, areas of high mussel CPUE were most-often found in predicted high quality habitat within persistent patches.

The less-predictive persistent habitat layer at Altair may be due to the abundance of deep pool habitats at the Altair site. These deeper areas qualify as persistent habitat due to low shear stress under all flow scenarios modeled. It should also be noted that modeling of higher flow scenarios could result in a decrease in persistent habitat availability at Altair. The 8,297 cfs flow rate modeled at Altair represents approximately the 90th percentile flow at this site. Although sporadic, even higher flows are important in structuring the mussel assemblage, as noted during

the mark-recapture study at this site following the 160,000 cfs event (Bonner et al. 2018). Regardless, validation results support that the combination of defining persistent habitat and calculating habitat suitability under base flow conditions within these areas is useful in modeling mussel habitat availability.

Environmental Flow Considerations - Altair

For the habitat modeling analysis above to be useful in evaluating environmental flow recommendations, results must be put in context of existing TCEQ Environmental Flow Standards for the lower Colorado River (TCEQ 2012). For the Altair site, the nearest gauge with an environmental flow standard is the Colorado River at Columbus (USGS gauge #08161000). Depending on season and hydrologic condition, subsistence standards at this gauge range from 190-534 cfs, and base flows range from 310-1,440 cfs (Table 6). Freshwater mussel habitat modeling at Altair shows that at 190 cfs, freshwater mussel PWUA for all categories is maintained at approximately 85-90% of maximum, suggesting that from a strictly habitat standpoint, this subsistence recommendation is protective. It should be noted that under subsistence flow conditions water quality considerations such as temperature and dissolved oxygen may influence mussel communities. Although considerable data on the influence of sub-lethal water quality stressors on these candidate mussel species was produced during Task 2 of this study (Bonner et al. 2018), no water quality modeling was conducted as part of this study.

At base flow levels of 310-1,440 cfs mussel PWUA is variable. At flows from 310-981 cfs mussel PWUA is maintained at greater than or equal to 80% of maximum for all categories. However, at flows between 1,000 cfs and 1,440 cfs, PWUA drops sharply, to 45-46% of maximum at 1,459 cfs. In the Columbus environmental flow standards, base flow levels exceed 1,000 cfs on three occasions – in March under Average conditions (1,020 cfs), in May under

Average conditions (1,316 cfs) and in June under Average conditions (1,440 cfs). This analysis suggests that current base flow standards for Average conditions in May and June at Columbus may temporarily limit mussel habitat availability.

Environmental Flow Considerations – La Grange

For the La Grange site, the nearest upstream gauge with an environmental flow standard is the Colorado River at Bastrop. Depending on season and hydrologic condition, subsistence flow standards at this gauge range from 123-275 cfs, and base flow standards range from 194-824 cfs (Table 6). Freshwater mussel habitat modeling at La Grange demonstrates that PWUA peaks at the 100 cfs flow rate for all categories modeled, maintaining greater than 92% of maximum for all categories from 50-250 cfs. This suggests that from a strictly-habitat-availability perspective, subsistence flow recommendations are protective of mussel habitat.

In the base flow range of 194-824 cfs, mussel habitat availability ranges from approximately 60-70% of maximum on the high end to greater than 95% of maximum at the low end. As at Altair, lower base flow standards maximize model predictions of freshwater mussel PWUA, whereas higher base flow recommendations result in more limited habitat predictions. However, at La Grange, even under the maximum base flow recommendations in the standards, mussel PWUA stays above 60% of maximum.

Pulse Flows and Freshwater Mussels

From a pulse flow perspective, higher flows limit habitat availability for mussels and larger pulses may result in downstream displacement when shear stress becomes too high for mussel persistence. However, these same pulses are important from an ecological perspective by increasing inputs of nutrients and organic matter that are key to mussel diets (Bonner et al. 2018,

Task 2.5) and maintaining habitat heterogeneity (Poff et al. 1997). Pulse flows also provide a variety of ecological services to fish, riparian, and wildlife communities (Poff et al. 1997). Further research is needed to elucidate relationships between mussel ecology and pulse flow events, and therefore, no analysis of pulse flow standards relative to mussels is presented herein.

Environmental Flow Considerations – Brazos Desktop Analysis

For most parameters (depth, velocity, Froude number, Reynolds number, substrate compaction, and shear stress) Little River unionids showed similar HSC to lower Colorado River unionids. However, substrate criteria were quite different due to differences in available habitat between the two systems. No boulder or bedrock substrates were encountered during surveys in the Little River basin, whereas these substrates showed high suitability in the lower Colorado River. Additionally, large differences in *C. houstonensis* HSC were apparent between systems. Species-specific HSC are based on smaller sample sizes than aggregate HSC, and therefore, are inherently more variable. Habitat modeling results presented above demonstrate that in the lower Colorado River, species-specific HSC for candidate mussels reacted similarly to aggregate HSC, and therefore, use of more consistent and statistically-robust aggregate HSC is likely sufficient for future studies.

Lower Colorado River mussel habitat modeling presented above demonstrates that mussel habitat availability peaks at flows lower than most fish habitat guilds used in previous instream modeling work in this basin (BIO-WEST 2008). Given this, and the observation that aggregate mussel HSC show similar utilization of most hydraulic variables between systems, similar results may be expected in the Brazos system, although additional site-specific modeling would be needed to confirm. A recent instream flow study conducted on the middle and lower Brazos River by the Texas Instream Flow Program (TIFP) included evaluation of mussel HSC

and persistent habitat (TIFP 2018). However, mussel habitat availability did not appear to be a major factor in setting instream flow recommendations during this study. In contrast, mussel thermal tolerance data was used to inform subsistence and base flow recommendations.

Conclusions

In conclusion, the two-step modeling approach presented above was successful in predicting mussel occurrence and abundance with mean CPUE data generally being higher in predicted high-quality habitat than in low-quality or non-persistent habitats. The approach of evaluating persistent habitat in combination with more traditional analysis of HSC and resulting WUA calculations provides a good method of accounting for persistent habitat across a wide-range of flow conditions while still recognizing selective habitat utilization of freshwater mussels. Species-specific criteria reacted similarly to aggregate criteria but were more variable and therefore less predictive. This suggests that aggregate mussel criteria based on more robust datasets may be sufficient for use in future studies, particularly when dealing with rare species and small sample sizes. The methods applied herein and the subsequent modeling results for the lower Colorado River will no doubt be useful in validating and refining instream flow standards in this basin, and potentially others, in the future.

It should be recognized that instream flow recommendations based solely on the mussel habitat modeling conducted above would result in lower base flow and potentially lower subsistence flow recommendations. However, a holistic approach is necessary when setting instream flow recommendations. While mussel habitat availability is an important consideration, it is only one component of many to be analyzed when developing ecologically-protective environmental flow recommendations. Mussel survival and recruitment could potentially be limited by water quality conditions under low flow situations. Applied research laboratory

studies conducted as a component of Task 2 of this study (Bonner et al. 2018) have provided crucial information regarding sublethal influences of water quality stressors on candidate species in the Colorado River basin. However, since this data became available, no water quality modeling studies have been conducted to integrate this new information with water quality data from the lower Colorado River.

Additionally, habitat availability for all organisms must be evaluated when setting instream flow recommendations. Previous studies have shown that habitat availability for most fish habitat guilds peak at higher flows than those for mussels presented above (BIO-WEST 2008). For the state-threatened Blue Sucker *Cycleptus elongatus*, habitat availability peaked at 2,000-2,500 cfs at the La Grange and Altair model sites (BIO-WEST 2008). High pulse flows, although they may potentially impact mussel persistence, are important for water availability and ecosystem disturbance within the riparian community (Stromberg et al. 2007). When setting instream flow recommendations, the mussel habitat modeling results presented above should be integrated with existing information for fish and riparian communities and should also include evaluation of sediment transport and other important physical components of a healthy riverine system. The above analysis fills a critical data gap in this process by providing information on mussel habitat availability in the lower Colorado River, and provides a new method for modeling mussel habitat in riverine systems.

Tables

Table 1. Results of mussel surveys at ten previously established LSWP intensive study sites on the Lower Colorado River. [a]*C. houstonensis*, [b]*C. petrina*, [c]*T. macrodon*

LSWP Site	Search Time (person-hours)	Mussel Abundance	CPUE (mussels/p-h)	Number of Candidate Species Present
Longhorn Dam	6	0	0.0	0
Utley	11	28	2.5	0
Bastrop	6	0	0.0	0
Smithville - US	6	0	0.0	0
Smithville - DS	6	0	0.0	0
La Grange[a]	11	74	6.7	1
Columbus[a,b]	10	88	8.8	2
Altair[a,b,c]	13	619	47.6	3
Wharton[a,b,c]	11	35	3.2	3
Lane City[b,c]	5	18	3.6	2
	85	862	10.1	

Table 2. Bed roughness values (k_s; cm) for each substrate type used in estimating shear stress. Values approximate median particle size for each substrate type from the Wentworth scale, except for bedrock. Values for bedrock were estimated based on perceived roughness of local bedrock material in comparison to other classes.

Substrate Class	k_s (cm)
Clay	0.0002
Silt	0.0016
Sand	0.05
Gravel	1.6
Cobble	6.4
Boulder	25
Bedrock	2

Table 3. Hydraulic model runs and associated water surface elevation calibration results.

Site	Discharge		Upstream			Mid-reach			Downstream		
	cms	cfs	Observed (m)	Predicted (m)	Δ (cm)	Observed (m)	Predicted (m)	Δ (cm)	Observed (m)	Predicted (m)	Δ (cm)
La Grange	1.42	50	NA	67.67	NA	NA	NA	NA	NA	66.11	NA
	2.83	100	NA	67.73	NA	NA	NA	NA	NA	66.21	NA
	7.08	250	NA	67.83	NA	NA	NA	NA	NA	66.34	NA
	12.74	450	67.97	67.93	4	66.61	66.57	4	66.61	66.60	1
						67.21	67.20	1			
	20.90	738	68.10	68.03	7	NA	NA	NA	66.60	66.62	-2
	56.63	2000	68.39	68.37	2	NA	NA	NA	67.01	67.02	-1
	243.81	8610	69.47	69.54	-7	NA	NA	NA	68.58	68.62	-2
Altair	2.83	100	NA	41.97	NA	NA	NA	NA	NA	38.53	NA
	9.81	287	42.40	42.33	7	NA	NA	NA	42.23	42.22	1
	14.87	525	42.43	42.46	-3	42.20	42.24	-4	42.24	42.24	0
						42.31	42.35	-4			
	27.78	981	42.74	42.69	5	NA	NA	NA	42.32	42.32	0
	41.39	1459	42.91	42.86	5	NA	NA	NA	42.36	42.36	0
	52.36	1849	43.00	42.98	2	NA	NA	NA	42.40	42.40	0
	234.95	8297	44.34	44.1	24	NA	NA	NA	42.77	42.77	0

Table 4. Model-predicted Persistent Weighted Usable Area (PWUA) from base flow rates at the Altair site.

Modeled Discharge (cms)	Modeled Discharge (cfs)	Aggregate Unionids		*C. houstonensis*		*C. petrina*	
		PWUA (m^2)	PWUA (% max)	PWUA (m^2)	PWUA (% max)	PWUA (m^2)	PWUA (% max)
2.83	100	50,336	76	42,781	75	65,024	76
8.13	287	66,072	100	55,987	98	85,116	100
14.87	525	52,626	80	45,718	80	67,994	80
27.78	981	62,113	94	57,345	100	79,301	93
41.39	1459	30,634	46	26,064	45	37,975	45
52.36	1879	27,138	41	22,824	40	32,920	39

Table 5. Model-predicted Persistent Weighted Usable Area (PWUA) from base flow rates at the La Grange site.

Modeled Discharge (cms)	Modeled Discharge (cfs)	Aggregate Unionids		*C. houstonensis*		*C. petrina*	
		PWUA (m^2)	PWUA (% max)	PWUA (m^2)	PWUA (% max)	PWUA (m^2)	PWUA (% max)
1.42	50	16,106	99	13,256	92	19,842	95
2.83	100	16,303	100	14,392	100	20,985	100
7.08	250	15,261	94	13,365	93	19,932	95
12.74	450	12,821	79	10,905	76	17,344	83
20.9	738	11,066	68	9,105	63	14,996	71
56.63	2000	8,872	54	6,986	49	12,032	57

Table 6. Ranges of TCEQ environmental flow standards for the lower Colorado River at Bastrop and Columbus. Specific subsistence and base flow standards vary depending on season and hydrologic condition.

Measurement Site	Environmental Flow Standards (cfs)				
	Subsistence	Base	2 per season	1 per 18 months	1 per 2 years
Bastrop	123-275	194-824	3000	8000	NA
Columbus	190-534	310-1440	3000	8000	27000

Figures

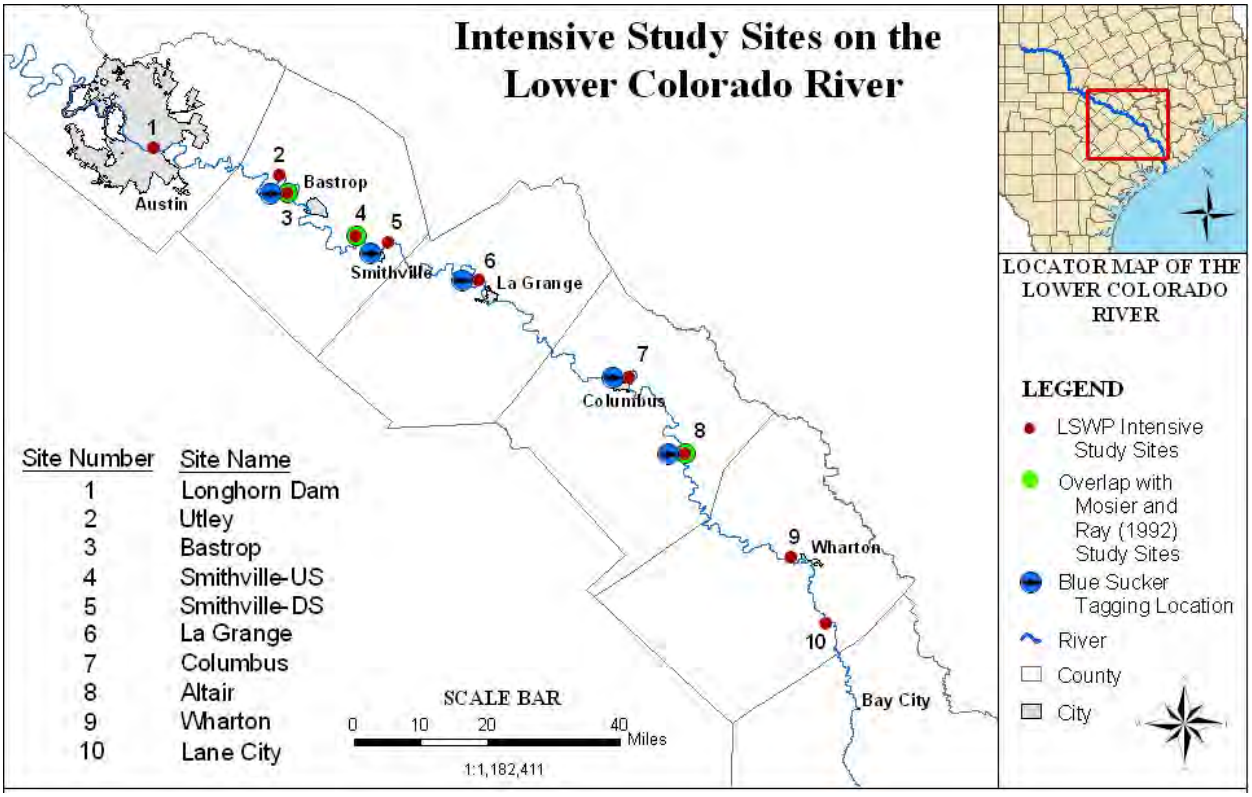

Figure 1. LSWP intensive study sites with existing hydraulic models.

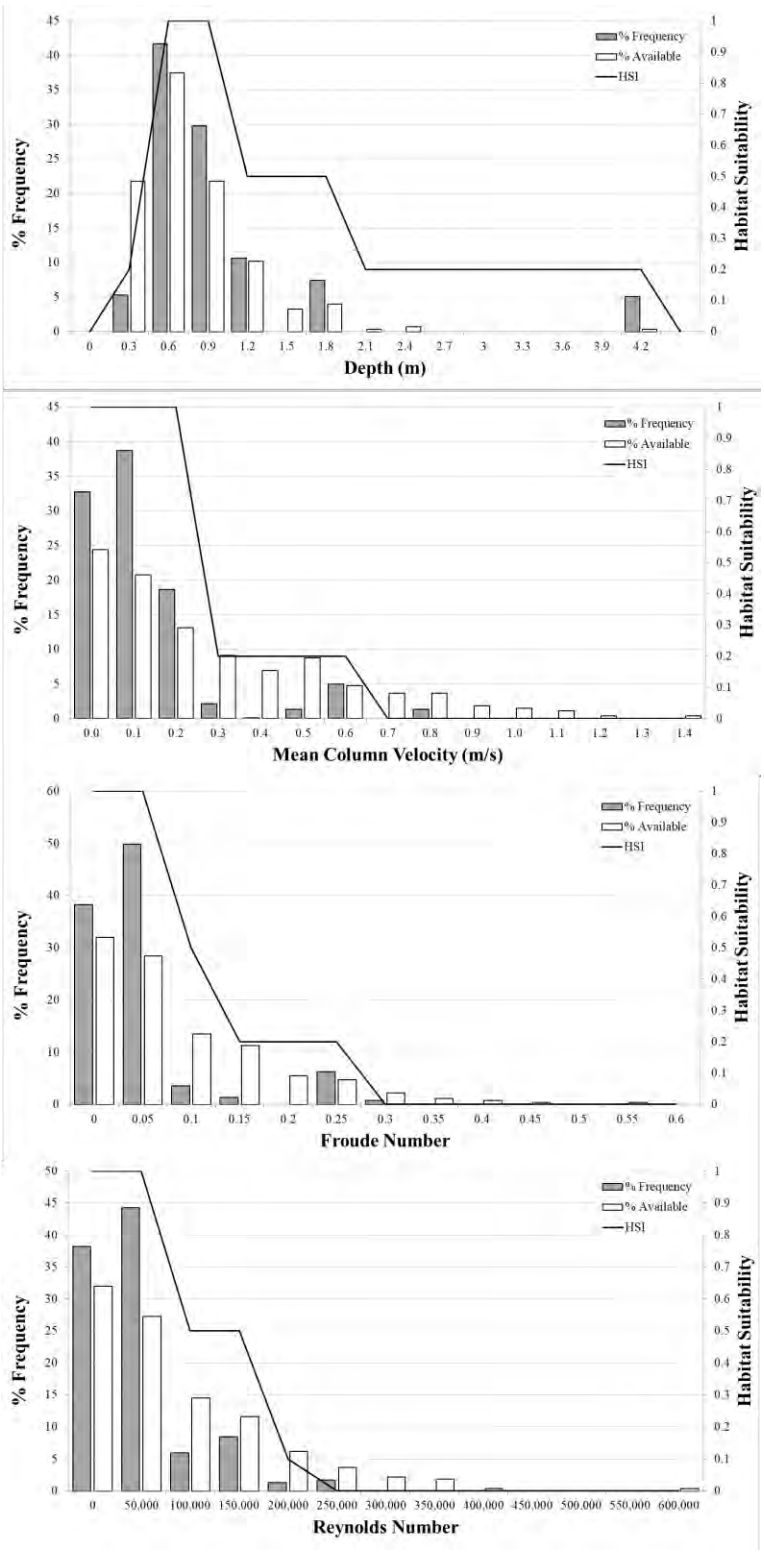

Figure 2. Percent frequency of occurrence (gray bars), percent frequency of habitats sampled (white bars), and habitat suitability values (black line) for lower Colorado River unionids (n = 2327) in relation to depth (m), mean column velocity (m/s), Froude number, and Reynolds number.

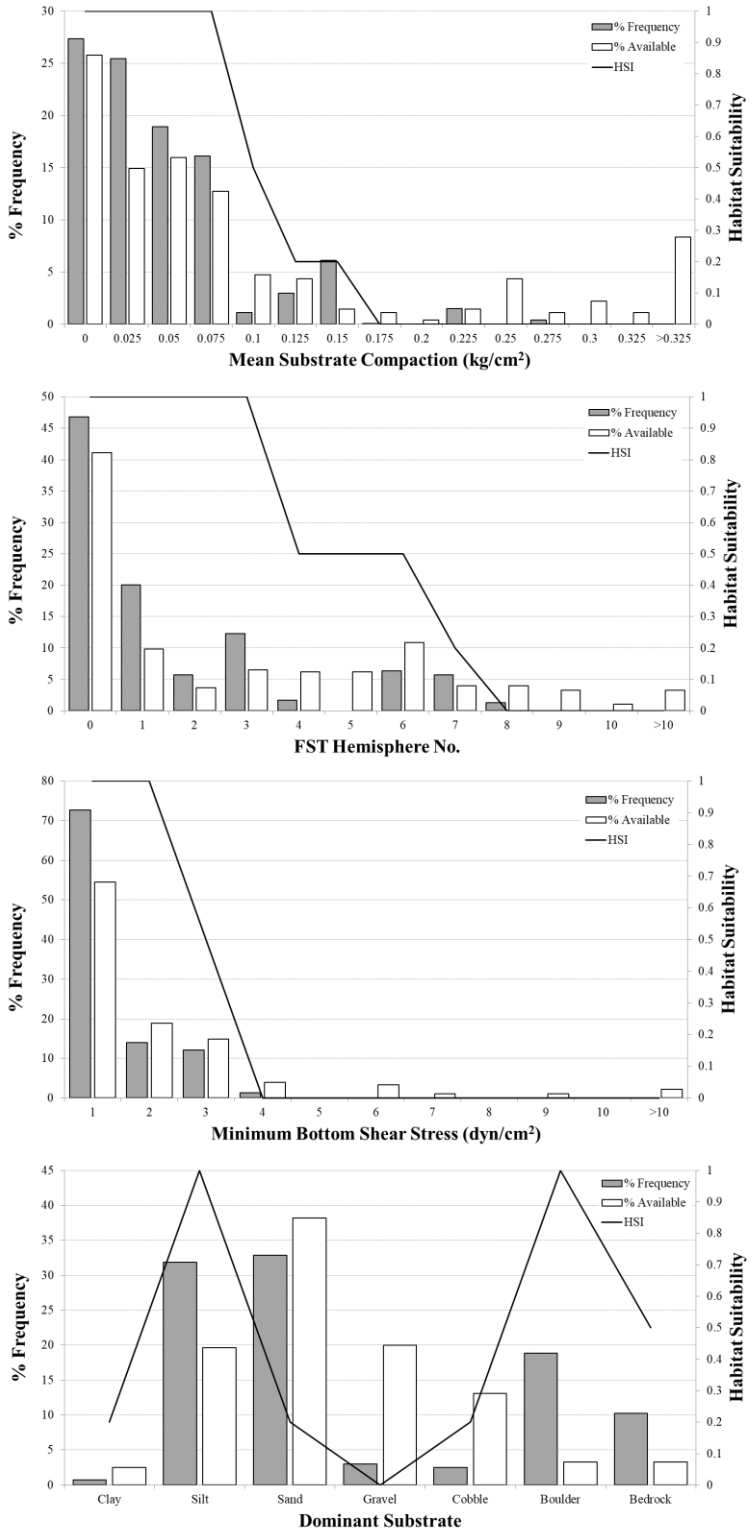

Figure 3. Percent frequency of occurrence (gray bars), percent frequency of habitats sampled (white bars), and habitat suitability values (black line) for lower Colorado River unionids (n = 2327) in relation to mean substrate compaction (kg/cm^2), FST hemisphere number, minimum bottom shear stress (dyn/cm^2), and dominant substrate.

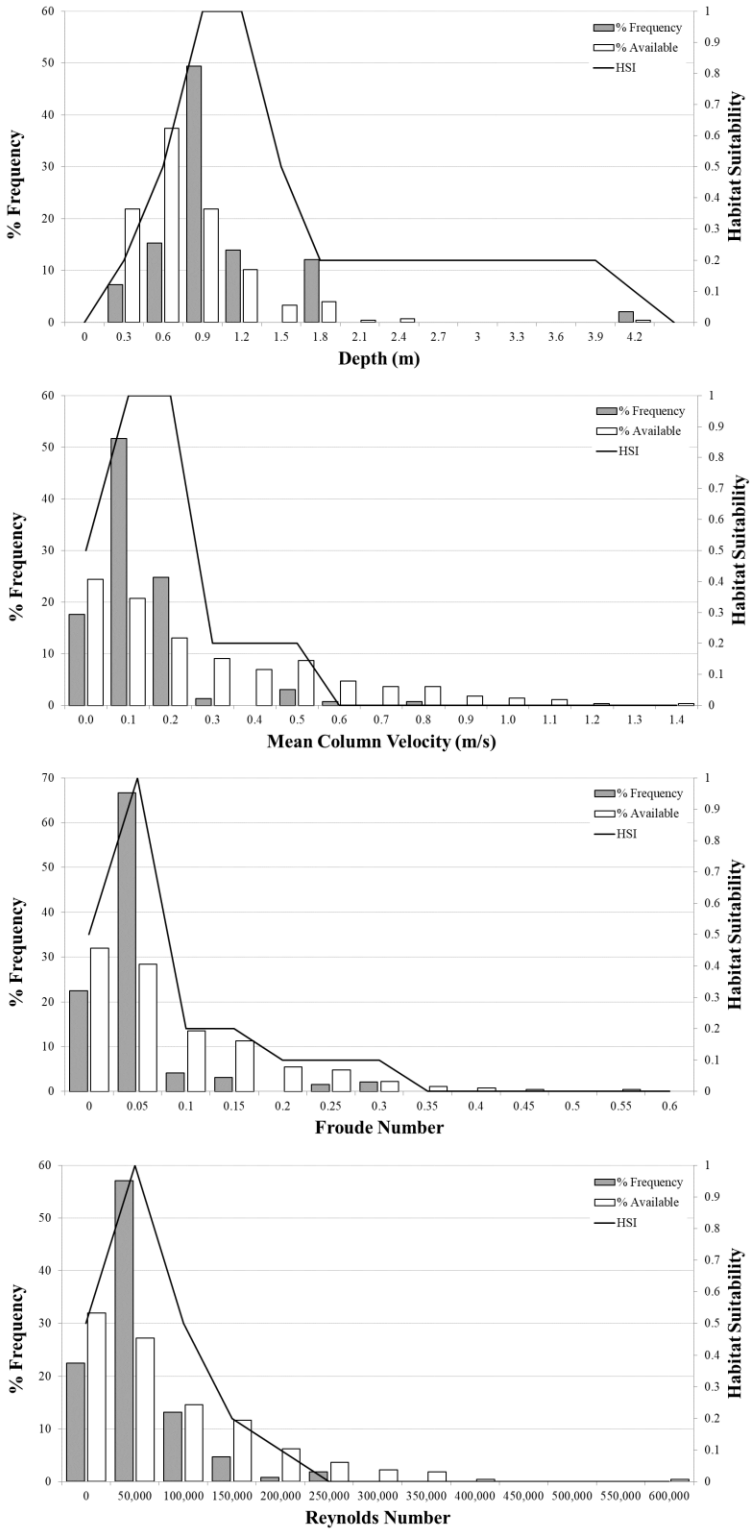

Figure 4. Percent frequency of occurrence (gray bars), percent frequency of habitats sampled (white bars), and habitat suitability values (black line) for lower Colorado River *C. houstonensis* (n = 387) in relation to depth (m), mean column velocity (m/s), Froude number, and Reynolds number.

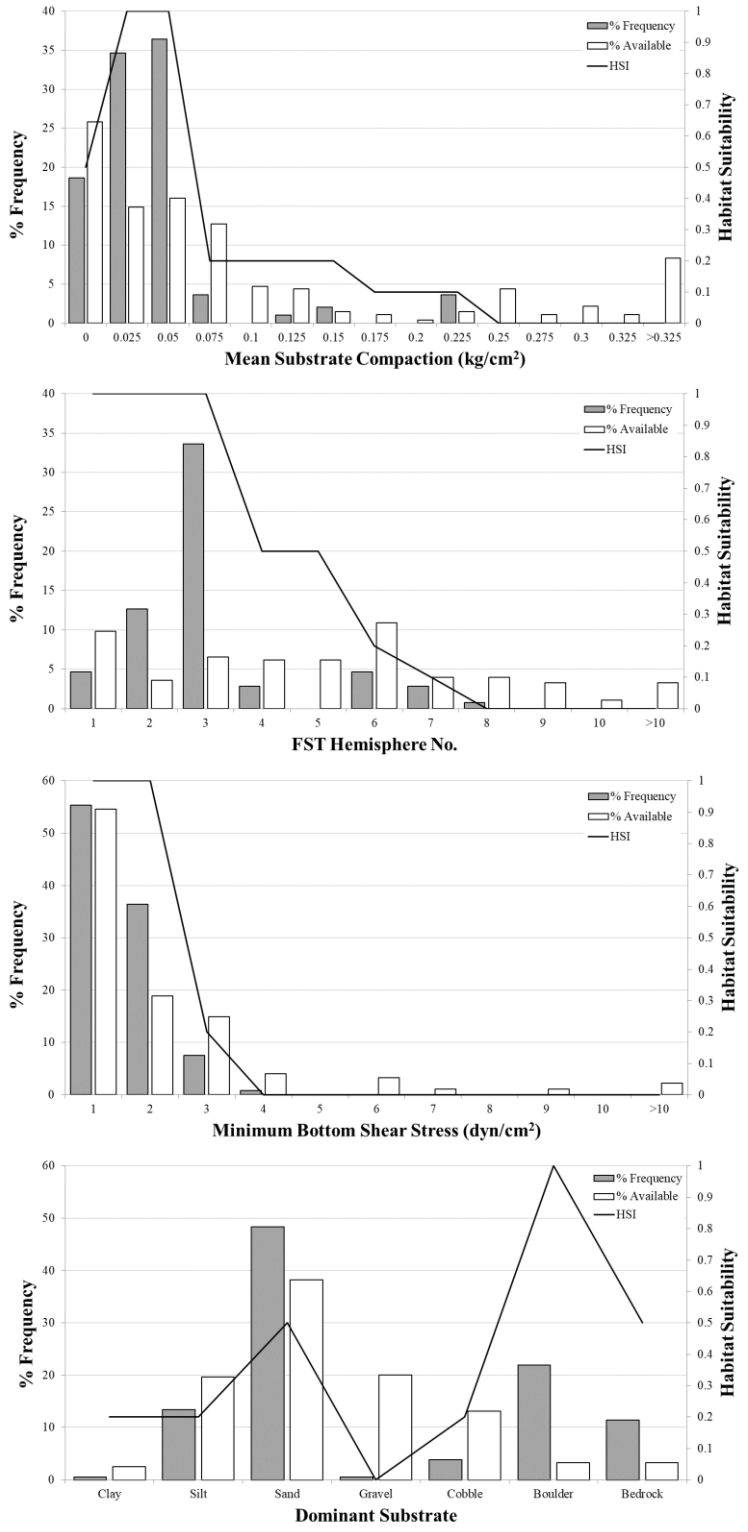

Figure 5. Percent frequency of occurrence (gray bars), percent frequency of habitats sampled (white bars), and habitat suitability values (black line) for lower Colorado River *C. houstonensis* (n = 387) in relation to mean substrate compaction (kg/cm^2), FST hemisphere number, minimum bottom shear stress (dyn/cm^2), and dominant substrate.

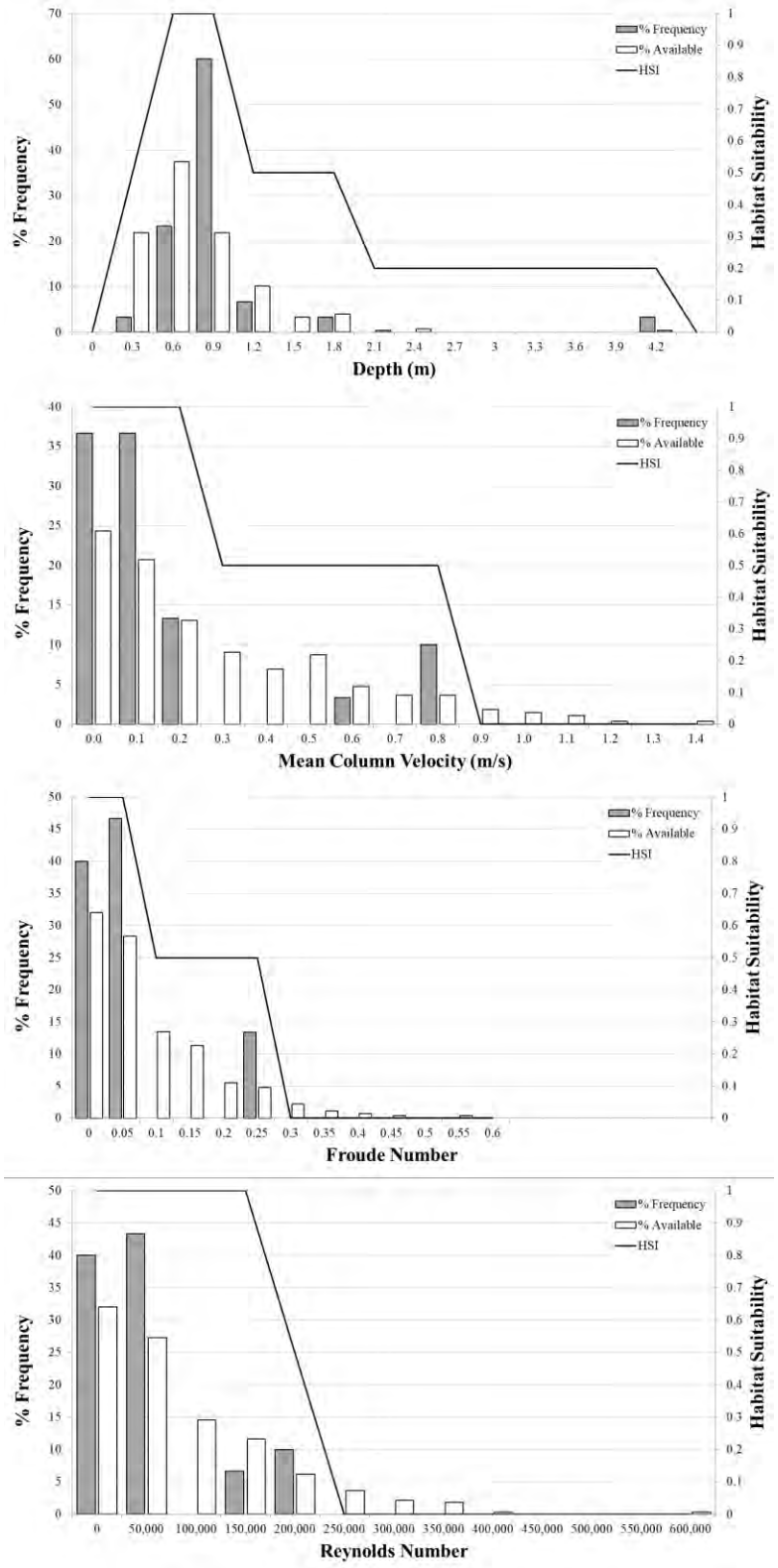

Figure 6. Percent frequency of occurrence (gray bars), percent frequency of habitats sampled (white bars), and habitat suitability values (black line) for lower Colorado River *C. petrina* (n = 30) in relation to depth (m), mean column velocity (m/s), Froude number, and Reynolds number.

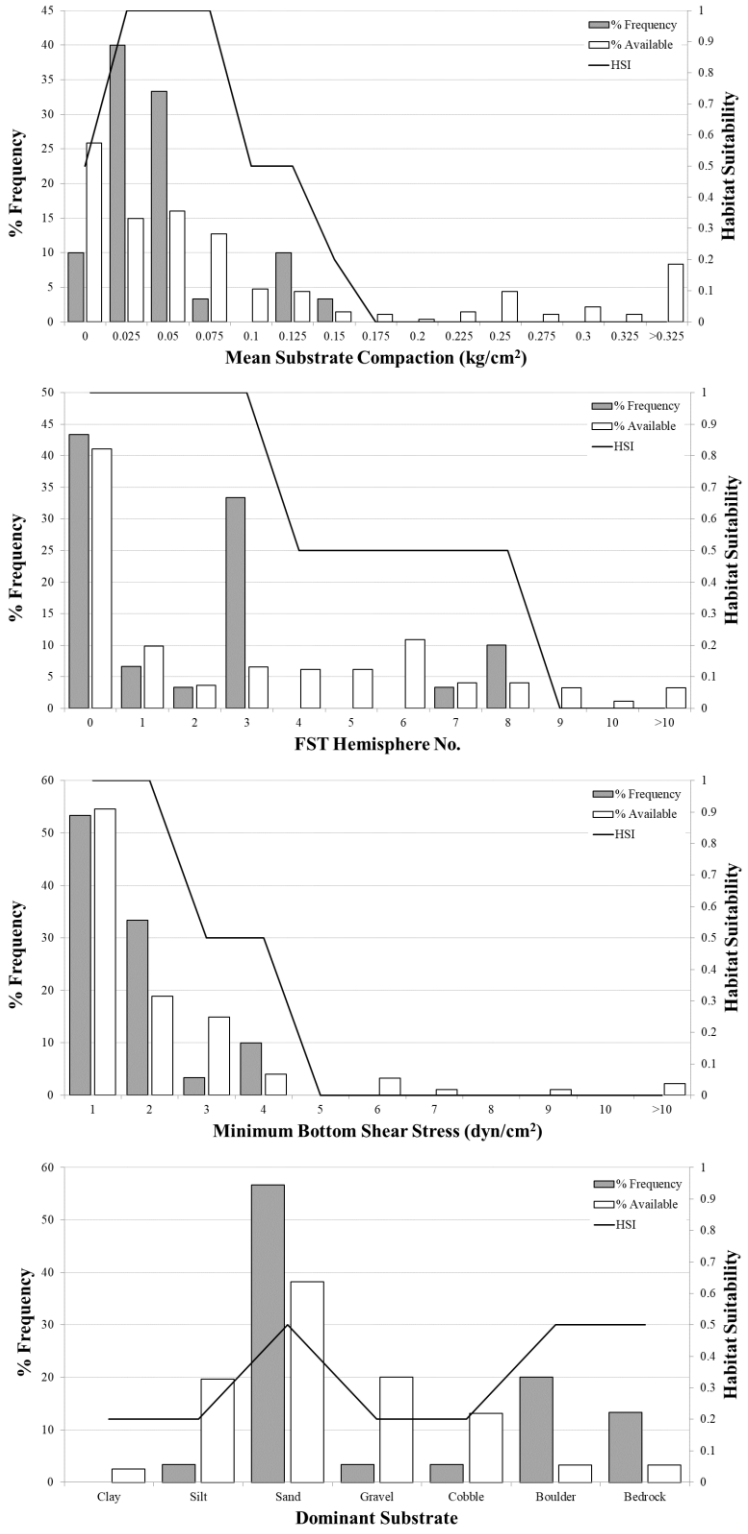

Figure 7. Percent frequency of occurrence (gray bars), percent frequency of habitats sampled (white bars), and habitat suitability values (black line) for lower Colorado River *C. petrina* (n = 30) in relation to mean substrate compaction (kg/cm^2), FST hemisphere number, minimum bottom shear stress (dyn/cm^2), and dominant substrate.

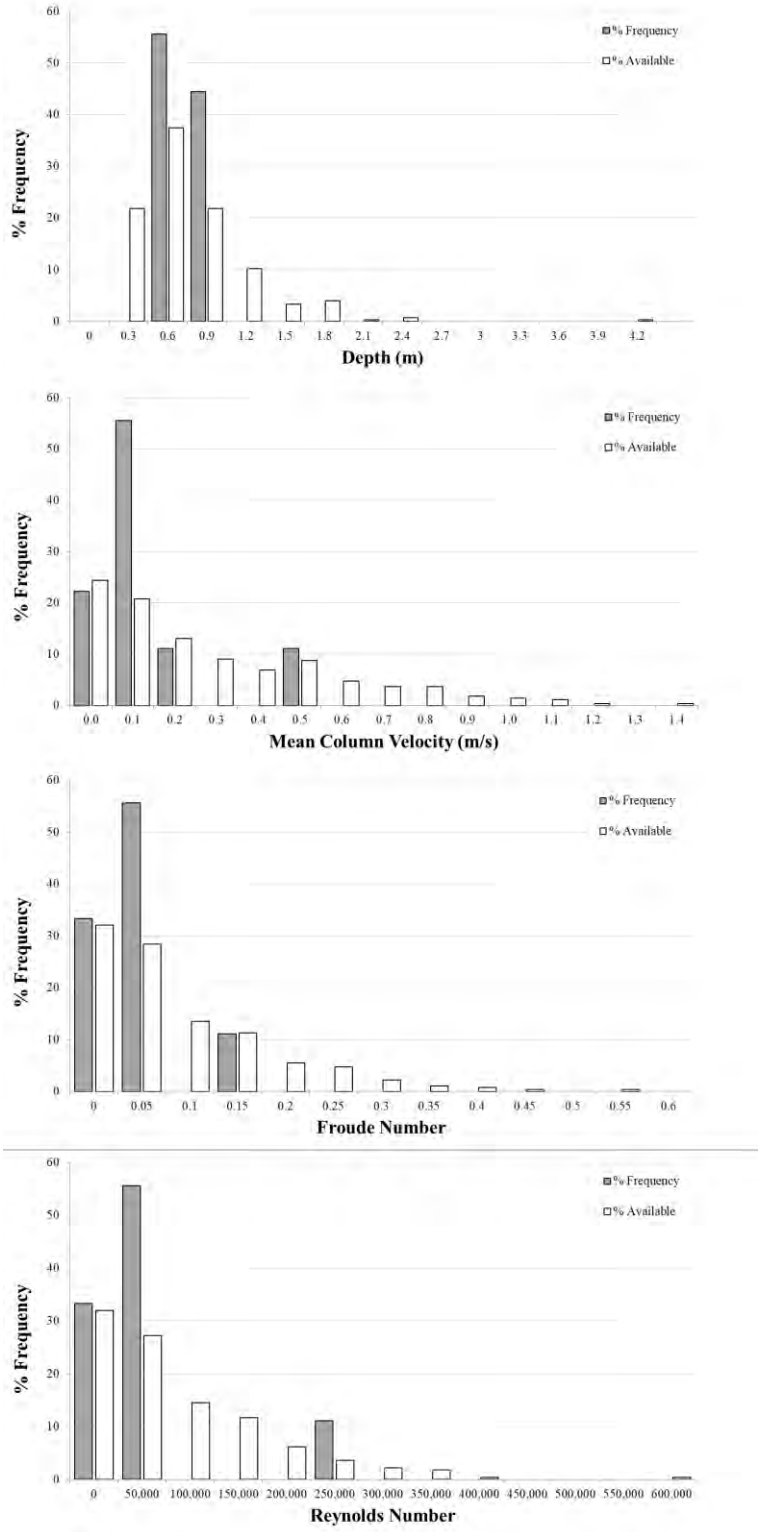

Figure 8. Percent frequency of occurrence (gray bars) and percent frequency of habitats sampled (white bars) for lower Colorado River *T. macrodon* (n = 9) in relation to depth (m), mean column velocity (m/s), Froude number, and Reynolds number. HSC were not generated for *T. macodon* due to insufficient sample size.

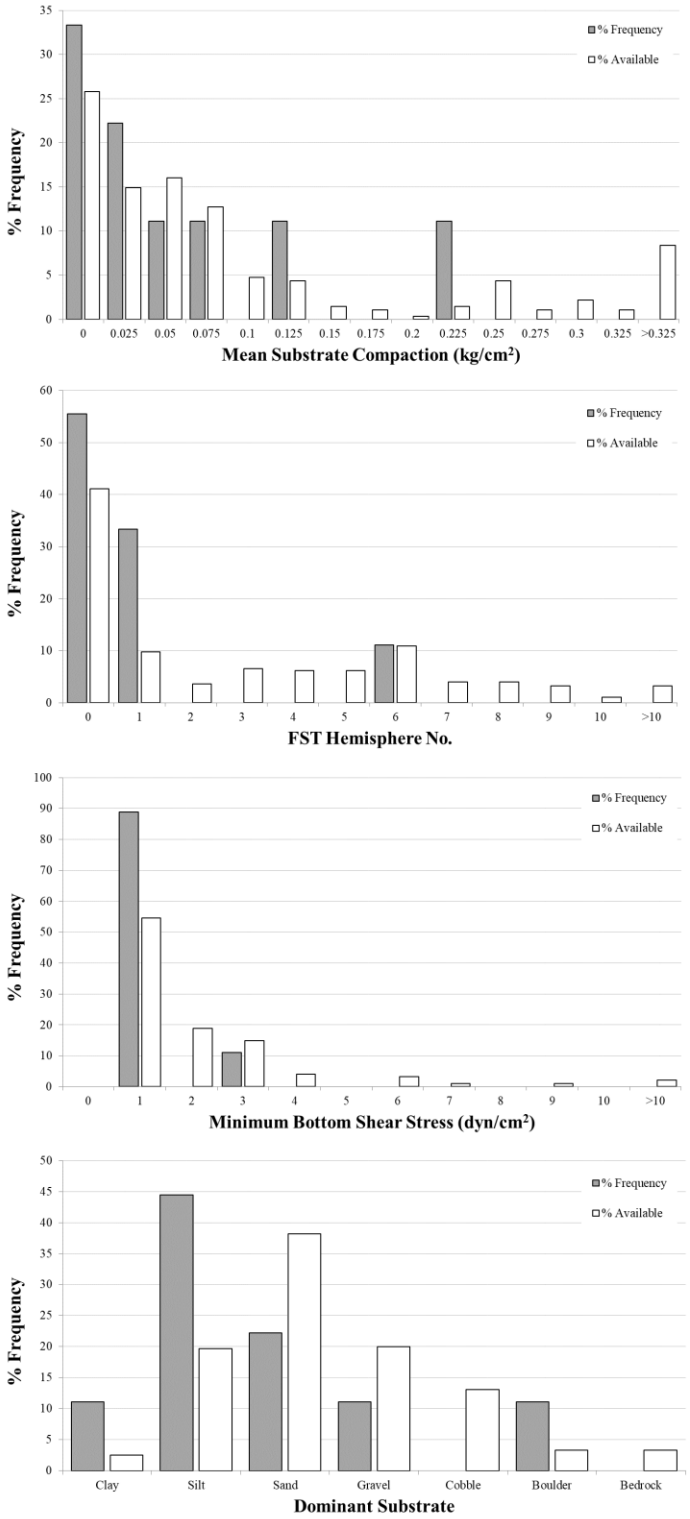

Figure 9. Percent frequency of occurrence (gray bars) and percent frequency of habitats sampled (white bars) for lower Colorado River *T. macrodon* (n = 9) in relation to mean substrate compaction (kg/cm^2), FST hemisphere number, minimum bottom shear stress (dyn/cm^2), and dominant substrate. HSC were not generated for *T. macodon* due to insufficient sample size.

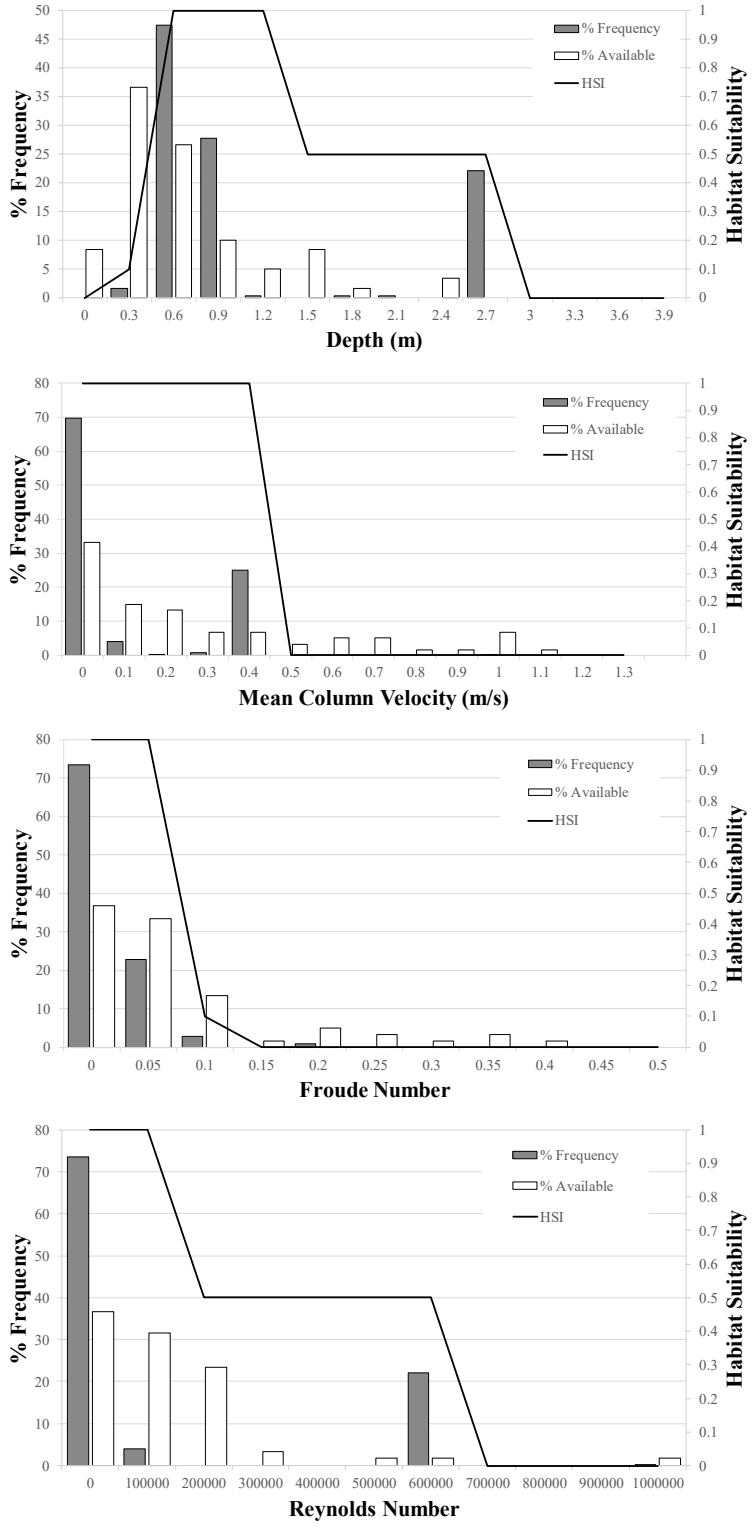

Figure 10. Percent frequency of occurrence (gray bars), percent frequency of habitats sampled (white bars), and habitat suitability values (black line) for Little River unionids (n = 320) in relation to depth (m), mean column velocity (m/s), Froude number, and Reynolds number.

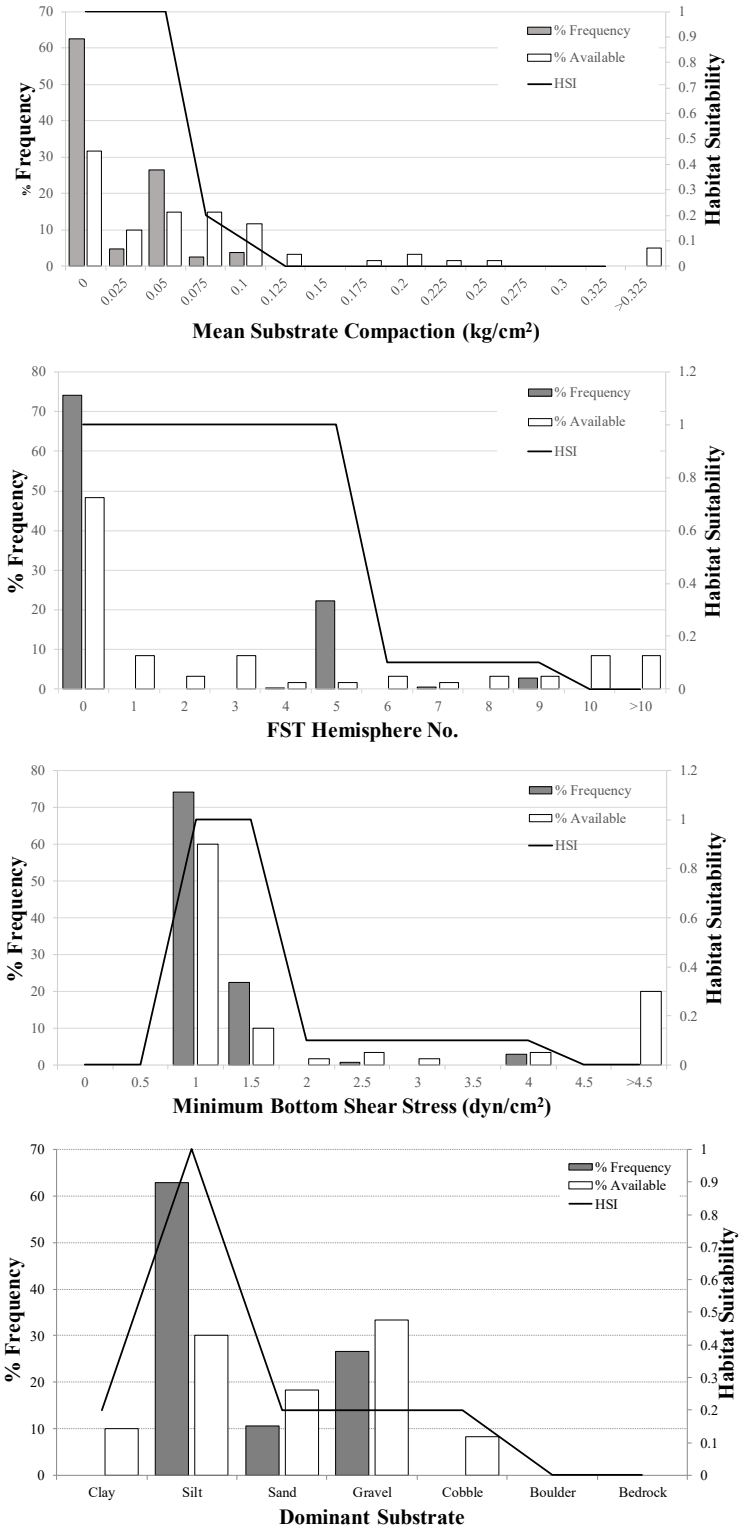

Figure 11. Percent frequency of occurrence (gray bars), percent frequency of habitats sampled (white bars), and habitat suitability values (black line) for Little River unionids (n = 320) in relation to mean substrate compaction (kg/cm^2), FST hemisphere number, minimum bottom shear stress (dyn/cm^2), and dominant substrate.

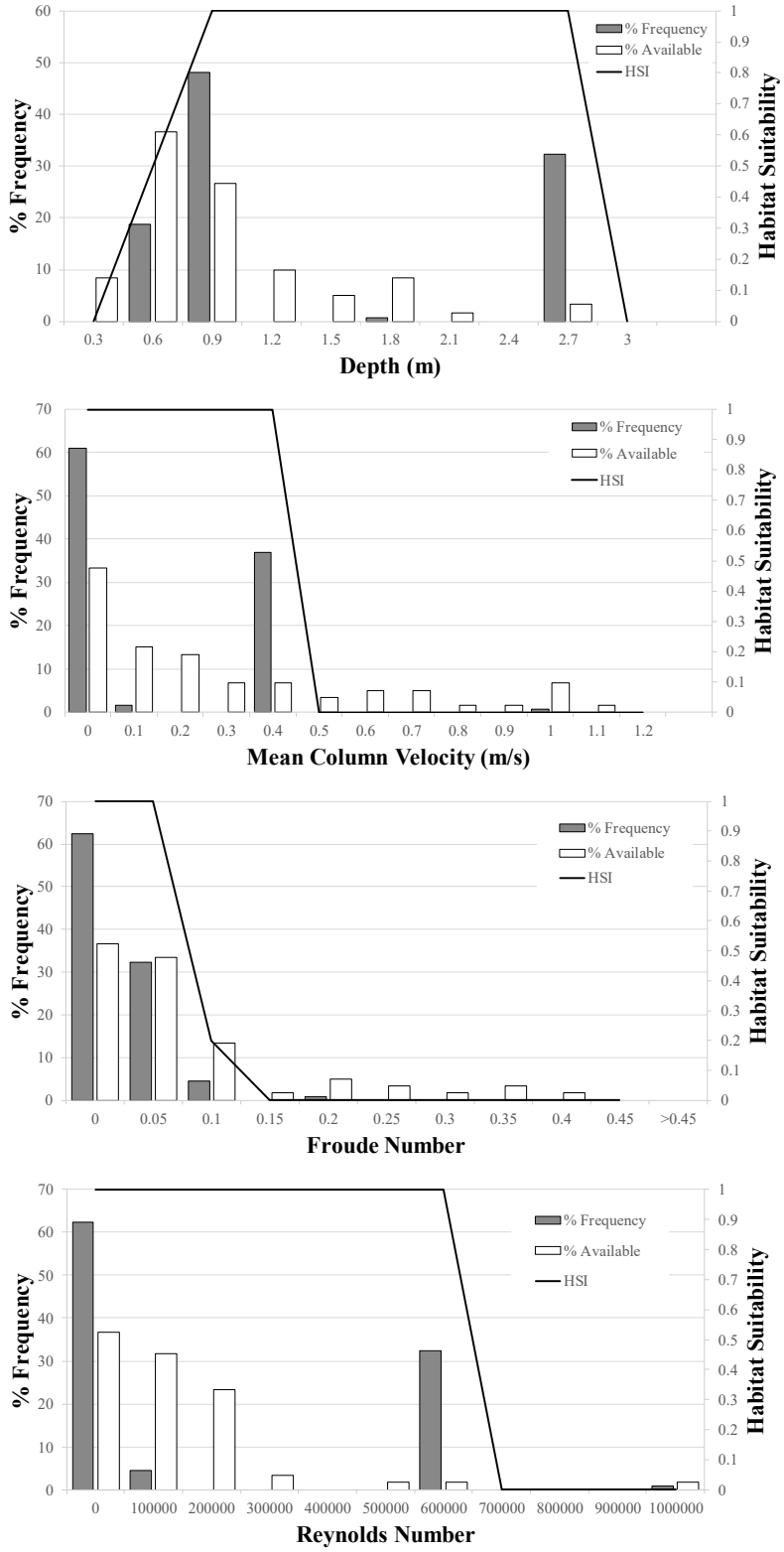

Figure 12. Percent frequency of occurrence (gray bars) and percent frequency of habitats sampled (white bars) for Little River *C. houstonensis* (n = 133) in relation to in relation to depth (m), mean column velocity (m/s), Froude number, and Reynolds number.

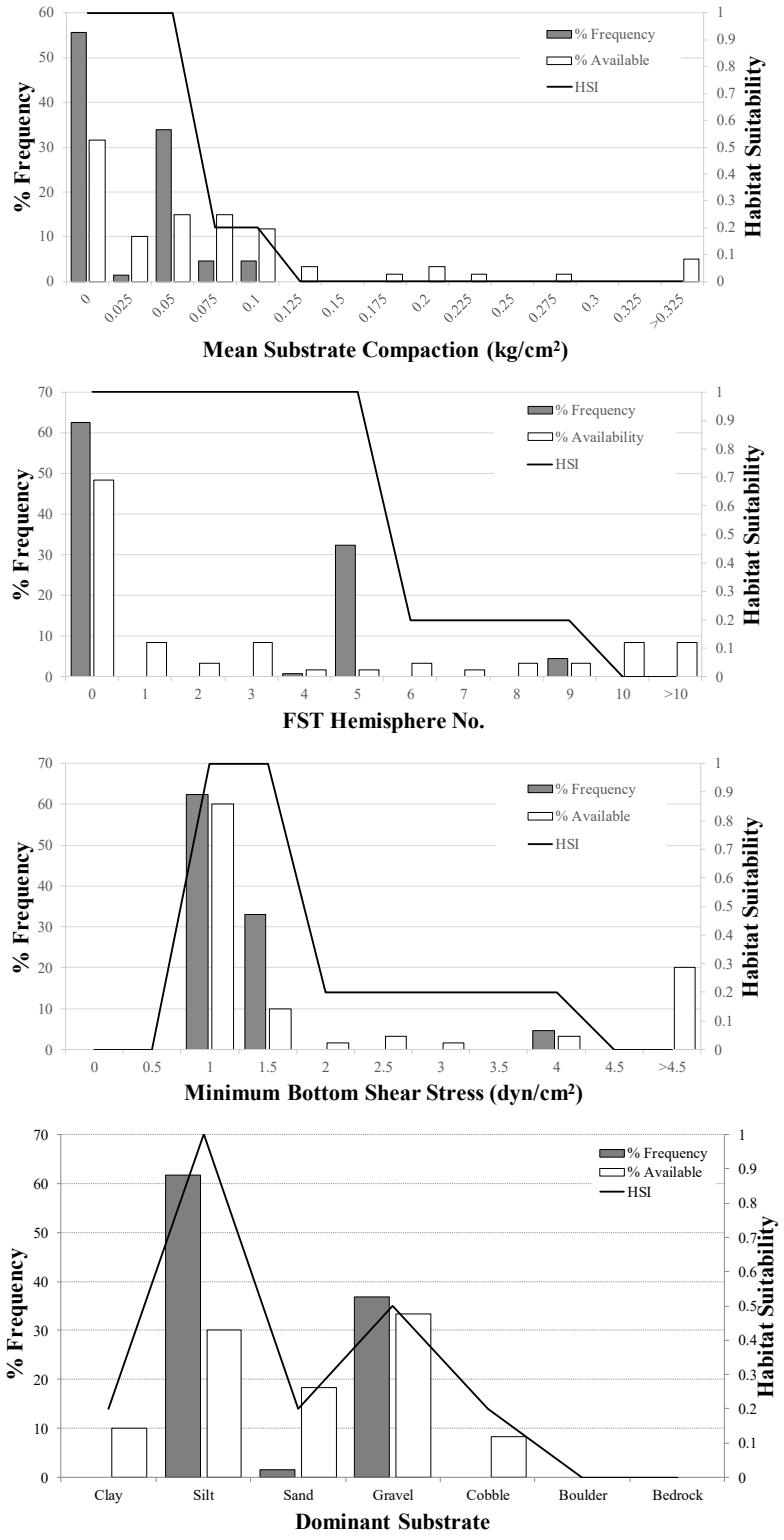

Figure 13. Percent frequency of occurrence (gray bars) and percent frequency of habitats sampled (white bars) for Little River *C. houstonensis* (n = 133) in relation to mean substrate compaction (kg/cm^2), FST hemisphere number, minimum bottom shear stress (dyn/cm^2), and dominant substrate.

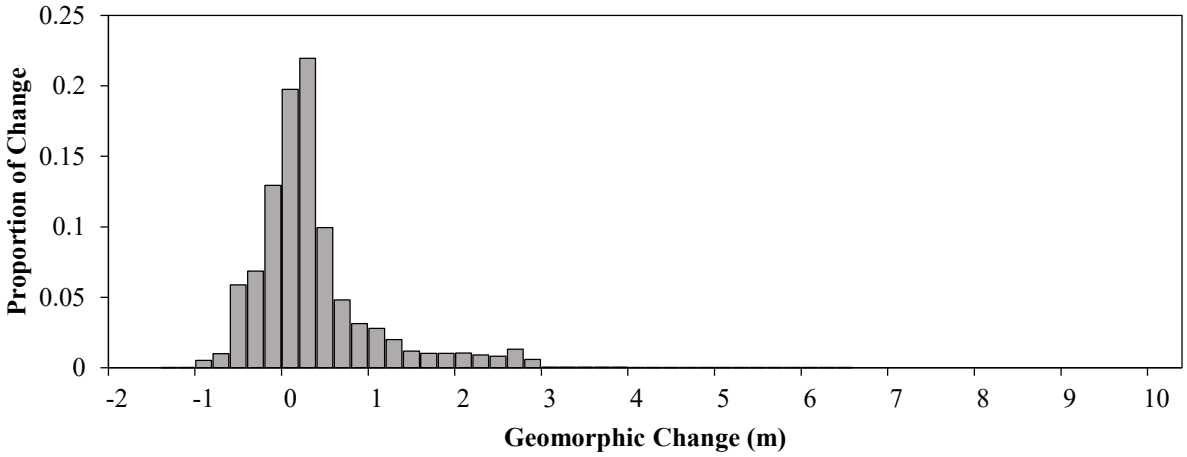

Figure 14. Histogram of changes in bed elevation between original model (2008) and updated model (2018) at the Altair site. Negative values represent deposition and positive values represent scour.

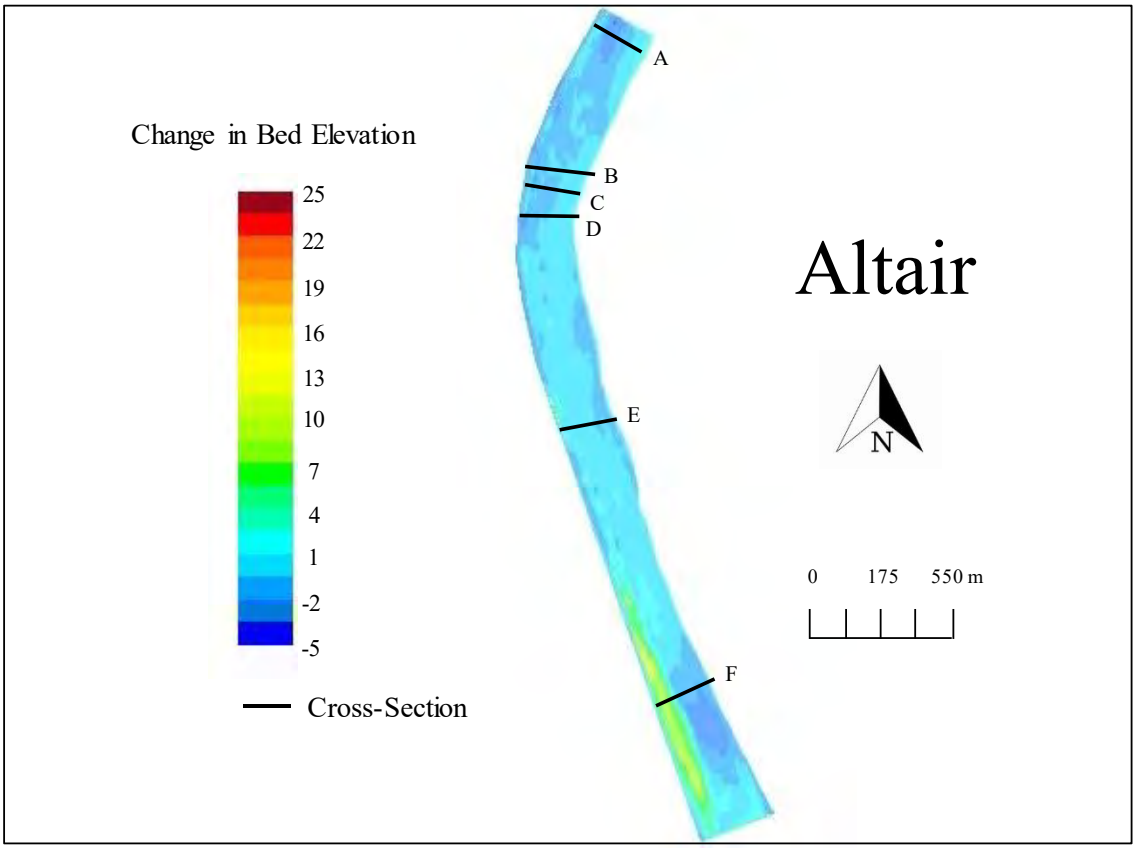

Figure 15. Map of change in bed elevation between original model (2008) and updated model (2018) at the Altair site. Negative values represent deposition and positive values represent scour.

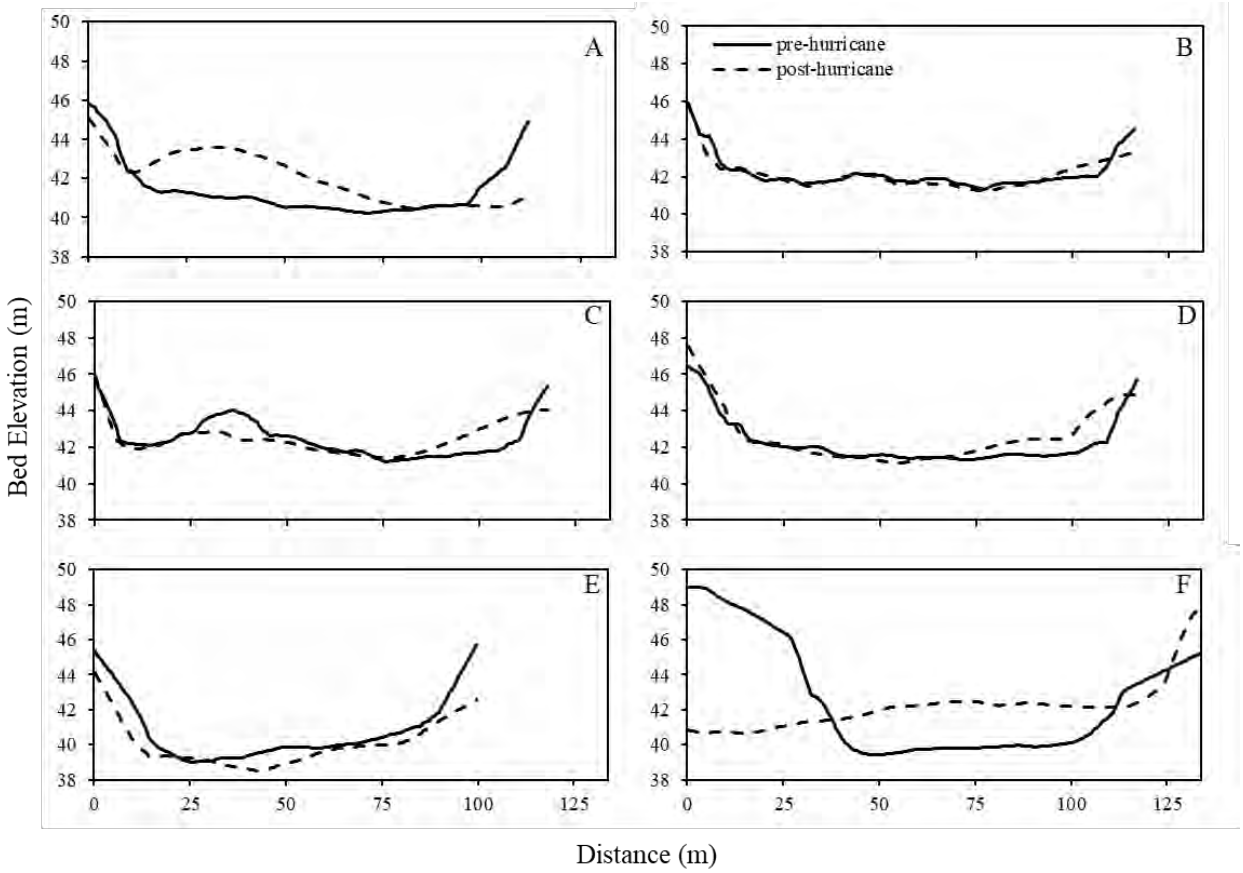

Figure 16. Cross-sections from the Altair site showing changes in bed elevation between the original model (pre-hurricane, 2008) and the updated model (post-hurricane, 2018). Cross-section locations are depicted in Figure 15.

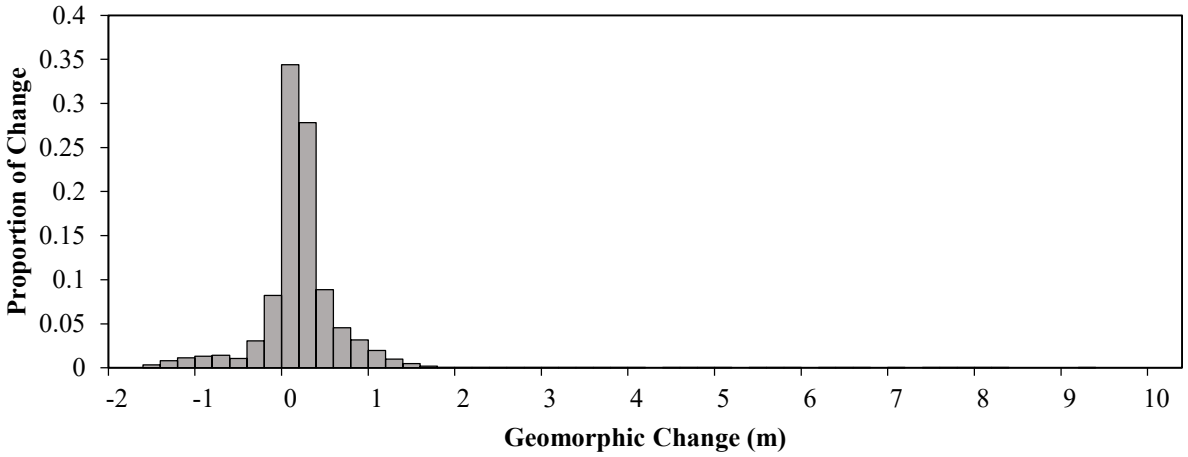

Figure 17. Histogram of changes in bed elevation between original model (2008) and updated model (2018) at the La Grange site. Negative values represent deposition and positive values represent scour.

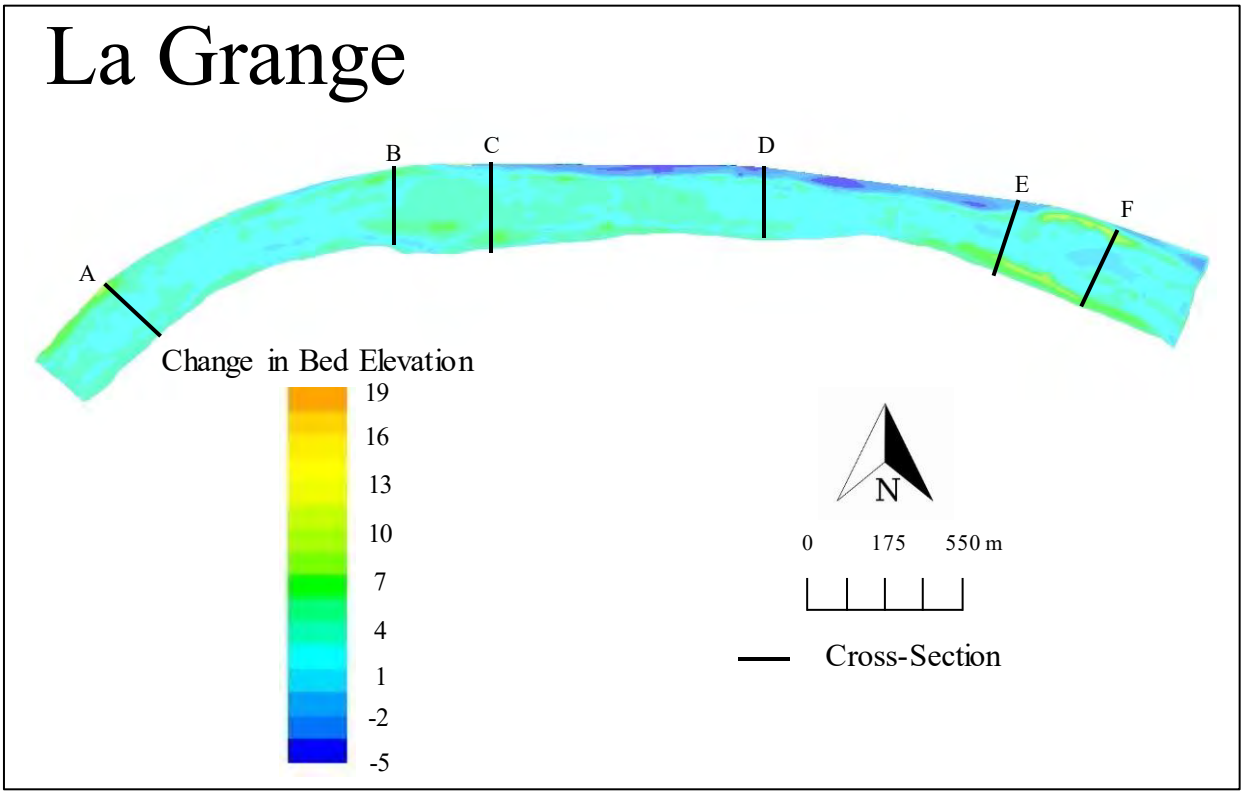

Figure 18. Map of change in bed elevation between original model (2008) and updated model (2018) at the La Grange site. Negative values represent deposition and positive values represent scour.

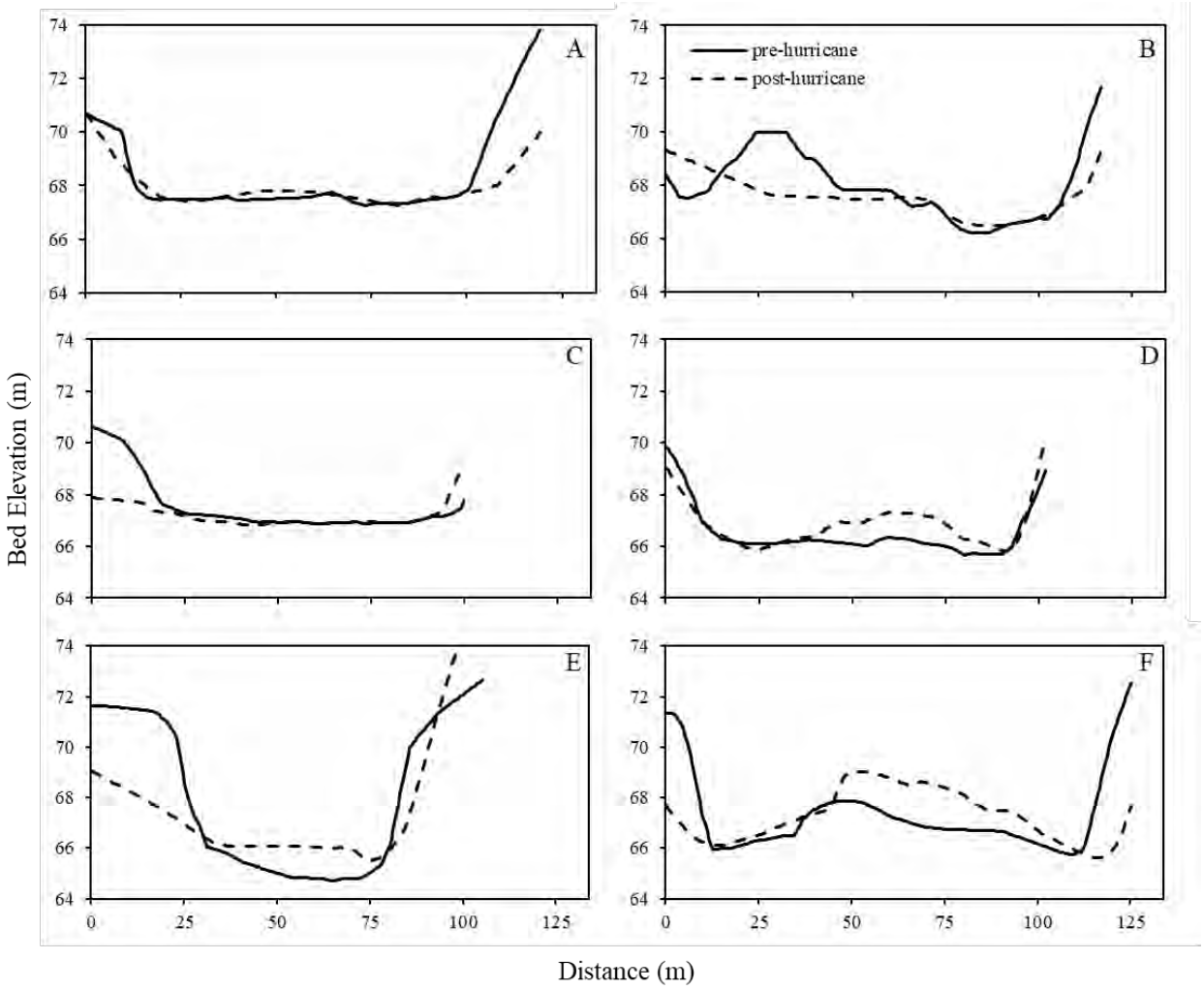

Figure 19. Cross-sections from the La Grange site showing changes in bed elevation between the original model (pre-hurricane, 2008) and the updated model (post-hurricane, 2018). Cross-section locations are depicted in Figure 18.

Figure 20. Map of persistent habitat at Altair.

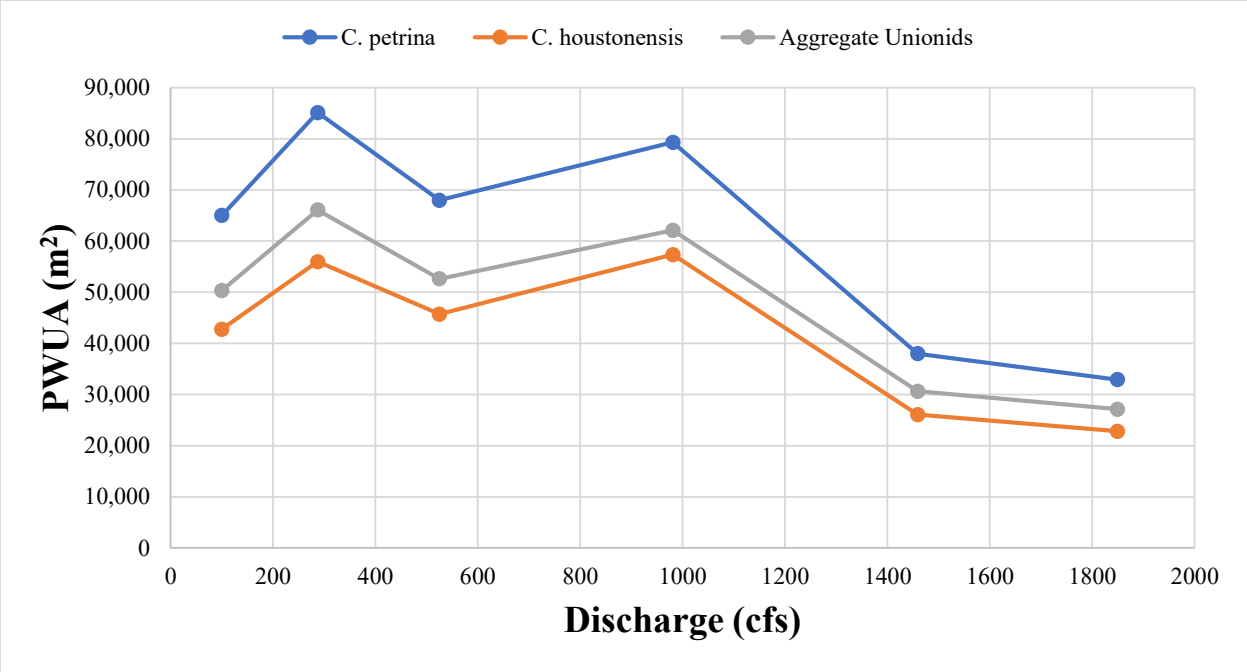

Figure 21. Persistent Weighted Usable Area (PWUA; m^2) to discharge relationships for *C. petrina*, *C. houstonensis*, and aggregate unionids from the Altair study site.

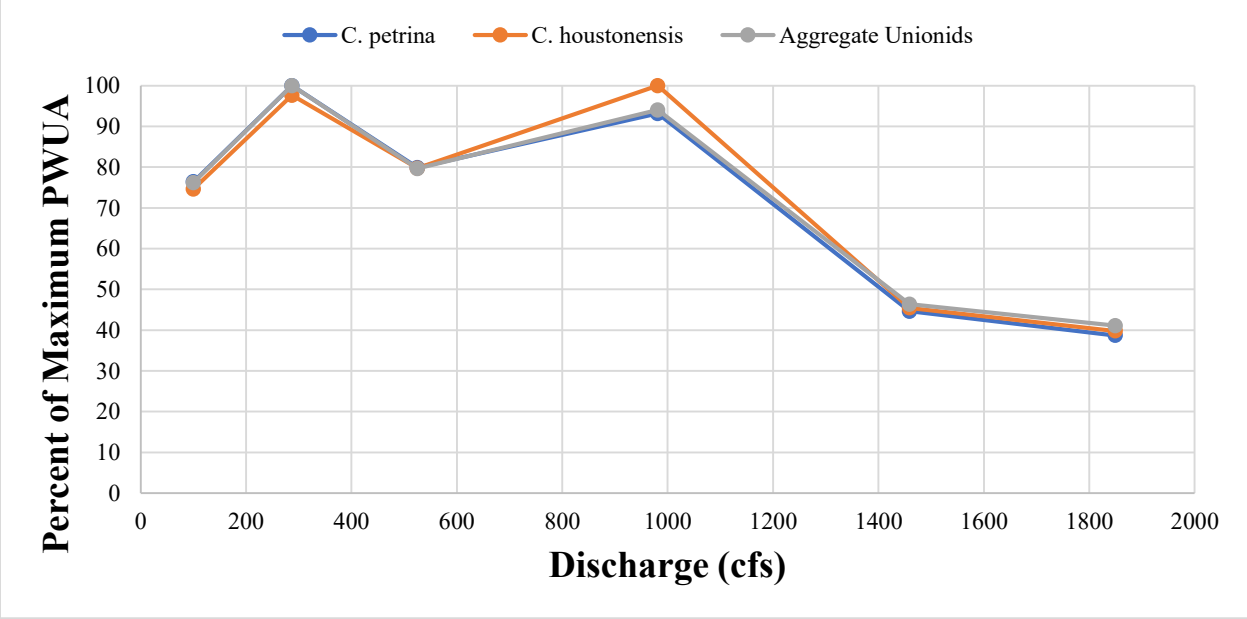

Figure 22. Percent of maximum PWUA to discharge relationships for *C. petrina*, *C. houstonensis*, and aggregate unionids from the Altair study site.

Figure 23. Map of persistent habitat at La Grange.

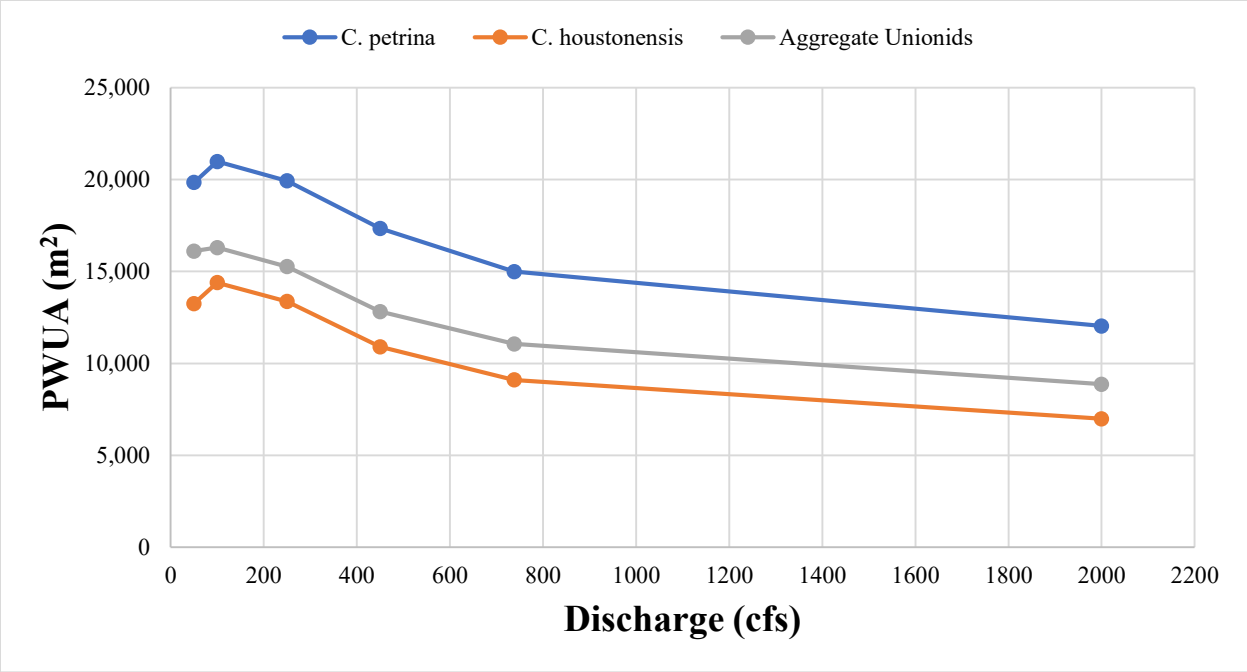

Figure 24. Persistent Weighted Usable Area (PWUA; m^2) to discharge relationships for *C. petrina*, *C. houstonensis*, and aggregate unionids from the La Grange study site.

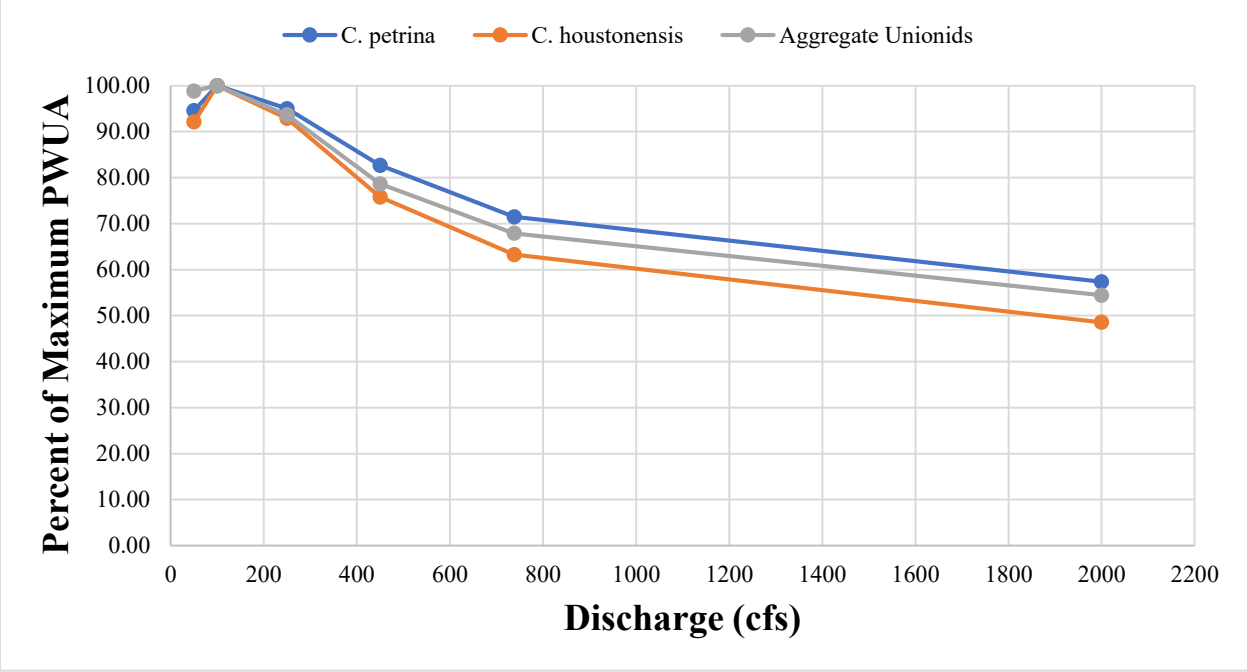

Figure 25. Percent of maximum PWUA to discharge relationships for *C. petrina*, *C. houstonensis*, and aggregate unionids from the La Grange study site.

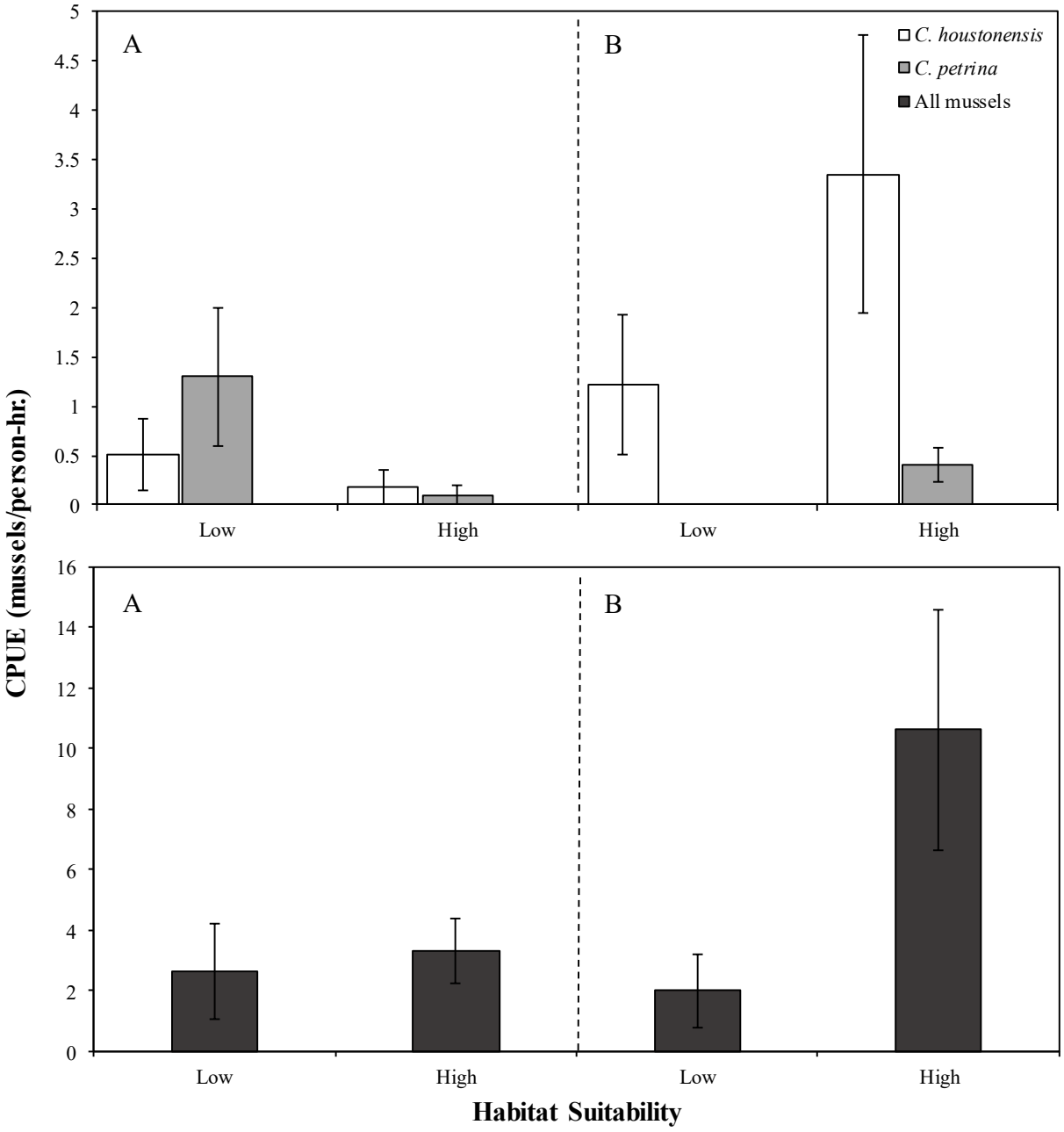

Figure 26. Mean catch-per-unit-effort (CPUE) of *C. houstonensis*, *C. petrina*, and aggregate mussels in low-quality (CSI<0.5) and high-quality (CSI>0.5) model-predicted habitat from non-persistent (A) and persistent (B) areas at the Altair site.

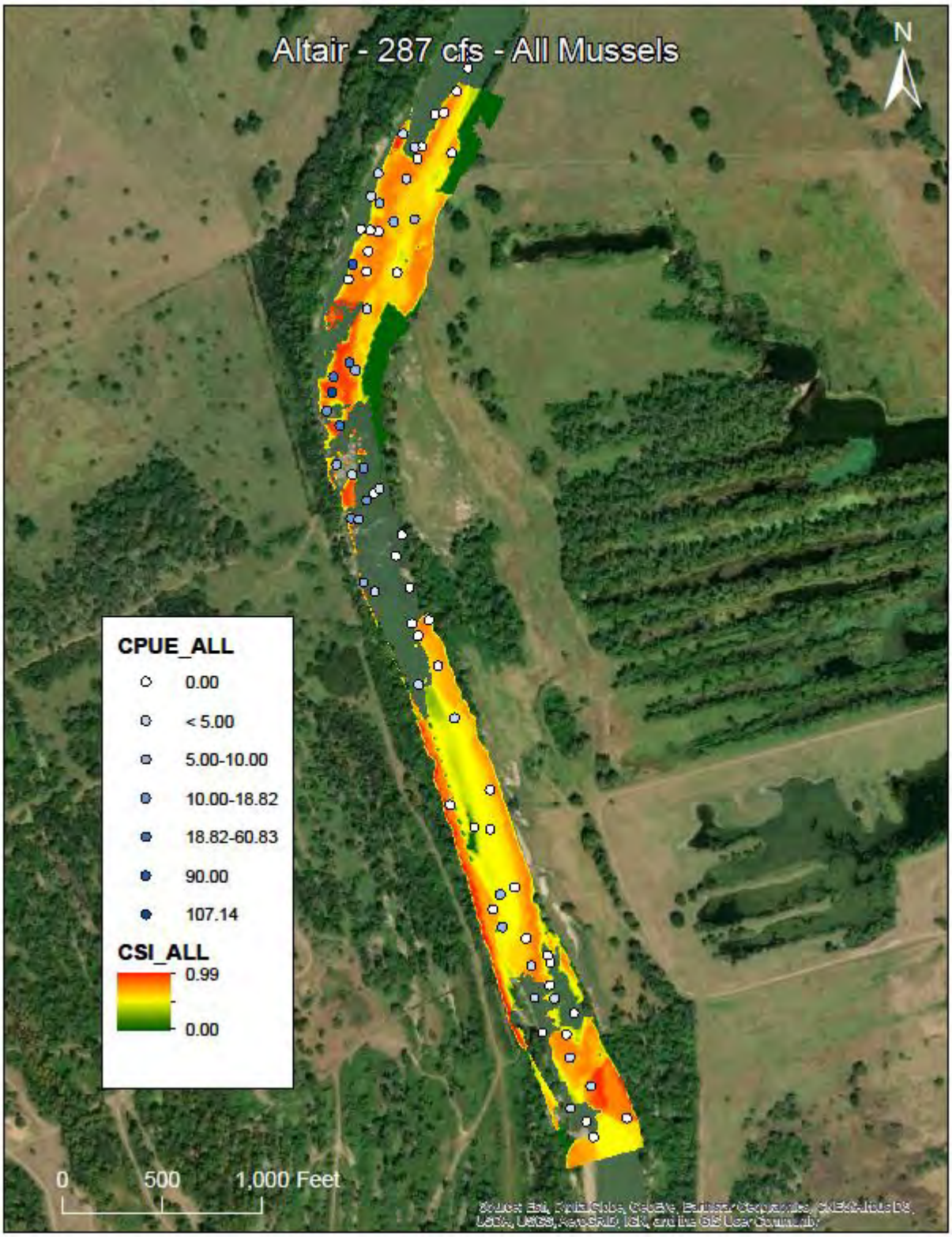

Figure 27. Model-predicted aggregate mussel Composite Suitability (CSI) in persistent habitats at the Altair site from the 287 cfs model run. Points represent aggregate mussel catch-per-unit-effort (CPUE) data from validation sampling efforts in summer 2018.

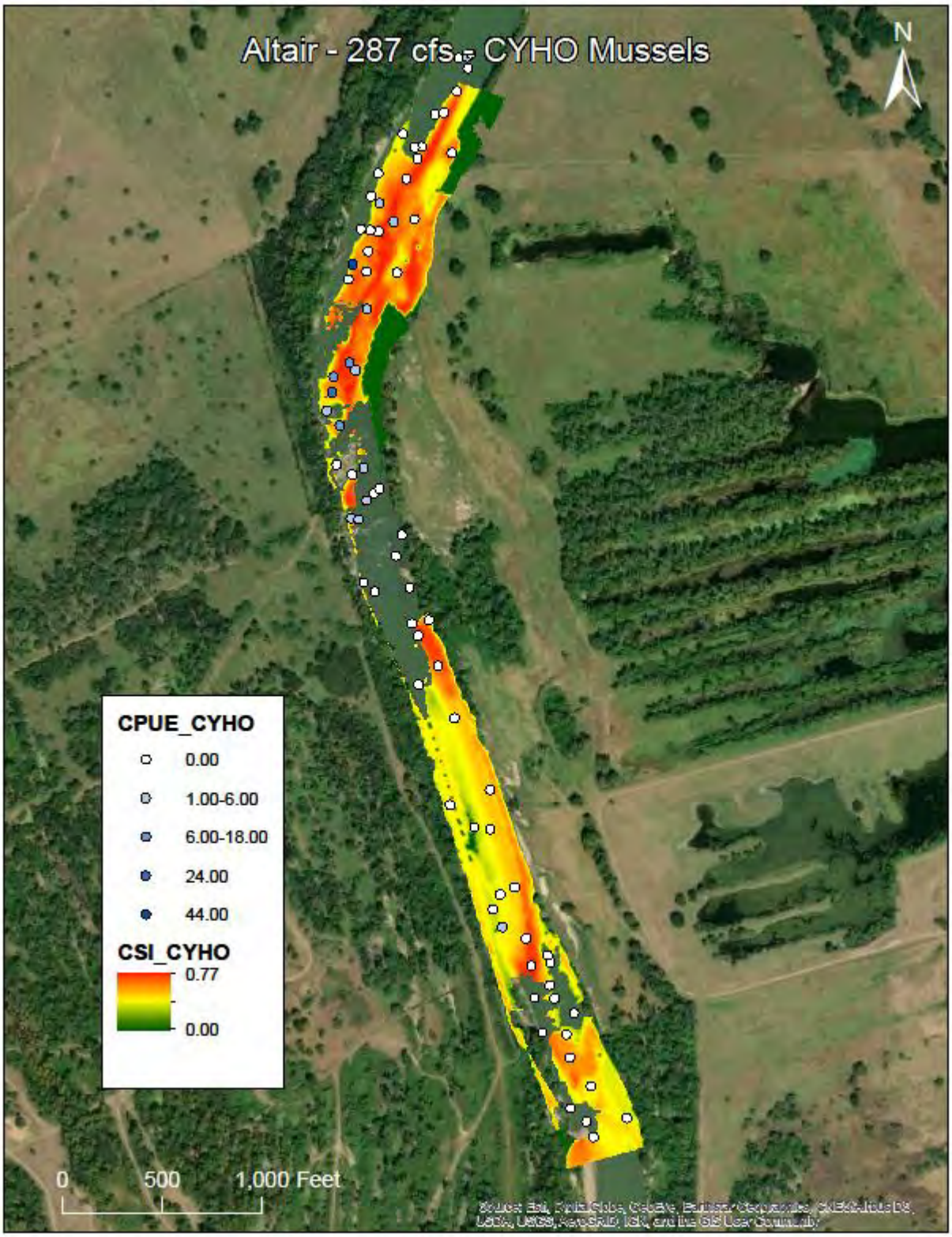

Figure 28. Model-predicted *C. houstonensis* Composite Suitability (CSI) in persistent habitats at the Altair site from the 287 cfs model run. Points represent *C. houstonensis* catch-per-unit-effort (CPUE) data from validation sampling efforts in summer 2018.

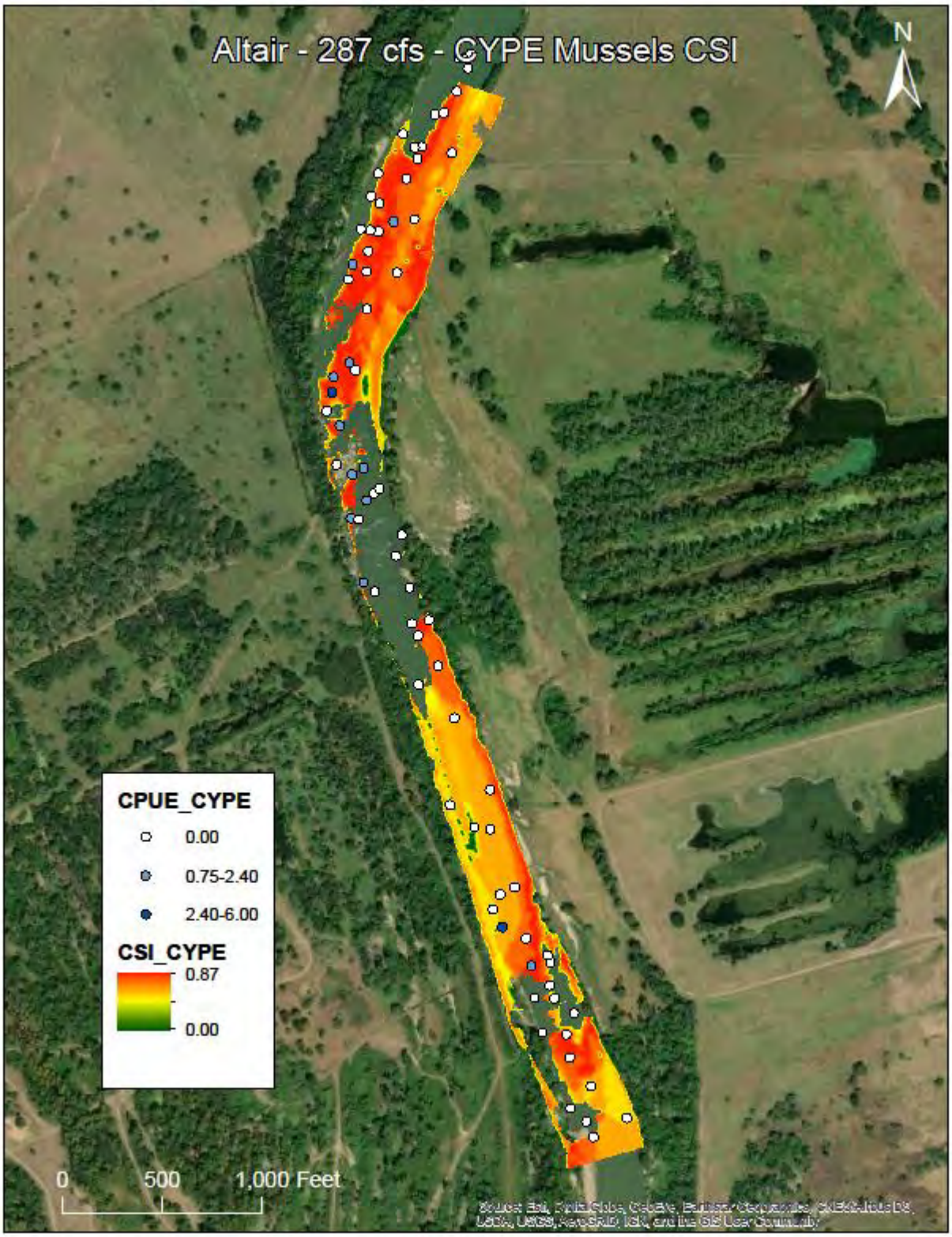

Figure 29. Model-predicted *C. petrina* Composite Suitability (CSI) in persistent habitats at the Altair site from the 287 cfs model run. Points represent *C. petrina* catch-per-unit-effort (CPUE) data from validation sampling efforts in summer 2018.

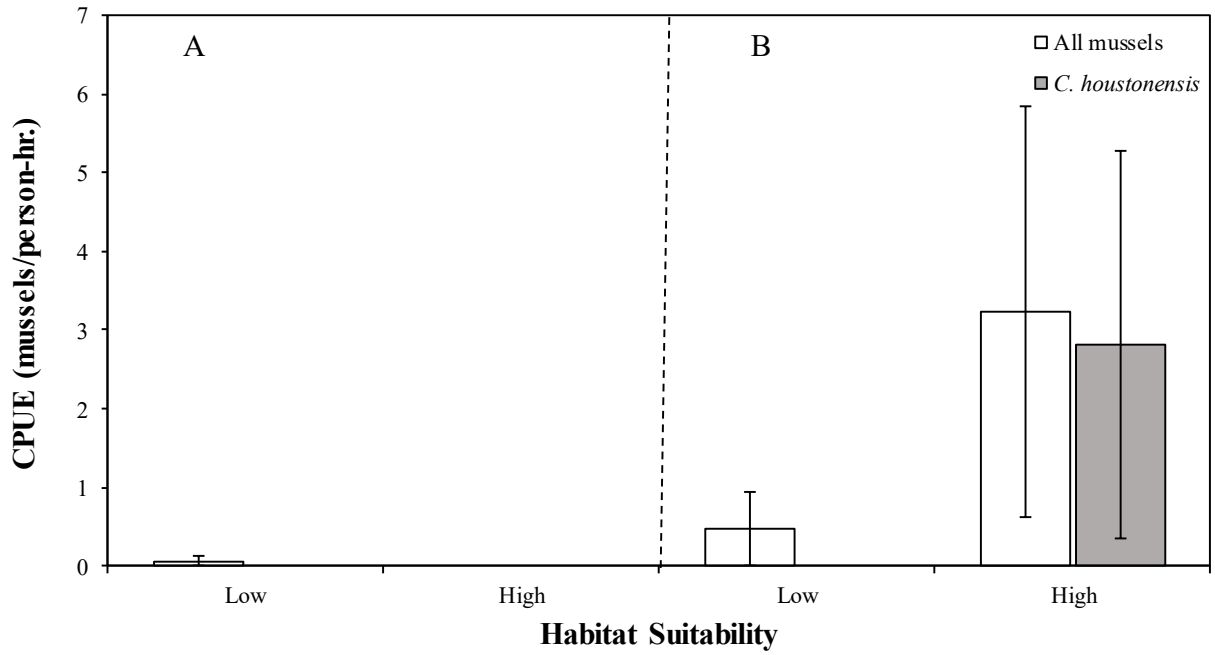

Figure 30. Mean catch-per-unit-effort (CPUE) of *C. houstonensis*, and aggregate mussels in low-quality (CSI<0.5) and high-quality (CSI>0.5) model-predicted habitat from non-persistent (A) and persistent (B) areas at the La Grange site.

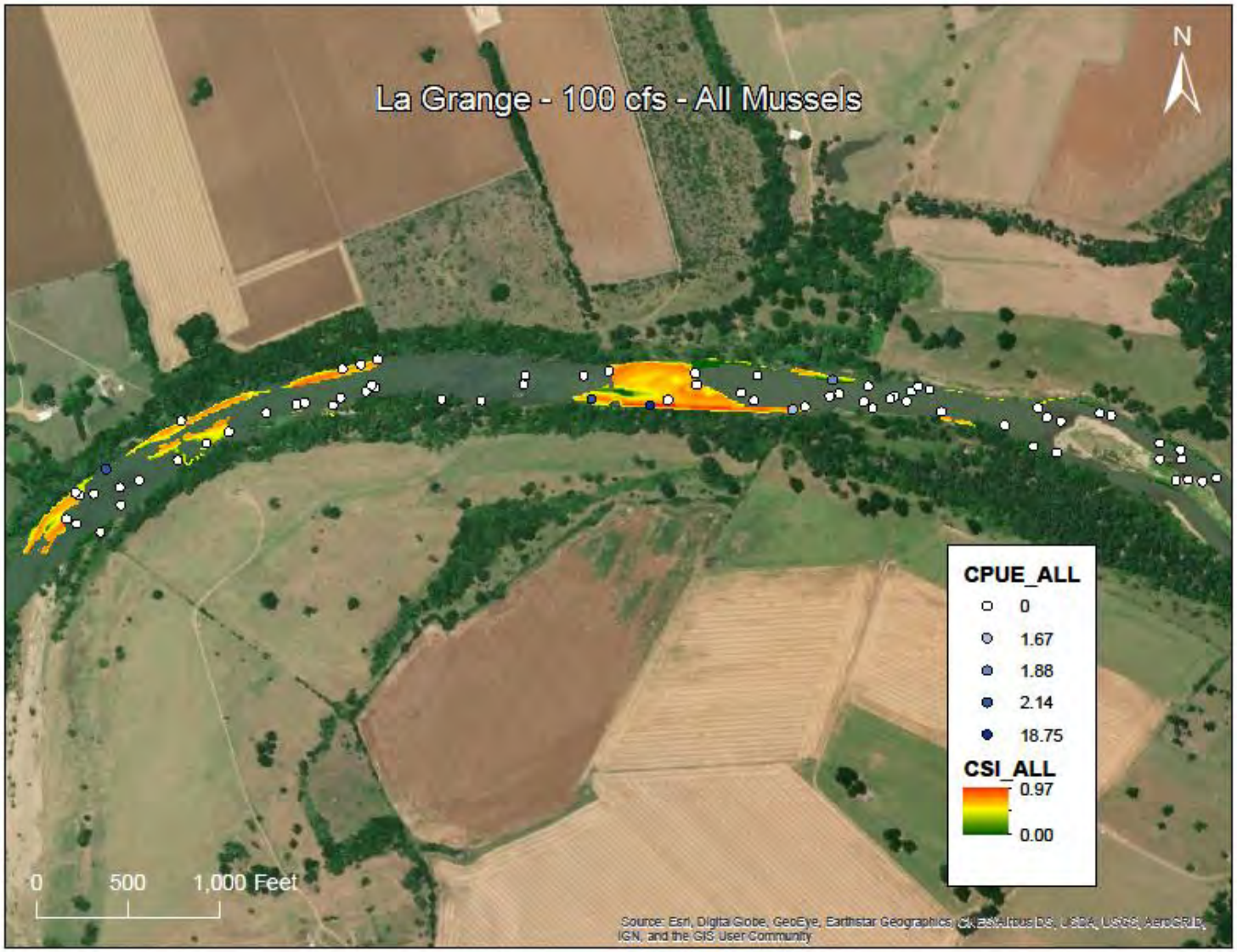

Figure 31. Model-predicted aggregate mussel Composite Suitability (CSI) in persistent habitats at the La Grange site from the 100 cfs model run. Points represent aggregate mussel catch-per-unit-effort (CPUE) data from validation sampling efforts in summer 2018.

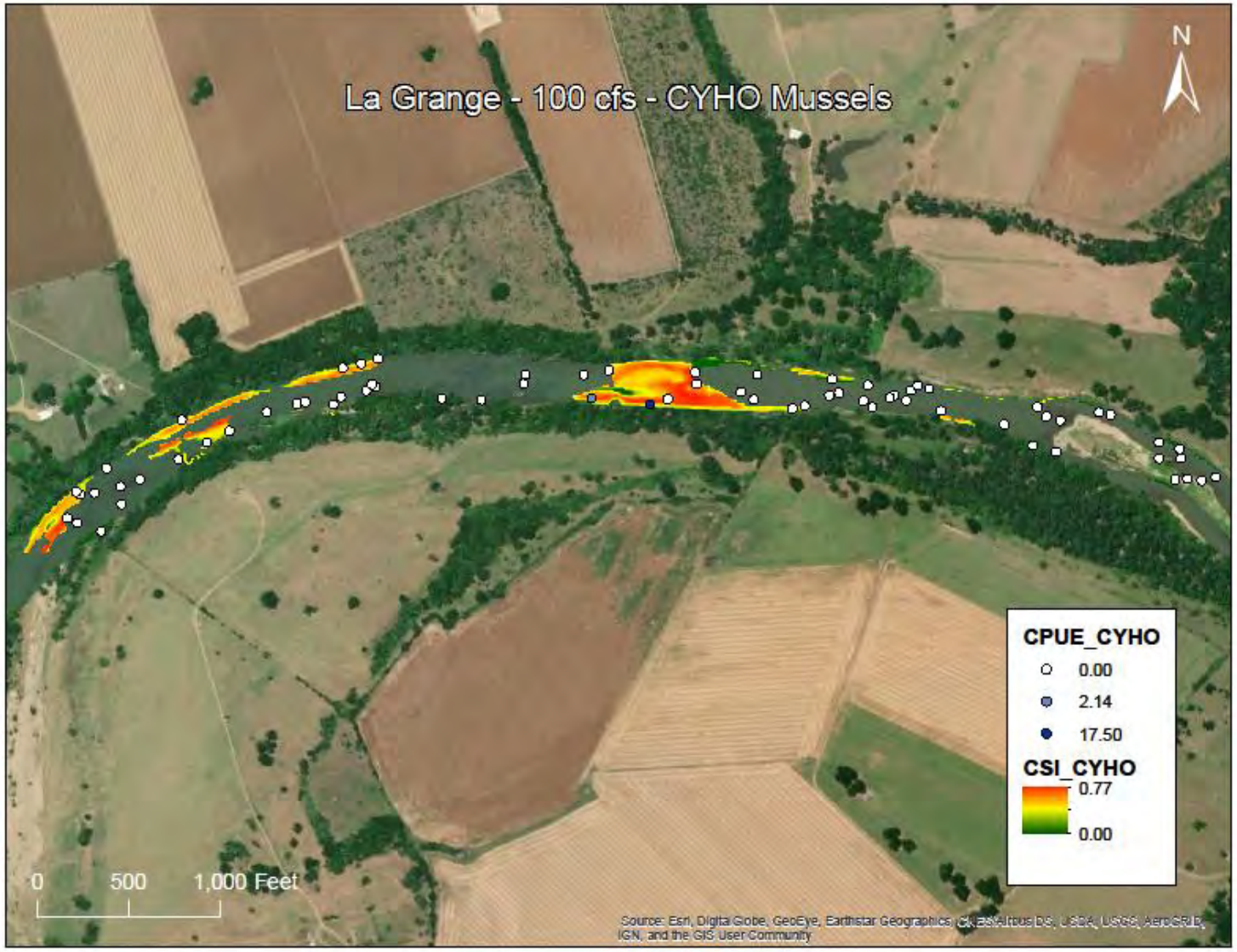

Figure 32. Model-predicted *C. houstonensis* Composite Suitability (CSI) in persistent habitats at the La Grange site from the 100 cfs model run. Points represent *C. houstonensis* catch-per-unit-effort (CPUE) data from validation sampling efforts in summer 2018.

References

BIO-WEST, Inc. 2008. Lower Colorado River, Texas Instream Flow Guidelines. Colorado River Flow Relationships to Aquatic Habitat and State Threatened Species: Blue Sucker. Report prepared for Lower Colorado River Authority (LCRA) and San Antonio Water System (SAWS) Water Project.

Bonner, T. H., E. L. Oborny, B. M. Littrell, J. A. Stoeckel, B. S. Helms, K. G. Ostrand, P. L. Duncan, and Jeff Conway. 2018. Multiple freshwater mussel species of the Brazos River, Colorado River, and Guadalupe River basins. Final Report to the Texas Comptroller of Public Accounts, February 28, 2018.

Bovee, K. D. 1986. Development and evaluation of habitat suitability criteria for use in the Instream Flow Incremental Methodology. Instream Flow Information Paper 21. U.S. Fish and Wildlife Service Biol. Rep. 86(7). 235 pp.

Gough, H. M., A. M. Hascho Landis, and J. A. Stoeckel. 2012. Behavoir and physiology are linked in responses of freshwater mussels to drought. Freshwater Biology 57:2356-2366.

Layzer, J. B., and L. M. Madison. 1995. Microhabitat use by freshwater mussels and recommendations for determining their instream flow needs. Regulated Rivers: Research and Management 10:329-345.

Maloney, K. O., W. A. Lewis, R. M. Bennett, and T. J. Waddle. 2012. Habitat persistence for sedentary organisms in managed rivers: the case for the federally endangered dwarf wedgemussel (*Alasmidonta heterodon*) in the Delaware River. Freshwater Biology 57:1315-1327.

Newton, T. J., S. J. Ziglerand, and B. R. Gray. 2015. Mortality, movement and behavior of native mussels during a planned water-level drawdown in the Upper Mississippi River. Freshwater Biology 60. DOI: 10.1111/fwb.12461.

Persinger, J. W., D. J. Orth, and A. W. Averett. 2010. Using habitat guilds to develop habitat suitability criteria for a warmwater stream fish assemblage. River Research and Applications (2010). DOI: 10.1002/rra.

Poff, N. L., J. D. Allan, M. B. Bain, J. R. Karr, K. L. Prestegaard, B. D. Richter, R. E. Sparks, and J. C. Stromberg. 1997. The Natural Flow Regime. BioScience 47:769-784.

Randklev, C. R., M. Cordova, J. Groce, E. Tsakiris, and B. Sowards. 2014. Freshwater mussel (Family: Unionidae) data collection in the middle and lower Brazos River. Report submitted to Texas Parks and Wildlife (TPWD) as part of TPWD Contract No. 424520.

Schwalb, A. N., and M. T. Pusch. 2007. Horizontal and vertical movement of unionid mussels in a lowland river. The North American Benthological Society 26:261-272.

Statzner, B., F. Kohmann, and A. G. Hildrew. 1991. Calibration of FST-hemispheres against bottom shear stress in a laboratory flume. Freshwater Biology (1991) 26: 227-231.

Steffler, P., and J. Blackburn. 2002. River2D hydraulic modeling program. http://www.river2d.ualberta.ca/

Strauss, R. E. 1979. Reliability estimates for Ivlev's electivity index, the forage ratio, and a proposed linear index of food selection. Transactions of the American Fisheries Society 108: 344-352.

Stromberg, J. C., V. B. Beauchamp, M. D. Dixon, S. J. Lite, and C. Paradzick. 2007. Importance of low-flow and high-flow characteristics to restoration of riparian vegetation along rivers in arid southwestern United States. Freshwater Biology 52(4): 651-679.

Texas Commission on Environmental Quality (TCEQ). 2012. Chapter 298 – Environmental Flow Standards for Surface Water; Subchapter D: Colorado and Lavaca Rivers, and Matagorda and Lavaca Bays. Effective August 30, 2012.

Texas Instream Flow Program (TIFP). 2018. Instream flow study of the middle and lower Brazos River. June 15, 2018. http://www.twdb.texas.gov/surfacewater/flows/instream/middle_lower_brazos/doc/BrazosRiverBasin_FinalRecommendationsReport_180615.pdf

Task 5: Captive Propagation

Principal Investigators: Ken Ostrand, Patricia Duncan, Jeff Conway
Addresses:
U.S. Fish and Wildlife Service, San Marcos Aquatic Resources Center, 500 E. McCarty Lane, San Marcos TX 78666
U.S. Fish and Wildlife Service, Uvalde National Fish Hatchery, 754 County Road 203 Uvalde, TX 78801
U.S. Fish and Wildlife Service, Inks Dam National Fish Hatchery, 345 Clay Young Road Burnet, Texas 78611
Email: Kenneth_Ostrand@fws.gov, patricia_duncan@fws.gov, jeff_conway@fws.gov

A.) March – Sept 2017: Texas fawnsfoot and false spike collection and transport to SMARC.

Adequate numbers of these species were not found during surveys in 2017. There are no suitable surrogate species because relatives are also rare and being considered for conservation status. Surveys for adequate numbers are ongoing.

B.) March – December 2017: glochidia extraction/fish infection for host fish determination.

Adequate numbers of Texas fawnsfoot were not found during surveys in 2018.

BIO-WEST, Inc. provided 2 gravid false spike to SMARC. These were used to infect shiners to determine practical host for captive propagation of false spike. SMARC will continue this work during 2019 if adequate numbers of false spike or Texas fawnsfoot are observed during surveys.

Multiple freshwater mussel species of the Brazos River, Colorado River, and Guadalupe River basins

CMD 1—6233CS

Supplemental Report II

February 28, 2020

Table of Contents

The Texas Comptroller of Public Accounts office provided financial assistance for this study. We thank R. Gulley, M. Hope, K. Horndeski, C. McDonald, and M. Salmon of the Texas Comptroller of Public Accounts office for their support and coordination of our research activities. We also thank staff from Austin Ecological Field Office, Texas Parks and Wildlife, Lower Colorado River Authority, and Brazos River Authority for their assistance and coordination among our partners.

The findings and conclusions in this report presented by U.S. Fish and Wildlife Service project team members do not necessarily represent the views of the U.S. Fish and Wildlife Service.

Task 4: Population-level responses of freshwater mussels to floods in a southwestern U.S.A. river using mark-recapture sampling

Contributing authors: V. Alex Sotola[1], Kyle T. Sullivan[2], Brad M. Littrell[2], Noland H. Martin[1], Daniel S. Stich[3], and Timothy H. Bonner[1]

Addresses: [1]Department of Biology, Texas State University, San Marcos, Texas 78666

[2]BIO-WEST, Inc. San Marcos, Texas 78666

[3]Biology Department, SUNY College at Oneonta, Oneonta, NY 13820

Principal Investigators: Tim Bonner and Brad Littrell

Email: TBonner@txstate.edu, blittrell@bio-west.com

Summary

1. Floods can directly affect riverine organisms by displacing them, and population-level responses to floods can vary depending on flood magnitude and organism mobility. Benthic organisms can resist displacement until substrates become unstable, whereas mobile organisms are more resistant. Freshwater mussels are benthic organisms with low mobility and limited research on their population-level responses to floods. This study provides novel insight to population-level responses of mussels to large floods (>500 m^3/s).

2. Population dynamics (i.e., detection probability, abundance, and apparent survival) in a closed robust design framework were estimated for four freshwater mussel species (*Cyclonaias petrina*, *C. pustulosa*, *Amblema plicata*, and *T. verrucosa*) from 2017 to 2019 at two sites within riffle habitats in the Colorado River, Texas, USA. During sampling, a flood occurred at both sites, each of which was in the 99th percentile of historical flows at their respective gages yet were of different magnitudes. Each species was affixed with shellfish tags, with *C. petrina* and *C. pustulosa* also being affixed with PIT tags. This allowed direct comparison of population-level estimates from data collected using each tag type.

3. There were site- and species-specific differences in estimated abundances and apparent survival during periods with the floods. Estimated abundances of PIT-tagged *C. petrina* and *C. pustulosa* were reduced 31 to 45% with the lesser flood magnitude (1,283 m^3/s). Estimated abundances of PIT-tagged *C. petrina* and *C. pustulosa* were reduced 73 to 80% with the greater flood magnitude (4,332 m^3/s). Reductions in estimated abundances were not detected for shellfish-tagged *A. plicata* and *T. verrucosa*. There were no differences in apparent survival at the upper site, while initially high apparent survival at the lower site was reduced during the interval with the flood. Population estimates from shellfish tags were generally lower and more variable than estimates from PIT tags indicating underestimation of population parameters.

4. Floods reduced the abundance of two species within riffle habitats at the two sites. Large floods, therefore, affect populations dynamics of mussels, but the fate of the displace mussels are unknown and, with limited inference, reach-scale effects are unknown. This study adds to the growing body of knowledge on vagile aquatic organism's resistance to large floods, although quantification of resiliency is needed to fully understand long-term fitness of mussels with large floods.

Introduction

Resistance and resiliency of riverine organisms to flooding are often-studied topics in population and community ecology (Power & Stewart, 1987; Grimm & Fisher, 1989; Flecker & Feifarek, 1994; Maltchik & Pedro, 2001; Franssen *et al.*, 2006; Robinson, 2012). Floods, generally defined as occurrences of water in usually dry areas (Jonkman & Kelman, 2005), indirectly affect riverine communities by altering physical (Peters *et al.*, 2016) and chemical (Talbot *et al.*, 2018) components of lotic systems. They also directly affect communities by displacing organisms (Cobb, Galloway & Flannagan, 1992), and generally have a variety of effects on ecosystem functions and services (Talbot *et al.*, 2018 and references therein). Additionally, they are considered essential components of the flow regime, maintaining ecological integrity of riverine communities (Poff *et al.*, 1997). Population-level responses of riverine organisms to floods vary widely, depending on several factors including flood magnitude, organismal biology (e.g. mobility), and instream habitats. Generally, populations are more resistant to small floods than large floods, though the effects will depend on stream geomorphic features and hydraulic forces (Robinson, 2012). Mobile organisms (e.g., fish and mammals) are more resilient to displacement effects (Crandall, Hayes & Ackland, 2003) due to their ability to escape or find appropriate refuge, whereas less mobile, sessile organisms (e.g., plants and some invertebrates), are particularly sensitive to flooding and resist displacement only until substrates become unstable (Cobb *et al.*, 1992).

Information about responses to floods is reported for a few populations of freshwater mussels, a group of benthic organisms with limited mobility. A flood in one southwest (USA) desert river (maximum daily flow: 26 m^3/s, percentile: 99^{th}, median flow: 0.20 m^3/s, drainage area: 890 km^2; USGS Station 08405500) had no detectable effect on mussel population dynamics (i.e., survival, growth) over a 15-year period (Inoue *et al.*, 2014). Moreover, the flood event was considered beneficial for mussel survival because it displaced fine sediments that accumulated during low flow periods (Inoue *et al.*, 2014). Floods in two northeastern (USA) creeks, Tonawanda Creek (maximum daily flows: 163 m^3/s, percentile: 99^{th}, median flow: 6.8 m^3/s, drainage area: 900 km^2; USGS Station 04218000) and French Creek (maximum daily flows: 479 m^3/s, percentile: 99^{th}, median flow: 38 m^3/s, drainage area: 2,040 km^2; USGS Station 03023100), had no detectable effects on mussel survival, occurrences, or composition over two decades, despite bed sediment mobilization occurring during more frequent floods (<2 year intervals) (Sansom *et al.*, 2018). Conversely, a flood described as a 100-year flood event on an ungaged, upland river in Scotland (Hastie *et al.*, 2001) was a potential conservation concern for a mussel population. An estimated 50,000 mussels, representing 4 to 8% of the total population, were displaced, stranded, and died. In other studies, the ability of freshwater mussels to resist floods are reported to depend on substrate stability and hydraulic variables related to substrate stability such as shear stress (Strayer, 1999; Morales *et al.*, 2006; Gangloff & Feminella, 2007; Zigler *et al.*, 2008; Allen & Vaughn, 2010; Randklev *et al.*, 2019), habitat type (Meador, Peterson & Wisniewski, 2011), channel geomorphology (Gangloff & Feminella, 2007), and shell morphology, behavior, and life-history strategies of the mussels (Allen & Vaughn, 2009; Goodding *et al.*, 2019; Randklev *et al.*, 2019). To date, empirical studies that directly assess

effects of floods on mussel population dynamics in large rivers are lacking, particularly in relation to large floods (e.g. >500 m^3/s).

In spring and summer 2017, two mark-recapture sites located in the upper and lower Colorado River, Texas (USA) —henceforth referred to as "upper site" and "lower site"— were established within riffle habitats to quantify population dynamics of mussel populations. Target species included *Cyclonaias petrina,* an endemic state-listed threatened species and a candidate species for listing by U.S. Fish and Wildlife Service, and *C. houstonensis*, another candidate species for listing, which was later synonymized with *C. pustulosa* (Johnson *et al.*, 2018). Additional target species were two common mussel species, *Tritogonia verrucosa* and *Amblema plicata*. Mark-recapture studies commonly use shellfish tags (Wisniewski *et al.*, 2013; Inoue *et al.*, 2014; Newton, Zigler & Gray, 2015) to estimate population dynamics such as abundances, immigration, emigration, and survival. However, burrowing tendencies of mussels can make them difficult to recapture in tactile surveys, leading to underestimates in population parameters (Strayer & Smith, 2003; Wisniewski *et al.*, 2013). Thus, to improve estimates of population parameters in this study and to additionally assess the effectiveness of shellfish tags, passive integrated transponder tags (PIT tags) were used on candidate species, in addition to shellfish tags on all target species in a closed robust design framework. During the study period, in August 2017, precipitation from Hurricane Harvey inundated the lower site with a peak flow of 4,332 m^3/s (percentile: 99^{th}, median flow: 44 m^3/s, drainage area: 110,000 km^2; USGS Station 08161000). In October 2018, precipitation from a frontal boundary inundated the upper site with a peak flow of 1,283 m^3/s (percentile: 99^{th}, median flow: 5.6 m^3/s, drainage area: 51,000 km^2; USGS Station 08147000). Both floods were classified as greater than one per five-year events (Buzan *et al.*, 2011).

The purpose of this study was to opportunistically assess population-level responses of four mussel species within riffle habitats following large (99th percentile, greater than one per five-year events) floods. Objectives were to quantify population-level responses (detection probability, estimated abundance, and apparent survival) of four mussel species (*C. pustulosa, C. petrina, T. verrucosa,* and *A. plicata*) using shellfish tags, in addition to PIT tags on two of the species (*C. petrina* and *C. pustulosa*). Estimation of population-level responses using shellfish tags and PIT tags on *C. petrina* and *C. pustulosa* enabled comparison of estimated population-level responses between two tag types. The latter objective will improve methods for estimating mussel responses as future work continues in assessing effects of flood events. Floods were expected to reduce abundance and apparent survival of the four mussel species with greater reductions at a peak flow of 4,332 m^3/s at the lower site than a peak flow of 1,283 m^3/s at the upper site unless substrate differences between sites mediated the decreases in abundance and apparent survival.

Methods

Field Sites— Two sites on the Colorado River with high densities of mussel species (Ruppel 2019) were chosen as mark-recapture locations. The upper site, located in the Colorado River near San Saba, Texas, was a riffle with mixture of cobble (60%), sand (25%), and gravel (15%) on the standard Wentworth scale (Wentworth, 1922). Water quality parameters were measured with a multiprobe meter (YSI-85) during sampling. Water temperature ranged from 15.1 to 29.6°C, dissolved oxygen ranged from 7.2 to 10.5 mg/l, and specific conductance ranged from 501 to 711 µS/cm during the study. The lower site, located in the lower Colorado River near Columbus, Texas, was a riffle with predominately cemented sandstone (70%) with interstitial pockets of sand (20%) and gravel (10%). Water temperature ranged from 20.8 to 31.7°C,

dissolved oxygen ranged from 7.5 to 10.9 mg/l, and specific conductance ranged from 574 to 712 µS/cm during the study.

Field sampling—Robust design mark-recapture methods (Pollock, 1982; Nichols & Pollock, 1990) were used to estimate detection probability, abundance, and apparent survival of freshwater mussels. Robust design methods consist of primary and secondary periods, where populations are assumed to be closed (i.e. no mortality or migration), and intervals, defined as the time between primary periods, where the populations are assumed to be open (i.e. mortality or migration can occur). At the upper site, mussels were initially captured and tagged in June 2017 and subsequently sampled during five primary periods over a three-year span (August and November 2017, April and August 2018, and April 2019). At the lower site, mussels were initially captured and tagged in March 2017 and sampled during five subsequent primary periods over two years (April, August, and November 2017; April and August 2018). Primary periods, consisting of three secondary periods (i.e. sampling events), were separated by three to four months; however, there were instances in which sampling had to be delayed several weeks for high flows to subside. Secondary periods were separated by about 24 hours. In total, there were five primary periods and four intervals at each sampling site.

For initial tagging and during subsequent primary and secondary periods, a 300-m^2 rectangular area was delineated within a riffle habitat at each site. The four corners were georeferenced so that the same area could be delineated during subsequent visits. During initial sampling, survey crews spread evenly across the downstream boundary and searched for mussels visually and tactilely moving upstream while crawling, floating, or snorkeling. Detected mussels were removed and placed into mesh bags kept in the river. Upon completion of the survey,

mussels were taken to a central processing station on the riverbank and identified morphologically to species. Mussels were then affixed with two laminated vinyl shellfish tags (Floy®) on each valve. For *C. petrina* and *C. pustulosa*, a PIT tag (Biomark ®) was also affixed to a valve. Cyanoacrylic glue (Loctite Gel Control Super Glue®) was used to affix tags to the mussel valves (Young & Isely, 2008; Ashton, Tiemann & Hua, 2017). Mussels were returned to the 300-m^2 rectangular area and placed in substrates with their posterior end in an upright position. For subsequent primary and secondary period sampling, the 300-m^2 rectangular areas were surveyed using a Biomark reader to locate PIT tagged individuals. After scanning, mussels were visually and tactilely captured, tagged, and returned as during initial tagging. For previously tagged mussels, the unique tag number per recaptured individual was recorded. Average person hours (p-h; calculated as total search time divided by number of people) ranged from 25.3 to 73.5 p-h at the upper site, and 4.6 to 36.0 p-h at the lower site. Mussel species with more than 15 total individuals captured were included in analyses. This included *C. petrina*, *C. pustulosa*, and *T. verrucosa* at the upper site, and *C. petrina*, *C. pustulosa*, and *A. plicata* at the lower site.

Hydrology—Discharge at the upper site, measured from USGS gage 08147000, ranged from 0.06 to 1,283 m^3/s throughout the duration of the study (Figure 1A). Discharge at the lower site, measured from USGS gage 08161000, ranged from 13 to 4,332 m^3/s (Figure 1B; Table 1). The flood at the upper site occurred during interval four, and the flood at the lower site occurred during interval two (Table 1). Median daily flow at the upper site (period of record: 1915–2017) was 5.6 m^3/s with a maximum peak flow of 5,409 m^3/s in 1938. Median daily flow at the lower

site (period of record: 1915–2017) was 44 m^3/s with a maximum peak flow of 4,642 m^3/s in 1935.

Data Analysis—A Bayesian closed robust design model (Pollock, 1982; Nichols & Pollock, 1990) was used to estimate apparent survival and abundance while accounting for imperfect detection separately for each species and site using methods and code modified from Riecke *et al.* (2018). Specifically, detection probability (p_t) was estimated as the probability an individual available for detection during time *t* was in fact detected during at least one secondary occasion, abundance (N_t) was estimated as the number of individuals in the study area during each primary period, and apparent survival (ϕ_t) was estimated as the probability an individual in the population at time *t* survived to time *t + 1* and did not permanently emigrate from the study area. Uninformative priors were used for all parameters; for detection probability and apparent survival a uniform distribution on the interval [0,1] was used. The probability (Pr) of losing one PIT tag or shellfish tag (t_1) or both tags (t_2) was estimated as:

$$\Pr[t_1] = \frac{l}{N}(1 - \frac{l}{N})$$

$$\Pr[t_2] = t_1^2$$

where *l* is the number of mussels observed with tag loss and *N* is the total number of tagged mussels (Reinert *et al.*, 1998; Meador *et al.*, 2011). In this study, the probability of losing a PIT tag was 0.053, the probability of losing a shellfish tag was 0.024, the probability of losing two shellfish tags was 0.00058, and the probability of losing a PIT and shellfish tag was 0.00127. The probability of not losing tags (1 - t_i) was calculated and was used as a constant multiplier on

apparent survival and estimated abundances in each model for each species depending on which type of tags were on each individual to account for tag loss in these estimates.

All model parameters were estimated using Markov Chain Monte Carlo methods in JAGS (Plummer 2003) written in the BUGS language, through R (R Core Team 2019) with the R2jags package (Su & Yajima, 2015, see Supplemental Information 5 for model code). A total of 15,000 iterations were used with a burn-in period of 5,000 iterations, and a thinning rate of 10 for each of three Markov chains to ensure sufficiently large effective sample sizes (range 140 to 3,000; mean of 2,385 for all parameters). Convergence was confirmed using visual inspection of trace plots and ensuring that the Gelman-Rubin statistic (Gelman & Rubin, 1992) was less than 1.10 for all parameters. All estimates are presented as posterior medians with 95% credible intervals (CRI) presented in Supplemental Tables 1-4.

Parameter estimates were compared between each primary period (p_t and N_t) or interval (ϕ_t) and the one directly preceding it in time to detect differences over time (i.e., t_1 and t_2 were compared, but not t_1 and t_3). For each MCMC iteration, the posterior estimate from time t was subtracted from the posterior estimate for time $t + 1$ to represent increases (+) or decreases (-) from one time to the next. Credible intervals (95% CRIs) were estimated around the differences, and if the CRI excluded zero, then the difference in estimates between periods was considered statistically significant.

Posterior estimates of detection probability, abundances, and apparent survival of *C. petrina* and *C. pustulosa* between PIT tag and shellfish tag data were compared using methods described above. The posterior estimates of the shellfish tag data were subtracted from the posterior estimates of the PIT tag data, and a 95% CRI for the difference was estimated. If the credible intervals excluded zero, the difference was interpreted as statistically significant.

Negative values indicated that the parameters from shellfish tag data were underestimated relative to those from PIT tag data, while positive values indicated that they were overestimated.

Results

Upper site

PIT tags were affixed to 442 *C. petrina* and 15 *C. pustulosa* among five primary periods with the 1,283 m^3/s flood occurring between primary periods 4 and 5 and during interval 4 (Table 2). For *C. petrina*, the probability of detecting a PIT-tagged individual ranged from 0.693 to 0.972 (Figure 2; Supplemental Table 1 & 2). Estimated abundances increased from 153 to 363 pre-flood (primary periods 1 - 4) and decreased to 249, a 31% decrease, after the flood (primary period 5; Table 3). Differences were not detected in apparent survival between intervals. For *C. pustulosa,* the probability of detecting a PIT-tagged individual ranged from 0.789 to 0.973. Estimated abundances generally increased from 6 to 11 pre-flood (primary periods 1 - 4) and decreased to 6, a 45% decrease, after the flood (primary period 5). Differences were not detected in apparent survival between intervals.

Shellfish tags were affixed to 442 *C. petrina*, 15 *C. pustulosa*, and 217 *T. verrucosa* across the five primary periods. For *C. petrina*, the probability of detecting a shellfish-tagged individual ranged from 0.335 to 0.958 (Figure 3; Supplemental Table 3 & 4). Estimated abundances ranged from 149 to 240 pre-flood (primary periods 1 - 3); differences in estimated abundances were not detected after the flood (primary periods 4 and 5). Apparent survival decreased from 0.978 during interval 2 to 0.706 during interval 3 pre-flood. For *C. pustulosa*, the probability of detecting a shellfish-tagged individual ranged from 0.639 to 0.958 among primary periods. Estimated abundances ranged from 4 to 7 pre-flood (primary periods 1 - 4); differences

in estimated abundances were not detected after the flood (primary periods 4 and 5). For *T. verrucosa*, the probability of detecting a shellfish-tagged individual ranged from 0.339 to 0.970 among primary periods. Estimated abundances ranged from 62 to 110 pre-flood (primary periods 1 - 3); differences in estimated abundances were not detected after the flood (primary periods 4 and 5). Differences were not detected in apparent survival between intervals for *C. pustulosa* or *T. verrucosa*.

Lower site

PIT tags were affixed to 120 *C. petrina* and 308 *C. pustulosa* among five primary periods with the 4,332 m^3/s flood occurring between primary periods 2 and 3 and during interval 2 (Table 2). For *C. petrina*, the probability of detecting a PIT-tagged individual ranged from 0.160 to 0.999 (Figure 4; Supplemental Table 1 & 2). Estimated abundances increased from 69 to 101 pre-flood (primary periods 1 and 2) and decreased to 28, a 73% decrease, after the flood (primary period 3). Apparent survival was 0.933 pre-flood (interval 1), decreased to 0.237 during the flood (interval 2), and increased to 0.796 after the flood (interval 3). For *C. pustulosa,* the probability of detecting a PIT-tagged individual ranged from 0.177 to 0.999. Estimated abundances increased from 150 to 264 pre-flood (primary periods 1 and 2), decreased to 53 after the flood (primary period 3), an 80% decrease, and increased to 133 in primary period 4. Apparent survival was 0.985 pre-flood (interval 1), decreased to 0.100 during the flood (interval 2), and increased to 0.919 after the flood (interval 3).

Shellfish tags were affixed to 117 *C. petrina*, 300 *C. pustulosa*, and 405 *A. plicata* among the five primary periods. For *C. petrina*, the probability of detecting a shellfish-tagged individual ranged from 0.084 to 0.999 (Figure 5; Supplemental Table 3 & 4). Estimated abundances decreased from 77 to 69 pre-flood (primary periods 1 and 2), decreased to 20 after the flood

(primary period 3), a 71% decrease, and decreased to zero between primary periods 4 and 5. Differences were not detected in apparent survival between intervals. For *C. pustulosa*, the probability of detecting a shellfish-tagged individual ranged from 0.087 to 1.0. Estimated abundances decreased from 202 to 163 pre-flood (primary periods 1 and 2), decreased to 68 after the flood (primary period 3), a 58% loss, and increased to 167 between primary periods 3 and 4, then decreased to 57 between primary periods 4 and 5. Apparent survival was 0.812 pre-flood (interval 1), decreased to 0.145 during the flood (interval 2), and increased to 0.844 after the flood (interval 3). For *A. plicata*, the probability of detecting a shellfish-tagged individual ranged from 0.135 to 1.0. Estimated abundances decreased from 283 to 97 pre-flood (primary periods 1 and 2); differences in estimated abundances were not detected after the flood. Differences were not detected in apparent survival between intervals.

Comparison of model estimates from PIT and shellfish tags

A total of 56 pairwise comparisons were conducted to compare detection probability, estimated abundances, and apparent survival between the two data types. Six (30%) of 20 comparisons of detection probability differed significantly; shellfish tag detection probabilities were underestimated in five (83%) of those six comparisons relative to PIT tags. Thirteen (65%) of the 20 estimated abundance comparisons differed; estimated abundances from shellfish tag data were underestimated in 10 (77%) of those 13 comparisons. Apparent survival estimates differed significantly between PIT tags and shellfish tags in one (6%) comparison; the shellfish tag estimate was lower than the PIT tag estimate in that one case. In 16 out of the 17 cases in which parameter estimates differed between tag types, there was also a change in the trend from one time period to the next (i.e. increase or decrease), indicating that these differences have the potential to influence the results of monitoring studies.

Discussion

Estimated abundances and apparent survival were directly quantified for four species of mussels during base flow and before and after large flood events, while accounting for imperfect detection. Our expectations that large floods would result in reductions of mussel abundances and decreases in apparent survival were partially supported. Estimated abundances, but not apparent survival, of PIT-tagged *C. petrina* and *C. pustulosa* were reduced with the lesser flood magnitude (i.e., 1,283 m^3/s), and estimated abundances and apparent survival of PIT-tagged *C. petrina* and *C. pustulosa* were reduced with the greater flood magnitude (i.e., 4,332 m^3/s). However, reductions in estimated abundances of mussels with shellfish tags were not detected for two (*T. verrucosa* at the upper site and *A. plicata* at the lower site*)* of the four species, and reductions in apparent survival were not detected for three (*C. petrina*, *T. verrucosa* and *A. plicata*) of the four species. Based on model comparisons, estimated abundances using shellfish tags generally underestimated abundances and were more variable relative to PIT tags, which might explain the lack of concordance in model estimates between PIT-tagged *C. petrina* and *C. pustulosa* (decreased in estimated abundances with floods) and *T. verrucosa* and *A. plicata* (no detectable effects in estimated abundances with floods). Alternatively, *T. verrucosa* and *A. plicata* might be more resistant to downstream displacement during flood events than *C. petrina* or *C. pustulosa*.

At both sites, the four mussel species persisted, yet abundances decreased ranging from 0 to 80% following two large floods (1,283 m^3/s and 4,332 m^3/s), which, to date, are the highest flows recorded in a study assessing influence of large floods on mussel populations. Combining estimated abundance decreases of different mussel species with two other studies (Inoue *et al.*,

2014; Sansom *et al.*, 2018) for a total of five flood events within drainage basins of different sizes and habitat types, mussel responses have an apparent non-linear relationship with peak flow, ranging between 25 m^3/s and 4,332 m^3/s. Abundances of mussels were unaffected by smaller peak flows (25 to 470 m^3/s; Inoue *et al.*, 2014; Sansom *et al.*, 2018) and reported herein to decrease from 0 to 45% among three species at 1,283 m^3/s and 0 to 80% among three species at 4,332 m^3/s. However, there are several confounding factors that, once quantified and replicated, could add robustness to explaining mussel abundance-peak flow relationships. Confounding factors include site-specific attributes, such as basin size, stream geomorphology, substrate type and stability, and habitat types, and species-specific attributes such as shell morphology and burrowing behavior (Strayer, 1999; Morales *et al.*, 2006; Gangloff & Feminella, 2007; Zigler *et al.*, 2008; Allen & Vaughn, 2010; Meador *et al.*, 2011; Randklev *et al.*, 2019). Observations during this study provide empirical support for two of the reported confounding factors and their influence of mussel-abundance flow relationship. Substrates at the upper site (i.e., sand, gravel, and cobble substrates) appeared to be less scoured than the substrates at the lower site (i.e., sand and cemented sandstone substrates), suggesting a substrate-stability influence on mussel displacement. In addition, *T. verrucosa* and *A. plicata* have medial sculptured shells, which are thought to enhance anchoring ability compared to other shell sculptures types (e.g. *C. petrina*) and unsculptured species (typical central Texas form of *C. pustulosa*; Watters, 1994; Allen & Vaughn, 2009; Hornbach, Kurth & Hove, 2010; Howells, 2014; Goodding *et al.*, 2019), although the influence of shell morphology on dislodgment resistance needs further assessment (Levine, Hansen & Gerald, 2014). Thus, targeted investigation into the relationship between peak flood discharge in different systems (e.g. small to large order rivers), habitats, substrate types, and among mussel species is warranted.

Notable limitations of this study, and other mark-recapture studies, are the unknown fate of the mussels displaced during flood events and the lack of power to infer mussel responses at the reach scale. Mussels displaced downstream have the potential to survive and establish new mussel beds (Hastie *et al.*, 2001), assuming they are deposited in suitable habitat. If deposited in non-suitable habitat, the fate is less certain given their low vagility. As for reach scale inference, mussel responses to floods are heterogenous within a reach. In a 3-km reach of the Delaware River, USA, mussel aggregations were less persistent in areas with scour and compared to areas with minimal scour following multiple floods (Maloney *et al.*, 2012). Therefore, 71% reductions in *C. petrina* and 80% reduction in *C. pustulosa* at the lower site with observed scour are likely overestimates of displaced *C. petrina* and *C. pustulosa* in the entire lower Colorado River. This is also supported by field surveys taken in the lower Colorado River during the same period, although the surveys were not specifically designed to assess effects of the Hurricane Harvey flood on the mussel community. Prior to the flood, Ruppel (2019) reported 10.4 mussels per habitat surveyed (N = 179) with species relative abundances of 16% for *C. pustulosa* and 1.4% for *C. petrina* from a total of 1,859 mussels collected. After the flood, 6.2 mussels per habitat (N = 66) were reported with species relative abundances of 21% for *C. pustulosa* and 0.9% for *C. petrina* from a total of 441 mussels collected. Although comparability of community effects pre-flood (March – August 2017) and after the flood (September & October 2017) have limitations (e.g., unequal sampling effort, different seasons, taken at different sites within the reach), numbers of mussels per habitat and community structure suggest that reach scale reductions were less than those reported from the mark-recapture site. In future studies, establishing a patchwork of mark-recapture sites within areas with various levels of scouring potential (e.g., numerous hydraulic and substrate types) would enable greater inferences into reach-scale effects.

With PIT tags and shellfish tags affixed to *C. petrina* and *C. pustulosa*, pairwise comparisons of model estimates using the closed robust design demonstrated that shellfish tags generally underestimated population parameters, as previously reported (Strayer & Smith, 2003; Kurth *et al.*, 2007; Wisniewski *et al.*, 2013). For example, the decrease in estimated abundance of *C. petrina* at the upper sites was 31% with PIT tags, but a decrease in estimated abundance was not detected with shellfish tags. However, the decrease in estimated abundance of *C. petrina* at the lower site was 73% with PIT tags and 71% with shellfish tags. In addition to lack of concordance in estimating abundance, detection probabilities using shellfish tags differed 75% of the time from PIT tags and were lower and more variable. This is corroborated by a previous study which found higher recapture rates for PIT tagged mussels (72 - 80%) relative to shellfish tagged mussels (30 - 47%; Kurth *et al.*, 2007). It should be noted that PIT tags have the potential to overestimate parameters relative to shellfish tags due to a higher probability of tag loss, but our analysis of PIT tag data included an estimation of tag loss. One potential mechanism for the discrepancy between shellfish and PIT tags is vertical migration through the substrate. Mussels migrate vertically for a variety of reasons, including reproduction, feeding, and thermoregulation, thus influencing the likelihood of capture with visual and tactile surveys to a large degree, and PIT tag surveys to a lesser extent because of their ability to detect subsurface mussels (Amyot & Downing, 1997; Watters, O'Dee & Chordas, 2001). However, despite the differences in estimates between the two tagging methods found in this study, the general patterns in the estimates were similar and reflect the effect of floods on mussel populations.

Studies geared towards resistance and resiliency of aquatic organisms to flooding are partly driven by the distinctly human perception that floods are devasting (i.e., considered natural disasters, destruction of human life and property). However, a differing ecological perspective

has been forming through time based on the tenets of the Flow Pulse Concept (Junk, Bayley & Sparks, 1989) and the Natural Flow Paradigm (Poff *et al.*, 1997). Where floods are a component of the natural flow regime and not exacerbated by anthropogenic alterations (Konrad, 2003), labeling of floods as a conservation concern due to apparent localized mortality of mussels (Hastie *et al.*, 2001) might overlook long-term ecosystem services and functions of floods. Neither of the floods documented in this study were the highest flow peaks measured by USGS since 1915. Previous to 1915 and extending back to the beginning of the Holocene, flow magnitudes in western gulf slope drainages of Texas were estimated to be four to eight times greater than current magnitudes (Baker & Penteado-Orellana, 1977; Sylvia & Galloway, 2006) and well within the likely timeframe of current species radiation within the Colorado River (Inoue *et al.*, 2019). Therefore, contemporary floods might not be a threat to the long-term viability of mussel populations given that mussels have some level of resistance to displacement (this study) despite evidence of 4 to 8% mortalities (Hastie *et al.*, 2001). However, more documentation is needed to quantify short-term mussel resistance (e.g., site-level and reach-level responses to floods while accounting for confounding factors), but more important, quantification of mussel population resiliency is needed to fully understand ecosystem services and functions and of large floods on the long-term fitness of mussel species.

Acknowledgements

Funded by Texas Comptroller of Public Accounts contract number CMD 1—6233CS. Special thank you to all undergraduate and graduate students at Texas State University who helped with field work, particularly David Ruppel, Cody Craig, Jeremy Maikoetter, Nicki Faucheux, Peter Pfaff, Marisa Quevedo, Danielle Terrell, Cameron Caldwell, Ryne Lehmann, Lauren Chappell, Rhys Woodruff, Anne Beckmann, and Erica Gomez. Additionally, thanks to BIO-West, Inc. researchers Jeff Jenkerson and Jubentino Guajardo. Thank you to Jess Jones and Chris Nice for friendly reviews prior to submission.

Data Availability Statement

Data and model code are available at https://github.com/vasotola/MusselMarkRecap

References

Allen D.C. & Vaughn C.C. (2009). Burrowing behavior of freshwater mussels in experimentally manipulated communities. *Journal of the North American Benthological Society* **28**, 93–100. https://doi.org/10.1899/07-170.1

Allen D.C. & Vaughn C.C. (2010). Complex hydraulic and substrate variables limit freshwater mussel species richness and abundance. **29**, 383–394. https://doi.org/10.1899/09-024.1

Amyot J.-P. & Downing J.A. (1997). Seasonal variation in vertical and horizontal movement of the freshwater bivalve. *Freshwater Biology* **37**, 345–354

Ashton M.J., Tiemann J.S. & Hua D. (2017). Evaluation of Costs Associated with Externally Affixing Pit Tags to Freshwater Mussels Using Three Commonly Employed Adhesives. *Freshwater Mollusk Biology and Conservation* **20**, 114. https://doi.org/10.31931/fmbc.v20i2.2017.114-122

Baker V.R. & Penteado-Orellana M.M. (1977). Adjustment to Quaternary Climatic Change by the Colorado River in Central Texas. *The Journal of Geology* **85**, 395–422. https://doi.org/10.1086/628315

Buzan D., Cook B.P, Fontenot M.M., Hardy T., Hoffpauir R.J., Kennedy K, Thornton O.W., Trungale J.F., Wakefield C. & Watters S.P. (2011). Colorado and Lavaca Rivers and Matagorda and Lavaca Bays Basin and Bay Expert Science Team. Environmental Flow Regime Recommendations Report

Cobb D.G., Galloway T.D. & Flannagan J.F. (1992). Effects of discharge and substrate stability

on density and species composition of stream insects. *Canadian Journal of Fisheries and Aquatic Sciences* **49**, 1788–1795. https://doi.org/10.1139/f92-198

Crandall R.M., Hayes C.R. & Ackland E.N. (2003). Application of the intermediate disturbance hypothesis to flooding. *Community Ecology* **4**, 225–232

Flecker A.S. & Feifarek B. (1994). Disturbance and the temporal variability of invertebrate assemblages in two Andean streams. *Freshwater Biology* **31**, 131–142. https://doi.org/10.1111/j.1365-2427.1994.tb00847.x

Franssen N.R., Gido K.B., Guy C.S., Tripe J.A., Shrank S.J., Strakosh T.R., *et al.* (2006). Effects of floods on fish assemblages in an intermittent prairie stream. *Freshwater Biology* **51**, 2072–2086. https://doi.org/10.1111/j.1365-2427.2006.01640.x

Gangloff M.M. & Feminella J.W. (2007). Stream channel geomorphology influences mussel abundance in southern Appalachian streams, U.S.A. *Freshwater Biology* **52**, 64–74. https://doi.org/10.1111/j.1365-2427.2006.01673.x

Gelman A. & Rubin D.B. (1992). Inference from iterative simulation using multiple sequences. *Statistical Science* **7**, 457–511. https://doi.org/10.2307/2246134

Goodding D.D., Williams M.G., Ford D.F., Williams L.R. & Ford N.B. (2019). Associations between substrate and hydraulic variables and the distributions of a sculptured and an unsculptured unionid mussel. *Freshwater Science* **38**, 543–553. https://doi.org/10.1086/704795

Grimm N.B. & Fisher S.G. (1989). Stability of Periphyton and Macroinvertebrates to Disturbance by Flash Floods in a Desert Stream. *Journal of the North American Benthological Society* **8**, 293–307. https://doi.org/10.2307/1467493

Hastie L.C., Boon P.J., Young M.R. & Way S. (2001). The effects of a major flood on an endangered freshwater mussel population. *Biological Conservation* **98**, 107–115. https://doi.org/10.1016/S0006-3207(00)00152-X

Hornbach D.J., Kurth V.J. & Hove M.C. (2010). Variation in Freshwater Mussel Shell Sculpture and Shape Along a River Gradient. *The American Midland Naturalist* **164**, 22–36. https://doi.org/10.1674/0003-0031-164.1.22

Howells, R.G. (2014). Field Guide to Texas Freshwater Mussels, Second Edition. BioStudies, Kerrville, Texas.

Inoue K., Harris J.L., Robertson C.R., Johnson N.A. & Randklev C.R. (2019). A comprehensive approach uncovers hidden diversity in freshwater mussels (Bivalvia: Unionidae) with the description of a novel species. *Cladistics* **36**, 88–113. https://doi.org/10.1111/cla.12386

Inoue K., Levine T.D., Lang B.K. & Berg D.J. (2014). Long-term mark-and-recapture study of a freshwater mussel reveals patterns of habitat use and an association between survival and river discharge. *Freshwater Biology* **59**, 1872–1883. https://doi.org/10.1111/fwb.12389

Johnson N.A., Smith C.H., Pfeiffer J.M., Randklev C.R., Williams J.D. & Austin J.D. (2018). Integrative taxonomy resolves taxonomic uncertainty for freshwater mussels being considered for protection under the U.S. Endangered Species Act. *Scientific Reports* **8**, 1–16. https://doi.org/10.1038/s41598-018-33806-z

Jonkman S.N. & Kelman I. (2005). An analysis of the causes and circumstances of flood disaster deaths. *Disasters* **29**, 75–97

Junk W.J., Bayley P.B. & Sparks R.E. (1989). The flood pulse concept. *International Large River Symposium*, 110–127

Konrad C.P. (2003). Effects of Urban Development on Floods. *U.S. Geological Survey* **d**, 1–4. https://doi.org/USGS Fact Sheet FS-076-03

Kurth J., Loftin C., Zydlewski J. & Rhymer J. (2007). PIT tags increase effectiveness of freshwater mussel recaptures. *Benthol. Soc* **26**, 253–260. https://doi.org/10.1899/0887-3593(2007)26[253:PTIEOF]2.0.CO;2

Levine T.D., Hansen H.B. & Gerald G.W. (2014). Effects of shell shape, size, and sculpture in burrowing and anchoring abilities in the freshwater mussel Potamilus alatus (Unionidae). *Biological Journal of the Linnean Society* **111**, 136–144. https://doi.org/10.1111/bij.12178

Maloney K.O., Lellis W.A., Bennett R.M. & Waddle T.J. (2012). Habitat persistence for sedentary organisms in managed rivers: The case for the federally endangered dwarf wedgemussel (Alasmidonta heterodon) in the Delaware River. *Freshwater Biology* **57**, 1315–1327. https://doi.org/10.1111/j.1365-2427.2012.02788.x

Maltchik L. & Pedro F. (2001). Responses of Aquatic Macrophytes to Disturbance by Flash Floods in a Brazilian Semiarid Intermittent Stream1. *Biotropica* **33**, 566. https://doi.org/10.1646/0006-3606(2001)033[0566:roamtd]2.0.co;2

McMullen L.E. & Lytle D.A. (2012). Quantifying invertebrate resistance to floods: A global-scale meta-analysis. *Ecological Applications* **22**, 2164–2175. https://doi.org/10.1890/11-1650.1

Meador J.R., Peterson J.T. & Wisniewski J.M. (2011). An evaluation of the factors influencing freshwater mussel capture probability, survival, and temporary emigration in a large lowland river. *Journal of the North American Benthological Society* **30**, 507–521. https://doi.org/10.1899/10-105.1

Morales Y., Weber L.J., Mynett A.E. & Newton T.J. (2006). Effects of substrate and hydrodynamic conditions on the formation of mussel beds in a large river. *Journal of the North American Benthological Society* **25**, 664–676. https://doi.org/10.1899/0887-3593(2006)25[664:eosahc]2.0.co;2

Newton T.J., Zigler S.J. & Gray B.R. (2015). Mortality, movement and behaviour of native mussels during a planned water-level drawdown in the Upper Mississippi River. *Freshwater Biology* **60**, 1–15. https://doi.org/10.1111/fwb.12461

Nichols J.D. & Pollock K.H. (1990). Estimation of recruitment from immigration versus in situ reproduction using Pollock's robust design. *Ecology* **71**, 21–26. https://doi.org/10.2307/1940243

Peters D.L., Caissie D., Monk W.A., Rood S.B. & St-Hilaire A. (2016). An ecological perspective on floods in Canada. *Canadian Water Resources Journal* **41**, 288–306. https://doi.org/10.1080/07011784.2015.1070694

Plummer, M. 2003. JAGS: A program for analysis of Bayesian graphical models using Gibbs sampling. *In* K. Hornik, F. Leisch, and A. Zeileis, editors. Proceedings of the 3rd International Workshop on Distributed Statistical Computing (DSC 2003), March 20–22, Vienna, Austria.

Poff N.L.R., Allan J.D., Bain M.B., Karr J.R., Prestegaard K.L., Richter B.D., *et al.* (1997). The natural flow regime: A paradigm for river conservation and restoration. *BioScience* **47**, 769–784. https://doi.org/10.2307/1313099

Pollock K.H. (1982). A Capture-Recapture Design Robust to Unequal Probability of Capture. *The Journal of Wildlife Management* **46**, 752–757

Power M.E. & Stewart A.J. (1987). Disturbance and Recovery of an Algal Assemblage Following Flooding in an Oklahoma Stream. *The American Midland Naturalist* **117**, 333–345

R Core Team. (2019). R: A language and environment for statistical computing. R Foundation for Statistical Computing, Vienna, Austria. URL https://www.R-project.org/.

Randklev C.R., Hart M.A., Khan J.M., Tsakiris E.T. & Robertson C.R. (2019). Hydraulic requirements of freshwater mussels (Unionidae) and a conceptual framework for how they respond to high flows. *Ecosphere* **10**. https://doi.org/10.1002/ecs2.2975

Reinert T.R., Wallin J., Griffin M.C., Conroy M.J. & Avyle M.J. Van Den (1998). Long-term retention and detection of oxytetracycline marks applied to hatchery-reared larval striped bass, Morone saxatilis. *Canadian Journal of Fisheries and Aquatic Sciences* **55**, 539–543

Riecke T. V., Leach A.G., Gibson D. & Sedinger J.S. (2018). Parameterizing the robust design in the BUGS language: Lifetime carry-over effects of environmental conditions during growth on a long-lived bird. *Methods in Ecology and Evolution* **2018**, 1–12. https://doi.org/10.1111/2041-210X.13065

Robinson C.T. (2012). Long-term changes in community assembly, resistance, and resilience following experimental floods. *Ecological Applications* **22**, 1949–1961. https://doi.org/10.1890/11-1042.1

Ruppel D.S. (2019). Facators influencing community structure of riverine organisms: implications for imperiled species management. Dissertation, Texas State University

Sansom B.J., Bennett S.J., Atkinson J.F. & Vaughn C.C. (2018). Long - term persistence of freshwater mussel beds in labile river channels. *Freshwater Biology* **63**, 1469–1481.

https://doi.org/10.1111/fwb.13175

Strayer D.L. (1999). Use of Flow Refuges by Unionid Mussels in Rivers Author (s): David L . Strayer Source : Journal of the North American Benthological Society , Vol . 18 , No . 4 (Dec ., 1999), Published by : The University of Chicago Press on behalf of the Society for. *The North American Benthological Society* **18**, 468–476

Strayer D.L. & Smith D.R. (2003). *A Guide to Sampling Freshwater Mussel Populations*.

Su, Y.S. & Yajima, M. (2015). R2jags: A package for running Jags from R. http://CRAN.R-project.org/package=R2jags (accessed on January 2019).

Sylvia D.A. & Galloway W.E. (2006). Morphology and stratigraphy of the late Quaternary lower Brazos valley: Implications for paleo-climate, discharge and sediment delivery. *Sedimentary Geology* **190**, 159–175. https://doi.org/10.1016/j.sedgeo.2006.05.023

Talbot C.J., Bennett E.M., Cassell K., Hanes D.M., Minor E.C., Paerl H., *et al.* (2018). The impact of flooding on aquatic ecosystem services. *Biogeochemistry* **141**, 439–461. https://doi.org/10.1007/s10533-018-0449-7

Watters G.T. (1994). Form and function of unionoidean shell sculpture and shape (Bivalvia). *American Malacological Bulletin* **11**, 1–20

Watters G.T., O'Dee S.H. & Chordas S. (2001). Patterns of vertical migration in freshwater mussels (Bivalvia: Unionoida). *Journal of Freshwater Ecology* **16**, 541–549. https://doi.org/10.1080/02705060.2001.9663845

Wentworth C.K. (1922). A Scale of Grade and Class Terms for Clastic Sediments. *The Journal of Geology* **30**, 377–392. https://doi.org/10.1086/622910

Wisniewski J.M., Shea C.P., Abbott S. & Stringfellow R.C. (2013). Imperfect Recapture: A

Potential Source of Bias in Freshwater Mussel Studies. *The American Midland Naturalist* **170**, 229–247. https://doi.org/10.1674/0003-0031-170.2.229

Young S.P. & Isely J.J. (2008). Evaluation of methods for attaching PIT tags and biotelemetry devices to freshwater mussels. *Molluscan Research* **28**, 175–178

Zigler S.J., Newton T.J., Steuer J.J., Bartsch M.R. & Sauer J.S. (2008). Importance of physical and hydraulic characteristics to unionid mussels: A retrospective analysis in a reach of large river. *Hydrobiologia* **598**, 343–360. https://doi.org/10.1007/s10750-007-9167-1

Table 1. Discharge values (m^3/s) for each sampling site for each interval (i.e., the time between primary periods; the first interval occurred between primary period one and primary period two). Included are median discharge, minimum discharge, and maximum discharge.

Site	Interval	Minimum	Median	Maximum
Upper	1	0.60	1.10	2.10
	2	1.11	1.81	76.46
	3	0.09	0.79	31.89
	4	0.06	11.02	1,270.29
Lower	1	21.58	33.61	52.25
	2	19.03	29.34	4,336.50
	3	12.97	17.36	618.89
	4	22.63	32.85	87.16

Table 2. The total number of mussels (Total N) sampled at each site, with survey gear for each species.

Site	Gear	Species	Total N
Upper	PIT tags	*C. petrina*	442
		C. pustulosa	15
	Shellfish tags	*C. petrina*	442
		C. pustulosa	15
		T. verrucosa	217
Lower	PIT tags	*C. petrina*	120
		C. pustulosa	308
	Shellfish tags	*C. petrina*	117
		C. pustulosa	300
		A. plicata	405

Table 3. Summary of estimated abundance and apparent survival of four mussel species after flood events at the upper and lower sites in the Colorado River. Estimated abundance percentage indicates the percent decrease in estimated abundance between the primary periods surrounding the flood for those comparisons which were significant. The letters "NS" represent no significant difference detected between primary periods (estimated abundance) or intervals (apparent survival). The symbol "--" represents species that did not have PIT tags.

		PIT-tagged		Shellfish-tagged	
Site	Species	Estimated abundance	Apparent survival	Estimated abundance	Apparent survival
Upper site	*C. petrina*	decreased 31%	NS	NS	NS
	C. pustulosa	decreased 45%	NS	NS	NS
	T. verrucosa	--	--	NS	NS
Lower site	*C. petrina*	decreased 73%	decreased	decreased 71%	NS
	C. pustulosa	decreased 80%	decreased	decreased 58%	decreased
	A. plicata	--	--	NS	NS

Figure 1. Discharge (m^3/s) plot of the upper (A) and lower (B) Colorado River throughout the duration of the study periods taken from USGS gages 08147000 (upper site) and 08161000 (lower site). Black dotted line denotes initial tagging event, black solid lines denote primary period sampling events.

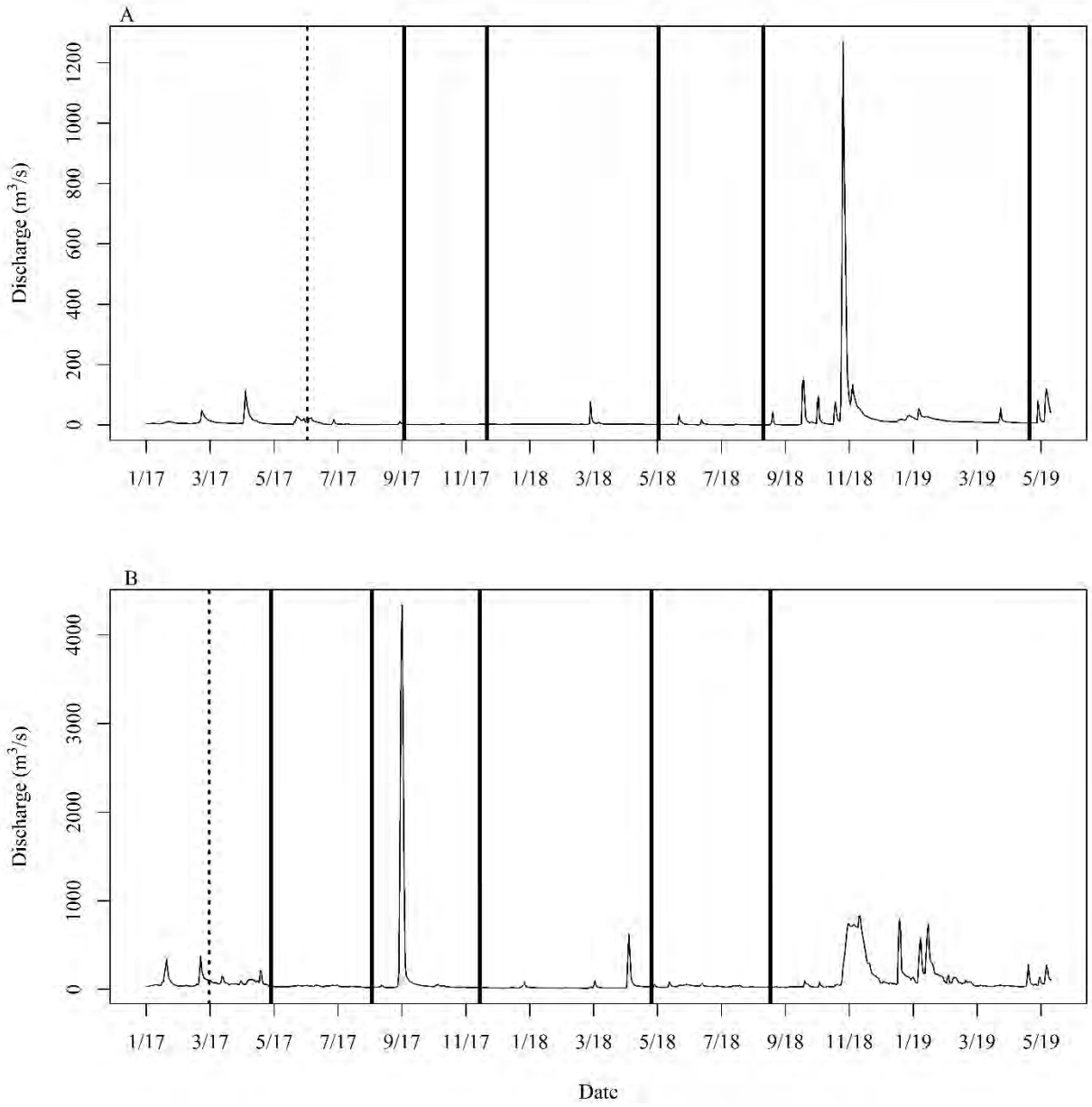

Figure 2. Boxplots depicting mark-recapture estimates of detection probability, estimated abundance, and apparent survival for *C. petrina* (A-C) and *C. pustulosa* (D-F) from the upper site on the Colorado River using PIT tag data. The flood occurred between primary period 4 and 5 and interval 4. An * indicates a significant difference between the primary period or interval and the one directly preceding it in time (i.e. *t-1* to *t*).

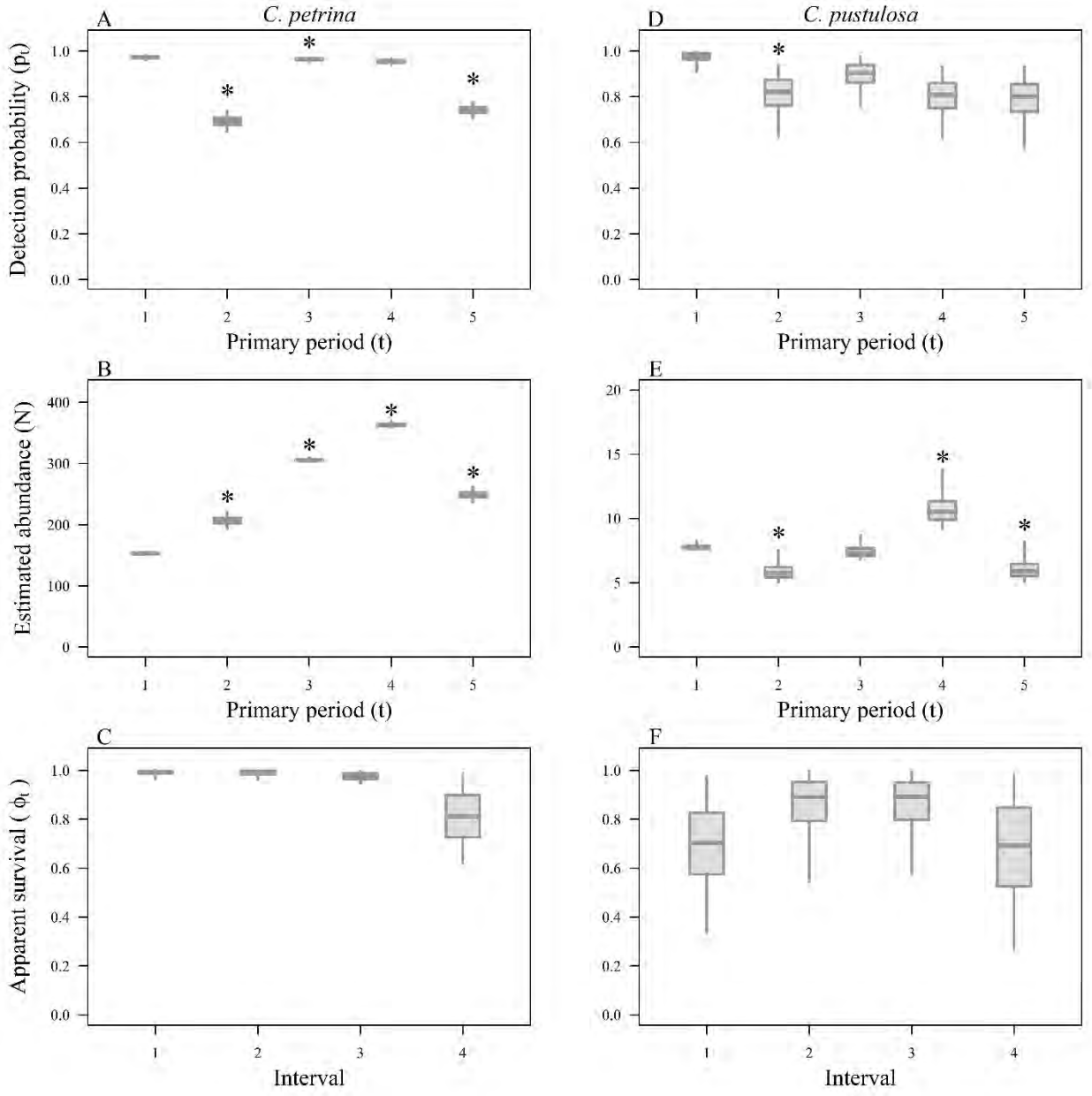

Figure 3. Boxplots depicting mark-recapture estimates of detection probability, abundance, and apparent survival for *C. petrina* (A-C), *C. pustulosa* (D-F), and *T. verrucosa* (G-I) from the upper site on the Colorado River using shellfish tag data. The flood occurred between primary period 4 and 5 and interval 4. An * indicates a significant difference between the primary period or interval and the one directly preceding it in time (i.e. *t-1* to *t*).

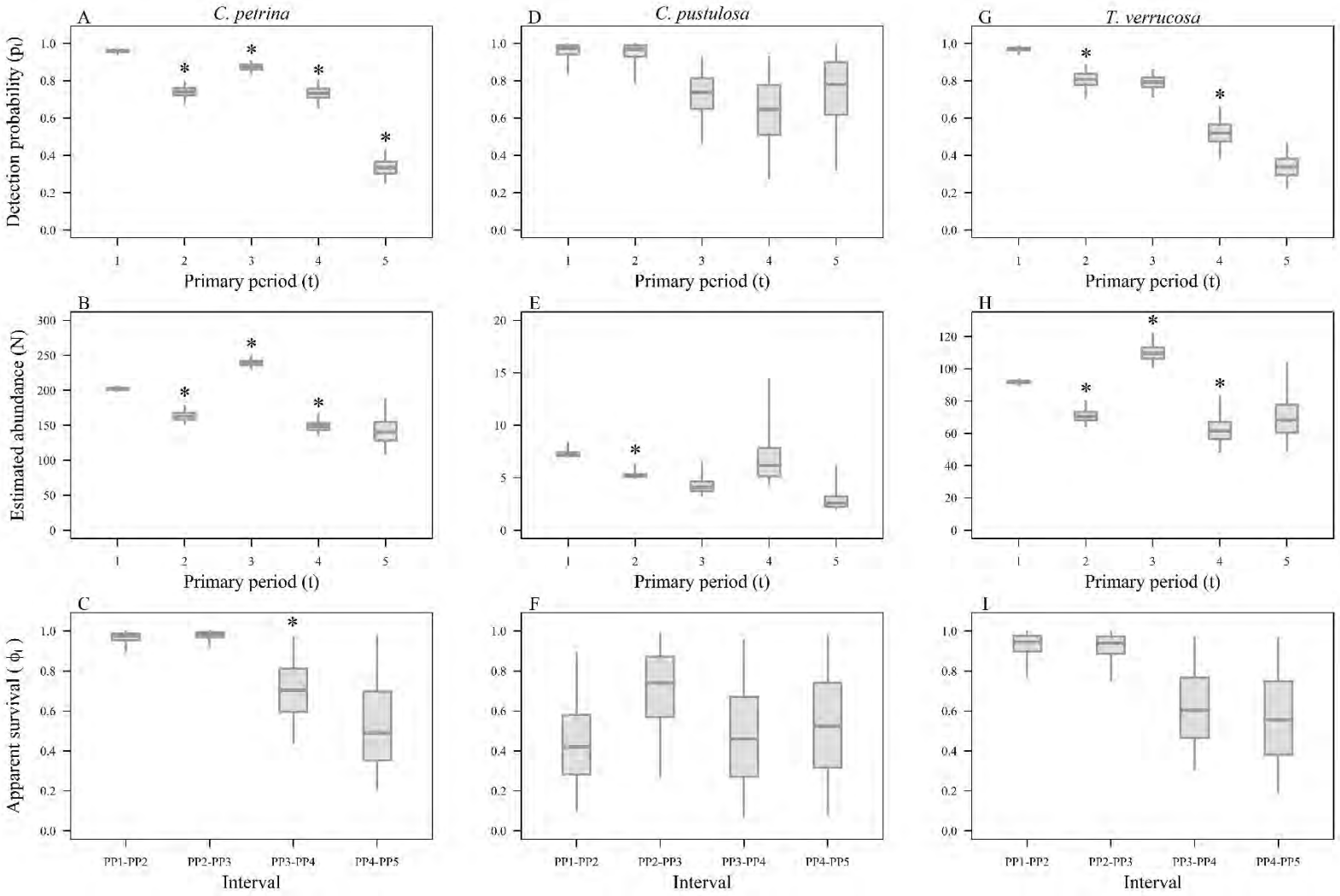

Figure 4. Boxplots depicting mark-recapture estimates of detection probability, abundance, and apparent survival for *C. petrina* (A-C) and *C. pustulosa* (D-F) from the lower site on the Colorado River using PIT tag data. The flood occurred between primary period 2 and 3 and interval 2. An * indicates a significant difference between the primary period or interval and the one directly preceding it in time (i.e. *t-1* to *t*).

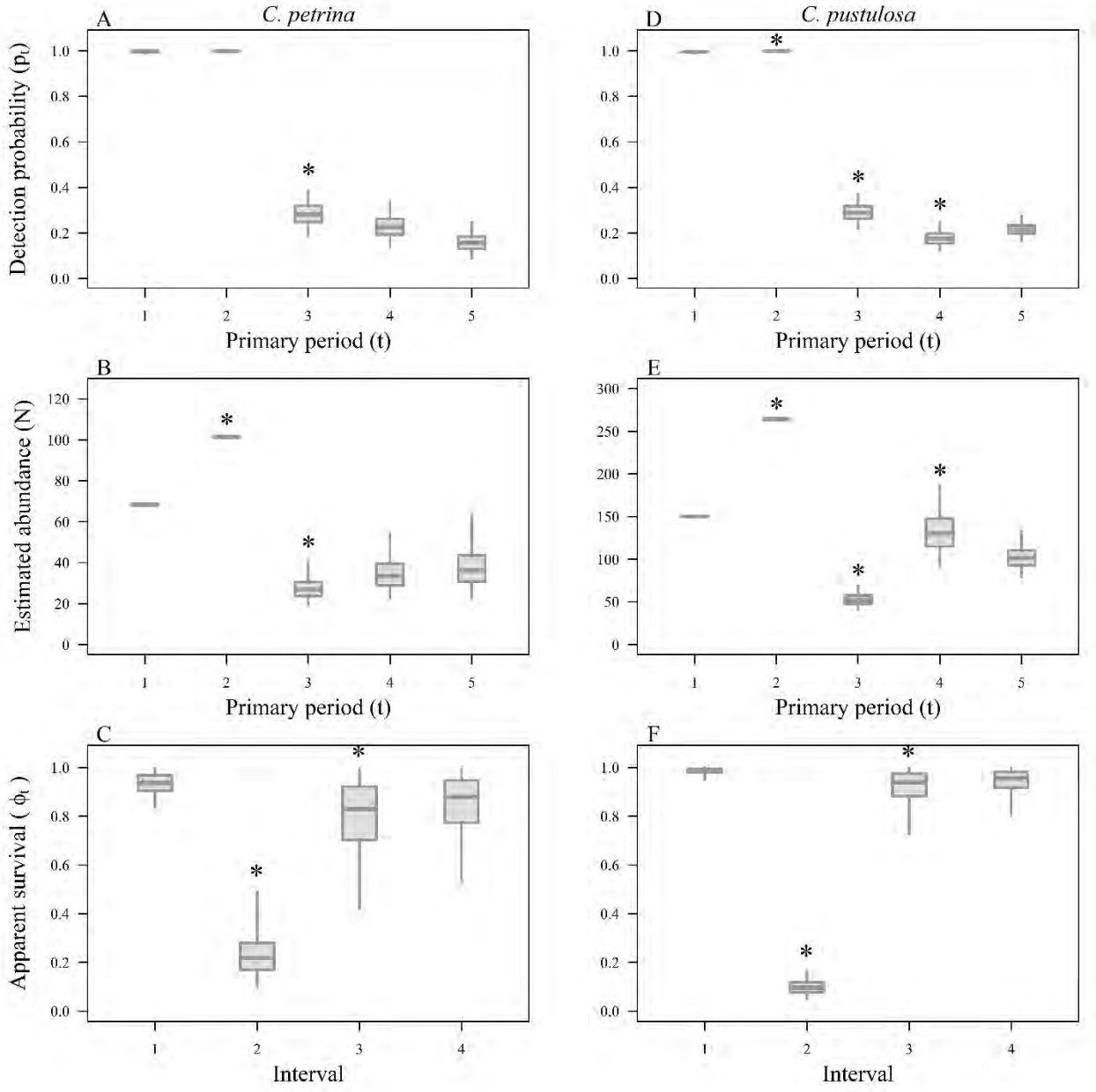

Figure 5. Boxplots depicting mark-recapture estimates of detection probability, abundance, and apparent survival for *C. petrina* (A-C), *C. pustulosa* (D-F), and *A. plicata* (G-I) from the lower site on the Colorado River using shellfish tag data. The flood occurred between primary period 2 and 3 and interval 2. An * indicates a significant difference between the primary period or interval and the one directly preceding it in time (i.e. *t-1* to *t*).

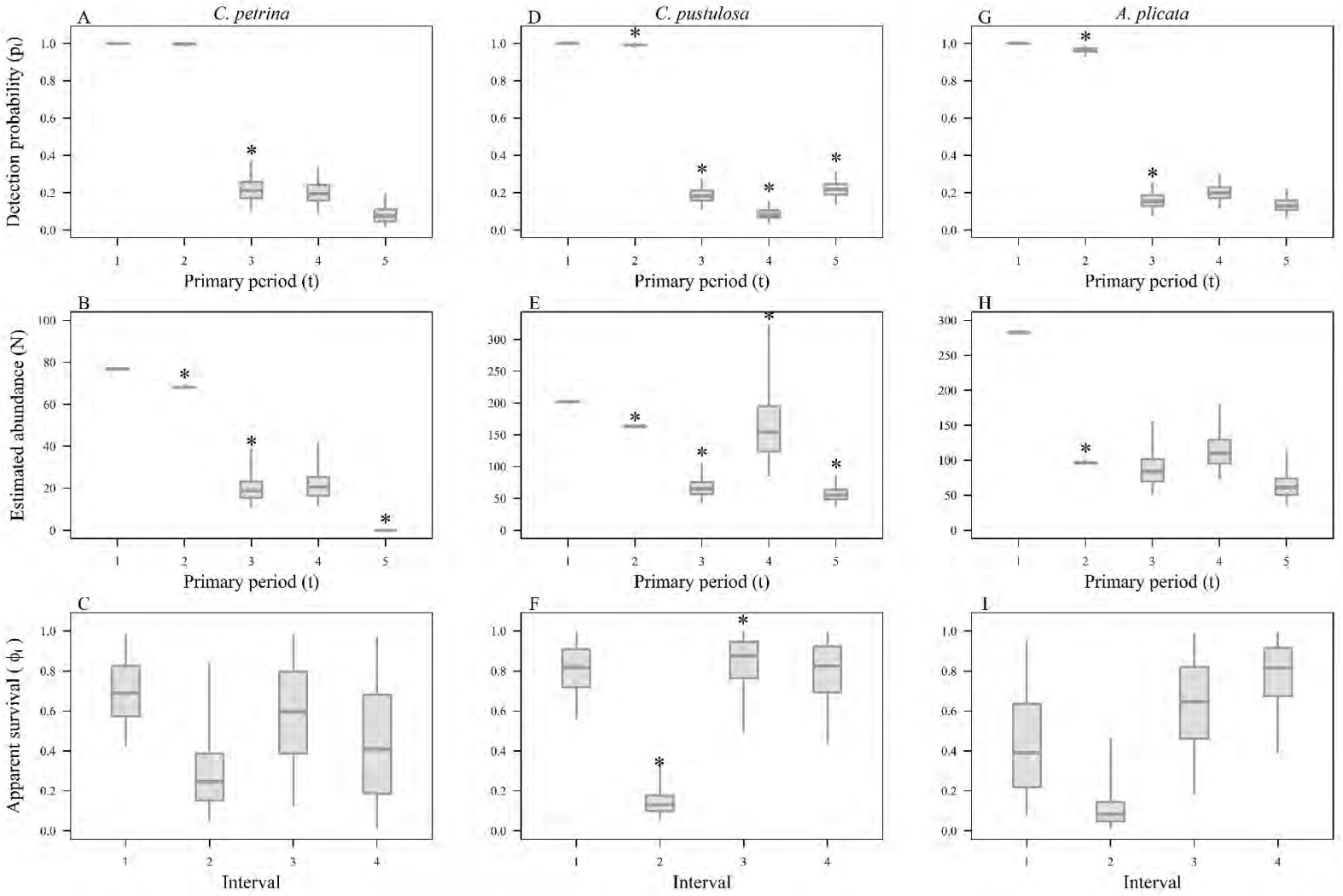

Supplemental Table 1. Mark-recapture median estimate, lower bound (LB), and upper bound (UB) credible intervals of detection probability and estimated abundances for each primary period (e.g. PP1 is primary period 1), and apparent survival for each interval for *C. petrina* and *C. pustulosa* from the upper and lower Colorado River via PIT surveys.

Site	Species	Parameter	Period	Estimate	LB	UB
Upper	*C. petrina*	Detection Probability	PP1	0.972	0.959	0.983
			PP2	0.693	0.647	0.739
			PP3	0.963	0.951	0.973
			PP4	0.954	0.94	0.967
			PP5	0.743	0.705	0.778
		Estimated Abundances	PP1	152.937	151.3	155.01
			PP2	206.563	193.378	220.87
			PP3	305.792	302.74	309.592
			PP4	363.252	358.331	368.917
			PP5	248.833	237.321	261.929
		Apparent Survival	Interval 1	0.99	0.965	1.0
			Interval 2	0.989	0.962	1.0
			Interval 3	0.975	0.94	0.998
			Interval 4	0.811	0.62	0.988
	C. pustulosa	Detection Probability	PP1	0.973	0.91	0.998
			PP2	0.812	0.626	0.942
			PP3	0.895	0.762	0.976
			PP4	0.8	0.619	0.931
			PP5	0.789	0.577	0.932
		Estimated Abundances	PP1	7.789	7.591	8.325
			PP2	5.894	5.028	7.565
			PP3	7.436	6.789	8.696
			PP4	10.78	9.155	13.775
			PP5	6.094	5.082	8.21
		Apparent Survival	Interval 1	0.695	0.34	0.976
			Interval 2	0.857	0.543	0.996
			Interval 3	0.862	0.576	0.996
			Interval 4	0.678	0.267	0.985
Lower	*C. petrina*	Detection Probability	PP1	0.996	0.989	0.999
			PP2	0.999	0.998	1.0
			PP3	0.284	0.187	0.392
			PP4	0.229	0.14	0.34
			PP5	0.16	0.089	0.249
		Estimated Abundances	PP1	68.461	68.239	68.916
			PP2	101.408	101.342	101.554

		PP3	27.642	19.338	40.556
		PP4	34.869	22.314	54.086
		PP5	38.105	22.8	64.034
	Apparent Survival	Interval 1	0.933	0.837	0.997
		Interval 2	0.237	0.1	0.49
		Interval 3	0.796	0.422	0.993
		Interval 4	0.845	0.53	0.995
C. pustulosa	Detection Probability	PP1	0.995	0.99	0.998
		PP2	0.999	0.999	1.0
		PP3	0.29	0.218	0.37
		PP4	0.177	0.122	0.247
		PP5	0.216	0.164	0.275
	Estimated Abundances	PP1	150.334	149.871	151.16
		PP2	264.389	264.277	264.575
		PP3	53.181	40.965	69.47
		PP4	132.787	92.102	186.389
		PP5	102.456	79.339	132.813
	Apparent Survival	Interval 1	0.985	0.951	1.0
		Interval 2	0.1	0.051	0.164
		Interval 3	0.919	0.727	0.998
		Interval 4	0.942	0.802	0.999

Supplemental Table 2. Median differences and lower bound (LB) and upper bound (UB) credible intervals between periods for each site, species, and parameter. Period column indicates which primary periods (e.g., 1-2 indicates PP1-PP2 comparison) or intervals (e.g., 1-2 indicates first and second interval comparison) were compared. An * in the period column indicates a significant difference between the respective periods or intervals. Data in this table are for PIT tag estimates.

Site	Species	Parameter	Periods	Median Difference	LB	UB
Upper	*C. petrina*	Detection Probability	1-2*	0.279	0.231	0.327
			2-3*	-0.270	-0.318	-0.223
			3-4	0.009	-0.009	0.026
			4-5	0.211	0.174	0.252
		Estimated Abundance	1-2*	-53.410	-68.158	-40.299
			2-3*	-99.511	-112.744	-84.314
			3-4*	-57.337	-63.831	-51.239
			4-5*	114.553	100.266	126.908
		Apparent Survival	1-2	0.001	-0.028	0.030
			2-3	0.013	-0.022	0.053
			3-4	0.162	-0.018	0.359
	C. pustulosa	Detection Probability	1-2*	0.152	0.016	0.351
			2-3	-0.079	-0.293	0.115
			3-4	0.090	-0.095	0.303
			4-5	0.008	-0.235	0.265
		Estimated Abundance	1-2*	2.021	0.190	2.924
			2-3	-1.590	-3.187	0.263
			3-4*	-3.132	-6.454	-1.237
			4-5*	4.574	1.923	8.071
		Apparent Survival	1-2	-0.171	-0.565	0.281
			2-3	-0.003	-0.363	0.336
			3-4	0.172	-0.237	0.649
Lower	*C. petrina*	Detection Probability	1-2	-0.003	-0.010	0.000
			2-3*	0.717	0.606	0.812
			3-4	0.056	-0.087	0.197
			4-5	0.069	-0.056	0.198
		Estimated Abundance	1-2*	-32.986	-33.219	-32.481
			2-3*	74.547	60.863	82.115
			3-4	-6.515	-28.290	10.295
			4-5	-2.502	-32.057	22.095
		Apparent Survival	1-2*	0.713	0.433	0.859
			2-3*	-0.608	-0.849	-0.033
			3-4	-0.043	-0.473	0.358
	C. pustulosa	Detection Probability	1-2*	-0.004	-0.009	-0.001
			2-3*	0.710	0.630	0.781

	3-4*	0.114	0.013	0.208
	4-5	-0.040	-0.119	0.049
Estimated Abundance	1-2*	-114.105	-114.567	-113.229
	2-3*	212.001	194.989	223.445
	3-4*	-77.466	-133.207	-35.925
	4-5	28.559	-21.258	89.693
Apparent Survival	1-2*	0.888	0.811	0.939
	2-3*	-0.839	-0.931	-0.609
	3-4	-0.013	-0.235	0.152

Supplemental Table 3. Mark-recapture median estimate, lower bound (LB), and upper bound (UB) credible intervals of detection probability and estimated abundances for each primary period (e.g. PP1 is primary period 1), and apparent survival for each interval for *C. petrina* (upper and lower sites), *C. pustulosa* (upper and lower sites), *T. verrucosa* (upper site), and *A. plicata* (lower site) via tactile surveys.

Site	Species	Parameter	Period	Estimate	LB	UB
Upper	*C. petrina*	Detection Probability	PP1	0.958	0.94	0.974
			PP2	0.741	0.676	0.802
			PP3	0.872	0.832	0.906
			PP4	0.734	0.659	0.801
			PP5	0.335	0.251	0.425
		Estimated Abundances	PP1	202.178	198.914	206.193
			PP2	163.465	150.6	178.857
			PP3	239.543	230.288	250.788
			PP4	148.773	135.952	165.209
			PP5	142.671	110.488	186.714
		Apparent Survival	Interval 1	0.967	0.896	0.999
			Interval 2	0.978	0.925	0.999
			Interval 3	0.706	0.447	0.973
			Interval 4	0.53	0.208	0.97
	C. pustulosa	Detection Probability	PP1	0.958	0.832	0.999
			PP2	0.946	0.774	0.999
			PP3	0.724	0.458	0.923
			PP4	0.639	0.297	0.933
			PP5	0.755	0.347	0.991
		Estimated Abundances	PP1	7.315	6.997	8.405
			PP2	5.304	4.998	6.45
			PP3	4.281	3.247	6.538
			PP4	6.922	4.282	13.451
			PP5	2.878	2.016	5.764
		Apparent Survival	Interval 1	0.44	0.109	0.893
			Interval 2	0.712	0.288	0.986
			Interval 3	0.489	0.076	0.963
			Interval 4	0.516	0.084	0.97
	T. verrucosa	Detection Probability	PP1	0.97	0.944	0.987
			PP2	0.805	0.709	0.883
			PP3	0.791	0.714	0.859
			PP4	0.521	0.385	0.658
			PP5	0.339	0.221	0.466
		Estimated Abundances	PP1	91.72	90.119	94.229

			PP2	70.975	64.503	80.309
			PP3	110.127	101.173	121.846
			PP4	62.495	48.582	83.025
			PP5	70.346	49.314	103.847
		Apparent Survival	Interval 1	0.928	0.774	0.998
			Interval 2	0.921	0.751	0.998
			Interval 3	0.619	0.308	0.97
			Interval 4	0.566	0.191	0.965
Lower	*C. petrina*	Detection Probability	PP1	0.999	0.998	1.0
			PP2	0.995	0.984	1.0
			PP3	0.221	0.109	0.364
			PP4	0.199	0.099	0.331
			PP5	0.084	0.018	0.199
		Estimated Abundances	PP1	76.954	76.906	77.092
			PP2	68.249	67.944	69.051
			PP3	20.024	10.967	36.539
			PP4	22.111	12.051	40.173
			PP5	0.0	0.0	0.0
		Apparent Survival	Interval 1	0.683	0.423	0.972
			Interval 2	0.311	0.06	0.827
			Interval 3	0.577	0.117	0.982
			Interval 4	0.451	0.018	0.969
	C. pustulosa	Detection Probability	PP1	1.0	0.999	1.0
			PP2	0.99	0.98	0.997
			PP3	0.184	0.116	0.262
			PP4	0.087	0.041	0.151
			PP5	0.219	0.144	0.313
		Estimated Abundances	PP1	201.796	201.751	201.908
			PP2	163.39	162.31	165.169
			PP3	68.093	45.694	103.405
			PP4	167.465	85.741	319.778
			PP5	56.933	38.231	83.01
		Apparent Survival	Interval 1	0.812	0.564	0.992
			Interval 2	0.145	0.059	0.284
			Interval 3	0.844	0.519	0.995
			Interval 4	0.798	0.444	0.993
	A. plicata	Detection Probability	PP1	1.0	1.0	1.0
			PP2	0.964	0.933	0.984
			PP3	0.16	0.084	0.252
			PP4	0.202	0.122	0.297
			PP5	0.135	0.071	0.217

Estimated Abundances	PP1	282.837	282.836	282.84
	PP2	96.481	94.437	99.617
	PP3	88.133	51.553	154.901
	PP4	114.331	73.908	179.96
	PP5	64.381	36.828	113.382
Apparent Survival	Interval 1	0.437	0.079	0.947
	Interval 2	0.118	0.014	0.462
	Interval 3	0.631	0.186	0.985
	Interval 4	0.779	0.395	0.991

Supplemental Table 4. Median differences and lower bound (LB) and upper bound (UB) credible intervals between periods for each site, species, and parameter. Period column indicates which primary periods (e.g., 1-2 indicates PP1-PP2 comparison) or intervals (e.g., 1-2 indicates first and second interval comparison) were compared. An * in the period column indicates a significant difference between the respective periods or intervals. Data in this table are for shellfish tag estimates.

Site	Species	Parameter	Periods	Median Diff	LB	UB
Upper	*C. petrina*	Detection Probability	1-2*	0.217	0.154	0.284
			2-3*	-0.131	-0.205	-0.058
			3-4*	0.137	0.063	0.220
			4-5*	0.400	0.283	0.505
		Estimated Abundance	1-2*	39.164	22.984	52.203
			2-3*	-76.319	-92.739	-58.018
			3-4*	91.015	72.236	107.476
			4-5	7.762	-38.887	41.997
		Apparent Survival	1-2	-0.008	-0.087	0.053
			2-3*	0.276	0.001	0.541
			3-4	0.201	-0.416	0.664
	C. pustulosa	Detection Probability	1-2	0.004	-0.134	0.195
			2-3	0.213	-0.035	0.508
			3-4	0.081	-0.314	0.496
			4-5	-0.123	-0.571	0.395
		Estimated Abundance	1-2*	2.015	0.781	3.184
			2-3	1.185	-1.321	2.637
			3-4	-1.998	-9.414	1.050
			4-5	3.448	-0.023	10.995
		Apparent Survival	1-2	-0.300	-0.776	0.383
			2-3	0.241	-0.462	0.801
			3-4	-0.036	-0.699	0.682
	T. verrucosa	Detection Probability	1-2*	0.162	0.081	0.263
			2-3	0.014	-0.100	0.129
			3-4*	0.270	0.117	0.423
			4-5	0.184	-0.001	0.363
		Estimated Abundance	1-2*	21.208	11.178	27.824
			2-3*	-38.862	-52.955	-26.525
			3-4*	48.239	25.937	65.392
			4-5	-6.683	-43.866	20.669
		Apparent Survival	1-2	0.005	-0.183	0.207
			2-3	0.314	-0.096	0.646
			3-4	0.043	-0.554	0.688
Lower	*C. petrina*	Detection Probability	1-2	0.003	-0.001	0.016
			2-3*	0.778	0.629	0.887

		3-4	0.020	-0.144	0.201
		4-5	0.114	-0.034	0.270
	Estimated Abundance	1-2*	8.786	7.895	9.038
		2-3*	49.812	31.628	57.317
		3-4	-1.805	-23.335	16.955
		4-5*	20.587	12.051	40.173
	Apparent Survival	1-2	0.388	-0.218	0.826
		2-3	-0.307	-0.837	0.538
		3-4	0.145	-0.672	0.832
C. pustulosa	Detection Probability	1-2*	0.009	0.003	0.020
		2-3*	0.808	0.727	0.875
		3-4*	0.097	0.006	0.191
		4-5*	-0.130	-0.233	-0.034
	Estimated Abundance	1-2*	38.532	36.609	39.487
		2-3*	97.492	59.562	117.727
		3-4*	-87.360	-252.186	-11.164
		4-5*	98.349	24.964	265.558
	Apparent Survival	1-2*	0.683	0.354	0.899
		2-3*	-0.734	-0.900	-0.330
		3-4	0.037	-0.379	0.462
A. plicata	Detection Probability	1-2*	0.035	0.016	0.067
		2-3*	0.807	0.705	0.884
		3-4	-0.043	-0.162	0.082
		4-5	0.068	-0.047	0.180
	Estimated Abundance	1-2*	186.518	183.221	188.399
		2-3	12.688	-58.774	45.627
		3-4	-26.202	-100.271	50.572
		4-5	48.032	-12.427	120.247
	Apparent Survival	1-2	0.295	-0.293	0.899
		2-3	-0.553	-0.929	0.182
		3-4	-0.135	-0.697	0.388

Supplementary Table 5. Median, lower bound (LB), and upper bound (UB) credible intervals of differences between parameter estimates from PIT tag and shellfish tag data for each species and both sites where a comparison was possible. If the median is negative, that indicates shellfish tag data underestimated parameter relative to PIT tag data, and overestimated if positive. An * in the period column indicates that zero is not included in the 95% credible intervals, and the posterior estimates of PIT and shellfish data are significantly different.

Site	Species	Parameter	Period	LB	Median	UB
Upper	*C. petrina*	Detection Probability	PP1	-0.036	-0.013	0.006
			PP2	-0.033	0.049	0.123
			PP3*	-0.133	-0.091	-0.055
			PP4*	-0.295	-0.219	-0.152
			PP5*	-0.497	-0.408	-0.312
		Estimated Abundance	PP1*	45.450	49.110	53.718
			PP2*	-61.583	-43.452	-22.897
			PP3*	-76.041	-66.537	-54.488
			PP4*	-228.658	-215.041	-197.705
			PP5*	-140.429	-108.053	-60.634
		Apparent Survival	PP1-PP2	-0.094	-0.270	0.022
			PP2-PP3	-0.066	-0.128	0.025
			PP3-PP4*	-0.529	-0.389	-0.001
			PP4-PP5	-0.683	-0.164	0.215
	C. pustulosa	Detection Probability	PP1	-0.141	-0.006	0.064
			PP2	-0.069	0.135	0.337
			PP3	-0.459	-0.161	0.069
			PP4	-0.538	-0.153	0.192
			PP5	-0.478	-0.009	0.302
		Estimated Abundance	PP1	-1.127	-0.552	0.602
			PP2	-2.335	-0.535	0.790
			PP3*	-4.863	-3.288	-0.718

			PP4	-8.172	-4.387	3.013
			PP5*	-5.663	-3.296	-0.119
		Apparent Survival	PP1-PP2	-0.724	-0.270	0.313
			PP2-PP3	-0.632	-0.128	0.314
			PP3-PP4	-0.840	-0.389	0.166
			PP4-PP5	-0.779	-0.164	0.490
Lower	*C. petrina*	Detection Probability	PP1	0.000	0.003	0.010
			PP2	-0.016	-0.003	0.001
			PP3	-0.219	-0.068	0.111
			PP4	-0.184	-0.032	0.138
			PP5	-0.190	-0.079	0.054
		Estimated Abundance	PP1*	8.008	8.530	8.751
			PP2*	-33.501	-33.242	-32.347
			PP3	-24.540	-8.004	11.146
			PP4	-35.951	-12.613	10.334
			PP5*	-64.034	-36.170	-22.800
		Apparent Survival	PP1-PP2	-0.532	-0.256	0.043
			PP2-PP3	-0.303	0.046	0.602
			PP3-PP4	-0.773	-0.208	0.357
			PP4-PP5	-0.910	-0.422	0.204
	C. pustulosa	Detection Probability	PP1*	0.001	0.004	0.010
			PP2*	-0.020	-0.008	-0.003
			PP3	-0.217	-0.107	0.001
			PP4*	-0.175	-0.090	-0.006
			PP5	-0.096	0.002	0.108
		Estimated Abundance	PP1*	50.626	51.522	51.937
			PP2*	-102.078	-101.123	-99.225
			PP3	-13.336	13.205	53.544

	PP4	-65.785	23.641	191.430
	PP5*	-81.700	-45.631	-9.915
Apparent Survival	PP1-PP2	-0.423	-0.160	0.009
	PP2-PP3	-0.066	0.038	0.190
	PP3-PP4	-0.425	-0.053	0.186
	PP4-PP5	-0.522	-0.114	0.104

Task 5 & 6: Captive breeding and development of aquaculture techniques and long-term captive rearing and holding.

Contributing Authors: Ashley Seagroves[1], Randy Gibson[1], Valentine Cantu[2], Patricia Duncan[2], Bailey Gaines[3], Scott Walker[3]

Adresses:[1] Aquatic Resources Center, 500 E. McCarty Ln., San Marcos, TX 78666
[2] Uvalde National Fish Hatchery, 754 County Rd 203, Uvalde, TX 78801
[3] Inks Dam National Fish Hatchery, 345 Clay Young Road, Burnet, TX 78611

Principal Investigator: Kenneth Ostrand[1]

Email: kenneth_ostrand@fws.gov

EXECUTIVE SUMMARY

INTRODUCTION

During 2017-2019, Texas State University contracted three U.S. Fish and Wildlife Service (USFWS) research and culture facilities in Texas to initiate mussel propagation programs and compare various culture techniques for candidate species of central Texas freshwater mussels. The emphasis of the work was primarily on comparing different water sources and diets: 1) San Marcos Aquatic Resources Center (SMARC) used commercially produced algae feed and fertilized pond water, 2) Uvalde National Fish Hatchery (UNFH) used well water and cultured algae, and 3) Inks Dam National Fish Hatchery (IDNFH) used lake water. Culture was focused primarily on three species (Texas Fatmucket, Texas Pimpleback, and Pimpleback) that were most accessible for collections or streamside infestations of host fish.

Pimpleback (*Cyclonaias pustulosa*) is the current name of four species found to be in synonymy. Those species were: Pimpleback (*Quadrula pustulosa*), Western Pimpleback (*Quadrula mortoni*), Smooth Pimpleback (*Quadrula houstonensis*), and Golden Orb (*Quadrula aurea*). Little to no work was performed on the Texas Fawnsfoot or the False Spike because of the rarity of these species and potential negative impacts to the wild population.

Preliminary Work and Lessons Learned

Initially all facilities purchased the necessary equipment for establishing a freshwater mussel propagation program and constructed various holding, rearing, and propagation systems specific to the facility. During the first two years of this project, very few juvenile mussels survived past four months in captivity. The primary issues contended with for successful production were water quality (especially dissolved oxygen and ammonia as result of source water, culture system design, and substrate particle size influences), predators and competitors in juvenile rearing systems (flatworms, annelids, chironomid larvae), and nutritional sources (freshwater mussel diets not fully understood and "wild water" considered beneficial for long-term holding and more successful growth of juveniles as compared to commercially produced algae diets). Each facility developed and refined techniques and adapted their culture program to contend with these and other facility-specific issues.

RESULTS

Texas Fatmucket (*Lampsilis bracteata*)

Most propagation success was achieve with Texas Fatmucket. Published knowledge about this species exists compared to the other mussel species including recent culture methods and host fish requirements (Seagroves et al. 2019). Texas Fatmucket is a long-term brooder, which allows more time throughout the year to collect gravid females. Gravidity is easily distinguished in the females and glochidia can be flushed out of the gills using a syringe. Gravid females can be held in refrigeration and later brought up to temperature when infestation of host fish for culture is most convenient. Propagation of Texas Fatmucket was exceptional at IDNFH using filtered lake water and up-wellers followed by pan systems with substrate > 400 µm. At IDNFH, the best results were achieved using Bluegill as a host. SMARC had some success using pond water continuously pumped into a beaker system supplemented by commercial feed and Large Mouth Bass as a host. UNFH had marginal success using commercial feed and cultured algae in a static beaker system and Green Sunfish as a host until juveniles succumbed to predation.

Texas Pimpleback (*Cyclonaias petrina*)

Members of the genus *Cyclonaias* are short-term brooders, which restrict the amount of time available during the season to collect gravid females. The shortened time-period can be an impediment to acquiring viable glochidia because timing of collection is crucial to success and, as occurred multiple times during this project, collection trips had to be cancelled due to unsafe river conditions. Additionally, handing of gravid females can trigger spontaneous abortion of conglutinates; therefore, requiring collection techniques to capture conglutinates if released with the hopes that most are viable. Propagation of Texas Pimpleback was successful at IDNFH using filtered river water and up-wellers followed by pan systems with substrate > 400 µm and Channel Catfish as a host. SMARC had marginal success with drop-offs in 2018 using Channel Catfish as a host, but no survival of juveniles likely due to water quality issues.

UNFH had marginal success using commercial feed and cultured algae in a static beaker system and Channel Catfish as a host until juveniles succumbed to predation.

Pimpleback (*Cyclonaias pustulosa*)

As mentioned previously, *Cyclonaias* species are short-term brooder and therefore poses more difficulty for culture as compared to long-term brooders. Propagation of Pimpleback was successful at IDNFH using filtered lake water and up-wellers followed by pan systems with substrate > 400 µm and Channel Catfish as a host. SMARC had some success with transformations using Channel Catfish as a host, but juveniles did not survive, likely due to water quality issues. UNFH also had successful transformations using Channel Catfish as a host, but juveniles did not survive, likely due to predation.

False spike (*Fusconaia mitchelli)* and Texas Fawnsfoot (*Truncilla macrodon*)

Limited work was performed with these species due their rarity in the wild and the absence of reliable source populations.

Costs

Initial costs for establishment of a mussel propagation program were expensive. These one-time, costs included construction of quarantine, holding and propagation systems (e.g. AHAB type systems), refurbishing buildings, outdoor augmentation of facilities (e.g. influent filter systems, effluent biosecurity systems, plumbing ponds for pumping water into buildings, etc.), purchasing necessary monitoring equipment (e.g. water quality meters and particle counters), and microscopes with cameras and measuring software needed for separating and counting juveniles. After aquaculture programs were initiated, then costs were reduced to labor followed by expendable supplies and aquatic holding system maintenance.

Most programs needed at least two full-time employees and used additional help during the peak mussel breeding season (spring and summer), but we recommend at least three to four full-time employees for a functional mussel propagation facility. Principal supply costs were for water filters required for successful rearing of juvenile mussels, reagents for monitoring equipment, commercial mussel food used when “wild water” is not available or at adequate levels to support the nutritional needs of the mussels, and fish food for hosts. Primary maintenance costs excluding utilities were for repairing and replacing equipment (e.g. pumps, chillers, heaters, blowers, UV sterilizers, and tanks) and repair and calibration of water quality equipment and particle counters.

DISCUSSION

Each facility experienced challenges establishing a mussel propagation program and developed the program accordingly. IDNFH had the greatest success using lake water and is refining the infrastructure and culture techniques for mass production and holding of freshwater mussels. “Wild

water" appears to be beneficial for growth and survival of juvenile mussels and essential for long term holding of adults.

The major drawbacks to using lake water is the expense for filtration, the seasonal and erratic fluctuations in water quality, and the danger of introducing deleterious organisms such as predacious worms. IDNFH is modifying their facility following protocols of other established mussel propagation facilities in order to ameliorate these issues. SMARC and UNFH did not have the same initial success but were limited by artificially cultured food sources. SMARC was able to use pond water as a nutrient source and eventually had success once water quality issues were eliminated through mechanically pumping pond water continually into the culture systems. SMARC is modifying the infrastructure, and refining its systems, pond management, and culture techniques to increase survival and growth of mussels and to increase the research capacity for future freshwater mussel conservation needs directed by the USFWS and stakeholders. UNFH was limited by using only cultured algae as a nutritional source for the mussels and predictably had marginal success. They are continuing to develop and refine techniques for freshwater algae culture to use when "wild water" is not available. Freshwater algae cultures would likely better provide for the basic nutritional requirements of freshwater mussels as compared to the commercially produced marine algae food that is currently used as the staple in mussel culture facilities. USFWS is evaluating various techniques to determine baseline heath and condition of freshwater mussels. Baseline health metrics can be used to assess wild populations and for guidance for captive propagation. Once a baseline is established for each species, then similar analysis of captive populations would help in determining if supplementation is needed to improve the health and condition of captive mussels and improve restoration activities and laboratory research of freshwater mussels.

FACILITY REPORTS

SAN MARCOS AQUATIC RESOURCES CENTER

Contributing Authors: Ashley Seagroves and Randy Gibson

INTRODUCTION

Description of Facility

The mussel program at the SMARC utilized two buildings and two ⅒ acre ponds. One of these buildings the "Holding House" was equipped with a quarantine room, aquatic tanks systems to hold and maintain host fish, and an isolated laboratory. All incoming species were transferred to the "Holding House" and held in quarantine indefinitely or until the USFWS's Southwestern Fish Health Unit, Dexter New Mexico had cleared them in an attempt to avoid the spread of possible pathogens. The "Holding House" building's tank systems were used to maintain host fish; where, each species was held in isolation. In addition, the "Holding House" building was also equipped with modified Aquatic Habitat Systems™ (AHAB). Fish inoculated with juvenile mussels were held within the AHAB systems until juvenile mussel drop offs from the host fish ceased. Viable juveniles mussels were then they were transferred from the AHAB systems to the" Test Pad" building. The "Test Pad" building receives pond water pumped in from the two ⅒ acre ponds used to rear algae and zooplankton that in turn feed mussels held within this building (Figure 1).

The "Holding House" laboratory is equipped with a variety of specialized equipment used solely for mussel culture. The equipment includes cross-polarizing microscopes and cameras that use computer software to measure and quantify juvenile mussel survival and growth. The laboratory is also equipped with a Beckman Multisizer that measures the size and quantifies the amounts of algae available for feeding mussels (Figure 2).

The SMARC used both managed pond water and commercial mussel feed (Nano 3600 (*Nannochloropsis*) and Shellfish Diet 1800, Reed Mariculture, Campbell, California) to rear juvenile and maintain adult mussels. Careful monitoring of ammonia and available food for mussels informs pond maintenance procedures, such as fertilizing or flushing ponds and adding catfish to keep filamentous algae at bay.

Description of Culture Systems

The SMARC mussel program utilized both AHAB (short-term) and long-term holding tanks for fish and mussels. AHABs were used during experiments or host fish inoculations, while long-term holding tanks are used before and after experiments, and for grow-out of propagated juvenile mussels. Each tank within the "Test Pad" building recirculated water and received a continuous low volume of pond water to supplement available food and maintain water turnover rates. Upon recirculation, water was chilled or heated to meet specified temperatures and passed through bio-filtration media to reduce level of toxic nitrogenous compounds including ammonia. Incoming pond water also passed through bio-filtration and was temperature conditioned in a sump system and then filtered to 5 µm to reduce the number of incoming predators of juvenile mussels (Figure 3). Well water was also available to the "Test Pad" building as an alternative water source, and was used to supplement tanks during occasional maintenance. The "Test Pad" building was equipped with environmental chambers that were used to maintain gravid mussels at colder temperatures so that glochidia release could be delayed, when necessary The "Holding House" building used water from Edward's Aquifer wells. Host fish infested with glochidia were held in AHAB tanks. These systems recirculated water through a heater, chiller, mechanical filter, and UV filter. They also allowed for the collection of juvenile mussels from individual fish (Figure 4). The quarantine room, within the "Holding House" building included a secondary AHAB system that was entirely flow-through. This second system allowed for the isolation of infested fish that arrived on station between fish health inspections. To accommodate a variety of species, grow-out systems were built with and without substrate. The up-welling and down-welling system held mussels without substrate on nylon mesh (Figure

5), which maintained relatively turbulent and oxygenated conditions. The pulse-flow beaker system held mussels with substrate and lower flow resulting in more static abiotic conditions (Figure 6).

Preliminary Work and Lessons Learned

Dewatering and desiccation studies on *Lampsilis bracteata* and *Cyclonaias petrina* took place in 1-year of this study. The dewatering study assessed both vertical and horizontal migration of waters in simulation of a drying river reach. The desiccation study assessed the duration of time that mussels could persist once dewatered, simulating extreme drought. The final report for these studies was competed January 2018. After these studies were completed, the surviving adult mussels (74 live on 31 Oct. 2018) were held in baskets in the ponds and later moved to the "Test Pad" building when pond water was made available.

The changing scope of mussel research from drought tolerance studies to propagation called for a nutrient-rich water source. SMARC used pond water supplemented with commercial mussel diets for mussel propagation but lacked a reliable method to deliver water to mussels. As a temporary solution, water was transported by truck in 100-gallon drums daily. Unfortunately, low survival of mussels in rearing systems called for a longer-term solution, as mortality was likely a byproduct of ammonia buildup in transportation tanks that could not drain fully. The availability of running pond water, as seen in the third year of this study, promoted survival of both adult and juvenile mussels in a variety of systems.

Another lesson learned for culture at SMARC was that flow-through rearing devices (i.e. Mucket Buckets) were labor intensive and unsuccessful. Constant clogging of screens by debris and calcium build-up resulted in reduced water quality and increased stress on juveniles during daily cleanings.

Other lessons learned early in this study informed future decisions regarding suitable substrate for

mussel rearing. Aside from water quality issues that may have impacted survival of juvenile mussels in the pan rearing system, the amount and type of substrate may have played a role in the buildup of ammonia. Anoxic conditions were observed within the substrate; thus, calling for substrate cleaning and replacement. However, the substrate was too large to adequately separate from mussels with a sieve, as mussels were roughly the same size as the substrate. Only pre-sieved substrate was used in year three of this study, which allowed for easier separation of juvenile mussels from substrate.

RESULTS

Success of juvenile mussel propagation varied among years, with the greatest number of live juvenile mussels produced in 2019 (Table 1). No juvenile mussels were produced in 2017 due to the emphasis of tolerance studies on mussels. Propagation efforts in 2018 resulted in a total of 2,598 live juvenile mussels from four species (Pimpleback, Texas Pimpleback, Texas Fatmucket, and False Spike) that survived for up to four months. Propagation in 2019 required several field outings to collect gravid mussels (Table 2) and resulted in a total of 5,067 live juvenile mussels from three species produced between June and September 2019. The October 2019 assessment included a total of 74 juvenile mussels from three *Lampsilis* species.

The pulse-flow beaker system currently contains three species of mussel including one rare and two common (used as surrogates for Texas Fatmucket). The common species, Louisiana Fatmucket (*Lampsilis hydiana*) and Yellow Sandshell (*Lampsilis teres*), were propagated in June, 2019 and September – October, 2019, respectively. The rare species Texas Fatmucket was propagated in August and September, 2019. Growth and survival assessments were conducted monthly. Of the four rearing systems used during this study, the pulse-flow beaker system had the greatest survival. While the pan system in 2018 and the up-wellers and down-wellers of 2019 resulted in no survival, all surviving juvenile mussels were housed in the pulse-flow beaker system. Survival in the beaker system with all species combined was 13% in the October 2019 monitoring event.

Texas Fatmucket (*Lampsilis bracteata*)— Texas Fatmucket propagation in 2019 began with the inoculation of 18 Green Sunfish and seven Largemouth Bass with glochidia from two Texas Fatmucket mussels on 9 July 2019. This resulted in a total of 1,975 live juvenile mussels (372 from Green Sunfish and 1,603 from Largemouth Bass). Mussels dropped from host fish between 22 July and 25 September 2019, and transformation success was 59% with both species combined (64% transformation for Largemouth Bass and 44% transformation for Green Sunfish). Transformation was calculated by dividing the number of live juveniles by the sum of all live and dead juvenile mussels along with all glochidia dropped from each fish. Shell length of juvenile Texas Fatmucket mussels ranged from 458 – 1004 µm in the October survival and growth assessment. The length of initial drop-offs increased from 293 µm ± 6 µm (mean ± SE, n=71, range 100-405 µm) in July, to 659 µm ± 19 µm (n=48, range 458-1004 µm) in October, with an estimated growth rate of 5.5 µm per day (Table 3, 4).

Texas Pimpleback (*Cyclonaias petrina*) - In 2019, SMARC personnel infested six Channel Catfish with Texas Pimpleback glochidia which resulted in no juvenile drop-offs (0% transformation). We attribute the absence of transformation to low glochidia viability caused by immature conglutinates, as there was a mixture of underdeveloped eggs and mature glochidia upon extraction. Future propagation efforts of Texas Pimpleback mussels will involve the collection of several gravid individuals that will be isolated among tanks. Upon the release of viable conglutinates from one individual, the rest of the individuals will be warmed to room temperature to promote the release of additional conglutinates. These efforts will aim to increase the number of glochidia available for host fish infestation and promote more fruitful propagation of juvenile mussels. In 2018, 892 juvenile drop-offs were achieved but did not survive past 4-months in captivity.

Pimpleback (*Cyclonaias pustulosa*) - In 2019, SMARC personnel inoculated two Channel Catfish with Texas Pimpleback glochidia which resulted in no juvenile drop-offs (0% transformation). We attribute the absence of transformation to low glochidia viability caused by immature conglutinates, as there was a mixture of underdeveloped eggs and mature glochidia upon extraction. Future propagation efforts of

Pimpleback mussels will involve the collection of several gravid individuals that will be isolated among tanks. Upon the release of viable conglutinates from one individual, the rest of the individuals will be warmed to room temperature to promote the release of additional conglutinates. This method will aim to increase the number of glochidia available for host fish inoculation and promote more fruitful propagation of juvenile mussels. In 2018, 116 juvenile drop-offs were recovered but did not survive past 4-months in captivity.

Texas Fawnsfoot (*Truncilla macrodon*) - SMARC did not propagate or collect any individuals during the 2019 season due the rarity of the species and the absence of a reliable source population.

False Spike (*Fusconaia mitchelli*) - SMARC did not propagate or collect any individuals during the 2019 season due the rarity of the species, absence of a reliable source population, and difficulty in acquiring appropriately sized host fish. In 2018, 1209 juvenile drop-offs were recovered but did not survive past 4-months in captivity.

Costs assessment

1. Personnel - One full time biologist (General Schedule (GS) 7/9) worked this project for the first 2-years and an Ecologist (GS-9) and Animal Caretaker (Wage Grade-5) took over during the last year. Part time assistance was required from other SMARC employees, students, interns, and volunteers throughout the project, especially during the mussel reproductive season in spring to early summer. Construction, maintenance, care, and propagation requires many hours and specialized skills. We recommend employing at least three to four full-time workers to successfully operate a mussel propagation program, as suggested by Program Supervisor Dr. Paul Johnson of the Alabama Aquatic Biodiversity Center in Montgomery, Alabama who has decades of experience with freshwater mollusk culture.

1. Infrastructure/Start-up Costs – Start-up cost for establishing a mussel propagation facility are expensive. Equipment needed for holding, culture, feeding, and monitoring are outlined below and some are specialized and costly (for example microscopes, particle counters,heater/chillers

and AHABs)

a. Establish Mussel Culture Building
    i. Plumb pond water to building
        1. Pond pumps, blower, filters, plumbing, earth moving equipment, sump, heater/chiller, biological filter
    ii. Mussel holding tanks
        1. Holding (insulated tanks, heater/chillers, biological filters, pumps, plumbing, baskets, tanks)
        2. Juvenile culture (up-weller/down-weller, beakers, flow-through etc.)
b. Multisizer 4e particle counter
c. Laboratory and field equipment (coolers, air pumps, mussel bags, ammonia analyzer, etc.)
d. Microscopes
    i. Cross-polarizing microscope with camera, field microscope, measuring software.
e. Building AHAB, fish holding, and culture equipment.
f. Establish fish health quarantine area

2. Culture Cost – Cost after establishing culture infrastructure is primarily in labor and some for maintenance of equipment (for example replacement of pumps, filters, and yearly particle counter calibration). Below is outline for basic culture costs.

a. Labor
    i. 3 - 4 Fulltime Employees
        1. Report writing, meetings, presentations
        2. Feeding mussels and fish, cleaning tanks
        3. Water quality testing: Multisizer, ammonia testing, fertilizing ponds
        4. Fish Health: diagnosing and treating ailments
        5. Fieldwork: collection, transport, boating, snorkel/SCUBA
        6. Fish pond maintenance: feeding, water quality, trap minnows as food
        7. Mussel food ponds: fertilize, water quality, pumps, blowers, plumbing
        8. Bio-security: Quarantine procedures, produce and follow HAACPs, etc.
        9. Microscope:
            a. Collecting samples and quantifying/measuring juvenile drop-offs and older juveniles.
        10. System maintenance, building
        11. Coordinating with hatcheries and obtaining host fish
        12. Acquiring and maintaining required training/certifications
b. Supplies
    i. Water filters, commercial mussel food, pond fertilizer, fish food, fish anesthesia/medications, water quality reagents, disinfectants, general lab supplies
c. Maintenance – utility fees, repair and replacement parts for culture systems, Multisizer 4e calibration
d. Travel
    i. Fieldwork, collect hatchery fish, meetings
e. Miscellaneous

DISCUSSION

The survival of juvenile mussels at the end of the study in 2019 may be attributed to the availability of pond water in the mussel building. Having two ponds available was beneficial when one pond would become overgrown with filamentous algae, or when one of the ponds required fertilization. One of the biggest challenges was continuously pumping water into the building. In the future, we will utilize larger pumps to avoid equipment failure. Additionally, we will make adjustments to the pond filtration system. Although filtering water to 5 µm reduced the number of predators in the juvenile culture systems, systems were not entirely devoid of predators. Chironomid larvae likely entered the tanks directly due to the opportunistic nature of winged invertebrates and the accessibility of the outdoor building. Though the chironomid larvae were not observed consuming juvenile mussels, the silk casings cast by chironomid larvae stuck to mussel shells thus trapping them or rendering them immobile. If this problem persists in future culture trials, Gnatrol might be used to prevent the residence of chironomid larvae following a procedure that was successful for IDNFH. The other drawback to filtering water to 5 µm is the high cost of filters which were rapidly exhausted in the summer months when algae counts were highest. To combat this issue, future efforts will include installing alternative filtration systems for adults and juvenile mussels. Alternative filtration will allow for finer filtration of pond water for young juvenile mussels susceptible to predators and coarser filtration for adult mussels that require a more diverse diet including larger algal particles. Adding a drum filter to remove larger particles will also help to improve the longevity of disposable filter cartridges.

The up-weller and down-weller systems showed some success early in the season, but the complex operation of the system made interim care on holidays and weekends more prone to issues. Future versions of this system will include more secure chambers to hold mussels in place and avoid accidental loss. Additional rearing systems will include a variety of static and turbulent systems. Static systems will include flow-through tank systems and pans, and turbulent systems will include modified up-weller and down-weller systems geared to house larger or smaller mussels.

Though the environmental chambers were useful for holding gravid mussels, the current system lacked circulation and required daily water changes. Future improvements to systems for holding gravid mussels in stasis will include a large industrial refrigerator that will be outfitted with pumps to allow for water recirculation in a temperature-controlled environment.

While AHAB systems are ideal for host fish studies that require observation of fish individually, collecting individual samples is a time- and labor-intensive endeavor. The ability to collect juvenile mussels detached from several fish at once promotes greater production for less effort. To accomplish this in the upcoming mussel season, the mussel program will incorporate circular self-siphoning tanks with a double standpipe for larger scale host fish infestations geared towards mass propagation. The flow-through AHAB in the quarantine room will be rebuilt to allow more space between tanks, and a drain for the sump will be installed to allow for recirculation, if necessary.

Using an outdoor building to house organisms in temperature-controlled tanks places a lot of strain on heater and chiller units. System failures due to thermal extremes are imminent, and future measures should be taken to relieve strain on systems and, by extension, mussels. To aid these efforts, the mussel building will be fitted for plastic panels to cover the screen windows and doors which will allow for better wind protection and insulation. Mussel tanks will be covered with similar panels to provide thermal protection, and large aquarium heaters will be added to each tank to remove some of the stress from in-line heaters during the winter months. Finally, sinks will be plumbed into the mussel building to allow for easier juvenile collection and monitoring.

TABLES AND FIGURES

Table 1. The number of live juvenile mussels produced at the SMARC between 2017 and 2019.

Species	Common Name	2017	2018	2019
Cyclonaias pustulosa (houstonensis)	(Smooth) Pimpleback	0	116	0
Cyclonaias petrina	Texas Pimpleback	0	892	0
Fusconaia mitchelli	False Spike	0	1209	0
Lampsilis bracteata	Texas Fatmucket	0	381	1975
Lampsilis hydiana	Louisiana Fatmucket	0	0	2604
Lampsilis teres	Yellow Sandshell	0	0	411
Truncilla macrodon	Texas Fawnsfoot	0	0	0

Table 2. Gravid Mussel Collection for 2019. The dates, locations, and numbers of gravid mussels collected during the 2019 season for juvenile mussel propagation.

Mussel	Num. Collected	Collected	Inoculated	Returned	Site
Lampsilis bracteata	2	6 June 2019	9 July 2019	18 July 2019	San Saba River near Menard, TX
Cyclonaias petrina	3	31 May 2019	7 June 2019	12 July 2019	Colorado River near San Saba, TX
Cyclonaias petrina	2	12 July 2019	NA	Remain on Site	Colorado River near San Saba, TX
Cyclonaias petrina	2	21 June 2019	26 June 2019	10 July 2019	Colorado River near Altair, TX
Cyclonaias pustulosa	4	21 June 2019	NA	10 July 2019	Colorado River near Altair, TX
Cyclonaias pustulosa	3	10 July 2019	16 July 2019	7 August 2019	Colorado River near Altair, TX
Lampsilis hydiana	5	15 May 2019	24 May 2019	Remain on Site	Guadalupe River near New Braunfels, TX

Table 3. Propagated juvenile Texas Fatmucket survival and growth that were recorded during monthly assessments in each system, and the shell lengths of a subset of mussels rounded to the nearest micrometer. NA refers to not applicable.

	Beakers		**Upweller/Downweller**	
2019	**Num. Juveniles**	**Shell length (µm)**	**Num. Juveniles**	**Shell length (µm)**
August	2	498 (n=1)	NA	NA
September	339	468 ± 11 SE (n=37)	0/0	NA
October	61	659 ± 19 SE (n=67)	NA	NA

Table 4. Growth Rate and Survival of Juveniles in 2019. Shell length, growth rate, survival, and the total number of juvenile mussels produced in 2019 for two species of *Lampsilis* mussel held in the pulse-flow beaker system.

Species	System	Max length observed (µm)	Max growth (µm/day)	Percent Survival	Total No. Produced
Texas Fatmucket	Beaker	1004	5.5	3.1	1975
Louisiana Fatmucket	Beaker	2844	26.3	0.5	2604

Figure 1. A SMARC ⅒ acre pond available dedicated to mussel nutrition at the SMARC. Photo Credit: USFWS

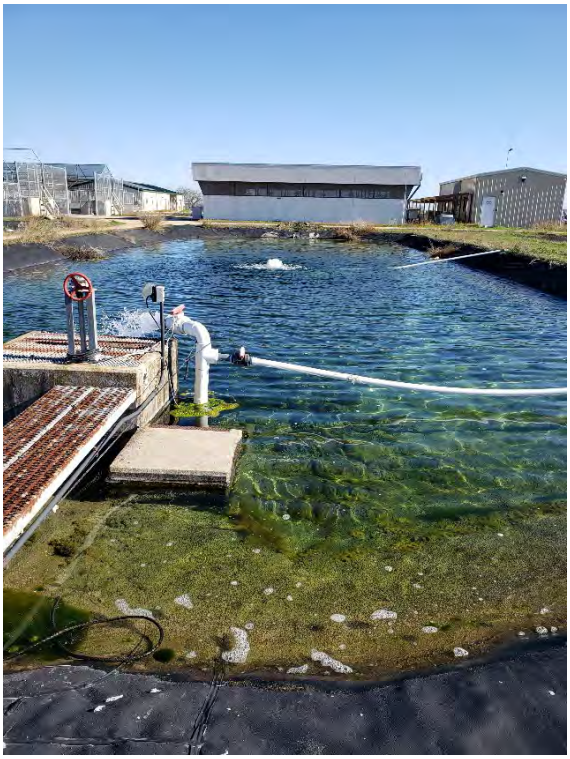

Figure 2. Beckman Coulter Multisizer 4e used to assess the quantity and type of algal cells present in mussel systems and ponds. Photo Credit: USFWS

Figure 3. SMARC pond water pumped into the mussel building shown in a circular sump on the back wall alongside two sets of filters, one with coarser filtration for adult mussels and one with finer filtration for juvenile mussels. Photo Credit: USFWS

Figure 4. Recirculating (AHAB) flow-through system for holding inoculated fish. Photo Credit: USFWS

Figure 5. The SMARC's up-welling and down-welling juvenile system (a) allowed for one down-weller (b, left) and one up-weller (b, right) per valve and implemented 150 µm mesh surrounding the mussels in each chamber. Photo Credit: USFWS

a)  b) 

Figure 6. The SMARC's pulse-flow beaker system included space for up to twenty 400 ml beakers to hold juvenile mussels. Photo Credit: USFWS

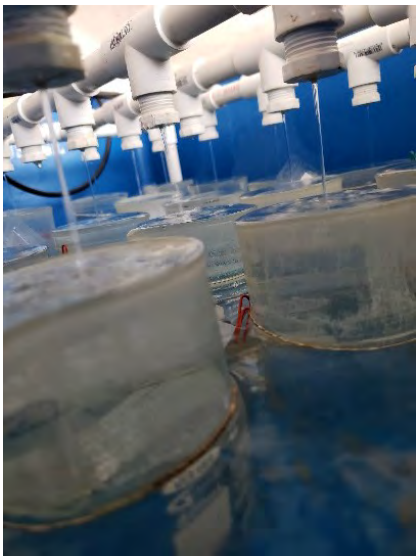

UVALDE NATIONAL FISH HATCHERY

Contributing Authors: Valentine Cantu and Patricia Duncan

INTRODUCTION

The UNFH is located in Southwest Texas between San Antonio and the Rio Grande. The facility is located on 100 acres of land with 50 ponds for fish and algal culture. There are a variety of potential fish hosts readily available both on station (i.e. station cultured channel catfish and minnows) and at the station's effluent drainage canal (i.e. a variety of sunfish, bass, minnows, and a native cichlid) that can readily be used for mussel propagation studies. The facility uses fresh well water (Temperature range = 21 to 25 ̊C) from the Austin Chalk formation (Spurgeon Well) and Edwards Aquifer (Wilson Well), pumped from one of two wells at a time. The extra well serves as a backup, during maintenance periods or should one fail. Both wells share a backup generator. The Quarantine Building (QB) and Refugia Building (RB) are equipped with separate emergency backup generators to protect against power outages. Each building is furnished with regenerative blowers to supply air to captive species and adjustable tmers to help maintain natural circadian rhythms. Magnetic booster pumps (Iwaki America In) are used in the QB to ensure that there is sufficient well water pressure available to tank systems.

Description of Systems and Culture Protocols

The mussel propagation project supported by Texas State University began in 2017, with the purchase of equipment and supplies, and construction of facilities.

Equipment

A Beckman Coulter Counter was purchased to provide accurate determination of algal and other feed items. An Olympus BX43 Phase Contrast Upright Custom Microscope System, which uses unique software (Cellsens), was purchased to measure larval stages of mussels. A complete recirculating Z-habitat system (Tecniplast) was purchased and installed in the QB to provide experimental space for fish hosts. A flow-through holding tank system or Quarantine Aquatic Mussel Habitat (QAMHAB) with four

aerated 20 gallon aquaria was custom designed in the Quarantine Building (QB) to hold mussels for prolonged periods. An algae feeder driven by a 50 GPD peristaltic pump (Stenner) was built onto the system to deliver a continuous drip of algae to feed mussels. All systems in the QB were designed to flow into a sand-filtered chlorinated system (SFCS; Figure 1) to prevent the spread of aquatic nuisance species (ANS; e.g. zebra mussels, Asian clams, red-rimmed melania snails), potentially introduced with mussel and fish hosts. The filtered, chlorinated effluent water first flows into an aerated retention tank and then flows onto an isolated leach field to evaporate as an additional precaution against escapement.

Construction

In 2018, construction and renovation of indoor tank systems continued at the facility's QB and RB. A chiller was added onto the Tecniplast Z-habitat system or AHAB1 (Figure 2). The QAMHAB in the QB (Figure 3) was renovated with a recirculating system and biological filter. A magnetic sump pump (Danner Manufacturing, Inc.) was used to recirculate water throughout the system. A fiberglass rack system was built to increase tank space to hold both mussels and fish hosts together for prolonged periods. The system was designed to hold infected fish hosts and to collect juveniles in 100 µm mesh bags after exposure to a glochidia bath or, alternatively, to allow "natural" infection of fish hosts by placing mussels with the fish, should mussels not release viable conglutinates or glochidia soon after being brought into captivity. Collection screens (100 µm) were used to monitor the "natural" release of glochidia from mussels. To reduce potential mussel stress and increase survival, tank systems were equipped with 2 KW inline water heaters (Aqua Logic Inc.) and independent 300 W aquarium heaters (Sunlight Supply Inc.). These helped warm well water to temperatures measured at their collection sites. Probiotic bacterial media (the Water Cleanser, Marine Easy Clean Australia) was added in individual units and in the sump as a substrate for bacterial growth. The water from each aquaria flowed through a 100 µm mesh collection screen so that glochidia could be regularly monitored and removed for infestation trials.

Mucket Buckets were constructed as designed by Barnhart (2005) to prepare for juvenile mussel

feed trials. The systems were designed with a small pump to recirculate water through isolated chambers made of PVC and 125 µm nylon mesh screens which held the juvenile mussels (Figure 4).

A mussel recirculating system or Refugia Aquatic Mussel Habitat (RAMHAB) was also constructed with a biological filter and lighting (12 hour day: 12 hour night timer) in the RB to hold non-gravid mussels collected in 2017 (Figure 5).

A recirculating Up-welling Juvenile Growth System (UJGS; Figure 12) was designed to replace the Mucket Buckets (Figure 4). Unlike the Mucket Buckets, the UJGS system was designed to eliminate biological waste, by modifying the system into a partial flow-through and recirculation system that would improve water quality and allow for continuous removal of wastes while feeding continuously. The UJGS allowed worms and debris to potentially pass out of the 155 µm screen of the juvenile chambers, while retaining juvenile mussels.

In 2019, construction and renovation of indoor mussel tank systems continued. An algal feeding system was added onto to the RAMHAB (Figure 5) for semi-continuous feeding of concentrated pond cultured algae. As part of the conditioning of mussels, after they were placed into the QAMHAB, the algal feeding system was utilized with the peristaltic pump supplying 1L/hour of live algae at 30 X 10^6 cells/ml to aquaria with gravid mussels. Further conditioning of the mussels was provided with gradual elevation of temperature and moderation of well water and recirculated water flows.

In 2019, a Static Juvenile Growth System (SJGS; Figure 11) was constructed to improve on the previous systems used in 2018. A static system similar to the Hruska Box (Hruska 1992). In a static container, it appeared easier to make sure that adequate amounts of food were available and that delicate early stages were not jostled by strong currents from air or flow. The SJGS utilized 500 ml polypropylene holding beakers set on a freestanding bulk storage rack.

To prepare for large scale production of freshwater mussel drop-offs, three 120 gallon rectangular flow- through tank systems or Big Blue Habitats (BBHAB1, 2, and 3) with similar plumbing (including double stand-pipe) and nylon screen collection features as the Recirculating Propagation System or RPS

(Barnhart, 2003) were constructed (Figure 9). A complete recirculating Zebrafish AHAB system (AHAB2, Aquaengineering, Figure 10**)** was purchased and installed in the QB to provide additional housing and experimental space for mussel propagation.

Collection

In August 2017, the first group of mussels were collected from the Lower Colorado River, Columbus, Texas with assistance from BIO-WEST Incorporated (BIO-WEST; Table 1). Pimpleback (*C. pustulosa*), Texas pimpleback (*C. petrina*) and Texas fawnsfoot (*T. macrodon*) were brought to the station's quarantine building to study basic culture techniques including nutritional and environmental requirements (i.e. water quality, flow, and sediment) necessary to provide optimum conditions for care of each mussel species.

In 2018, UNFH collaborated and coordinated efforts with SMARC, IDNFH, and BIO-WEST to collect gravid females from the lower and middle sections of the Colorado River (See Table 2). Pimpleback (*C. pustulosa*) and Texas Pimpleback (*C. petrina*) were collected and brought to the station's QB to for infestation of fish hosts.

In 2019, staff members from IDNFH coordinated collection efforts with UNFH to collect gravid females. Mussels were collected from the middle and lower sections of the Colorado River and the San Saba River for infestation trials (Table 3). Texas fatmucket (*L. bracteata*), pimpleback (*C. pustulosa*), and Texas pimpleback (*C. petrina*) were collected and brought to the station's QB for fish hosts and juvenile feed growth trials.

In 2018 and 2019, mussels were transported back to the QB in coolers with mussels placed in source water with soft filter material surrounding them to prevent excessive motion, in plastic bags. Air bubblers were used to produce gentle aeration which was kept near the top of the water level. Coolers were not closed completely, leaving a gap for air circulation. In the QB mussels were slowly acclimated to the water temperature in the aquaria by gradual addition of aquaria water into a bag holding the mussels until acclimation to the system water temperature was achieved. Prior to mussels coming on

station, temperatures of the holding systems were adjusted to approximate the temperature of the collection.

Feeding

Wild stock mussels were held in the QAMHAB and batch fed 9 ml of an equal concentration mix of Shellfish diet 1800 (Reed Mariculture Inc. USA) and Nano 3600 (Reed Mariculture Inc. USA) three times daily. To maintain optimum water quality and remove wastes, staff siphoned weekly, adjusted air flows, maintained air stones in holding containers, and adjusted well-water flows.

Supplemental Feeding

Supplemental feeding of live algal cultures of *Nannochloropsis* sp., *Nannochloris* sp. and *Chlorella* sp. were provided to gravid mussels once daily during the conditioning period. The pure strains of algae were cultured from microalgae disks (Florida Aquafarms) following the vendor's instructions. Conditioning of the mussels with the manipulation of temperatures, water flows, and varied feeding regimes on this system were used as a means to attempt to trigger the release of glochidia. Conditioning regimes have been regularly used in the propagation of various bivalve species in hatcheries to stimulate spawning activity and larval production (Walne 1980, Castagna and Krauter 1981). Mussel species in the RB were fed 9 ml of an equal concentrated mix of Shellfish diet 1800 and Nano 3600 three times daily and batch- fed live *Nannochloris* sp., *Chlorella* sp., and *Nannochloropsis* sp. weekly.

Live algal culture systems were initiated in response to the difficulty of obtaining commercially available microalgae during the government shutdown, which occurred from December 26 to January 28. Pure cultures of live *Nannochloris* sp., *Nanochloropsis* sp. and *Chlorella* sp. were initially started indoors in sterile 4.5 oz. specimen cups (VWR Scientific) and later transferred into disinfected 5 gallon buckets (Figure 6), which were located in the QB under a bank of grow lights with suitable wavelengths for the growth of the target algal species. At the same time, algal cultures containing a variety of pond algal species were started outdoors in 20 gallon containers (Figure 7, Rubbermaid Feed and Seed) using a modified version of the Wells-Glancy method (Wells 1927). Seed algal cultures were obtained by

selecting 5 gallons of water from a Channel Catfish pond, during a good algal bloom, and filtering it through a 10 µm filter bag. This filtered water was added to a clean, disinfected, dry 20-gallontranslucent container, filled with well water, and the suggested amount of fertilizer (Pro line algae food part A and B, Pentair Aquatic Ecosystem) was added following manufacturer guidelines. The containers with the algal blooms were covered by a 150 µm nylon mesh and were placed in a partially sheltered area with good exposure to the sun. Depending on freshwater mussel size, cultured outdoor algae was sieved through a 10 µm or 5 µm, 32" x 7" felt mesh bag with a poly ring mouth (Pentair Aquatic Ecosystem). Both motile and non-motile algae (microflagellates, diatoms and green algal species) were produced from outdoor cultures seeded from catfish ponds (Figure 8). The live algae was intended to increase the overall nutritional value of the mussel food supply.

Production

For all trials, mussels were maintained on station. When conglutinates were released by mussels, either on the way to the culture facility, or weeks later during the extended trials, water volume in aquaria with fish hosts was reduced to about four liters. Conglutinates were mechanically separated with a turkey baster. Light aeration was added to help mix the bath solution for infestation, reduce stress in fish hosts and allow exposure of hosts to a concentrated solution of glochidia for 30 minutes in a small volume of water.

In 2018, glochidia were estimated by moving collection mesh bags (Midwest Filter, LLC) into a 1 L plastic beaker, and filling the sample with well water up to 1 L. While mixing the sample with a turkey baster, three samples were transferred with a 3 ml disposable pipette into a circular acrylic zooplankton counting wheel (Wildlife Supply Company), and then counted under a dissection microscope to determine the number of glochidia per liter (Patterson et al. 2018).

In 2019, mussels were monitored for release of glochidia in concentrations sufficient to conduct infestation trials with host fish. For the Texas fatmucket, a variety of fish hosts were utilized in an effort to obtain increased numbers of juveniles for later feeding trials. After infestation periods of at least 30

minutes with glochidia in a lightly aerated 5 gallon bucket, fish were removed, separated by species and put into the ZHAB aquaria, which were fitted with 120 µm filter bag to catch any drop offs. To reduce handling stress, recent drop-offs (juveniles) were left in the 120 µm mesh bag for 1 week before pouring them through sieves to quantify them. The bags were monitored weekly to collect any drop-offs that could then be moved into the SJGS for the first stage of growth.

For infestation trials with the Texas Pimpleback and the Pimpleback, groups of channel catfish were infested with glochidia in a 5 gallon bucket for 30 minutes and then fish were transferred into the 120 gallon tank fitted with a 120 µm screen for later removal of drop offs and placement into the SJGS for initial rearing..

Mussel drop-offs were placed in the SJGS for the rearing period. Mussels were initially placed in each container with well water and 100 ml of 5-µm filtered algal bloom water at the same temperature of the water from where the drop-offs had been collected. The water was changed in each container three times per week. Representative samples of mussels from each collection date were removed daily and monitored for behavior and feeding. Mussel populations in the individual SJGS containers were periodically spread from one into two containers to provide more space as required. Water changes were provided three times a week with replacement of a mixture of well water and 5-µm filtered algal bloom water.

In 2018, staff tested a variety of readily available fish hosts for pimpleback (*C. pustulosa*) and Texas pimpleback (*C. petrina*) infestation in glochidia baths (Table 2) including Channel Catfish (CC), Green Sunfish (GSF), Bluegill (BG), Warmouth (WM), and Rio Grande Cichlids (RGC).

RESULTS

In 2018, most conglutinates and fragments (8 of 11; 73%) were released within the first 48 hours; while three of 11 (27 %) were released after 48 hours. On one occasion, a pimpleback mussel released

two viable conglutinate fragments two weeks after being brought into captivity. Pimpleback mussels continued to release viable glochidia (5% to 95% viable) up to 33 days after mussels were collected (Table 2). Although up to 30 conglutinate fragments were released from mussels and the glochidia viability reached as high as 95% (Table 2) in 2018, infestation was low, resulting in low juvenile drop-off rates and insufficient juveniles. On one occasion of eleven conglutinate release events, glochidia numbers and viability from conglutinates were high enough to result in a low juvenile drop off rate (Juveniles = 15; Table 2) two weeks after being brought into captivity. This pimpleback mussel collected on May 31, released two conglutinate fragments (total glochidia = 1,111 to 1,667, total glochidia in 4 liter dilution bath = 278 to 417 glochidia per liter, 95% viability) on June 14, resulting in 15 viable juvenile drop-offs from channel catfish. A summarized table of the total juvenile drop-offs can be found on Table 4.

In the 2018 trials, juveniles with debris were transferred into the Mucket Bucket recirculating system (Figure 4) and checked weekly; however, none of the juveniles survived more than a week. Gravid females collected from Lampasas (middle Colorado River) appeared to provide mature conglutinates with visible bivalve shell, but most perished during transported from SMARC to the UNFH. Although no juvenile drop-offs were obtained after infestation baths from this reach of the river, post- mortem examination of the gills of several species of fish host showed encapsulation of glochidia. A summarized table of the total infestation rates can be found on Table 5.

Texas Fatmucket (*Lampsilis bracteata*)— In 2019, two Texas fatmucket mussels were collected by UNFH staff from the wild and brought into captivity for infestation trials (Table 3). Staff tested a variety of readily available fish hosts on station to glochidia infestation baths including Green Sunfish (GSF), Bluegill (BG), Rio Grande Cichlids (RGC), Warmouth (WM), Sailfin Mollies, and Mexican Tetras (MT; Table 3). UNFH staff infested 34 GSF, 22 RGC, 19 BG, 4 WM, 4 MSM and 3 MT with Texas fatmucket glochidia which resulted in 2,793 juvenile drop-offs. On one occasion, a Texas fatmucket released glochidia (84.6% viable) 18 days after being brought into captivity.

Although this was the lowest total number of juveniles of any species produced at the UNFH, this

was the first year we produced Texas pimpleback juveniles. Of the six fish host species infested with Texas pimpleback mussels, GSF resulted in the highest drop-off rate of 2,051 (62 juveniles/fish) while RGC and BG resulted in the second and third highest drop-off rates of 576 (36 juveniles/fish) and 158 (36 juveniles/fish) respectively (Figure 13 and 14). Two different species mortalities were found with capsulated glochidia (Table 3). We suspect that most mortalities occurred due to antagonistic interactions with other fish held in the same container. GSF had the highest mean gill intensity of capsules (269.1± 367.8 SD, N=7, Total = 1,884, Range = 4 – 916). BG had the next highest mean gill intensity of capsules (72.0 ± 73.51 SD, N =3, Total = 216, Range 4 – 150).

Texas fatmucket juveniles were doing well initially, but unsuccessful quarantine procedures for host fish caught from the station effluent canal, led to contamination of parasitic worms, which killed all Texas fatmucket juveniles. When CC, which were propagated and held in ponds on the station were used as hosts, we observed a lower concentration of worms compared to the concentration in the fish species from the effluent canal. Unfortunately, the young mussels were especially vulnerable to the worms at the early stage of development. Texas fatmucket juvenile drop-offs reached a mean size of 270.7± 8.3 µm in the UJGS, surviving only about 4 weeks in the system. As other species of mussel juveniles grew to around 500-600 µm. Although no Texas fatmucket juvenile mussels survived to reach 1 mm, the drop offs lived long enough to show good juvenile development before succumbing to parasites.

Pimpleback (*Cyclonaias pustulosa*)— In 2019, UNFH staff collected eight pimpleback mussels and infested 35 CC with glochidia, resulting in a drop-off of 157,744 juveniles, the highest number of juveniles produced for any mussel species for the past two years at UNFH (Table 4). We attributed this higher juvenile transformation from gill larvae in fish hosts to mussel juveniles partly to the improved system designs used in 2019 compared to 2018 (Total pimpleback mussels = 60). CC mortalities infested with pimpleback glochidia had a mean gill intensity of 314.1 capsules ± 362.1 SD, N=17, Total = 5,339, Range = 12 – 11,400. Average juvenile drop-offs reached a size of 530.3 ± 40.3 µm in the UJGS, surviving 6 weeks in the system. High numbers of juvenile pimplebacks were collected and sustained in culture until mid-August. There were problems with worm contamination, but many of the mussels had

grown large enough to close their shell when worms approached. There may have been cross-contamination of worms from containers with Texas fatmucket juveniles, since few worms were seen with the CC. However, smaller mussels (< 500 µm) exposed to worms perished despite efforts to remove the worms.

A sudden die off of the surviving mussels occurred in 2019 and was attributed to a sudden decrease in room temperature (by 7 °C) after two aquatic heater/chiller units were turned off. Because of the relatively small volume of the containers holding the juveniles, the temperature drop would have occurred rapidly and remained cool. No pimpleback mussels survived to reach 1 mm.

Texas Pimpleback (*Cyclonaias petrina*)— In 2019, eight Texas pimpleback mussels were collected by UNFH staff from the wild and used for infection trials (Table 3). Of the six species tested, four fish species were found to be infested with capsulated glochidia. A CC had the highest gill infestation of 1,008 capsules per fish. This CC jumped out of its experimental container and died. A WM was infested with 186 capsules per fish, and a GS with six capsules per fish. The GS also died, likely due to competitive interactions from other fish held in the same container. A total of 23 CC were infested with Texas pimpleback glochidia, which resulted in 32,077 juvenile drop-offs (Table 4). In 2018, only 30 juveniles developed from CC gill larvae. Ten of 13 conglutinate release events or 77% (Table 3) were released later than expected for most short-term brooders. On one occasion, a Texas pimpleback mussel released 50 partially viable conglutinate fragments (41.7 % viable) 33 days after being brought into captivity, which is about 4 weeks longer (27 days) than last year's longest release time of six days of conglutinate (5% viability) by this species. Viable conglutinates were released two weeks longer than in 2018, 33 versus 14 days later, while viable glochidia (100% viable) were released up to 14 days later (Table 3). CC mortalities infested with Texas pimpleback glochidia had a slightly higher mean gill intensity of 3,666.3 capsules ± 349.6 SD, N=3, Total = 1.099, range = 6 - 704. Juvenile Texas pimpleback mussels reached a size of 600 µm in the UJGS surviving 5 weeks in the system before the low temperature event (described above) appeared to cause the sudden mortality of all juveniles.

We were unable to produce juvenile mussels (>1 mm) for controlled feeding studies. Thus, these studies were not accomplished.

Lessons Learned

In 2017, basic systems and methods were developed for care and maintenance of pimpleback and Texas pimpleback mussels in captivity. We did not produce any mussels in 2017. By 2018, systems and methods were refined to afford the improved performance of the combination flow-through and recirculation system for better care of mussels in the QB.

Alga cultures were rotated so that harvest occurred with each batch within 48 hours of starting a new culture in the container. Cultures were eliminated, and new cultures started, when there were signs of any contamination. While the initial, temporary, set up of single cell culture in the QB in buckets was successful for a short time, it became contaminated and was discarded after two months. The management of pond blooms based on a modified Wells-Glancy method proved to be more successful and more easily managed with desirable species; and the cultures were longer lasting. The mussels demonstrated a positive feeding response to species in the algal blooms and the single cell species offered as food. An immediate active feeding response was repeatedly observed by UNFH staff when mussels were fed the live algal species or species from the algal blooms. UNFH staff noted a delayed feeding response when commercial algal feeds were presented to the mussels. When only commercial algal feeds were offered, and the systems were operated with both recirculating and flowing water with the bacterial probiotic media, the delay of the active feeding response was extended.

In the 2018 trials, we found the Mucket Bucket recirculating system contained high numbers of predacious round and flatworms, a possible major factor leading to juvenile mortality.

It is too early to assess the reliability and advantages of the new UJGS design, since 100% of the cultured juvenile mussels died before reaching the size to place them into the system.

Recommendations

For the construction and operation of a freshwater mussel propagation facility that propagates and conducts research on two or three species of mussels, we recommend at least two full-time (GS-9, GS-7, or GS-5) trained personnel (or one full-time and two part time personnel) for the construction and setup of mussel systems, collection and acclimation of mussels, conducting trials, enumerating larvae and juveniles under microscopes, mussel care (e.g. daily monitoring and maintenance, feeding, and cleaning of systems, and water quality). For proposal writing, planning, and reporting, two employees (GS-11, GS-12, or GS-13) working part-time on the project are recommended.

To prevent the spread of ANS into our local watershed, we used a SFCS (Figure 1) that flows onto an isolated leach field to evaporate and includes the holding containers, ceramic air stones, mesh screen, sand, sump pump, plumbing, and chlorine tablets. We recommend using biosecurity measures that help prevent the spread of ANS.

For the detection and collection of conglutinates, glochidia, and juveniles from wild-caught freshwater female mussels and fish hosts, we preferred using the QAMHAB system (Figure 3) over the factory designed AHAB system (Figure 2). Of the two recirculating systems, the QAMHAB system proved to be more reliable than the AHAB system for long-term infestation trials. During 2018 and 2019 trials, the AHAB system failed three times, each resulting in fish host and juvenile mortalities. Unlike the AHAB system, the QAMHAB system was designed with well water inputs and aeration into each individual holding container. The QAMHAB system was designed with backup systems to keep aquatic species alive should any two of the recirculation, well water, or aeration systems fail. The QAMHAB system also had larger holding containers (20-gallon aquaria) that can be used to hold larger fish hosts with mussels together over extended periods to allow for the “natural” release of conglutinates or glochidia. Due to the difficulty of visually finding pronounced inflated or discolored gills in Texas pimpleback and pimpleback females in the field, it was not uncommon to collect and bring in females

with premature fertilized ovaries into captivity. In comparison with the AHAB system, the QAMHAB's nylon filters were more accessible and easier to replace and required much less maintenance. Another advantage is that the QAMHAB system cost about a quarter of cost for the AHAB system used in the trial.

For the mass production of targeted juvenile species, we preferred using the BBHAB system (Figure 10) over the QAMHAB and AHAB systems. Unlike the other systems, this system is designed with a 120- gallon holding container to provide more room for infected fish hosts in a single container. The well water flow in conjunction with aeration and the swimming action of fish hosts helped move juveniles drop-offs through a double stand-pipe and into a single nylon collection bag. We used up to 19 infested CC hosts (TL = 27 cm) resulting in more drop offs (Total = 156,830 juveniles) than any other system designed thus far (Table 2 and Table 3). No antagonistic behaviors were observed among the catfish. On two or three occasions, 100% of the fish hosts survived after the pump to the well water supply failed, presumably due to the continued aeration. The BBHAB system costs was much less than the AHAB system and the QAMHAB system.

Despite the previous record of the AHAB system's unreliability, high maintenance, and higher cost, advantages included having more holding containers (N = 70) than other systems used; which was ideal for infesting multiple fish hosts simultaneously. The system is suitable for short-term replicated infection trials that might include finding suitable fish hosts for target mussel species. The system might be more reliable by adding a cartridge filter system with freshwater well water inputs and aeration into each container and adding a drain to help remove wastes.

Costs

The total estimated upfront cost to conduct this project the first year, included staff training, labor, tank system renovation, equipment, and supplies. These estimates include costs of pre-existing fiberglass tank systems and renovation of tank systems, renovation of building space, and renovation of infrastructure, but did not include costs of existing infrastructure, buildings, ponds, vehicles and fuel used

for collections, utilities, assistance from maintenance personnel and volunteers, and fish hosts readily available on station for trials. Annual re-occurring costs after the first year included continued staff labor, consumable laboratory and field supplies, live algae food, and commercially available algae. Training costs were completely covered by the UNFH which included sending a staff member to a "Freshwater Mussel Propagation and Restoration" course, freshwater mussel books, USFWS Non-motorized Boat Training, USFWS Motor Boat Training, Snorkel Training, and CPR and First Aid training. Labor costs included costs for GS-5 to GS-12 staff to assist with the project.

DISCUSSION

Progress was made at UNFH in collecting, identifying gravid mussels, and creating different systems to successfully care for adult and juvenile mussels. In 2019, a great deal of improvements were made in demonstrating and refining protocols for the infestation of host fish with three different species of mussels.

Host species for the *L. bracteata* were demonstrated to provide juveniles. Preliminary results demonstrated that the Rio Grande Cichlid has potential as a host and we have this fish readily available in the effluent canal at the hatchery. These fish also remained in good condition as a host fish which is a characteristic necessary to allow the time needed for drop-offs to fully develop. Future trials should be conducted with the Rio Grande Cichlid because of its favorable characteristics as a host fish and availability. Although we were able to get *L. bracteata* juveniles from different host species, they were lost due to contamination with worms. Further protocols must be developed to prevent contamination with worms and other predators of young juvenile mussels. There was little contamination with worms when station propagated and cultured Channel Catfish were used as host fish. Methods developed with the propagation of *C. petrina* in 2019, demonstrated that our protocols had greatly reduced worm infestation with this mussel, however, improvements are still needed. It might take capture and treatment of host fish for longer periods to remove parasites in the future.

There is also the potential contamination of well water that travels through an extensive pipe system before it reaches the QB. In the last trial with the *C. petrina*, when well water was filtered through a 1 µm bag filter, no worms were observed. In future trials, well water should be filtered for the culture systems of the earliest stages of juvenile mussels. Also, efforts to close the areas where the juvenile mussels are grown should also be employed to reduce the chances of contamination. In particular, closing areas for culture should reduce the incidence of potential airborne fungal spores that proved to be another problem which affected mussel survival.

Progress was made in developing conditioning protocols for the three species of mussels tested that served to prolong the time period for infestation of hosts. With each mussel species, and the use of different conditioning regimes, viable glochidia that were capable of providing infestations were available weeks after the mussels were collected. Creating opportunities for infestation over time might provide increased numbers of juvenile mussels. Further work is needed, however, to refine and determine reliable conditioning protocols for each species.

In future mussel work, temperature control of the environment surrounding the juvenile mussels should be a priority. The early stages of mussels should be placed in a temperature-controlled environment where great swings in temperature will not occur. The QB where mussels were located during the past two growing seasons, was kept at cooler temperatures due to the necessary requirements of other species on station sharing the same area. With the ubiquitous nature of airborne fungal spores, we suspect that the cooler temperatures possibly enhanced fungal growth (Post 1987, Tucker and Robinson 1990). In the future, environmental temperatures should be set at temperatures close to those juveniles would experience during development. In warmer temperatures, faster development can occur, which may increase survivability. In future growth trials, the earliest stages of drop-offs mussels should be placed in a large incubator, which will provide temperature control and provide an enclosed area to lessen contamination from other sources, whether fungal spores or worms.

It was unfortunate that we did not have survival of juvenile mussels necessary to conduct controlled

feeding studies at UNFH to date. We were able to demonstrate good growth and survivability of three species of juvenile mussels when fed a combination of cultured algae and 5-µm filtered algal blooms, when there were no predators in culture units and when temperatures were stable. Future work is necessary to determine optimum combinations and feeding regimes of different algal species and feeds for improved growth and survival of different sizes of mussels.

Table 1. FY 2017 collection dates, number of mussels collected / species, collection location, field temperature, aquarium temperature, days in trial, total conglutinates and fragments, total glochidia, percent viability, number of fish host species, number of juveniles / fish species, length of juveniles, number of capsules / fish species mortality. QAMHAB = Aquarium Mussel Habitat. P = Pimpleback, TPB = Texas Pimpleback, TFF = Texas Fawnsfoot. LCR = Lower Colorado River, Col = Columbus, TX.

Collection Date	Number of Mussel collected / Species	Collection Location	Field Temp. (˚C)	Aquarium Temp. (˚C)	Days in Trial	Total Conglutinates and Fragments	Total Glochidia	Percent Viability	Number of Fish Host Species	Number of Juveniles / Fish Species	Length of Juveniles (µm ± SD)	Width of Juveniles (µm ± SD)	Number of Capsules / Fish Species Mortality	Size TL (mm)
3-Aug-17	30 P (QAMHAB)	LCR (Col)	31.4	24.3	–	–	–	–	–	–	–	–	–	–
3-Aug-17	15 TPB (QAMHAB)	LCR (Col)	31.4	24.3	–	–	–	–	–	–	–	–	–	–
3-Aug-17	2 TFF (QAMHAB)	LCR (Col)	31.4	24.3	–	–	–	–	–	–	–	–	–	–

Table 2. FY 2018 collection dates, number of mussels collected / species, collection location, field temperature, aquarium temperature, days in trial, total conglutinates and fragments, total glochidia, percent viability, number of fish host species, number of juveniles / fish species, length of juveniles, number of capsules / fish species mortality. P = Pimpleback, TPB = Texas Pimpleback, TFM = Texas Fatmucket. QAMHAB = Quarantine Aquarium Mussel Habitat, AHAB = Aquatic Habitat. LCR = Lower Colorado River, MCR = Middle Colorado River, ALT = Altiar, LAMP = Lampasas, CC = Channel Catfish, BG = Bluegill, GSF = Green Sunfish, RGC = Rio Grande Cichlid, WM = warmouth.

Collection Date	Number of Mussel collected / Species	Collection Location	Field Temp. (˚C)	Aquarium Temp. (˚C)	Days in Trial	Total Conglutinates and Fragments	Total Glochidia	Percent Viability	Number of Fish Host Species	Number of Juveniles / Fish Species	Length of Juveniles (µm ± SD)	Width of Juveniles (µm ± SD)	Number of Capsules / Fish Species Mortality	Size TL (mm)
30-Apr-18	3 P (QAMHAB)	LCR[a] (ALT)	–[b]	20.1	–	0	0	–	–	–	–	–	–	–
7-May-18	1 TPB (AHAB)	MCR[a] (LAMP)	b	22.4, 22.4, 21.8, 25.2	2, 13, 14, 35	30, 0, 0, 0	2,778 – 3,333, 0, 0, 0	95, - - -	, 5 GSF, 3 BG	0	–	–	6 / GSF, 0 / BG	89.1, 77.7
	1 TPB	MCR[a]	b	22.4,	0,	0,	0,	-					0 / GSF,	61.9,
7-May-18	(QAMHAB)	(LAMP)	–	22.4	2	3,	111 – 556	0	2 GSF	0	–	–	0 / GSF	84.8
	2 TPB	MCR[a]	b	22.4,	0,	0,	0,	-,						
7-May-18	(AHAB1)	(LAMP)	–	22.4, 22.6	2, 21	30 0	2,778 – 3,333, 0	95, -	1 CC	0	–	–	1008 / CC	270
18-May-18	1 TPB (QAMHAB	MCR[a]	b –	22.4	0	30	2,778 – 3,333	0	, 2 GSF,	0	–	–	, 0/ GSF, 0 / GSF,	76.9, 54.4,
	)	(LAMP)							2 BG,				0 / BG, 0 / BG,	57.6, 93.8
31-May-18	2 P (AHAB1)		30.6	22.4, 26.3, 24.3, 25.5	0, 33, 40, 62	0, 0, 0, 0	0, 2,778 – 3,333, 2,778 – 3,333 0	-, 95, 0 -	1 CC	30 / CC,	256.6 ± 12.7	206.0 ± 15.2	–	–
	1 P	LCR		22.4,	0,	0,	0,	-,						
31-May-18	(AHAB1)	(ALT)	30.6	25.2 25.5	1, 36	0, 0,	1,111 – 1,667 0	95 -	1 CC	15 / CC	256.6 ± 12.7	206.0 ± 15.2	–	–
31-May-18	1 P (AHAB1)	12-	Jun-18	22.4, 2 TPB (AHAB)	0, AHAB) LCR (ALT	3,)	2,778 to 3,333, LCR (ALT)	0, 30.6	25.4,					

14,	2,	95,	1 CC						15 / CC	256.6 ± 12.7	206.0 ± 15.2	_	_	
	1,111 – 1,667,		1 CC, 26.3 1 WM, 25.2 1 BG, 24.3 1 BG	30, 33	0, 0	0, 111 - 556	-, 5		0	_	_	0 / BG, 0 / BG, 186 / WM	61.9, 55.9, 124.3	
		30.3		0, 3. 4	0, 0	1,111 – 1,667 0	95 -, -							

[a] Mussels collected by IDNF and SMARC and later picked up by UNFH.

[b] Temperatures collected by IDNF and SMARC

Table 2. *(cont.)*

Collection Date	Number of Mussel collected / Species	Collection Location	Field Temp. (°C)	Aquarium Temp. (°C)	Days in Trial	Total Conglutinates and Fragments	Total Viable Glochidia	Percent Viability	Number of Fish Host Species	Number of Juveniles / Fish Species	Length of Juveniles (µm ± SD)	Width of Juveniles (µm ± SD)	Number of Capsules / Fish Species Mortality	Size TL (mm)
12-Jun-18	1 TPB (AHAB1)	LCR (ALT)	30.3	25.2, 26.2	0, 20	0, 0	1,111 – 1,667, 0	95, -	1 CC	30 / CC	256.6 ± 12.7	206.0 ± 15.2	–	–
12-Jun-18	1 P (QAMHAB)	LCR (ALT)	30.3	25.2, 25.4	0, 2	0, 0	0, 111 - 556	-, 0	1 BG	0	–	–	0 / BG	69.1
28-Jun-18	2 P (QAMHAB)	LCR (ALT)	32.5	25.2 26.3	0, 5	0’ 0	0, 111 - 556	-, 0	5 BG, 1 RGC	0	–	–	0 / BG, 0 / BG 0 / BG 0 / BG 0 / BG, 0 / RGC	71.9, 53.5, 65.9, 57.9, 59.5, 80.9
28-Jun-18	2 TPB (AHAB1)	LCR (ALT)	32.5	25.2 26.3	0, 5	0, 0	0, 3	-, 5	1 CC, 1 GSF	0	–	–	0 / GSF	63.0
2-Aug-18	1 TPB (QAMHAB)	LCR (ALT)	31.2	25.4 25.3	0 1	0 4	– 1,111 to 1,667	– 0	1 BG	0	–	–	0 / BG	75.83
2-Aug-18	1 TPB (AHAB1)	LCR (ALT)	31.2	25.4 25.3 27.4 25.5 28.0 27.7	0 1 4 6 24 27	0 15 3 2 0 0	0 2,778 to 3,333 1,111 to 1,667 1,111 to 1,667 111 to 556 111 to 556	- 0 0 5 0 0	1 CC, 6 GB	0	–	–	–	–
2-Aug-18	2 P (AHAB1)	LCR (ALT)	31.2	25.4 25.3 28.3 28.1 28.3 27.4 27.3 27.4 27.2 27.5 27.7	0 1 4 6 17 18 19 20 21 24 26	0 4 0 0 0 0 0 0 0 0 0	0 1,111 to 1,667 0 0 111 to 556 111 to 556 111 to 556 111 to 556 111 to 556 1,111 to 1,667 111 to 556	- 0 - - 95 95 0 0 0 0 0	6 GSF	0	–	–	0 / GSF	67.1

Table 3. FY 2019 collection dates, number of mussels collected / species, collection location, field temperature, aquarium temperature, days in trial, total conglutinates and fragments, total glochidia, percent viability, number of fish host species, number of juveniles / fish species, length of juveniles, number of capsules / fish species mortality. SPB = Smooth Pimpleback, TPB = Texas Pimpleback, TFM = Texas Fat Mucket. QAMHAB = Aquarium Mussel Habitat, AHAB = Aquatic Habitat, and BBHAB = Big Blue Habitat. LCR = Lower Colorado River, MCR = Middle Colorado River, ALT = Altiar, LAMP = Lampasas, HWY190 = Highway 190 Bridge, SSR = San Saba River, CC = Channel Catfish, BG Bluegill, GSF = Green Sunfish, MSM = Sailfin Molly, MT = Mexican tetra, RGC = Rio Grande Cichlid, WM = Warmouth.

Collection Date	Number of Mussels collected/ Species	Collection Location	Field Temp. (˚C)	Aquarium Temp. (˚C)	Days in Trial	Total Conglutinates and Fragments	Total Viable Glochidia	Percent Viability	Number of Fish Host Species	Number of Juveniles / Fish Species	Length of Juveniles (µm ± SD)	Width of Juveniles (µm ± SD)	Number of Capsules / Fish Specie Mortality	Size TL (mm)
	3 TPB	MCR[a]												
2-Jun-19	(QAMHAB)	(190)	–[b]	23.1	0	2	0	0	–	–	–	–	–	–
6-Jun-19	2 TFM (AHAB1)	SSR	27.9	22.7 24.8 23.7 24.8 24.2 28.2 31.8 27.6 22.7 22.9 28.2	0 2 5 8 11 14 22 38 0 6 14	0 0 0 0 0 0 0 0 0 0 0	0 30 921 0 0 0 0 0 0 24,600 0	– 100 95 – – – – – – 92.7 –	, 1 RGC 11 GSF, 2 BG,	29 /RGC, 5 / GSF, 1097 / GSF, 23 / BG,	270.7 ± 8.3	221.8 ± 8.2	, ,	, , ,
			27.9	29.7 31.8 29.3 27.6	20 22 31 38	0 0 0 0	0 0 0 0	– – – –	4 WM, 1 MT	4 / WM, 5 / GSF, 1 / GSF, 4 / MT	270.7 ± 8.3	221.8 ± 8.2	0 / GSF	60.12
			27.9	22.7 23.2 24.8 23.5 26.3 28.2 31.8 30.6 27.7 29.3 27.6	0 7 8 10 12 14 22 24 25 31 38	0 3 0 0 0 0 0 0 0 0 0	0 66,300 0 0 0 0 0 0 0 0 0	– 96.8 – – – – – – – – –	1 5GSF, 7 BG, 10 RGC	255 / GSF, 70 / BG, 24 / RGC, 478 / GSF, 32 / BG, 283 / RGC, 2 / BG, 5 / GSF, 1 / RGC	270.7 ± 8.3	221.8 ± 8.2	150 / BG, 6 / GSF, 4 / GSF, 14 / GSF, 0 / GSF, 0 / GSF, 70 / GSF, 222 / GSF, 0 / GSF, 0 / GRGC, 0 / GSF	50.0 55.0, 50.5, 60.9, 61.6, 55.8, 106.7 , 125.0 , 54. 6, 63.3, 47.5

Table 3. *(cont.)*

Collection Date	Number of Mussel collected/ Species	Collection Location	Field Temp. (°C)	Aquarium Temp. (°C)	Days in Trial	Total Conglutinates and Fragments	Total Viable Glochidia	Percent Viability	Number of Fish Host Species	Number of Juveniles / Fish Species	Length of Juveniles (µm ± SD)	Width of Juveniles (µm ± SD)	Number of Capsules / Fish Specie Mortality	Size TL (mm)
6-Jun-19	2 TFM (AHAB1)	SSR	27.9	22.7 25.5 23.5 27.0 28.2 31.9 31.8 31.5 29.3 28.8 27.6	0 9 10 13 14 21 22 28 31 32 38	0 14 0 0 0 0 0 0 0 0 0	0 185,000 0 0 0 0 0 0 0 0 0	– 96.2 - - - - - - - - -	8 GSF, 8 BG, 11 RGC, 2 MT, 4 MSM,	349 / GSF, 25 / BG, 95 / RGC, 1 / MT, 0 / MSM,	270.7 ± 8.3	221.8 ± 8.2	2 / BG6, 916 / GSF, 4 / BG, 652 / GSF, 6 / R 0 / GSF, 0 / MM, 0 / MM	75.0, 89.3, 60.3, 94.3, 70.6, 74.4, 61.5, 71.2
			27.9	22.7 26.3 28.2 30.1	0 12 14 18	0 0 0 1	0 7,650 5 3900	– 77.3 100 84.6 6	2 BG	6 / BG	270.7 ± 8.3	221.8 ± 8.2	–	–
21-Jun-19	4 P (AHAB1)	LCR (ALT)	30.3	23.5 29.7 28.9 29.8 30.3 30.3	0 1 2 3 6 7	8 26 34 – – –	Combined Combined 112,200 – – –	– – 74.3 – – –	11 CC	914 / CC	493.5 ± 28.0	520.3 ± 40.3	732 / CC, 702 / CC, 40 / CC, 32 / CC, 348 / CC, 86 / CC, 1140 / CC, 46 / CC, 40 / CC, 86 / CC, 12 / CC	295.0, 275.0, 250.0, 255.0, 2450., 250.0, 220.0, 255.0, 240.0, 240.0, 265.0
	(AHAB1)		30.3	29.2 29.8 30.3 30.3	0 3 6 7	8 3 0 0	Combined 379,000 0 0	– 94.6 – –	5 CC	0	493.5 ± 28.0	520.3 ± 40.3	140 / CC, 994 / CC, 222 / CC, 346 / CC, 356 / CC,	265.0, 255.0, 250.0, 270.0, 250.0
	(BBHAB 1)		30.3	29.2 29.7 29.8	0 1 3	8 15 3	0 0 379,000	– – 94.6	19 CC	156,830 / CC	493.5 ± 28.0	520.3 ± 40.3	0	-
21-Jun-19	1 TPB (AHAB1)	LCR (ALT)	30.3	29.3 29.1 29.6 32.6	60 1 2 6	1 6 12 0	Combined Combined 7,500 0	– – 64 –	2 CC	154 / CC	471.5 ± 42.6	371.1 ± 61.4	6 / CC, 389 / CC	265.0, 260.0

Table 3. *(cont.)*

Collection Date	Number of Mussel collected / Species	Collection Location	Field Temp. (˚C)	Aquarium Temp. (˚C)	Days in Trial	Total Conglutinates and Fragments	Total Viable Glochidia	Percent Viability	Number of Fish Host Species	Number of Juveniles / Fish Species	Length of Juveniles (µm ± SD)	Width of Juveniles (µm ± SD)	Number of Capsules / Fish Specie Mortality	Size TL (mm)
				29.3	0	0	0	_						
	(AHAB1)		30.3	29.9	3	16	17,000	91.2	1 CC	0	_	_	704 / CC	270.0
				32.6	6	0	0	_						
	4 P			27.4	0	0	0	__						
10-Jul-19	(QAMHAB	LCR (ALT)	32.0	26.1	6	4	1872	0	_	_	_	_	_	_
	)			26	15	4	7006	0						
	4 TPB			27.8	0	combined	0	_	_					
	(QAMHAB	LCR		28.0	2	30	58,250	97.4	8 CC,					
10-Jul-19	)	(ALT)	32	28.6	4	20	19,600	73.3	4 CC,	31,900 / CC	471.5 ± 42.6	371.1 ± 61.4	_	_
	(BBHAB2)			25.7	12	20	15	_	_					
				25.6	15	10	51	_	_					
	(QAMHAB			29.9	33	50	3,000	41.7						
	)			31.1	34	24	0	_	11 CC	23 / CC	471.5 ± 42.6	371.1 ± 61.4	_	_
	(BBHAB3)			30.9	35	11	0	_						

Table 4: Total juvenile mussels produced at the UNFH in 2018 and 2019.

Year	Mussel Species	Number of Juveniles Produced
2018	Pimpleback *Cyclonaias pustulosa*	60
	Texas Pimpleback *Cyclonaias petrina*	30
	Total	90
2019	Pimpleback *Cyclonaias pustulosa*	157,744
	Texas Pimpleback *Cyclonaias petrina*	32,077
	Texas Fatmucket *Lampsilis bracteata*	2,793
	Total	192,614

Table 5: Fish hosts infected by Texas Pimpleback *Cyclonaias petrina* from different reaches of the Colorado River at the UNFH in 2018.

Fish Species	**Colorado River Reach**	**Number of Gill Capsules per fish**
Channel Catfish *Ictalurus punctatus*	Middle	1008
Warmouth *Lepomis gulosus*	Lower	186
Green Sunfish *Lepomis cyanellus*	Middle	6

Figure 1. A chlorinated sand filter system at the UNFH Quarantine Building used to prevent to the spread of ANS and disease into the local watershed. Photo Credit: USFWS

Figure 2. A Tecniplast technician installing a chiller onto a state of the art AHAB system (AHAB1). Photo Credit: USFWS

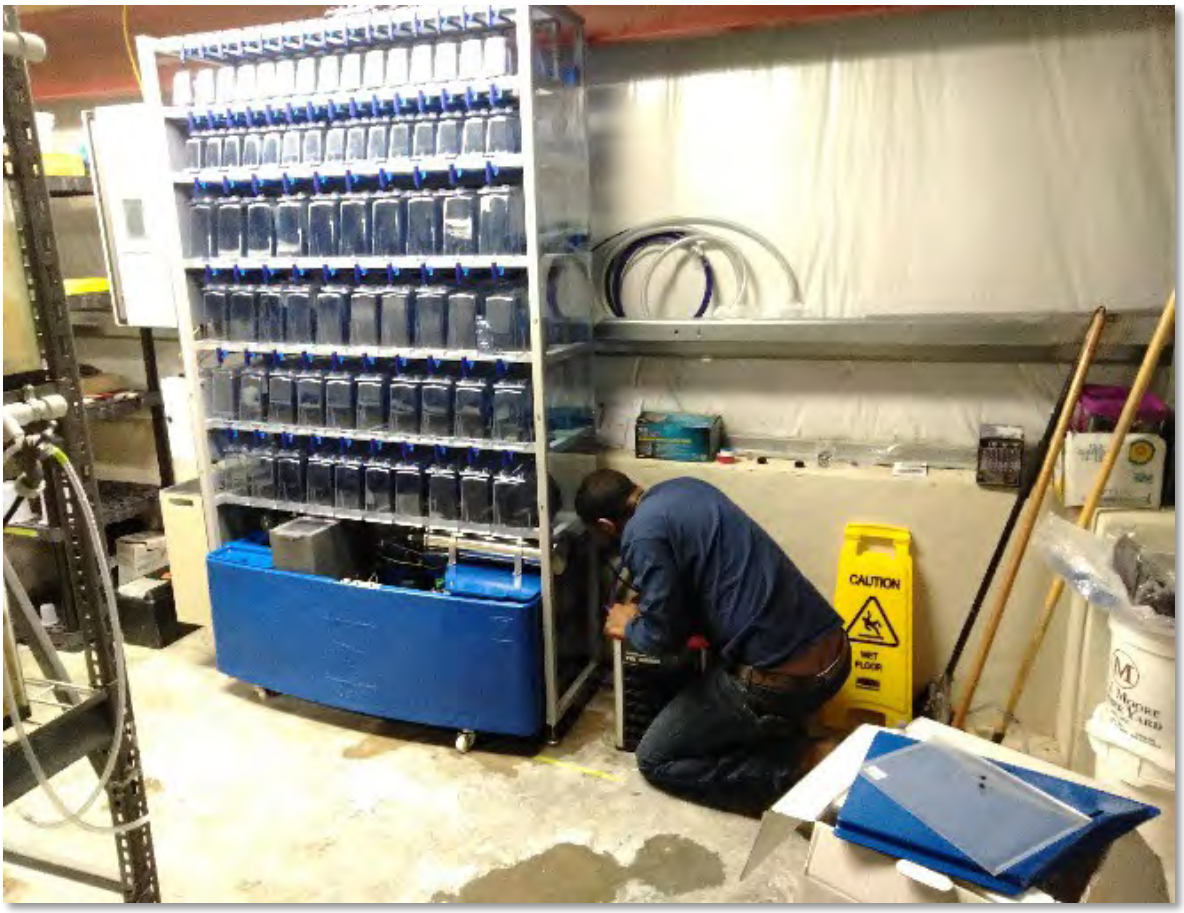

Figure 3. A renovated temperature controlled mussel flow-through system (QAMHAB) capable of holding mussels and fish hosts together for prolonged periods. Photo Credit: USFWS

Figure 4. Barnhart (2005) Freshwater mussel Mucket Buckets for juvenile mussels produced in 2018. Photo Credit: USFWS

.

Figure 5. In 2018, a Aquatic Mussel Habitat (RAMHAB) recirculating system was built to hold non-gravid freshwater mussels collected in 2017. In 2019, a feeding system was designed to pump concentrated algae from a 10-gallon container (white container on right side) into freshwater mussel containers (black containers left side) with a peristaltic pump. Photo Credit: USFWS

.

Figure 6. Live indoor algal cultures that started up during the government shutdown as a backup food supply. Pure cultures include *Chlorella* sp. and *Nannochloropsis* sp. Photo Credit: USFWS

Figure 7. Live outdoor algal cultures grown outside in high concentrations in 20-gallon food-grade containers. The algae was used to increase the nutritional value of the mussel food supply. A 10 µm or 5µm 32” x7" mm felt mesh bag with a poly ring mouth (upper left) was used to sieve algae for freshwater adult and juvenile mussels. Photo Credit: USFWS

Figure 8. Outdoor pond cultures provide a variety of algal species, which include both motile and non-motile algae. Flagella on some of these single celled algae are not detectable in the photograph. Photo Credit: USFWS

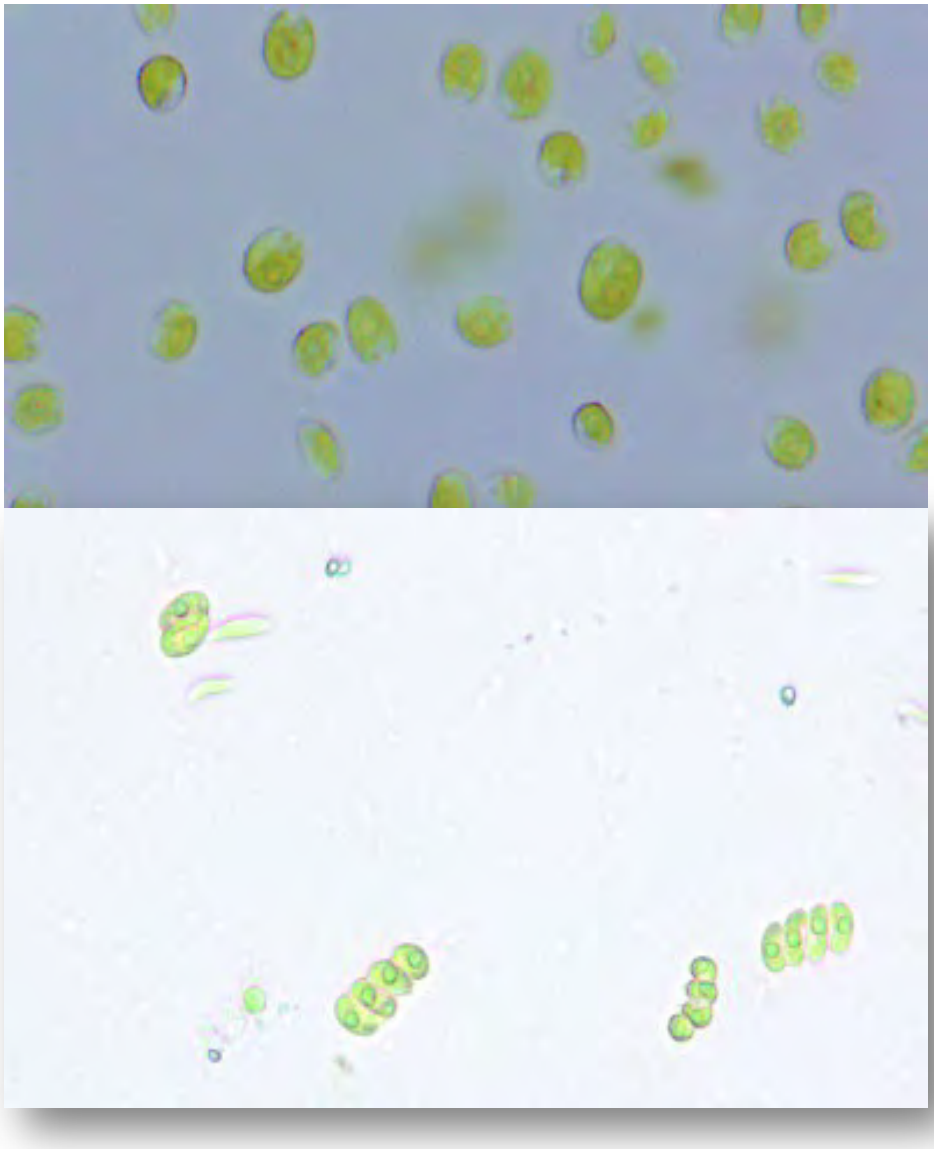

Figure 9. The UNFH mussel culture facility currently has three flow-through systems or Big Blue Habitats (BBHAB1, 2, and 3) designed to maintain large numbers of infected catfish hosts. Nylon collection bags were used to collect high concentrations of juvenile mussels that drop off from large numbers of fish hosts. There are two BBHAB systems below the previously built QAMHAB system. Only one can be seen in this photo. Photo Credit: USFWS

Figure 10. A complete recirculating Zebrafish AHAB system (AHAB2) was installed to provide additional experimental space for mussel propagation at the Station's Quarantine Building (QB). Photo Credit: USFWS

Figure 11. The Static Juvenile Growth System (SJGS) was set up to grow the juveniles to 1 mm in length in the static systems before subjecting the delicate drop-offs to the potential negative effects of the dead algal treatments and turbulence produced by the up-welling system. Photo Credit: USFWS

Figure 12. The Up-welling Juvenile Growth System (UJGS) has a pump that recirculates water from a 5-gallon bucket into a 20-gallon basin. To eliminate waste, fresh well water was added from a manifold and excess water exits a standpipe on the 5-gallon bucket that drains down into a basin with a sump pump. The advantage to this system was that three independent systems with three replicates each may be setup to test different feed treatments simultaneously. Photo Credit: USFWS

Figure 13. A graph showing the total juvenile drop-off rate of six different fish host species infected with L. bracteata glochidia. N = number of fish hosts that resulted in drop-offs. GSF = Green Sunfish, RGC = Rio Grande Cichlid, BG = Bluegill, MT = Mexican Tetra, WM = Warmouth, and MSM = Sailfin Molly. Photo credit: USFWS.

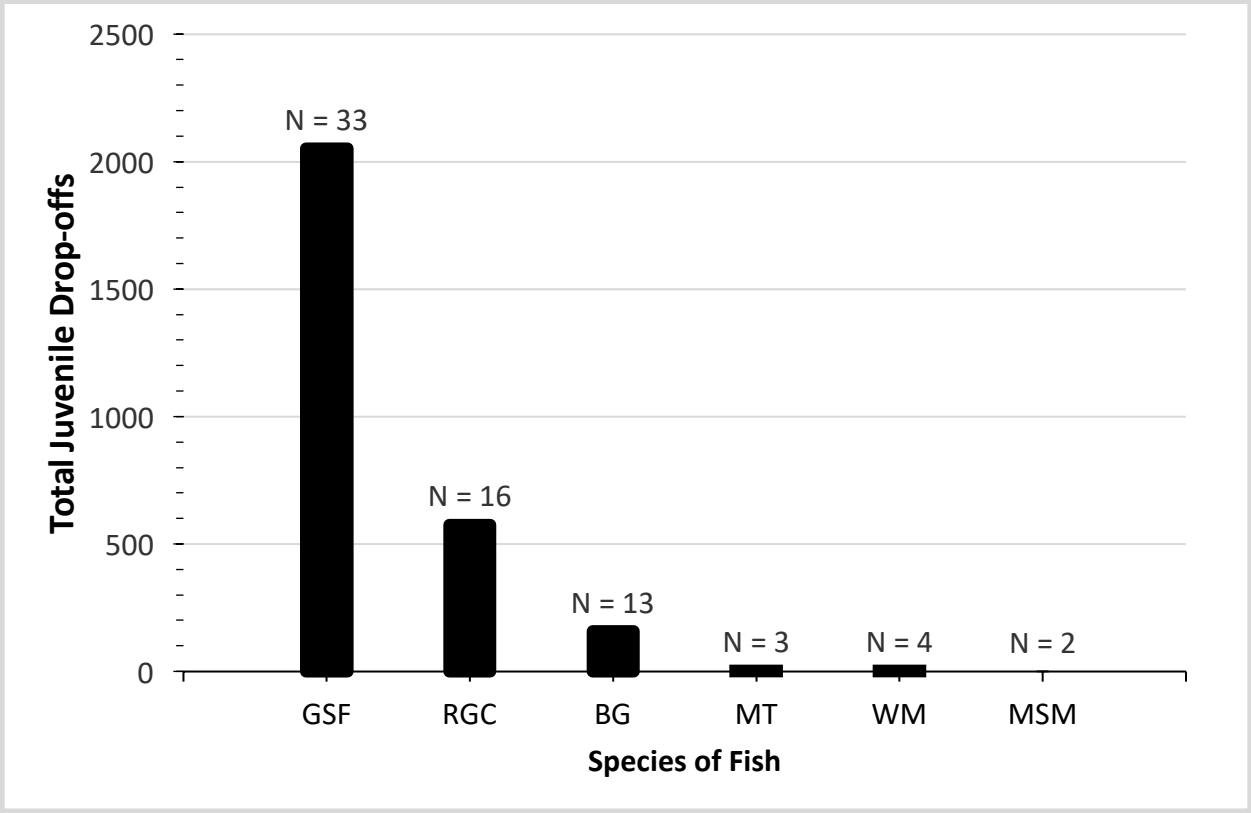

Figure 14. A graph showing the number of juvenile drop-offs per fish for six different fish host species infested with *L. bracteata* glochidia. N = number of fish hosts that resulted in drop-offs. GSF = Green Sunfish, RGC = Rio Grande Cichlid, BG = Bluegill, MT = Mexican Tetra, WM = Warmouth, and MSM = Sailfin Molly. Photo credit: USFWS.

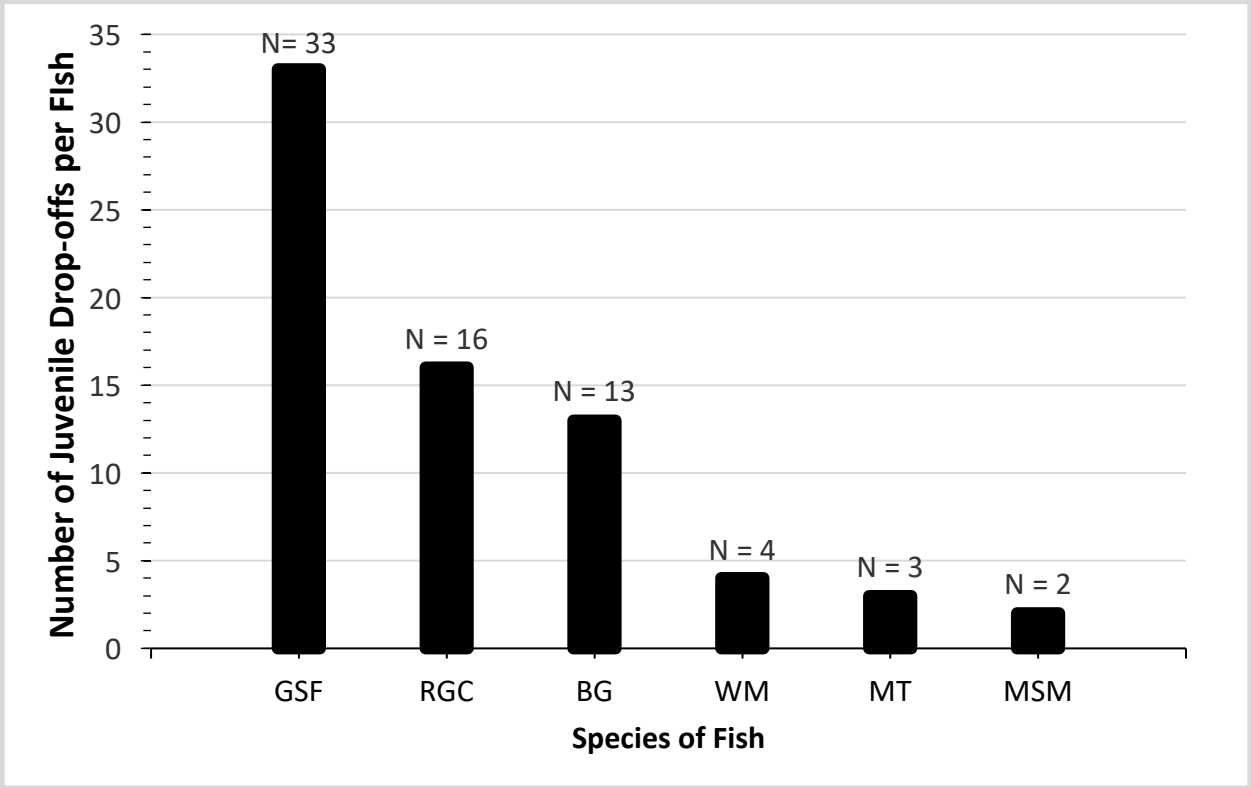

References

Barnhart, M. C., 2006. Buckets for muckets: a compact system for rearing juvenile freshwater mussels. Aquaculture 254: 227–233.

Castagna, M. and J.N. Krauter. 1984. Manual for Growing the Hard Clam *Mercenaria.* Special Report in Applied Marine Science and Ocean Engineering No. 249. Virginia Institute of Marine Science, Gloucester Point, Virginia. 110 p.

Duncan, P. L. 1986. The use of crab meal as a supplemental food for juvenile hard clams, *Mercenaria mercenaria.* Master's thesis. Virginia Institute of Marine Science. College of William and Mary. Gloucester Point, Virginia.

Gatenby, C.M., R.J. Neves and B.C. Parker. 1996. Influence of sediment and algal food on cultured juvenile freshwater mussels. Journal of the North American Benthological Society. 15:597–609.

Gatenby, C.M., B.C. Parker and R.J. Neves. 1997. Growth and survival of juvenile rainbow mussels, *Villosairis* (Lea 1829) (Bivalvia: Unionidae), reared on algal diets and sediment. American Malacological Bulletin. 14:57–66.

Heasman, M.P., T.M. Sushames, J.M. Diemar, W.A. O'Connor, and L.A .Foulkes. 2001. Production of microalgal concentrates for aquaculture part 2: Development and evaluation of harvesting, preservation, storage and feeding technology. NSW Fisheries Final Report Series No. 34, ISSN 1440-3544.

Hruska, J. 1992. The freshwater pearl mussel in south Bohemia: evaluation of the effect of temperature on reproduction, growth and age structure of the population. Archiv fur Hydrobiologie. 126:181–91.

Johnson, N. A., Smith, C. H., Pfeiffer, J. M., Randklev, C. R., Williams, J. D., and J. D. Austin. 2018. Integrative taxonomy resolves taxonomic uncertainty for freshwater mussels being considered for protection under the U.S. Endangered Species Act. Scientific Reports, 8, 15892.

Mair, R. A. 2013. A suitable diet and culture system for rearing freshwater mussels at White Sulphur Springs National Fish Hatchery, West Virginia. Master's thesis, Virginia Polytechnic Institute and State University, Blacksburg.

Patterson, M.A., R.A. Mair, N.L. Eckert, C.M. Gatenby, T. Brady, J.W. Jones, B.R. Simmons, J.L. Devers. 2018. Freshwater Mussel Propagation for Restoration. Cambridge University Press, Cambridge.

Post, G. 1987. Textbook of Fish Health. T. F. H. Publications. Neptune City, New Jersey. 288 p.

Tucker, C.S. and E.H. Robinson. 1990. Channel Catfish Farming Handbook. Van Nostrand Reinhold. New York, New York. 454 p.

Walne, P. R. 1979. Culture of Bivalve Molluscs 50 years' experience at Conwy. Fishing News Books Ltd, Farnham Surrey England. 185 p.

Wells, W.F. 1927. Report of the experimental shellfish station. Report of the Rep. No. 16, pp. 1–22. New York State Conservation Department.

INKS DAM NATIONAL FISH HATCHERY FACILITY REPORT

Contributing Authors: Bailey Gaines and Scott Walker

INTRODUCTION

Increased concern over the status of native freshwater mussels in the Colorado River watershed of Texas prompted efforts to evaluate the viability of freshwater mussel propagation in a hatchery setting. Inks Dam National Fish Hatchery (IDNFH) was one of three facilities chosen as a potential site for mussel propagation due in part to its unique water source(s). IDNFH utilizes both well water and surface water (Inks Lake) to support aquatic animal husbandry. For freshwater mussel propagation, the main goal of IDNFH was to determine if water sourced from Inks Lake could support the dietary needs of adult freshwater mussel broodstock as well as growth and survival of transformed juvenile mussels. Beginning in FY-2017, IDNFH initiated freshwater mussel propagation activities which included modifications to existing hatchery infrastructure, collection of broodstock mussels, and acquisition of host fish. IDNFH collected and brought on station Texas Fatmucket (*Lampsilis bracteata*), Texas Pimpleback (*Cyclonaias petrina*), and Pimpleback (*Cyclonaias pustulosa*) for research and development of propagation programs for each of the three species (Figure 1).

Facility Food Source

Surface water for IDNFH is collected from Inks Lake via a 30” pipeline, mechanically filtered to 50 µm, and distributed throughout the hatchery. In February 2017, facility staff began using a Beckman Coulter Multisizer 4e particle analyzer to measure amount and size of particles in influent lake water post filtration (Figure 2). Amount and size of particles measured remained consistent from 2017 to 2019 with average number/ml = 28,346 (± 8,488) and average particle size = 3.84 µm (±0.321). The composition of these particles is unknown; however, likely make-up of a wild water source includes bacteria, phytoplankton, zooplankton, and organic detritus.

Preliminary Work and Lessons Learned

From 2017 to 2019, rearing equipment and propagation techniques at IDNFH evolved based on efficiency of use, propagation successes, propagation failures, and the innovative adaptation of techniques found to be successful at other mussel rearing facilities.

Infrastructure Improvements – FY-2017

The first mussel holding system built at IDNFH was completed in early 2017 and was an outdoor flow- through system comprised of six independent 5-ft. circular tanks (Figure 3). The intended purpose of the system was to hold adult broodstock collected from the wild. The system was used for that purpose in 2017; but in 2018, facility staff determined the system was better suited for holding host fish in quarantine and adult mussels were transferred to a temperature-controlled building.

After propagation efforts transitioned to a temperature controlled building, FY-2017 gravid broodstock and infested host fish were held in a three-tiered Z-habitat type system with on-board temperature control, UV sterilization, and automatic water exchanges (Figures 4 and 5). The Z-habitat system was equipped with 150 µm mesh screens on the outfalls of each tank containing infested host fish. Mesh screens were checked regularly for the presence of transformed juvenile mussels (Figure 6). Transformed juveniles were then placed in a flow-through pan system with commercially available swimming pool filter sand substrate (Figure 7). The flow-through pan system utilized incoming lake water from the facility's main water line. Water flowed into each pan through a short piece of flexible 3/8 inch hose, circulated in the pan, and then exited through a central PVC standpipe. Filter screens were placed under each pan to prevent escapement of juveniles that made their way over the pan's standpipe. In August 2017, supplemental aeriation was added to each pan in response to anoxic incoming lake water. Prior to a low dissolved oxygen (DO) event, supplemental aeration was not used due to concerns that the aeration within each pan would cause juveniles to be circulated within the water column and out the standpipe.

Freshwater Mussel Acquisition and Collection – FY-2017

In April 2017, IDNFH staff met with SMARC staff to collect adult mussels from the Llano River at Farm to Market Road 1871 (FM 1871 site) southwest of Mason, TX (Table 1). Approximately 40 Texas Pimpleback and 40 Texas Fatmucket were encountered during sampling and four of each species were brought back to IDNFH for holding trials and potential use as broodstock.

IDNFH staff next accompanied BIO-WEST Inc. to a site on the Lower Colorado River near Altair, TX. This site produced multiple mussels. Pimpleback and Texas Pimpleback (12 and 11, respectively) were collected and brought back to IDNFH for holding trials and broodstock use.

In mid-May, Inks Dam staff traveled to multiple sites on the Llano River in search of additional mussel sampling locations for Texas Fatmucket and Texas Pimpleback. Although freshwater mussels were encountered at some of the sites visited, they were not found in sufficient numbers to warrant collection. Lack of success at alternative collection sites prompted IDNFH staff to return to the Llano River FM 1871 site in Late-May and again in Mid-July for broodstock collection of Texas Fatmucket and Texas Pimpleback. In May, two Texas Fatmucket and five Texas Pimpleback were collected and in July, two Texas Fatmuckets and three Texas Pimpleback were collected. All were retained at IDNFH for holding and future use as broodstock. The Llano River FM 1871 site was visited on three occasions in FY-2017; however, collection efforts were conducted in separate reaches on each trip so as not to repeatedly sample from the same group of mussels.

Captive Propagation of Juveniles FY-2017 – Texas Fatmucket

IDNFH hatchery staff, with the assistance of SMARC and Ecological Services staff, infested Bluegill *(Lepomis macrochirus*) and Green Sunfish *(Lepomis cyanellus)* using glochidia from two gravid Texas Fatmucket on June 20, 2017 (Figure 8). Staff estimated 2,300 metamorphosed juveniles were collected and stocked into the flow-through pan system (Table 2). Supplemental feed was not offered.

Juvenile Rearing FY-2017

The juvenile mussels experienced good growth over the first month, increasing in size from approximately 250 µ to 1000 µ. As previously stated, anoxic influent water (dissolved oxygen < 0.5 mg/L) from the hatchery water source (Inks Lake) was experienced in early August, 2017 and led to near total mortality of the juvenile mussels. Two survivors were found in the system following the anoxic event and were kept in the flow-through pan system with supplemental aeriation until the system was upgraded in FY-2018. The continued growth and survival of these two juvenile Texas Fatmucket lent credence to the belief that freshwater mussels could be reared at IDNFH on filtered lake water without supplemental feeding.

Infrastructure Improvements – FY-2018

Improvements to freshwater mussel rearing systems at IDNFH began in November 2017 with the installation of shallow bottomed flow-through indoor raceway tanks (Figure 9). These tanks were used to hold adult mussels from collection efforts. The tanks were supplied with lake water and supplemental aeration. Mussels were placed in perforated plastic trays containing sand and gravel substrate. The perforated sides allowed water flow over the mussels. The decision to move adult mussels from a pre-existing outdoor flow-through system to an indoor system was made so that staff could more closely monitor mussel health and behavior. In particular, when adult female Texas Fatmuckets engaged in lure-display and when Texas Pimplebacks and Pimplebacks expelled conglutinates.

In addition to the raceway tanks, considerable improvements were made to the facility's flow-through pan system. The original pan system consisted of 9 – 12 inch diameter pans with sand substrate. The system was completely flow-through and did not have supplemental aeration in the pans for fear that agitation of the water might lead to escapement loss of newly transformed juveniles. Because poor water quality was considered the single primary cause of mortality from the previous year, a new pan system was designed that included a sump to aerate incoming water and mitigate low dissolved oxygen concentrations. The system was modified for recirculation capabilities and expanded from 9 pans to 36

(Figure 10). The system was completed in February 2018 and utilized locally sourced sand filtered to < 400 µm so as to allow juvenile mussels to be separated from the substrate at a smaller size for enumeration and survival assessment. Two new Z-habitat type rearing systems were also installed during FY-2018 (Figure 11).

The Z-habitat type systems were used to hold host fish infested with mussel glochidia.

Freshwater Mussel Acquisition and Collection – FY-2018

In December 2017, IDNFH received five gravid Texas Fatmucket obtained by BIO-WEST Inc. during a reservoir draw-down in Llano, Texas. Subsequently, a total of eleven collections/acquisitions took place during FY-2018 (Table 3). Collection efforts involving hatchery staff for FY-2018 began in February with trips to the Colorado River approximately one mile south of the HWY 190 Bridge crossing between San Saba and Lometa, Texas (HWY 190 site). The purpose of the trips was to identify locations of freshwater mussel assemblages (beds) and to check for gravid Texas Pimpleback females. Hatchery staff accompanied employees of BIO-WEST Inc., and the first gravid mussel collection occurred on April 18, 2018. The next collection site visited by hatchery staff was the Llano River at Farm to Market Road 1871 (FM 1871 site) southwest of Mason, Texas. The FM 1871 site was visited on May 22, 2018 and three gravid female Texas Pimpleback were collected and transferred to the hatchery.

Inks Dam NFH and SMARC staff next accompanied BIO-WEST Inc. for collection on the Lower Colorado River Hwy 90 crossing near Altair, TX (Altair site). The Altair site is known to have mussel beds containing Pimpleback. The first collection at the Altair site occurred on June 12, 2018 and the last collection was on August 2, 2018. A total of 31 Pimpleback females were collected from the Altair site.

On July 2, 2018, hatchery staff collected two Texas Fatmucket from the Bois d'arc Road crossing of the San Saba River west of Menard, TX (Bois d'arc site). On July 19, staff returned to the Bois d'arc site and collected two additional gravid Texas Fatmucket females.

All freshwater mussel collections during FY-2018 were conducted under the authority of, and in accordance with, appropriate State and Federal permits. During FY-2018, attempts were made to return

broodstock to their location of collection when feasible. The return of collected broodstock was discussed at length prior to its implementation. Criteria for the return of mussels to their collection site were that mussels collected upriver from IDNFH and Inks Lake would only be returned if they had been quarantined in their source water (brought back from their point of collection) and not exposed to mussels from other locations or water supplied from Inks Lake. Mussels collected downstream (i.e. Lower Colorado at Altair) could be returned without the need for quarantine while at IDNFH.

With the exception of two mussels, all of the Pimpleback collected were returned to their collection site by the end of FY-2018. With the exception of four Texas Pimpleback that were returned to the Hwy 190 site and three Texas Pimpleback that were returned to the Altair site, the Texas Pimpleback and Texas Fatmucket collected during FY-2018 remained at the hatchery at the end of FY-2018.

Captive Propagation of Juveniles FY-2018 – Texas Fatmucket

Host infestations for FY-2018 began on December 8, 2017 using a single gravid Texas Fatmucket collected by BIO-WEST Inc. from a reservoir drain-down in Llano, Texas (Table 4). Twenty-six Green Sunfish were used as hosts with an estimated 49,000 glochidia attached to host fish (50% attachment). Transformed juveniles were detected 10 days later with a total of 548 recovered. The low number of successful transformations may have been attributed to the host fish. The Green Sunfish used had been used in FY-2017 and may have developed immunity to glochidial infestation.

Host infestations using Texas Fatmucket glochidia occurred again on May 15, 2018. The source of the glochidia was a single female from the previously mentioned reservoir draw-down in Llano, Texas. Locally sourced (Colorado River next to Inks Dam NFH) sunfish species were used as hosts and included Bluegill (*Lepomis macrochirus*), Redbreast Sunfish (*Lepomis auritus*), Longear Sunfish (*Lepomis megalotis*), Green Sunfish (*Lepomis cyanellus*), and Warmouth (*Lepomis gulosus*). In total, 24 fish were infested with 31,975 glochidia (72% attachment). No transformed juveniles were recovered from this infestation and by May 28 all of the host fish had died. It is thought that the host fish mortalities were

either due to handling stress during hook and line capture, stress due to glochidial infestation, or a combination of the two.

Unexpectedly, adult Texas Fatmucket held over from 2017 spawned in captivity and were used as broodstock during FY-2018. It is reasonable to assume sperm casting occurred in the indoor raceway system. The possibility of viable Texas Fatmucket sperm entering the facility is extremely low; and although hermaphrodism in freshwater mussels has been reported, it has not been reported for Texas Fatmucket. An estimated 42,750 viable glochidia from the 2017 Texas Fatmucket where obtained on June 11, 2018 when the mussel unexpectedly expelled conglutinates. While lure display is the primary means of Texas Fatmucket attracting and infesting its host fish, it is evident that this species can resort to a secondary strategy. Conglutinates salvaged from the raceway were viable and were used to infest 81 Bluegill. Estimated number of attached glochidia was 19,550 (46% attachment). Additional glochidia (expelled as conglutinates and not enumerated) were obtained on June 18 and 19 and used to infest 15 Green Sunfish by direct glochidia application to the gills via pipette. Transformed juveniles (1,250) were recovered by staff and placed in the semi-closed flow-through pan system.

On July 9, 2018, glochidia from the two Texas Fatmucket collected from the Bois d'arc site (July 2 collection) were harvested using the syringe method. An estimated 141,211 viable glochidia were used to infest 13 Green Sunfish and 57 Bluegill Sunfish. Percent attachment was not calculated for this infestation and host fish experienced high mortality; however, transformed juveniles were recovered and placed in the semi-closed flow-through pan system. Additional infestations using Texas Fatmucket glochidia occurred on July 30 and August 15, but resulted in few transformed juveniles. The total number of transformed juvenile Texas Fatmucket recovered during FY-2018 was 2,683.

Captive Propagation of Juveniles FY-2018 – Texas Pimpleback

Collection of viable, fully developed glochidia from gravid Texas Pimpleback females proved difficult in FY-2018. As a whole, freshwater mussels categorized as short term brooders (i.e. Texas Pimpleback) present challenges to propagation that are more profound than those found in long term

brooders (i.e., Texas Fatmucket). Rather than relying on a mantle lure to attract host fishes, Texas Pimpleback expel glochidia in packets called “conglutinates”. The conglutinate packets are thought to resemble a prey item that host fish attempt to eat and thus become infested with glochidia. One of the main difficulties in working with members of the Quadrulini Tribe (of which *Cyclonaias* is a member genus) is that collected female’s will often abort conglutinates in response to handling (Figure 12). The problem of spontaneous abortion of conglutinates is further compounded by abortions that occur before glochidia contained in conglutinates are fully developed. To mitigate against loss of glochidia during mussel collection, hatchery staff placed newly collected mussels and native water in round plastic containers with screw top lids. Although this prevented the loss of conglutinates, it did not prevent spontaneous abortion. As noted earlier, the first Texas Pimpleback collection occurred on April 18, 2018. Over the next several days, the mussels aborted over 100 conglutinates, none of which contained fully formed glochidia. The first viable glochidia were obtained from the mussels collected on May 7, 2018 and were used to infest Channel Catfish (*Ictalurus punctatus*) on the same day (Table 5). The mussels released conglutinates over the next three days and the glochidia obtained were used to infest Channel Catfish and Fathead Minnows (*Pimephales promelas*). In total, glochidia obtained from the two mussels collected on May 7 were used to infest 52 Channel Catfish and 170 Fathead Minnows. The infested host fish were placed in Z-habitat units and separated by species so that transformed mussels would be collected on different screens. Channel Catfish mortality was high for the above infestation(s), but did result in recovery of transformed juvenile drop-offs that were placed in the previously described pan-system. The Fathead Minnow infestations resulted in poor attachment and only 17 total transformed juvenile drop-offs.

Furthermore, gill examination of channel catfish on May 12th showed heavy gill loading from both May 8 and May 9 infestations while gill examination of Fathead Minnows from the same infestations showed no visible glochidia attachment. Based on these results, staff believe Fathead Minnow to be a poor host for Texas Pimpleback.

Channel Catfish infestations occurred again on May 17, 2018 when 30 fish were used as hosts for

an estimated 10,500 Texas Pimpleback glochidia. The host fish were placed in a Z-habitat unit. The following day, 46 Channel Catfish were infested with 17,575 glochidia and placed in a Z-habitat. Both infestations resulted in recovered transformed juvenile drop-offs which were placed in the pan system. The total number of transformed juvenile Texas Pimpleback recovered and enumerated during FY-2018 was 5,331.

Captive Propagation of Juveniles FY-2018 – Pimpleback

As with Texas Pimpleback, collection of viable glochidia from Pimpleback for host fish infestation was hampered by the mussel's brood strategy and aversion to handling (Table 6). This was seen on our first collection trip to the Hwy 190 site when the mussel collected expelled conglutinates with under- developed glochidia. Pimpleback were not brought on site until May 24, 2018 when SMARC staff delivered five mussels previously collected from the Altair site. Although the mussels expelled conglutinates, they did not contain viable glochidia.

The first batch of viable glochidia (~20%) were recovered on June 16, 2018 from mussels collected on June 12 and an estimated 4,484 glochidia were used to infest Channel Catfish and placed in a Z-habitat unit. The infestation resulted in transformed juvenile drop-offs with initial recovery taking place on July 3, 2018.

The next infestation occurred on June 29 with 1,850 viable glochidia obtained from two mussels collected from the Altair site on June 12. Six Channel Catfish were infested and placed in a Z-habitat unit. The infestation resulted in transformed juvenile drop-offs which were placed in the pan-system.

The final Pimpleback infestation occurred on August 3, 2018 when 70 Channel Catfish were infested with glochidia obtained from Altair site mussels collected the day before. Glochidia quality was very poor and the infestation did not result in transformed juvenile drop offs. The total number of Pimpleback transformed juvenile drop offs recovered in FY-2018 was 1,205.

Juvenile Rearing during FY-2018

Transformed juveniles were recovered for each mussel species ranging in size from 200 to 300 µm. Glochidia collected from Z-habitat screens were transferred to a flow through/partial recirculating pan system. Incoming water from Inks Lake was constantly added to the system resulting in a 100% water exchange every 2-3 hours. Each pan was filled with sand sieved to <400 µm making initial growth monitoring problematic; however, it was expected that as mussels grew, they could be separated from the substrate with the appropriate size sieve. In addition to the Z-habitat units, a 4-foot circular holding tank was used as overflow for Channel Catfish infested with Texas Pimpleback glochidia. Transformed juvenile Texas Pimpleback were present in the bottom of the circular tank but were not enumerated. At the request of partners, 150 juvenile Texas Pimplebacks (200 – 350 µm) were siphoned from the bottom of the circular tank and transferred to Dr. Jim Stoeckel for respirometry research as part of a cooperative agreement with Auburn University.

Total mortality of juvenile mussels occurred soon after stocking in the pan-system as well as the circular tank. Microscopic examination of substrate post stocking yielded only empty shells, none of which exceeded 400 µm in length. A definitive cause for mortality is not known. Hypotheses to explain juvenile mortality included predation by micro invertebrate predators that exist in the wild water source, substrate size preference of juvenile mussels, or a lack of an age specific food source for juvenile mussels in incoming water FY-2018. However, wild caught adults and FY-2017 juvenile Texas Fatmucket showed growth on the same water source (Figure 13).

Infrastructure Improvements – FY-2019

FY-2019 system additions and modifications began in October 2018. Need for increased efficiency in the collection of juvenile drop-offs justified transition away from Z-habitat units to larger “batch” style drop-off collection tanks. The relatively small individual tank size of the Z-habitat was believed to be a cause of increased stress to infested host fish. Furthermore, drop-off recovery from the Z-habitat systems, while useful in host fish determination work, is not as efficient for mussel production when using larger

numbers of host fish or larger bodied hosts. To address this need, four – 30" diameter cone bottomed circular tanks were installed and used as a juvenile drop-off recovery system (see Juvenile Rearing during FY- 2019, this document**).** Poor juvenile survival from FY-2018 prompted changes to previously used juvenile mussel culture techniques and the addition of multiple juvenile rearing systems. Hypotheses for poor survival was predation by invertebrates present in the incoming lake water and substrate size used in the pan-system. For FY-2019, a total of 10 different aquaculture systems for host-fish, juvenile, and sub-adult mussels were built and/or modified to allow for multiple rearing conditions. The goal of using multiple rearing systems was to stock them concurrent with one another in order to assess which system is best suited for rearing freshwater mussels at IDNFH.

An additional set of raceway tanks was installed which are similar to the set that houses adult mussels/broodstock (Figure 14). The new set contained six raceway tanks allowing for the construction of a paired set of juvenile up-wellers and down-wellers in the center four tanks and wash-down sinks for cleaning and sorting of mussel drop-offs and juveniles on each end. The paired sets of up-wellers and down-wellers were configured with the option of either lake water directly from the facility's main water line ("unfiltered") or lake water from the facility's main water line filtered with a 20-µm cartridge filter ("filtered"). This allowed for the pairwise comparison of a replicate set of up-wellers and down-wellers run on filtered vs. unfiltered lake water. The four systems utilized chambers, enclosed by micron mesh on both ends, which contained juvenile mussels. The design of the chambers allowed for monitoring of growth and survival without having to sort through substrate.

A modification was also made to the existing semi-closed flow-through pan-system. The two sided system was set up to run on two independent sumps which allowed the relatively simple modification of adding filtration of the incoming water to just one of the two sides. Three cartridge filters were plumbed in series to allow for an incremental stepdown of filter cartridge micron size and an increase in total filter capacity (Figure 15). Half of the pan-system used filtered lake water and the other half used unfiltered lake water. Two substrate sizes, < 400 µm and > 400 µm, were used to evaluate substrate size on growth

and survival of newly transformed juveniles. Although monitoring of the pan-systems was more cumbersome than in the up-weller/down-weller systems, it did allow for presence/absence observations.

Next, a large flow-through up-weller system was built using a 30” x 70” x 36” rectangular fiberglass tank and 12” PVC wells (Figure 16). The system was designed to hold larger size-class juvenile mussels once they outgrew the 2 inch wells of the smaller up-wellers and down-wellers. Two-inch bulkhead fittings were installed in the walls of the rectangular tank and plumbed as drain lines. Each 12-inch pan was fitted with 500 µm mesh screen on the bottom side and a 2” outflow near the top edge. The system was designed so that water up-wells through the screen, over the mussels, and through the outflow pipe.

Mussels stocked into this system were large enough that filtration for invertebrate predators was not needed.

In addition to improvements made to freshwater mussel culture systems, lab stools, cabinetry, and desktop space were installed allowing biologists to sit rather than stand while using the microscopes. A stainless steel lab sink, drying rack for glassware, and hot water heater were installed to aid in cleaning equipment (Figure 17).

Freshwater Mussel Acquisition and Collection – FY-2019

A total of 12 collections took place in FY-2019 (Table 7). No new sites were identified or visited. River collection trips began in late March and continued as needed through August. One trip was made to The Llano River, three to the San Saba River, four to the middle Colorado River, and five to the lower Colorado River. Brood Stock were collected at all sites except the Llano River.

Heavy rains and high flows limited sampling efforts on the Colorado River both at the Hwy. 190 site and at Altair. Two unsuccessful sampling trips were made to the Hwy. 190 site and IDNFH staff eventually determined that river flow for this site needed to be at or below 750 cfs and a gauge height of 3.55ft as measured by the Hwy 190 USGS gauging station for safe and effective mussel sampling.

An increased effort was made in FY-2019 to return collected broodstock after glochidia had been collected (Figure 18). The same quarantine protocol and return criteria were used as established the previous year. In addition to returning more broodstock to their collection sites, a trial streamside harvest of Texas Fatmucket glochidia was performed. Instead of collecting two gravid individuals and bringing them to Inks Dam NFH for a total harvest of glochidia, four gravid mussels were brought streamside where only one of their two gills was harvested. The harvested glochidia were kept in a container with source water to be taken back to IDNFH for an infestation later that evening while the adult mussels were returned to the river with a gravid gill intact to contribute to natural reproduction.

Late in the collection season (July 17), a trip was made to the San Saba River site to collect a pair of Male Texas Fatmucket. A gravid female was also collected at this time for one additional infestation and the two males will be held over winter with other females to further investigate the ability of Texas Fatmucket to become gravid in captivity.

RESULTS

Captive Propagation of Juveniles FY-2019 – Texas Fatmucket

Infestations for FY-2019 began in late March with glochidia collected from two gravid Texas Fatmucket. One mussel contributed 110,000 glochidia and the second 152,000 (Table 8). Both batches were combined and used to infest 59 Bluegill and 90 Green Sunfish in a single infestation bath. Due to cooler water temperatures this early in the spring (avg. 18°C), the attachment period was extended and the first drop-offs were seen at 26 days after infestation (Table 8). A total of 367 drop-offs were recovered from 90 Green Sunfish and a total of 3,860 drop-offs were recovered from 59 Bluegill.

The second Texas Fatmucket infestation occurred on June 6 after the successful streamside harvest of glochidia from a single gill from 4 mussels. Glochidia from one of the four females had a clumpy appearance at the streamside harvest and was later confirmed to be non-viable. Contributions from the other three Texas Fatmucket yielded an estimated 238,000 glochidia that were used to infest 150+

Bluegill. At an average water temperature of 23℃, drop offs were seen in 13 days and by day 22 concluded with a total of 11,604 juvenile drop-offs.

A third infestation was conducted on July 30th using glochidia from one gravid Texas Fatmucket collected on July 17. 56,700 glochidia were harvested and used to infest 75 Bluegill. High host fish mortality in this batch yielded very low drop-off numbers.

Captive Propagation of Juveniles FY-2019 – Texas Pimpleback

Texas Pimpleback propagation began sooner than expected when an early site visit on April 4 produced a gravid female mussel with viable glochidia a month earlier than was observed the prior year (Table 9). On April 7, 44,600 glochidia were released and used to infest 60, 4.5-inch Channel Catfish for 20 minutes before being placed in one of the drop-off recovery circulars (Figure 19). The following day, an additional 45,300 glochidia were released and used to infest 45 additional Channel Catfish again for 20 minutes. At 19 ℃, the host fish attachment period ranged from 22 to 41 days and produced a total of 1603 juvenile drop-offs. As juvenile drop-offs were collected they were enumerated and split into separate batches and stocked into each of the eight different rearing system treatments (Figure 20).

High flows kept Inks Dam NFH staff from accessing Texas Pimpleback sampling sites again until the last day of May. Glochidia from this collection began to be released June 4 and continued through June 8. In total, 116 Channel Catfish were infested with 100,000+ glochidia resulting in 1736 recovered juvenile drop-offs.

Captive Propagation of Juveniles FY-2019 – Pimpleback

High river flow kept IDNFH staff out of the river until much later in the season than would have been preferred. It was fortunate that the opportunity to collect gravid short-term brooders was not completely obscured by of high river flows. Two collections did however yield gravid Pimpleback from the Altair site (Table 10). The first infestation of Channel Catfish with Pimpleback glochidia was conducted on June 22 when 55 Channel Catfish were infested with 86,600 glochidia for 30 minutes in 3

gallons of water under light aeration. Juvenile drop-offs (5,651) were recovered between 6 and 16 days after the infestation at an average water temperature of 25℃.

A second infestation of Channel Catfish with Pimpleback occurred on July 18 from mussels collected on July 10 at the Altair site. 24,400 glochidia were used to infest 20 Channel Catfish for 40 minutes resulting in a total of 4,088 recovered juvenile drop-offs. As with the other mussel species produced in FY-2019, juvenile drop-offs were collected, enumerated, and split into separate batches and stocked into each of the eight different rearing treatment scenarios.

Juvenile Rearing during FY-2019

Hatchery staff did not use the Z-habitat units previously used in FY-2017 and 2018 for mussel transformation and drop-off. In an effort to save time and ease collection of transformed juveniles, IDNFH staff installed four – 30" diameter cone bottomed circular tanks (Figure 21). After glochidial infestation, host fish were placed in the circular tanks. Incoming lake water was filtered through a 20-micron cartridge filter before entering each tank. Each tank was equipped with double standpipes. The outer standpipe had openings in the bottom and the inner standpipe was solid. Circular flow in each tank helped any mussel drop-offs move to the center of the tank, through the outer standpipe, and up and over the inner standpipe. The drain line of each tank was fitted with a mesh sock to catch mussel drop-offs. All four tanks drained to a common sump so that the mesh socks were always immersed in water.

Newly transformed juveniles from each species were stocked into each of eight different rearing systems for growth and survival analysis. The treatments included two general system types; chambered (meaning screens on both ends) flow-through and a partial flow-through pan system. Within the chambered setup, four different treatments were tested including: up-welling chambers run on unfiltered incoming lake water (unfiltered up-wellers), up-welling chambers run on filtered (20µm) incoming lake water (filtered up-wellers), down-welling chambers run on unfiltered incoming lake water (unfiltered down-wellers), and down-welling chambers run on filtered (20µm) incoming lake water (filtered down-wellers). Within the partial flow-through pan system, the following four treatments were also tested:

pans run on unfiltered incoming lake water with a substrate size of <400µm (unfiltered pan <400µm), pans run on unfiltered lake water with a substrate size of >400 µm (unfiltered pan >400µm), pans run on lake water filtered to 5µm with a substrate size of <400µm (filtered pan <400µm), and pans run on lake water filtered to 5µm with a substrate size of >400µm (filtered pan >400µm).

During the grow-out period, regular maintenance and monitoring was required on all systems. The chambered weller systems were initially fitted with 150µm mesh screens. Screen cleaning was usually required daily for the unfiltered treatments and every other day to every third day for the filtered treatments. The cartridge filters for the filtered systems would last a varying amount of time depending on the particulate load of the incoming lake water but one to four days was a normal interval between cartridge filter changes. Pan systems required considerably less daily maintenance; however, the cartridge filters required similar exchange intervals to the weller systems and flows to each pan required a daily check. Line clogging to each individual pan would eventually occur and would require cleaning. Line clogging occurred at a higher rate in the unfiltered pans versus the filtered pans.

Juvenile mussels showed growth throughout the summer and growth rates are reported based on data collected in mid-September with growth times of 77 to 144 days. Growth rate varied by species as well as by rearing system. The highest growth rates were seen in Texas Fatmucket followed by Pimpleback and Texas Pimpleback. Growth rates were also higher in filtered systems when compared to unfiltered.

Survival data was also collected in mid-September. System comparisons were consistent across species with the filtered systems outperforming the unfiltered, up-wellers outperforming down-wellers and >400µm substrate pans outperforming <400µm substrate pans. In all species, up-welling chambers run on filtered lake water showed the best survival (Figure 22). The filtered pan system showed the next highest survival but at roughly 50% of that seen in the filtered up-wellers. On the bottom end, both the unfiltered down-wellers and the unfiltered pan system with substrate <400µ showed no survival.

Total numbers surviving were enumerated by microscope counts in mid-September of each well

or pan depending on the system (Table 11). Totals were: Texas Fatmucket - 2,537 with an overall survival rate of 15.2%; Texas Pimpleback - 289 with an overall survival rate of 5.4%; and Pimpleback – 492 with an overall survival rate of 5%.

Costs

Initial startup costs at IDNFH included costs for alterations to existing buildings to provide culture space. At IDNFH, approximately 1,200 square feet of available space was retro-fitted for mussel culture. High cost laboratory equipment for mussel culture at IDNFH included microscopes, water quality monitoring meters, and a particle analyzer for evaluation of potential food source(s). Although the high cost equipment made initial start-up expensive, their expected life span should make them one-time purchases. Additional one-time purchases/acquisitions at IDNFH included host fish holding tanks, juvenile drop-off recovery systems, adult mussel holding systems, and juvenile culture systems. Although those items varied in price/value, the limiting factor for their installation at IDNFH was available space rather than cost. Additional costs for start-up included consumable items such as glassware, culture equipment, plumbing supplies, and water filtration equipment. Consumable items should be taken into consideration when budgeting for mussel culture; however, their overall costs are relatively low compared to the one- time purchases listed above.

Personnel cost was also a major expenditure. A minimum of two full time employees were needed to effectively source/collect broodstock and conduct daily animal care. Field sampling required the use of a motor boat and sampling gear which included speculums for checking females for gravidity, calipers, mesh sampling bags, snorkeling equipment, dive equipment, and live mussel transport containers.

Host fish infestations and host fish acquisition and care also incurred expense. Depending on the species of mussel, host fish where either readily available or somewhat difficult to obtain at the appropriate time needed for infestation. At IDNFH, staff used outdoor culture ponds and flow through fiberglass tanks to hold host fish. In some cases, host fish were held in quarantine so as not to jeopardize other production programs at the facility. Maintenance of ponds and care of host fish both incurred

expense.

DISCUSSION

FY-2019 production outcomes at IDNFH were the result of lessons learned during the previous two years. At the end of FY-2017, two Texas Fatmuckets were produced; however, their cohorts did not survive.

Our initial hypothesis that anoxic culture conditions were responsible for low survival may have been correct, but it did not take into account the possibility of predation by invertebrates in our water supply. Never the less, the survival of two mussels demonstrated that mussel culture using water from Inks Lake (without supplemental feeding) was possible.

Confidence was high going into FY-2018 because we had corrected the system issue that led to anoxic conditions. In addition, substrate size was not considered to be a significant variable at that time and was changed to a finer particle size to aid in separating juvenile mussels, via sieve, from the substrate. As we eventually learned in FY-2019, all three mussel species in the unfiltered pans with <400µm substrate had no survival. Although we cannot say with certainty that the smaller particle size used in FY-2018 was the sole cause of mortality, we can say that <400 µm substrate is inappropriate for the three mussel species evaluated in our semi-closed flow-through pan system. Extensive microscope work in FY-2018 searching through substrate for mussels that were no longer present also revealed to us the abundance of micro- invertebrates that had colonized our systems through the incoming lake water. This observation prompted the need to test additional filtration immediately prior to water entering each system. Aerial colonization of aquatic systems by chironomid sp. larvae also proved problematic. While chironomids were not believed to predate on the juvenile mussels, they did appear to contribute to mortality either through harassment or by the use of juvenile mussels in the construction of their chironomid tubes. Control of chironomids with a 24 hour 10 ppm treatment of Gnatrol WGD was effective.

Diversification of rearing methods in FY-2019 enhanced our ability to evaluate which rearing

methods worked best at IDNFH. Filtered water proved to be essential given the predators present in the incoming lake water. Filtration also reduced the cleaning frequency of all juvenile mussel systems tested and improved system functionality. Filtered up-wellers outperformed everything else tested two to one. Of the four “weller” systems tested, they not only performed the best, but required the least amount of maintenance. They were however higher maintenance than any of the pan systems which had the lowest daily maintenance of all the systems tested.

The infrastructure for the juvenile rearing systems used in FY-2019 can be easily modified to retain the properties of what was shown to be most efficient and productive. Further, the systems can be expanded and refined to optimize freshwater mussel rearing at IDNFH. We see a need to further test juvenile mussel culture through the addition of UV sterilization vs non-sterilized incoming water, temperature optimizations, additional substrate sizes, stocking densities, and filtration size.

Figures and Captions

Figure 1. Freshwater mussels collected from the Colorado River watershed for use in propagation at Inks Dam NFH. From left to right: Texas Fatmucket (*Lampsilis bracteata*), Texas Pimpleback (*Cyclonaias petrina*) and Pimpleback (*Cyclonaias pustulosa*). Photo Credit: USFWS.

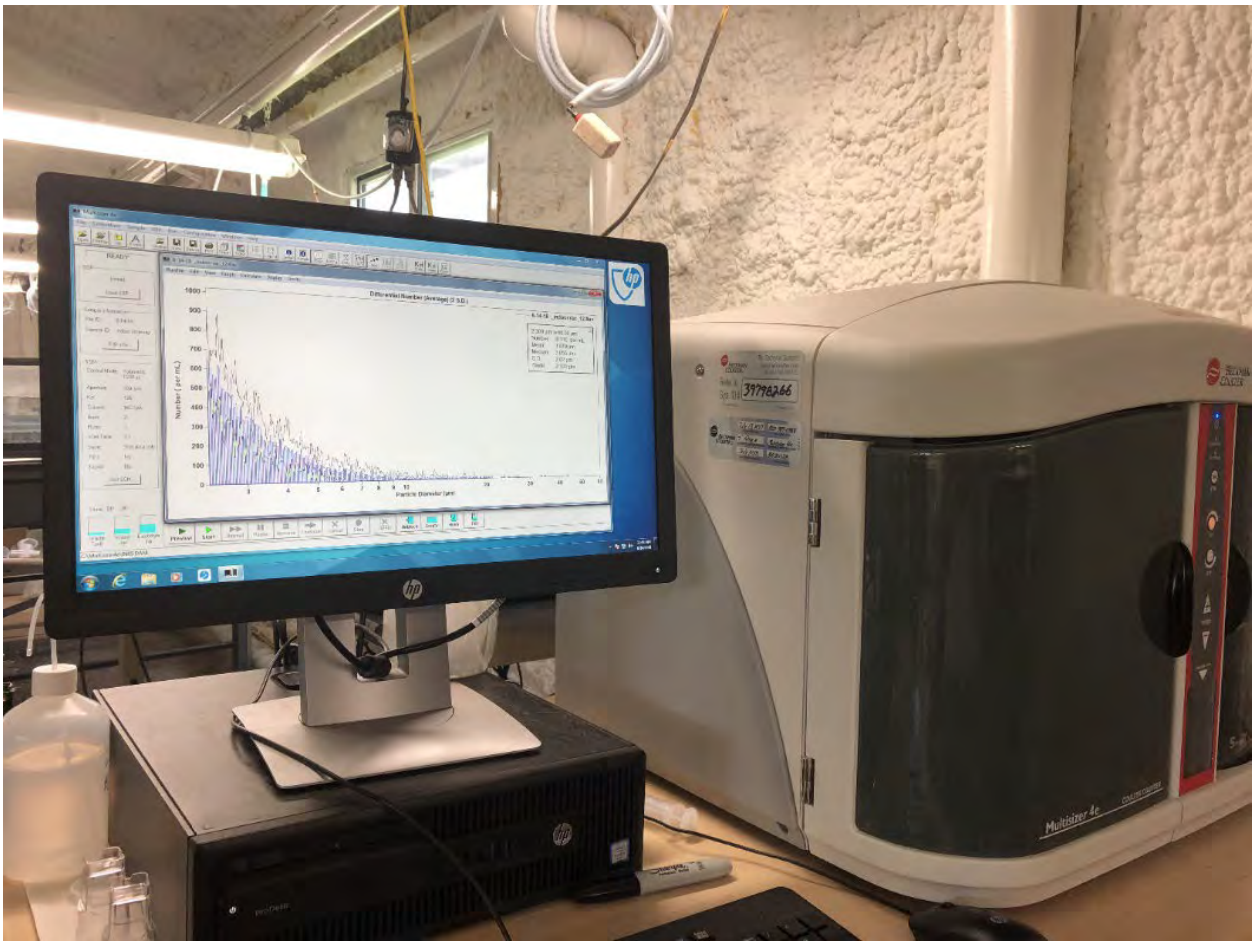

Figure 2. Beckman Coulter Multisizer 4e particle analyzer at Inks Dam NFH. Photo Credit: USFWS

Figure 3. Outdoor flow-through freshwater mussel holding tanks at Inks Dam NFH. Photo Credit: USFWS

Figure 4. Gravid female Texas Fatmucket displaying its lure inside Z-habitat tank at IDNFH. Photo Credit: USFWS

Figure 5. Hatchery staff stock infested host fish into a Z-habitat unit at IDNFH. Photo Credit: USFWS

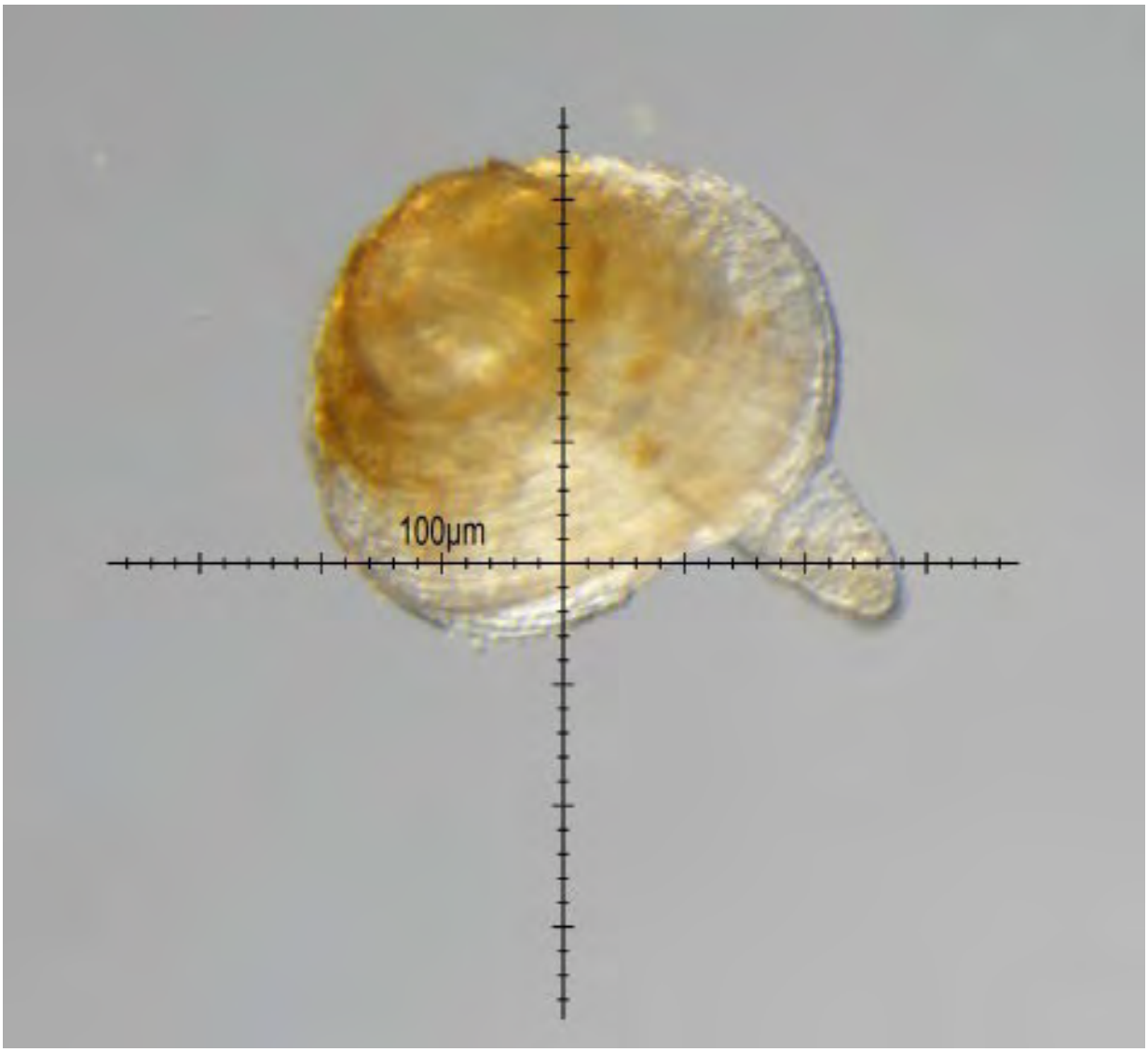

Figure 6. Newly metamorphosed juvenile Texas Fatmucket (*Lampsilis bracteata*) at IDNFH. Photo Credit: USFWS

Figure 7. Flow-through juvenile mussel rearing system at IDNFH. Photo Credit: USFWS.

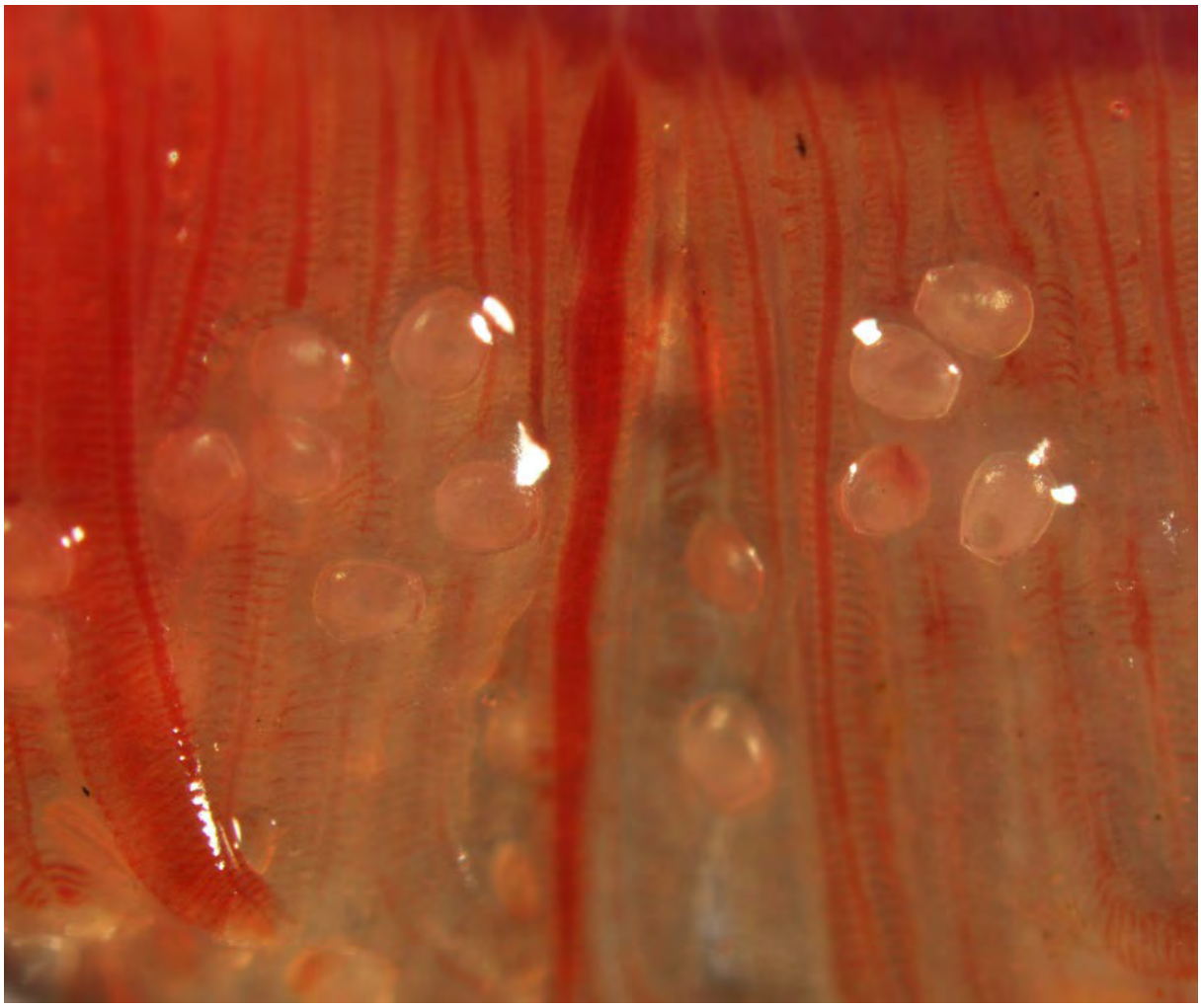

Figure 8. Gill sample from a Green Sunfish showing infestation of Texas Fatmucket glochidia. Photo Credit: USFWS

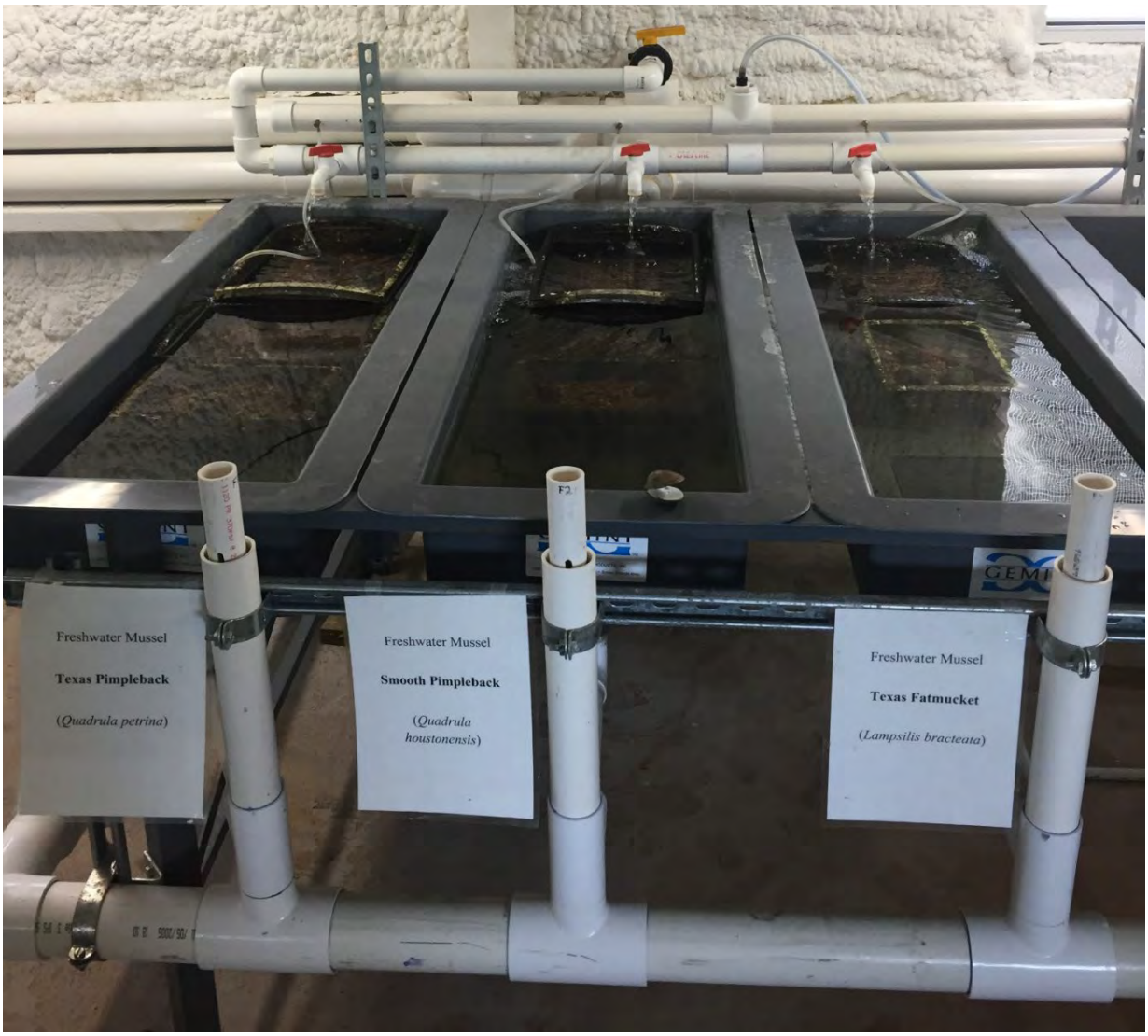

Figure 9. Indoor flow-through raceways for holding adult freshwater mussels. Photo Credit: USFWS

Figure 10. Semi-closed flow-through pan system(s) with total recirculation capability for juvenile freshwater mussel rearing at Inks Dam NFH. Photo Credit: USFWS

Figure 11. Z-habitat systems used in freshwater mussel propagation during FY-2018 at Ink Dam NFH. Photo Credit: USFWS

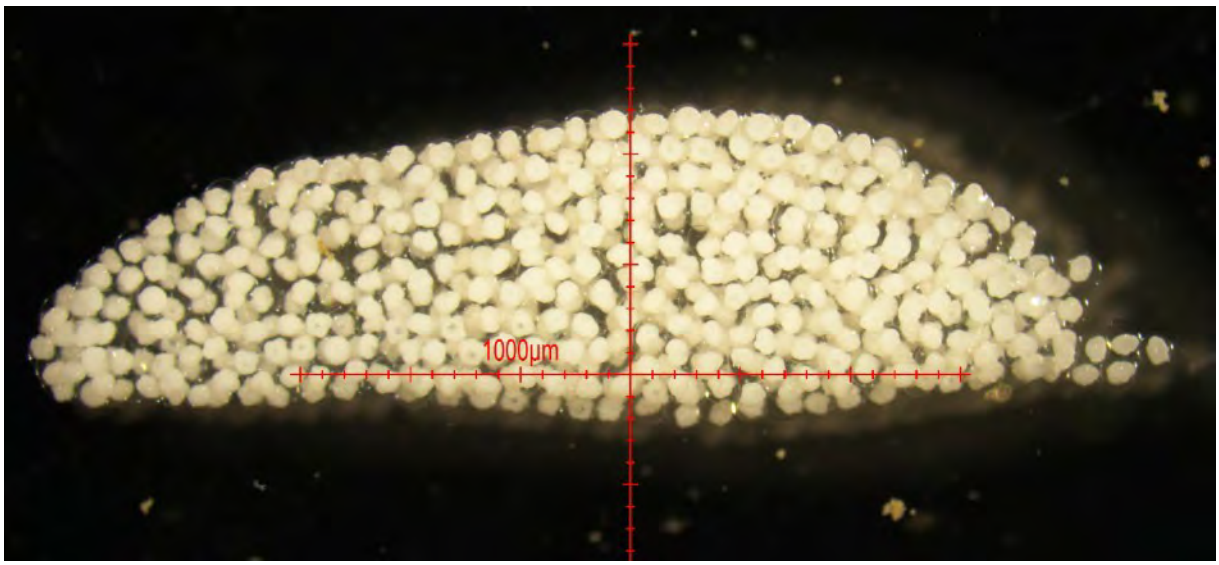

Figure 12. Under-developed Texas Pimpleback (Cyclonaias petrina) glochidia inside aborted conglutinate packet. Photo Credit: USFWS

Figure 13. FY-2017 captive reared Texas Fatmucket (*Lampsilis bracteata*) in August 2018. Photo Credit: USFWS

Figure 14. Paired flow-through filtered vs. unfiltered up-wellers and down-wellers. Photo Credit: USFWS

Figure 15. Paired semi-closed filtered vs. unfiltered pan systems. Photo Credit: USFWS

Figure 16. (Left) Large flow-through up-weller system. (Right) single large up-weller stocked with juvenile Texas Fatmuckets (*Lampsilis bracteata*). Photo Credit: USFWS

Figure 17. Microscopes, lab desk space, and sink used in freshwater mussel propagation at IDNFH. Photo Credit: USFWS

Figure 18. Texas Fatmucket broodstock tagged and returned to the San Saba River. Photo credit USFWS

Figure 19. Texas Pimpleback (*Cyclonaias petrina*) conglutinates (top right). Photo credit: USFWS

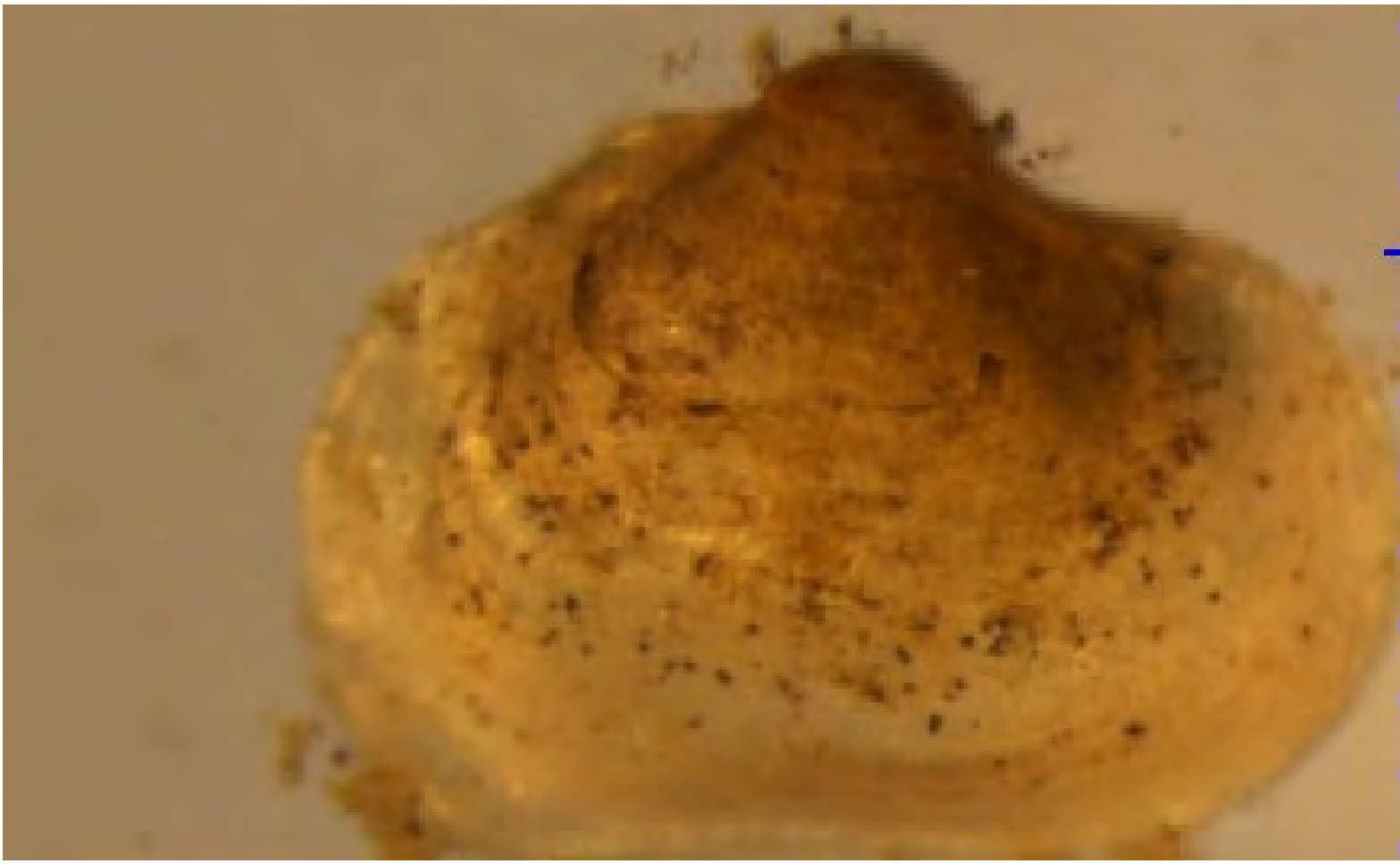

Figure 20. Texas Pimpleback (*Cyclonaias petrina*) after 64 days of growth in an unfiltered up-weller. Length is approximately 1400 µm. Photo credit: USFWS

Figure 21. Four tank juvenile mussel collection system at IDNFH. Photo Credit: USFWS.

Figure 22. Texas Fatmuckets (*Lampsilis bracteata*) in a filtered up-weller at Inks Dam NFH. Photo credit USFWS

Tables and Captions

Table 1. Freshwater mussel collection and acquisition during FY-2017.

Date	Species	Collection Site	Collector(s)	No.	No. Returned
4/20/2017	Texas Fatmucket	Llano River, FM 1871	IDNFH / SMARC	4	0
4/20/2017	Texas Pimpleback	Llano River, FM 1871	IDNFH / SMARC	4	0
5/3/2017	Texas Pimpleback	Colorado River, Altair	IDNFH / Bio-West	11	0
5/3/2017	Pimpleback	Colorado River, Altair	IDNFH / Bio-West	12	0
5/16/2017	Texas Fatmucket	Llano River, Simonsville Rd.	IDNFH	1	0
5/16/2017	Texas Fatmucket	Llano River, CR 102	IDNFH	1	0
5/16/2017	Texas Pimpleback	Llano River, CR 102	IDNFH	2	0
5/31/2017	Texas Fatmucket	Llano River, FM 1871	IDNFH / Bio-West	2	0
5/31/2017	Texas Pimpleback	Llano River, FM 1871	IDNFH / Bio-West	5	0
7/18/2017	Texas Fatmucket	Llano River, FM 1871	IDNFH	2	0
7/18/2017	Texas Pimpleback	Llano River, FM 1871	IDNFH	3	0
			Totals	**47**	**0**
			Total Retained	**47**	

Table 2. Texas Fatmucket (*Lampsilis bracteata*) infestation data during FY-2017.

Infestation Date	Number of Host Fish	Host Fish Species	Number of Glochidia	Glochidia attached to fish	Infestation Time (min)	Drop-off Recovery System	Number of Days on Fish	System Temperature (˚C)	Drop-offs Recovered
6/20/2017	18/18	Bluegill and Green Sunfish	-	-	-	Z-habitat	10 to 14	23	2300

Table 3. Freshwater mussel collection and acquisition during FY-2018.

Date	Species	Collection Site	Collector(s)	No.	No. Returned
12/3/2017	Texas Fatmucket	Llano Reservoir, Llano TX	Bio-West	5	0
4/18/2018	Texas Pimpleback	Colorado River, Hwy 190	IDNFH / Bio-West	1	0
4/18/2018	Pimpleback	Colorado River, Hwy 190	IDNFH / Bio-West	1	1
4/28/2018	Texas Pimpleback	Colorado River, Hwy 190	IDNFH / Bio-West	2	2
5/7/2018	Texas Pimpleback	Colorado River, Hwy 190	IDNFH / Bio-West	2	2
5/17/2018	Texas Pimpleback	Colorado River, Hwy 190	IDNFH / Bio-West	6	0
5/22/2018	Texas Pimpleback	Llano River, FM 1871	IDNFH	3	0
5/24/2018	Pimpleback	Colorado River, Altair	SMARC	5	5
6/12/2018	Pimpleback	Colorado River, Altair	IDNFH / SMARC	5	5
6/28/2018	Pimpleback	Colorado River, Altair	IDNFH / SMARC	3	3
7/2/2018	Texas Fatmucket	San Saba River, Bois d'arc Rd.	IDNFH	2	0
7/19/2018	Texas Fatmucket	San Saba River, Bois d'arc Rd.	IDNFH	2	0
8/2/2018	Pimpleback	Colorado River, Altair	IDNFH / SMARC	23	22
8/2/2018	Texas Pimpleback	Colorado River, Altair	IDNFH / SMARC	3	3
			Totals	**63**	**43**
			Total Retained	**20**	

Table 4. Texas Fatmucket infestation data during FY-2018.

Infestation Date	Number of Host Fish	Host Fish Species	Number of Glochidia	No. Glochidia attached to fish	Infestation Time (min)	Drop-off Recovery System	Number of Days on Fish	System Temperature (˚C)	Number of Drop-offs Recovered
12/8/2017	26	Green Sunfish	96,000	48,000	-	Z-habitat	10 to 16	25	548
5/15/2018	24	Assorted Spp.	44,275	31,975	20	Z-habitat	-	24	0
6/11/2018	81	Bluegill	42,750	19,550	30	Z-habitat	14 to 20	24	1,235
6/18/2018	10	Bluegill				Z-habitat			
6/25/2018	15	Green Sunfish	25,050	7,800	40	Z-habitat	17 to 23	24	860
7/4/2018	2	Green Sunfish	-	-	direct application to gills	Z-habitat	-	-	0
7/9/2018	57/13	Bluegill and Green Sunfish	141,211	-	-	Z-habitat	-	-	40
8/15/2018	70	Bluegill	55,500	-	-	-	-	-	0
								Total	**2,683**

Table 5. Texas Pimpleback infestation data during FY-2018.

Infestation Date	Number of Host Fish	Host Fish Species	Number of Glochidia	No. Glochidia attached to fish	Infestation Time (min)	Drop-off Recovery System	Number of Days on Fish	System Temperature (˚C)	Number of Drop-offs Recovered
5/7/2018	12	Channel Catfish	-	-	-	Z-habitat	-	24	-
5/8/2018	10	Channel Catfish	-	-	-	Z-habitat	4 to 19	24	10
5/8/2018	90	Fathead Minnow	-	-	-	Z-habitat	13	24	1
5/9/2018	80	Fathead Minnow	107,700	44,800	30	Z-habitat	12 to 17	24	16
5/9/2018	30	Channel Catfish	107,700	44,800	30	Z-habitat	-	24	-
5/10/2019	10	Channel Catfish	50,400	-	-	Z-habitat	9 to 15	24	508
5/17/2018	30	Channel Catfish	25,500	10,500	10	Z-habitat	6 to 18	24	4,796
5/18/2018	46	Channel Catfish	37,575	17,575	25	circular	-	24	-
5/19/2018		Channel Catfish	7,500	-	-	circular	-	-	-
								Total	**5,331**

Table 6. Pimpleback infestation data during FY-2018.

Infestation Date	Number of Host Fish	Host Fish Species	Number of Glochidia	No. Glochidia attached to fish	Infestation Time (min)	Drop-off Recovery System	Number of Days on Fish	System Temperature (˚C)	Number of Drop-offs Recovered
6/13/2018	6	Channel Catfish	6,884	-	60	Z-habitat	-	-	1,200
6/29/2018	6	Channel Catfish	1,850	-	30	Z-habitat	-	-	5
8/3/2018	70	Channel Catfish	-	-	-	Z-habitat	-	-	-
								Total	**1,205**

Table 7. IDNFH Freshwater mussel collection and acquisition during FY-2019.

Date	Species	Collection Site	Collector(s)	No.	No. Returned
3/25/2019	Texas Fatmucket	San Saba R., Bois d'arc Rd.	IDNFH/Austin ES	2	2
4/4/2019	Texas Pimpleback	Colorado River, Hwy 190	IDNFH/Austin ES	5	5
4/19/2019	Texas Pimpleback	Colorado River, Hwy 190	IDNFH	0	0
5/1/2019	Texas Fatmucket	Llano River, FM 1871	IDNFH	0	0
5/7/2019	Texas Pimpleback	Colorado River, Hwy 190	IDNFH	0	0
5/31/2019	Texas Pimpleback	Colorado River, Hwy 190	IDNFH/Bio-West/SMARC	3	3
6/6/2019	Texas Fatmucket	San Saba R., Bois d'arc Rd.	IDNFH/SMARC/Uvalde	4*	4
6/21/2019	Pimpleback	Colorado River, Altair	IDNFH/SMARC/Uvalde	5	5
6/212019	Texas Pimpleback	Colorado River, Altair	IDNFH/SMARC/Uvalde	1	1
7/10/2019	Pimpleback	Colorado River, Altair	IDNFH/SMARC/Uvalde	4	4
7/12/2019	Texas Pimpleback	Colorado River, Hwy 190	IDNFH/SMARC	2	0
7/16/2019	Pimpleback	Colorado River, Altair	IDNFH/SMARC	3	3
7/16/2019	Texas Pimpleback	Colorado River, Altair	IDNFH/SMARC	1	0
7/18/2019	Texas Fatmucket	San Saba R., Bois d'arc Rd.	IDNFH/SMARC	3	0
			Total	**33**	**27**
			Total Retained	**6**	

* Harvested a single gill from each mussel streamside and returned mussels to collection point.

Table 8. Texas Fatmucket (*Lampsilis bracteata*) infestations during FY-2019.

Infestation Date	Number of Host Fish	Host Fish Species	Number of Glochidia	No. Glochidia attached to fish	Infestation Time (min)	Drop-off Recovery System	Number of Days on Fish	System Temperature (˚C)	Number of Drop-offs Recovered
3/27/2019	90	Green Sunfish	262,000	-	10	Circular	26 to 55	18	367
	59	Bluegill				Circular	26 to 41	18	3,860
6/6/2019	150+	Bluegill	238,000	-	30	Circular	13 to 22	23	11,604
7/30/2019	75	Bluegill	56,700	-	45	Circular	13 to 22	28	13
								Total	**15,844**

Table 9. Texas Pimpleback (*Cyclonaias petrina*) infestations during FY-2019.

Infestation Date	Number of Host Fish	Host Fish Species	Number of Glochidia	No. Glochidia attached to fish	Infestation Time (min)	Drop-off Recovery System	Number of Days on Fish	System Temperature (˚C)	Number of Drop-offs Recovered
4/7/2019	60	Channel Catfish	44,600	18,244	20	Circular	22 to 41	19	1,603
4/8/2019	45	Channel Catfish	45,300	24,600	20	Circular			
6/4/2019	7	Channel Catfish	2,700	-	45	Circular	9 to 24	23	1,736
6/5/2019	35	Channel Catfish	31,400	-	30	Circular			
6/6/2019	20	Channel Catfish	19,200	-	35	Circular			
6/7/2019	5	Channel Catfish	-	-	20	Circular			
6/8/2019	49	Channel Catfish	49,000	-	30	Circular			
								Total	**3,339**

Table 10. Pimpleback (*Cyclonaias pustulosa*) infestation data during FY-2019.

Infestation Date	Number of Host Fish	Host Fish Species	Number of Glochidia	No. Glochidia attached to fish	Infestation Time (min)	Drop-off Recovery System	Number of Days on Fish	System Temperature (˚C)	Number of Drop-offs Recovered
6/22/2019	55	Channel Catfish	86,600	-	35	Circular	6 to 16	25	5,651
7/18/2019	20	Channel Catfish	24,400	-	40	Circular	10 to 13	28	4,088
								Total	**9,739**

Table 11. FY-2019 growth and survival of three freshwater mussel species where F↓ is filtered down-weller, F↑ is filtered up-weller, U↓ is unfiltered down-weller, U↑ is unfiltered up-weller, FPS is filtered pan system, and UPS is unfiltered pan system.

Species	System	Maximum length observed (µm)	Maximum growth (µm/day)*	Percent Survival	Total No. Produced
Texas Fatmucket	F↓	6,000	74.7	14.3	664
	F↑	6,500	60.1	27.7	1,026
	U↓	0	N/A	0.0	0
	U↑	3,600	25.8	9.2	47
	FPS <400µm	3,000	28.7	5.8	88
	FPS >400µm	3,800	41.3	17.5	688
	UPS <400µm	0	N/A	0.0	0
	UPS >400µm	4,600	31.3	9.2	47
Texas Pimpleback	F↓	0	N/A	0	0
	F↑	3,500	26.6	15.8	113
	U↓	0	N/A	0	0
	U↑	0	N/A	0	0
	FPS <400µm	1,600	11.0	0.4	2.0
	FPS >400µm	2,800	26.9	7.4	172
	UPS <400µm	0	N/A	0	0
	UPS >400µm	2400	16.4	0.4	2
Pimpleback	F↓	2,600	37.3	3.8	49
	F↑	2,300	32.0	12.3	304
	U↓	N/A	N/A	N/A	N/A
	U↑	0	0	0.0	0
	FPS <400µm	1,400	17.7	3.0	18
	FPS >400µm	2,200	24.1	6.6	119
	UPS <400µm	0	0	0.0	0
	UPS >400µm	1,300	14.4	0.1	2

*Daily growth rate assumes a starting length of 250 µm for newly transformed juveniles.